

**ENANTIOSELECTIVE CYCLOPROPANATIONS OF ALLENES AND THEIR  
APPLICATION TO THE TOTAL SYNTHESIS OF CLAVINE ALKALOIDS**

by

Stephanie R. McCabe

B.Sc (Adv) (Hons), The Australian National University, 2012

Submitted to the Graduate Faculty of

The Kenneth P. Dietrich School of Arts and Sciences in partial fulfillment

of the requirements for the degree of

Doctor of Philosophy

University of Pittsburgh

2018

UNIVERSITY OF PITTSBURGH  
THE KENNETH P. DIETRICH SCHOOL OF ARTS AND SCIENCES

This dissertation was presented

by

Stephanie R. McCabe

It was defended on

May 4th, 2018

and approved by

Dennis P. Curran, Distinguished Service Professor of Chemistry and Bayer Professor,

Department of Chemistry

Kazunori Koide, Associate Professor, Department of Chemistry

Jelena M. Janjic, Associate Professor, School of Pharmacy and Graduate School of

Pharmaceutical Sciences, Duquesne University

Dissertation Advisor: Peter Wipf, Distinguished University Professor, Department of

Chemistry

Copyright © by Stephanie R. McCabe

2018

# ENANTIOSELECTIVE CYCLOPROPANATIONS OF ALLENES AND THEIR APPLICATION TO THE TOTAL SYNTHESIS OF CLAVINE ALKALOIDS

Stephanie R. McCabe, PhD

University of Pittsburgh, 2018

The first section of this thesis describes the development of an enantioselective synthesis of terminally unsubstituted methylenecyclopropanes. The key feature of this approach is a  $\text{Rh}_2(\text{S-TBPTTL})_4$ -mediated catalytic asymmetric cyclopropanation of unsubstituted allene to produce enantioenriched methylenecyclopropanes bearing alkyl or activated ester functionalities. This method was successfully applied to the enantioselective total synthesis of cycloclavine.

The second section of this thesis describes the development of an improved 12 steps/5.2% overall yield racemic total synthesis of the clavine alkaloid cycloclavine. The first enantioselective total syntheses of the unnatural enantiomer (–)-cycloclavine and the natural enantiomer (+)-cycloclavine were also accomplished in 8 steps/7.1%(brsm) overall yield and 8 steps/4% overall yield, respectively. Noteworthy features of this approach include a strain-promoted intramolecular Diels-Alder reaction followed by a highly regioselective aerobic  $\alpha,\beta$ -dehydrogenation to form a key enone intermediate in >99.5:0.5 *er* after crystallization. Additional noteworthy features include the enone 1,2-addition of a novel TEMPO-carbamate aminomethyl carbanion and an IMDAF reaction to install the indole core. The mechanism of thermolysis of the new TEMPOC amine protecting-group was investigated. Finally, the natural and unnatural enantiomers were evaluated for their ability to bind to several neurotransmitter receptors in radioligand binding assays.



## TABLE OF CONTENTS

<b>1.0</b>	<b>ENANTIOSELECTIVE CYCLOPROPANATIONS OF ALLENES .....</b>	<b>1</b>
<b>1.1</b>	<b>INTRODUCTION .....</b>	<b>1</b>
<b>1.1.1</b>	<b>Methylenecyclopropane: Structure and Properties .....</b>	<b>1</b>
<b>1.1.2</b>	<b>Biological Profile of Natural and Synthetic Methylenecyclopropanes .....</b>	<b>3</b>
<b>1.1.3</b>	<b>Synthesis of Methylenecyclopropanes .....</b>	<b>4</b>
<b>1.1.3.1</b>	<b>Cyclopropyl Ring Formation .....</b>	<b>5</b>
<b>1.1.3.2</b>	<b>Exocyclic Olefin Formation .....</b>	<b>7</b>
<b>1.1.4</b>	<b>Synthesis of Chiral Methylenecyclopropanes .....</b>	<b>10</b>
<b>1.1.5</b>	<b>Enantioselective Cyclopropanations of Allenes .....</b>	<b>14</b>
<b>1.2</b>	<b>RESULTS AND DISCUSSION .....</b>	<b>16</b>
<b>1.2.1</b>	<b>Cyclopropanations with <math>\alpha</math>-Alkyl Diazoesters .....</b>	<b>17</b>
<b>1.2.2</b>	<b>First Strategy: Enantioselective Cyclopropanation/Elimination .....</b>	<b>19</b>
<b>1.2.3</b>	<b>Second Strategy: Enantioselective Cyclopropanation of a Silyl Allene ....</b>	<b>21</b>
<b>1.2.4</b>	<b>Third Strategy: Enantioselective Cyclopropanation of Allene .....</b>	<b>25</b>
<b>1.3</b>	<b>CONCLUSIONS .....</b>	<b>36</b>
<b>2.0</b>	<b>TOTAL SYNTHESIS OF CLAVINE ALKALOIDS .....</b>	<b>38</b>
<b>2.1</b>	<b>INTRODUCTION .....</b>	<b>38</b>
<b>2.1.1</b>	<b><i>Ergot</i> Alkaloids .....</b>	<b>38</b>

2.1.2	Clavine Alkaloids: Structure and Biological Profile.....	40
2.1.3	Cycloclavine: Isolation and Structure.....	42
2.1.4	Cycloclavine: Biosynthesis .....	43
2.1.5	Synthetic Approaches to Cycloclavine .....	46
2.1.5.1	Szántay's Total Synthesis of (±)-Cycloclavine (2008).....	46
2.1.5.2	Wipf's Total Synthesis of (±)-Cycloclavine (2011).....	47
2.1.5.3	Brewer's Total Synthesis of (±)-Cycloclavine (2014).....	49
2.1.5.4	Cao's Formal Synthesis of (±)-Cycloclavine (2014).....	51
2.1.5.5	Opatz' Formal Synthesis of (±)-Cycloclavine (2016).....	53
2.1.5.6	Cao's Formal Synthesis of (+)-Cycloclavine (2017).....	54
2.1.5.7	Bisai's Formal Synthesis of (+)- and (-)-Cycloclavine (2018).....	56
2.2	RESULTS AND DISCUSSION.....	59
2.2.1	Retrosynthetic Analysis of (±)-Cycloclavine.....	59
2.2.2	Synthesis of the Key Tricyclic Ketone.....	60
2.2.3	Ketone Dehydrogenation.....	64
2.2.4	Completion of the Synthesis of (±)-Cycloclavine.....	70
2.2.5	Retrosynthetic Analysis of (-)-Cycloclavine .....	71
2.2.6	Synthesis of the Indoline-Fused Cyclopropane Core.....	72
2.2.7	Ketone Dehydrogenation and Enantiomeric Enrichment.....	74
2.2.8	Studies of Furanyl Lithium Additions to Enones.....	77
2.2.9	IMDAF Reaction and Completion of the Synthesis.....	90
2.2.10	Synthesis of (+)-Cycloclavine .....	94
2.2.11	Attempted Analogue Synthesis by Late Stage Derivatization .....	102

2.2.12	TEMPO-Carbamate Thermolysis Studies.....	108
2.2.13	Radioligand Binding Assays.....	111
2.3	CONCLUSIONS.....	115
3.0	EXPERIMENTAL.....	117
3.1	GENERAL EXPERIMENTAL.....	117
3.2	EXPERIMENTAL PROCEDURES.....	119
3.2.1	CHAPTER ONE EXPERIMENTAL PART .....	119
3.2.2	CHAPTER TWO EXPERIMENTAL PART: (±)-2.1 .....	152
3.2.3	CHAPTER TWO EXPERIMENTAL PART: (-)-2.1 .....	164
3.2.4	CHAPTER TWO EXPERIMENTAL PART: (+)-2.1 .....	185
APPENDIX A .....		208
APPENDIX B .....		230
BIBLIOGRAPHY.....		323

## LIST OF TABLES

Table 1-1 Catalytic Asymmetric Cyclopropanation of Vinyl Halides.....	20
Table 1-2 Catalytic Asymmetric Cyclopropanation of DMPS Allene .....	24
Table 1-3 Catalytic Asymmetric Cyclopropanation of Allene: Diazo Ester Screen .....	29
Table 1-4 Catalytic Asymmetric Cyclopropanation of Allene: Catalyst Screen .....	32
Table 2-1 Optimization of the Intramolecular Methylenecyclopropane Diels-Alder Reaction ...	62
Table 2-2 Optimization of the Dehydrogenation of 3-Phenylcyclohexanone under Stahl Conditions.....	65
Table 2-3 Enone 1,2-Addition: Metal, Organolithium Reagent and Additive Screen.....	78
Table 2-4 Enone 1,2-Addition: Amine Protecting Group Screen.....	85
Table 2-5 Transmetallation/Addition of TEMPO-carbamate <b>2.149</b> on a Model System .....	87
Table 2-6 Optimization of the IMDAF Cyclization on a Model System .....	91
Table 2-7 A Comparison of the Literature and Synthetic <sup>1</sup> H NMR Spectra of Cycloclavine ....	100
Table 2-8 A Comparison of the Literature and Synthetic <sup>13</sup> C NMR Spectra of Cycloclavine ...	101
Table 2-9 Thermolysis of the TEMPOC-Protected Indole .....	109
Table 2-10 Radioligand Binding Studies.....	114
Table A-1 Data Collection and Structure Refinement for Methylenecyclopropane <b>1.105</b> .....	210
Table A-2 Atomic Coordinates and Equivalent Isotropic Atomic Displacement Parameters (Å <sup>2</sup> ) for Methylenecyclopropane <b>1.105</b> .....	211

Table A-3 Bond Lengths (Å) for Methylene cyclopropane <b>1.105</b> .....	212
Table A-4 Bond Angles (°) for Methylene cyclopropane <b>1.105</b> .....	213
Table A-5 Anisotropic Atomic Displacement Parameters (Å <sup>2</sup> ) for Methylene cyclopropane <b>1.105</b> . .....	214
Table A-6 Hydrogen Atomic Coordinates and Isotropic Atomic Displacement Parameters (Å <sup>2</sup> ) for Methylene cyclopropane <b>1.105</b> .....	215
Table A-7 Data Collection and Structure Refinement for Ketone (±)- <b>2.86</b> .....	217
Table A-8 Atomic Coordinates and Equivalent Isotropic Atomic Displacement Parameters (Å <sup>2</sup> ) for Ketone (±)- <b>2.86</b> . .....	218
Table A-9 Bond Lengths (Å) for Ketone (±)- <b>2.86</b> .....	218
Table A-10 Bond Angles (°) for Ketone (±)- <b>2.86</b> .....	219
Table A-11 Anisotropic Atomic Displacement Parameters (Å <sup>2</sup> ) for Ketone (±)- <b>2.86</b> .....	220
Table A-12 Hydrogen Atomic Coordinates and Isotropic Atomic Displacement Parameters (Å <sup>2</sup> ) for Ketone (±)- <b>2.86</b> .....	221
Table A-13 Date Collection and Structure Refinement for Allylic Alcohol (±)- <b>2.111</b> .....	223
Table A-14 Atomic Coordinates and Equivalent Isotropic Atomic Displacement Parameters (Å <sup>2</sup> ) for Allylic Alcohol (±)- <b>2.111</b> .....	224
Table A-15 Bond lengths (Å) for Allylic Alcohol (±)- <b>2.111</b> .....	225
Table A-16 Bond Angles (°) for Allylic Alcohol (±)- <b>2.111</b> .....	226
Table A-17 Anisotropic Atomic Displacement Parameters (Å <sup>2</sup> ) for Allylic Alcohol (±)- <b>2.111</b> .....	228
Table A-18 Hydrogen atomic coordinates and isotropic atomic displacement parameters (Å <sup>2</sup> ) for allylic alcohol (±)- <b>2.111</b> .....	229

## LIST OF FIGURES

Figure 1-1 Properties of methylcyclopropane and methylenecyclopropane.....	2
Figure 1-2 Geometric properties of cyclopropane and methylenecyclopropane .....	2
Figure 1-3 Select methylenecyclopropane-containing natural products.....	4
Figure 1-4 Selected methylenecyclopropane nucleosides .....	4
Figure 1-5 Methylenecyclopropane Diels-Alder reaction <i>en route</i> to cycloclavine.....	16
Figure 1-6 Proposed cyclopropanation of an allene or alkene with a diazopropanoate .....	16
Figure 1-7 Competing $\beta$ -hydride migration and cyclopropanation pathways .....	17
Figure 1-8 First strategy to access enantioenriched methylenecyclopropane <b>1.65</b> .....	19
Figure 1-9 Cyclopropanation/protodesilylation strategy .....	22
Figure 1-10 Retrosynthetic analysis of methylenecyclopropane <b>1.65</b> .....	25
Figure 1-11 X-ray of <b>1.105</b> and attempts to upgrade the <i>ee</i> by crystallization.....	30
Figure 1-12 Selected chiral catalysts .....	31
Figure 1-13 a) Proposed transition states for the asymmetric cyclopropanation of allene with diazoester <b>1.99</b> b) possible conformations of dirhodium carboxylate catalysts.. .....	35
Figure 2-1 Lysergic acid and clavine subclasses and representative Ergot alkaloid pharmaceuticals.....	39
Figure 2-2 Tricyclic, tetracyclic and rearranged <i>clavine</i> alkaloids.....	40
Figure 2-3 Therapeutically relevant clavine alkaloids.....	41

Figure 2-4 Cycloclavine numbering and the methyl bromide salt derivative.....	42
Figure 2-5 Retrosynthetic analysis of (±)-cycloclavine.....	60
Figure 2-6 Classical methods for the dehydrogenation of ketones to enones.....	64
Figure 2-7 Proposed mechanism for the Pd(II)-catalyzed aerobic dehydrogenation of ketones..	67
Figure 2-8 Correlation between enolate stability and ring junction stereochemistry in <i>cis</i> and <i>trans</i> decalins .....	68
Figure 2-9 Regioselectivity in the enolization of <i>trans</i> -enolate <b>2.99</b> .....	69
Figure 2-10 Retrosynthetic analysis of (–)-cycloclavine .....	72
Figure 2-11 Enantiomeric enrichment by recrystallization to upgrade the <i>er</i> of tricycle <b>2.85</b> and SFC chromatograms of the a) racemic standard and b) enantioenriched enone <b>2.85</b> .....	76
Figure 2-12 Requisite enone 1,2-addition.....	77
Figure 2-13 Thiol addition/elimination strategy to mask the enone and facilitate a 1,2-addition reaction.....	81
Figure 2-14 Key 1D-NOE correlations for the allylic alcohol diastereomers .....	88
Figure 2-15 Key ROESY correlations for allylic alcohol diastereomers <b>2.111</b> and <i>epi</i> - <b>2.111</b> ....	89
Figure 2-16 X-ray structure of the major diastereomer <b>2.111</b> .....	90
Figure 2-17 Enantiomeric enrichment of the excess enantiomer by crystallization SFC chromatograms of the a) racemic standard and b) enantioenriched ketone <i>ent</i> - <b>2.85</b> .....	98
Figure 2-18 Comparison of the CD spectra of cycloclavine enantiomers .....	102
Figure 2-19 Ergoline core and the structure of selected monoamine neurotransmitters .....	111
Figure 3-1 Chiral GC resolution of racemic <b>1.81</b> .....	120
Figure 3-2 Chromatogram of enantiomerically enriched of ester <b>1.81</b> .....	120
Figure 3-3 Racemic standard .....	126

Figure 3-4 Enantioenriched ester derivatives .....	127
Figure 3-5 SFC chromatograms of racemic standard and imide derived from enantioenriched ester <b>1.101</b> .....	133
Figure 3-6 SFC chromatograms of racemic standard and imide <b>2.87</b> derived from enantioenriched mother liquor sample of methylenecyclopropane <b>1.105</b> .....	139
Figure 3-7 Mosher ester derivative: racemic standard.....	141
Figure 3-8 Enantioenriched Mosher ester derivatives .....	142
Figure 3-9 SFC chromatogram of imide <b>2.87</b> derived from the reaction with Rh <sub>2</sub> ( <i>R</i> -DOSP) <sub>4</sub> ..	144
Figure 3-10 SFC chromatogram of imide <b>2.87</b> derived from the reaction with Rh <sub>2</sub> ( <i>R</i> -BTCP) <sub>4</sub>	145
Figure 3-11 SFC chromatogram of imide <b>2.87</b> derived from the reaction with Rh <sub>2</sub> ( <i>S</i> -PTTL) <sub>4</sub> .	145
Figure 3-12 SFC chromatogram of imide <b>2.87</b> derived from the reaction with Rh <sub>2</sub> ( <i>S</i> -PTAD) <sub>4</sub>	146
Figure 3-13 SFC chromatograms of racemic standard and imide <b>2.87</b> derived from the cyclopropanation with dirhodium catalyst <b>1.117</b> .....	151
Figure 3-14 Representative SFC chromatogram showing racemic standard and enantiomerically enriched imide <b>2.87</b> using conditions b).....	166
Figure 3-15 SFC chromatograms of the racemic standard and enantioenriched enone <b>2.85</b> after recrystallization.....	170
Figure 3-16 SFC chromatogram of racemic standard and enantioenriched amide <i>ent</i> - <b>2.87</b> (87:13 <i>er</i> ).....	189
Figure 3-17 Representative SFC chromatograms of a) racemic standard b) enone <i>ent</i> - <b>2.85</b> before recrystallization and c) enantioenriched enone <i>ent</i> - <b>2.85</b> after recrystallization (batch 1) .....	194
Figure 3-18 Overlaid CD spectra of (–)- and (+)-cycloclavine.....	198
Figure 3-19 Thermolysis experiment 1: crude <sup>1</sup> H NMR spectrum.....	203



Figure 3-20 Thermolysis experiment 2: crude $^1\text{H}$ NMR spectrum.....	204
Figure 3-21 Thermolysis experiment 3: crude $^1\text{H}$ NMR spectrum.....	205
Figure 3-22 Thermolysis experiment 4: crude $^1\text{H}$ NMR spectrum.....	206
Figure A-1 ORTEP structure of methylenecyclopropane <b>1.105</b> .....	209
Figure A-2 ORTEP structure of ketone ( $\pm$ )- <b>2.86</b> .....	216
Figure A-3 ORTEP structure of allylic alcohol ( $\pm$ )- <b>2.111</b> .....	222

## LIST OF SCHEMES

Scheme 1-1 Synthesis of methylenecyclopropane by Gragson .....	5
Scheme 1-2 Synthesis of methylenecyclopropanes by alkylidenecarbene addition to an olefin....	6
Scheme 1-3 Methylenecyclopropane formation by carbenoid addition to an allene.....	6
Scheme 1-4 Methylenecyclopropane formation by an addition/elimination sequence .....	7
Scheme 1-5 Methylenecyclopropane formation by elimination of HX.....	8
Scheme 1-6 Methylenecyclopropane formation by elimination of HY .....	8
Scheme 1-7 Methylenecyclopropane formation by elimination of XY .....	9
Scheme 1-8 Methylenecyclopropane formation by double bond isomerization and allylic alcohol reduction .....	10
Scheme 1-9 Enzymatic resolution of prochiral methylenecyclopropyl diol.....	10
Scheme 1-10 Conversion of enantiopure cyclobutane into a chiral methylenecyclopropane .....	11
Scheme 1-11 Methylenecyclopropane synthesis by a [3,3]-sigmatropic rearrangement .....	11
Scheme 1-12 Synthesis of chiral methylenecyclopropanes from enantiopure cyclopropenes .....	13
Scheme 1-13 Catalytic asymmetric Michael addition to nitroalkenes.....	13
Scheme 1-14 Rh <sub>2</sub> ( <i>S</i> -DOSP) <sub>4</sub> catalyzed enantioselective cyclopropanation of phenylallene.....	14
Scheme 1-15 Ru(II)-Ph-Pheox catalyzed asymmetric cyclopropanation of cyclohexylallene.....	15
Scheme 1-16 Rh <sub>2</sub> ( <i>S</i> -IBAZ) <sub>4</sub> catalyzed cyclopropanation of phenylallene with an α-cyano diazo ester .....	15

Scheme 1-17 Fox's approach for the enantioselective cyclopropanation of $\alpha$ -alkyl- $\alpha$ -diazoesters .....	18
Scheme 1-18 Hashimoto's approach for the enantioselective cyclopropanation of diazopropanoates.....	19
Scheme 1-19 Attempted elimination reactions to form methylenecyclopropane <b>1.84</b> .....	21
Scheme 1-20 Preparation of alkyl diazopropanoates by alkylation and Regitz diazo transfer reactions .....	22
Scheme 1-21 Resolution of enantioenriched esters with ( <i>R</i> )-(-)-MTPACl to assess <i>ee</i> .....	23
Scheme 1-22 Precedent for metal carbenoid cyclopropanations of allene .....	25
Scheme 1-23 Synthesis of diazo substrates bearing an activated ester.....	26
Scheme 1-24 Trial cyclopropanation of allene with ethyl diazopropanoate.....	27
Scheme 1-25 Resolution of enantioenriched esters with ( <i>R</i> )-(-)-MTPACl to assess <i>er</i> .....	27
Scheme 1-26 Synthesis of dirhodium catalyst <b>1.117</b> .....	33
Scheme 1-27 Cyclopropanation of allene using Rh <sub>2</sub> ( <i>S</i> -4,7-DPPTTL) <sub>4</sub> .....	34
Scheme 2-1 Early stage transformations in the biosynthesis of cycloclavine .....	44
Scheme 2-2. Late stage transformations in the biosynthesis of cycloclavine.....	45
Scheme 2-3 Potential mechanisms of the <i>EasH</i> mediated biosynthetic cyclopropanation .....	46
Scheme 2-4 Total synthesis of (±)-cycloclavine by Szántay .....	47
Scheme 2-5 Total synthesis of (±)-cycloclavine by Petronijevic and Wipf .....	49
Scheme 2-6 Total synthesis of (±)-cycloclavine by Brewer .....	51
Scheme 2-7 Formal total synthesis of (±)-cycloclavine by Cao .....	52
Scheme 2-8 Synthesis of pyrrolinone <b>2.61</b> .....	53
Scheme 2-9 Formal total synthesis of (±)-cycloclavine by Netz and Opatz.....	54

Scheme 2-10 Synthesis of aldehyde <b>2.67</b> .....	55
Scheme 2-11 Formal total synthesis of (+)-cycloclavine by Cao .....	56
Scheme 2-12 Formal total synthesis of (+)-cycloclavine by Bisai .....	58
Scheme 2-13 Key $\alpha$ -aminoxylation in the formal synthesis of (–)-cycloclavine .....	59
Scheme 2-14 Synthesis of the key amino silyloxy diene ( $\pm$ )- <b>2.91</b> .....	61
Scheme 2-15 Formation of ketones ( $\pm$ )- <b>2.86</b> and ( $\pm$ )- <i>epi</i> - <b>2.86</b> and the relative configuration of ketone ( $\pm$ )- <b>2.86</b> .....	63
Scheme 2-16 Partial conversion of enol ethers ( $\pm$ )- <b>2.91</b> and ( $\pm$ )- <i>epi</i> - <b>2.91</b> to the undesired enone ( $\pm$ )- <b>2.93</b> .....	63
Scheme 2-17 Pd(II)-mediated aerobic oxidation of ketone ( $\pm$ )- <b>2.86</b> to enone ( $\pm$ )- <b>2.85</b> .....	66
Scheme 2-18 Pd <sup>II</sup> -mediated aerobic oxidation of ketone ( $\pm$ )- <i>epi</i> - <b>2.86</b> to enone ( $\pm$ )- <b>2.93</b> .....	67
Scheme 2-19 Completion of the synthesis of ( $\pm$ )-cycloclavine .....	70
Scheme 2-20 Synthesis of vinylogous imide <b>2.87</b> and SFC chromatograms of the a) racemic standard and b) enantioenriched imide <b>2.87</b> .....	73
Scheme 2-21 Conversion of vinylogous imide <b>2.87</b> into tricyclic ketones <b>2.86</b> and <i>epi</i> - <b>2.86</b> .....	74
Scheme 2-22 Pd(II)-mediated aerobic oxidation of ketone <b>2.86</b> to enone <b>2.85</b> .....	75
Scheme 2-23 Attempts to chemoselectively reduce an amide in the presence of an enone .....	79
Scheme 2-24 Synthesis of pyrone <b>2.121</b> and attempted enone 1,2-addition .....	80
Scheme 2-25 Intermolecular Diels-Alder reaction of pyrone <b>2.120</b> and cyclohexenone .....	81
Scheme 2-26 Enone protection by a thiol addition/elimination strategy in Wipf's synthesis of (–)-tuberostemonine .....	82
Scheme 2-27 Thiol conjugate addition, ketone 1,2-addition .....	83

Scheme 2-28 Synthesis of stannanes <b>2.139-2.141</b> via a Curtius rearrangement/ alkylation sequence.....	84
Scheme 2-29 Synthesis of stannane <b>2.149</b> .....	86
Scheme 2-30 Transmetallation/addition sequence using the optimized TEMPO furanyllithium reagent.....	87
Scheme 2-31 Thermal deprotection of TEMPOC-protected indole <b>2.151</b> .....	92
Scheme 2-32 Attempts to convert the equatorial diastereomer <i>epi</i> - <b>2.111</b> into indole <b>2.110</b> .....	93
Scheme 2-33 Completion of the synthesis of (–)-cycloclavine .....	94
Scheme 2-34 Synthesis of the dirhodium catalyst Rh <sub>2</sub> ( <i>R</i> -TBPTTL) <sub>4</sub> .....	95
Scheme 2-35 Synthesis of enantiomerically enriched vinylogous amide ( <i>ent</i> - <b>2.87</b> ) and SFC chromatograms of the a) racemic standard and b) enantioenriched amide <b>2.87</b> .....	96
Scheme 2-36 Synthesis of enantioenriched tricyclic enone <i>ent</i> - <b>2.85</b> .....	97
Scheme 2-37 Completion of the synthesis of (+)-cycloclavine .....	99
Scheme 2-38 Attempted <i>N</i> -CH <sub>3</sub> functionalization and hydrogenation of (+)-cycloclavine .....	103
Scheme 2-39 Attempted hydrogenation of amide <i>ent</i> - <b>2.110</b> .....	104
Scheme 2-40 Procter’s reductive ring-opening of a cyclopropyl amide using SmI <sub>2</sub> /NEt <sub>3</sub> /H <sub>2</sub> O. ....	105
Scheme 2-41 Synthesis of cyclopropyl amide model system and SmI <sub>2</sub> -mediated ring opening .....	106
Scheme 2-42 Attempted radical reduction of amide <i>ent</i> - <b>2.110</b> .....	107
Scheme 2-43 TEMPOC protection of indole.....	108
Scheme 2-44 Proposed mechanism for the major ionic thermolysis pathway .....	110
Scheme 2-45 Proposed mechanism for the minor radical pathway of thermolysis.....	110

## LIST OF ABBREVIATIONS

<i>p</i> -ABSA	..... <i>para</i> -acetamidobenzenesulfonyl azide
Ac	.....acetyl
AIBN	.....azobisisobutyronitrile
ATD	.....aluminium tris(2,6-di- <i>tert</i> -butyl-4-methylphenoxide)
BTPCP	.....(4-bromophenyl)-2,2-diphenylcyclopropanecarboxylato
Bn	.....benzyl
Boc	..... <i>tert</i> -butoxycarbonyl
<i>n</i> -BuLi	..... <i>n</i> -butyllithium
<i>s</i> -BuLi	..... <i>s</i> -butyllithium
brsm	.....based on recovered starting material
cat	.....catalytic
catMETium	.....Tricyclohexylphosphine[4,5-dimethyl-1,3-bis(2,4,6-trimethylphenyl)imidazol-2-ylidene][2-thienylmethylene] ruthenium(II) dichloride
COD	.....1,5-cyclooctadiene
cy	.....cyclohexyl
d	.....day(s)
DABCO	.....1,4-diazabicyclo[2.2.2]octane

DBU .....1,8-diazabicyclo[5.4.0]undec-7-ene  
 DCE.....dichloroethane  
 DDQ.....2,3-dichloro-5,6-dicyano-1,4-benzoquinone  
 dec .....decomposed  
 DHP .....dihydropyran  
 DIBAL-H .....diisobutylaluminium hydride  
 DMAP .....4-dimethylaminopyridine  
 DMF .....*N,N*-dimethylformamide  
 DMPS.....dimethylphenylsilyl  
 DMSO .....dimethylsulfoxide  
 DOSP .....*N*-(*p*-dodecylphenylsulfonyl)prolinato  
*dr* .....diastereomeric ratio  
*Eas*.....ergot alkaloid synthesis  
 EC<sub>50</sub>.....effective concentration of 50% of maximal response  
*ee* .....enantiomeric excess  
*ent*.....enantiomer  
 eq/equiv .....equivalent(s)  
 esp ..... $\alpha,\alpha,\alpha',\alpha'$ -tetramethyl-1,3-benzenedipropionate  
*er* .....enantiomeric ratio  
 EtOAc .....ethyl acetate  
 Exp. ....experimental  
 GABA .....gamma-aminobutyric acid  
*gem* .....geminal

h.....hour(s)  
 HIV ..... human immunodeficiency virus  
 HMPA.....hexamethylphosphoramide  
 HRMS .....high-resolution mass spectroscopy  
 IBAZ .....isobutyl-2-oxaazetidine-4-carboxylate  
 IBX..... 2-iodoxybenzoic acid  
 IMDAF.....intramolecular Diels-Alder furan  
 IR.....infrared spectroscopy  
 IC<sub>50</sub>.....the half-maximum inhibitory concentration  
 LAH .....lithium aluminum hydride  
 LCMS.....liquid chromatography mass spectroscopy  
 LDA .....lithium diisopropylamide  
 LiHMDS .....lithium bis(trimethylsilyl)amide  
*m*CPBA .....*meta*-chloroperoxybenzoic acid  
 MEM.....2-methoxyethoxymethyl ether  
 min .....minute(s)  
 Ms .....methanesulfonyl  
 MTBE .....methyl *tert*-butyl ether  
 MTPA ..... $\alpha$ -methoxy- $\alpha$ -trifluoromethylphenylacetic acid  
 NAD .....nicotinamide adenine dinucleotide  
 NaHMDS .....sodium bis(trimethylsilyl)amide  
 NMR .....nuclear magnetic resonance  
 NMO ..... *N*-methyl-morpholine-*N*-oxide



NMP ..... *N*-methyl-2-pyrrolidone  
 NOE ..... nuclear Overhauser effect  
 Ns (nosyl).....4-nitrobenzenesulfonyl  
 ON.....overnight  
 PARP .....poly (ADP-ribose) polymerase  
 Pcp.....pentachlorophenyl  
 PDT .....product  
 Pfp.....pentafluorophenyl  
 Pheox.....2-[(4*S*)-4,5-dihydro-4-phenyl-2-oxazolyl-*N*]phenyl  
 Piv .....pivaloyl  
 PMB .....*p*-methoxybenzyl  
 PPh<sub>3</sub>.....triphenylphosphine  
 ppm .....parts per million  
 PTAD .....(1-adamantyl)-(N-phthalimido)acetato  
 PTTL.....*N*-phthaloyl-*tert*-leucine  
 Py .....pyridine  
 ROESY .....rotating frame Overhauser effect spectroscopy  
 rt.....room temperature  
 SFC .....supercritical fluid chromatography  
 SM.....starting material  
 Su .....succinimidyl  
 TASF.....tris(dimethylamino)sulfonium difluorotrimethylsilicate  
 TBAF .....tetrabutylammonium fluoride

TBPTTL .....*N*-tetrabromophthaloyl-*tert*-leucine  
 TBS .....*tert*-butyldimethylsilyl  
 TEMPO .....2,2,6,6-tetramethyl-1-piperidinyloxy  
 Tf.....trifluoromethanesulfonyl  
 TFA .....trifluoroacetic acid  
 THF .....tetrahydrofuran  
 THP .....tetrahydropyran  
 TLC .....thin layer chromatography  
 TMDS .....1,1,3,3-tetramethyldisiloxane  
 TMP .....tetramethylpiperidine  
 TMS .....trimethylsilyl  
 TPA .....triphenylacetate  
 TPTA.....tri-*p*-tolylaminium  
 Ts.....toluenesulfonyl

## PREFACE

First I would like to thank my advisor, Prof. Peter Wipf for providing me with the opportunity to work in his group. I am grateful for the exceptional training and mentorship that I have received from him over the years. Prof. Wipf's dedication and drive for excellence in organic chemistry is truly remarkable and I am grateful to have worked for an advisor who continually challenges his students to achieve their best. I would also like to express my appreciation to my thesis committee, Prof. Dennis Curran, Associate Prof. Kazunori Koide and Prof. Jelena Janjic for overseeing my research and providing helpful feedback and advice. I would also like to thank Dr Curran for his guidance on my research proposal.

I wish to express my gratitude to all Wipf group members past and present. I've had the privilege to work with many outstanding and talented people during my time in graduate school. Firstly, I would like to thank Filip for pioneering the early work on the cycloclavine project and for paving the way for my graduate studies. I would also like to thank Kara and Josh for their constant friendship and for proofreading numerous drafts over the years. Additionally, I would like to thank Evan, Alex, Raf and Chaemin for their help and friendship. I would also like to thank my wonderful family for their unconditional love and support. Last but not least, I would like to thank James for his constant encouragement, love and unwavering support every step of the way. Without him this would not have been possible.

## 1.0 ENANTIOSELECTIVE CYCLOPROPANATIONS OF ALLENES

### 1.1 INTRODUCTION

#### 1.1.1 Methylenecyclopropane: Structure and Properties

The study and preparation of strained carbocycles has captivated synthetic and theoretical chemists for decades. Adolf Von Baeyer first introduced the concept of ring strain in 1885.<sup>1,2</sup> At the time numerous compounds containing five- and six-membered rings had been synthesized or isolated from natural sources. In contrast, smaller three- and four-membered rings had not been prepared despite considerable effort. This observation led von Baeyer to hypothesize that three and four membered rings were less stable due to ring strain.<sup>1</sup>

Methylenecyclopropanes are a unique subset of strained carbocycles with high ring strain energy (40.9 kcal/mol). This high ring strain can be largely attributed to the inherent angle strain caused by the deviation of the internal angles from the ideal  $sp^2$  bond angle of  $120^\circ$  and the ideal  $sp^3$  bond angle of  $109.5^\circ$  to  $\sim 64^\circ$  and partly because of the torsional strain imparted by eclipsing C–H bonds on adjacent carbons (Figure 1-1). The introduction of the exocyclic double bond in methylenecyclopropane (**1.1**) increases the ring strain by ca. 11 kcal/mol relative to methylcyclopropane (**1.2**). Studies by Wiberg revealed that the additional ring strain arises in part from the incorporation of a trigonal  $sp^2$  center in the ring.<sup>3</sup> The replacement of two relatively

strong C-H bonds (110.5 kcal/mol) in methylcyclopropane (**1.2**) with relatively weaker allylic C-H bonds in methylenecyclopropane (**1.1**) (99.3 kcal/mol) has also been reported to contribute to the added ring strain.<sup>4</sup>



**Figure 1-1** Properties of methylcyclopropane and methylenecyclopropane

The unique bonding characteristics of methylenecyclopropane (**1.1**) have been studied by several spectroscopic methods. Allen *et al.* showed that the exocyclic methylene distorts the C–C bond lengths in the cyclopropyl ring (Figure 1-2). Analysis of equilibrium geometries obtained from microwave and Raman studies show that the C1–C2 and C1–C3 bonds are 1.457 Å in methylenecyclopropane (**1.1**), which is slightly shorter than the bonds in the parent cyclopropane (**1.3**) (1.512 Å).<sup>5</sup> In contrast, the opposite C2–C3 bond in methylenecyclopropane (**1.1**) was determined to be 1.542 Å, which is marginally longer than the parent cyclopropane (**1.3**) C–C bonds (1.512 Å).

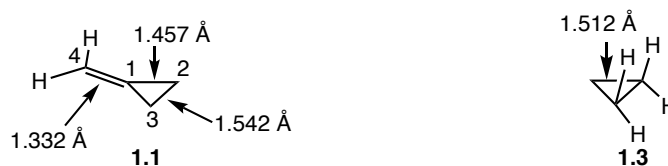


**Figure 1-2** Geometric properties of cyclopropane and methylenecyclopropane

### 1.1.2 Biological Profile of Natural and Synthetic Methylenecyclopropanes

Methylenecyclopropanes are found in several biologically active natural products and synthetic drug candidates. Amphimic acids A, B and C are a group of naturally occurring C<sub>27</sub> or C<sub>28</sub> methylenecyclopropane containing unsaturated fatty acids originally isolated from an Australian sea sponge of the genus *Amphimedon* at the Great Barrier Reef (Figure 1-3).<sup>6</sup> These natural products exhibited inhibitory activity against human DNA topoisomerase I in preliminary biological evaluations. Amphimic acid A proved to be a potent inhibitor of human topoisomerase I with an IC<sub>50</sub> of 0.47  $\mu$ M. Amphimic acid B and C were less potent exhibiting an IC<sub>50</sub> of 0.72 and 6.7  $\mu$ M respectively. The natural product G1499-2 was isolated from a culture broth of *Cytophaga johnsonii* and was characterized by the presence of a methylenecyclopropane substituent on a 4-quinolinone core.<sup>7</sup> G1499-2 showed moderate antibiotic activity against *flavobacterium* 1980 and *Staphylococcus aureus*. Hypoglycin A is a naturally occurring non-proteinogenic amino acid isolated from unripened fruit of the Ackee tree.<sup>8</sup> Its metabolite methylenecyclopropane acetyl CoA was identified as the causative agent of Jamaican vomiting sickness and is known to reduce blood glucose levels leading to hypoglycemia.<sup>9,10</sup> Clinical features of the illness include hypoglycemia, cerebral edema, convulsions and vomiting, which can progress to coma and in severe cases death.

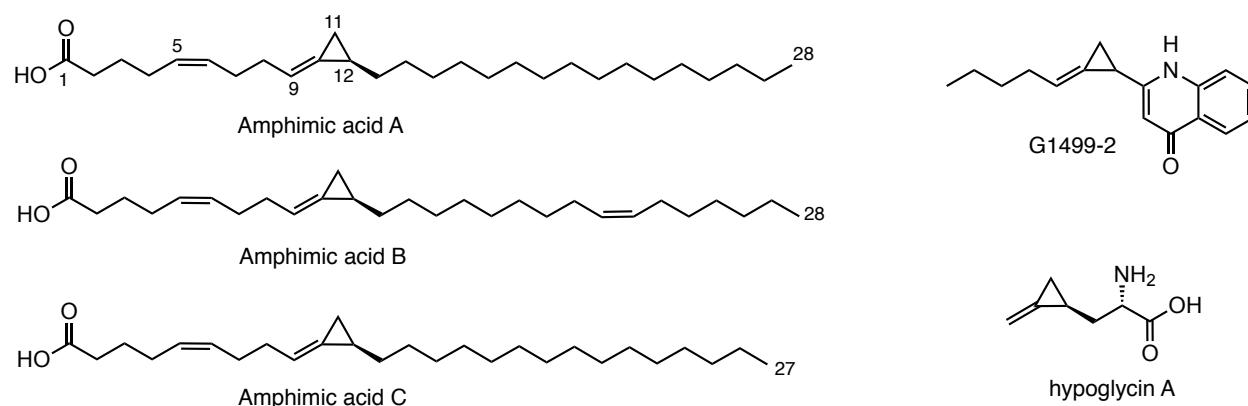


**Figure 1-3** Select methylenecyclopropane-containing natural products

Several methylenecyclopropane nucleosides possess potent antiviral activities. Cyclopropavir is a potent inhibitor of human cytomegalovirus with an  $EC_{50}$  of  $0.46 \mu\text{M}$  and is currently undergoing early stage clinical trials for the treatment of this viral disease.<sup>11</sup> Cyclopropavir also demonstrated antiviral activity against Epstein-Barr virus and human herpesvirus HHV-6 and HHV-8. The analogue (*S*)-synaguanol exhibited a broader spectrum of antiviral properties including anti-hepatitis B and anti-HIV activity.<sup>12</sup>

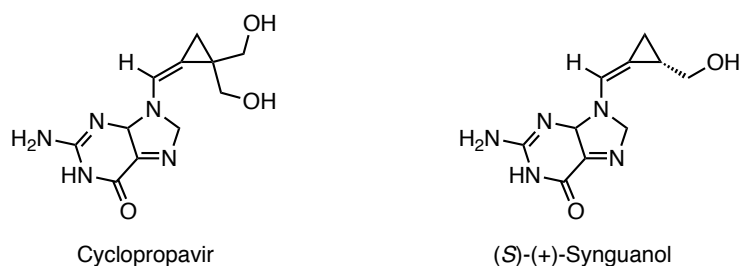
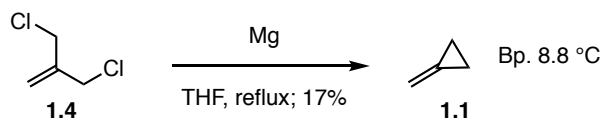


**Figure 1-4** Selected methylenecyclopropane nucleosides

### 1.1.3 Synthesis of Methylenecyclopropanes

Despite their high strain energy, many methylenecyclopropanes are surprisingly stable. The parent hydrocarbon **1.1** was first synthesized in 1952 by Gragson who showed that the

reaction of 3-chloro-(2-chloromethyl)-1-propene (**1.4**) with magnesium in refluxing THF formed methylenecyclopropane (**1.1**) in 17% yield after fractional distillation (Scheme 1-1).<sup>13</sup> The boiling point was determined to be 8.8 °C.



**Scheme 1-1** Synthesis of methylenecyclopropane by Gragson

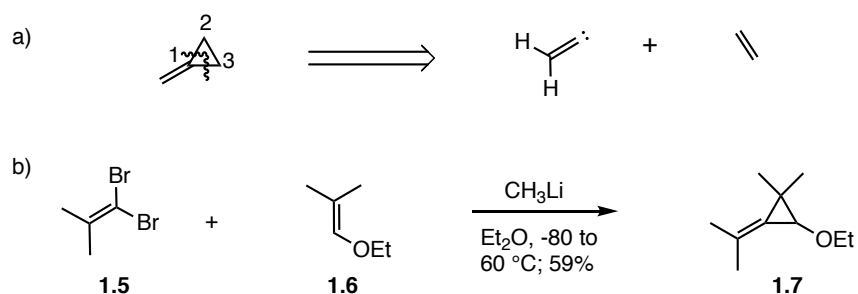
Numerous synthetic methods have since emerged to construct methylenecyclopropanes. These syntheses have been the subject of several comprehensive reviews and can be broadly classified into two major groups,<sup>14,15,16,17</sup> specifically, reactions that form the cyclopropane ring or reactions that form the exocyclic olefin from a pre-formed cyclopropane. The following section provides a brief overview of these approaches.

### 1.1.3.1 Cyclopropyl Ring Formation

The addition of a carbene to an unsaturated alkene or allene is one of the most extensively utilized and general methods to form methylenecyclopropanes. Two variants of this reaction have been developed.

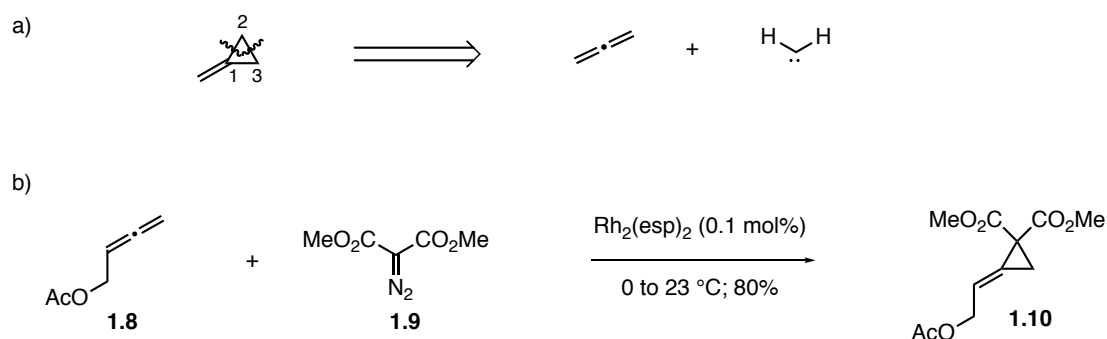
The first approach involves the addition of an alkylidenecarbene to an olefin to forge the cyclopropyl ring through C1–C2 and C1–C3 bond formation (Scheme 1-2a). The alkylidenecarbene substrate is typically generated by a base-mediated, thermal or photochemically induced 1,1-elimination of a substituted alkene.<sup>17</sup> One example of this alkylidenecarbene cyclopropanation is the reaction of 1,1-dibromo-2-methyl-1-propene (**1.5**) and vinyl ether **1.6** with methyllithium to form methylenecyclopropane **1.7** in 59% yield (Scheme 1-2b).<sup>18</sup>





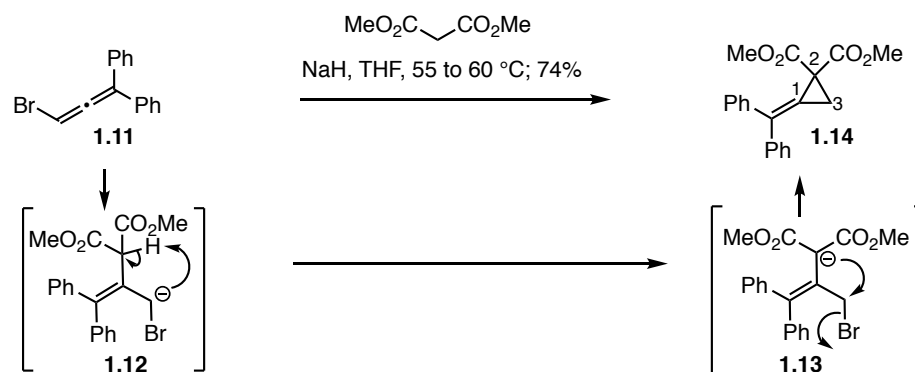
**Scheme 1-2** Synthesis of methylenecyclopropanes by alkylidenecarbene addition to an olefin

The second variant of this approach involves the cyclopropanation of an allene with a diazo carbenoid to forge the cyclopropyl ring through C1–C2 and C2–C3 bond formation (Scheme 1-3a). Highly stereoselective variants of this reaction have been developed, particularly in the presence of transition metal catalysts like rhodium, ruthenium and copper complexes. For example, during their synthetic studies toward members of the *Melodinus* alkaloid family, the Stoltz group showed that the reaction of homoallenyl acetate **1.8** with dimethyl 2-diazomalonate **1.9** in the presence of 0.1 mol% of the dirhodium complex  $\text{Rh}_2(\text{esp})_2$  formed the *E*-isomer **1.10** in 80% yield (Scheme 1-3b).<sup>19</sup>



**Scheme 1-3** Methylenecyclopropane formation by carbenoid addition to an allene

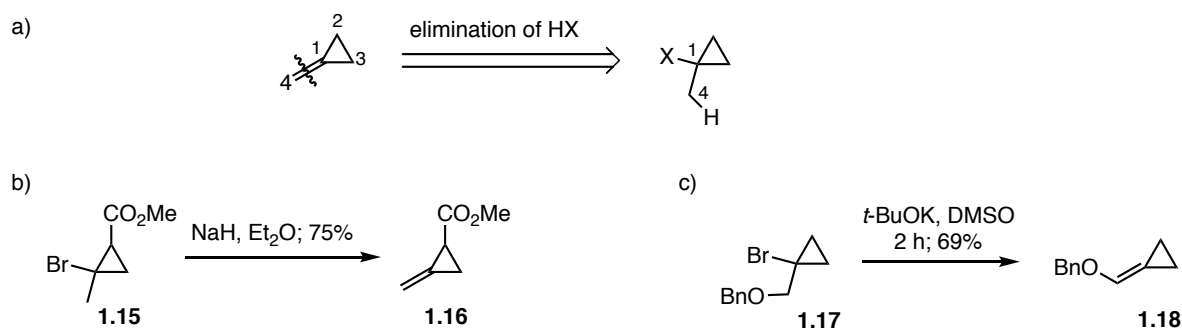
Huang *et al.* have reported a stepwise variant of this strategy in which methylenecyclopropanes were synthesized through sequential formation of the C1–C2 and C2–C3 bonds (Scheme 1-4).<sup>20</sup> In this approach, a base-mediated intermolecular cyclization of bromoallene **1.11** and dimethyl malonate proceeded smoothly to deliver methylenecyclopropane **1.14** in 74% yield. Various mono- and disubstituted aryl bromoallenes were tolerated. The mechanism is proposed to involve initial attack of the dimethyl malonate carbanion on the central carbon of the bromoallene **1.11** to generate intermediate **1.12**. An intramolecular proton transfer then forms the allylic anion **1.13**. Finally, an intramolecular substitution reaction of carbanion **1.13** produces methylenecyclopropane **1.14**.



**Scheme 1-4** Methylenecyclopropane formation by an addition/elimination sequence

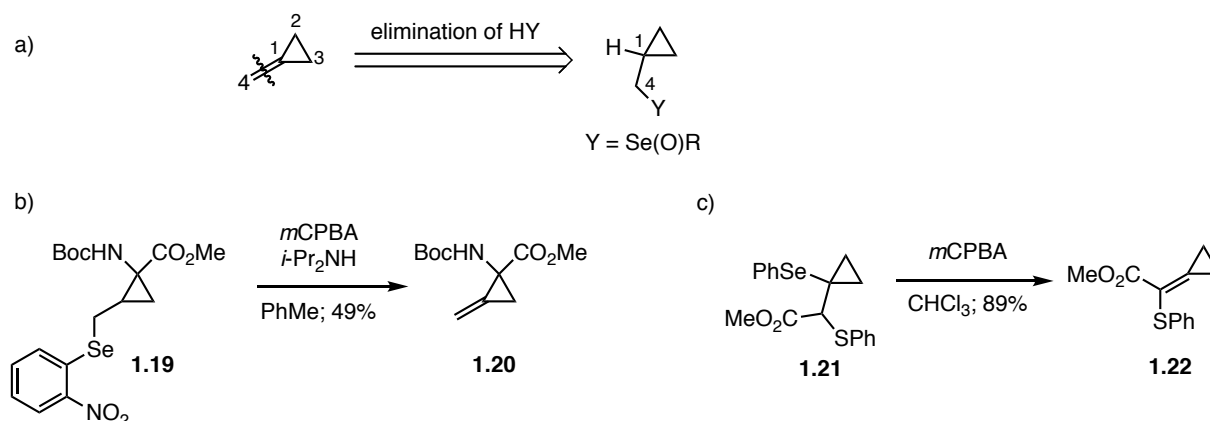
### 1.1.3.2 Exocyclic Olefin Formation

The conversions of 1-alkylcyclopropanes to the corresponding olefins by elimination reactions are among the most widely utilized and practical methods to form methylenecyclopropanes. For example, tertiary halides **1.15** and **1.17** readily undergo dehydrohalogenation upon treatment with base to form methylenecyclopropanes **1.16** and **1.18** in 75% and 69% yield respectively (Scheme 1-5b and 1-5c).<sup>21,22</sup>



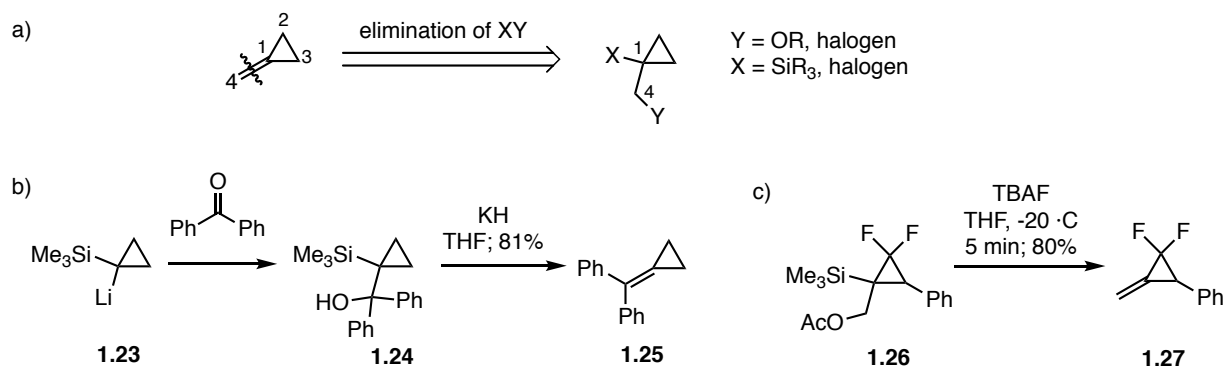
**Scheme 1-5** Methylenecyclopropane formation by elimination of HX

The dehydro-elimination of a non-halogen group like a selenoxide is another practical way to synthesize methylenecyclopropanes (Scheme 1-6a). Liu and colleagues showed that the oxidation of cyclopropyl selenide **1.19** with *m*CPBA formed the corresponding selenoxide, which then underwent *syn*-elimination to form olefin **1.20** (Scheme 1-6b).<sup>23</sup> The de Meijere group demonstrated that the oxidation of the phenylselenenyl group in **1.21** with *m*CPBA followed by  $\beta$ -elimination produced the corresponding  $\alpha,\beta$ -unsaturated ester **1.22** in 89% yield (Scheme 1-6c).<sup>24</sup>



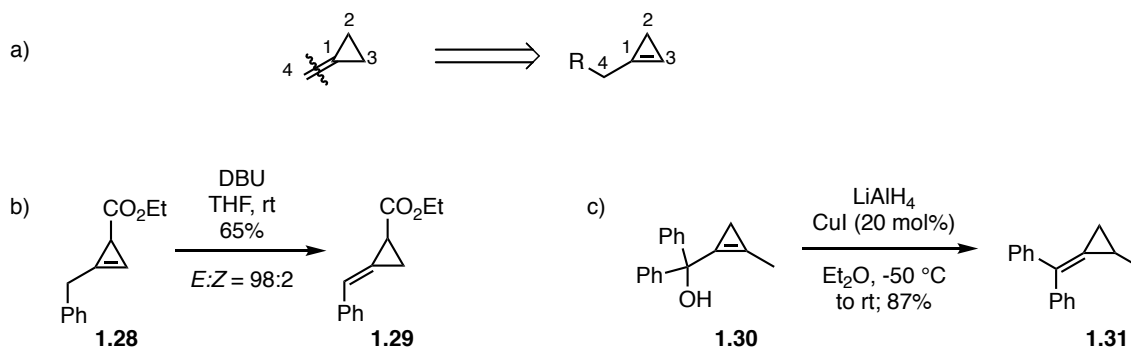
**Scheme 1-6** Methylenecyclopropane formation by elimination of HY

Finally, the elimination of an XY group is also frequently exploited to form methylenecyclopropanes from cyclopropane precursors (Scheme 1-7a). For example, lithiated cyclopropane **1.23** reacted with benzophenone to give intermediate  $\beta$ -hydroxy silane **1.24**. This intermediate then underwent a Peterson elimination upon treatment with KH to afford methylenecyclopropane **1.25** in 81% yield (Scheme 1-7b).<sup>25</sup> Taguchi demonstrated that the reaction of  $\beta$ -hydroxy silane **1.26** with TBAF at low temperatures in THF formed the corresponding difluorosubstituted methylenecyclopropane **1.27** in 80% yield (Scheme 1-7c).<sup>26</sup>



**Scheme 1-7** Methylenecyclopropane formation by elimination of XY

Alkylcyclopropenes can be transformed into methylenecyclopropanes by isomerizations or nucleophilic displacement reactions (Scheme 1-8a). Shi *et al.* showed that arylcyclopropene **1.28** could be converted into the *E*-methylenecyclopropane **1.29** in 65% yield by a DBU-mediated isomerization (Scheme 1-8b).<sup>27</sup> Marek developed a copper-catalyzed addition of LiAlH<sub>4</sub> to cyclopropenylcarbinol **1.30** to form methylenecyclopropane **1.31** in 87% yield (Scheme 1-8c). The reaction proceeds through a formal S<sub>N</sub>2' reaction to produce the methylenecyclopropane exclusively.<sup>28</sup> Hydroalumination of the cyclopropenyl alkene was not observed.

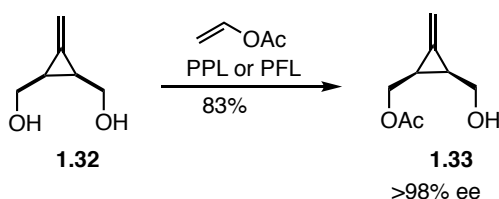


**Scheme 1-8** Methylenecyclopropane formation by double bond isomerization and allylic alcohol reduction

Other, albeit less widely utilized methods to form methylenecyclopropanes include the rearrangement of metal-allyl complexes, Wittig reactions, Horner-Wadsworth-Emmons reactions, Horner-Wittig olefinations and rearrangement reactions of cyclobutyl carbenes.<sup>15</sup>

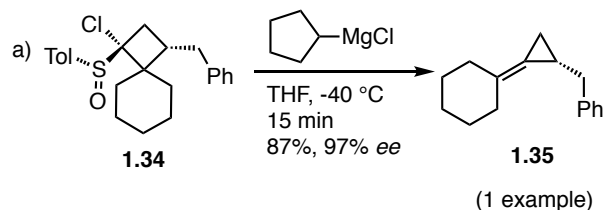
### 1.1.4 Synthesis of Chiral Methylenecyclopropanes

Methods to access enantioenriched methylenecyclopropanes are limited. Most approaches rely on enzymatic resolution or the use of chiral substrates and have narrow substrate scope. For example, the desymmetrization of prochiral alcohols by a lipase-catalyzed acylation is commonly used to produce enantiopure alcohols. The reaction of prochiral diol **1.32** with *Pseudomonas fluorescens* lipase AK or porcine pancreas lipase produced monoacetate **1.33** in >98% *ee* (Scheme 1-9).<sup>29</sup>



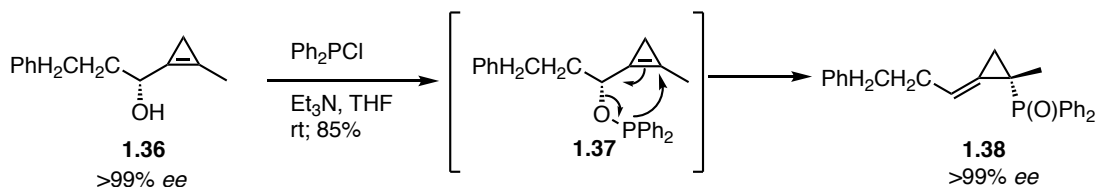
**Scheme 1-9** Enzymatic resolution of prochiral methylenecyclopropyl diol

The majority of protocols to form chiral methylenecyclopropanes rely on the use of enantiomerically pure starting materials. For example, the Satoh group showed that the reaction of the enantiopure sulfoxide **1.34** with cyclopentylmagnesium chloride generated the corresponding magnesium carbenoid, which underwent spontaneous rearrangement to provide methylenecyclopropane **1.35** in 87% yield and 97% *ee* (Scheme 1-10).<sup>30</sup>



**Scheme 1-10** Conversion of enantiopure cyclobutane into a chiral methylenecyclopropane

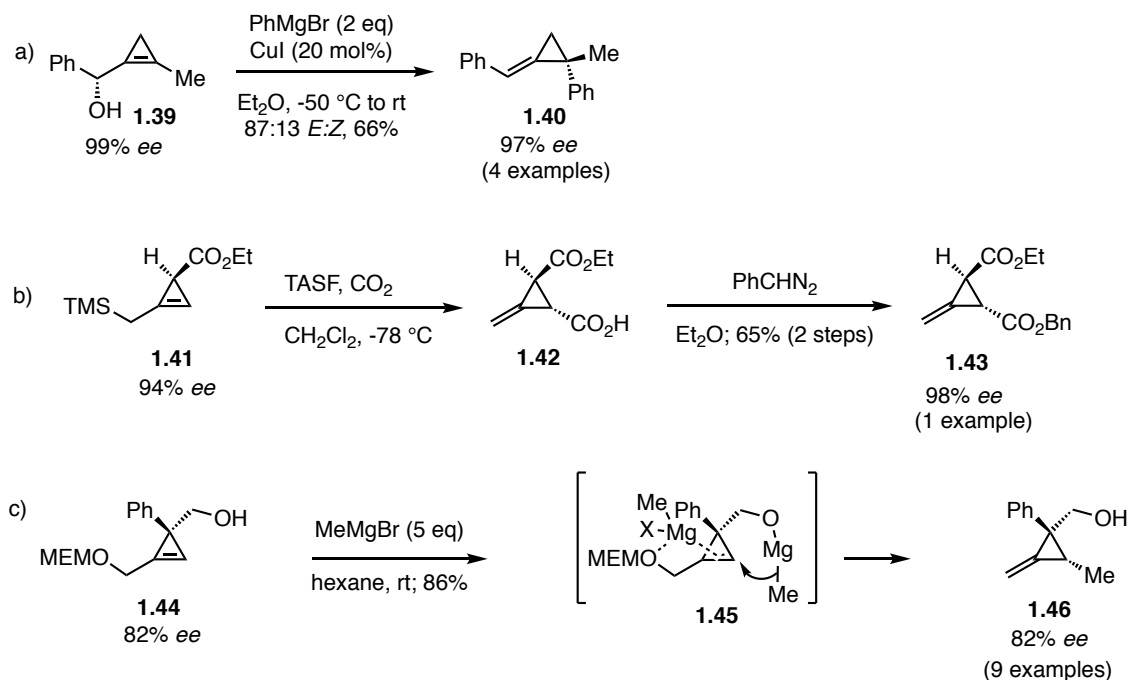
When enantiopure alcohol **1.36** was reacted with chlorodiphenylphosphane at room temperature, intermediate **1.37** formed and a spontaneous [3,3]-sigmatropic rearrangement occurred to form diphenylphosphine oxide derivative **1.38** in 85% yield and with complete transfer of chirality (Scheme 1-11).<sup>31</sup>



**Scheme 1-11** Methylenecyclopropane synthesis by a [3,3]-sigmatropic rearrangement

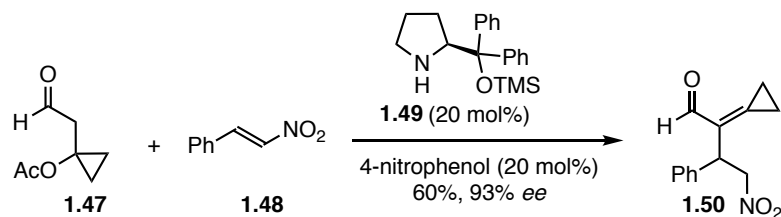
In the last decade, significant advances have been made in the synthesis of chiral methylenecyclopropanes from enantioenriched cyclopropene precursors. The Marek group showed that the reaction of cyclopropenylcarbinols like **1.39** with excess Grignard reagent in the presence of substoichiometric amounts of CuI produced enantiopure methylenecyclopropanes

such as **1.40** in good yield and diastereoselectivity (Scheme 1-12a).<sup>32</sup> Excellent retention of chirality from chiral cyclopropene **1.39** (99% *ee*) to methylenecyclopropane **1.40** (97% *ee*) was observed. Corey demonstrated that the reaction of enantiopure cyclopropenyl ester **1.41** with TASF at -78 °C under an atmosphere of CO<sub>2</sub> generated a methylenecyclopropane carboxylic acid intermediate **1.42**, which upon esterification with phenyldiazomethane gave the chiral methylenecyclopropane **1.43** in 65% yield over two steps and 98% *ee* (Scheme 1-12b).<sup>33</sup> Notable contributions to this area have been made by the Fox group who showed that enantiomerically pure alkylcyclopropenes could be converted to methylenecyclopropanes in high yield and with broad substrate scope by a nucleophilic displacement reaction (Scheme 1-12c).<sup>34,35</sup> Under optimized conditions they found that the reaction of cyclopropenyl alcohol **1.44** with excess MeMgBr proceeded with excellent regio- and diastereoselectivity to form methylenecyclopropane **1.46** in 86% yield and 82% *ee*. The free alcohol is proposed to chelate one equivalent of Grignard reagent to direct the delivery of the reagent from the same face in a pseudo-intramolecular manner. A second equivalent of the Grignard reagent is proposed to act as a Lewis acid to coordinate the MEM ether and olefin and block delivery of the Grignard to the more substituted position of the double bond.



**Scheme 1-12** Synthesis of chiral methylenecyclopanes from enantiopure cyclopropanes

A catalytic asymmetric Michael addition of aldehyde **1.47** to a series of nitrostyrenes in the presence of organocatalyst **1.49** has been reported (Scheme 1-13). The reaction between aldehyde **1.47** and nitrostyrene **1.48** in the presence of catalytic amounts of the chiral prolinol catalyst **1.49** and 4-nitrophenol as an acid co-catalyst furnished methylenecyclopropane **1.50** in 63% yield and 93% *ee*. A variety of electron deficient and electron rich aryl substituents and a 2-thienyl substituent were tolerated on the olefin component, giving the corresponding methylenecyclopropanes in moderate yields (27-60%) and high enantiomeric excesses (85-99% *ee*).<sup>36</sup>

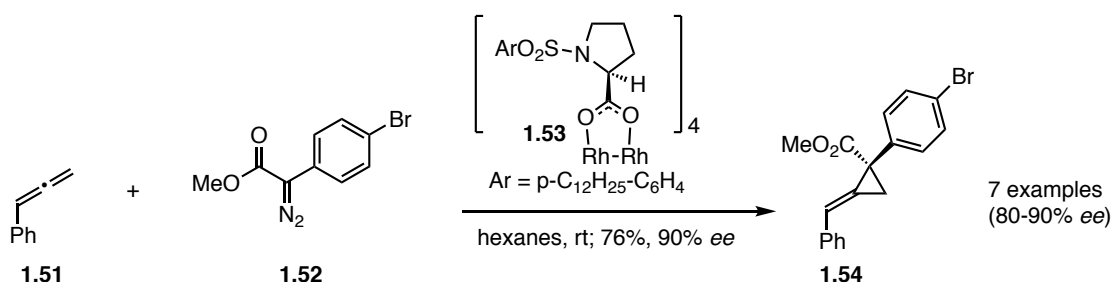


**Scheme 1-13** Catalytic asymmetric Michael addition to nitroalkenes



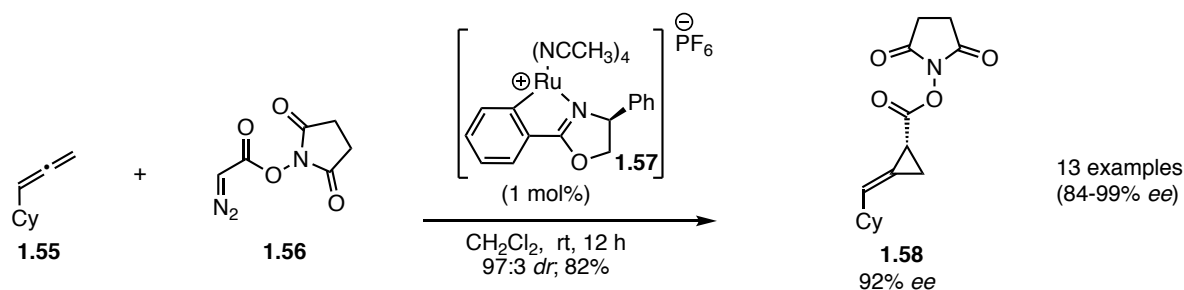
### 1.1.5 Enantioselective Cyclopropanations of Allenes

Only three transition metal catalyzed enantioselective cyclopropanations of substituted allenes with diazoesters have been reported.<sup>37</sup> This is surprising given the wide array of chiral catalysts available for the analogous reaction with alkyl olefins and styrenes. Gregg *et al.* developed a  $\text{Rh}_2(\text{S-DOSP})_4$  catalyzed cyclopropanation of diazoester **1.52** with several mono- and 1,1-disubstituted allenes to form methylenecyclopropanes in 80-90% *ee*. One example includes the cyclopropanation of phenylallene **1.51** with ester **1.52** to produce methylenecyclopropane **1.54** in 76% yield and 90% *ee* (Scheme 1-14).<sup>38</sup>



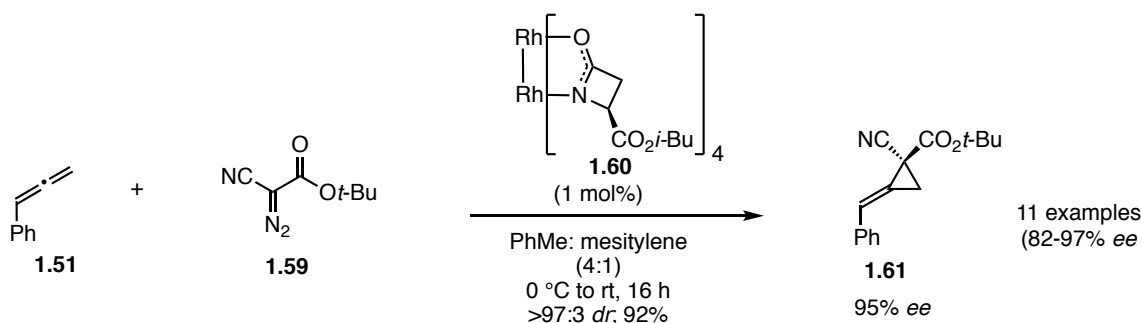
**Scheme 1-14**  $\text{Rh}_2(\text{S-DOSP})_4$  catalyzed enantioselective cyclopropanation of phenylallene

Iwasa reported that  $\text{Ru(II)-Ph-Pheox}$  (**1.57**) was an excellent catalyst for the asymmetric cyclopropanation of allenes with succinimidyl diazoacetate (Scheme 1-15).<sup>39</sup> Methylenecyclopropane products were obtained in high enantiomeric excesses ranging from 84-99% *ee*. The  $\text{Ru(II)-Ph-Pheox}$  catalyzed cyclopropanation of cyclohexylallene with succinimidyl diazo acetate proceeded smoothly at room temperature to form methylenecyclopropane **1.58** in 82% yield and 92% *ee* with excellent selectivity for the *E*-isomer.



**Scheme 1-15** Ru(II)-Ph-Pheox catalyzed asymmetric cyclopropanation of cyclohexyllallene

Finally, Charette showed that chiral dirhodium complex  $\text{Rh}_2(\text{S-IBAZ})_4$  (**1.60**) can catalyze the enantioselective cyclopropanation of diaceptor diazoesters with several mono- and 1,1-disubstituted allenes (Scheme 1-16).<sup>40</sup> The reaction between phenylallene **1.51** and diazo ester **1.59** in the presence of catalytic  $\text{Rh}_2(\text{S-IBAZ})_4$  delivered methylenecyclopropane **1.61** in 92% yield and 95% *ee*.



**Scheme 1-16**  $\text{Rh}_2(\text{S-IBAZ})_4$  catalyzed cyclopropanation of phenylallene with an  $\alpha$ -cyano diazo ester

A major limitation of these methods is the restriction of the allene component to substituted allenes, especially arylallenes. Expanding the scope of the allene substitution is necessary to further improve the utility of this methodology. We were thus interested in developing a method to access terminally unsubstituted methylenecyclopropanes in an enantioselective manner.

## 1.2 RESULTS AND DISCUSSION

The Wipf group has an ongoing interest in the synthesis and application of terminally unsubstituted methylenecyclopropanes. During the group's first total synthesis of cycloclavine the methylenecyclopropane **1.62** was converted into methylenecyclopropyl diene **1.63** and subjected to an intramolecular Diels-Alder reaction to forge the indoline-fused cyclopropane core **1.64** of the natural product (±)-cycloclavine (Figure 1-5).<sup>41</sup>

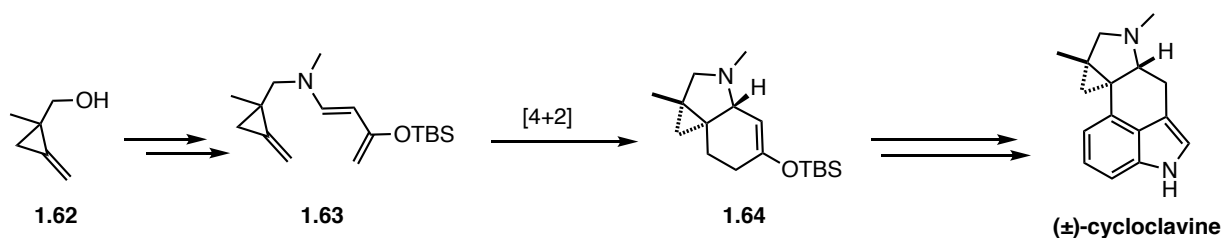


**Figure 1-5** Methylenecyclopropane Diels-Alder reaction *en route* to cycloclavine

In order to accomplish an enantioselective synthesis of cycloclavine, we sought to develop an enantioselective synthesis of a terminally unsubstituted methylenecyclopropane like **1.65** (Figure 1-6). To achieve this goal, we envisioned that methylenecyclopropane **1.65** could be formed through an enantioselective cyclopropanation of diazopropanoate **1.66** with an allene **1.67** using a transition metal catalyst and chiral ligand. Alternatively, an approach could use the reaction of diazopropanoate **1.66** with olefin **1.68**, followed by exocyclic alkene formation.

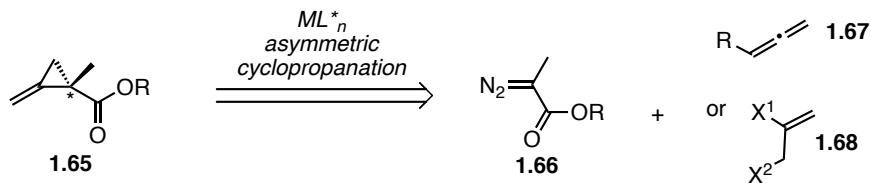


**Figure 1-6** Proposed cyclopropanation of an allene or alkene with a diazopropanoate

### 1.2.1 Cyclopropanations with $\alpha$ -Alkyl Diazoesters

Diazopropanoates like **1.66** are difficult substrates for metal-mediated cyclopropanations because of the propensity of the corresponding metal carbenoid **1.70** to undergo competing  $\beta$ -hydride elimination to form an acrylic ester **1.71** rather than the desired intermolecular cyclopropanation to form cyclopropane ester **1.69** (Figure 1-7).

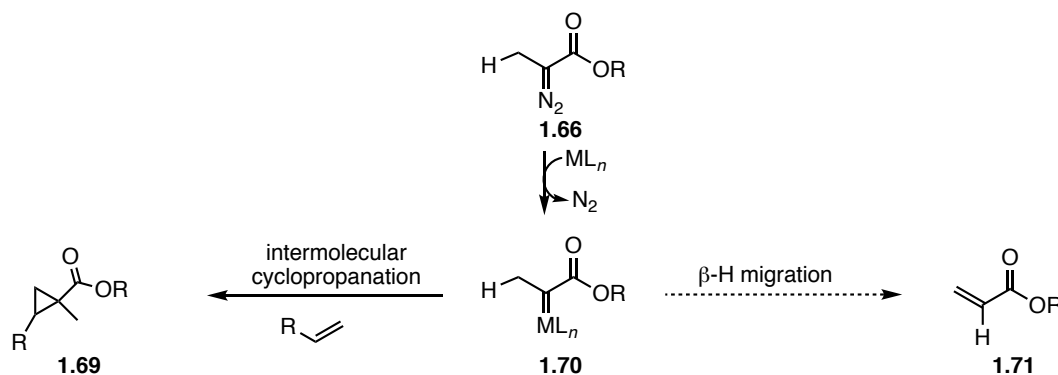
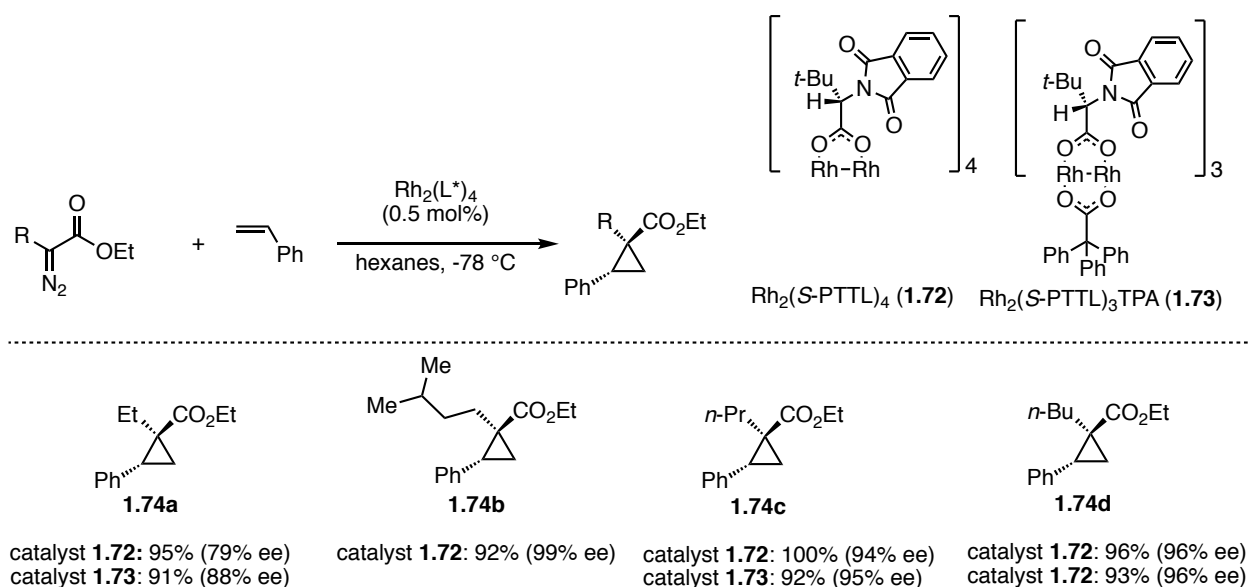


**Figure 1-7** Competing  $\beta$ -hydride migration and cyclopropanation pathways

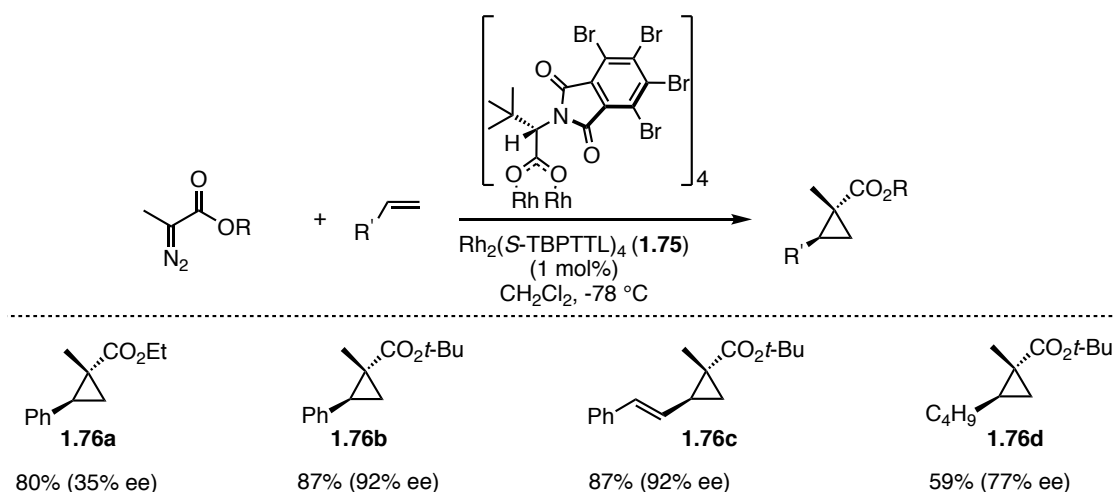
In the past decade, several methods have emerged that address these limitations. In a landmark study, Fox *et al.* found that dirhodium complexes with sterically hindered carboxylate ligands in conjunction with low reaction temperatures effectively promoted intermolecular cyclopropanations over the competing  $\beta$ -H migration pathway.<sup>42</sup> The achiral catalyst tetrakis(triphenylacetato) dirhodium(II)  $Rh_2(TPA)_4$  was particularly effective at converting a range of  $\alpha$ -alkyl- $\alpha$ -diazoesters to the corresponding cyclopropanes in high yield and with excellent diastereoselectivity.<sup>42</sup> The Fox group subsequently reported an enantioselective variant of this reaction using bulky carboxylate ligands derived from *L*-*tert*-leucine. The *N*-imido-*tert*-leucinate complexes  $Rh_2(S-PTTL)_4$  (**1.72**) and  $Rh_2(S-PTTL)_3TPA$  (**1.73**) were identified as the most effective catalysts providing cyclopropanes in high enantiomeric excesses (Scheme 1-17).

The level of enantioinduction was sensitive to the length of the  $\alpha$ -alkyl side chain. High levels of enantioinduction were obtained for diazoesters incorporating a long side chain. The corresponding methylenecyclopropane esters **1.74a-1.74d** were obtained in high *ee*'s ranging from 79-96% *ee*.



**Scheme 1-17** Fox's approach for the enantioselective cyclopropanation of  $\alpha$ -alkyl- $\alpha$ -diazoesters

Recently, Hashimoto *et al.* showed that the substrate scope of these reactions could be further expanded to include diazopropanoates when the dirhodium complex  $\text{Rh}_2(\text{S-TBPTTL})_4$  (**1.75**) was used as the catalyst (Scheme 1-18).<sup>43</sup> The use of sterically bulky esters with styrene derivatives as the olefin component led to high levels of enantioinduction (86-92% *ee* for esters **1.76a-1.76d**).



**Scheme 1-18** Hashimoto's approach for the enantioselective cyclopropanation of diazopropanoates

## 1.2.2 First Strategy: Enantioselective Cyclopropanation/Elimination

Our first approach to form the enantioenriched methylenecyclopropane **1.65** is outlined in Figure 1-8. We proposed that the chiral methylenecyclopropane **1.65** could be obtained *via* sequential Rh(II)-catalyzed asymmetric cyclopropanation and elimination reactions.

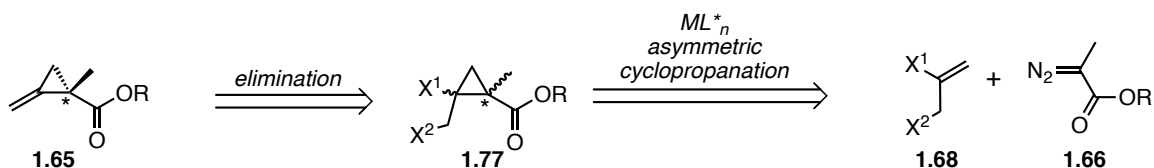
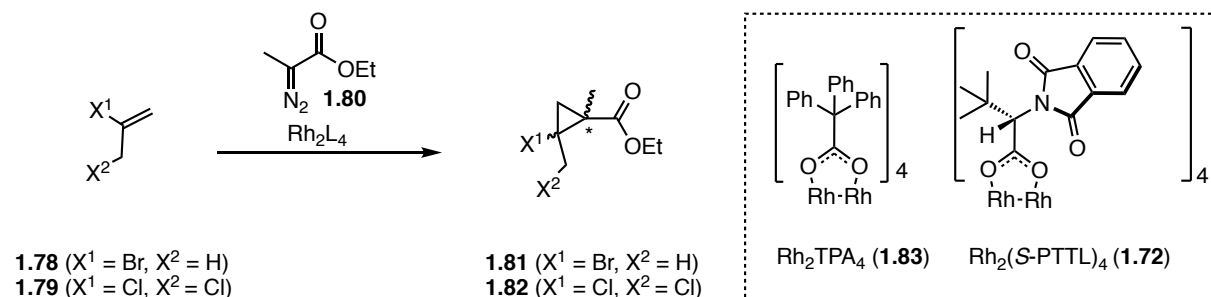


**Figure 1-8** First strategy to access enantioenriched methylenecyclopropane **1.65**

Dirhodium catalysts  $\text{Rh}_2\text{TPA}_4$  (**1.83**) and  $\text{Rh}_2(\text{S-PTTL})_4$  (**1.72**) were prepared according to literature protocols and screened in the cyclopropanation of ethyl 2-diazopropanoate (**1.80**) and 2-bromopropene (**1.78**) (Table 1-1, Entries 1-3) or 2,3-dichloroprop-1-ene (**1.79**) (Table 1-1, Entry 4).<sup>43,44</sup> Unfortunately, the desired cyclopropane was obtained at best in a moderate yield of

39% and a poor *er* of 62:38 when Rh<sub>2</sub>(S-PTTL)<sub>4</sub> (**1.72**) was employed as the catalyst and 2-bromopropene (**1.78**) as the vinyl halide (Table 1-1, Entry 3).

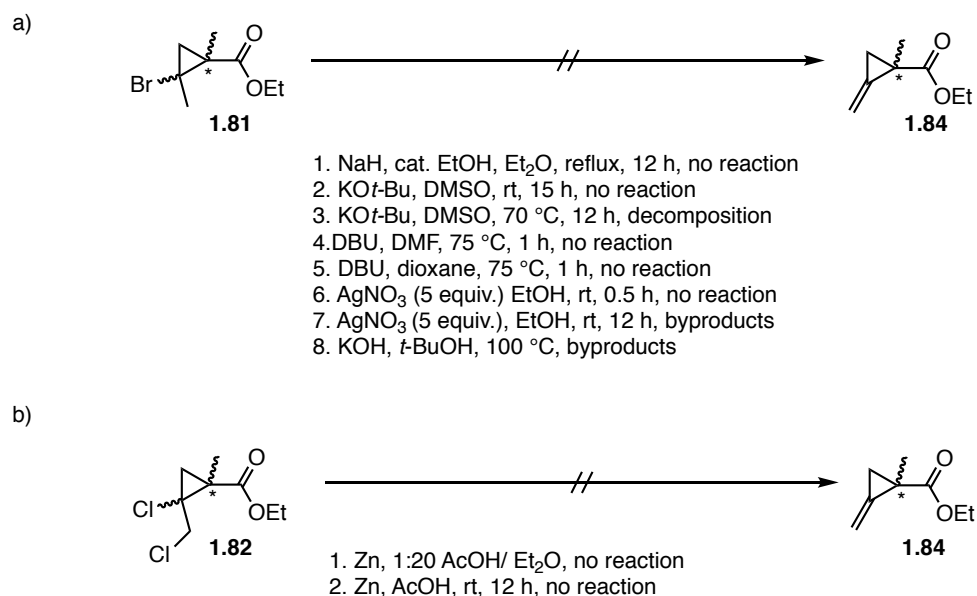
**Table 1-1** Catalytic Asymmetric Cyclopropanation of Vinyl Halides



Entry	Substrate	Catalyst	Solvent	Yield	<i>er</i>
1	<b>1.78</b>	Rh <sub>2</sub> (OAc) <sub>4</sub>	CH <sub>2</sub> Cl <sub>2</sub>	0%	-
2	<b>1.78</b>	<b>1.83</b>	CH <sub>2</sub> Cl <sub>2</sub>	8% <sup>a</sup>	-
3	<b>1.78</b>	<b>1.72</b>	hexanes	39% <sup>a</sup>	62.4: 37.6 <sup>b,c</sup>
4	<b>1.79</b>	<b>1.72</b>	hexanes	26% <sup>a</sup>	ND <sup>d</sup>

<sup>a</sup>isolated yield; <sup>b</sup>*ee* determined by chiral GC; <sup>c</sup>absolute configuration was not determined; <sup>d</sup>not determined.

All attempts to convert cyclopropane **1.81** to the corresponding methylenecyclopropane using a variety of bases including NaH, KO*t*-Bu, DBU and KOH and in the presence of superstoichiometric silver nitrate (Scheme 1-19) failed. Additionally, no reaction was observed when vicinal dichloride **1.82** was subjected to a zinc-mediated dehalogenation reaction.



**Scheme 1-19** Attempted elimination reactions to form methylenecyclopropane **1.84**

The poor enantioinduction in the cyclopropanation step combined with the failure of tertiary halides to undergo an elimination reaction to the corresponding methylenecyclopropane forced us to revise our strategy.

### 1.2.3 Second Strategy: Enantioselective Cyclopropanation of a Silyl Allene

We reasoned that using an allene in the asymmetric cyclopropanation would provide direct access to a functionalized methylenecyclopropane, thus circumventing the problematic elimination step. Retrosynthetically, we expected that terminal methylenecyclopropanes such as **1.65** could be formed from the corresponding vinyl silanes **1.85** by a protodesilylation reaction (Figure 1-9). The substituted methylenecyclopropane **1.85** could in turn be synthesized by a rhodium(II) carboxylate catalyzed enantioselective cyclopropanation of a silyl allene **1.86** and a



diazopropanoate **1.66**. Furthermore, we hoped that the silyl group would facilitate the cyclopropanation through the well-documented  $\beta$ -silicon effect.<sup>38</sup>

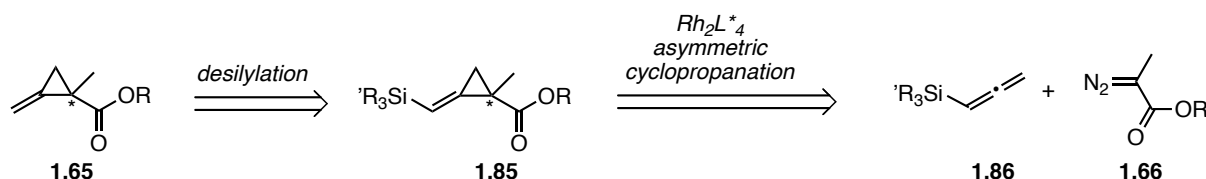
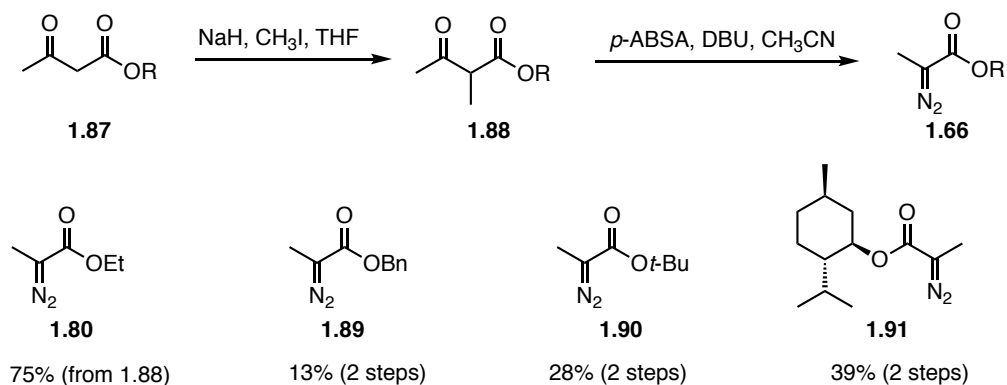


**Figure 1-9** Cyclopropanation/protodesilylation strategy

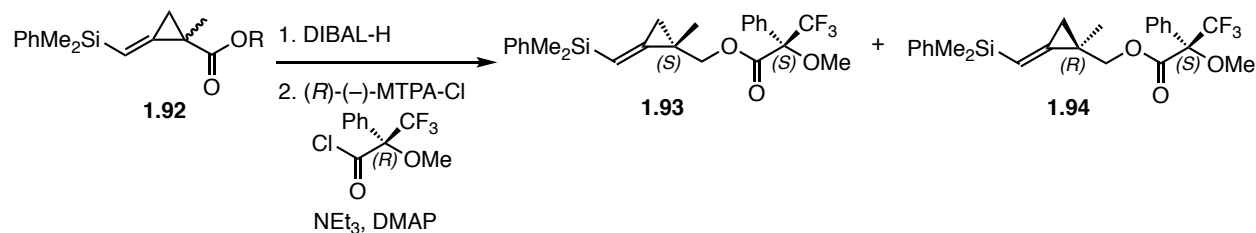
The syntheses of the known diazo ester substrates **1.80** and **1.89-1.91** are outlined in Scheme 1-20. The two-step protocol began with the deprotonation of  $\beta$ -ketoesters **1.87** with NaH followed by alkylation of the carbanion intermediate with methyl iodide. The methylated products **1.88** were then converted into the diazo esters **1.66** by a Regitz diazo transfer reaction.<sup>45,46</sup>



**Scheme 1-20** Preparation of alkyl diazopropanoates by alkylation and Regitz diazo transfer reactions

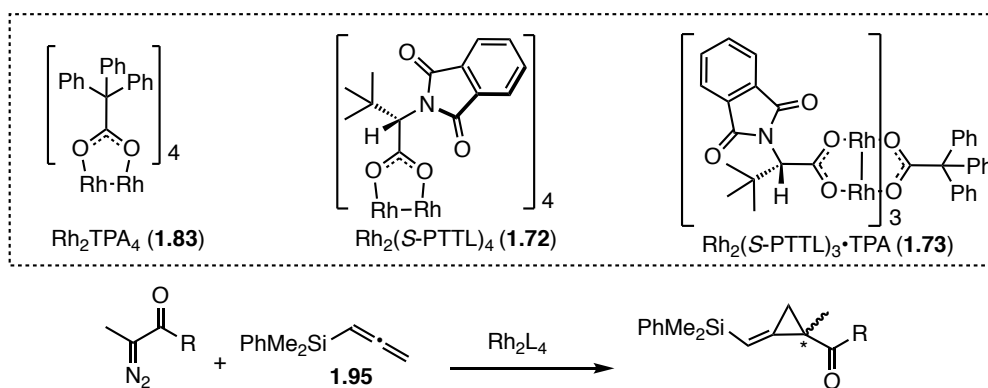
In order to establish the *ee* of the methylenecyclopropane products, the ester products were reduced to the corresponding alcohols and reacted with (*R*)-(-)-MTPACl to give the diastereomeric Mosher ester adducts **1.93** and **1.94** (Scheme 1-21). The *dr* was determined by NMR analysis of the crude reaction mixture and reflects the enantiomeric enrichment obtained in

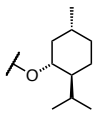
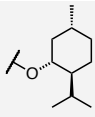
the prior cyclopropanation step. Complete conversion of the alcohol to the ester is important for accurate *dr* measurements due to differing rates of formation of the (*S,S*)- and (*R,S*)-diastereomers.<sup>47</sup>



**Scheme 1-21** Resolution of enantioenriched esters with (*R*)-(-)-MTPACl to assess *ee*

Our investigation commenced with a catalyst screen using the reaction of ethyl diazopropanoate with DMPS allene as a model system (Table 1-2, Entries 1-3). We were pleased to see that the reaction proceeded smoothly in the presence of the achiral catalyst  $\text{Rh}_2(\text{TPA})_4$  to form the desired methylenecyclopropane in 60% yield (Table 1-2, Entry 1). Next, chiral catalysts **1.72** and **1.73** were evaluated. The dirhodium complex  $\text{Rh}_2(\text{S-PTTL})_3 \cdot \text{TPA}$  (**1.73**) formed the desired methylenecyclopropane, albeit in a low yield of 31% and a poor *er* of 69:31 (Table 1-2, Entry 2). Switching to  $\text{Rh}_2(\text{S-PTTL})_4$  (**1.72**) resulted in a better yield of 61% and an improved *er* of 76:24 (Table 1-2, Entry 3). Using  $\text{Rh}_2(\text{S-PTTL})_4$  (**1.72**) as the optimal catalyst we then examined the cyclopropanation of different ester substrates. Unfortunately, the benzyl, *t*-butyl and menthyl diazo esters **1.89-1.91** resulted in moderate yields and poor *er*'s in all cases (Table 1-2, Entries 4-6). The best result was obtained using a menthyl diazo ester **1.91** in the presence of the achiral catalyst  $\text{Rh}_2(\text{TPA})_4$  (**1.83**) (Table 1-2, Entry 7), which gave the methylenecyclopropane adduct in a good yield of 83% and an *er* of 19:81.

**Table 1-2** Catalytic Asymmetric Cyclopropanation of DMPS Allene

Entry	R	Catalyst	Solvent	T (°C)	Yield (%)	<i>er</i> <sup>a,b</sup>
1	OEt ( <b>1.80</b> )	<b>1.83</b>	CH <sub>2</sub> Cl <sub>2</sub>	-78	60	50:50
2	OEt ( <b>1.80</b> )	<b>1.73</b>	hexanes	-78	31	69:31
3	OEt ( <b>1.80</b> )	<b>1.72</b>	hexanes	-78	64	76:24
4	OBn ( <b>1.89</b> )	<b>1.72</b>	hexanes	-78	41	72:28
5	<i>Ot</i> -Bu ( <b>1.90</b> )	<b>1.72</b>	hexanes	-78	34	68:32
6	 ( <b>1.91</b> )	<b>1.72</b>	hexanes	-78	62	73:27
7	 ( <b>1.91</b> )	<b>1.83</b>	CH <sub>2</sub> Cl <sub>2</sub>	-78	83	19:81 <sup>c</sup>

<sup>a</sup>based on analysis of MTPA-ester derivative; <sup>b</sup>the absolute configuration was not determined; <sup>c</sup>favours the opposite enantiomer.

In addition to the modest enantioinduction observed in the reaction, all attempts to convert the vinylsilane to the terminal methylenecyclopropane failed. Attempts to remove the silyl group using nucleophilic fluoride conditions gave no reaction or decomposition under harsher conditions (TBAF 5 eq., 80 °C, overnight). Additional attempts to cleave the analogous TMS or TBS methylenecyclopropane with reagents such as TBAF, HF•pyridine and AgF also failed to deliver the desired product. Overall, the poor enantioinduction combined with the failure to promote protodesilylation of the vinylsilane products forced us to further revise our strategy.

### 1.2.4 Third Strategy: Enantioselective Cyclopropanation of Allene

For our third-generation strategy we planned to exploit the asymmetric cyclopropanation of a diazopropanoate with unsubstituted allene (**1.96**) to form the chiral methylenecyclopropane **1.65** (Figure 1-10).

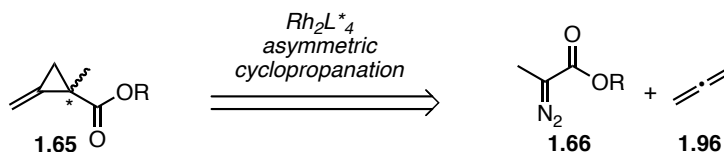
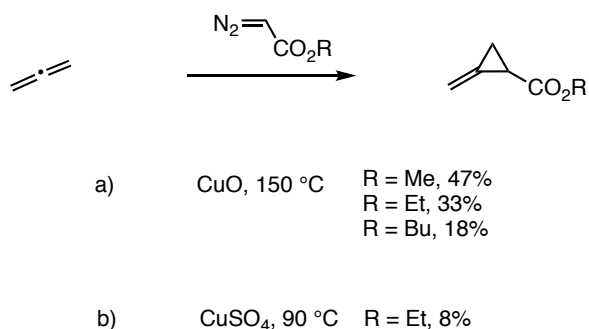


**Figure 1-10** Retrosynthetic analysis of methylenecyclopropane **1.65**

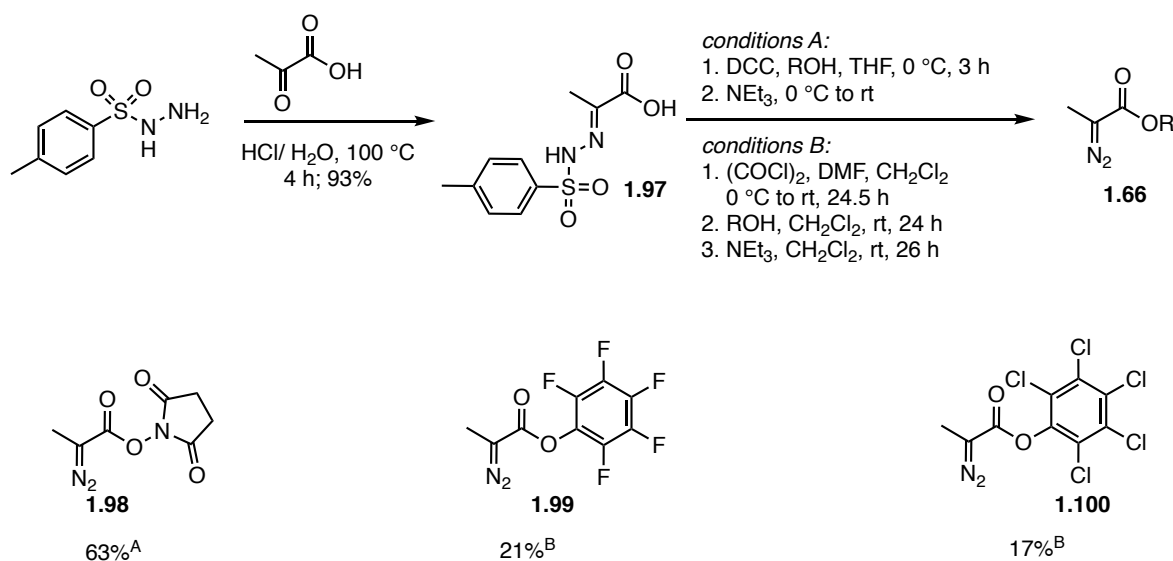
Allene is an ideal, atom-economical precursor to methylenecyclopropanes. However, the successful use of allene in an enantioselective metal carbenoid cyclopropanation remained uncertain because only two metal-mediated cyclopropanations of allene were reported in the literature, and both reactions gave poor yields of racemic product (Scheme 1-22).<sup>48,49</sup>



**Scheme 1-22** Precedent for metal carbenoid cyclopropanations of allene

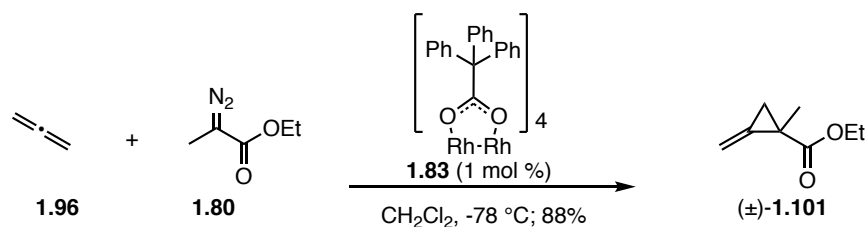
Our efforts began with the synthesis of a series of activated esters to screen in the asymmetric cyclopropanation reaction (Scheme 1-23). The condensation of pyruvic acid with tosyl hydrazine under acidic conditions provided hydrazone **1.97** in 93% yield. The resulting

hydrazone was treated with *N*-hydroxy succinimide under Steglich esterification conditions, followed by triethylamine to deliver the diazo ester **1.98** in 63% yield. Alternatively, hydrazone **1.97** could be converted into the acid chloride followed by esterification with pentafluorophenol or pentachlorophenol to deliver the corresponding ester intermediates. Base-mediated diazo formation produced diazo esters **1.99** and **1.100** in 21% and 17% yield, respectively.



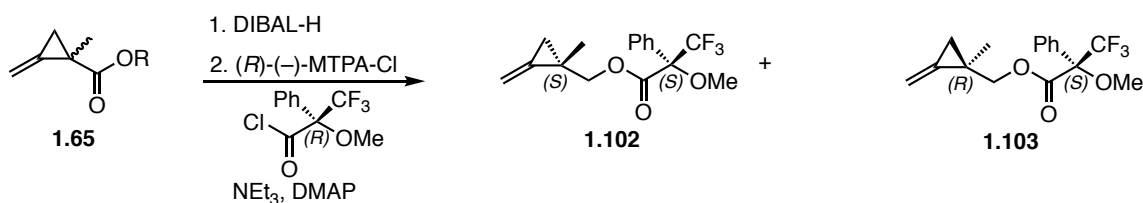
**Scheme 1-23** Synthesis of diazo substrates bearing an activated ester

With the requisite diazo esters in hand, we first explored the feasibility of the key cyclopropanation of unsubstituted allene. We were delighted to see that the reaction of ethyl diazopropanoate **1.80** and allene **1.96** proceeded smoothly at low temperature in the presence of a catalytic amount of the achiral dirhodium catalyst Rh<sub>2</sub>(TPA)<sub>4</sub> **1.83** to afford the desired methylenecyclopropane (±)-**1.101** in 88% yield (Scheme 1-24).



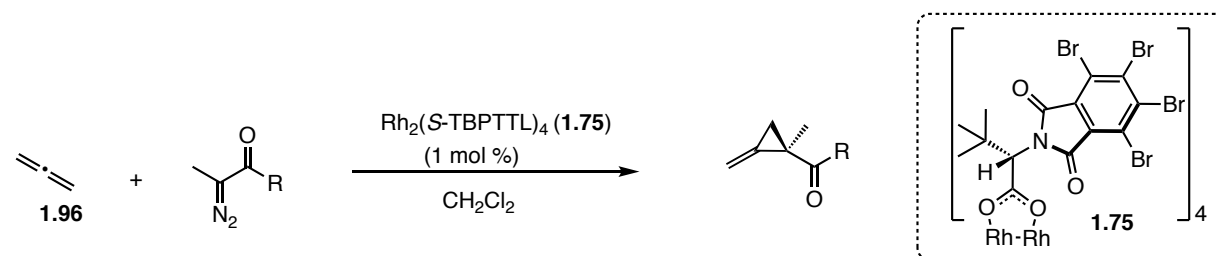
**Scheme 1-24** Trial cyclopropanation of allene with ethyl diazopropanoate

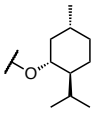
Next, a substrate screen was conducted to identify the optimal diazo ester. The dirhodium catalyst  $\text{Rh}_2(\text{S-TBPTTL})_4$  (**1.75**) was chosen for initial enantioselective conversions because of its successful use in a related cyclopropanation of diazopropanoates and styrene derivatives.<sup>43</sup> The enantiomeric excess of the ester product was evaluated by reduction of the ester to the alcohol and derivatization as the Mosher ester using the same protocol employed earlier for the methylenecyclopropyl silanes (Scheme 1-25). The absolute configuration of the major enantiomer was tentatively assigned at this stage by comparing the optical rotation sign of the ester products **1.65** to the reported optical rotation sign of related compounds of known absolute configuration.<sup>43</sup> The absolute configuration of the methylenecyclopropanes **1.65** was unambiguously determined the completion of the synthesis of enantiomerically pure cycloclavine.



**Scheme 1-25** Resolution of enantioenriched esters with  $(R)$ -(-)-MTPACl to assess *er*

We found that both the reaction outcome and degree of enantioinduction was influenced by the nature of the ester. Unfortunately, the menthyl diazo ester **1.91** failed to deliver the desired methylenecyclopropane (Table 1-3, Entry 4). However, a moderate *er* of 81:19 was obtained with the ethyl diazopropanoate **1.80** (Table 1-3, Entry 1). Pleasingly, the sterically demanding *t*-butyl diazopropanoate **1.90** delivered the best *er* at low temperatures (Table 1-3, Entries 2 and 3). However, for additional transformations, methylenecyclopropanes bearing a Weinreb amide or activated ester to facilitate direct aminolysis were more attractive (Table 1-3, Entries 5-8). Disappointingly, the Weinreb amide **1.104** failed to deliver the expected methylenecyclopropane (Table 1-3, Entry 5). In contrast, we were pleased to see that the activated ester diazo compounds **1.98**, **1.99** and **1.100** were compatible with the reaction conditions. A moderate degree of enantioinduction was obtained with the succinimide **1.98** and pentachlorophenyl **1.100** diazopropanoates (Table 1-3, Entries 6 and 7). Gratifyingly, the pentafluorophenyl diazopropanoate **1.99** provided better enantioinduction, delivering the desired methylenecyclopropane in a good *er* of 87:13 and a high yield of 86% (Table 1-3, Entry 8).

**Table 1-3** Catalytic Asymmetric Cyclopropanation of Allene: Diazo Ester Screen

Entry	R	T (°C)	Yield	<i>er</i> <sup>a</sup>
1	OEt ( <b>1.80</b> )	-78	20-62 <sup>b</sup>	81:19 <sup>c</sup>
2	<i>Or</i> -Bu ( <b>1.90</b> )	-78	51	91:9 <sup>d</sup>
3	<i>Or</i> -Bu ( <b>1.90</b> )	-98 to -80	47	93:7 <sup>d</sup>
4	 ( <b>1.91</b> )	-78	0	-
5	NMeOMe ( <b>1.104</b> )	-78	0	-
6	OSu <sup>e</sup> ( <b>1.98</b> )	-78 <sup>f</sup> to rt	27	77:23 <sup>d</sup>
7	OPcp <sup>g</sup> ( <b>1.100</b> )	-78	74 <sup>h</sup> (84) <sup>i</sup>	77:23 <sup>d</sup>
8	OPfp <sup>j</sup> ( <b>1.99</b> )	-78	86	87:13 <sup>c</sup>

<sup>a</sup>the absolute configuration was assigned based on literature<sup>43</sup> and the specific rotation of (–)-cycloclavine; <sup>b</sup>variable isolated yields due to volatility of product; <sup>c</sup>*er* determined by SFC analysis of derivative **2.87**; <sup>d</sup>*er* was determined by <sup>1</sup>H NMR analysis of the diastereomeric Mosher esters; <sup>e</sup>succinimidyl; <sup>f</sup>negligible conversion at -78 °C; <sup>g</sup>pentachlorophenyl; <sup>h</sup>reaction on 0.2 mmol scale; <sup>i</sup>reaction on 9 mmol scale; <sup>j</sup>pentafluorophenyl.

Since the pentachlorophenyl methylenecyclopropane **1.105** was obtained as a crystalline solid we attempted to upgrade the *er* by preferential crystallization of the excess enantiomer (Figure 1-11).<sup>50</sup> Interestingly, after two crystallizations from boiling heptanes we found that the mother liquor had been enriched from an *er* of 77:23 to 88:12. Switching solvent and crystallizing the mother liquor a third time from boiling 1,2-dichloroethane only slightly enriched the mother liquor to an *er* of 90:10. An x-ray crystal structure of methylenecyclopropane **1.105** was obtained confirming the structure of the product.





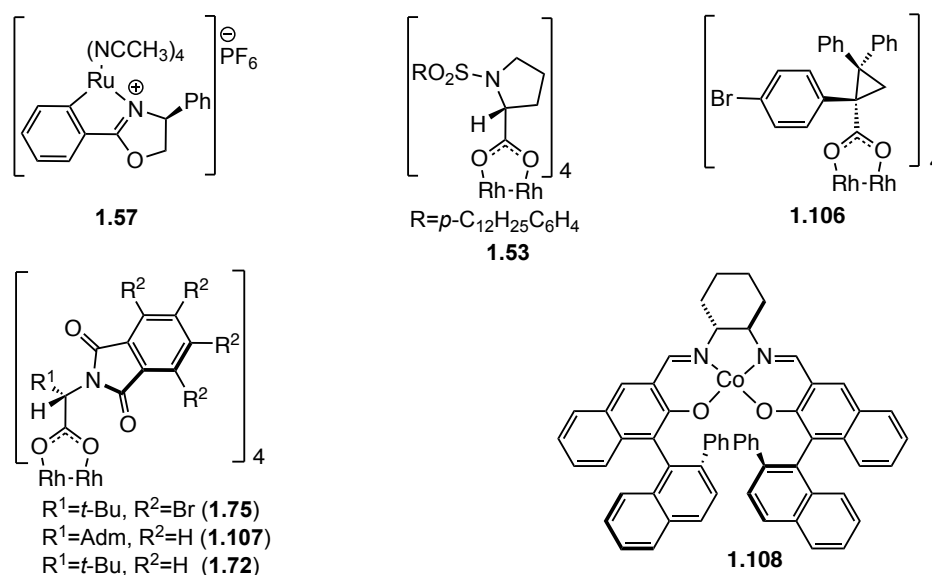
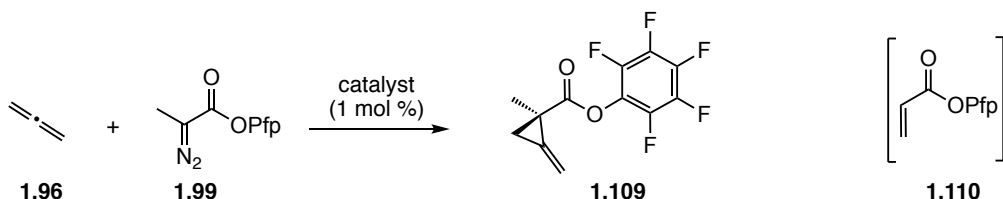


**Figure 1-12** Selected chiral catalysts

The chiral catalysts in Figure 1-12 were evaluated in the reaction of allene (**1.96**) and pentafluorophenyl diazopropanoate (**1.99**) to form methylenecyclopropane **1.109** (Table 1-4). We found that the reaction of Ru(II)-Ph-Pheox (**1.57**) did not deliver the desired methylenecyclopropane. Instead, upon warming the reaction from  $-78\text{ }^\circ\text{C}$  to room temperature, full conversion to the undesired  $\beta$ -H elimination product **1.110** was observed (Table 1-4, Entry 1). Davies' proline based catalyst  $\text{Rh}_2(\text{R-DOSP})_4$  (**1.53**) provided the desired methylenecyclopropane in a moderate yield of 61%. Unfortunately, negligible enantioinduction was observed (Table 1-4, Entry 2). Similarly, the chiral cyclopropane catalyst **1.106** delivered the desired product in moderate yields and with poor enantioinduction (Table 1-4, Entry 3). Next, we evaluated different Rh(II) catalysts with sterically hindered carboxylate ligands. The dirhodium catalysts  $\text{Rh}_2(\text{S-PTTL})_4$  (**1.72**) and  $\text{Rh}_2(\text{S-PTAD})_4$  (**1.107**) led to slight improvements in *er* to  $\sim 70:30$  (Table 1-4, Entries 4-5). The (salen)cobalt(II) catalyst **1.108** showed no catalytic activity (Table 1-4, Entry 6). Overall, Hashimoto's tetrabromophthaloyl *tert*-leucine dirhodium

catalyst **1.75** remained the optimal catalyst, giving desired cyclopropane **1.109** in a high yield with a good *er* of 87:13 (Table 1-4, Entry 7).

**Table 1-4** Catalytic Asymmetric Cyclopropanation of Allene: Catalyst Screen

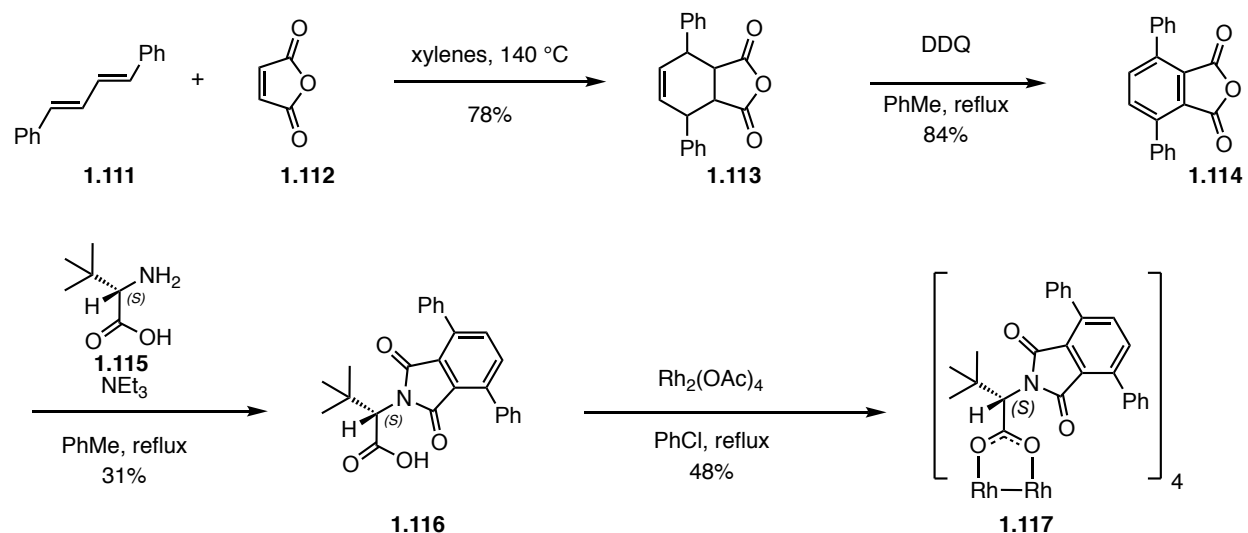


Entry	Catalyst	Solvent	T (° C)	Product	Yield (%)	<i>er</i> <sup>a</sup> (SFC)	R/S
1	[Ru(II) ( <i>S</i> )-Ph-Pheox]PF <sub>6</sub> ( <b>1.57</b> )	CH <sub>2</sub> Cl <sub>2</sub>	-78 to rt	<b>1.110</b>	ND	-	-
2	Rh <sub>2</sub> ( <i>R</i> -DOSP) <sub>4</sub> ( <b>1.53</b> )	hexanes	-78	<b>1.109</b>	61	53:47	<i>R</i>
3	Rh <sub>2</sub> ( <i>R</i> -BTPCP) <sub>4</sub> ( <b>1.106</b> )	CH <sub>2</sub> Cl <sub>2</sub>	-78	<b>1.109</b>	59	59:41	<i>S</i>
4	Rh <sub>2</sub> ( <i>S</i> -PTTL) <sub>4</sub> ( <b>1.72</b> )	hexanes	-78	<b>1.109</b>	83	72:28	<i>R</i>
5	Rh <sub>2</sub> ( <i>S</i> -PTAD) <sub>4</sub> ( <b>1.107</b> )	hexanes	-78	<b>1.109</b>	84	73:27	<i>R</i>
6	Co(II)-salen ( <b>1.108</b> ) <sup>b</sup>	THF	-78 to rt	NR	-	-	-
7	Rh <sub>2</sub> ( <i>S</i> -TBPTTL) <sub>4</sub> ( <b>1.75</b> )	CH <sub>2</sub> Cl <sub>2</sub>	-78	<b>1.109</b>	86	87:13	<i>R</i>

<sup>a</sup>the ester was derivatized as the vinylogous imide **2.87** for SFC analysis; <sup>b</sup>10 mol% NMI was employed in the reaction

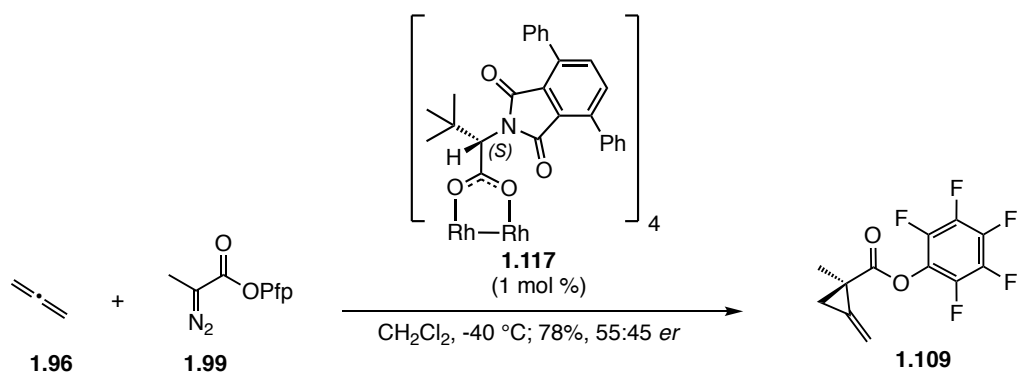
Given the success of the sterically demanding dirhodium tetrabromophthaloyl-*tert*-leucine catalyst, we synthesized a novel sterically demanding dirhodium catalyst **1.117**, reasoning that the 4,7-diphenyl substitution pattern on the phthalimide ring would impose greater steric demand than the corresponding bromide substituents, hopefully leading to greater differentiation between the enantiotopic faces of the allene (Scheme 1-26). The synthesis of the catalyst began with a Diels-Alder reaction of diphenylbutadiene **1.111** and maleic anhydride

**1.112** to afford bicycle **1.113** in 78% yield. DDQ oxidation delivered phthalic anhydride **1.114** which was reacted with *S*-*tert*-leucine (**1.115**) in the presence of triethylamine to form phthalimide **1.116**. A ligand exchange reaction generated the dirhodium catalyst **1.117** in 48% yield.



**Scheme 1-26** Synthesis of dirhodium catalyst **1.117**

Unfortunately, when allene was reacted with pentafluorophenyl diazopropanoate (**1.99**) in the presence of the novel dirhodium catalyst  $\text{Rh}_2(\text{S-4,7-DPPTTL})_4$  (**1.117**) no reaction occurred at  $-78\text{ }^\circ\text{C}$  and the reaction had to be warmed to  $-40\text{ }^\circ\text{C}$  before conversion was observed. Disappointingly, virtually no enantioinduction was observed in this reaction (55:45 *er*, Scheme 1-27).



**Scheme 1-27** Cyclopropanation of allene using  $\text{Rh}_2(\text{S-4,7-DPPTTL})_4$

An X-ray structure of the catalyst  $\text{Rh}_2(\text{S-TBPTTL})_4$  (**1.75**) was obtained by Hashimoto and coworkers. The X-ray structure revealed that the dirhodium complex adopts a  $C_4$  symmetric chiral crown conformation in the solid state form.<sup>55</sup> This same conformation was reported for the related catalyst  $\text{Rh}_2(\text{S-PTTL})_4$  and other phthalimide based catalysts.<sup>53,56</sup> In this conformation the four phthalimide moieties are oriented on the same face and form four halogen bonds between a carbonyl of the phthalimide and a bromide substituent on an adjacent ligand (Figure 1-13a). The four *tert*-butyl groups are oriented on the opposite face and block approach from that face. Assuming the chiral crown conformation is formed in solution, Hashimoto proposed a plausible stereochemical pathway to explain the high levels of enantioselectivity observed using  $\text{Rh}_2(\text{S-TBPTTL})_4$  in the enantioselective cyclopropanation of alkynes and  $\alpha$ -alkyl- $\alpha$ -diazoesters.<sup>55</sup> Their hypothesis was supported by DFT calculations of the proposed transition states. According to their analysis transition state A should be strongly favored over transition state B in our system due to the unfavorable steric repulsion that arises between the pentafluorophenyl ester and the tetrabromophthalimido ligand in transition state B (Figure 1-13a).

In the case of the dirhodium 4,7-diphenylphthaloyl *tert*-leucine [ $\text{Rh}_2(\text{S-4,7-DPPTTL})_4$ ] complex, the poor *er* of 55:45 obtained suggests that there is negligible differentiation between

the enantiotopic faces of the allene substrate with this catalyst. Davies *et al.* have shown that chiral dirhodium carboxylate catalysts commonly exist in  $C_1$ ,  $C_2$ ,  $C_4$ , or  $D_2$  symmetric conformations (Figure 1-13b).<sup>56,57</sup> Charette has postulated the chiral crown conformation of the tetrahalogenated phthalimido dirhodium catalysts is stabilized in solution by the halogen-bonding interactions.<sup>56</sup> In contrast, non-halogenated complexes, which lack this stabilizing interaction, may be less rigid in solution leading to scrambling of the ‘all up’ conformation. Furthermore, poor levels of enantioinduction were also observed with the  $\text{Rh}_2(\text{DOSP})_4$  catalyst (*er* 53:47; Table 1-4, Entry 2). Davies proposed that this catalyst adopts a  $D_2$  symmetric conformation in solution.<sup>58</sup> This result indicates the  $D_2$  symmetric conformation is not effective at inducing high levels of enantioinduction in the cyclopropanation of allene with pentafluorophenyl diazopropanoate.

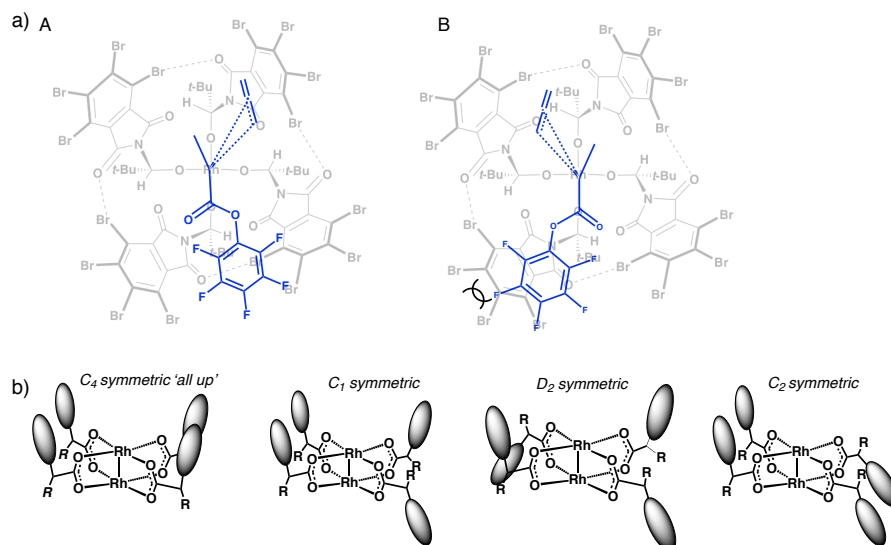


**Figure 1-13** a) Proposed transition states for the asymmetric cyclopropanation of allene with diazoester **1.99** b) possible conformations of dirhodium carboxylate catalysts. (Figure 1-13 b was reprinted with permission from Lindsay, V. N. G.; Lin, W.; Charette, A. B. *J. Am. Chem. Soc.* **2009**, *131*, 16383. Copyright 2009 American Chemical Society).

Thus the poor levels of enantioinduction observed for the novel  $[\text{Rh}_2(S\text{-}4,7\text{-DPPTTL})_4]$  complex could be due to the scrambling of the optimal  $C_4$  chiral crown complex in solution which could give rise to a large number of possible transition states and lead to low overall enantioselectivity. Alternatively, the poor enantioinduction could be rationalized by a preference for an ineffective conformation of the catalyst such as the  $D_2$  conformation which is known to lead to poor enantioinduction in this system.

### 1.3 CONCLUSIONS

$\alpha$ -Methyl diazopropanoates were shown to be effective metal carbenoid precursors for asymmetric cyclopropanation reactions with dimethylphenylsilyl allene and unsubstituted allene. Key features of this chapter include the first use of unsubstituted allene in a catalytic asymmetric cyclopropanation reaction to deliver a range of methylenecyclopropanes bearing alkyl or activated ester moieties. This reaction is the most direct and atom-economical method to form methylenecyclopropanes with a terminal olefin. Although the mechanism of enantioinduction remains unclear, we determined that the degree of enantioinduction depends on the identity of the transition metal ion, the steric and electronic properties of the chiral ligand and the temperature.

Overall, the dirhodium complex  $\text{Rh}_2(S\text{-TBPTTL})_4$  (**1.75**) was identified as the optimal catalyst for enantioselective conversions. The *tert*-butyl diazopropanoate (**1.90**) and the pentafluorophenyl diazopropanoate (**1.99**) were identified as the best substrates for enantioselective conversions, providing the corresponding methylenecyclopropanes in 47% yield/93:7 *er* and 86% yield/87:13 *er* respectively. The optimal solvent for the reaction was

dichloromethane. Looking forward to an enantioselective synthesis of cycloclavine, we selected the pentafluorophenyl diazopropanoate for further synthetic operations, hoping that the *er* could be further upgraded from 87:13 through recrystallization of a crystalline intermediate later in the synthesis.



## 2.0 TOTAL SYNTHESIS OF CLAVINE ALKALOIDS

### 2.1 INTRODUCTION

#### 2.1.1 *Ergot* Alkaloids

The *ergot* alkaloids are a large group of structurally diverse indole-containing natural products produced by *Clavicipitaceae* and *Trichocomaceae* fungi.<sup>59</sup> These fungi are known to invade grass species causing ergot, a disease that is recognized by the replacement of healthy kernels with dark sclerotia that contain high concentrations of ergot alkaloids.<sup>59,60</sup> Susceptible host plants include cultivated cereals like rye, sorghum, pearl millet, triticale, barley and oats as well as several species of wild grasses.<sup>61</sup> Historically, ergot alkaloids have had a major impact on human health and agriculture. During the Middle Ages, ingestion of ergot contaminated grains led to fatal epidemics of ergotism across central Europe.<sup>59</sup> Two forms of the disease are described clinically. Convulsive ergotism is characterized by hallucinations, fever and convulsions, whereas, gangrenous ergotism is characterized by burning sensations in the limbs followed by gangrene caused by potent and long-lasting vasoconstriction.<sup>62</sup> Ergotism in humans and livestock is rare in modern times because of the strict regulations governing the permissible amount of ergot in grain. However, ergotism can still cause economic loss when commercial grains are downgraded or discarded due to ergot contamination.<sup>63</sup>

Structurally ergot alkaloids can be classified into the lysergic acid or clavine subclasses based on the oxidation state of the C8 substituent (Figure 2-1). The lysergic acid subclass, which comprises both lysergic acid amides and ergopeptines have a C8 substituent at the carboxylic acid oxidation level. In contrast, the clavine subclass typically possess a C8 substituent at the alkane or alcohol oxidation state.<sup>64</sup> *Ergot* alkaloids have an astonishingly diverse spectrum of pharmacological activity that covers numerous therapeutic areas including CNS diseases, obstetrics and oncology. These alkaloids bear a strong structural resemblance to natural neurotransmitters like serotonin, dopamine and adrenalin and as such the biological activities of these alkaloids have been attributed to agonistic or antagonistic activity toward neurotransmitter receptors. For example, the naturally occurring alkaloid ergotamine has been used to treat migraines, bromocriptine has been used to treat Parkinson's disease and ergonovine is a front-line pharmaceutical for the treatment of post-partum haemorrhage.<sup>65,66</sup>

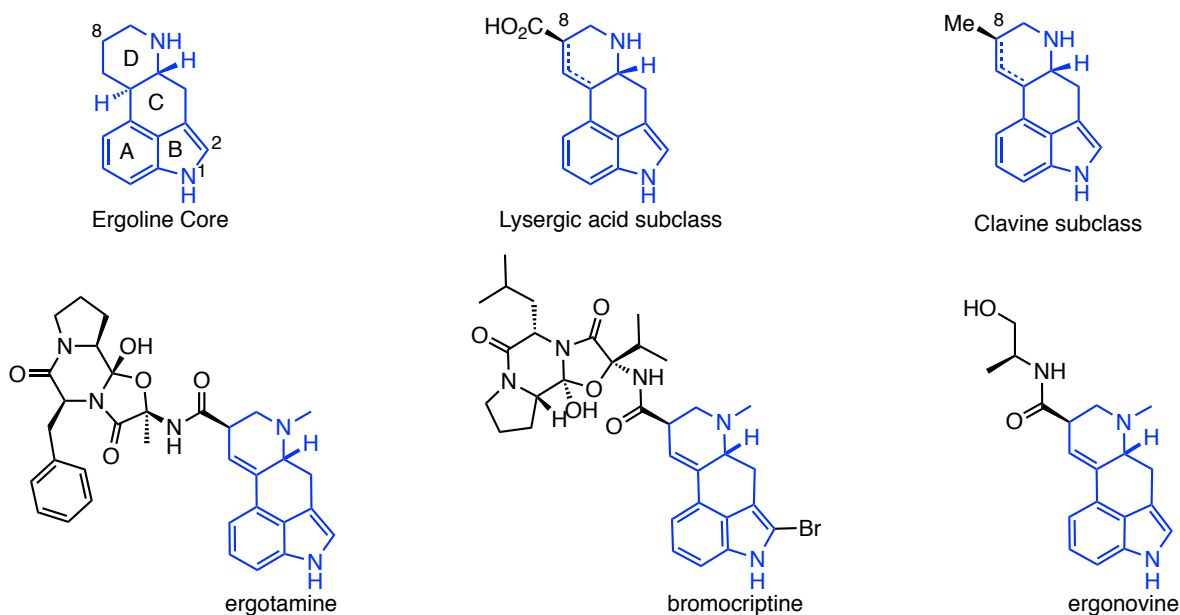


**Figure 2-1** Lysergic acid and clavine subclasses and representative Ergot alkaloid pharmaceuticals

### 2.1.2 Clavine Alkaloids: Structure and Biological Profile

The clavine alkaloids can be divided into three distinct groups based on their biosynthetic origin and structure (Figure 2-2).<sup>59</sup> The tricyclic clavines are formed during the early stages of ergot alkaloid biosynthesis and serve as precursors to more complex tetracyclic clavines. The tetracyclic clavines are either advanced intermediates or the end products of the biosynthetic pathway and possess a common tetracyclic core. They differ in the presence and location of an olefin in the D-ring and the identity of the C8 substituent. The rearranged clavine alkaloid subgroup possesses a rearranged ergoline skeleton and are the products of diverted biosynthetic pathways off the primary route leading to tetracyclic clavines. These rare alkaloids include (+)-cycloclavine (+)-(2.1), rugulovasine A (2.2) and aurantioclavine (2.3)

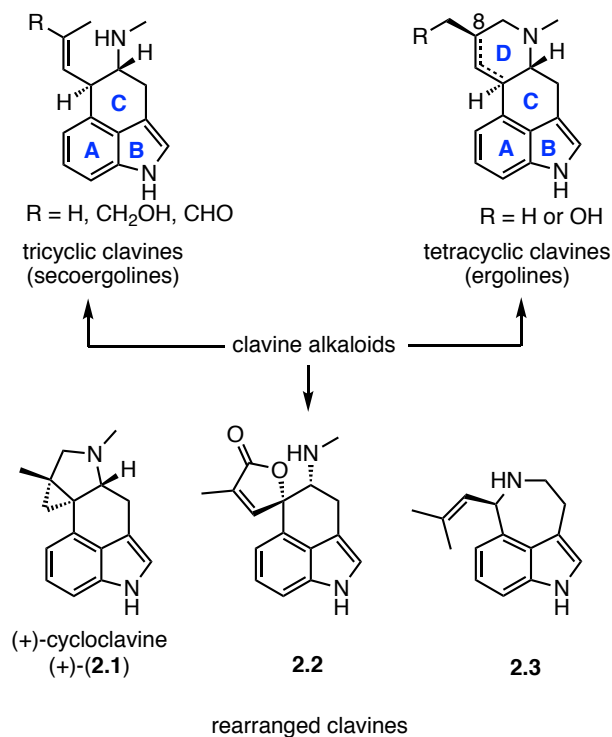


**Figure 2-2** Tricyclic, tetracyclic and rearranged *clavine* alkaloids

Lysergic acid amides and ergopeptines have been extensively used in drug development.<sup>59</sup> In contrast, the therapeutic potential of clavine alkaloids remains relatively unexplored. Several natural clavines possess promising anti-cancer properties. Pibocin B exhibited moderate cytotoxicity against mouse Ehrlich carcinoma cells with an ED<sub>50</sub> of 25  $\mu\text{g/mL}$  (Figure 2-3).<sup>67</sup> Fumigaclavine C showed cytotoxic activity against the human breast cancer cell line MCF-7 and the mouse leukemia cell line P388.<sup>68</sup> Several marketed drugs are structurally related to clavine alkaloids. The PARP inhibitor rucaparib is used to treat advanced ovarian cancer and strongly resembles the rearranged clavine alkaloids aurantioclavine (**2.3**) and clavicipitic acid.<sup>69</sup> The semi-synthetic alkaloid pergolide has been used to treat early-onset Parkinson's disease.<sup>70</sup> Clavine alkaloids have also demonstrated promising insecticidal activities. For example, cycloclavine and the methyl carbamate derivative **2.4** induced a mortality of 75% at 300 ppm in several species of aphids compared to untreated controls. Furthermore, the methyl carbamate **2.4** also induced 75% mortality in diamond black moth, orchid thrips, red spider mite and striped flea beetle at a concentration of 300 ppm.<sup>71</sup>

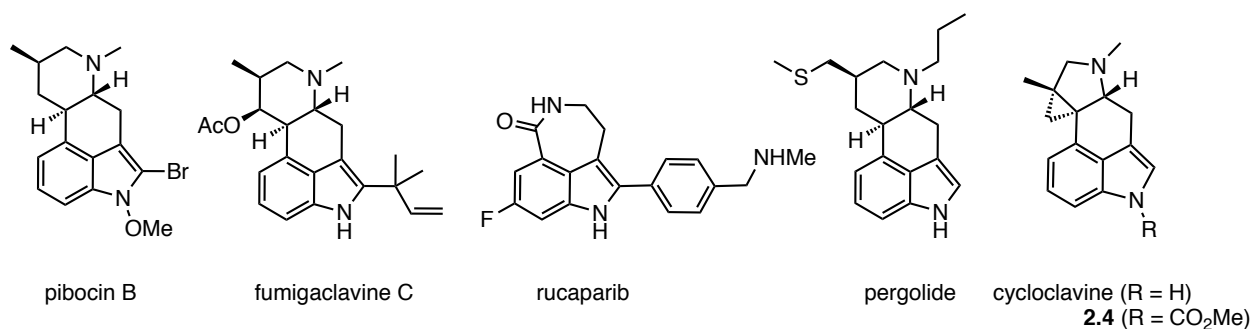


**Figure 2-3** Therapeutically relevant clavine alkaloids

### 2.1.3 Cycloclavine: Isolation and Structure

(+)-Cycloclavine (+)-(2.1) was first isolated from seeds of the African morning glory shrub (*Ipomea hildebrandtii*) in 1969.<sup>72</sup> The natural product was characterized using a combination of NMR spectroscopy, IR, elemental analysis, specific rotation and X-ray analysis (Figure 2-4). The relative and absolute configuration was unambiguously assigned through X-ray analysis of the methyl bromide salt (+)-(2.1)•CH<sub>3</sub>Br. Following the initial isolation, cycloclavine has subsequently been isolated in Japan from a culture of the fungus *Aspergillus japonicus*.<sup>73</sup>

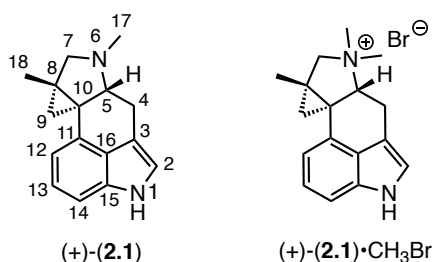


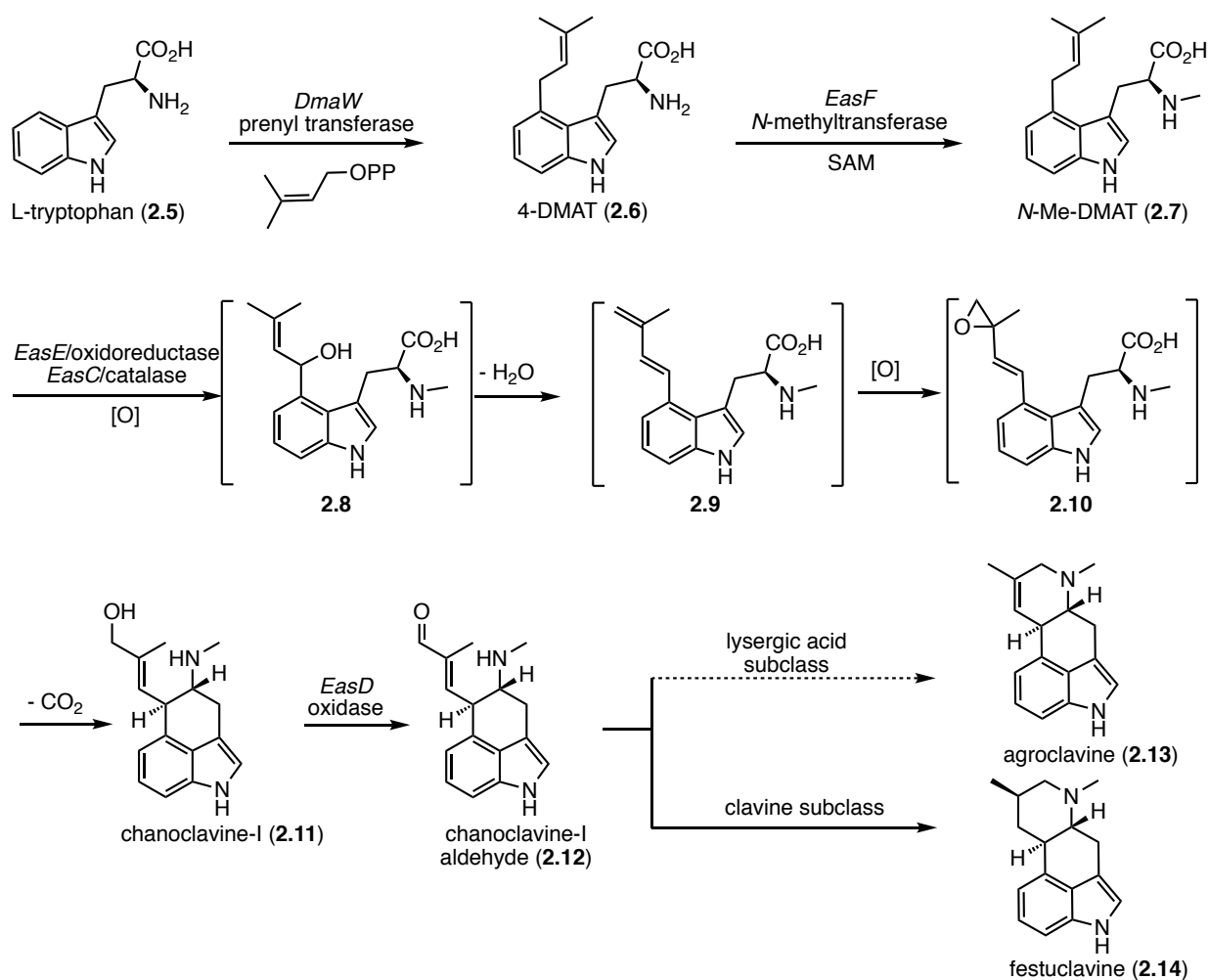
**Figure 2-4** Cycloclavine numbering and the methyl bromide salt derivative

Cycloclavine has attracted considerable attention as a target for total synthesis campaigns due to its unprecedented skeleton, which features a pyrrolidine-fused cyclopropane in place of the piperidine ring that is common in other ergot alkaloids. This unique connectivity presents a noteworthy synthetic challenge, particularly in regard to the diastereo- and enantiocontrol that is required to forge the *trans*-hydroindoline ring system at C5/C10 and the appended cyclopropane, which contains vicinal all-carbon quaternary stereocenters.

#### 2.1.4 Cycloclavine: Biosynthesis

In recent years, remarkable advances have been made in elucidating the biogenetic origin of ergot alkaloids. While the early biosynthetic transformations leading to the ergoline scaffold are well understood, the roles of the mid to late pathway genes involved in the structural derivatization of the ergoline core are less clear and have been the subject of intensive investigations. In 2012 a biosynthetic gene cluster containing eight genes was identified in the genome of the cycloclavine producer *Aspergillus japonicus*.<sup>74</sup>

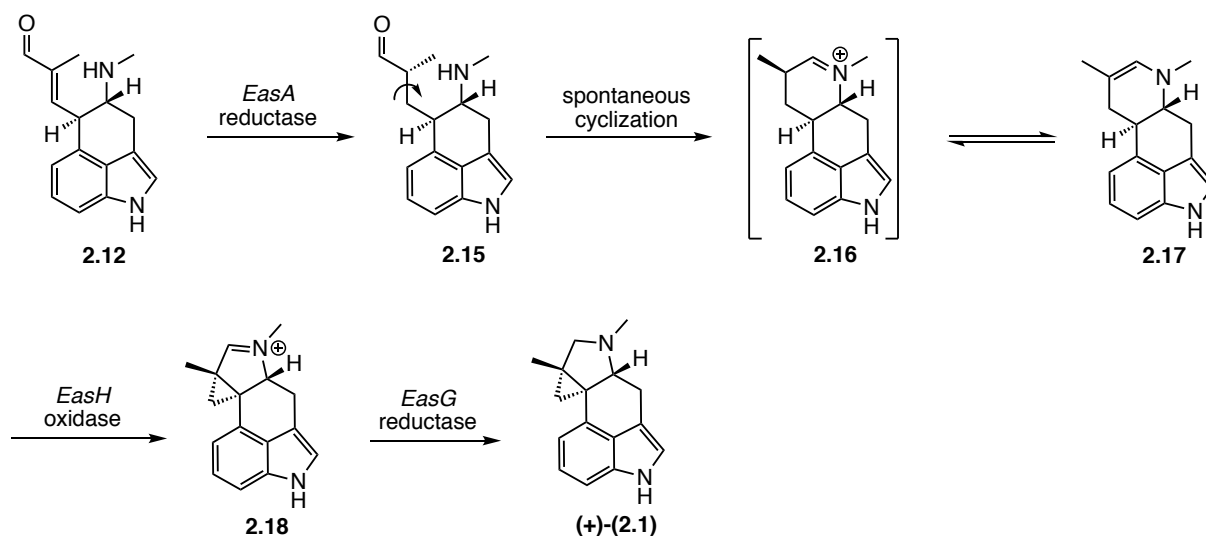
In 2015, the O'Connor group proved that this gene cluster is responsible for the biosynthesis of cycloclavine by reconstituting the entire eight enzyme pathway in a host yeast strain with excellent production levels ( $>500 \text{ mg L}^{-1}$ ).<sup>75</sup> Cycloclavine biosynthesis begins with prenylation of L-tryptophan (**2.5**) to produce 4-dimethylallyltryptophan (4-DMAT) (**2.6**) (Scheme 2-1). Next, *N*-methylation of the primary amine is catalyzed by *easF* in the presence of a *S*-adenosyl methionine (SAM) cofactor. The resulting *N*-methylated amine **2.7** can be converted into chanoclavine-I (**2.11**) through sequential oxidation, decarboxylation and cyclization reactions. Oxidation of chanoclavine-I gives chanoclavine-I aldehyde (**2.12**) the last common biosynthetic precursor of all ergot alkaloids. At this point the biosynthetic pathway branches off to produce agroclavine (**2.13**) in the biosynthesis of lysergic acid alkaloids or festuclavine (**2.14**) in the biosynthesis of clavine alkaloids.



**Scheme 2-1** Early stage transformations in the biosynthesis of cycloclavine

The incorporation of an *EasH*-derived oxidase into the gene cluster was pinpointed as the enzyme responsible for diverting the biosynthetic pathway to accumulate cycloclavine instead of festuclavine and other clavine alkaloid end products. *EasH* is a non-heme iron and  $\alpha$ -ketoglutarate-dependent oxidase that works in conjunction with a flavoenzyme encoded by *EasA* and an NADPH-dependent oxidoreductase *EasG* to convert chanoclavine-I aldehyde (**2.12**) to cycloclavine (Scheme 2-2).<sup>76</sup> This sequence begins with the *EasA* mediated conjugate reduction of enal **2.12**.<sup>77</sup> The resulting aldehyde **2.15** undergoes a spontaneous cyclisation to generate iminium intermediate **2.16**. The iminium ion is then converted to the corresponding

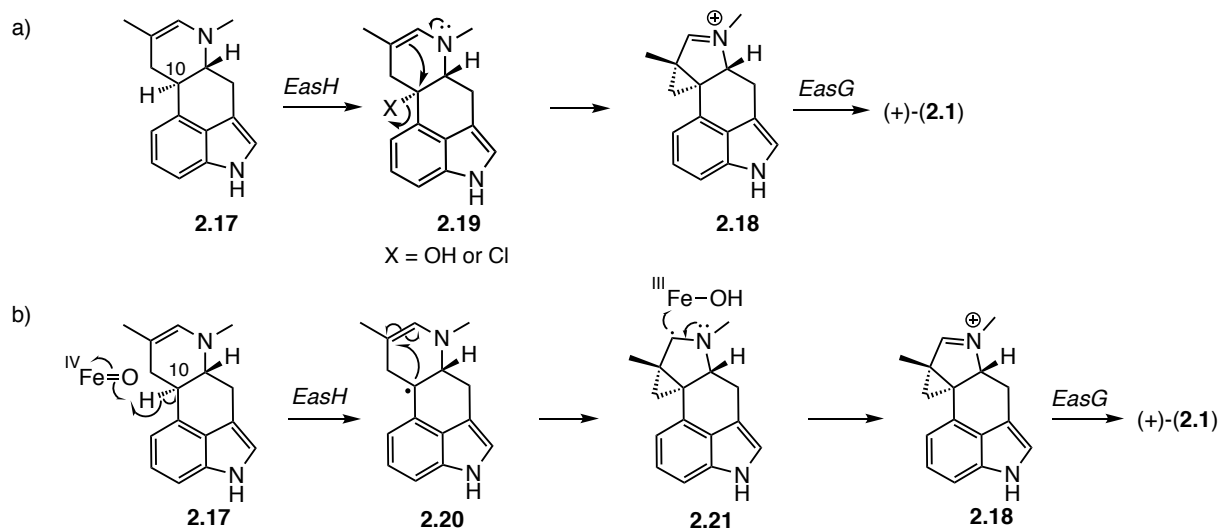
enamine **2.17**, which undergoes an intramolecular cyclopropanation to generate the pyrrolidinium-fused cyclopropane **2.18**. Reduction of iminium ion **2.18** affords cycloclavine.



**Scheme 2-2.** Late stage transformations in the biosynthesis of cycloclavine

O'Connor *et al.* proposed two plausible mechanisms for the ring contraction/cyclopropanation reaction catalyzed by *EasH*.<sup>76</sup> Since  $\alpha$ -ketoglutarate dependent enzymes are known to catalyze hydroxylation and halogenation reactions, one potential pathway involves hydroxylation or halogenation of the C10 benzylic methine in enamine **2.17** to form intermediate **2.19** (Scheme 2-3a). A ring contraction reaction then furnishes the cyclopropyl moiety **2.18**.<sup>78,79</sup> Alternatively, radical abstraction of the C10 methine in enamine **2.17** by an iron cofactor, followed by an intramolecular radical addition across the enamine **2.20** gives the rearranged intermediate **2.21** (Scheme 2-3b). Oxidation of the resulting radical **2.21** could generate the pyrrolidinium-fused cyclopropane **2.18**. Reduction of the iminium ion delivers cycloclavine.





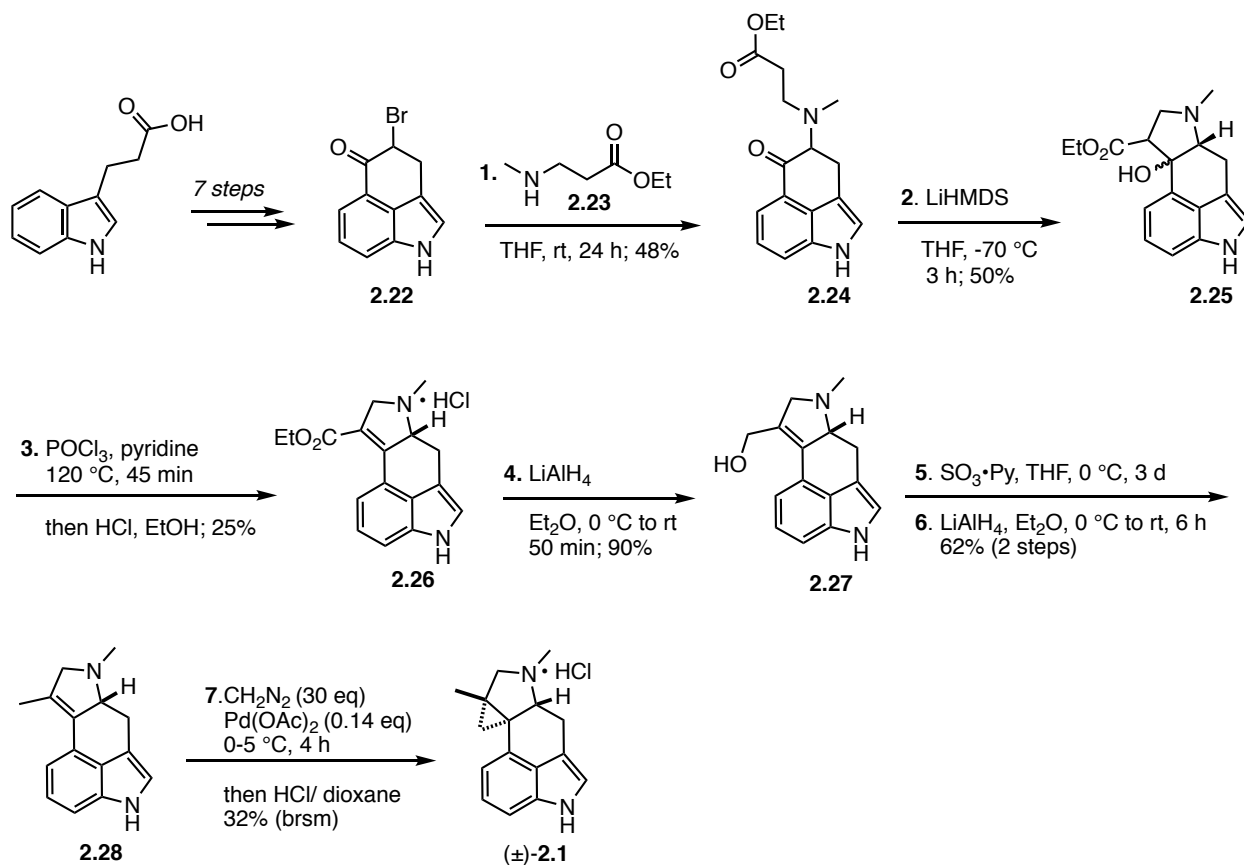
**Scheme 2-3** Potential mechanisms of the *EasH* mediated biosynthetic cyclopropanation

## 2.1.5 Synthetic Approaches to Cycloclavine

### 2.1.5.1 Szántay's Total Synthesis of (±)-Cycloclavine (2008)

In 2008 Szántay published the first total synthesis of (±)-cycloclavine.<sup>80</sup> Their approach used 4-bromo Uhle's ketone **2.22** as an advanced starting material in which the A, B and C-rings of the natural product are present and featured the late-stage formation of the cyclopropane E-ring (Scheme 2-4). The tricyclic ketone **2.22** was prepared in seven steps from 3-indolepropionic acid.<sup>81,82</sup> The D-ring was then forged in two steps by sequential alkylation of ketone **2.22** with 3-methylaminopropanoate **2.23** followed by LiHMDS-mediated ring closure to produce β-hydroxy ester **2.25**. The tertiary alcohol **2.25** underwent elimination when treated with POCl<sub>3</sub> in pyridine and the resulting amine was isolated as the hydrochloride salt **2.26**. Next, the α,β-unsaturated ester **2.26** was reduced to the allylic alcohol **2.27** by LiAlH<sub>4</sub> which was then deoxygenated by sequential treatment with SO<sub>3</sub>•Py and LiAlH<sub>4</sub>. Finally, cyclopropanation of olefin **2.28** with excess diazomethane in the presence of palladium acetate gave (±)-cycloclavine (±)-(2.1), which

was isolated as the hydrochloride salt in a modest yield of 32% (brsm). In summary, the synthesis was accomplished in 7 steps and 1% overall yield (brsm) from 4-bromo Uhle's ketone **2.22**.



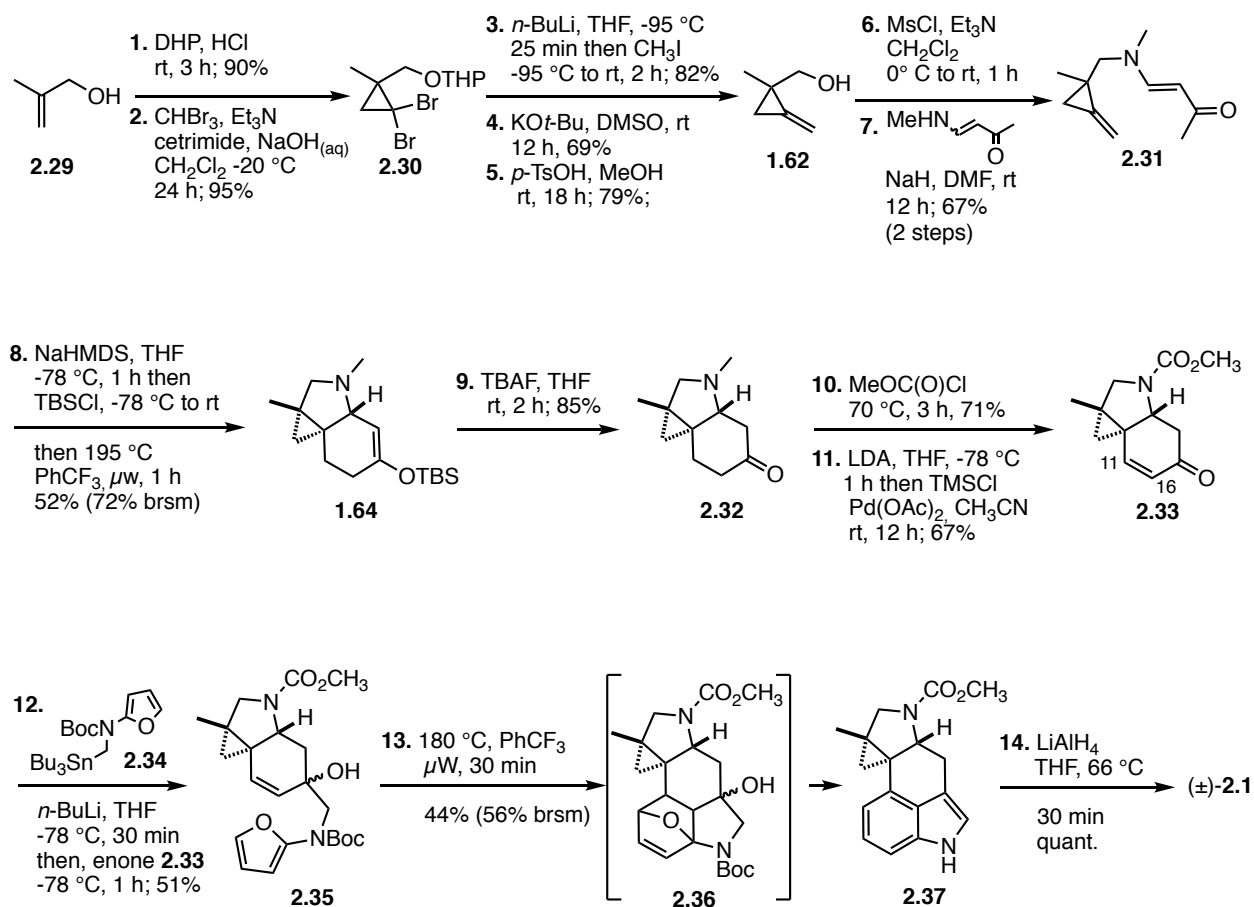
**Scheme 2-4** Total synthesis of (±)-cycloclavine by Szántay

### 2.1.5.2 Wipf's Total Synthesis of (±)-Cycloclavine (2011)

The Wipf group has an on-going interest in the synthesis of 3,4-disubstituted indoles using an intramolecular Diels-Alder furan (IMDAF) reaction.<sup>83,84,85,86</sup> As such, we were initially drawn to cycloclavine because it contains this indole substitution pattern and due to the synthetically intriguing pyrrolidine fused cyclopropane ring system, which is unique among clavine alkaloids. The groups' first total synthesis of cycloclavine was accomplished by Dr. Filip Petronijevic in 2011 (Scheme 2-5).<sup>41</sup> The synthesis began with the treatment of allylic alcohol

**2.29** with 2,3-dihydropyran and catalytic HCl to form the corresponding THP ether (Scheme 2-5). The protected allylic alcohol was then subjected to a cyclopropanation reaction with bromoform and NaOH under phase transfer conditions to deliver *gem*-dibromocyclopropane **2.30**. Exposure of cyclopropane **2.30** to one equivalent of *n*-BuLi at -95 °C gave the mono-lithiated cyclopropane which was quenched with methyl iodide to afford the tertiary bromide. A KO*t*-Bu mediated dehydrobromination followed by acid-catalyzed THP cleavage furnished methylenecyclopropane **1.62**. The primary alcohol **1.62** was then activated as the mesylate and alkylated with the anion of 4-(methylamino)but-3-en-2-one to form the diene precursor **2.31**. Next, the key intramolecular Diels-Alder reaction with the pendant methylenecyclopropane dienophile was attempted. The methyl ketone **2.31** underwent enolization when added to a solution of NaHMDS in THF at -78 °C. The resulting enolate was trapped *in situ* with TBSCl to deliver the reactive silyloxy diene intermediate. Gratifyingly, when this key diene was irradiated at 195 °C for 1 h in the microwave, a highly diastereoselective Diels-Alder cycloaddition occurred to give the cyclic enol ether adduct **1.64** as a single diastereomer. The silyl enol ether was converted to ketone **2.32** upon treatment with TBAF. With the tricyclic ketone in hand, attention shifted to the installation of the 3,4-disubstituted-indole core. Unfortunately, dehydrogenation of ketone **2.32** failed under standard Saegusa-Ito conditions possibly due to the coordination of the basic tertiary amine to the palladium catalyst. This problem was circumvented by a dealkylative protection of the amine with methyl chloroformate followed by a Saegusa-Ito dehydrogenation to successfully introduce the olefin **2.33** at C11/C16. Transmetalation of stannane **2.34** with *n*-BuLi formed the organolithium reagent, which was treated with enone **2.32** to deliver the expected tertiary alcohol **2.35**. The alcohol **2.35** was then subjected to a microwave promoted IMDAF reaction to form intermediate **2.36**, which then

underwent a double dehydrative aromatization sequence under the reaction conditions to furnish indole **2.37** in 44% yield. Finally,  $\text{LiAlH}_4$  reduction of carbamate **2.37** afforded cycloclavine in quantitative yield. Overall, the total synthesis proceeded in 14 steps and 1.2 % yield.

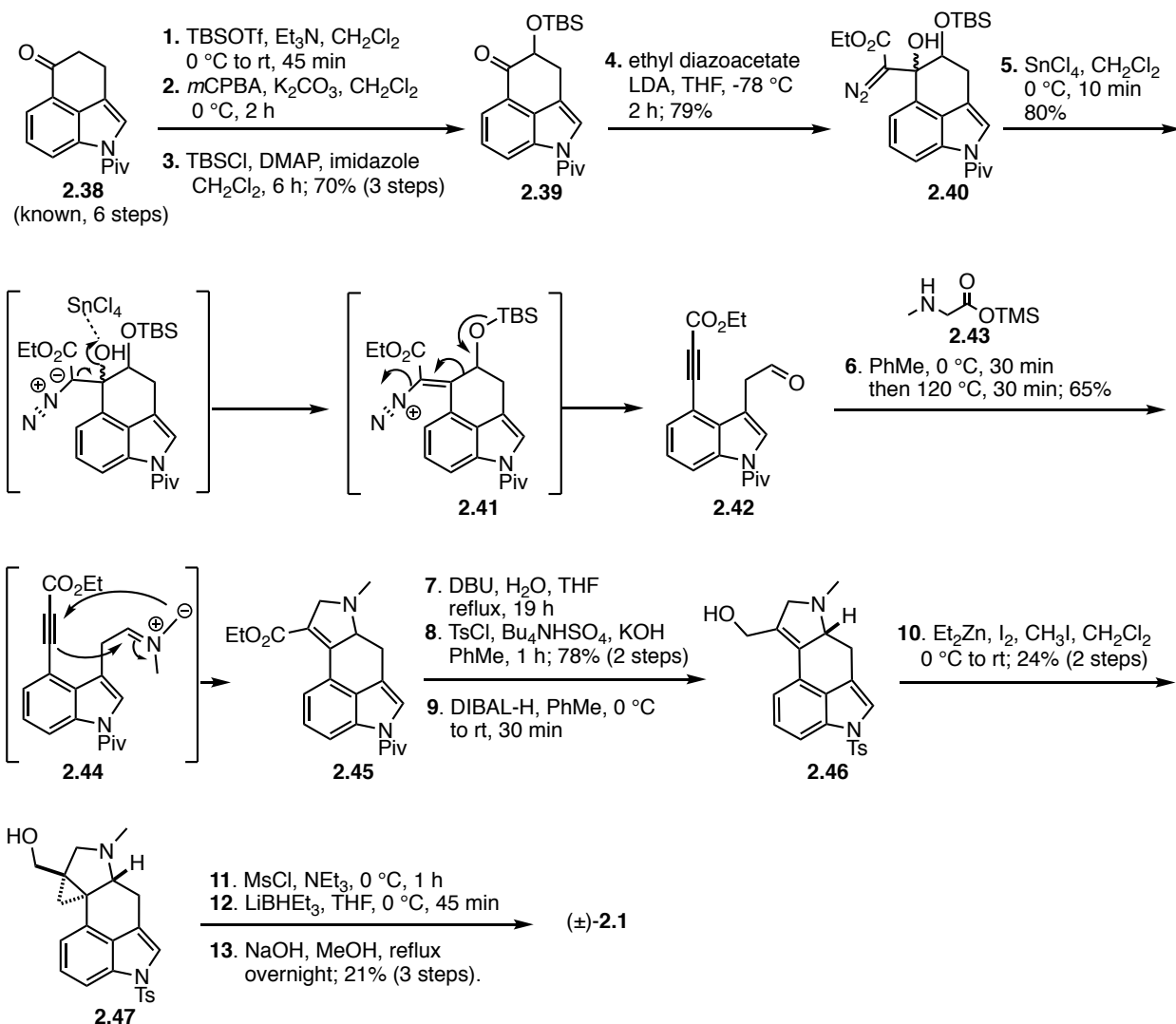


**Scheme 2-5** Total synthesis of (±)-cycloclavine by Petronijevic and Wipf

### 2.1.5.3 Brewer's Total Synthesis of (±)-Cycloclavine (2014)

Brewer's 2014 racemic total synthesis of cycloclavine featured an interesting fragmentation/1,3-dipolar cycloaddition sequence that was originally developed by their group for the synthesis of polycyclic 2,5-dihydropyrroles.<sup>87,88</sup> Brewer used a similar strategy to Szántay by using Uhle's ketone derivative **2.38** as an advanced tricyclic starting material, focusing on the elaboration of the pyrrolidine D-ring and cyclopropane E-ring.<sup>81</sup> First, ketone **2.38** was subjected

to a Rubottom oxidation to form an intermediate  $\alpha$ -hydroxy ketone that was immediately converted to corresponding TBS ether **2.39** (Scheme 2-6). An aldol-like addition of ethyl lithiodiazoacetate produced diazo ester **2.40** as an inseparable mixture of diastereomers. The key fragmentation reaction proceeded smoothly when diazo ester **2.40** was treated with  $\text{SnCl}_4$  at 0 °C to form the tethered aldehyde ynoate **2.42**. Aldehyde **2.42** was then condensed with sarcosine silyl ester **2.43** and heated at 120 °C in toluene to generate the azomethine ylide intermediate **2.44**. This ylide underwent an intramolecular 1,3-dipolar cycloaddition to give the expected 2,5-dihydropyrrole **2.45** in 65% yield. Pivalate deprotection provided the protecting-group-free indole and intercepted Szántay's synthesis. The Brewer group also explored alternative cyclopropanation conditions. They found that the tetrasubstituted olefin was unreactive toward diazomethane and Corey-Chaykovsky conditions. They reasoned that reduction of the ester to the corresponding allylic alcohol might enable an alcohol directed cyclopropanation to occur. Reduction of the ester with DIBAL-H proceeded smoothly to give alcohol **46**. Unfortunately, attempts to promote a Simmons-Smith cyclopropanation with various metals including Zn, Sm, Pd, Mg and Cr failed. Only Charette's *gem*-dizinc carbenoid cyclopropanation protocol provided the desired cyclopropane **2.47**, albeit in a low yield of 24%. Mesylation of the primary alcohol **2.47** followed by hydride displacement provided the deoxygenated product. The synthesis was completed by hydrolysis of the sulfonamide to give cycloclavine ( $\pm$ )-**2.1**. In summary, Brewers approach provided the racemic natural product in 13 steps and 1.1% overall yield from tricycle **2.38**.

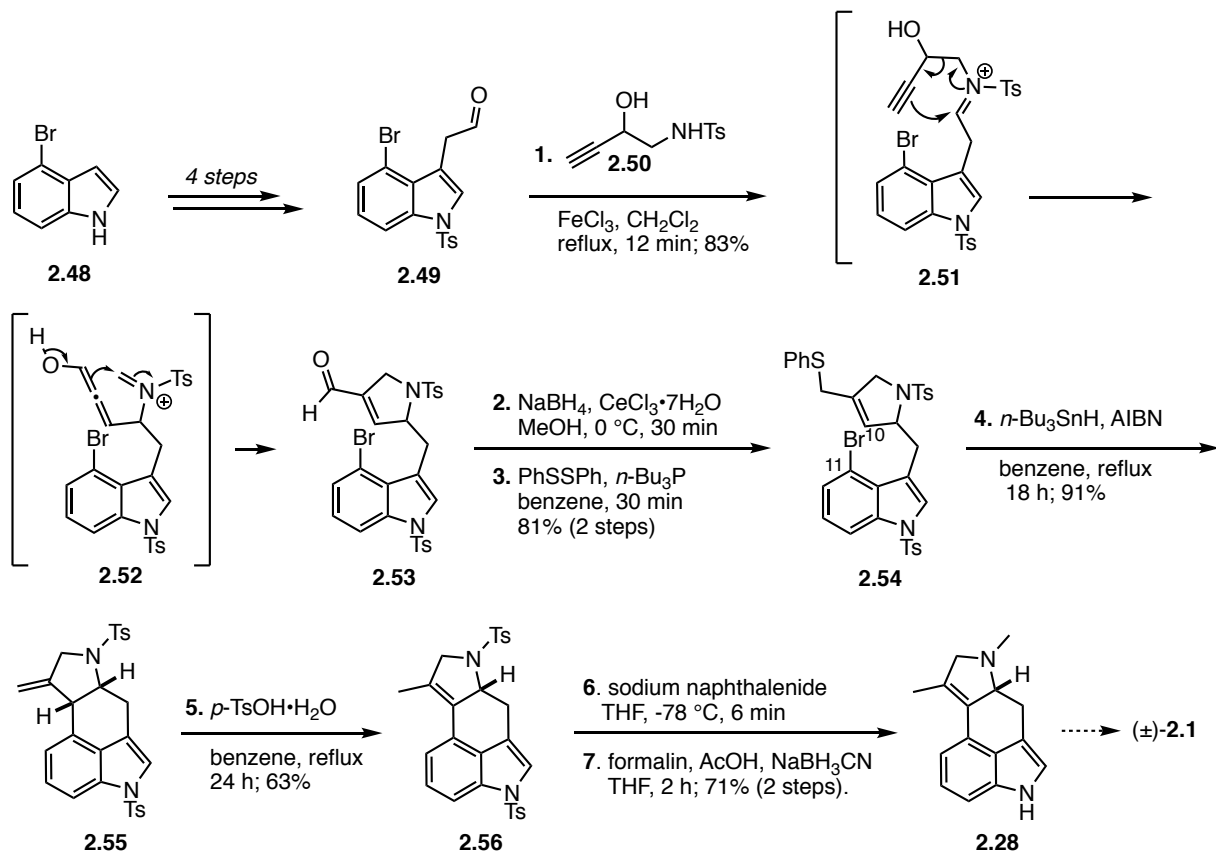


**Scheme 2-6** Total synthesis of (±)-cycloclavine by Brewer

#### 2.1.5.4 Cao's Formal Synthesis of (±)-Cycloclavine (2014)

In 2014, the Cao group published a concise synthesis of Szántay's amine **2.28** using an aza-cope Mannich reaction and radical cyclization strategy (Scheme 2-7).<sup>89</sup> The indole starting material **2.49** was formed in four steps and 72% overall yield from 4-bromoindole. A FeCl<sub>3</sub>-promoted condensation of aldehyde **2.49** and 2-hydroxy homopropargylamine (**2.50**) formed the iminium ion intermediate **2.51**. This underwent an aza-Cope reaction to form enol **2.52**, which further reacted in a spontaneous intramolecular Mannich reaction to afford dihydropyrrole **2.53**

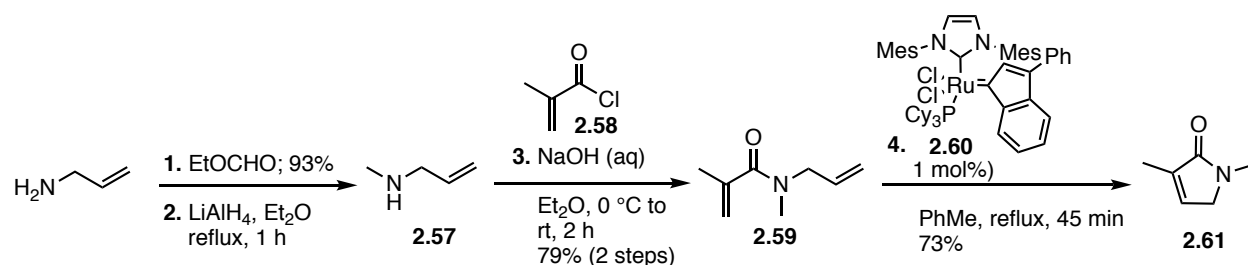
in 83% yield. The aldehyde was reduced with NaBH<sub>4</sub> to the corresponding alcohol, which was immediately converted to sulfide **2.54**. The final challenge of the synthesis was to close the C-ring from precursor **2.54** by a C10/11 bond formation. Initial attempts to perform an intramolecular Heck reaction were low yielding. However, an alternative radical initiated ring closure gave the desired tetracycle **2.55** in an excellent yield of 91%. Next, the exocyclic olefin **2.55** was isomerized to the tetrasubstituted olefin **2.56** using *p*-TsOH•H<sub>2</sub>O in refluxing benzene. Finally, Szántay's intermediate **2.28** was accessed by sodium naphthalenide-mediated global cleavage of the tosyl groups and selective *N*-methylation of the aliphatic amine, thereby completing the formal synthesis of cycloclavine in 27% yield and 7 steps from known aldehyde **2.49**.



Scheme 2-7 Formal total synthesis of ( $\pm$ )-cycloclavine by Cao

### 2.1.5.5 Opatz' Formal Synthesis of (±)-Cycloclavine (2016)

In 2016, the Opatz group reported a convergent formal synthesis of (±)-cycloclavine.<sup>90</sup> Their approach centred on a late-stage formation of the C-ring through the combination of a D-ring fragment and the indole AB-ring. The synthesis of the D-ring started with methylation of allylamine using a two-step protocol involving sequential formylation, then LiAlH<sub>4</sub> reduction (Scheme 2-8). *N*-Allylmethylamine (**2.57**) was acylated with methacryloyl chloride **2.58** to afford amide **2.59**. Ring closing metathesis with catalytic amounts of catMETium **2.60** afforded the D-ring fragment **2.61** in 73% yield.

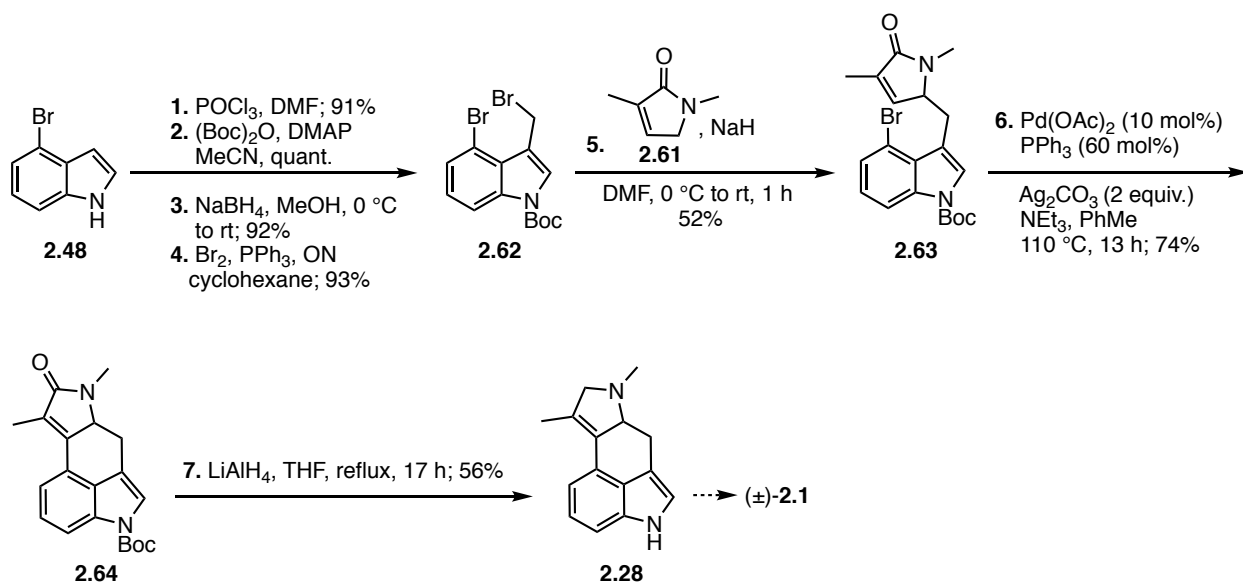


Scheme 2-8 Synthesis of pyrrolinone **2.61**

The A-B fragment **2.62** was synthesized in four steps and 78% overall yield from 4-bromoindole (**2.48**) (Scheme 2-9). Pyrrolinone **2.61** was deprotonated with NaH to form the corresponding anion, which underwent a highly regioselective alkylation with bis-bromoindole **2.62** in 52% yield. The regioselective alkylation at the  $\gamma$ -position of the anion rather than the  $\alpha$ -position was attributed to the steric demand imposed on the  $\alpha$ -position by the bulky bromine substituent in the S<sub>N</sub>2 transition state. Gratifyingly, the key Ag<sub>2</sub>CO<sub>3</sub> promoted intramolecular Heck reaction of aryl bromide **2.63** afforded tetracycle **2.64** in 74% yield. Reduction of the lactam to the tertiary amine with LiAlH<sub>4</sub> was accompanied by Boc-cleavage to deliver amine



**2.28**, which intercepted Szántay's route and thus completed the formal synthesis of cycloclavine in 17% yield and 7 steps to cycloclavine precursor **2.48**.

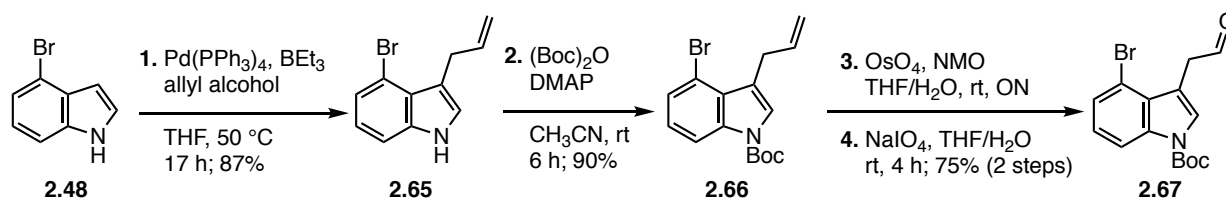


**Scheme 2-9** Formal total synthesis of (±)-cycloclavine by Netz and Opatz

#### 2.1.5.6 Cao's Formal Synthesis of (+)-Cycloclavine (2017)

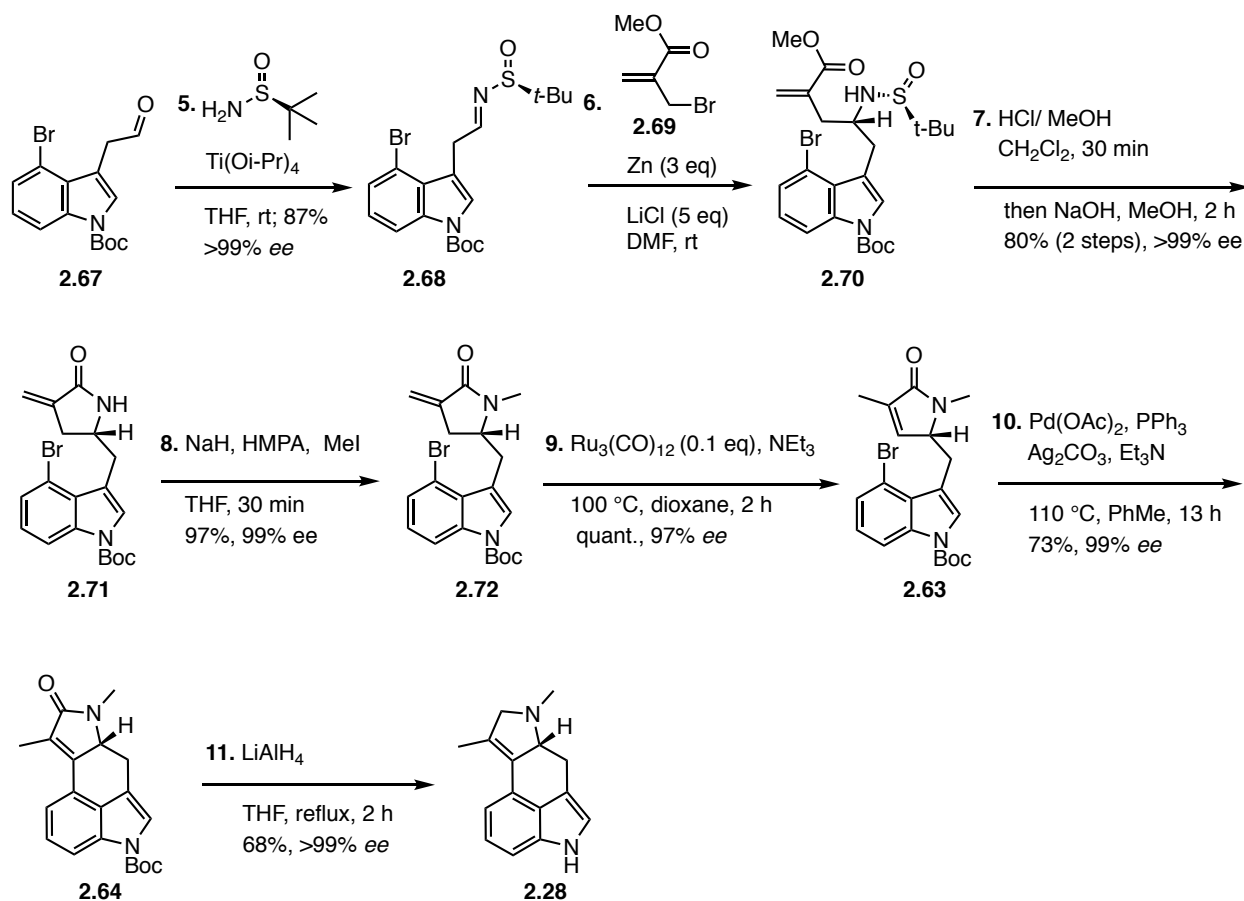
In 2017, the Cao group reported the first enantioselective formal synthesis of the natural enantiomer (+)-cycloclavine.<sup>91</sup> A key feature of the synthesis was a Barbier-type addition to a chiral *N-tert*-butanesulfinyl imine to set the absolute configuration of the secondary amine.

The synthesis commenced with a 4-step gram-scale preparation of known aldehyde **2.67** (Scheme 2-10). 2-Bromoindole (**2.48**) was subjected to a regioselective C3-allylation to form 3-allyl indole **2.65**. The free indole was then Boc-protected and the olefin **2.66** subjected to oxidative cleavage conditions with  $\text{OsO}_4/\text{NaIO}_4$  to afford aldehyde **2.67** in 75% over two steps.



Scheme 2-10 Synthesis of aldehyde **2.67**

The known aldehyde **2.67** was then reacted with (*S*)-2-methylpropane-2-sulfinamide in the presence of  $\text{Ti}(\text{O}i\text{-Pr})_4$  to form the chiral imine **2.68** in 87% yield and >99% *ee* by chiral HPLC analysis (Scheme 2-11). The crucial Barbier addition of 2-(bromomethyl)acrylate **2.69** to imine **2.68** proceeded smoothly to produce sulfinamide **2.70**. This product was immediately subjected to an acid mediated cleavage of the sulfinyl auxiliary followed by a base promoted intramolecular ester aminolysis to form lactam **2.71**. Methylation of the lactam delivered **2.72** in 97% yield. The exocyclic methylene lactam **2.72** was then isomerized to pyrrolinone **2.63** by heating the lactam in dioxane at 100 °C in the presence of  $\text{Ru}_3(\text{CO})_{12}$ . Finally, the C-ring was forged by an intramolecular Heck reaction using Opatz' conditions and the resulting lactam **2.64** was reduced with  $\text{LiAlH}_4$  in refluxing THF to deliver Szántay's amine **2.28** in 68% yield and >99% *ee*. Overall, the first formal synthesis of (+)-cycloclavine was accomplished in 11 steps and 19.7% yield from commercially available 4-bromoindole (**2.48**).



**Scheme 2-11** Formal total synthesis of (+)-cycloclavine by Cao

### 2.1.5.7 Bisai's Formal Synthesis of (+)- and (–)-Cycloclavine (2018)

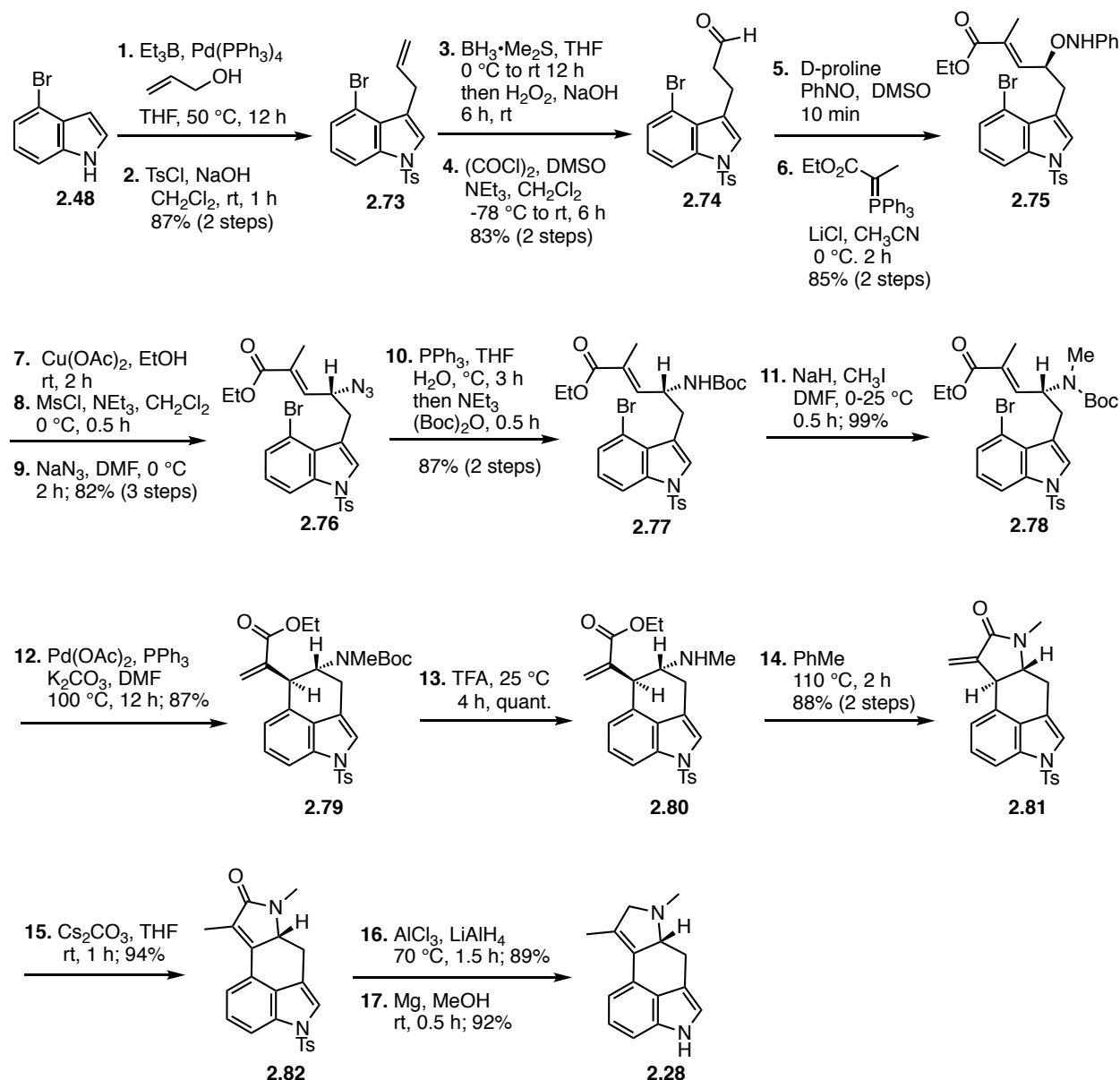
Bisai's enantioselective formal synthesis of both the natural and unnatural enantiomer of cycloclavine further highlights the utility of the intramolecular Heck reaction in the total synthesis of clavine alkaloids.<sup>92</sup> The absolute configuration of the secondary amine was set using a key enantioselective  $\alpha$ -aminoxylation reaction followed by a  $\text{S}_{\text{N}}2$  inversion with  $\text{NaN}_3$ .

The synthesis began with a palladium-catalyzed allylation of 4-bromoindole (**2.48**) with allyl alcohol in the presence of triethylborane to form 3-allyl-4-bromoindole (Scheme 2-12). The indole nitrogen was then protected as the tosylate **2.73** and subjected to a hydroboration/oxidation/Swern oxidation sequence to give aldehyde **2.74** in 83% yield over two

steps. The vital  $\alpha$ -aminoxylation reaction was initiated by treating aldehyde **2.74** with a catalytic amount of D-proline, followed by the addition of nitrosobenzene to afford the expected  $\alpha$ -aminoxy intermediate. This compound was immediately reacted with the stabilized Wittig reagent ethyl 2-(triphenylphosphoranylidene)propionate to provide the *E*-ester **2.75** exclusively in 85% yield over two steps and 96% *ee*.

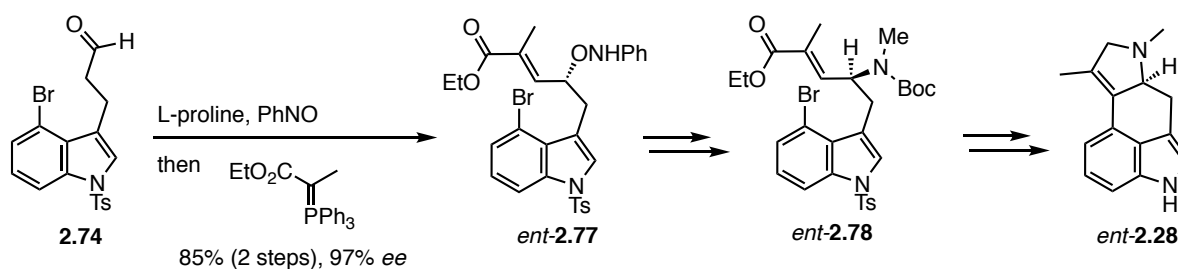
With the chiral ester **2.75** in hand, their attention moved to the elaboration of the allylic amine precursor **2.78** for the Heck cyclization. N-O cleavage of the hydroxylamine ether **2.75** was accomplished with anhydrous Cu(OAc)<sub>2</sub>. The resulting secondary alcohol was converted to the mesylate and subjected to a S<sub>N</sub>2 reaction with NaN<sub>3</sub> to deliver azide **2.76** in 82% yield over three steps. The azide moiety was reduced to the corresponding amine under Staudinger conditions and the free amine protected *in situ* as the Boc carbamate **2.77**. Finally *N*-methylation of the amino group provided the cyclization precursor **2.78**. The crucial intramolecular Heck reaction proceeded smoothly when 4-bromoindole **2.78** was reacted with Pd(OAc)<sub>2</sub>, PPh<sub>3</sub> and K<sub>2</sub>CO<sub>3</sub> in DMF at 100 °C for 12 h to afford tricycle **2.79** in 87% yield.

The final sequence to form the D-ring was initiated by Boc deprotection to form secondary amine **2.80**. When amine **2.80** was heated in toluene at reflux an intramolecular ester aminolysis occurred to give the tetracyclic lactam **2.81**. The exocyclic double bond in **2.81** was then isomerized upon treatment with Cs<sub>2</sub>CO<sub>3</sub> in THF to give pyrrolinone **2.82**. Finally, lactam reduction and indole deprotection completed the formal synthesis of (+)-cycloclavine in 17 steps and 25.5% overall yield.



**Scheme 2-12** Formal total synthesis of (+)-cycloclavine by Bisai

To complete a formal synthesis of the unnatural enantiomer, the catalytic enantioselective  $\alpha$ -aminoxylation reaction was carried out with L-proline instead of D-proline to provide the enantiomer of the hydroxylamine ether *ent*-**2.77** in 97% *ee* (Scheme 2-13). This material was carried through the same sequence to form the enantiomeric amine *ent*-**2.78** that was then converted into the enantiomer of Szántay's amine *ent*-**2.28**.



**Scheme 2-13** Key  $\alpha$ -aminoxylation in the formal synthesis of (-)-cycloclavine

## 2.2 RESULTS AND DISCUSSION

### 2.2.1 Retrosynthetic Analysis of ( $\pm$ )-Cycloclavine

Before embarking on an enantioselective total synthesis of cycloclavine, we planned to carry out an improved racemic synthesis of the natural product. The original 14-step/1.2% overall yield racemic synthesis was revised and an improved version that retains the innovative double Diels-Alder approach to the ABCD-ring system was envisaged (Figure 2-5). We aimed to install the indole last through an IMDAF reaction from enone **2.85**. Given the challenge in installing the C11/C16 double bond in the original synthesis, a key modification of the revised route was to protect the tertiary amine as the amide, which we anticipated would allow a direct regioselective oxidation to access enone **2.85** from ketone **2.86**. A strain-promoted intramolecular methylenecyclopropane Diels-Alder reaction leads retrosynthetically to diene precursor **2.87**. The amide **2.87** could be synthesized by an amidation reaction of vinylogous amide **2.88** and methylenecyclopropane carboxylic acid **2.89**. The methylenecyclopropane could in turn be generated through a literature reported  $\text{Rh}_2(\text{OAc})_4$  catalyzed cyclopropanation reaction between ethyl diazoacetate and 2-bromopropene.

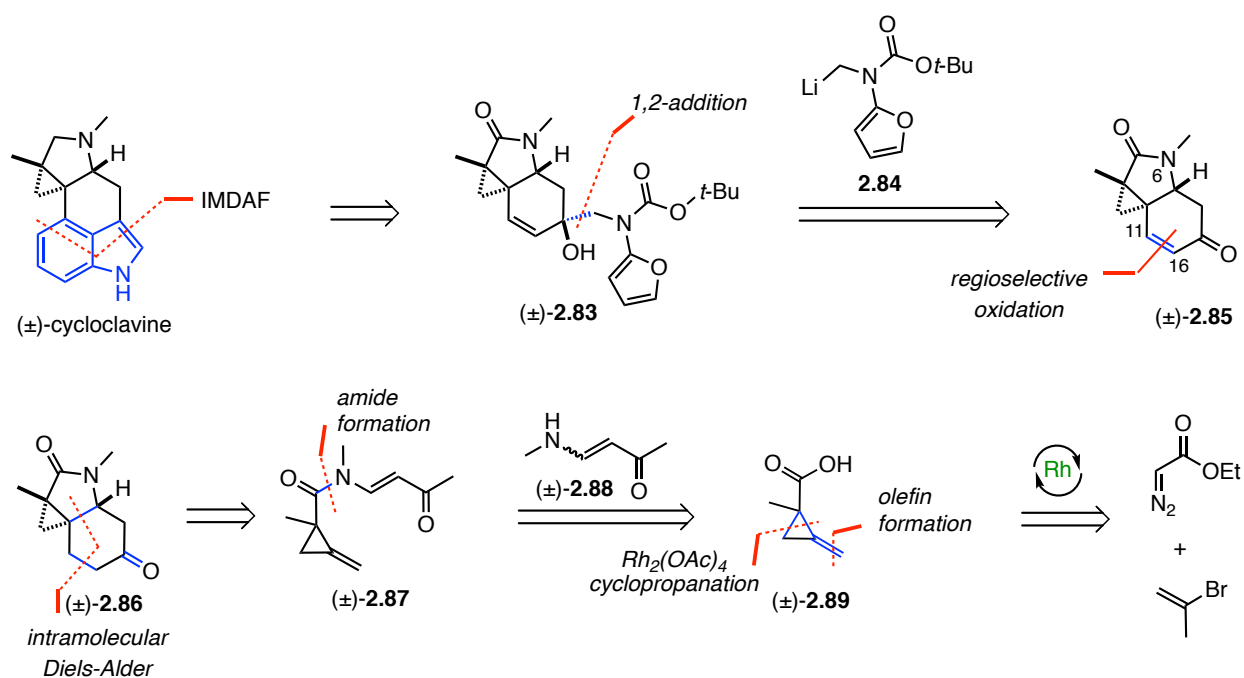
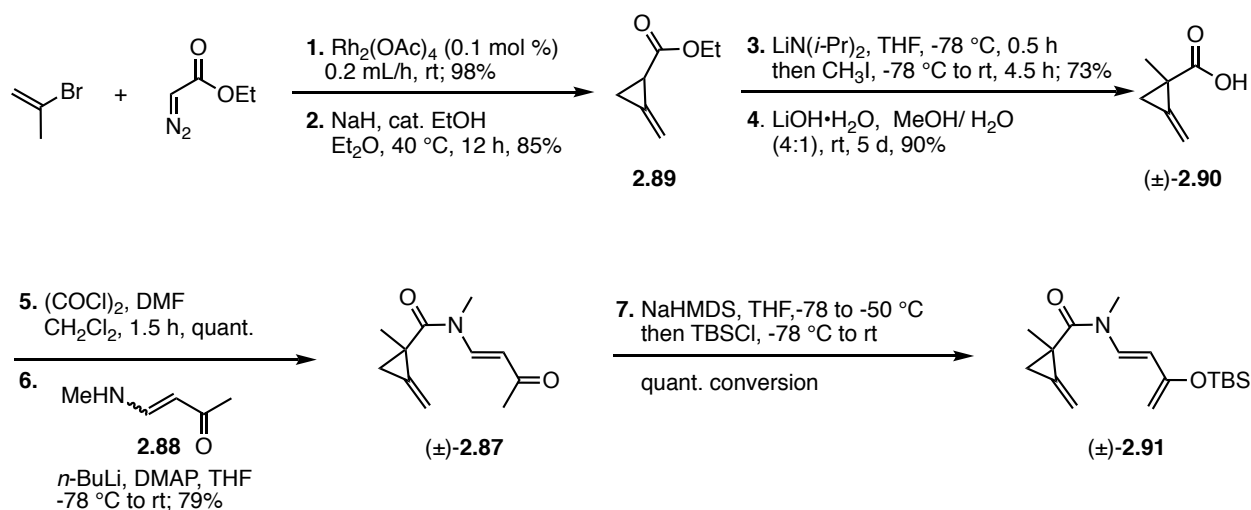


Figure 2-5 Retrosynthetic analysis of (±)-cycloclavine

## 2.2.2 Synthesis of the Key Tricyclic Ketone

The first portion of the synthesis was focused on the formation of the tricyclic cyclopropa[*c*]indoline core of the natural product. Our approach to tricycle **2.86** began with the known reaction of 2-bromopropene and ethyl diazoacetate in the presence of 0.1 mol%  $\text{Rh}_2(\text{OAc})_4$  to form an intermediate tertiary cyclopropyl bromide (Scheme 2-14).<sup>93</sup> This intermediate underwent an elimination reaction upon treatment with NaH to form the known methylenecyclopropane **2.89** in 83% yield over two steps.<sup>93</sup> The methylenecyclopropane **2.89** underwent enolization when reacted with the sterically hindered base  $\text{LiN}(i\text{-Pr})_2$  at  $-78^\circ\text{C}$  to form the corresponding enolate which was subsequently quenched with  $\text{CH}_3\text{I}$  to form the  $\alpha$ -methyl ester in 73% yield. Saponification of the ester with excess  $\text{LiOH}\cdot\text{H}_2\text{O}$  in  $\text{MeOH}/\text{H}_2\text{O}$  afforded the methylenecyclopropane carboxylic acid (±)-**2.90** in 90% yield. The ester was

converted to the corresponding acid chloride using the Vilsmeier reagent, which was generated *in situ* by the reaction of oxalyl chloride and DMF. The acyl chloride was then coupled to the anion of the vinylogous amide **2.88** to produce the vinylogous imide ( $\pm$ )-**2.87** in 79% yield. The vinylogous imide was added to a solution of NaHMDS at -78 °C to form the corresponding enolate. We found that it was crucial to allow the reaction to warm to -50 °C over 1 h after the vinylogous imide had been added to ensure complete enolization. The enolate was quenched at -78 °C by the addition of TBSCl to form the highly reactive amino silyloxy diene ( $\pm$ )-**2.91**.



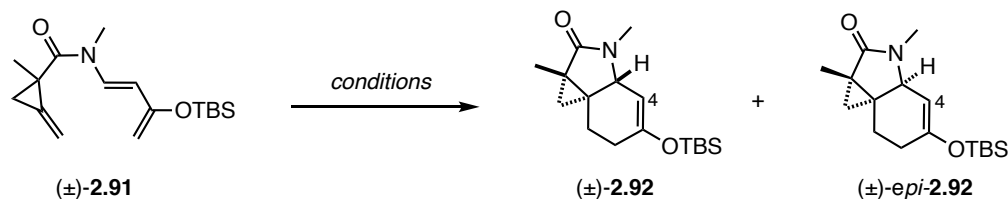
**Scheme 2-14** Synthesis of the key amino silyloxy diene ( $\pm$ )-**2.91**

With the diene in hand, we were positioned to explore the key strain-promoted methylenecyclopropane Diels-Alder [4+2] cycloaddition (Table 2-1). When a solution of crude silyl enol ether ( $\pm$ )-**2.91** was heated in trifluorotoluene at 150 °C under microwave irradiation for 25 min, it underwent an *anti*-selective intramolecular Diels-Alder reaction with the pendant methylenecyclopropane. The expected Diels-Alder adducts were formed in a 2.2:1 ratio ( $\pm$ )-**2.92**: ( $\pm$ )-*epi*-**2.92** based on NMR analysis (Table 2-1, Entry 1). While this result was promising, we sought to improve the diastereomeric ratio to further favor the desired *trans*-ring fusion product



(±)-**2.92**. Lowering the temperature to 110 °C led to an improved diastereomeric ratio of 3.7:1 (±)-**2.92**: (±)-*epi*-**2.92** (Table 2-1, Entry 3). Switching the solvent to THF and carrying the reaction out at 100 °C further increased the *dr* to 4.1:1 (Table 2-1, Entry 4). Attempts to conduct the Diels-Alder reaction using the Lewis acid Et<sub>2</sub>AlCl led to silyl deprotection to form amide **2.87** (Table 2-1, Entry 5). Overall, heating the diene in THF at 100 °C for 25 min under microwave irradiation was identified as the optimum conditions for the Diels-Alder reaction.

**Table 2-1** Optimization of the Intramolecular Methylene cyclopropane Diels-Alder Reaction

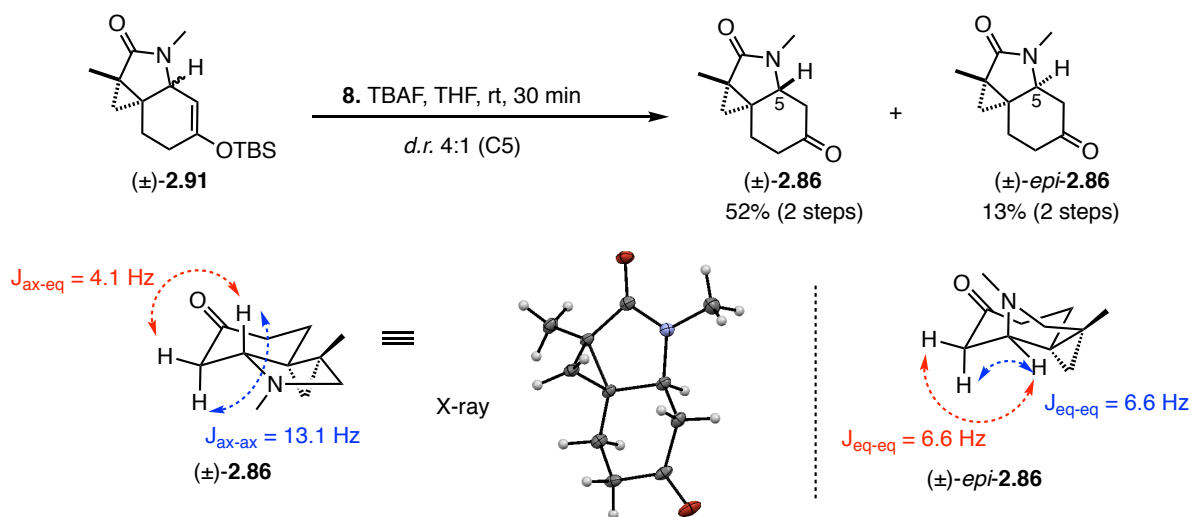


Entry	Conditions	Product Ratio ( <sup>1</sup> H NMR) <sup>a</sup>	
		(±)- <b>2.92</b>	(±)- <i>epi</i> - <b>2.92</b>
1	PhCF <sub>3</sub> , 150 °C, μw, 25 min	2.2	1
2	PhCF <sub>3</sub> , 130 °C, μw, 25 min	2.9	1
3	PhCF <sub>3</sub> , 110 °C, μw, 25 min	3.7	1
4	THF, 100 °C, μw, 25 min	4.1	1
5	Et <sub>2</sub> AlCl, CH <sub>2</sub> Cl <sub>2</sub> , -78 to -40 °C	Amide <b>2.87</b>	

<sup>a</sup>the C4 vinyl proton in (±)-**2.92** (δ 5.05 ppm) and (±)-*epi*-**2.92** (δ 5.01 ppm) were integrated in the crude <sup>1</sup>H NMR spectrum to assign the *dr* of crude enol ether adducts

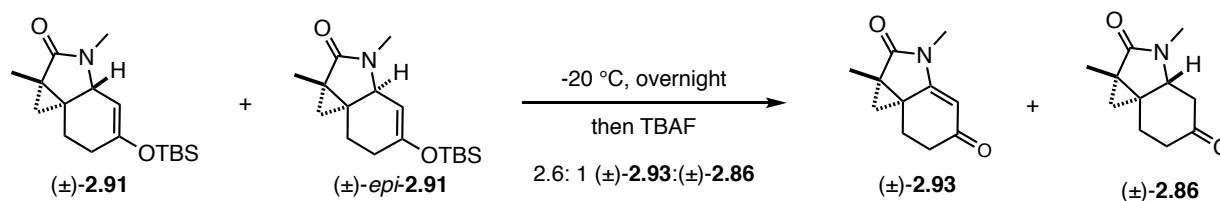
The crude enol ether products were directly subjected to TBAF cleavage at room temperature to afford diastereomers of ketone (±)-**2.86** in a 4:1 *dr* at C(5) (Scheme 2-15). The diastereomers could be separated by chromatography on SiO<sub>2</sub>. The ring-junction configuration of the major diastereomer was assigned as the *trans*-diastereomer (±)-**2.86** through analysis of the vicinal coupling constants. The ring junction methine showed a vicinal coupling constant of *J* = 13.1 Hz to the adjacent axial proton and a coupling constant of *J* = 4.1 Hz to the adjacent

equatorial proton. A single crystal X-ray structure of ( $\pm$ )-**2.86** confirmed this assignment. In contrast, the ring junction methine H5 in the minor *cis*-diastereomer appeared as an apparent triplet at  $\delta$  3.73 ppm with a coupling constant of  $J = 6.6$  Hz to the adjacent equatorial proton and a coupling constant of  $J = 6.6$  Hz to the adjacent axial proton.



**Scheme 2-15** Formation of ketones ( $\pm$ )-**2.86** and ( $\pm$ )-*epi*-**2.86** and the relative configuration of ketone ( $\pm$ )-**2.86**

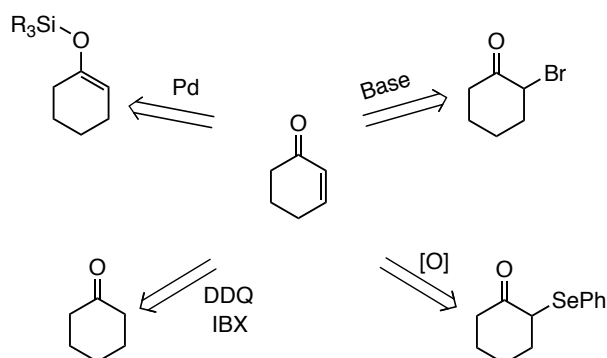
We found that it was important to perform the enolization, Diels-Alder cycloaddition and TBS-enol ether cleavage sequence directly without storage of the intermediate enol ethers (Scheme 2-16). The Diels-Alder adducts ( $\pm$ )-**2.91** and ( $\pm$ )-*epi*-**2.91** exhibited limited stability when stored overnight in the freezer before TBAF cleavage, with a partial conversion to the undesired regioisomer ( $\pm$ )-**2.93** occurring. This undesired side reaction could be completely avoided by subjecting the crude enol-ether adducts directly to TBAF.



**Scheme 2-16** Partial conversion of enol ethers ( $\pm$ )-**2.91** and ( $\pm$ )-*epi*-**2.91** to the undesired enone ( $\pm$ )-**2.93**

### 2.2.3 Ketone Dehydrogenation

The next challenge in the synthesis was to perform a regioselective dehydrogenation of the tricyclic ketone ( $\pm$ )-**2.86** to enone ( $\pm$ )-**2.85**. Traditional two-step methods for this conversion include  $\alpha$ -bromination/dehydrobromination,  $\alpha$ -selenation/oxidative elimination or a Saegusa-Ito reaction, which proceeds via a Pd(II)-mediated dehydrosilylation of a silyl enol ether (Figure 2-6).<sup>94,95,96,97</sup> Alternatively, stoichiometric oxidants like 2-iodoxybenzoic acid (IBX) and 2,3-dichloro-5,6-dicyano-1,4-benzoquinone (DDQ) can be employed to access the enone directly; however, the use of stoichiometric oxidant is not atom economical (Figure 2-6).

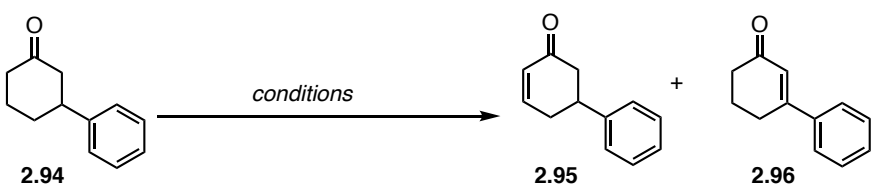


**Figure 2-6** Classical methods for the dehydrogenation of ketones to enones

We were particularly inspired by work carried out by Diao and Stahl who showed that catalytic amounts of  $\text{Pd}_2(\text{TFA})_2$  in the presence of DMSO (0.1 eq) and an atmosphere of oxygen promoted the direct dehydrogenation of cyclic ketones to the corresponding enones in high yields for a wide range of substrates.<sup>98</sup> This one-step protocol is especially appealing because it uses catalytic Pd(II) and molecular  $\text{O}_2$ , an atom-economical reagent as the stoichiometric oxidant.

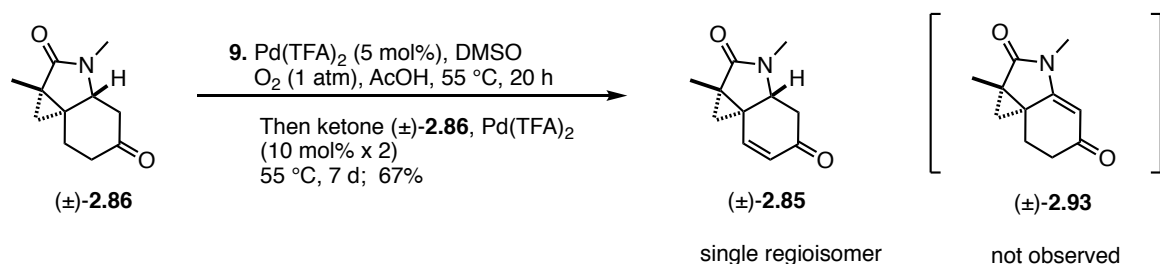
Initial optimizations were conducted on the dehydrogenation of 3-phenylcyclohexanone (**2.94**) (Table 2-2). When ketone **2.94** was subjected to Stahl's conditions of 5 mol% Pd(TFA)<sub>2</sub>, 10 mol% DMSO in AcOH (0.2 M) at 80 °C for 12 h under an atmosphere of oxygen, enones **2.95** and **2.96** were obtained in a 1.7:1 mixture of regioisomers in a combined yield of 63%. Pre-activating the catalytic system overnight prior to the addition of the ketone and performing the reaction at a lower temperature of 55 °C led to a more regioselective reaction and an improved ratio of 2.17:1 of **2.95**: **2.96**.

**Table 2-2** Optimization of the Dehydrogenation of 3-Phenylcyclohexanone under Stahl Conditions

		
Conditions	Product Ratio ( <sup>1</sup> H NMR)	
	2.95	2.96
ketone <b>2.94</b> , Pd(TFA) <sub>2</sub> (0.05 eq), O <sub>2</sub> (1 atm), AcOH (0.2 M), DMSO (0.1 eq), 80 °C, 12 h	1.7	1
1. Pd(TFA) <sub>2</sub> (0.05 eq), O <sub>2</sub> (1 atm), AcOH (0.2 M), DMSO (0.1 eq) 55 °C, 20 h 2. ketone <b>2.94</b> , 55 °C, 2 d	2.17	1

Using the conditions optimized on the model system, the dehydrogenation of tricyclic ketone (±)-**2.86** was attempted. We were pleased to see that under the optimal conditions, the reaction of ketone (±)-**2.86** with 5 mol% of Pd(TFA)<sub>2</sub> and 10 mol% DMSO in AcOH under an atmosphere of oxygen at 55 °C for 7 days proceeded with excellent regioselectivity, forming the

less-substituted enone ( $\pm$ )-**2.85** exclusively (Scheme 2-17). During the reaction it was necessary to add additional catalyst (2 x 10 mol%) to drive the reaction to completion.



**Scheme 2-17** Pd(II)-mediated aerobic oxidation of ketone ( $\pm$ )-**2.86** to enone ( $\pm$ )-**2.85**

The proposed catalytic cycle is outlined in Figure 2-7.<sup>98,99</sup> The reaction is initiated by the formation of a palladium(II) enolate that exists in a tautomeric equilibrium of *O*- and *C*-bound palladium enolates ( $\pm$ )-**2.98** and ( $\pm$ )-**2.99**. When the *C*-bound palladium tautomer ( $\pm$ )-**2.98** forms, the proximity of the palladium center to the  $\beta$ -hydrogen can facilitate  $\beta$ -hydrogen elimination to form enone ( $\pm$ )-**2.85**. The resulting Pd(II)-hydride intermediate undergoes reductive elimination to form an equivalent of carboxylic acid and Pd(0) species **2.101**. The Pd(0) species can be oxidized by molecular oxygen to form the  $\eta^2$ -peroxo complex **2.102**. Protonolysis generates complex **2.103** which can react with a second equivalent of carboxylic acid to regenerate the active Pd(II) catalyst.<sup>100</sup> Kinetic and computational experiments support the mechanism for the conversion of palladium(II)-hydride intermediate **2.100** to the palladium(II) peroxide complex **2.103**.<sup>100,101</sup>

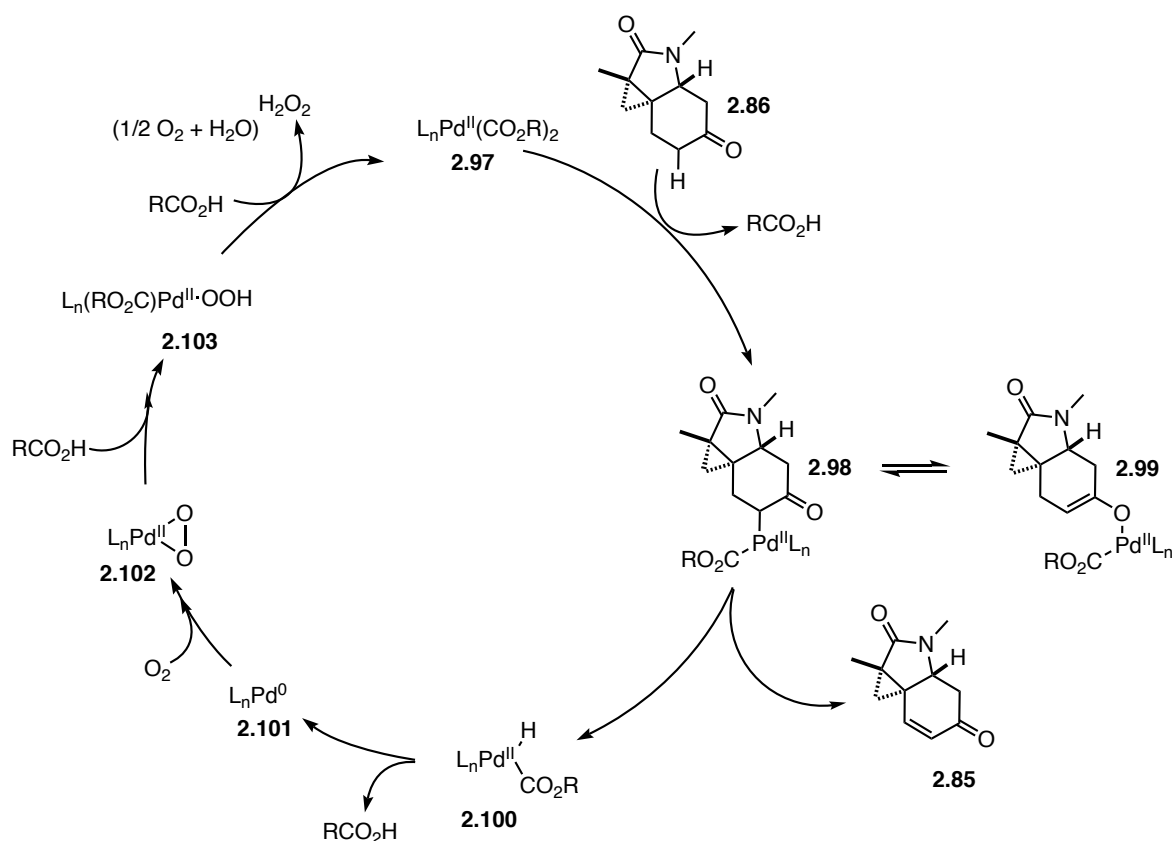
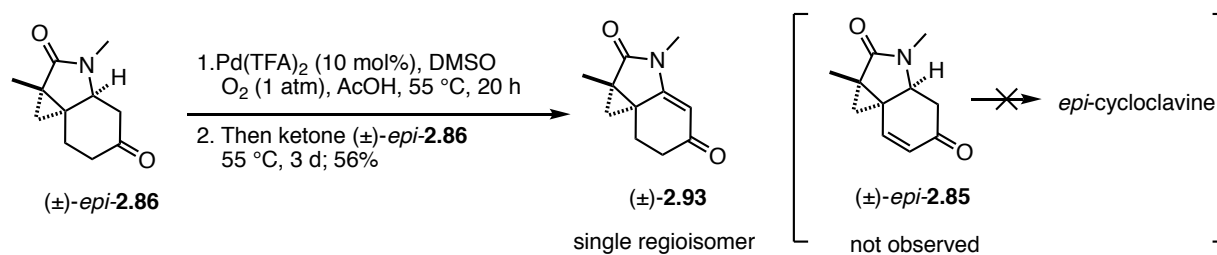


**Figure 2-7** Proposed mechanism for the Pd(II)-catalyzed aerobic dehydrogenation of ketones

We also investigated whether the Pd(II) catalyst would impart similar regioselectivity in the oxidation of the minor *cis*-diastereomer ( $\pm$ )-*epi*-**2.86** to form enone ( $\pm$ )-*epi*-**2.85**, an intermediate in Wipf and Petronijevic's route to *epi*-cycloclavine.<sup>41</sup> However, when ( $\pm$ )-*epi*-**2.86** reacted with Pd(TFA)<sub>2</sub> and DMSO in AcOH under an atmosphere of oxygen at 55 °C for 3 days, the more substituted regioisomer ( $\pm$ )-**2.93** was formed exclusively in 56% yield (Scheme 2-18).



**Scheme 2-18** Pd<sup>II</sup>-mediated aerobic oxidation of ketone ( $\pm$ )-*epi*-**2.86** to enone ( $\pm$ )-**2.93**

The complete switch in regioselectivity for the *trans* and *cis* diastereomers parallels results obtained for the enolization of *trans* and *cis* 2-decalones (Figure 2-8). The *trans* or *cis* stereochemistry at the decalin ring junction governs the regioselectivity of enolate formation due to torsional strain in the enolate transition state.<sup>102,103</sup> House and Trost showed that a 1:1 mixture of *trans*-enol acetates **2.104** and **2.105** could be equilibrated in the presence of catalytic *p*-toluenesulfonic acid at 100 °C to give equilibrium mixtures having the compositions indicated in Figure 2-8.<sup>102</sup> The *trans*-2-decalone was shown to favor the 2,3-enol acetate **2.105** (Figure 2-8a). In contrast, when the same experiment was performed on *cis*-2-decalone, the 1,2-enol acetate **2.106** was favored (Figure 2-8b).

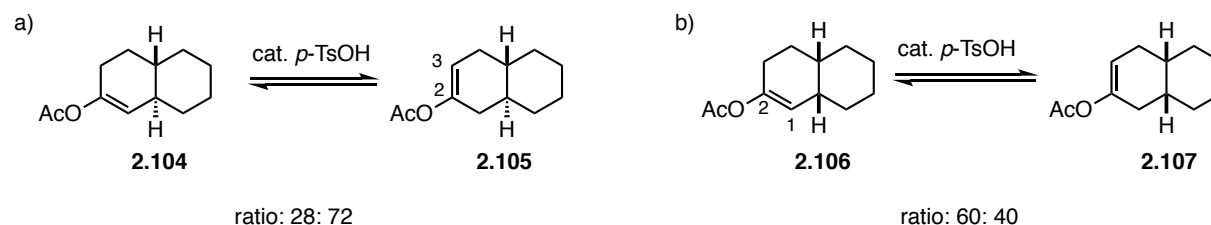
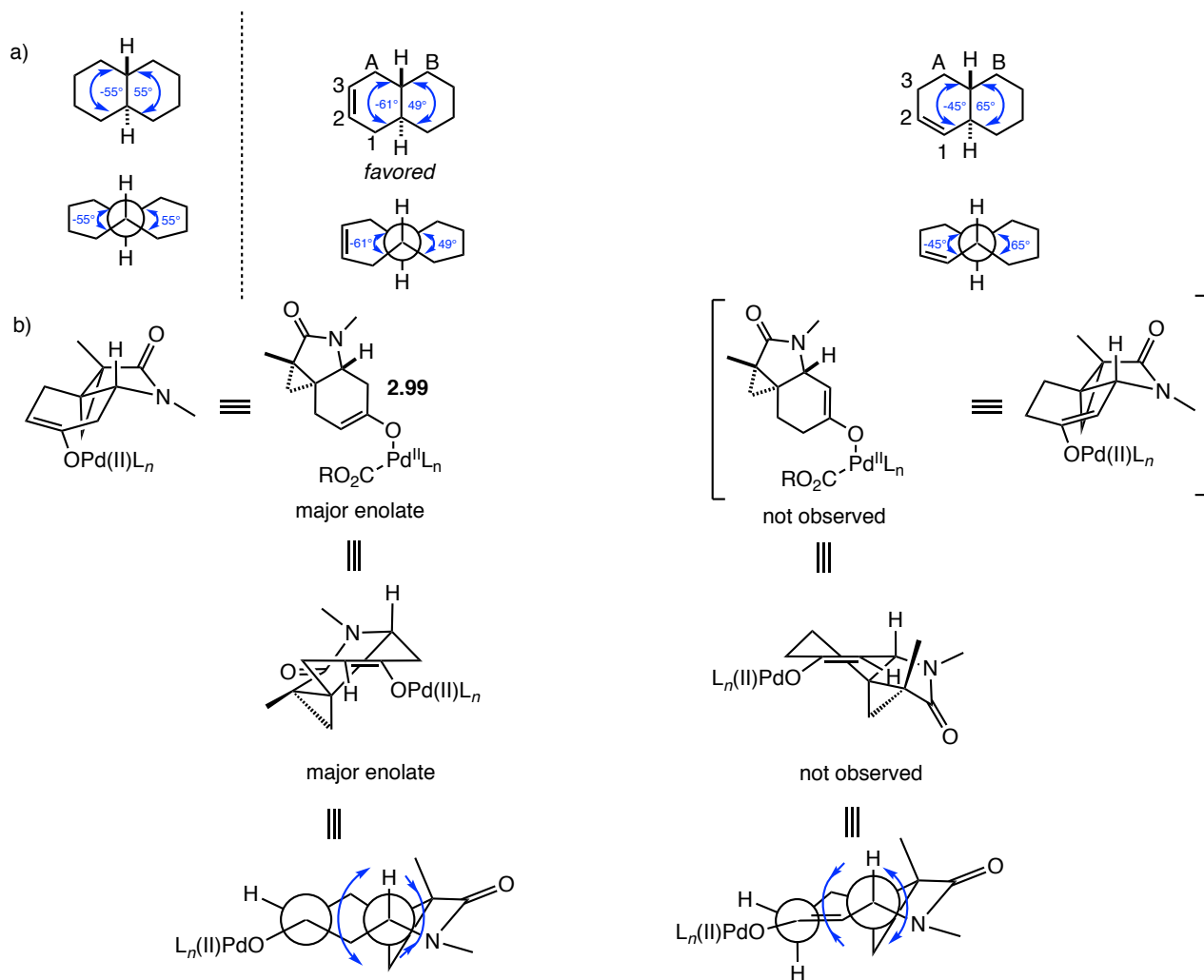


**Figure 2-8** Correlation between enolate stability and ring junction stereochemistry in *cis* and *trans* decalins

The torsional effects that have been proposed to govern the regiochemistry of enolization in *cis* and *trans*-decalones has been investigated in greater detail in relevant *cis*- and *trans*-octalins (Figure 2-9a).<sup>103,104</sup> The introduction of a double bond at the 1,2 position of the parent decalin leads to an opening of the saturated ring B by approximately 10° (from +55° to +65°) and causes a corresponding ring closure by 10° in the unsaturated ring A (from -55° to -45°). In contrast the introduction of a double bond at the 2,3-position of the parent decalin leads to a ring opening of 6° in the unsaturated A-ring (from -55° to -61°) and a corresponding ring-closure by 6° in the saturated B ring (from 55° to 49°). Overall, this means that the double bond at the 2,3-

position is more favorable as it imparts less torsional strain in the transition state leading to the *trans*-fused octalin product.

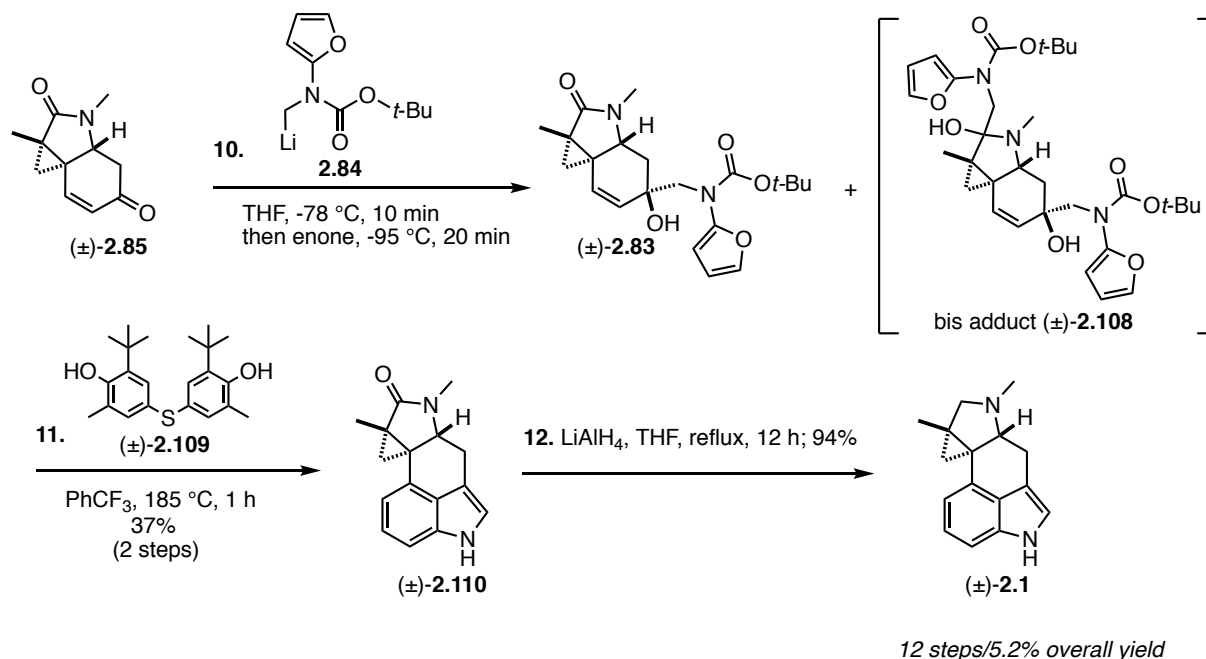


These effects are presumably amplified in the smaller 5,6-fused ring system, rationalizing the regioselectivity observed for the conversion of *trans*-ketone ( $\pm$ )-**2.86** to the less substituted enone ( $\pm$ )-**2.85** and the conversion of *cis*-ketone ( $\pm$ )-*epi*-**2.86** to the more substituted enone ( $\pm$ )-**2.93** and accordingly, indicates that regioselectivity is due to substrate control rather than governed by catalyst effects.



## 2.2.4 Completion of the Synthesis of (±)-Cycloclavine

With enone (±)-**2.85** in hand, our attention turned to the installation of the amino furan side chain. We were pleased to see that the reaction of Boc-carbamate stabilized methyllithium reagent **2.84** with racemic enone (±)-**2.85** delivered the desired tertiary alcohol (±)-**2.83** (Scheme 2-19). However, the addition was hampered by incomplete consumption of enone (±)-**2.85** and the formation of a byproduct tentatively assigned as the bis-addition product (±)-**2.108** by LCMS. This byproduct was likely formed *via* a second addition of the furanyl lithium reagent to the amide. The crude allylic alcohol was subjected directly to an IMDAF reaction in the presence of Kishi's radical inhibitor **2.109**. At best, indole (±)-**2.110** was isolated in 37% yield over two steps.  $\text{LiAlH}_4$  reduction delivered racemic cycloclavine (±)-**2.1** in 94% yield. Overall the revised racemic synthesis was completed in 12 steps and 5.2% overall yield.



Scheme 2-19 Completion of the synthesis of (±)-cycloclavine

### 2.2.5 Retrosynthetic Analysis of (–)-Cycloclavine

In order to accomplish an enantioselective total synthesis of cycloclavine and develop an efficient route to either enantiomer, we revised our 12 steps/5.2% racemic synthesis. We intended to employ the same endgame strategy where the indole AB-ring would be installed by an enone 1,2-addition/IMDAF sequence from enone **2.85** (Figure 2-10). The key enone **2.85** would be synthesized from ketone **2.86** using the improved one-step regioselective aerobic dehydrogenation optimized during the racemic synthesis. The intramolecular Diels-Alder reaction to form ketone **2.86** would be retained. The main feature of the revised enantioselective route is a significantly improved strategy to access the vinylogous imide **2.87**. We anticipated that the amide linkage in **2.87** could be generated by direct aminolysis of an activated ester with vinylogous amide **2.88**. The key methylenecyclopropane moiety could be accessed *via* a chiral metal-mediated asymmetric cyclopropanation of a diazo ester **1.99** with allene **1.96**, thereby providing a way to set the absolute configuration of either enantiomer of cycloclavine **2.1** from the outset of the synthesis. The successful implementation of this two-step approach to **2.87** would represent a major improvement compared to our previous synthesis, which required six steps to access intermediate ( $\pm$ )-**2.87**.

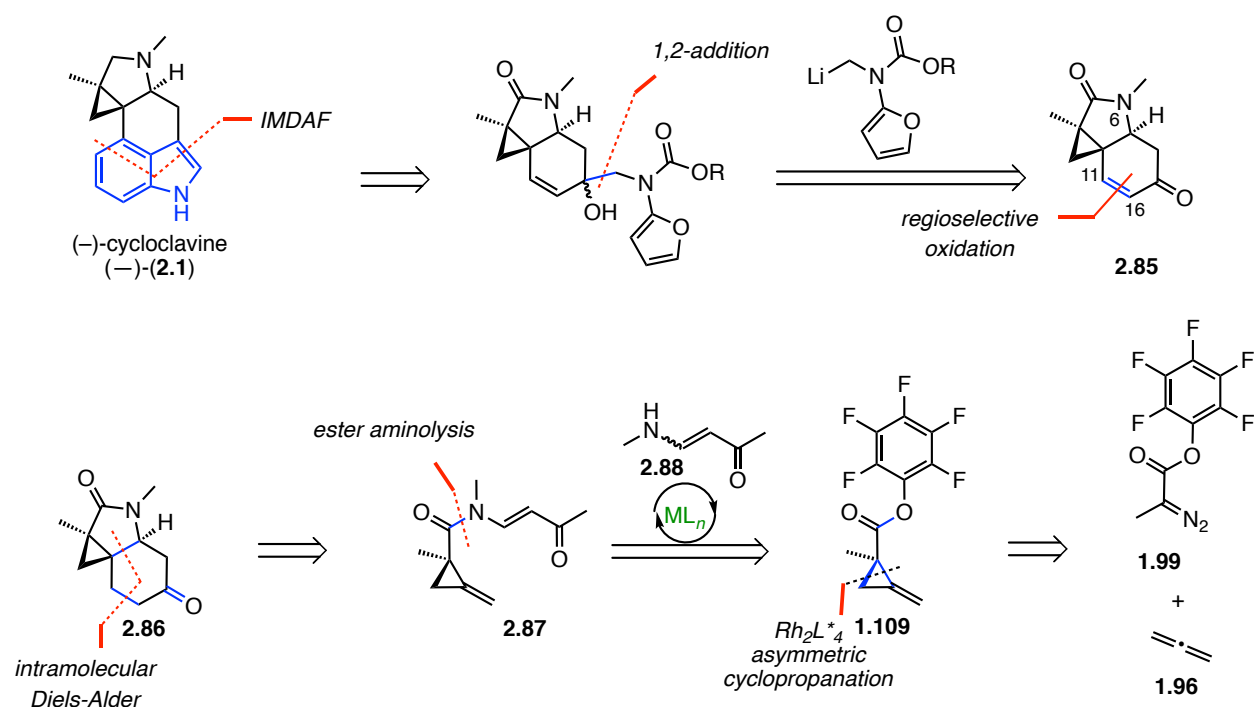
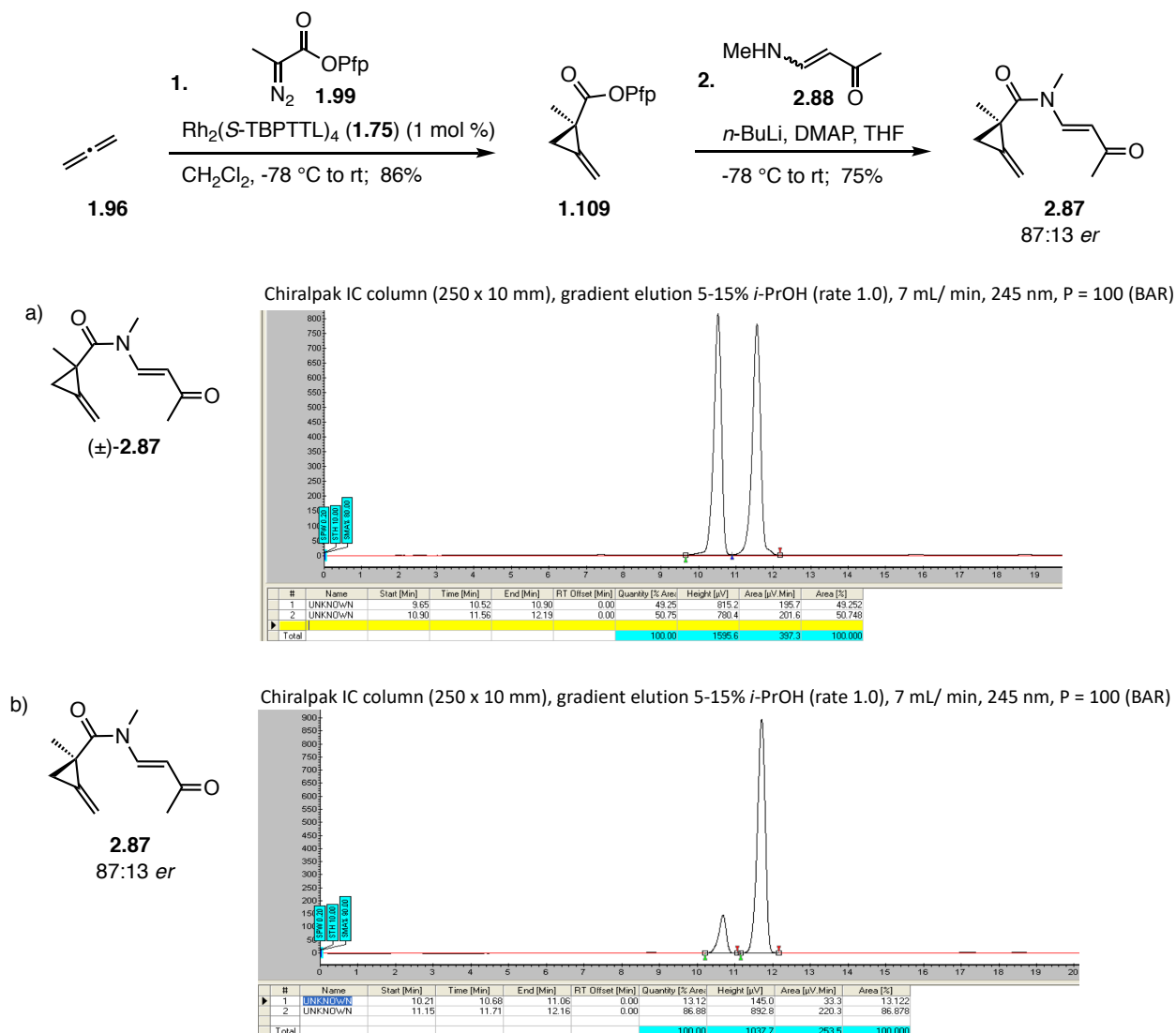


Figure 2-10 Retrosynthetic analysis of (-)-cycloclavine

## 2.2.6 Synthesis of the Indoline-Fused Cyclopropane Core

Our initial efforts were directed toward the assembly of the indoline-fused cyclopropane core. The synthesis began with an enantioselective cyclopropanation of allene **1.96** with diazo ester **1.99** in the presence of 1 mol% dirhodium complex  $Rh_2(S\text{-TBPTTL})_4$  to form methylenecyclopropane **1.109** in 86% yield (Scheme 2-20). The vinylogous amide **2.88** was deprotonated with *n*-BuLi at -78 °C in THF, then acylated with activated ester **1.109** to afford the vinylogous imide **2.87**. Interestingly, the *E/Z* ratio of **2.88** proved to be inconsequential as both isomers produced the *E*-alkene product **2.87**, probably due to rapid isomerization of the enamine upon deprotonation and preferential acylation of the *E*-enamide. Chiral SFC analysis of imide

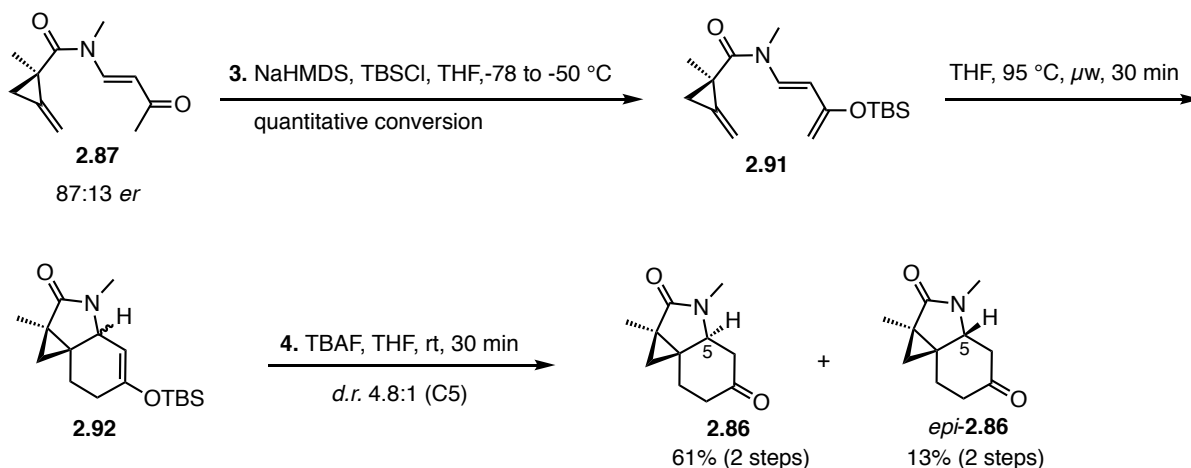
**2.87** revealed an 87:13 *er*, reflecting the enantiomeric enrichment obtained in the prior cyclopropanation step.



**Scheme 2-20** Synthesis of vinylogous imide **2.87** and SFC chromatograms of the a) racemic standard and b) enantioenriched imide **2.87**

Treatment of amide **2.87** with NaHMDS formed the corresponding enolate, which was trapped *in situ* with TBSCl to deliver the highly reactive amino silyloxy diene **2.91** that was used directly without purification (Scheme 2-21). Subjection of diene **2.91** to microwave irradiation at

95 °C triggered an *anti*-selective intramolecular Diels-Alder [4+2] cycloaddition with the pendant methylenecyclopropane to form a mixture of cyclic enol ethers **2.92**. An improvement in *dr* from 4:1 to 4.8:1 was observed by lowering the temperature of the Diels-Alder reaction from 100 °C to 95 °C. The resulting diastereomeric enol ether products were directly subjected to TBAF cleavage at room temperature to afford separable diastereomers of ketone **2.86** and *epi*-**2.86** in 4.8:1 *dr*.

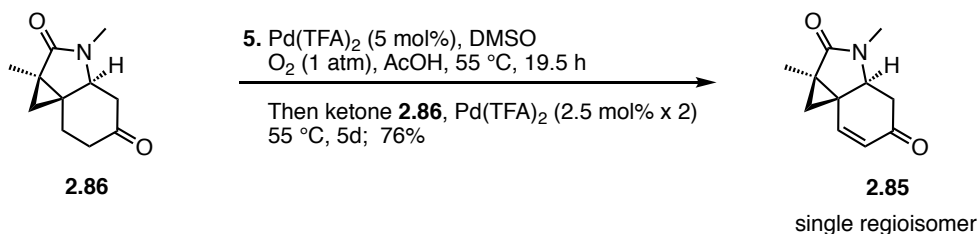


**Scheme 2-21** Conversion of vinylogous imide **2.87** into tricyclic ketones **2.86** and *epi*-**2.86**

## 2.2.7 Ketone Dehydrogenation and Enantiomeric Enrichment

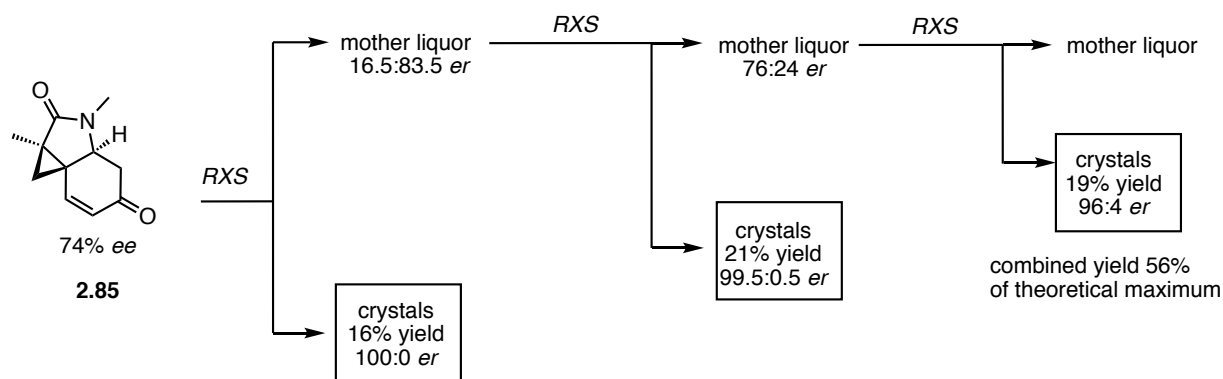
We next attempted the key aerobic dehydrogenation. We were pleased to see that the reaction of ketone **2.86** with 5 mol% of Pd(TFA)<sub>2</sub>, and 10 mol% DMSO in AcOH under an atmosphere of oxygen at 55 °C for 5 days proceeded with excellent regioselectivity, forming the less-substituted enone **2.85** exclusively in 76% yield (Scheme 2-22). Over the course of the reaction it was necessary to add additional catalyst to drive the conversion to completion. In contrast to earlier work in the racemic synthesis, which employed an additional 2 x 10 mol% of

the Pd(TFA)<sub>2</sub> catalyst, we found that the loading of the additional palladium complex could be decreased to 2 x 2.5 mol%.

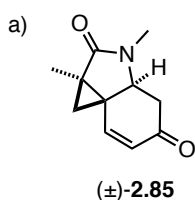


**Scheme 2-22** Pd(II)-mediated aerobic oxidation of ketone **2.86** to enone **2.85**

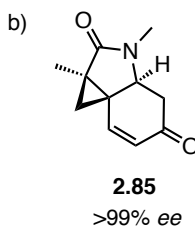
After generating an enantiomeric excess by a partially selective synthesis, the preferential crystallization of the major enantiomer from a supersaturated solution can be exploited to obtain enantiomerically enriched material.<sup>50</sup> Enone **2.85** was obtained as a crystalline solid and we were delighted to discover that it proved highly suitable for further enantiomeric enrichment via preferential crystallization of the major enantiomer to provide tricycle **2.85** in high enantiomeric purity (up to >99.5:0.5 *er* by chiral SFC analysis). A typical enrichment protocol is outlined in Figure 2-11. A crystalline sample of enone **2.85** was dissolved in a 15:1 solution of boiling MTBE/1,2-DCE. The solution was cooled to room temperature, treated with a seed crystal and allowed to stand at -20 °C overnight during which time white needle shaped crystals of the excess enantiomer formed. The mother liquor was removed and the crystals washed with MTBE, dried and analyzed by chiral SFC to determine the enantiomeric purity of the crystallized material. The chromatogram of the racemic compound (±)-**2.85** was used as a standard for comparison. After three rounds of crystallization the excess enantiomer of enone **2.85** was obtained in a combined yield of 56% of the theoretical maximum yield. Representative chromatograms are depicted in Figure 2-11 showing the racemic standard, and enone **2.85** after enantiomeric enrichment by crystallization.



recrystallization conditions: 15: 1 boiling MTBE/DCE, seed crystal, -20 °C, overnight



Chiralpak IC column (250 x 10 mm), gradient elution: 1-30% *i*-PrOH (rate 1.0), 5.5 mL/min, 254 nm, P=100 (BAR)



Chiralpak IC column (250 x 10 mm), gradient elution: 1-30% *i*-PrOH (rate 1.0), 5.5 mL/min, 254 nm, P=100 (BAR)

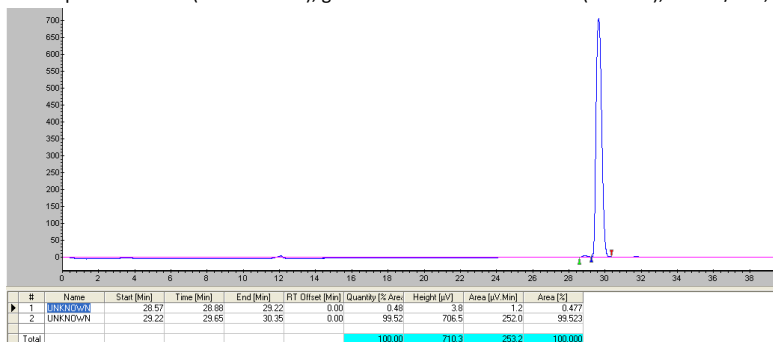


**Figure 2-11** Enantiomeric enrichment by recrystallization to upgrade the *er* of tricycle **2.85** and SFC chromatograms of the a) racemic standard and b) enantioenriched enone **2.85**

## 2.2.8 Studies of Furanyl Lithium Additions to Enones

The next challenge of the synthesis was to perform a chemoselective addition of a furanyl amino methyl lithium reagent to an enone (Figure 2-12). During the racemic synthesis, this reaction suffered from low yields and poor chemoselectivity due to the formation of an undesired byproduct, which was tentatively identified as the bis-adduct by LCMS resulting from the addition of a second equivalent of organolithium reagent to the amide.

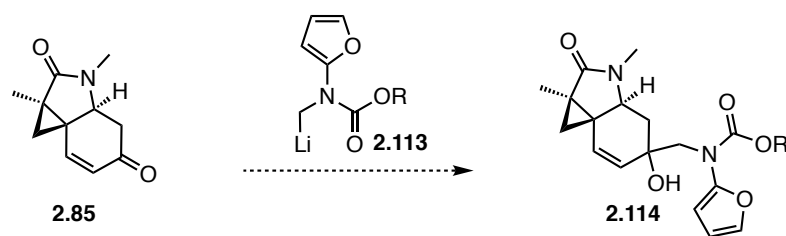


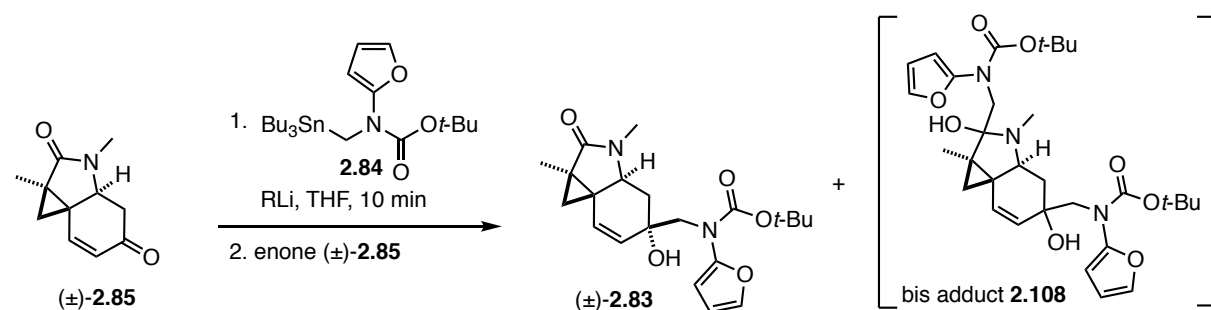
Figure 2-12 Requisite enone 1,2-addition

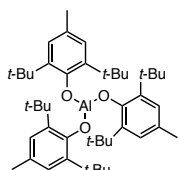
To address this chemoselectivity problem, we first attempted to optimize the addition reaction by varying the additive, base and metal (Table 2-3). The addition of TMEDA afforded the desired allylic alcohol ( $\pm$ )-**2.83**, albeit in a low yield of 20% (Table 2-3, Entry 1). Disappointingly, recovered starting material was obtained when  $\text{CeCl}_3$  was used as an additive (Table 2-3, Entry 2). We next investigated the use of the Lewis acid ATD **2.115** as an additive in the reaction (Table 2-3, Entry 3).<sup>105</sup> We reasoned that the bulky Lewis acid would preferentially coordinate the more Lewis basic amide carbonyl, blocking the addition of the organolithium to the amide and thus directing the attack to the enone. Unfortunately, this reaction was not chemoselective and low yielding. An attempt to transmetallate the furanyllithium reagent to the corresponding titanium reagent prior to ketone addition also failed, delivering recovered starting material (Table 2-3, Entry 4). Shifting focus, we next screened different bases while reasoning



that the steric and electronic properties of the base may influence the chemoselectivity of the addition if a tin-ate complex formed during the transmetallation reaction. No reaction occurred when PhLi was used as the base (Table 2-3, Entry 5). Transmetallation with *s*-BuLi followed by enone addition led to the bis-adduct exclusively by LCMS (Table, 2-3, Entry 6). Lastly, the use of 1-hexynyl lithium at -40 °C resulted in acetylide addition to the enone (Table 2-3, Entry 7).

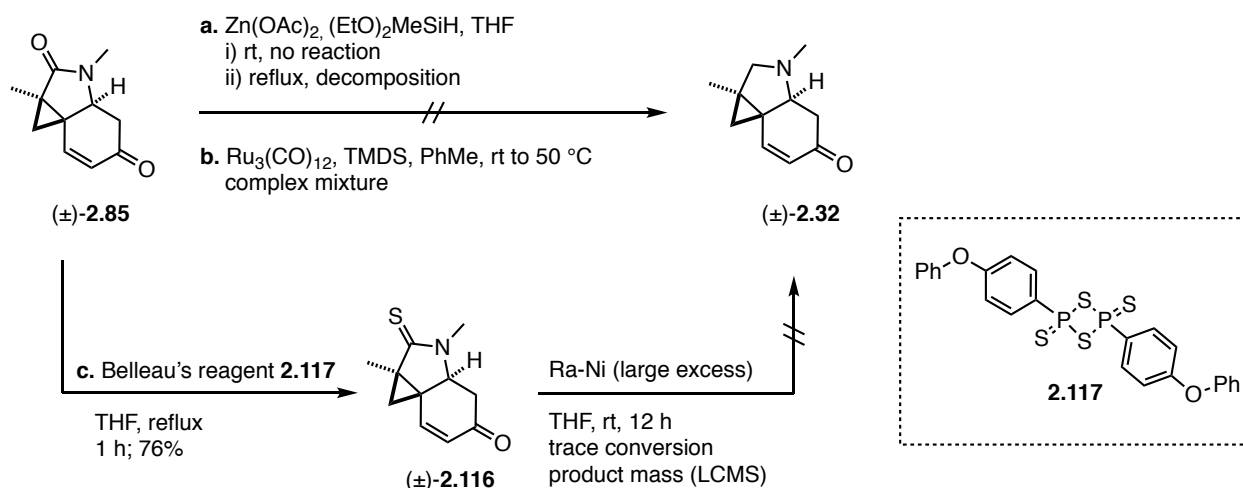
**Table 2-3** Enone 1,2-Addition: Metal, Organolithium Reagent and Additive Screen



Entry	R <sub>1</sub> Li	Eq.	Additive	T (°C)	Time	Yield
1	<i>n</i> -BuLi	1.3	TMEDA (1.3 eq)	-90	10 min	20% (±)- <b>2.83</b>
2	<i>n</i> -BuLi	1.3	CeCl <sub>3</sub> (1.1 eq) <sup>a</sup>	-90	1.5 h	RSM (±)- <b>2.85</b>
3	<i>n</i> -BuLi	1.5	 <b>2.115</b> (1.5 eq) <sup>b</sup>	-90	5 min	25% (±)- <b>2.83</b> + bis adduct <b>2.108</b>
4	<i>n</i> -BuLi	1.5	Ti( <i>i</i> -PrO) <sub>3</sub> Cl (3 eq) <sup>c</sup>	-78 to -40	10 min	RSM (±)- <b>2.85</b>
5	PhLi	1.5	-	-90	5 min	RSM (±)- <b>2.85</b>
6	<i>s</i> -BuLi	1.5	-	-90	5 min	bis-adduct <b>2.108</b> (LCMS)
7	1-hexynyl lithium	1.5	-	-40	5 min	1-hexynyl lithium addition to enone

<sup>a</sup>the enone was added to a solution of CeCl<sub>3</sub> in THF and stirred for 30 min before the resulting mixture was cooled to -90 °C and treated with the furanyl lithium reagent by cannula transfer; <sup>b</sup>the ATD prepared as a 0.25 M solution in 9:1 PhMe/THF; <sup>c</sup>after Ti addition the resulting solution was stirred for 40 min for transmetallation prior to the addition of the enone.

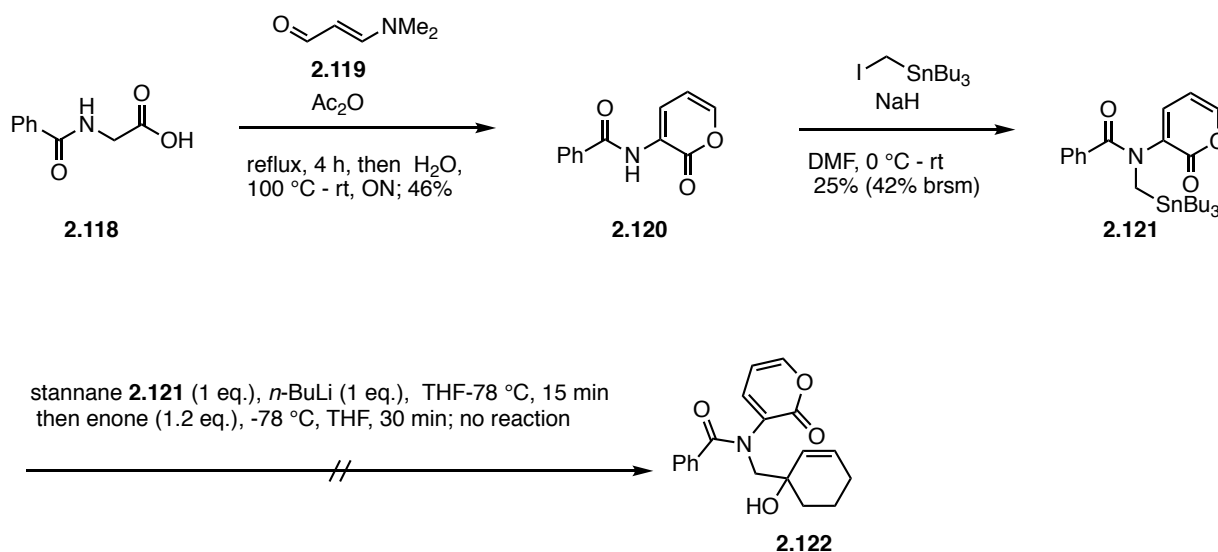
We next attempted to reduce the tertiary amide prior to the addition step. To this end, direct reduction of the tertiary amide was attempted using Beller's conditions (Scheme 2-23a).<sup>106</sup> Unfortunately, when amide ( $\pm$ )-**2.85** was treated with  $\text{Zn}(\text{OAc})_2$  and  $(\text{EtO})_2\text{MeSiH}$  in THF at room temperature, no reaction occurred. An attempt to force the reaction at reflux in THF resulted in decomposition. Reduction with  $\text{Ru}_3(\text{CO})_{12}$  and 1,1,3,3-tetramethyldisiloxane (TMDS) gave a complex mixture of products in which reduction of the olefin was evident (Scheme 2-23b).<sup>107</sup> Using a stepwise strategy, enone ( $\pm$ )-**2.85** was converted into the thioamide ( $\pm$ )-**2.116** using Belleau's reagent **2.117** in 76% yield (Scheme 2-23c). Unfortunately, a chemoselective reduction of the thioamide with Ra-Ni only delivered trace amine by LCMS ( $\pm$ )-**2.32**.



**Scheme 2-23** Attempts to chemoselectively reduce an amide in the presence of an enone

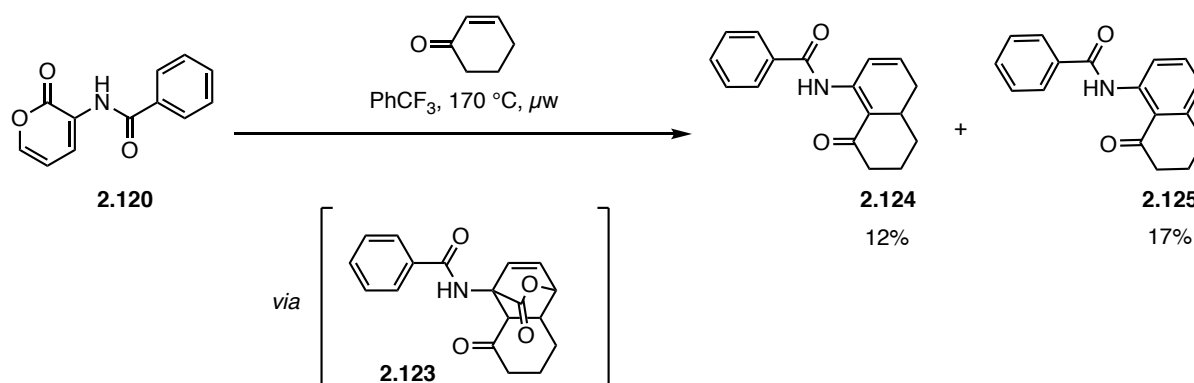
Given the poor results obtained thus far with the enone 1,2-addition of a furanyl aminomethyl lithium reagent and the low yields in the subsequent Diels-Alder reaction, we next investigated pyrone **2.121** as a heterocyclic replacement for the furan moiety. We hoped that the pyrone aminomethyl lithium reagent would lead to a more chemoselective enone 1,2-addition and a higher yielding IMDAF cycloaddition, facilitated by the extrusion of  $\text{CO}_2$ . The synthesis of

the pyrone reagent began with the reaction of hippuric acid with the 3-amino acrolein **2.119** to deliver pyrone **2.120** in 46% yield (Scheme 2-24). The pyrone **2.120** was deprotonated with NaH then treated with tributyl(iodomethyl)stannane to form stannane **2.121** in modest yield. Unfortunately, when stannane **2.121** was subjected to the Sn-Li exchange/enone 1,2-addition sequence, no product **2.122** was obtained and decomposition of the pyrone reagent was observed under the reaction conditions.



**Scheme 2-24** Synthesis of pyrone **2.121** and attempted enone 1,2-addition

An intramolecular variant of this reaction was also attempted. When pyrone **2.120** was reacted with cyclohexenone under microwave irradiation at  $170^\circ\text{C}$ , enone **2.124** was formed in 12% yield along with the protected aniline **2.125** in 17% yield (Scheme 2-25). Product **2.124** was likely formed by a ring opening reaction of the initial Diels-Alder Adduct **2.123** followed by elimination and double bond isomerization into conjugation with the enone. The amide **2.125** was probably formed from **2.124** by elimination to form the aromatized product. While these results were promising, the low yield and the need for further synthetic conversions to access the desired indole led us to explore alternative routes.



**Scheme 2-25** Intermolecular Diels-Alder reaction of pyrone **2.120** and cyclohexenone

We next attempted to mask the enone by the conjugate addition of a thiol (Figure 2-13). We reasoned that the resulting ketone **2.126** would be more electrophilic than the enone precursor, leading to greater electronic differentiation and better chemoselectivity for the ketone over the amide in the 1,2-addition reaction.

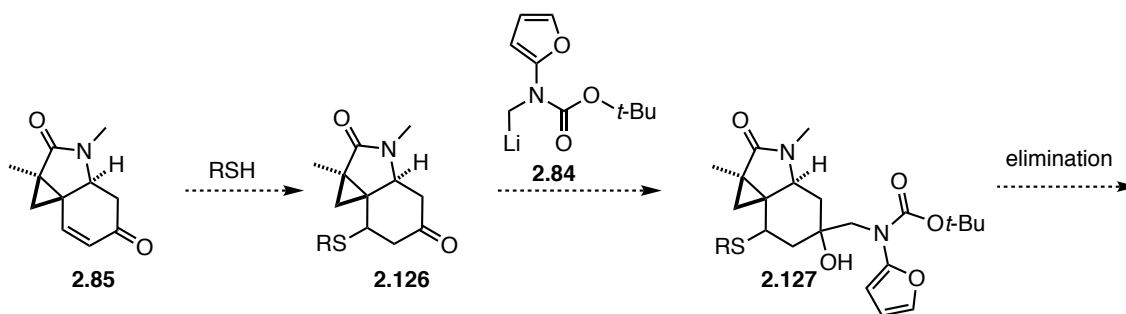
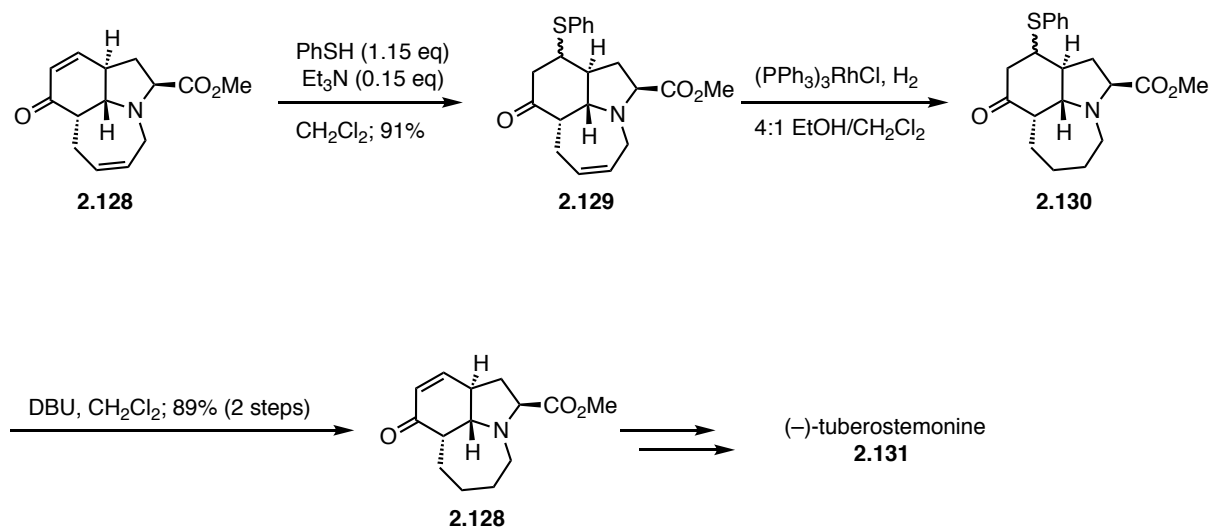


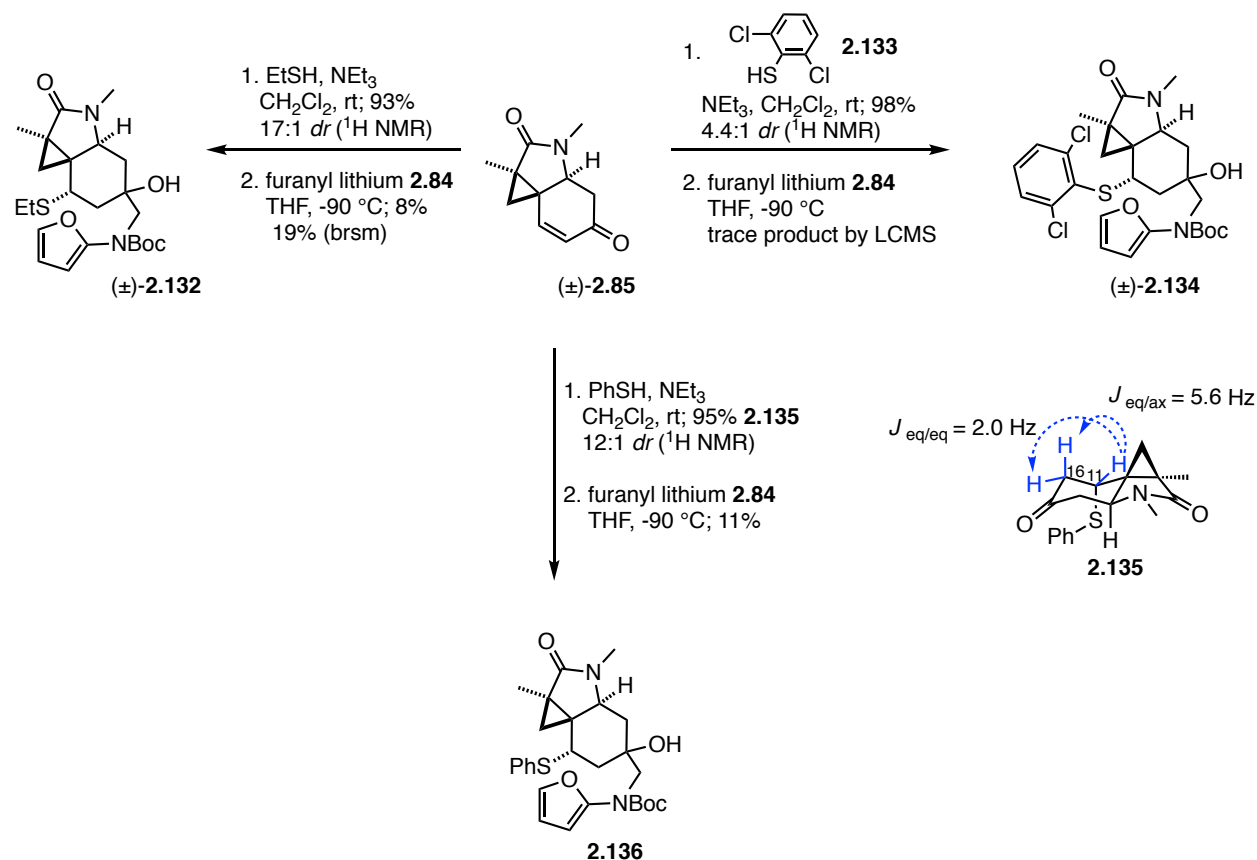
**Figure 2-13** Thiol addition/elimination strategy to mask the enone and facilitate a 1,2-addition reaction

The Wipf group has successfully employed a similar strategy in the total synthesis of the natural product (–)-tuberostemonine (Scheme 2-26).<sup>108,109</sup> They found that the conjugate addition of thiophenol to enone **2.128** proceeded smoothly when the reaction was performed in the presence of a catalytic amount of  $\text{Et}_3\text{N}$  (0.15 eq). After olefin reduction, the enone was regenerated by a DBU-mediated thiol elimination to afford tricycle **2.128**.<sup>110</sup>



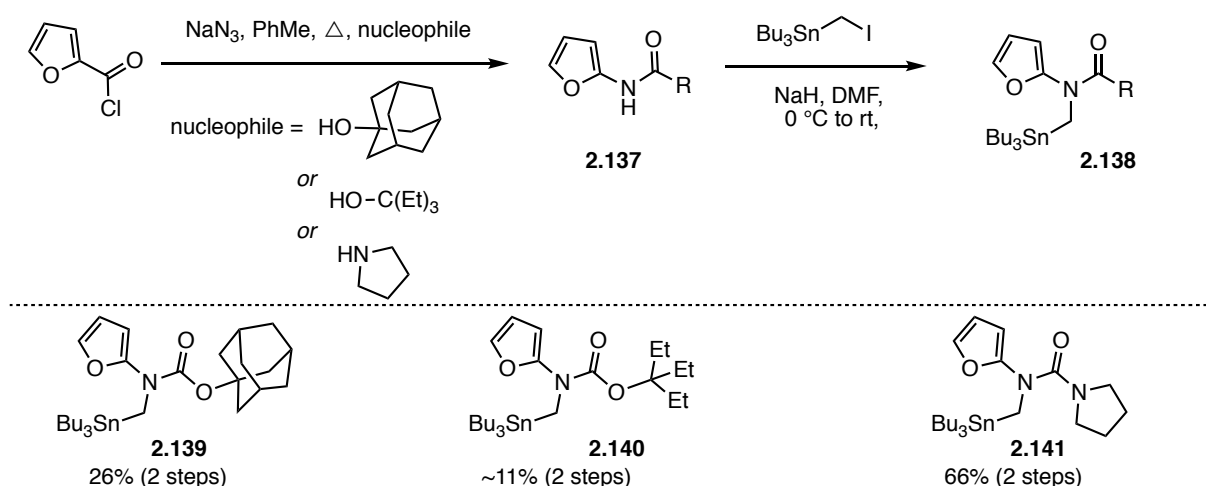
**Scheme 2-26** Enone protection by a thiol addition/elimination strategy in Wipf's synthesis of (-)-tuberostemonine

Using this protocol, we synthesized several thiol derivatives in high yield. The relative stereochemistry of the intermediate thiols was assigned by analysis of vicinal coupling constants (Scheme 2-27). For example, the major diastereomer **2.135** from the conjugate addition of thiophenol to enone **2.85** exhibited coupling constants of  $J = 5.6$  and  $2.0$  Hz between the C11 methine and adjacent C16 axial and equatorial protons, indicating the C11 methine had an equatorial orientation. The minor diastereomer showed a coupling constant of  $J = 13.2$  Hz between the minor C11 axial methine and adjacent C16 axial proton and a coupling constant of  $J = 4.0$  Hz between the C11 axial methine and adjacent C16 equatorial proton. Unfortunately, the subsequent addition reaction with the organolithium reagents afforded the addition adducts **2.132**, **2.134** and **2.136** in low yields ranging from trace conversion to 11% yield at best.



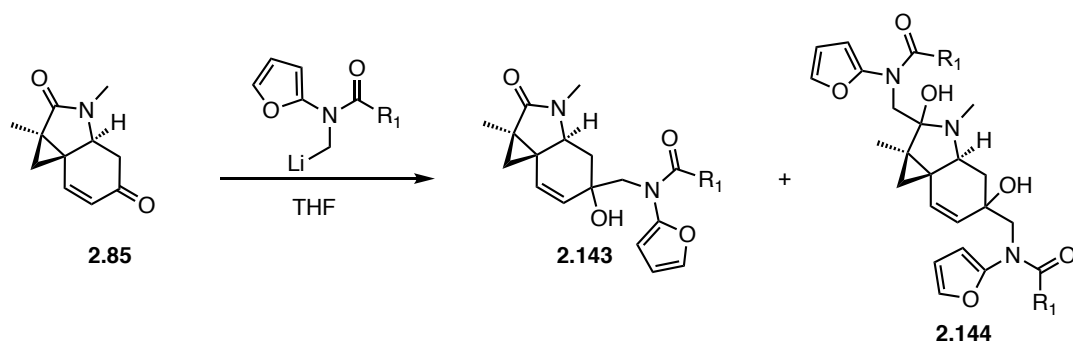
**Scheme 2-27** Thiol conjugate addition, ketone 1,2-addition

We next surveyed different organolithium reagents, exchanging the Boc-group for other sterically demanding carbamate protecting groups and a urea derivative. The stannane reagents **2.139-2.141** were prepared from 2-furoyl chloride *via* a Curtius rearrangement followed by *N*-alkylation (Scheme 2-28). The adamantyl and triethyl carbamates proved low yielding and were characterized by <sup>1</sup>H NMR and screened directly in the addition step without further characterization. The pyrrolidine urea was isolated in high yields of 66% over two steps.



**Scheme 2-28** Synthesis of stannanes **2.139-2.141** via a Curtius rearrangement/ alkylation sequence

The stannanes were then evaluated in the transmetalation/1,2-addition to enone **2.85** (Table 2-4). When enone **2.85** was reacted with excess *N*-adamantanyl organolithium reagent, the desired allylic alcohol was formed in low yield along with recovered starting material and trace bis-addition product by LCMS (Table 2-4, Entry 1). Unfortunately, when the crude alcohol was subjected to a thermal IMDAF cyclization, the reaction proceeded with only trace conversion. Disappointingly, the triethylcarbamate derivative was not chemoselective (Table 2-4, Entry 2). We also evaluated a pyrrolidine urea-based protecting group. The 1,2-addition of this furanyl lithium reagent afforded the allylic alcohol, albeit in a low yield of 6% (Table 2-4, Entry 3). Further investigation of this reaction using cyclohexenone as a model system showed that the reagent was unstable and was prone to protodestannylation and demethylation side reactions. We reasoned that the instability of the pyrrolidine urea furanyl lithium was due to  $\alpha$ -lithiation on the pyrrolidine ring, which could facilitate reagent decomposition.

**Table 2-4** Enone 1,2-Addition: Amine Protecting Group Screen

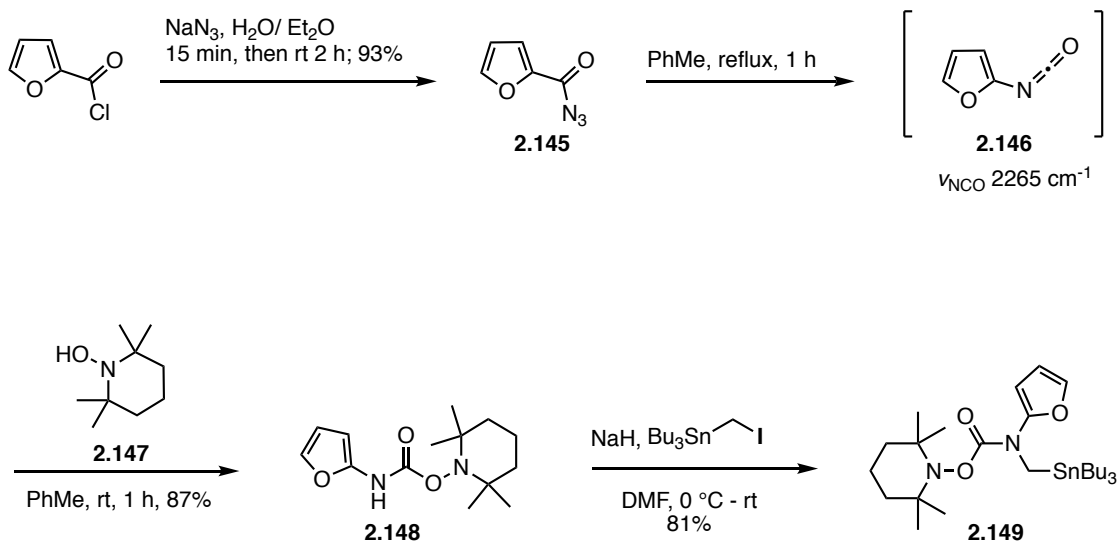
Entry	R <sup>1</sup>	R <sup>1</sup> -M (eq)	T (° C)	Time (min)	Product ratio	Yield
1		1.9	-78	30	<b>2.143</b> and <i>epi</i> - <b>2.143</b> + trace <b>2.144</b> and <i>epi</i> - <b>2.144</b> + SM	50% <sup>a,b</sup>
2		1.2	-90	20	~ 1:1 ( <b>2.143</b> + <i>epi</i> - <b>2.143</b> : <b>2.144</b> + <i>epi</i> - <b>2.144</b> ) <sup>a</sup>	ND <sup>a,b</sup>
3		2	-90	20	<b>2.143</b> + SM	6%

<sup>a</sup>product distribution based on LCMS trace; <sup>b</sup>no reaction or trace conversion in the IMDAF reaction

Hoping to avoid reagent degradation, a novel TEMPO-carbamate (TEMPOC) **2.149** was developed (Scheme 2-29). We anticipated that the tetramethyl substitution pattern at the  $\alpha$ -position of the piperidine ring would result in a more stable furanyllithium reagent. Additionally, we hoped that employing a TEMPO moiety instead of a tetramethylpiperidine ring would avoid severe steric hindrance that could lead to sluggish reactivity in the latter organolithium reagent. The TEMPO carbamate was synthesized according to the sequence outlined in Scheme 2-29. 2-Furoyl chloride was reacted with NaN<sub>3</sub> in H<sub>2</sub>O/Et<sub>2</sub>O to form the known acyl azide **2.145**.<sup>111</sup> Heating acyl azide **2.145** in toluene at reflux for 1 h promoted a Curtius rearrangement to afford the intermediate isocyanate **2.146**. IR analysis showed full conversion to the isocyanate as

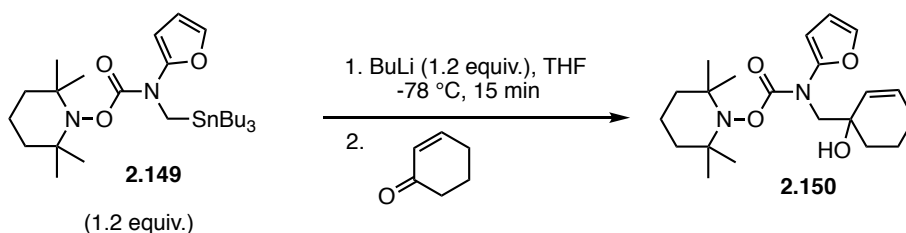


evidenced by the characteristic isocyanate stretching frequency at  $2265\text{ cm}^{-1}$ . The isocyanate was cooled to room temperature and quenched with the reduced TEMPO hydroxylamine **2.147** to give the desired carbamate **2.148** in 87% yield. The protected furan **2.148** was deprotonated by NaH at  $0\text{ }^{\circ}\text{C}$  and treated with tributyl(iodomethyl)stannane to afford the *N*-alkylation product **2.149** in 81% yield.



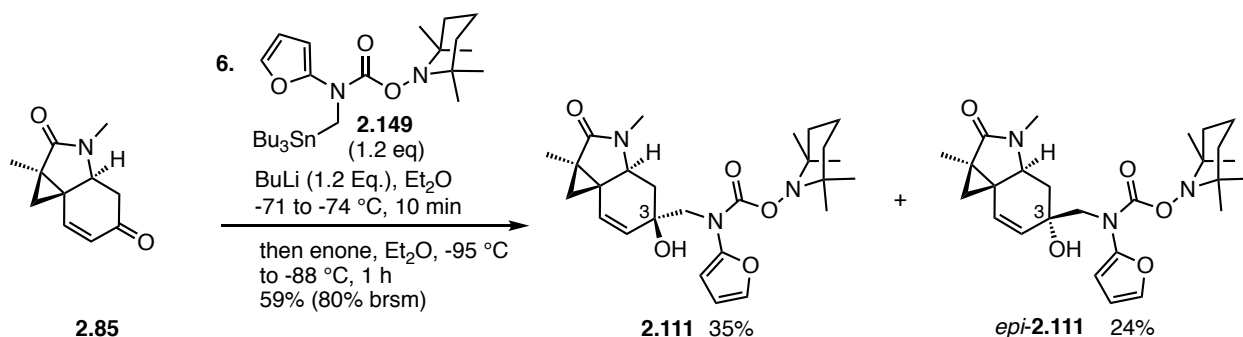
**Scheme 2-29** Synthesis of stannane **2.149**

With the key stannane **2.149** in hand, we tested the transmetallation/enone 1,2-addition sequence on cyclohexenone as a model system (Table 2-5). We were pleased to see that stannane **2.149** underwent facile transmetallation when treated with *n*-BuLi at  $-78\text{ }^{\circ}\text{C}$ . The addition of neat cyclohexenone delivered the expected allylic alcohol **2.150** in 88% yield (Table 2-5, Entry 1). When cyclohexenone was added to the furanyllithium species at even lower temperatures of  $-90\text{ }^{\circ}\text{C}$  for 30 min, the reaction proceeded smoothly to deliver the allylic alcohol **2.150** in a comparable yield of 89% (Table 2-5, Entry 2).

**Table 2-5** Transmetallation/Addition of TEMPO-carbamate **2.149** on a Model System

Entry	Conditions	Yield
1	-78 °C, 30 min	88%
2	-90 °C, 30 min	89%

Using these optimized conditions, we next attempted the Sn/Li transmetallation and subsequent 1,2-addition sequence on the enantioenriched enone **2.85** (Scheme 2-30). A thermocouple thermometer was employed to continuously monitor the internal temperature of the reaction. A solution of stannane **2.149** in Et<sub>2</sub>O was cooled to -71 °C, treated with *n*-BuLi and stirred for 10 min to facilitate transmetallation. The resulting furanyllithium intermediate was then cooled to -94 °C and treated with enone **2.85** to afford allylic alcohols **2.111** and *epi*-**2.111** as separable diastereomers in 1.5:1 *dr* and 59% yield (80% brsm). We found that performing the reaction at these low temperatures led to a cleaner reaction profile and favoured the allylic alcohol **2.111**.

**Scheme 2-30** Transmetallation/addition sequence using the optimized TEMPO furanyllithium reagent

The relative configuration of the addition adducts **2.111** and *epi*-**2.111** were established through a combination of X-ray and NMR spectroscopy. The 1D-NOE spectra of the allylic alcohol diastereomers **2.111** and *epi*-**2.111** are shown in Figure 2-14. Selective irradiation of the ring junction methine H5 in the axial diastereomer **2.111** showed a key correlation to the H2/2' methylene, indicating these protons are located on the same face. In contrast, no correlation was observed between the ring junction methine H5 and the H2/2' methylene in the minor equatorial diastereomer *epi*-**2.111**, supporting the assignment.

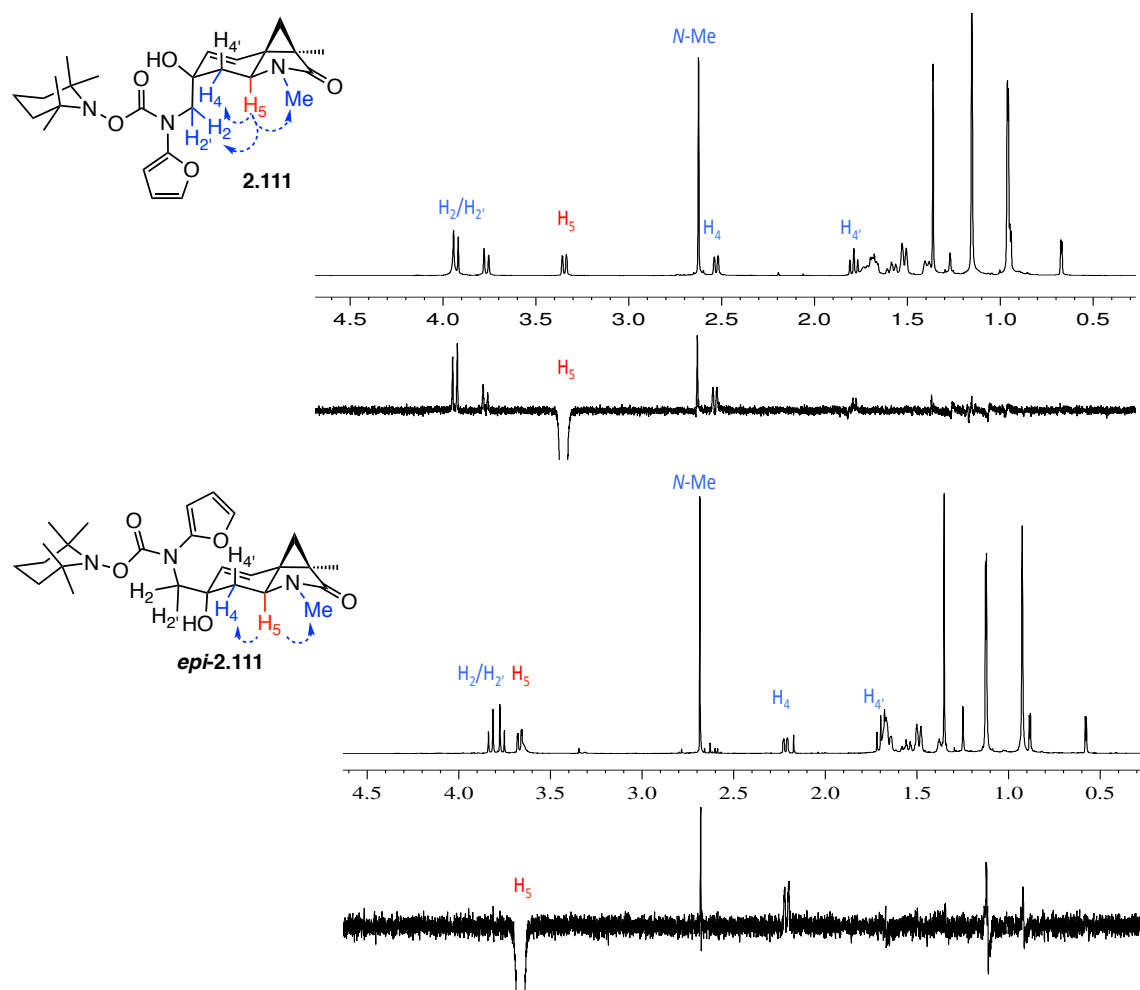


**Figure 2-14** Key 1D-NOE correlations for the allylic alcohol diastereomers

2D ROESY correlations also supported the assignment of the two diastereomers. Key features of the 2D ROESY spectra of both diastereomers are shown in Figure 2-15. In the spectrum of the major diastereomer **2.111**, there is a cross peak correlation between the ring junction methine H5 and the H2/2' methylene was observed. This correlation is absent in the minor diastereomer *epi*-**2.111**.

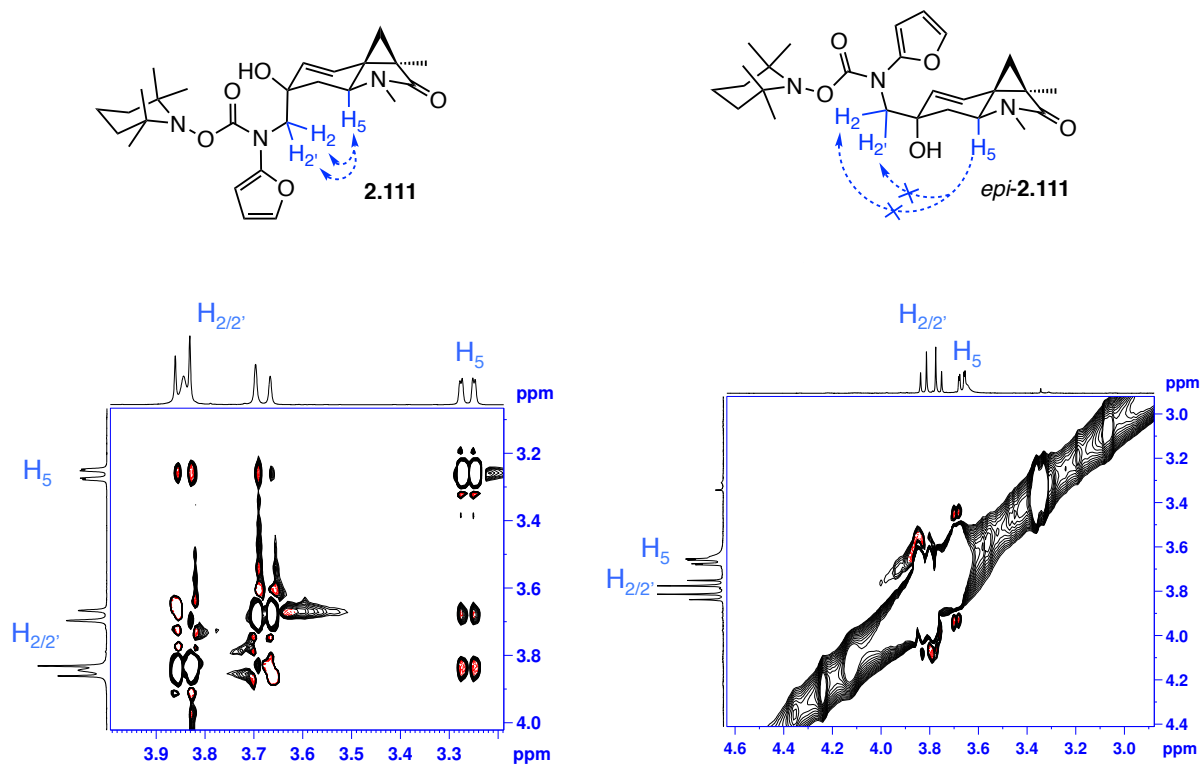


**Figure 2-15** Key ROESY correlations for allylic alcohol diastereomers **2.111** and *epi*-**2.111**

In addition to the 1D-NOE and 2D-ROESY data, the relative configuration and structure of the major diastereomer **2.111** was unambiguously confirmed by X-ray analysis of a single crystal (Figure 2-16).

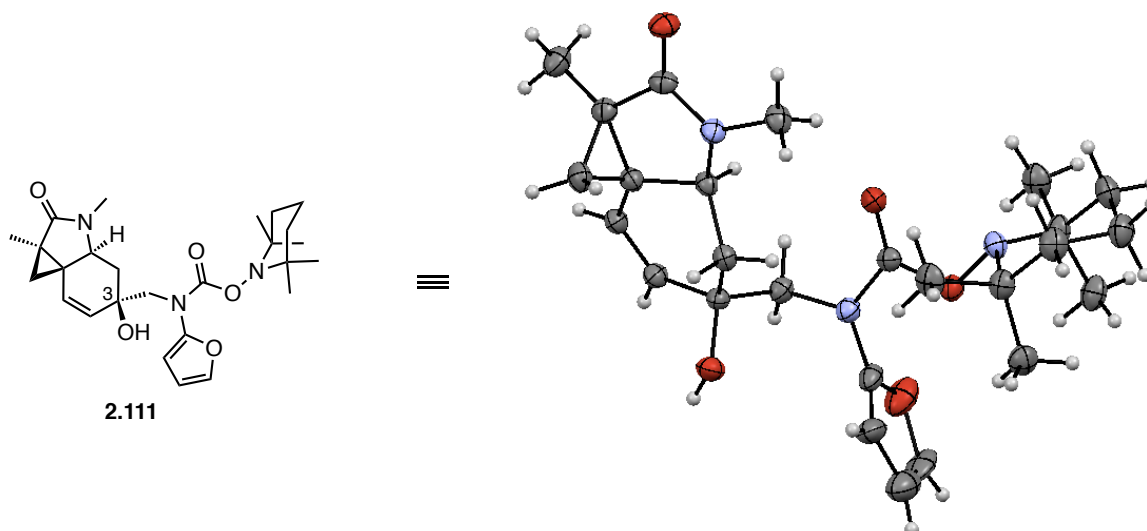


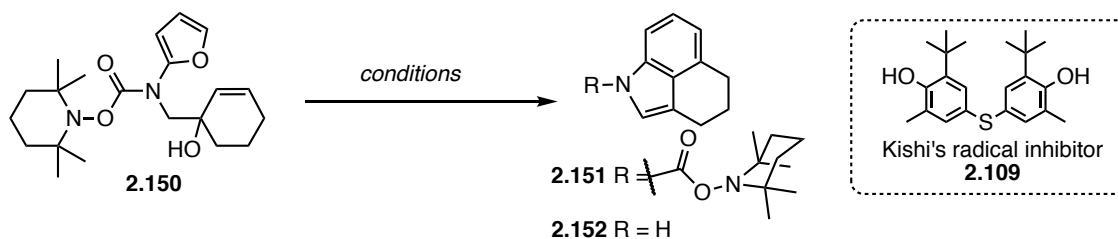
**Figure 2-16** X-ray structure of the major diastereomer **2.111**

### 2.2.9 IMDAF Reaction and Completion of the Synthesis

The last challenge of the synthesis was to carry out an IMDAF cycloaddition to form the indole. This reaction was first investigated using allylic alcohol **2.150** as a model system to test whether the new TEMPOC protecting group was compatible with the IMDAF reaction conditions. The reaction failed under Lewis acidic conditions (Table 2-6, Entry 4) and no reaction occurred when the allylic alcohol **2.150** was subjected to microwave irradiation in trifluorotoluene in the presence of Kishi's radical inhibitor **2.109** at temperatures below 140 °C (Table 2-6, Entry 1). However, at 140 °C, in the presence of radical inhibitor **2.109**, trace consumption of **2.150** was observed (Table 2-6, Entry 2) and we were encouraged that increasing the temperature to 160 °C led to full consumption of the starting material and the appearance of possible intermediates by LCMS (Table 2-6, Entry 3). Moving to conventional thermal heating we next investigated different solvent effects. While reaction at 130 °C in chlorobenzene (Table 2-6, Entry 9) led to decomposition, several other aromatic solvents were found to promote the

IMDAF cyclization. The reaction proceeded with full conversion by  $^1\text{H}$  NMR when carried out in mesitylene, xylenes and toluene (Table 2-6, Entries 10, 8 & 7). Conventional heating in toluene at 130 °C in a sealed tube were the most effective conditions, affording the protected indole **2.151** in 51% isolated yield (Table 2-6, Entry 7). We also found that the presence of substoichiometric  $\text{Pd}(\text{PPh}_3)_4$  and  $\text{P}(\text{O}i\text{-Pr})_3$  promoted the cycloaddition (Table 2-6, Entries 5 & 6) in low yields, possibly through the intermediacy of a putative  $\pi$ -allyl palladium complex. When the reaction mixture was heated for 37 h (Table 2-6, Entry 6), the protecting-group-free indole **2.152** was obtained in 40%.

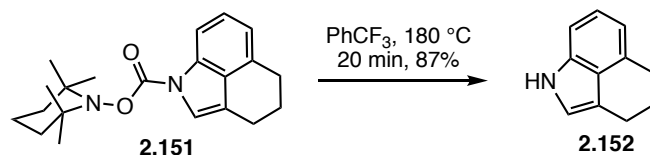
**Table 2-6** Optimization of the IMDAF Cyclization on a Model System



Entry	Solvent	Additive	$\Delta$	T (°C)	Time	Yield
1	$\text{PhCF}_3$	<b>2.109</b>	$\mu\text{W}$	120	0.5 h	NR
2	$\text{PhCF}_3$	<b>2.109</b>	$\mu\text{W}$	140	0.5 h	SM (major), trace intermediates <sup>a</sup>
3	$\text{PhCF}_3$	<b>2.109</b>	$\mu\text{W}$	160	0.5 h	Intermediates <sup>a,b</sup>
4	$\text{PhMe}$	$\text{BF}_3 \cdot \text{OEt}_2$	-	-30	5 min	0
5	NMP	$\text{Pd}(\text{PPh}_3)_4$ (10mol%), $\text{P}(\text{O}i\text{-Pr})_3$ (20 mol%)	$\mu\text{w}$	130	2 h	~ 15% 1:1 <b>2.151</b> : <b>2.152</b> (25% brsm)
6	NMP	$\text{Pd}(\text{PPh}_3)_4$ (5 mol%), $\text{P}(\text{O}i\text{-Pr})_3$ (20 mol%)	$c^c$	120- 130	37 h	40% <b>2.152</b>
7	$\text{PhMe}$	-	$c^c$	130	10 d	51% <sup>c</sup> <b>2.151</b>
8	Xylenes	-	$c^c$	140	4 d	ND <sup>d</sup>
9	$\text{C}_6\text{H}_5\text{Cl}$	-	$c^c$	130	4 d	0 <sup>b</sup>
10	Mesitylene	-	$c^c$	130	4 d	28% <sup>d</sup>

<sup>a</sup>observed in LCMS trace; <sup>b</sup>decomposition; <sup>c</sup>conventional heating in an oil bath; <sup>d</sup>full conversion by  $^1\text{H}$  NMR.

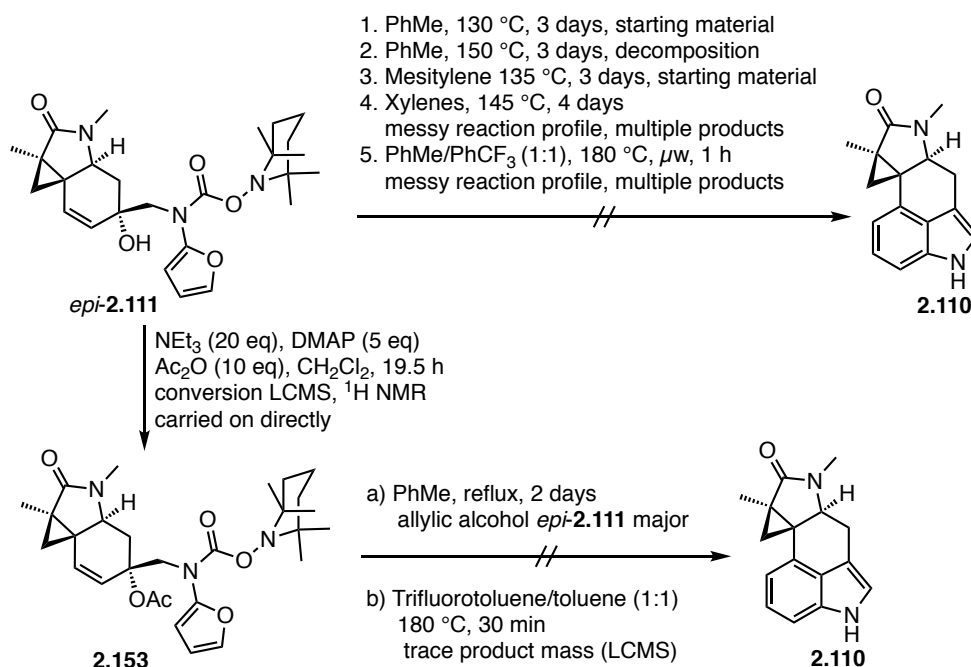
The protected indole **2.151** was converted to the free indole **2.152** by a thermal cleavage of the TEMPO carbamate-protecting group (Scheme 2-31). We found that the thermolysis proceeded smoothly at an elevated temperature of 180 °C in trifluorotoluene under microwave irradiation for 20 min to provide the protecting group free indole **2.152** in 87% yield on small scale.



**Scheme 2-31** Thermal deprotection of TEMPOC-protected indole **2.151**

Given the success with the model system, we next attempted the IMDAF reaction on the allylic alcohol diastereomers **2.111** and *epi*-**2.111**. Disappointingly, when the equatorial diastereomer *epi*-**2.111** was heated at 130 °C in toluene for 3 days, only starting material was observed (Scheme 2-32). Unfortunately, an attempt to force the conversion of *epi*-**2.111** to indole **2.110** at higher temperatures of 150 °C for 3 days failed and decomposition was noted. Several additional aromatic solvents were also evaluated without success. For example when alcohol *epi*-**2.111** was heated in mesitylene at 135 °C for 3 days only starting material was observed. Both the reaction of the allylic alcohol in xylenes at 145 °C for 4 days and in a solution of PhMe/PhCF<sub>3</sub> under microwave irradiation at 180 °C for 1 h led to multiple unidentified products. We also pursued a different strategy where alcohol *epi*-**2.111** was treated with NEt<sub>3</sub>, DMAP and Ac<sub>2</sub>O in CH<sub>2</sub>Cl<sub>2</sub>. The corresponding acetate **2.153** was detected by LCMS and <sup>1</sup>H NMR and taken up directly in toluene and heated at reflux for 2 days. Unfortunately the major product was consistent with the deprotected alcohol *epi*-**2.111** and attempts to convert this compound to

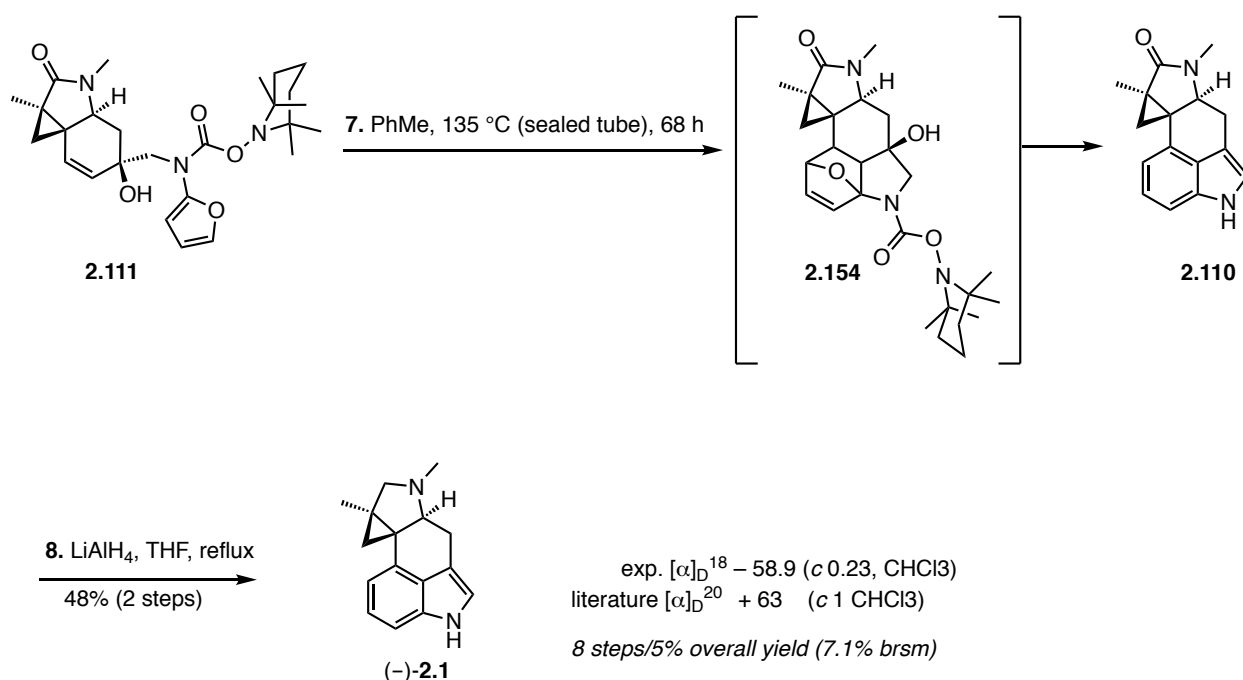
indole **2.110** in a 1:1 mixture of PhMe/PhCF<sub>3</sub> at 180 °C in the microwave only formed trace product mass by LCMS.



**Scheme 2-32** Attempts to convert the equatorial diastereomer *epi*-**2.111** into indole **2.110**

In contrast, we were delighted to see that the axial diastereomer **2.111** was more reactive and could be cleanly converted into to indole **2.110** when heated in a sealed tube for 68 h at 135 °C (external temperature) (Scheme 2-33). Fortuitously, the initial Diels-Alder adduct **2.154** underwent aromatization accompanied by the thermolysis of the TEMPOC protecting group under the reaction conditions to afford the protecting group free indole **2.110**. The tertiary amide **2.110** was then reduced with excess LiAlH<sub>4</sub> in refluxing THF to afford (–)-cycloclavine, (–)-**(2.1)**, in 48% over two steps. The specific rotation of the unnatural enantiomer was –58.9 (*c* 0.23, CHCl<sub>3</sub>), which was consistent in magnitude but opposite in sign to the literature value for the natural enantiomer, which was +63 (*c* 1, CHCl<sub>3</sub>). Overall, the synthesis of (–)-cycloclavine was accomplished in 8 steps and 5% (7.1% brsm) yield.

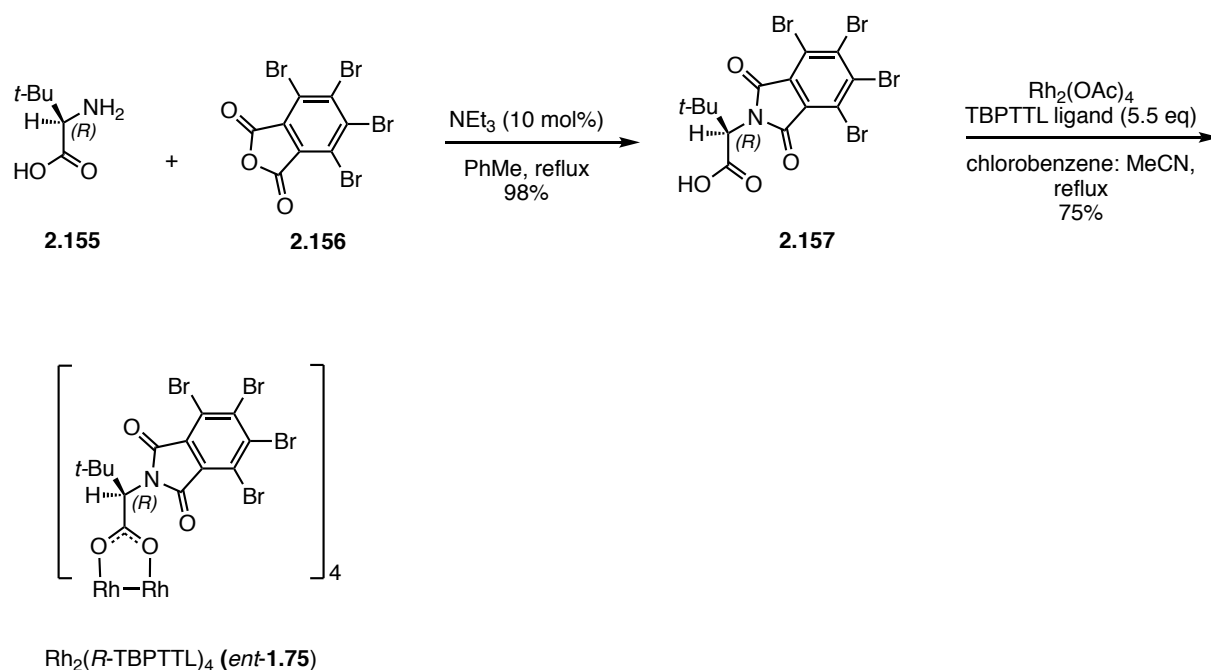




**Scheme 2-33** Completion of the synthesis of (-)-cycloclavine

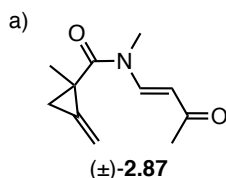
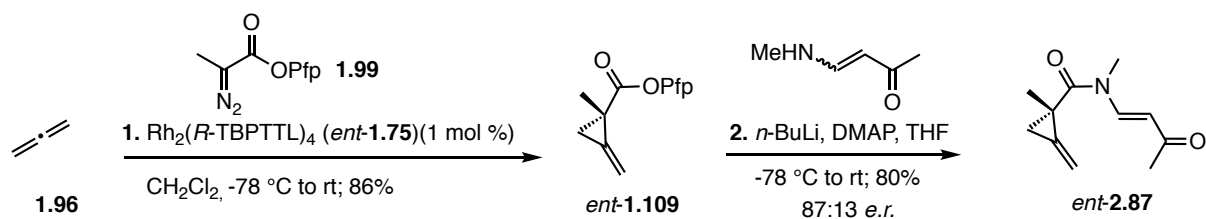
### 2.2.10 Synthesis of (+)-Cycloclavine

In order to synthesize the natural enantiomer, (+)-cycloclavine, we required the enantiomer of the catalyst  $\text{Rh}_2(\text{S-TBPTTL})_4$  (**1.75**). The dirhodium complex  $\text{Rh}_2(\text{R-TBPTTL})_4$  (*ent*-**1.75**) was prepared from *D-tert*-leucine using the route outlined in Scheme 2-34. *D-tert*-Leucine (**2.155**) reacted with tetrabromophthalic anhydride (**2.156**) and  $\text{NEt}_3$  (0.1 eq) in toluene at reflux to provide *N*-tetrabromophthaloyl-(*R*)-*tert*-leucine (TBPTTL) (**2.157**) in 98% crude yield. A ligand exchange reaction was then carried out by reacting  $\text{Rh}_2(\text{OAc})_4$  with excess TBPTTL ligand in a chlorobenzene/ $\text{CH}_3\text{CN}$  mixture at  $130^\circ\text{C}$  to form the dirhodium catalyst  $\text{Rh}_2(\text{R-TBPTTL})_4$  (*ent*-**1.75**) in 75% yield.

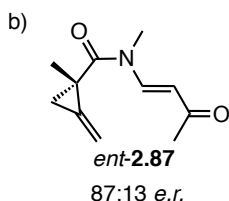
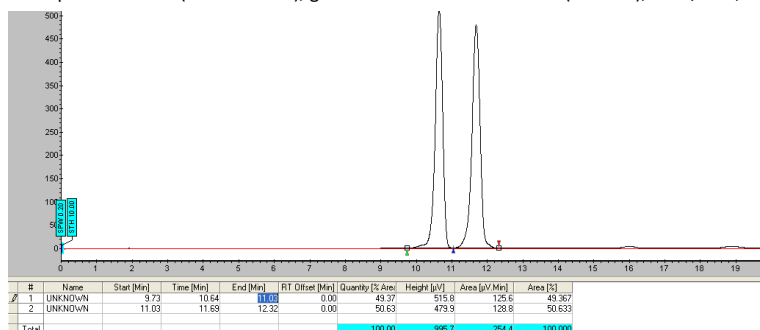


**Scheme 2-34** Synthesis of the dirhodium catalyst  $\text{Rh}_2(R\text{-TBPTTL})_4$

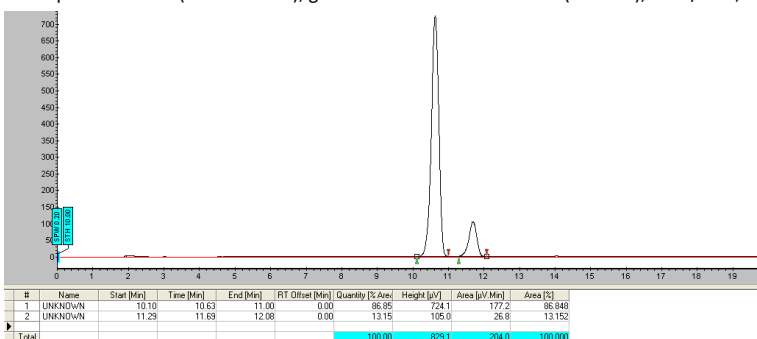
With the requisite catalyst in hand, the synthesis of (+)-(**2.1**) began with the cyclopropanation of allene **1.96** and diazopropanoate **1.99** in the presence of 1 mol% of the dirhodium catalyst  $\text{Rh}_2(R\text{-TBPTTL})_4$  (*ent*-**1.75**) to form the enantiomerically enriched methylenecyclopropane *ent*-**1.109** in 86% yield (Scheme 2-35). This reaction was successfully performed on scales up to 9.0 g. Ester aminolysis gave the vinylogous imide *ent*-**2.87** in 80% yield and 87:13 *er*. The SFC chromatograms for the racemic standard and enantiomerically enriched vinylogous amide are shown in Scheme 2-35. As expected, the opposite enantiomer was enriched when  $\text{Rh}_2(R\text{-TBPTTL})_4$  (*ent*-**1.75**) was employed as the catalyst in the cyclopropanation reaction.



Chiralpak IC column (250 x 10 mm), gradient elution 5-15% *i*-PrOH (rate 1.0), 7 mL/min, 245 nm, P = 100 (BAR)



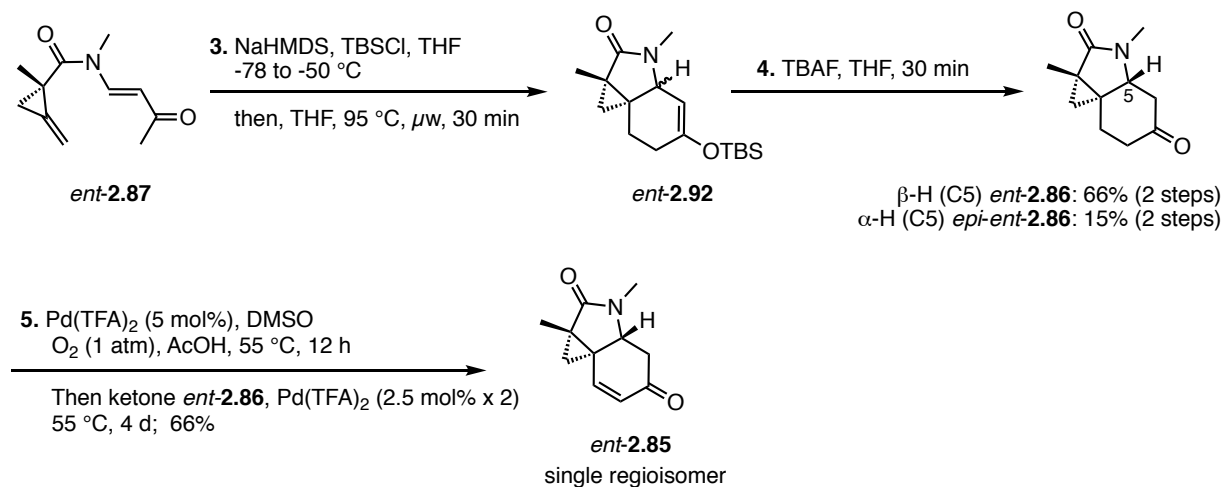
Chiralpak IC column (250 x 10 mm), gradient elution 5-15% *i*-PrOH (rate 1.0), 7 mL/min, 245 nm, P = 100 (BAR)



**Scheme 2-35** Synthesis of enantiomerically enriched vinyllogous amide (**ent-2.87**) and SFC chromatograms of the a) racemic standard and b) enantioenriched amide **2.87**

The vinyllogous imide **ent-2.87** was reacted with NaHMDS in THF between -78 and -50 °C to form the enolate which was trapped with TBSCl to form the corresponding TBS enol ether (Scheme 2-36). When heated at 95 °C in THF in the microwave, the enol ether underwent the intramolecular strain-promoted Diels-Alder reaction, followed by TBAF cleavage of the silyl enol ether to form the desired *trans*-adduct **ent-2.86** in 66% yield on gram scale along with the

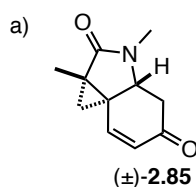
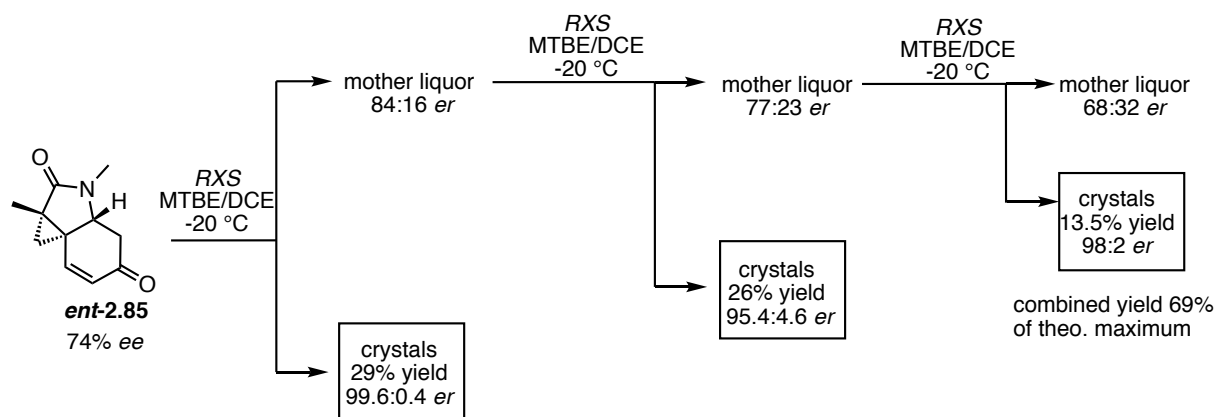
*cis*-adduct *epi-ent-2.86* in 15% yield. Dehydrogenation of ketone *ent-2.86* under modified Stahl conditions gave the corresponding enone **2.85** in 66% as a single regioisomer.



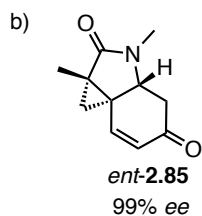
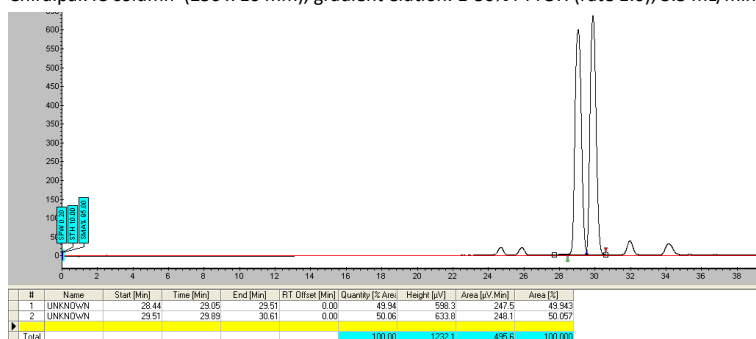
**Scheme 2-36** Synthesis of enantioenriched tricyclic enone *ent-2.85*

Enone **2.85** was obtained as a crystalline solid and we were pleased to see that the excess enantiomer could be enriched by recrystallization from 87:13 *er* to >99% *er* using the same protocol employed in the earlier synthesis of (–)-cycloclavine.

A typical enrichment procedure for ketone *ent-2.85* is outlined in Figure 2-17. Chiral SFC analysis was used to evaluate each batch for enantiomeric purity. For example, the first round of crystallization provided crystals of 99.5:0.5 *er*, the second recrystallization provided crystals of 91% *ee* and the third recrystallization provided crystals of 96% *ee*. Overall the combined yield was 69% of the theoretical maximum. Representative chromatograms are depicted in Figure 2-17, showing the racemic standard and enone *ent-2.85* after enantiomeric enrichment by crystallization.



Chiralpak IC column (250 x 10 mm), gradient elution: 1-30% *i*-PrOH (rate 1.0), 5.5 mL/min, 254 nm, P=100 (BAR)



Chiralpak IC column (250 x 10 mm), gradient elution: 1-30% *i*-PrOH (rate 1.0), 5.5 mL/min, 254 nm, P=100 (BAR)

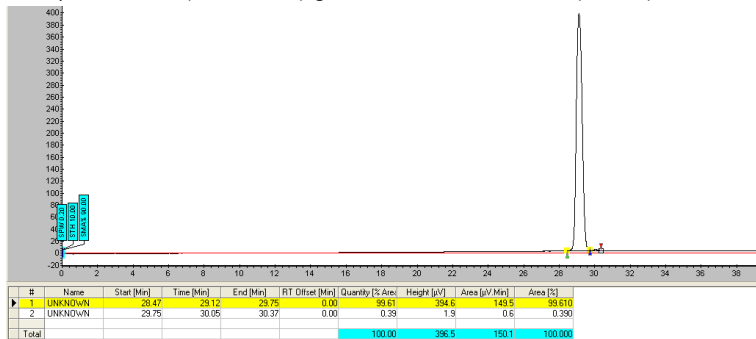
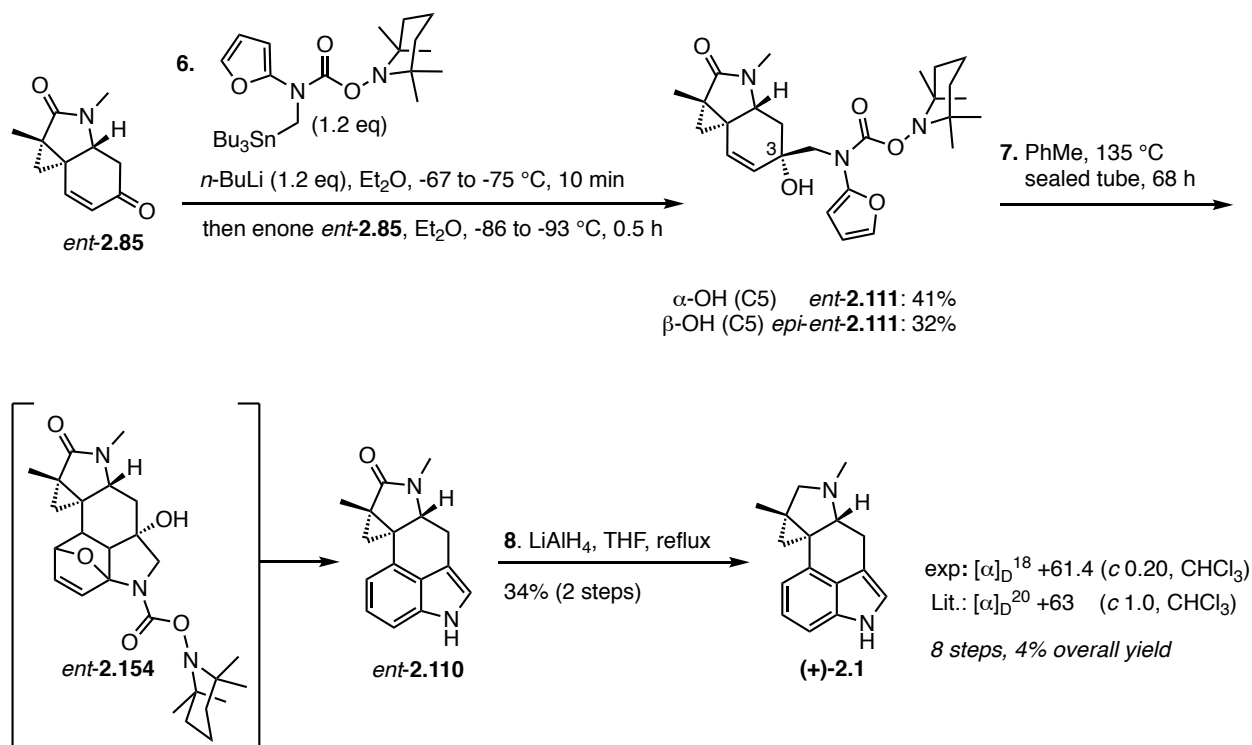


**Figure 2-17** Enantiomeric enrichment of the excess enantiomer by crystallization SFC chromatograms of the a) racemic standard and b) enantioenriched ketone **ent-2.85**

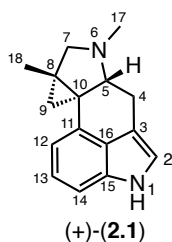
The final task of the synthesis was to install the indole core. The stannane **2.149** underwent transmetalation to the corresponding furanyl lithium reagent when treated with *n*-BuLi at low temperature (Scheme 2-37). Addition of the enantioenriched enone **ent-2.85** delivered the desired allylic alcohols, which could be separated by chromatography on SiO<sub>2</sub> to

give *ent*-**2.111** and *epi-ent*-**2.111** in 41% and 32% respectively. Allylic alcohol *ent*-**2.111** underwent the final IMDAF reaction to deliver intermediate *ent*-**2.154**. The initial Diels-Alder adduct underwent aromatization and cleavage of the TEMPOC protecting group under the reaction conditions to form indole *ent*-**2.110**. Amide reduction delivered the natural enantiomer (+)-**2.1** in 34% over two steps. Overall, the synthesis of (+)-cycloclavine was accomplished in 8 steps and 4% yield. The specific rotation of the synthetic material was determined to be +61.4 (*c* 0.2, CHCl<sub>3</sub>), which was consistent with the literature value +63 (*c* 1, CHCl<sub>3</sub>).



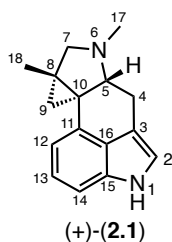
**Scheme 2-37** Completion of the synthesis of (+)-cycloclavine

The <sup>1</sup>H and <sup>13</sup>C NMR data for (+)-cycloclavine were consistent with the previously reported data for the natural compound (Tables 2-7 and 2-8).

**Table 2-7** A Comparison of the Literature and Synthetic  $^1\text{H}$  NMR Spectra of Cycloclavine

Atom #	Wipf and Petronijevic's synthetic ( $\pm$ )- <b>2.1</b> $^1\text{H}$ NMR, $\text{CDCl}_3$ , 700 MHz <sup>a</sup> $\delta$ (ppm), multiplicity J, # H	Our synthetic (+)- <b>2.1</b> $^1\text{H}$ NMR, $\text{CDCl}_3$ , 500 MHz <sup>b</sup> $\delta$ (ppm), multiplicity J, # H
1	7.92, bs, 1 H	7.89, bs, 1 H
14	7.15, d, $J = 8.4$ Hz, 1H	7.13 dd, $J = 8.0, 0.5$ Hz, 1 H
13	7.10, ap. t, $J = 7.7$ Hz, 1 H	7.09, ap. t, $J = 7.8$ Hz, 1 H
2	6.91, s, 1 H	6.90, ap. t, $J = 1.8$ Hz, 1 H
12	6.84, d, $J = 7.0$ Hz, 1 H	6.82, dd, $J = 7.0, 0.5$ Hz, 1 H
7 <sub>A</sub>	3.17, d, $J = 9.1$ Hz, 1 H	3.15, d, $J = 9.0$ Hz, 1 H
4 <sub>A</sub>	3.15, dd, $J = 14.0, 4.2$ Hz, 1 H	3.13, dd, $J = 13.8, 3.8$ Hz, 1 H
5	2.79, dd, $J = 11.2, 3.5$ Hz, 1 H	2.78, dd, $J = 11.5, 4.0$ Hz, 1 H
4 <sub>B</sub>	2.61, t, $J = 12.6$ Hz, 1 H	2.63-2.57, m, 1 H
7 <sub>B</sub>	2.42, d, $J = 8.4$ Hz, 1 H	2.40, d, $J = 8.5$ Hz, 1 H
17	2.37, s, 3 H	2.36, s, 3H
18	1.70, s, 3 H	1.69, s, 3 H
9 <sub>A</sub>	1.61, d, $J = 2.8$ Hz, 1 H	1.60, d, $J = 3.5$ Hz, 1 H
9 <sub>B</sub>	0.46, d, $J = 3.5$ Hz, 1 H	0.45, d, $J = 3.5$ Hz, 1 H

<sup>a</sup>the solvent reference for Wipf and Petronijevic's sample was:  $^1\text{H}$   $\delta$  7.27 ( $\text{CDCl}_3$ ); <sup>b</sup>the solvent reference for our synthetic material (+)-**2.1** was:  $^1\text{H}$   $\delta$  7.26 ( $\text{CDCl}_3$ ).

**Table 2-8** A Comparison of the Literature and Synthetic  $^{13}\text{C}$  NMR Spectra of Cycloclavine

Atom #	Wipf and Petronijevic's synthetic ( $\pm$ )- <b>2.1</b> $^{13}\text{C}$ NMR, $\text{CDCl}_3$ , 175 MHz $\delta$ (ppm)	Our synthetic (+)- <b>2.1</b> $^{13}\text{C}$ NMR, $\text{CDCl}_3$ , 150 MHz $\delta$ (ppm)
11	135.4	135.6
15	133.5	133.7
16	128.7	128.8
13	122.9	123.1
2	118.1	118.2
3	113.2	113.5
12	110.3	110.5
14	107.9	108.1
5	69.6	69.8
7	65.6	65.7
17	39.9	40.1
8	34.4	34.5
10	27.8	27.9
4	24.9	25.1
9	24.2	24.4
18	16.5	16.6

<sup>a</sup>the solvent reference for Wipf and Petronijevic's sample was:  $^{13}\text{C}$   $\delta$  77.0 ( $\text{CDCl}_3$ ); <sup>b</sup>the solvent reference for our synthetic material (+)-**2.1** was:  $^{13}\text{C}$   $\delta$  77.16 ( $\text{CDCl}_3$ ).



The overlaid circular dichroism (CD) spectra for (+)- and (–)-cycloclavine are shown in Figure 2-18. As expected, the CD spectra of the enantiomers were approximately equal in magnitude but opposite in sign. The natural enantiomer (+)-**2.1** had a positive cotton effect while the unnatural enantiomer (–)-**2.1** displayed a negative cotton effect.

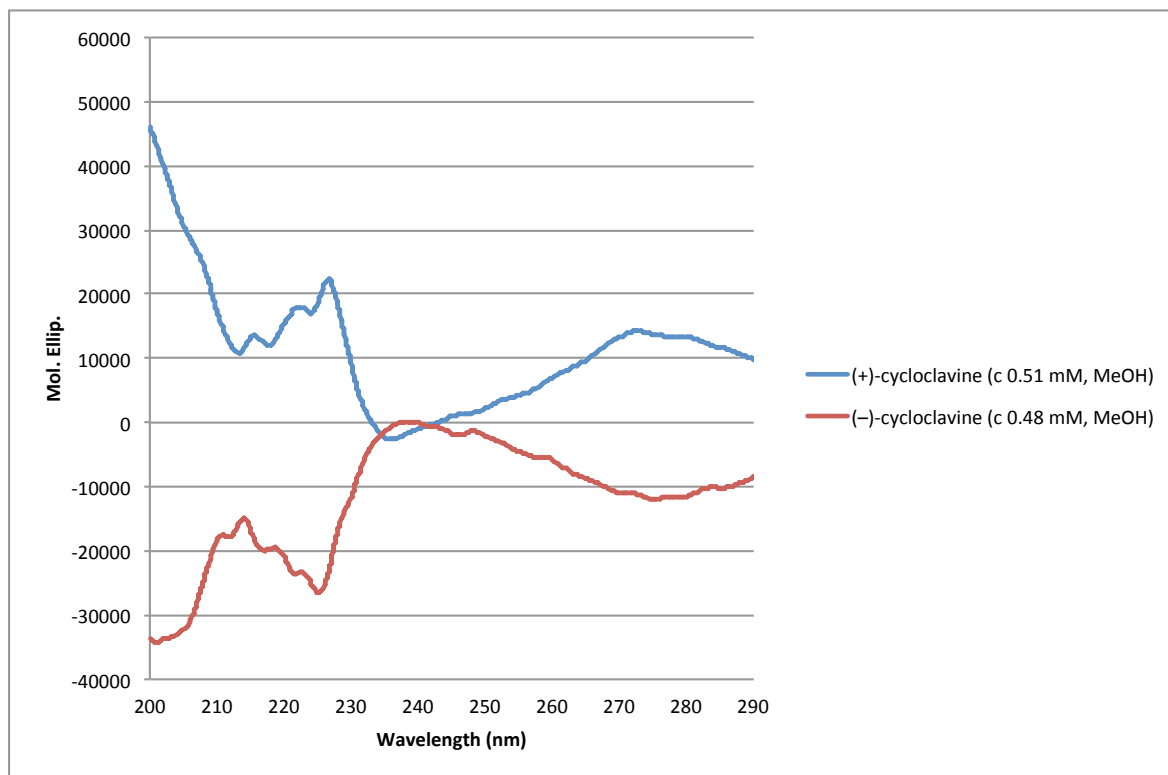


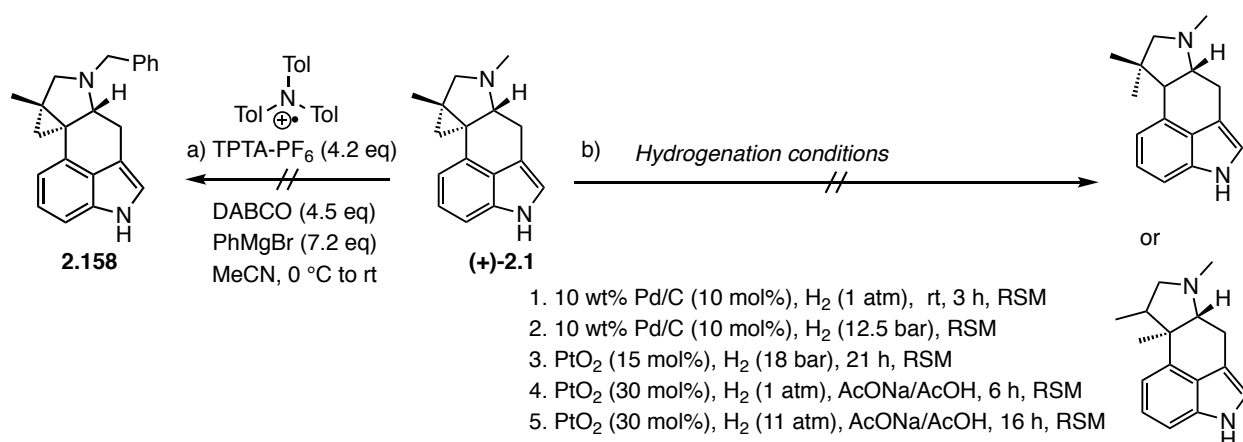
**Figure 2-18** Comparison of the CD spectra of cycloclavine enantiomers

### 2.2.11 Attempted Analogue Synthesis by Late Stage Derivatization

We were also interested in synthesizing analogues of cycloclavine by carrying out late-stage site-selective modifications to the cycloclavine core. The Murphy group has reported a highly selective C–H functionalization of *N*-CH<sub>3</sub> groups using the radical cation DABCO<sup>•+</sup> and Grignard reagents.<sup>112</sup> They demonstrated the utility of this method in the site-selective functionalization of several natural products and pharmaceutical agents. The proposed

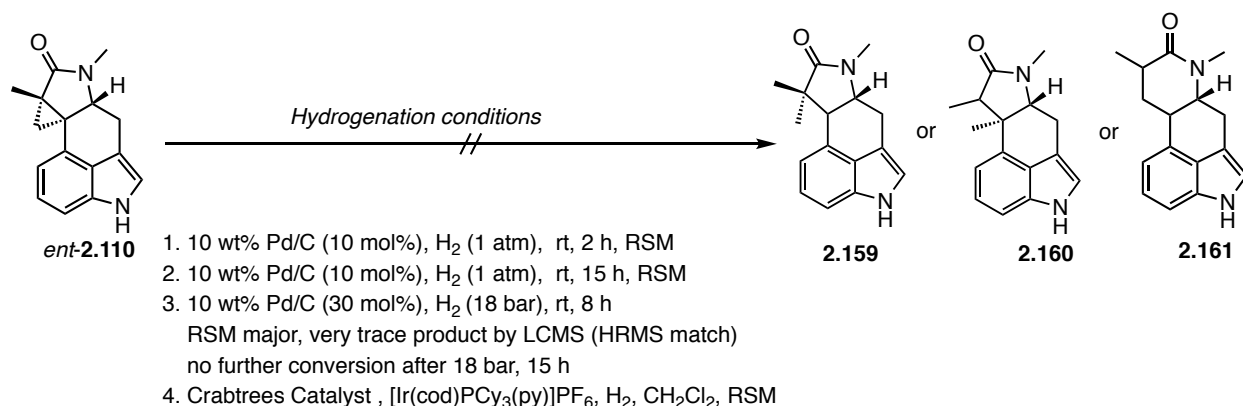
mechanism involves conversion of the *N*-CH<sub>3</sub> group to the corresponding iminium ion by two sequential single electron transfers in the presence of excess DABCO<sup>+</sup>. The iminium ion then reacts with excess Grignard reagent to form a variety of *N*-alkylated products. Unfortunately, in our hands the reaction of (+)-cycloclavine with DABCO<sup>+</sup> and PhMgBr gave a messy reaction profile with multiple unidentified products (Scheme 2-38a).

We next attempted hydrogenation of the cyclopropane C–C bond to form the hydrogenated ring-opening product (Scheme 2-38b). The unactivated tetrasubstituted cyclopropane in (+)-cycloclavine is a highly challenging substrate for hydrogenation due to the severe steric hindrance imposed by the vicinal quaternary stereocenters upon interaction with the Pd/C catalytic system.<sup>113</sup> However, we hoped that the release of ring-strain upon reductive ring opening of the cyclopropane would provide a driving force for the reaction. Unfortunately the substrate proved unreactive under classic hydrogenation conditions of 10% Pd/C under an atmosphere of hydrogen. Furthermore, no reaction occurred when (+)-**2.1** was subjected to harsher hydrogenation conditions of 18 bar in a Parr hydrogenator. Switching catalysts to PtO<sub>2</sub> in AcOH/AcONa under H<sub>2</sub> at 11 atm gave recovered starting material.<sup>114</sup>



**Scheme 2-38** Attempted *N*-CH<sub>3</sub> functionalization and hydrogenation of (+)-cycloclavine

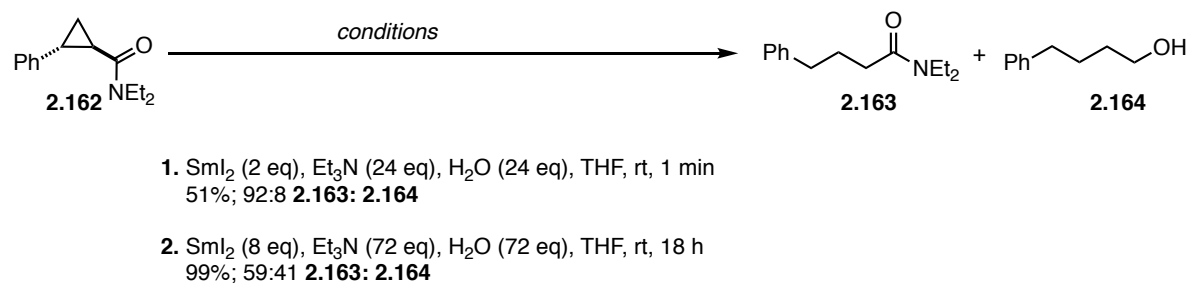
We next examined the hydrogenation of the tertiary amide precursor *ent*-**2.110** reasoning that the proximal Lewis-basic amide carbonyl could coordinate the metal center and thereby facilitate the desired hydrogenation reaction (Scheme 2-39). The amide did not react under the standard conditions of 10 mol% of Pd/C (10wt%)/H<sub>2</sub> (1 atm). Higher catalyst loadings of 30 mol% Pd/C (10wt%) and increased pressure of 18 bar in the Parr hydrogenator led to recovered starting material along with trace conversion by LCMS. The Crabtree catalyst is commonly used for the hydrogenation of unfunctionalized tri- and tetrasubstituted alkenes. Unfortunately, no reaction occurred when this catalyst was used on our system.



**Scheme 2-39** Attempted hydrogenation of amide *ent*-**2.110**

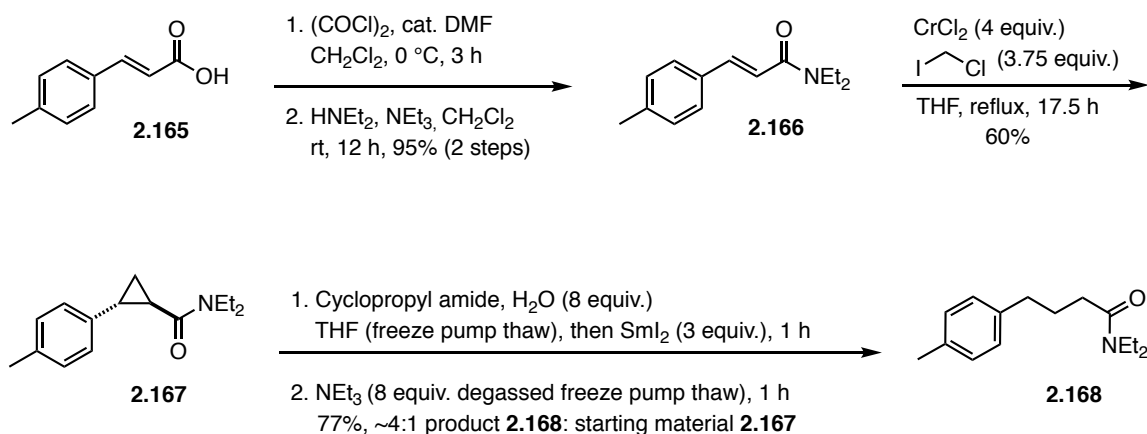
The SmI<sub>2</sub>/H<sub>2</sub>O/NEt<sub>3</sub> reagent has recently emerged as one of the most powerful samarium-based reducing agents ( $E^\circ = -2.8$  V) and is capable of reducing challenging substrates like carboxylic acids and amides, which were generally considered to lie outside the reducing range of SmI<sub>2</sub>.<sup>115</sup> Proctor and coworkers reported that the reduction of cyclopropyl amides to alcohols can be achieved using the SmI<sub>2</sub>/NEt<sub>3</sub>/H<sub>2</sub>O system.<sup>116</sup> This reaction represents the first general method to form ketyl-type radicals from unactivated amides. In a relevant experiment Proctor showed that the reaction of amide **2.162** with SmI<sub>2</sub> (2 eq), Et<sub>3</sub>N (24 eq) and H<sub>2</sub>O (24 eq) in THF at room temperature for 1 min lead to a 92:8 ratio of amide **2.163** to alcohol **2.164** (Scheme 2-

40). Using a larger excess of the  $\text{SmI}_2\text{-Et}_3\text{N-H}_2\text{O}$  reagent over longer reaction times of 18 h led to increased formation of the alcohol **2.164**.



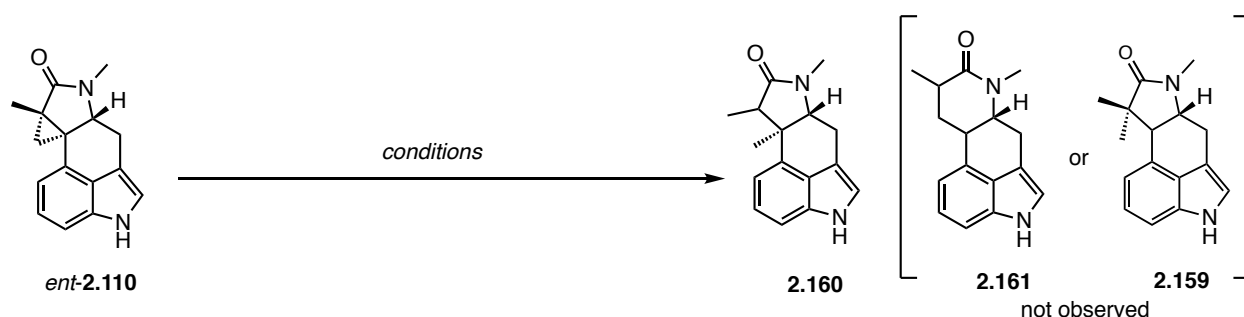
**Scheme 2-40** Procter's reductive ring-opening of a cyclopropyl amide using  $\text{SmI}_2/\text{NEt}_3/\text{H}_2\text{O}$

We initially tested the reaction on cyclopropyl amide **2.167** as a model system. The cyclopropyl amide was synthesized from acrylic acid **2.165** according to the sequence outlined in Scheme 2-41. Acrylic acid **2.165** was reacted with oxalyl chloride and catalytic DMF to form the acyl chloride, then subjected to an amidation reaction with  $\text{HNEt}_2$  and  $\text{NEt}_3$  to form the acrylic amide **2.166** in 95% yield. Amide **2.166** was subjected to a chromium carbene mediated cyclopropanation to give cyclopropyl amide **2.167**. We hoped that by employing relatively short reaction times the conversion could be halted at the ring-opened tertiary amide product without over-reduction to the alcohol. We were pleased to see when a degassed solution of cyclopropyl amide **2.167** and  $\text{H}_2\text{O}$  in THF was treated with  $\text{SmI}_2$  (3 eq) then  $\text{NEt}_3$  for 1 h the desired ring-opened adduct was obtained in 77% as an inseparable 4:1 mixture of ring-opened amide **2.168** to starting material **2.167**.



**Scheme 2-41** Synthesis of cyclopropyl amide model system and SmI<sub>2</sub>-mediated ring opening

The amide *ent*-**2.110** was subjected to reduction with the SmI<sub>2</sub>/amine/H<sub>2</sub>O system. However, only partial conversion to product was observed by LCMS under the same conditions identified on the model system and no further conversion was observed when additional SmI<sub>2</sub> (3 eq) was added (Scheme 2-42). Moving to harsher conditions we reacted amide *ent*-**2.110** with a large excess of SmI<sub>2</sub> (24 eq), NEt<sub>3</sub> (72 eq) and H<sub>2</sub>O (72 eq). Consumption of the starting material was observed and a cyclopropyl cleavage product tentatively assigned as the amide **2.160** was formed in low yields. Insufficient material prevented full characterization. Screening other additives including HMPA and H<sub>2</sub>O in combination with SmI<sub>2</sub> gave recovered starting material. An attempt to reduce the cyclopropane with Bu<sub>3</sub>SnH/AIBN also failed. We also investigated a small scale Birch-type reduction. Amide *ent*-**2.110** was reacted with excess lithium metal in dry EtNH<sub>2</sub> for 5 min at 0 °C. We were pleased to see that the reduction product **2.160** was obtained in ~36% yield, however full characterization was again hampered by insufficient material. Unfortunately, an attempt to conduct the reaction on scale led to over reduction and a messy reaction profile.



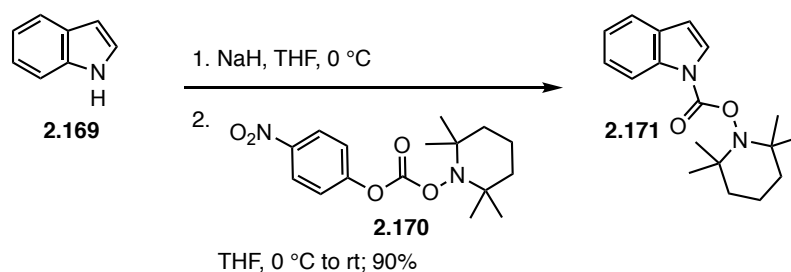
1.  $\text{SmI}_2$  (3 equiv.), degassed  $\text{NEt}_3$  (8 equiv.), degassed  $\text{H}_2\text{O}$  (8 equiv.), THF, 15 min then  $\text{SmI}_2$  (3 equiv.), 15 min
2.  $\text{SmI}_2$  (total 24 equiv.), degassed  $\text{NEt}_3$  (72 equiv.), degassed  $\text{H}_2\text{O}$  (72 equiv.), THF, 4 h  
**2.160** (0.75 mg, ~11.5%), other over-reduction byproducts (by LCMS)
3.  $\text{SmI}_2$  (0.07 M in THF) (5 eq), HMPA (25 eq), degassed by freeze pump thaw, 1.5 h, RSM
4.  $\text{SmI}_2$  (0.07 M in THF) (10 eq),  $\text{H}_2\text{O}$  (500 eq.), degassed by freeze pump thaw, 30 min, RSM
5.  $\text{SmI}_2$  (0.07 M in THF) (4 eq), HMPA (20 eq),  $\text{NEt}_3$  (10 eq.), degassed by freeze pump thaw, RSM
6.  $\text{HSnBu}_3$  (5 equiv.), AIBN (2 equiv.), RSM
7. Li (~12 eq), anhydrous  $\text{EtNH}_2$ , 0 °C, 5 min; ~36% **2.160**
8. Li (~14 eq), anhydrous  $\text{EtNH}_2$ , 0 °C, 5 min; over reduction

**Scheme 2-42** Attempted radical reduction of amide **ent-2.110**

In summary, attempts to perform late stage derivatization reactions on the natural product (+)-cycloclavine and the precursor amide **ent-2.110** proved challenging. Both the natural product and amide precursor **ent-2.110** proved unreactive toward hydrogenation conditions. Radical-mediated reduction with excess  $\text{SmI}_2/\text{H}_2\text{O}/\text{NEt}_2$  or Li metal/ $\text{EtNH}_2$  proved partially successful delivering small quantities of a reduction product **2.160** along with over reduction products. Overall, the successful implementation of a radical mediated reduction to obtain meaningful quantities of product in a reproducible manner was hindered by an inability to control a mono-reduction reaction on small scale and in the presence of excess reducing reagent.

### 2.2.12 TEMPO-Carbamate Thermolysis Studies

We also investigated the thermolytic cleavage of the novel TEMPO-carbamate protecting group that was employed in our synthesis of cycloclavine. We decided to study the thermolytic cleavage on a model system. To this end indole **2.169** was deprotonated with NaH followed by *N*-acylation with the mixed anhydride **2.170** to form the TEMPO-carbamate **2.171** in 90% yield (Scheme 2-43).

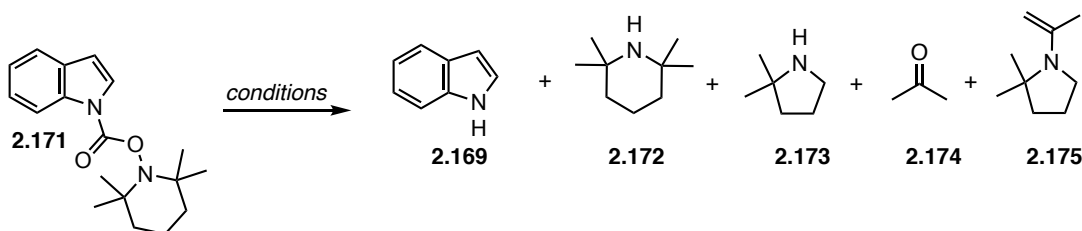


Scheme 2-43 TEMPOC protection of indole

To gain insight into the mechanism of cleavage, the protected indole **2.171** was subjected to thermolysis in toluene-*d*<sub>8</sub> (Table 2-9) and the resulting products were analyzed by NMR spectroscopy. We found that heating indole **2.171** at 150 °C for 20 h cleanly afforded the desired protecting-group free indole **2.169** along with a 3.6:1 ratio of pyrrolidine **2.173**: tetramethylpiperidine (TMP) **2.172** (Table 2-9, Entry 1). When degassed solvent was employed (Table 2-9, Entry 2), a 2.3:1:0.98 ratio of pyrrolidine **2.173**:TMP **2.169**:enamine **2.175** (tentatively assigned) was observed. Thermolysis at 150 °C with 4 equivalents of water (Table 2-9, Entry 3) led to indole **2.169** in an isolated yield of 87% along with a 3.4:1 ratio of pyrrolidine **2.173**:TMP **2.172**. Interestingly, when the thermal cleavage was conducted at lower temperatures of 135-140 °C (Table 2-9, Entry 4), a 1.8:1 ratio of **2.173**:**2.172** was observed. Only trace

conversion was observed when the thermolysis was conducted at 120 °C in benzene-*d*6 overnight (Table 2-9, Entry 5).

**Table 2-9** Thermolysis of the TEMPOC-Protected Indole

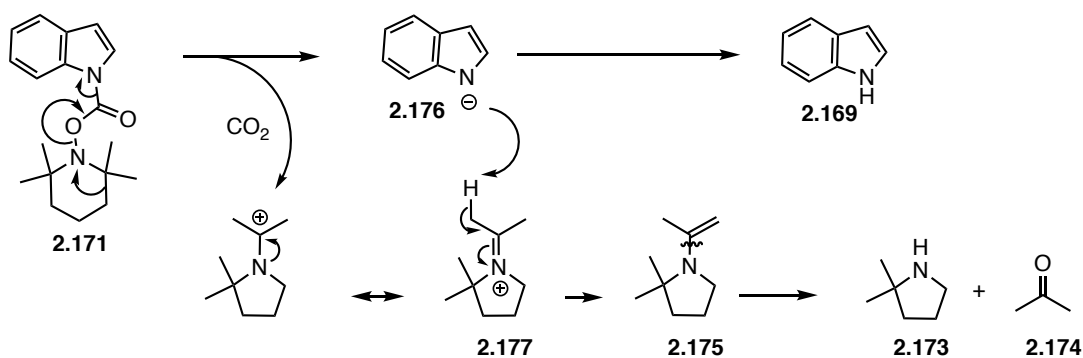


Entry	Conditions <sup>a</sup>	Thermolysis Product Ratio			
		2.172	2.173	2.174	2.175
1	150 °C, PhMe- <i>d</i> 8 (1 M), 20 h	1	3.6	ND <sup>b</sup>	0
2	150 °C, PhMe- <i>d</i> 8 (1 M, degassed), 9 h	1	2.3	ND <sup>b</sup>	0.98
3	150 °C, PhMe- <i>d</i> 8 (1 M), H <sub>2</sub> O (4 eq), 21.5 h <sup>c</sup>	1	3.4	ND <sup>b</sup>	0
4	135-140 °C, PhMe- <i>d</i> 8 (1 M), 32.5 h	1	1.8	ND <sup>b</sup>	Trace
5	120 °C, C <sub>6</sub> D <sub>6</sub> (1 M), 12 h	SM major, trace conversion			

<sup>a</sup>all reactions were carried out in a sealed tube, using conventional heating in an oil bath; <sup>b</sup>not determined; <sup>c</sup>isolated yield 87%.

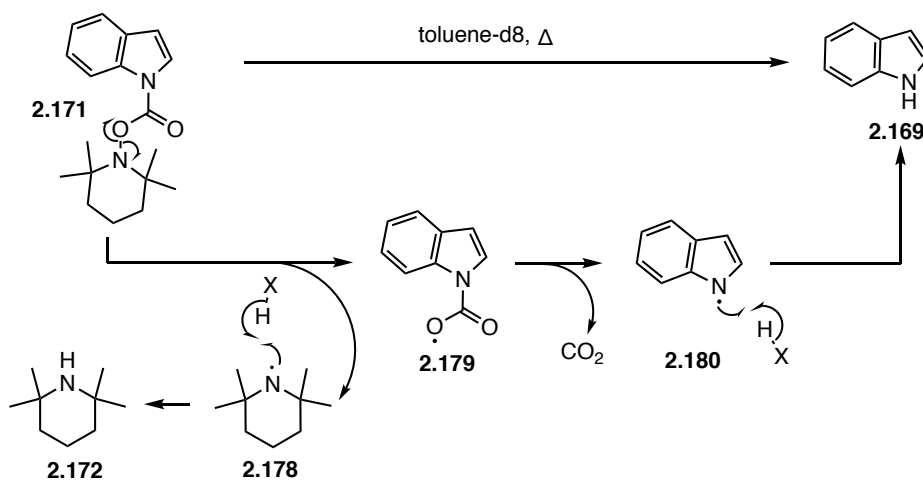
These studies support a deprotection mechanism that occurs through a mixed mechanistic pathway. The major ionic cleavage is outlined in Scheme 2-44. When indole **2.171** is heated in a sealed tube in toluene-*d*8 at temperatures above 135 °C, a ring contraction and extrusion of CO<sub>2</sub> occurs to form indole anion **2.176** and iminium ion **2.177**. Subsequent proton transfer affords the protecting-group-free indole **2.169** and enamine **2.175**. The enamine **2.175** can be cleaved under the reaction conditions to form acetone **2.174** and pyrrolidine **2.173**.





**Scheme 2-44** Proposed mechanism for the major ionic thermolysis pathway

The minor thermolysis product tetramethylpiperidine (**2.172**) is most likely generated through a separate radical-mediated pathway (Scheme 2-45). A plausible mechanism involves homolysis of the N-O bond upon thermolysis in toluene-*d*<sub>8</sub>. The resulting tetramethylpiperidine radical **2.178** undergoes a radical abstraction from a proton source to generate tetramethylpiperidine **2.172**. The carboxyl radical **2.179** is proposed to undergo rapid decarboxylation to generate CO<sub>2</sub> and an indole radical **2.180**, which can undergo a second proton abstraction to generate indole **2.169**. While the proton source in the reaction remains unclear the toluene solvent or residual H<sub>2</sub>O are potential sources.



**Scheme 2-45** Proposed mechanism for the minor radical pathway of thermolysis

### 2.2.13 Radioligand Binding Assays

Ergot alkaloids display an extraordinarily broad spectrum of biological activity spanning multiple therapeutic fields including infectious diseases, CNS disorders, obstetrics and oncology. This diverse biological profile has been attributed to their ability to mimic or block the binding of natural neurotransmitters like serotonin, dopamine, noradrenalin and adrenalin to their receptors.

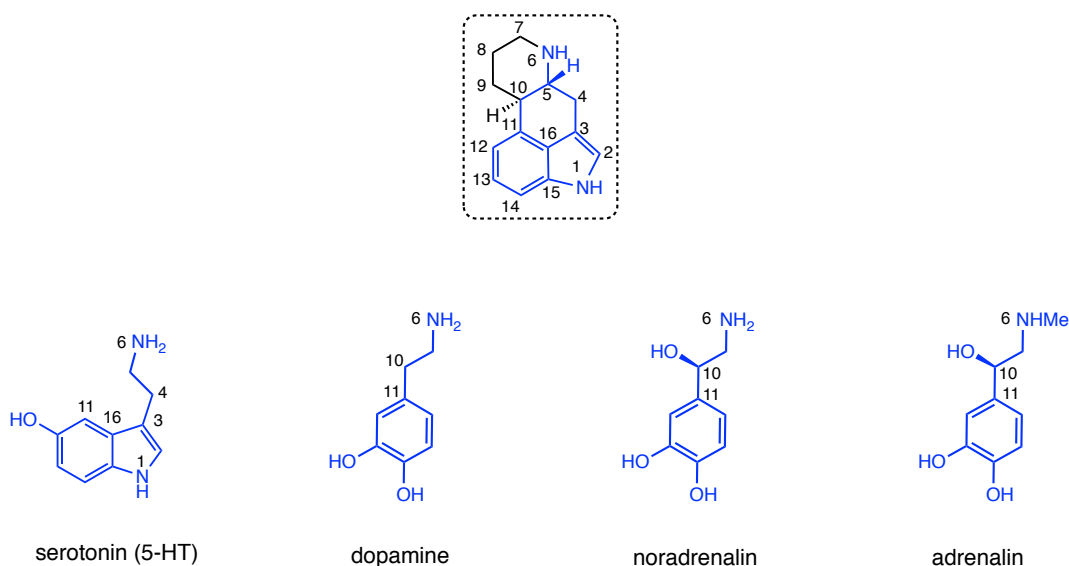


**Figure 2-19** Ergoline core and the structure of selected monoamine neurotransmitters

While cycloclavine demonstrated promising insecticidal and antiparasitic activity, its broader biological profile remains unknown. We were thus interested in testing the binding affinity of our synthetic materials to several neurotransmitter receptors. Radioligand-binding assays were carried out to determine the affinity of each enantiomer for dopamine and serotonin receptor subtypes (Table 2-10). In these experiments both enantiomers of cycloclavine were evaluated for their ability to outcompete a radioligand control for binding to a neurotransmitter

receptor target. The results are expressed as a percent inhibition of the controls specific binding to the receptor.

The results are summarized in Table 2-10 along with the reported radioligand binding data for lysergic acid diethylamide (LSD) at 10  $\mu$ M for comparison.<sup>117</sup> Neither enantiomer showed significant binding to the GABAA, histamine H<sub>1</sub>, muscarinic M<sub>2</sub> and M<sub>5</sub>, nicotinic acetylcholine  $\alpha$ 4 $\beta$ 2, cytosine and the orexin OX<sub>1</sub> receptors at 10  $\mu$ M. The enantiomers exhibited moderate affinity for the adrenergic  $\alpha$ <sub>1</sub> receptor and the  $\kappa$ -opiate receptor. The natural enantiomer showed 57% radioligand displacement at the adrenergic  $\alpha$ <sub>1</sub> receptor and 73% displacement at the  $\kappa$ -opiate receptor. The unnatural enantiomer showed 59% radioligand displacement at the adrenergic  $\alpha$ <sub>1</sub> receptor and 75% radioligand displacement the  $\kappa$ -opiate receptor. Interestingly, the natural enantiomer (+)-**2.1** exhibited a high affinity for both dopamine and serotonin receptor subtypes at 10  $\mu$ M (Table 2-10, Entries 9-13). When re-evaluated at 1  $\mu$ M, (+)-**2.1** showed high affinity for the dopamine D<sub>3</sub> receptor (75% inhibition) and quantitative binding to serotonin receptor subtypes (Table 2-10, entries 11-13). In contrast, while the unnatural enantiomer (–)-**2.1** showed significant binding to 5-HT<sub>1A</sub> and 5-HT<sub>2A</sub> at 10  $\mu$ M, when re-evaluated at 1  $\mu$ M it exhibited moderate affinity (Table 2-10, Entry 12-13). The unnatural enantiomer (–)-**2.1** exhibited modest affinity for the dopamine receptor subtypes (Table 2-10, Entries 9-11). Overall, these studies identified serotonin and dopamine receptor subtypes as potential biological targets for the natural enantiomer.

G-protein coupled dopamine receptors (D<sub>1</sub>-D<sub>5</sub>) are widely expressed in the brain and periphery and mediate all physiological functions of the neurotransmitter dopamine including locomotion, emotion, endocrine regulation, reward and learning.<sup>118</sup> Specific dopamine agonists or antagonists can enhance or reduce the physiological activities of dopamine. For example

dopamine D<sub>3</sub> receptor agonists have neuroprotective effects and have been used as anti-Parkinson's agents, whereas dopamine D<sub>3</sub> antagonists show antipsychotic activity.<sup>119,120,121</sup>

The neurotransmitter serotonin modulates a wide range of neuropsychological activities. For example, agonists of 5-HT<sub>1A</sub>, which is primarily located in the CNS, have been used to treat anxiety and depression.<sup>122</sup> Non-selective agonists like ergotamine have been used to treat migraines.<sup>123</sup> The 5-HT<sub>2A</sub> receptor is widely expressed throughout the CNS. In the periphery, it is highly expressed in platelets, where it facilitates platelet aggregation, and it is also expressed in several cell types of the cardiovascular system. For example, it is present on smooth arterial muscle where it mediates vasoconstriction.<sup>124,125</sup> Agonists of 5-HT<sub>2A</sub> are well known for their psychoactive properties and hallucinogenic effects.<sup>126</sup> The psychedelic drugs LSD, psilocin and mescaline are full or partial agonists of this receptor.<sup>127,128</sup> Antagonists of 5-HT<sub>2A</sub> are widely used as antipsychotic drugs have been used to treat hypertension.<sup>129,130,131</sup>

The unnatural enantiomer exhibited stronger binding to the 5-HT<sub>1A</sub> receptor (75% inhibition) compared to the 5-HT<sub>2A</sub> receptor (51% inhibition). This differential activity is particularly interesting, because the development of therapeutics without hallucinogenic effects is desired. In the future, functional assays could be performed to determine whether the natural and unnatural enantiomers of cycloclavine are inhibitors or activators of the serotonin 5-HT<sub>1A</sub> and 5-HT<sub>2A</sub> receptor subtypes. With this information in hand, the downstream consequences on the physiological processes mediated by these receptors can be probed.

**Table 2-10** Radioligand Binding Studies<sup>a</sup>

Entry	Receptor	(+)-cycloclavine		(-)-cycloclavine		LSD <sup>117</sup>
		10 $\mu$ M	1 $\mu$ M	10 $\mu$ M	1 $\mu$ M	10 $\mu$ M
1	GABAA, muscimol, central	9 <sup>rat</sup>	-	-9 <sup>rat</sup>	-	-2 <sup>rat</sup>
2	Histamine H <sub>1</sub>	17	-	27	-	85 <sup>rat</sup>
3	Muscarinic M <sub>2</sub>	-1	-	-3	-	2
4	Muscarinic M <sub>5</sub>	11	-	15	-	15
5	Nicotinic acetylcholine $\alpha$ 4 $\beta$ 2, cytisine	9	-	11	-	-2.5
6	Orexin OX <sub>1</sub>	23	-	6	-	-
7	Adrenergic $\alpha$ <sub>1</sub> , non-selective	57 <sup>rat</sup>	-	59 <sup>rat</sup>	-	-
8	Opioid $\kappa$ (OP2, KOP)	73	-	75	-	29
9	Dopamine D <sub>1</sub>	91	-	30	-	30
10	Dopamine D <sub>2L</sub>	81	-	14	-	14
11	Dopamine D <sub>3</sub>	93	75	64	32	64
12	Serotonin (5-HT <sub>1A</sub> )	97	97	91	73	100
13	Serotonin (5-HT <sub>2A</sub> )	103	103	89	51	93

<sup>a</sup>bioassay measures binding affinity toward receptor by displacement of a radioligand at 10 and 1  $\mu$ M of compound (>50% of max stimulation or inhibition is defined as significant).

## 2.3 CONCLUSIONS

The clavine alkaloids are an important group of indole containing alkaloids that belong to the well-known ergot alkaloid family. Ergot alkaloids were among the first fungal-derived natural products identified and have since been a rich source of pharmaceutical agents with diverse applications in obstetrics and the treatment of a variety of diseases, including CNS disorders, migraine and cancer. Cycloclavine is a structurally intriguing member of the rare rearranged clavine alkaloids. It is unique among clavine alkaloids, possessing an unprecedented pyrrolidine-fused cyclopropane ring with vicinal all carbon quaternary stereocenters in place of the piperidine common for other clavine alkaloids. Synthetic studies have been particularly valuable in facilitating access to the racemic form as well as both enantiomers of cycloclavine.

Herein, we describe the development of an improved racemic synthesis of cycloclavine that proceeded in 12 steps/5.2% overall yield compared to our 14 step/1.2% overall yield original synthesis. The key feature of the revised racemic route was the application of a regioselective aerobic dehydrogenation to form a bicyclic enone. We also describe the development and completion of the first enantioselective synthesis of the unnatural enantiomer (–)-cycloclavine (–)-(2.1) that was completed in 8 steps/7.1% overall yield from allene. Noteworthy features of the synthesis include the first application of the enantioselective cyclopropanation of allene described in Chapter 1. Additional significant features include the development and application of a TEMPO-carbamate as a new amine protecting-group that can be cleaved by thermolysis. Mechanistic studies were performed to elucidate the mechanism of thermolytic deprotection and showed that cleavage of the TEMPOC group proceed *via* a mixed mechanistic pathway involving a major ionic mechanism of thermolysis, and a minor homolytic mechanism of

cleavage. The first total synthesis of the natural enantiomer (+)-cycloclavine was also accomplished in 8 steps and 4% overall yield from allene using  $\text{Rh}_2(R\text{-TBPTTL})_4$  (*ent*-**1.75**) as the catalyst for the enantioselective cyclopropanation and the same route used to synthesize (–)-**2.1** thereafter. In an attempt to synthesize analogues of the natural product, several late-stage derivatization reactions on the cycloclavine core were carried out. A partially successful single electron reduction was identified. Further work is required to optimize this reaction and provide meaningful quantities of cycloclavine derivatives. Lastly, the synthetic materials were evaluated in radioligand binding assays with several potential target receptors. The natural enantiomer showed quantitative binding to the serotonin receptors 5-HT<sub>1A</sub> and 5-HT<sub>2A</sub> at 1  $\mu\text{M}$ . Overall, these studies identified serotonin and dopamine receptor subtypes as potential biological targets for the natural enantiomer.

### 3.0 EXPERIMENTAL

#### 3.1 GENERAL EXPERIMENTAL

All glassware was dried in an oven at 140 °C for at least 2 h prior to use. All air and moisture-sensitive reactions were performed under a dry N<sub>2</sub> atmosphere. Reactions carried out at 0 °C employed an ice bath and reactions carried out at -78 °C employed a dry ice/acetone bath. THF and Et<sub>2</sub>O were distilled over sodium/benzophenone ketyl, Et<sub>3</sub>N, CH<sub>2</sub>Cl<sub>2</sub> and toluene were distilled from CaH<sub>2</sub>. All other materials were obtained from commercial sources and used as received. Microwave reactions were performed in a Monowave microwave synthesis reactor. Infrared spectra were obtained from neat solids or oils on ATR FT-IR spectrometers. Melting points were determined in open capillary tubes and are uncorrected. High- resolution mass spectra were obtained on a Q-TOF MS or a Thermo Scientific Exactive Orbitrap LC-MS. <sup>1</sup>H and <sup>13</sup>C NMR spectra were obtained at 300, 400, 500, 600 or 700 MHz NMR in CDCl<sub>3</sub> unless otherwise specified. <sup>13</sup>C NMR spectra were obtained at 100, 125, or 150 MHz using a proton-decoupled pulse observed peak. Chemical shifts (δ) are reported in parts per million with the residual solvent peak used as an internal standard δ <sup>1</sup>H/<sup>13</sup>C (Solvent); 7.26/77.16 (CDCl<sub>3</sub>); 7.16/128.06 (C<sub>6</sub>D<sub>6</sub>), 5.32/54.00 (CD<sub>2</sub>Cl<sub>2</sub>) and 2.08/20.43 (PhMe-*d*8) and are tabulated as follows: chemical shift, multiplicity (s = singlet, d = doublet, t = triplet, q = quartet, m = multiplet), and coupling constant(s), number of protons. Reactions were monitored by thin layer



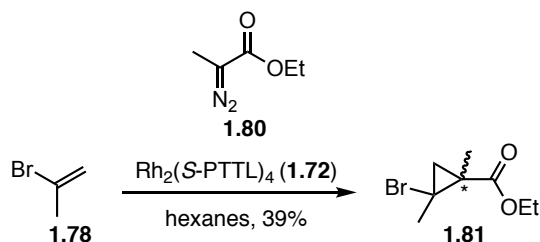
chromatography analysis (pre-coated silica gel 60 F254 plates, 250  $\mu\text{m}$  layer thickness) and visualization was accomplished with a  $\text{KMnO}_4$  solution (1.50 g of  $\text{KMnO}_4$ , 10 g of  $\text{K}_2\text{CO}_3$ , and 1.25 mL of 10%  $\text{NaOH}$  in 200 mL of  $\text{H}_2\text{O}$ ) when needed. Flash chromatography was performed using  $\text{SiO}_2$  (40-63  $\mu\text{m}$ ). Optical rotations were measured on a polarimeter equipped with a sodium lamp. Specific rotation values were calculated using the equation:

$$[\alpha]_{\lambda}^T = (100 \cdot a) / (l \cdot c)$$

Where  $[\alpha]$  represents the specific rotation of the sample in ( $10^{-1} \cdot \text{deg} \cdot \text{cm}^2 \cdot \text{g}^{-1}$ ),  $T$  indicates ambient temperature in  $^{\circ}\text{C}$ ,  $\lambda$  indicates wavelength ( $D$  is used to indicate the sodium line,  $\lambda = 589$  nm),  $a$  indicates the measured optical rotation,  $l$  indicates the path length in decimeters and  $c$  indicates the concentration in g/100 mL. All enantiomeric excesses were determined by analytical SFC separations using a ChiralPak IC column.

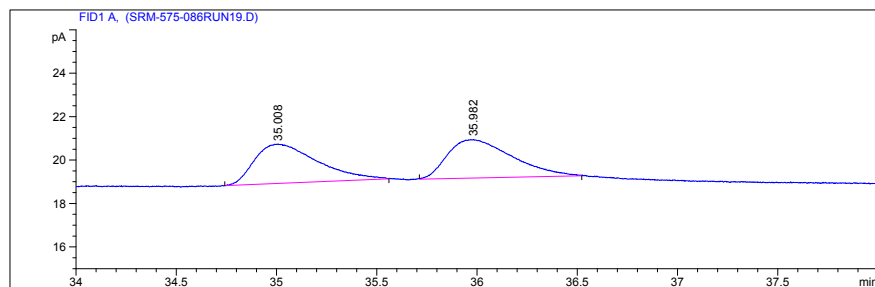
## 3.2 EXPERIMENTAL PROCEDURES

### 3.2.1 CHAPTER ONE EXPERIMENTAL PART



**Ethyl 2-bromo-1,2-dimethylcyclopropane-1-carboxylate (1.81).** An oven dried flask was charged with  $\text{Rh}_2(\text{S-PTTL})_4$  (**1.72**) (0.018 g, 0.012 mmol) and 2-bromopropene (0.50 mL, 5.6 mmol) in anhydrous hexanes (14.1 mL) under an atmosphere of nitrogen. The solution was cooled to  $-78\text{ }^\circ\text{C}$  and treated with a solution of diazopropanoate **1.80** (0.60 g, 4.7 mmol) in anhydrous hexanes (2.3 mL) *via* syringe pump at a rate of 1 mL/h. After the addition was complete, the reaction was allowed to warm to room temperature, concentrated and purified by chromatography on  $\text{SiO}_2$  (0-10%  $\text{Et}_2\text{O}$ /pentane) to deliver ester **1.81** (0.40 g, 39%, ~62:38 *er*) as a clear and colorless oil:  $[\alpha]_D^{20} + 26$  ( $c$  1,  $\text{CHCl}_3$ ); IR (ATR) 2975, 2937, 1726, 1456, 1361, 1286, 1178, 1122  $\text{cm}^{-1}$ ;  $^1\text{H}$  NMR (300 MHz,  $\text{CDCl}_3$ )  $\delta$  4.17 (q,  $J = 7.1$  Hz, 2 H), 1.83 (s, 3 H), 1.71 (d,  $J = 6.6$  Hz, 1 H), 1.57 (s, 3 H), 1.27 (t,  $J = 7.1$  Hz, 3 H), 1.11 (d,  $J = 6.3$  Hz, 1 H);  $^{13}\text{C}$  NMR (100 MHz,  $\text{CDCl}_3$ )  $\delta$  171.7, 61.4, 42.4, 30.4, 28.9, 26.1, 21.6, 14.4; HRMS (ESI) $^+$   $m/z$  calcd for  $\text{C}_8\text{H}_{14}^{79}\text{BrO}_2$  (M+H) 221.0177, found 221.0168.

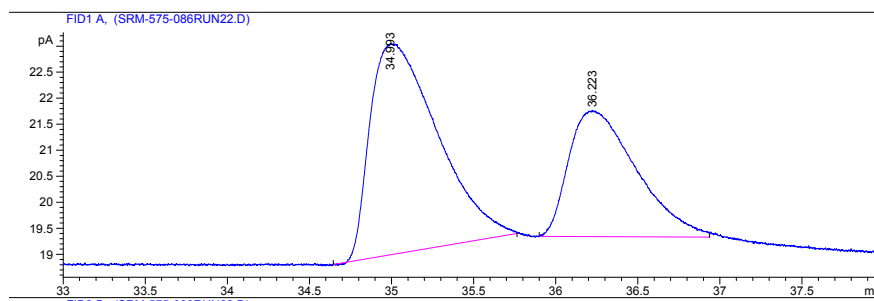
Chiral GC conditions: Astec CHIRALDEX G-TA capillary column (20m x 0.25mm x 0.12  $\mu\text{m}$  film thickness):  $60\text{ }^\circ\text{C}$  (hold for 3 min) then  $0.25\text{ }^\circ\text{C}/\text{min}$  to  $63\text{ }^\circ\text{C}$  (hold for 10 min), then  $0.50\text{ }^\circ\text{C}/\text{min}$  to  $65\text{ }^\circ\text{C}$  (hold for 3 min), then  $0.50\text{ }^\circ\text{C}/\text{min}$  to  $75\text{ }^\circ\text{C}$  (hold for 1 min), helium gas, 3.6 mL/min, average velocity 53 cm/sec, P = 16.50 psi.



Signal 1: FID1 A,

Peak #	RetTime [min]	Type	Width [min]	Area [pA*s]	Height [pA]	Area %
1	35.008	BB	0.2565	39.43559	1.81126	49.86148
2	35.982	BB	0.2620	39.65471	1.77601	50.13852

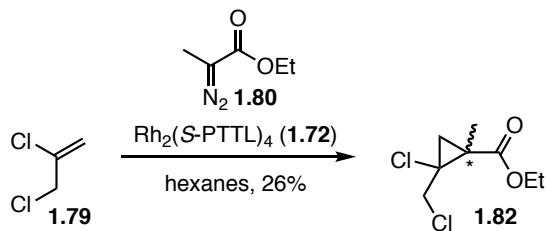
**Figure 3-1** Chiral GC resolution of racemic **1.81**



Signal 1: FID1 A,

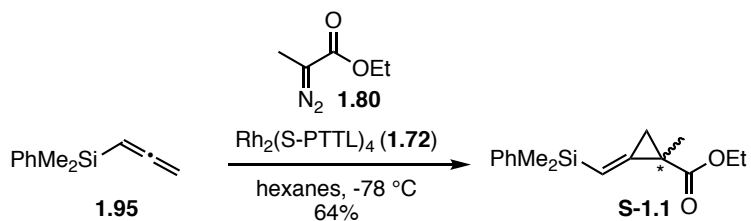
Peak #	RetTime [min]	Type	Width [min]	Area [pA*s]	Height [pA]	Area %
1	34.993	BB	0.3324	115.23926	4.05727	62.42364
2	36.223	BV	0.3349	69.36909	2.42399	37.57636

**Figure 3-2** Chromatogram of enantiomerically enriched of ester **1.81**



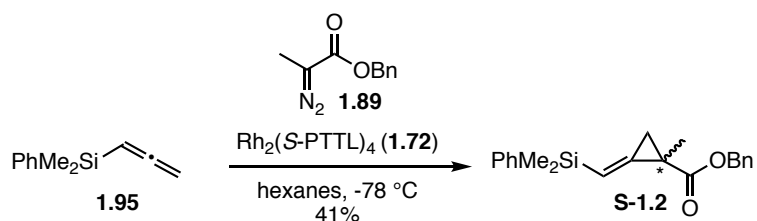
**Ethyl 2-chloro-2-(chloromethyl)-1-methylcyclopropane-1-carboxylate (1.82).** An oven dried flask charged with  $\text{Rh}_2(\text{S-PTTL})_4$  (**1.72**) (0.052 g, 0.037 mmol) and vinyl chloride

**1.79** (0.15 mL, 1.6 mmol) in anhydrous hexanes (2.8 mL) was cooled to -78 °C and treated with a solution of diazopropanoate **1.80** (0.10 g, 0.78 mmol) in anhydrous hexanes (0.5 mL) *via* syringe pump at a rate of 1 mL/h. After the addition was complete, the mixture was allowed to warm to room temperature and concentrated. The resulting residue was purified by chromatography on SiO<sub>2</sub> (0-10% Et<sub>2</sub>O/pentane) to deliver vicinal dichloride **1.82** (0.043 g, 26%) as a clear and colorless oil and single diastereomer: IR (ATR) 2982, 2937, 1719, 1456, 1297, 1223, 1154, 1059, 725 cm<sup>-1</sup>; <sup>1</sup>H NMR (300 MHz, CDCl<sub>3</sub>) δ 4.21 (qd, *J* = 7.1, 2.9 Hz, 2 H), 4.04 (d, *J* = 12.3 Hz, 1 H), 3.95 (d, *J* = 12.3 Hz, 1 H), 1.96 (d, *J* = 6.6 Hz, 1 H), 1.57 (s, 3 H), 1.30 (t, *J* = 7.2 Hz, 3 H), 1.26 (d, *J* = 6.6 Hz, 1 H); <sup>13</sup>C NMR (100 MHz, CDCl<sub>3</sub>) δ 171.4, 62.0, 54.4, 50.6, 31.7, 29.4, 18.4, 14.2; HRMS (ESI)<sup>+</sup> *m/z* calcd for C<sub>8</sub>H<sub>13</sub>Cl<sub>2</sub>O<sub>2</sub> (M+H) 211.0293, found 211.0283.



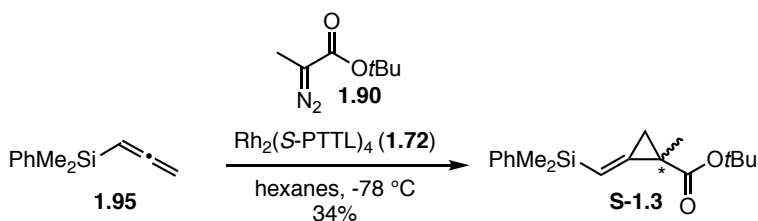
**Ethyl (*E*)-2-((dimethyl(phenyl)silyl)methylene)-1-methylcyclopropane-1-carboxylate (**S-1.1**).** An oven-dried flask charged with Rh<sub>2</sub>(S-PTTL)<sub>4</sub>•2EtOAc (**1.72**) (0.0028 g, 0.0020 mmol) in anhydrous hexanes (2.3 mL) was treated with DMPS allene **1.95** (0.082 g, 0.47 mmol) and cooled to -78 °C under an atmosphere of nitrogen. The cooled solution was treated with a solution of ethyl 2-diazopropanoate **1.80** (0.050 g, 0.39 mmol) in anhydrous hexanes (1.1 mL) *via* syringe pump at a rate of 1 mL/h. After the addition was complete, the mixture was allowed to warm to room temperature and concentrated. The crude residue was purified by chromatography on SiO<sub>2</sub> (0-5% Et<sub>2</sub>O/hexanes) to deliver ester **S-1.1** (0.069 g, 64%) as a clear

and colorless oil:  $^1\text{H}$  NMR analysis of the diastereomeric Mosher ester derivatives showed an *er* ~76: 24.  $[\alpha]_D^{20} + 12.7$  (*c* 1,  $\text{CHCl}_3$ ); IR (ATR) 3066, 2960, 2930, 2908, 1717, 1456, 1426, 1290, 1137, 1111, 833, 729  $\text{cm}^{-1}$ ;  $^1\text{H}$  NMR (400 MHz,  $\text{CDCl}_3$ )  $\delta$  7.54-7.53 (m, 2 H), 7.36-7.35 (m, 3 H), 6.10 (ap. d,  $J = 2.4$  Hz, 1 H), 4.10 (qd,  $J = 7.2, 0.9$  Hz, 2 H), 2.06 (dd,  $J = 9.2, 2.0$  Hz, 1 H), 1.38 (s, 3 H), 1.31 (dd,  $J = 9.2, 2.4$  Hz, 1 H), 1.23 (t,  $J = 7.2$  Hz, 3 H), 0.41 (s, 3 H), 0.40 (s, 3 H);  $^{13}\text{C}$  NMR (100 MHz,  $\text{CDCl}_3$ )  $\delta$  173.6, 147.5, 139.1, 133.9, 129.1, 127.9, 113.3, 60.7, 22.8, 19.7, 18.8, 14.3, -1.9, -2.2; HRMS (ESI+) *m/z* calcd for  $\text{C}_{16}\text{H}_{23}\text{O}_2\text{Si}$  (*M*+*H*) 275.14618, found 275.14787.



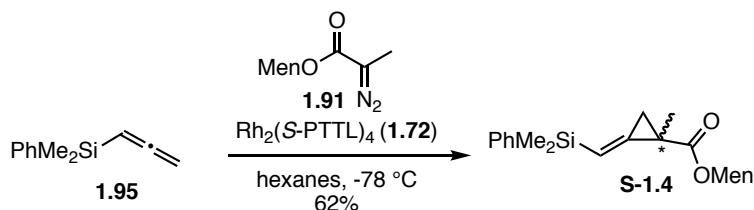
**Benzyl (E)-2-((dimethyl(phenyl)silyl)methylene)-1-methylcyclopropane-1-carboxylate (S-1.2).** An oven-dried round bottom flask containing  $\text{Rh}_2(\text{S-PTTL})_4 \cdot 2\text{EtOAc}$  (**1.72**) (0.0019 g, 0.0013 mmol) in anhydrous hexanes (1.6 mL) was treated with DMPS allene **1.95** (0.055 g, 0.32 mmol) and cooled to  $-78\text{ }^\circ\text{C}$  under an atmosphere of nitrogen. The resulting cooled solution was treated with a solution of benzyl 2-diazopropanoate **1.89** (0.050 g, 0.26 mmol) in anhydrous hexanes (0.75 mL) via syringe pump at a rate of 1 mL/h. After the addition was complete, the mixture was allowed to warm to room temperature and concentrated. The crude residue was purified by chromatography on  $\text{SiO}_2$  (0-2%  $\text{Et}_2\text{O}$ /hexanes) to deliver enantiomerically enriched ester **S-1.2** (0.036 g, 41%) as a clear and colorless oil.  $^1\text{H}$  NMR analysis of the diastereomeric Mosher ester derivatives showed an *er* ~72: 28: IR (ATR) 3066, 2954, 2928, 1720, 1454, 1426, 1292, 1247, 1135, 1123, 911, 837, 731  $\text{cm}^{-1}$ ;  $^1\text{H}$  NMR (400 MHz;

CDCl<sub>3</sub>)  $\delta$  7.53-7.51 (m, 2 H), 7.34-7.28 (m, 8 H), 6.13 (t,  $J$  = 2.6 Hz, 1 H), 5.15 (d,  $J$  = 12.8 Hz, 1 H), 5.06 (d,  $J$  = 12.8 Hz, 1 H), 2.11 (dd,  $J$  = 9.4, 2.6 Hz, 1 H), 1.41 (s, 3 H), 1.34 (dd,  $J$  = 9.4, 2.6 Hz, 1 H), 0.41 (s, 3 H), 0.40 (s, 3 H); <sup>13</sup>C NMR (100 MHz, CDCl<sub>3</sub>)  $\delta$  173.5, 147.1, 138.9, 136.4, 133.9, 129.1, 128.6, 128.1, 127.9, 127.7, 113.7, 66.3, 22.8, 19.8, 18.8, -2.0, -2.2; DEPT-135 (100 MHz, CDCl<sub>3</sub>)  $\delta$  133.9 (CH), 129.1 (CH), 128.6 (CH), 128.1 (CH), 127.9 (CH), 127.7 (CH), 113.7 (CH), 66.3 (CH<sub>2</sub>), 19.8 (CH<sub>2</sub>), 18.8 (CH<sub>3</sub>), -2.0 (CH<sub>3</sub>), -2.2 (CH<sub>3</sub>); HRMS (ESI+)  $m/z$  calcd for C<sub>21</sub>H<sub>25</sub>O<sub>2</sub>Si (M+H) 337.16183, found 337.16505.



***tert*-Butyl (E)-2-((dimethyl(phenyl)silyl)methylene)-1-methylcyclopropane-1-carboxylate (S-1.3).** An oven-dried round bottom flask charged with Rh<sub>2</sub>(S-PTTL)<sub>4</sub>•2EtOAc (**1.72**) (0.0018 g, 0.0013 mmol) in anhydrous hexanes (1.5 mL) was treated with DMPS allene **1.95** (0.054 g, 0.31 mmol) and cooled to -78 °C under an atmosphere of nitrogen. The resulting cooled solution was treated with a solution of *tert*-butyl 2-diazopropanoate **1.90** (0.040 g, 0.26 mmol) in anhydrous hexanes (0.7 mL) via syringe pump at a rate of 1 mL/h. After the addition was complete, the reaction was allowed to stir for 1 h at -78 °C before the mixture was allowed to warm to room temperature and concentrated. The residue was purified by chromatography on SiO<sub>2</sub> (0-2% Et<sub>2</sub>O/hexanes) to deliver ester **S-1.3** (0.026 g, 34%) as a clear and colorless oil. <sup>1</sup>H NMR analysis of the diastereomeric Mosher ester derivatives showed an *er* ~68: 32: IR (ATR) 3068, 2969, 2930, 1713, 1456, 1426, 1377, 1305, 1247, 1141, 837 cm<sup>-1</sup>; <sup>1</sup>H NMR (400 MHz; CDCl<sub>3</sub>)  $\delta$  7.55-7.52 (m, 2 H), 7.36-7.32 (m, 3 H), 6.07 (t,  $J$  = 2.4 Hz, 1 H), 1.97 (dd,  $J$  = 9.2, 2.4

Hz, 1 H), 1.40 (s, 9 H), 1.33 (s, 3 H), 1.25 (dd,  $J = 9.2, 2.4$  Hz, 1 H), 0.40 (s, 3 H), 0.38 (s, 3 H);  $^{13}\text{C}$  NMR (100 MHz;  $\text{CDCl}_3$ )  $\delta$  172.9, 148.1, 139.2, 134.0, 129.1, 127.9, 112.7, 80.3, 28.1, 23.7, 19.5, 18.8, -1.9, -2.2; HRMS (ESI+)  $m/z$  calcd for  $\text{C}_{18}\text{H}_{27}\text{O}_2\text{Si}$  (M+H) 303.17748, found 303.18031.



**(1*R*,2*S*,5*R*)-2-Isopropyl-5-methylcyclohexyl**

**(*E*)-2-**

**((dimethyl(phenyl)silyl)methylene)-1-methylcyclopropane-1-carboxylate (**S-1.4**).** An oven-dried round bottom flask charged with  $\text{Rh}_2(\text{S-PTTL})_4 \cdot 2\text{EtOAc}$  (**1.72**) (0.0015 g, 0.0011 mmol) in anhydrous hexanes (1.0 mL) was treated with DMPS allene **1.95** (0.044 g, 0.25 mmol) and cooled to  $-78\text{ }^\circ\text{C}$  under an atmosphere of nitrogen. The resulting cooled solution was treated with a solution of menthyl diazoacetate **1.91** (0.050 g, 0.21 mmol) in anhydrous hexanes (0.50 mL) at a rate of 1 mL/h. After the addition was complete, the reaction was allowed to stir at  $-78\text{ }^\circ\text{C}$  for 7h before the mixture was allowed to warm to room temperature. The solvent was subsequently removed and the residue was purified by chromatography on  $\text{SiO}_2$  (0-2%  $\text{Et}_2\text{O}$ /hexanes) to deliver ester **S-1.4** (0.050 g, 62%) as a clear and colorless oil and as an inseparable mixture of diastereomers which were directly subjected to derivatization as the Mosher ester adducts. HRMS (ESI+)  $m/z$  calcd for  $\text{C}_{24}\text{H}_{37}\text{O}_2\text{Si}$  (M+H) 385.25573, found 385.25922.  $^1\text{H}$  NMR analysis of the diastereomeric Mosher ester derivatives showed an *er* ~73: 27.





**(*E*)-2-((Dimethyl(phenyl)silyl)methylene)-1-methylcyclopropyl)methanol (S-1.6).** A solution of methylenecyclopropane ( $\pm$ )-**S-1.1** (0.063 g, 0.23 mmol) in CH<sub>2</sub>Cl<sub>2</sub> (1.5 mL) was cooled to 0 °C and treated with DIBAL-H (0.62 mL, 1M in hexanes, 0.62 mmol) and stirred at 0 °C for 1 h. The reaction was treated successively with deionized H<sub>2</sub>O (0.025 mL), 15% NaOH (0.025 mL) and deionized H<sub>2</sub>O (0.062 mL), dried (MgSO<sub>4</sub>) and filtered through a pad of Celite washing with EtOAc to deliver alcohol **S-1.6** (0.050 g, 93%) as a clear and colorless oil, which was used directly without further purification. **Diastereomeric Mosher esters (1.93 & 1.94):** A solution of alcohol **S-1.6** (0.015 g, 0.065 mmol) in CH<sub>2</sub>Cl<sub>2</sub> (1.0 mL) under an inert atmosphere was treated sequentially with crude acid chloride (*R*)-(-)-MTPA-Cl<sup>47</sup> (0.032 g, 0.13 mmol), using CH<sub>2</sub>Cl<sub>2</sub> (0.5 mL) to complete transfer, anhydrous NEt<sub>3</sub> (0.027 mL, 0.19 mmol) and DMAP (0.0010 g, 0.0081 mmol). The resulting clear and colorless solution was stirred at room temperature for 5 h during which time the solution became clear and pale yellow. The reaction was filtered through a small pad of florisil (washing with 20% EtOAc/hexanes) and concentrated under reduced pressure to give crude Mosher ester adducts **193** and **194**. <sup>1</sup>H NMR analysis of the crude reaction mixture showed ~ 1.1 ratio of vinyl protons: HRMS (ESI+) *m/z* calcd for C<sub>24</sub>H<sub>31</sub>O<sub>3</sub>NF<sub>3</sub>Si [M+NH<sub>4</sub>]<sup>+</sup> 466.20198, found 466.2045

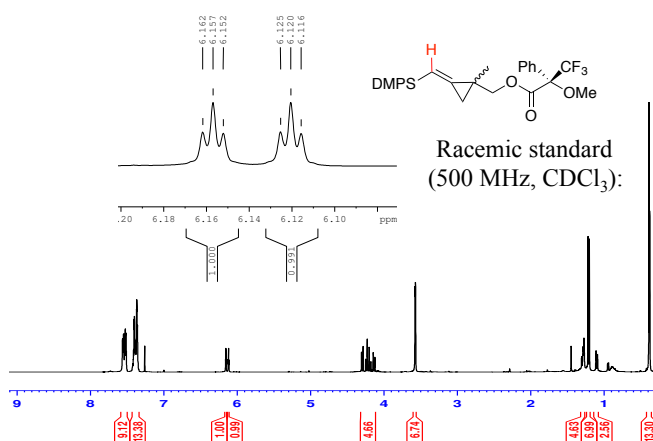


**Figure 3-3** Racemic standard

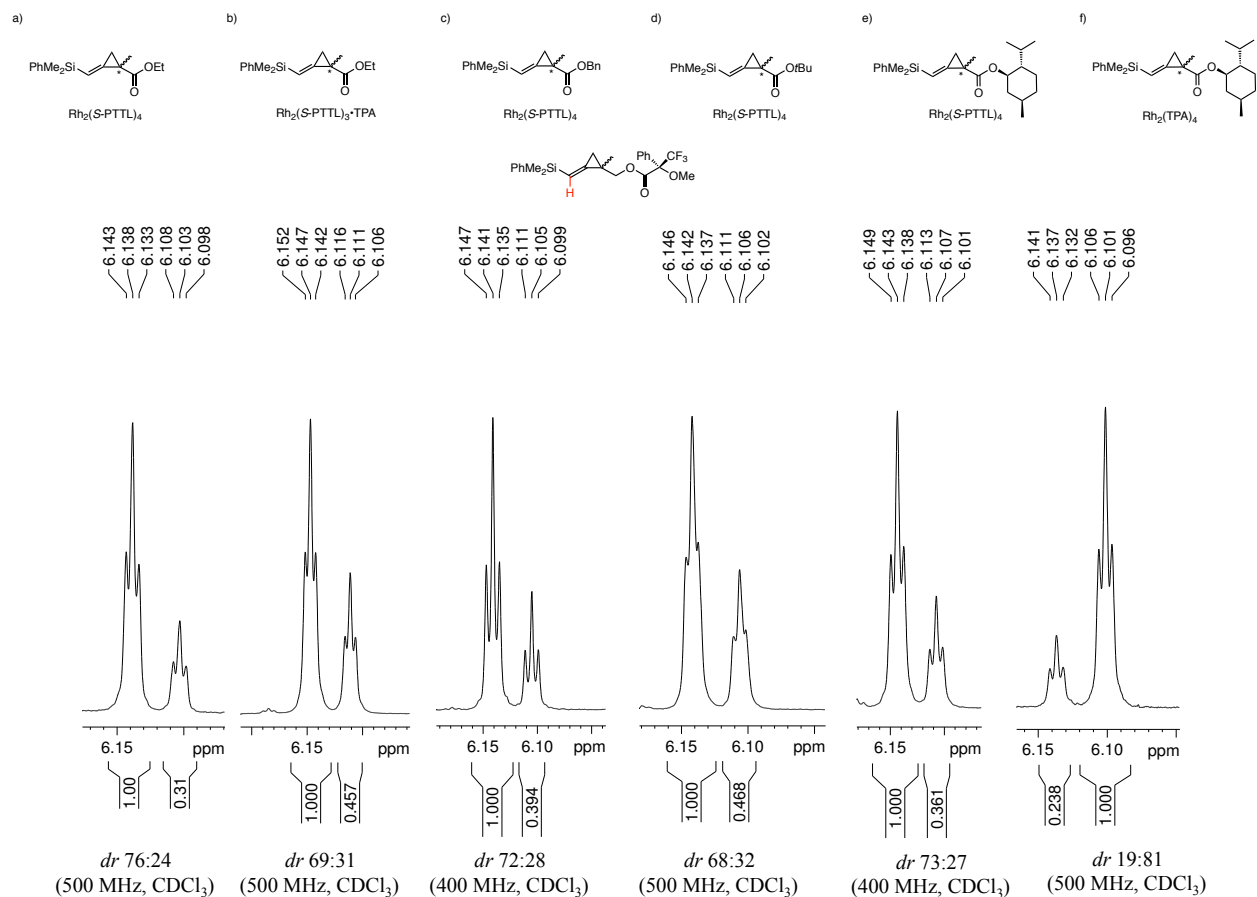
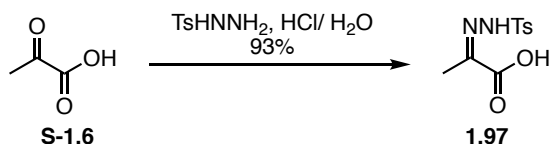


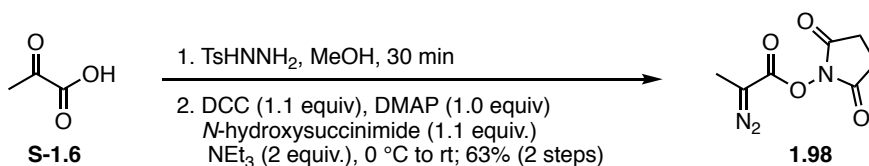
**Figure 3-4** Enantioenriched ester derivatives

a) Ethyl derivative (Table 1-2, entry 3, 500 MHz, CDCl<sub>3</sub>); (b) ethyl derivative (Table 1-2, entry 2, 500 MHz, CDCl<sub>3</sub>); (c) benzyl derivative (Table 1-2, entry 4, 400 MHz, CDCl<sub>3</sub>); (d) *t*-butyl derivative (Table 1-2, entry 5, 500 MHz, CDCl<sub>3</sub>); (e) menthyl derivative (Table 1-2, entry 6, 400 MHz, CDCl<sub>3</sub>); (f) menthyl derivative (Table 1-2, entry 7, 500 MHz, CDCl<sub>3</sub>)



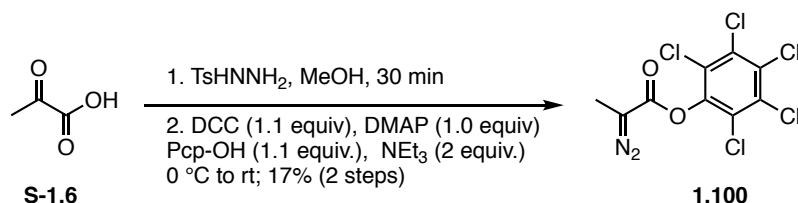
**2-(2-Tosylhydrazono)propanoic acid (1.97).** A solution of *p*-toluenesulfonyl hydrazide (5.00 g, 26.3 mmol) in H<sub>2</sub>O (25 mL) was treated sequentially with 2.5M HCl (12.5 mL) and pyruvic acid **S-1.6** (2.24 mL, 31.6 mmol) and the resulting heterogeneous mixture was heated at 100 °C for 4 h. The reaction was cooled to room temperature and the white precipitate collected

by vacuum filtration, washing with cold H<sub>2</sub>O (3 x) and dried under high vacuum to deliver 2-(2-tosylhydrazono)propanoic acid **1.97** (6.29 g, 93%) as a white solid: Mp 158.4-159.6 °C; IR (ATR) 3546, 3215, 2930, 1690, 1596, 1340, 1166, 1121, 1083, 907, 786 cm<sup>-1</sup>; <sup>1</sup>H NMR (400 MHz, DMSO-d<sub>6</sub>) δ 12.8 (bs, 1 H), 11.1 (s, 1 H), 7.76 (d, *J* = 8.4 Hz, 2 H), 7.41 (d, *J* = 8.0 Hz, 2 H), 2.38 (s, 3 H), 1.93 (s, 3 H); <sup>13</sup>C NMR (100 MHz, DMSO-d<sub>6</sub>) δ 165.2, 145.3, 143.8, 136.0, 129.7, 127.4, 21.0, 13.1; HRMS (LCMS ESI<sup>+</sup>) *m/z* calcd for C<sub>10</sub>H<sub>13</sub>N<sub>2</sub>O<sub>4</sub>S 257.0591, found 257.0587.

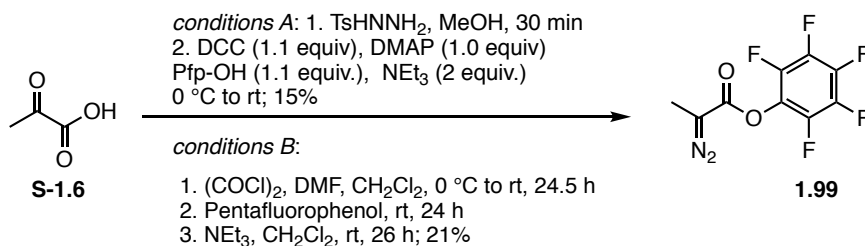


**2,5-Dioxopyrrolidin-1-yl 2-diazopropanoate (1.98).** Prepared using a modified protocol originally reported by Maruoka *et al.*<sup>132</sup> A solution of *p*-toluenesulfonyl hydrazide (1.07 g, 5.56 mmol) in MeOH (3 mL) was treated with pyruvic acid (**S-1.6**) (0.395 mL, 5.56 mmol) and the resulting clear and colorless solution stirred for 30 min at room temperature. The reaction was concentrated under reduced pressure to remove the MeOH and placed under high vacuum for 15 min to deliver 2-(2-tosylhydrazono)propanoic acid (**1.97**) as a white foam that was immediately taken up in THF (55 mL) and cooled to 0 °C. The solution was treated with *N*-hydroxysuccinimide (0.726 g, 6.12 mmol) and DCC (1.38 g, 6.12 mmol) and the resulting solution stirred at 0 °C for 3 h. The reaction was then treated with triethylamine (0.948 mL, 6.68 mmol) and the resulting yellow mixture was stirred for 20 h warming slowly to room temperature. The mixture was filtered through a pad of Celite (washing with 50% EtOAc/hexanes) and the solvent removed under reduced pressure. The viscous brown residue was purified by chromatography on SiO<sub>2</sub> (20-30% EtOAc/hexanes) to deliver 2,5-

dioxopyrrolidin-1-yl 2-diazopropanoate (**1.98**) (0.695 g, 63%) as a yellow solid: IR (ATR) 2958, 2947, 2095 ( $\nu = \text{N}_2$ ), 1730, 1635, 1364, 1200, 1075  $\text{cm}^{-1}$ ;  $^1\text{H}$  NMR (500 MHz,  $\text{CDCl}_3$ )  $\delta$  2.78 (s, 4 H), 2.58 (s, 3 H)



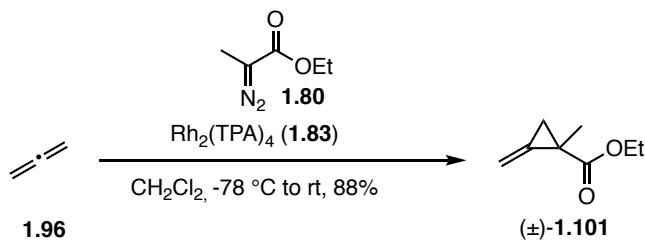
**Perchlorophenyl 2-diazopropanoate (1.100).** A solution of *p*-toluenesulfonyl hydrazide (1.07 g, 5.56 mmol) in MeOH (3 mL) was treated with pyruvic acid (**S-1.6**) (0.395 mL, 5.56 mmol) and the clear and colorless solution stirred for 30 min at room temperature. The reaction was concentrated under reduced pressure and then placed under high vacuum for 15 min to deliver 2-(2-tosylhydrazono)propanoic acid **1.97** as a white foam which was immediately dissolved in THF (55 mL), cooled to 0  $^\circ\text{C}$  and treated sequentially with pentachlorophenol (1.63 g, 6.12 mmol) and DCC (1.38 g, 6.12 mmol). The resulting cream mixture was stirred at 0  $^\circ\text{C}$  for 3 h during which time it turned yellow and then orange. The reaction was then treated with triethylamine (0.948 mL, 6.68 mmol) and the resulting orange, heterogeneous mixture was stirred for 24 h warming slowly to room temperature. The mixture was filtered through a pad of (washing with 50%  $\text{Et}_2\text{O}$ /hexanes) and the solvent was removed under reduced pressure. The brown viscous residue was purified by chromatography on  $\text{SiO}_2$  (3%  $\text{Et}_2\text{O}$ /hexanes) to deliver perchlorophenyl 2-diazopropanoate **1.100** (0.331 g, 17%) as a yellow solid: IR (ATR) 2984, 2937, 2091 ( $\nu = \text{N}_2$ ), 1722, 1465, 1454, 1392, 1361, 1325, 1064, 712  $\text{cm}^{-1}$ ;  $^1\text{H}$  NMR (300 MHz,  $\text{CD}_2\text{Cl}_2$ )  $\delta$  2.08 (bs, 3 H).



**Perfluorophenyl 2-diazopropanoate (1.99).** *Conditions A:* A solution of *p*-toluenesulfonyl hydrazide (10.7 g, 56.2 mmol) in MeOH (30 mL) was treated with pyruvic acid **S-1.6** (3.95 mL, 56.2 mmol). The resulting clear and colorless solution was stirred at room temperature for 0.5 h then concentrated to deliver 2-(2-tosylhydrazono)propanoic acid **1.97** as a white foam which was immediately dissolved in CH<sub>2</sub>Cl<sub>2</sub> (576 mL), cooled to 0 °C and treated sequentially with DCC (13.9 g, 61.8 mmol) and DMAP (6.87 g, 56.2 mmol). The resulting mixture was stirred at 0 °C for 30 min then treated with pentafluorophenol (11.4 g, 61.8 mmol) in CH<sub>2</sub>Cl<sub>2</sub> (5 mL). The reaction was allowed to stir at 0 °C for 5 h then treated with triethylamine (15.9 mL, 112 mmol) and the resulting yellow mixture was stirred for 12 h while warming slowly to room temperature. The mixture was filtered through a pad of Florisil (washing with CH<sub>2</sub>Cl<sub>2</sub>) and the filtrate was carefully concentrated under reduced pressure. The crude residue was purified by chromatography on SiO<sub>2</sub> (0-2% Et<sub>2</sub>O/hexanes) to deliver **1.99** (2.21 g, 15%) as a yellow oil: IR (ATR) 2940, 2094 (ν=N<sub>2</sub>), 1721, 1655, 1515, 1474, 1338, 1297, 1147, 1055, 992, 713 cm<sup>-1</sup>; <sup>1</sup>H NMR (300 MHz, C<sub>6</sub>D<sub>6</sub>) δ 1.20 (s, 3 H).

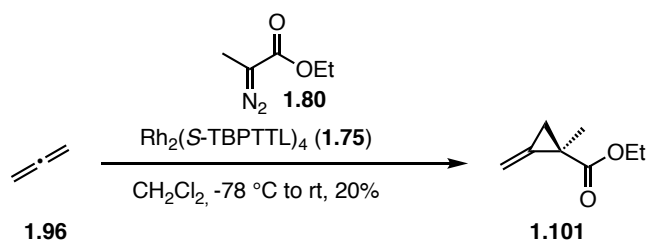
*Conditions B:* A suspension of 2-(2-tosylhydrazono)propanoic acid **1.97** (8.00 g, 31.2 mmol) in CH<sub>2</sub>Cl<sub>2</sub> (336 mL) under an atmosphere of argon (balloon) was cooled to 0 °C and treated sequentially with oxalyl chloride (4.10 mL, 46.8 mmol) and DMF (0.0121 mL, 0.156 mmol) upon the addition of which gas evolution was observed. The resulting suspension was stirred at 0 °C warming to room temperature 24.5 h during which time the white solid gradually

went into solution becoming clear and pale yellow. The reaction was then treated dropwise with a solution of pentafluorophenol (8.62 g, 46.8 mmol) in CH<sub>2</sub>Cl<sub>2</sub> (13 mL) and the resulting clear and pale yellow solution allowed to stir at room temperature for 24 h. The reaction was then treated with NEt<sub>3</sub> (8.87 mL, 62.4 mmol) during the addition of which a white gas evolved and the solution became orange/ yellow color. The resulting orange solution was allowed to stir at room temperature for 26 h then filtered through a pad of florisil (washing with CH<sub>2</sub>Cl<sub>2</sub>) and concentrated. The resulting yellow was purified by chromatography on SiO<sub>2</sub> (0-1% Et<sub>2</sub>O/hexanes) to deliver diazopropanoate **1.99** (1.76 g, 21%) as a yellow oil: <sup>1</sup>H NMR (300 MHz, C<sub>6</sub>D<sub>6</sub>) δ 1.21 (s, 3 H).



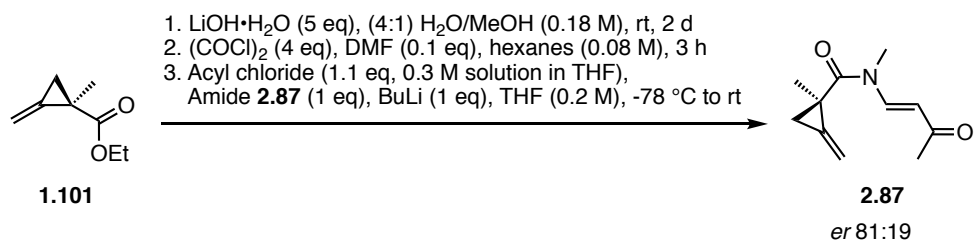
**Ethyl 1-methyl-2-methylenecyclopropane-1-carboxylate (±-1.101).** An oven-dried three neck flask fitted with a nitrogen inlet, a dry-ice condenser and septum was charged with Rh<sub>2</sub>(TPA)<sub>4</sub>•2EtOAc (**1.83**) (0.0060 g, 0.0039 mmol) and CH<sub>2</sub>Cl<sub>2</sub> (3.6 mL) and the resulting green solution cooled to -78 °C and treated dropwise with an excess of condensed allene (**1.96**) (10 drops). The resulting purple/brown solution was then treated with a solution of ethyl diazopropanoate **1.80** (0.10 g, 0.78 mmol) in anhydrous CH<sub>2</sub>Cl<sub>2</sub> (1 mL) via syringe pump at a rate of 1 mL/h. After the addition was complete, the mixture was allowed to warm to room temperature. The reaction was concentrated and the resulting green residue purified by chromatography on SiO<sub>2</sub> (10% Et<sub>2</sub>O/hexanes) to deliver methylenecyclopropane ethyl ester (±)-**1.101** (0.096 g, 88%) as a clear and very pale yellow oil. <sup>1</sup>H NMR analysis of the diastereomeric

Mosher ester derivatives showed an *er* ~50: 50: IR (ATR) 2902, 2978, 2934, 1719, 1459, 1445, 1389, 1379, 1299, 1284, 1171, 1141, 1094, 1031  $\text{cm}^{-1}$ ;  $^1\text{H}$  NMR (400 MHz;  $\text{CDCl}_3$ )  $\delta$  5.45 (t,  $J$  = 2.8 Hz, 1 H), 5.42 (t,  $J$  = 2.0 Hz, 1 H), 4.13 (dq,  $J$  = 10.8, 7.2 Hz, 1 H), 4.09 dq,  $J$  = 10.8, 7.2 Hz, 1 H), 2.01 (dt,  $J$  = 8.9, 2.5 Hz, 1 H), 1.39 (s, 3 H), 1.31 (dt,  $J$  = 8.7, 2.2 Hz, 1 H), 1.23 (t,  $J$  = 7.2 Hz, 3 H);  $^{13}\text{C}$  NMR (100 MHz;  $\text{CDCl}_3$ )  $\delta$  173.7, 137.9, 102.7, 60.9, 23.2, 19.0, 18.9, 14.3; HRMS (ESI+)  $m/z$  calcd for  $\text{C}_8\text{H}_{13}\text{O}_2$  ( $\text{M}+\text{H}$ ) 141.09101, found 141.09199.



**Ethyl (*R*)-1-methyl-2-methylenecyclopropane-1-carboxylate (1.101).** An oven-dried three neck flask fitted with a nitrogen inlet, a dry-ice condenser and septum was charged with  $\text{Rh}_2(\text{S-TBPTTL})_4$  (1.75) (0.029 g, 0.012 mmol) and  $\text{CH}_2\text{Cl}_2$  (6.5 mL) and the resulting green solution cooled to  $-78^\circ\text{C}$  (dry ice, acetone bath) and treated dropwise with an excess of condensed allene gas (1.96) (ca. 0.50 g, 13 mmol). The resulting green solution was then treated with a solution of diazopropanoate 1.80 (0.15 g, 1.17 mmol) in anhydrous  $\text{CH}_2\text{Cl}_2$  (1.2 mL) *via* syringe pump at a rate of approximately 1 mL/h. The resulting solution was allowed to stir at  $-78^\circ\text{C}$  for 1 h before warming to room temperature. The resulting green residue was concentrated and purified by chromatography on  $\text{SiO}_2$  (0-1%  $\text{Et}_2\text{O}$ /hexanes to deliver methylenecyclopropane 1.101 (0.032 g, 20%) as a clear and pale yellow oil:  $^1\text{H}$  NMR (400 MHz;  $\text{CDCl}_3$ )  $\delta$  5.45 (t,  $J$  = 2.8 Hz, 1 H), 5.42 (t,  $J$  = 2.0 Hz, 1 H), 4.13 (dq,  $J$  = 10.8, 7.1 Hz, 1 H), 4.09 dq,  $J$  = 10.8, 7.2 Hz, 1 H), 2.01 (dt,  $J$  = 8.8, 2.4 Hz, 1 H), 1.39 (s, 3 H), 1.31 (dt,  $J$  = 8.8, 2.4 Hz, 1 H), 1.23 (t,  $J$  = 7.2

Hz, 3 H). The *er* was determined to be 81:19 by derivatization as the amide **2.87** using the same protocol developed in the synthesis of (±)-cycloclavine and analyzed by chiral SFC.



SFC resolution of racemic (±)-**2.87** [Chiralpak IC column (250 x 10 mm), gradient elution 5-15% *i*PrOH (rate 1.0), 7 mL/ min, 245 nm, P = 100 (BAR)]:

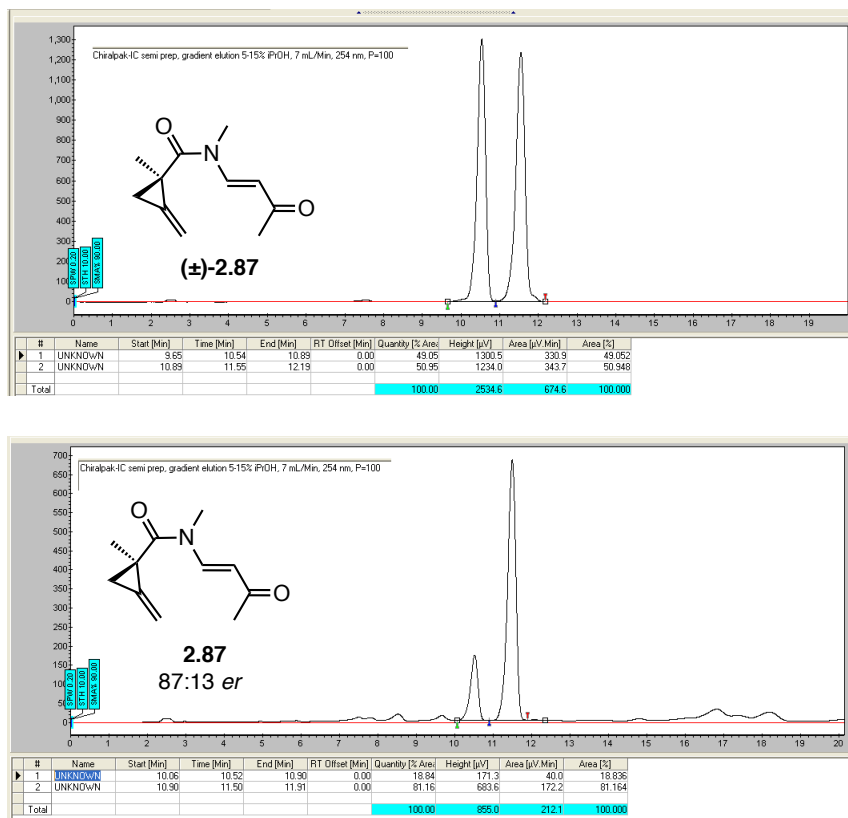
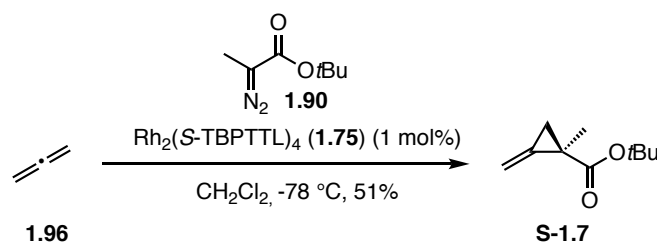
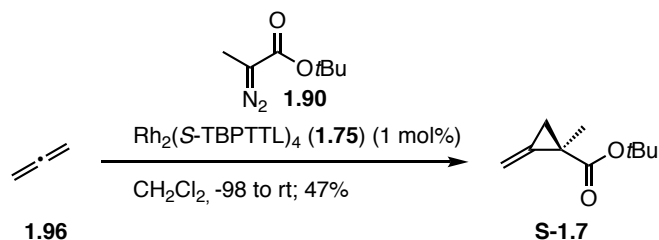


**Figure 3-5** SFC chromatograms of racemic standard and imide derived from enantioenriched ester **1.101**

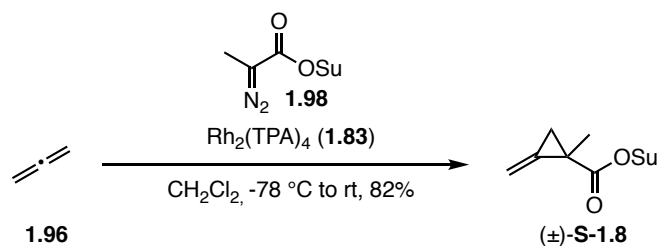




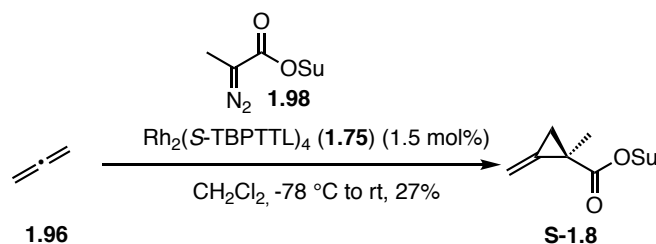
***tert*-Butyl (*R*)-1-methyl-2-methylenecyclopropane-1-carboxylate (S-1.7).** An oven-dried three neck flask fitted with a nitrogen inlet, a dry-ice condenser and septum was charged with  $\text{Rh}_2(\text{S-TBPTTL})_4$  (**1.90**) (0.00803 g, 0.00320 mmol) and  $\text{CH}_2\text{Cl}_2$  (3.2 mL) under an atmosphere of nitrogen. The resulting clear, green solution was cooled to  $-78\text{ }^\circ\text{C}$  and treated dropwise with condensed allene (6 liquid drops, 0.500 g, 12.5 mmol). The clear, purple reaction mixture was then treated with a solution of *tert*-butyl 2-diazopropanoate **1.90** (0.0500 g, 0.320 mmol) in  $\text{CH}_2\text{Cl}_2$  (0.9 mL) slowly at a rate of  $\sim 1\text{ mL/h}$  during which time the solution became brown/ yellow in color. The reaction was stirred at  $-78\text{ }^\circ\text{C}$  for 3 h after which time TLC indicated the complete consumption of the diazo starting material. The reaction was allowed to warm to room temperature and purified directly by chromatography on  $\text{SiO}_2$  (2-5%  $\text{Et}_2\text{O}$ /hexanes) to deliver *tert*-butyl 1-methyl-2-methylenecyclopropane-1-carboxylate **S-1.7** (0.0275 g, 51%) as a clear and colorless oil.  $^1\text{H}$  NMR analysis of the diastereomeric Mosher ester derivatives showed an *er*  $\sim 91: 9$ : IR (ATR) 2978, 2934, 1716, 1478, 1458, 1392, 1368, 1311, 1297, 1256, 1221, 1189, 1141, 1097, 888,  $733\text{ cm}^{-1}$ ;  $^1\text{H}$  NMR (400 MHz;  $\text{CDCl}_3$ )  $\delta$  5.42 (t,  $J = 2.8\text{ Hz}$ , 1 H), 5.37 (t,  $J = 2.0\text{ Hz}$ , 1 H), 1.94 (dt,  $J = 8.8, 2.4\text{ Hz}$ , 1H), 1.41 (s, 9 H), 1.34 (s, 3 H), 1.24 (dt,  $J = 8.8, 2.4\text{ Hz}$ , 1 H);  $^{13}\text{C}$  NMR (100 MHz;  $\text{CDCl}_3$ )  $\delta$  172.9, 138.2, 102.1, 80.4, 28.1, 24.1, 19.0, 18.7; unable to obtain a HRMS on the sample due to volatility issues.



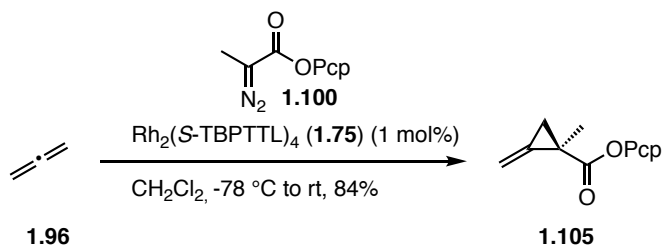
***tert*-Butyl (*R*)-1-methyl-2-methylenecyclopropane-1-carboxylate (S-1.7).** An oven dried three neck flask fitted with a nitrogen inlet, a dry-ice condenser and septum was charged with  $\text{Rh}_2(\text{S-TBPTTL})_4$  (**1.75**) (0.00803 g, 0.00320 mmol) and  $\text{CH}_2\text{Cl}_2$  (3.2 mL) under an atmosphere of nitrogen. The resulting clear, green solution was cooled to ca.  $-98\text{ }^\circ\text{C}$  (external temperature, 2:1  $\text{Et}_2\text{O}$ /pentane liquid  $\text{N}_2$  bath) and treated dropwise with condensed allene (7 drops). The reaction was then treated with a solution of *tert*-butyl 2-diazopropanoate **1.90** (0.0500 g, 0.320 mmol) in  $\text{CH}_2\text{Cl}_2$  (0.9 mL) slowly at a rate of  $\sim 1\text{ mL/h}$  maintaining the external temperature between  $-95$  to  $-98\text{ }^\circ\text{C}$ . The resulting solution was stirred for 1 h maintaining the external temperature below  $-95\text{ }^\circ\text{C}$  after which time TLC indicated major diazo starting material. The reaction was allowed to warm to  $-80\text{ }^\circ\text{C}$  at which point TLC indicated some desired product formation. The reaction was let stir at this temperature for a further 2 h then allowed to warm slowly to room temperature, and concentrated. The resulting residue was filtered through a pad of florisil washing with 10%  $\text{Et}_2\text{O}$ /petroleum ether to deliver methylenecyclopropane **S-1.7** (0.025 g, 47%) as a clear and colorless oil:  $^1\text{H}$  NMR (400 MHz;  $\text{CDCl}_3$ )  $\delta$  5.42 (ap. t,  $J = 2.6\text{ Hz}$ , 1 H), 5.37 (ap. t,  $J = 2.0\text{ Hz}$ , 1 H), 1.94 (dt,  $J = 8.8, 2.4\text{ Hz}$ , 1 H), 1.41 (s, 9 H), 1.34 (s, 3 H), 1.25 (dt,  $J = 8.8, 2.1\text{ Hz}$ , 1 H)



**2,5-Dioxopyrrolidin-1-yl 1-methyl-2-methylenecyclopropane-1-carboxylate (±)-(S-1.8).** An oven-dried three neck flask fitted with a nitrogen inlet, a dry-ice condenser and septum was charged with  $\text{Rh}_2\text{TPA}_4 \cdot 2\text{EtOAc}$  (**1.83**) (0.00388 g, 0.00254 mmol) and  $\text{CH}_2\text{Cl}_2$  (2.5 mL) and the resulting green solution cooled to  $-78\text{ }^\circ\text{C}$  (dry ice/ acetone bath) and treated dropwise with an excess of condensed allene gas **1.96** (0.500 g, 12.5 mmol). The resulting purple/ maroon solution was then treated with a solution of 2,5-dioxopyrrolidin-1-yl 2-diazopropanoate **1.98** (0.100 g, 0.507 mmol) in anhydrous  $\text{CH}_2\text{Cl}_2$  (0.7 mL) *via* syringe pump at a rate of 1 mL/h during which time the solution turned a yellow/brown color. After the addition was complete, the mixture was allowed to warm to room temperature, concentrated and the resulting green oil purified by chromatography on  $\text{SiO}_2$  (60%  $\text{Et}_2\text{O}$ /hexanes) to deliver methylenecyclopropane (±)-**S-1.8** (0.0873 g, 82%) as a clear and pale yellow oil: IR (ATR) 2993, 2984, 1771, 1728, 1428, 1364, 1199, 1064, 1023, 813  $\text{cm}^{-1}$ ;  $^1\text{H}$  NMR (300 MHz;  $\text{CDCl}_3$ )  $\delta$  5.68 (t,  $J = 2.7$  Hz, 1 H), 5.56 (t,  $J = 2.0$  Hz, 1 H), 2.81 (s, 4 H), 2.32 (dt,  $J = 9.3, 2.4$  Hz, 1 H), 1.59 (dt,  $J = 9.3, 2.4$  Hz, 1 H), 1.51 (s, 3 H);  $^{13}\text{C}$  NMR (125 MHz)  $\delta$  169.2, 169.1, 135.3, 105.0, 25.7, 21.3, 20.8, 18.4; DEPT-135 ( $\text{CDCl}_3$ )  $\delta$  105.0 ( $\text{CH}_2$ ), 25.7 ( $\text{CH}_2$ ), 20.8 ( $\text{CH}_2$ ), 18.4 ( $\text{CH}_3$ ); HRMS (ASAP)  $m/z$  calcd for  $\text{C}_{10}\text{H}_{11}\text{NO}_4$  209.0688, found 209.0710.



**2,5-Dioxopyrrolidin-1-yl (*R*)-1-methyl-2-methylenecyclopropane-1-carboxylate (S-1.8).** An oven-dried three neck flask fitted with a nitrogen inlet, a dry-ice condenser and septum was charged with  $\text{Rh}_2(\text{S-TBPTTL})_4$  (**1.75**) (0.0140 g, 0.00560 mmol) and  $\text{CH}_2\text{Cl}_2$  (2.75 mL) and the resulting green solution cooled to  $-87^\circ\text{C}$  (acetone/cryocool) and treated dropwise with an excess of condensed allene gas (0.700 g, 17.5 mmol). The resulting solution was then treated with a solution of 2,5-dioxopyrrolidin-1-yl 2-diazopropanoate (**1.98**) (0.110 g, 0.558 mmol) in anhydrous  $\text{CH}_2\text{Cl}_2$  (0.8 mL) via syringe pump at a rate of 1 mL/h during which time the solution became yellow/green in color. After the addition was complete, the solution was stirred at  $-87^\circ\text{C}$  for 4 h during which time no conversion occurred. The reaction was then allowed to warm to  $-78^\circ\text{C}$  for 2 h after which time  $^1\text{H}$  NMR analysis showed minor conversion to product. Additional catalyst was added (0.00700 g) and the reaction was allowed to warm to room temperature. The reaction was concentrated and purified by chromatography on  $\text{SiO}_2$  (25-30% EtOAc/hexanes) to deliver 2,5-dioxopyrrolidin-1-yl 1-methyl-2-methylenecyclopropane-1-carboxylate **S-1.8** (0.0310 g, 27%) as a clear and pale yellow oil:  $^1\text{H}$  NMR analysis of the diastereomeric Mosher ester derivatives showed an *er* ~77:23.  $^1\text{H}$ -NMR (400 MHz;  $\text{CDCl}_3$ )  $\delta$  5.67 (t,  $J = 2.8$  Hz, 1 H), 5.55 (t,  $J = 2.2$  Hz, 1 H), 2.80 (s, 4 H), 2.30 (dt,  $J = 9.2, 2.4$  Hz, 1 H), 1.58 (dt,  $J = 9.4, 2.5$  Hz, 1 H), 1.50 (s, 3 H).



**Perchlorophenyl (*R*)-1-methyl-2-methylenecyclopropane-1-carboxylate (1.105).** An oven-dried three neck flask fitted with a nitrogen inlet, a dry-ice condenser and septum was charged with  $\text{Rh}_2(\text{S-TBPTTL})_4$  (**1.75**) (0.0413 g, 0.0165 mmol) and  $\text{CH}_2\text{Cl}_2$  (8.0 mL) and the resulting green solution cooled to  $-78^\circ\text{C}$  and treated dropwise with an excess of condensed allene gas **1.96** (0.570 g, 14.2 mmol). The resulting green solution was then treated with a solution of perchlorophenyl 2-diazopropanoate (**1.100**) (0.574 g, 1.65 mmol) in anhydrous  $\text{CH}_2\text{Cl}_2$  (2.9 mL) via syringe pump at a rate of 1 mL/h. The resulting solution was allowed to stir at  $-78^\circ\text{C}$  for 1.5 h before warming to room temperature. The residue was purified by chromatography on  $\text{SiO}_2$  (0-3%  $\text{Et}_2\text{O}$ /hexanes) to deliver methylenecyclopropane **1.105** (0.496 g, 84%) as a white solid.  $^1\text{H}$  NMR analysis of the diastereomeric Mosher ester derivatives showed an *er* ~77:23: MP  $106.2\text{--}108.5^\circ\text{C}$ ; IR (ATR) 2973, 2934, 1745, 1442, 1388, 1361, 1288, 1255, 1214, 1134, 1103, 1086, 1033, 984, 955, 905, 888, 767  $\text{cm}^{-1}$ ;  $^1\text{H}$  NMR (500 MHz;  $\text{CD}_2\text{Cl}_2$ )  $\delta$  5.67 (t,  $J = 2.8$  Hz, 1 H), 5.58 (t,  $J = 2.0$  Hz, 1 H), 2.37 (dt,  $J = 9.5, 2.5$  Hz, 1 H), 1.63 (dt,  $J = 9.3, 2.5$  Hz, 1 H), 1.53 (s, 3 H);  $^{13}\text{C}$  NMR (100 MHz;  $\text{CD}_2\text{Cl}_2$ )  $\delta$  170.0, 144.9, 136.8, 132.4, 131.7, 128.4, 104.5, 23.4, 20.4, 18.8; DEPT-135 ( $\text{CD}_2\text{Cl}_2$ , 125 MHz)  $\delta$  104.5 ( $\text{CH}_2$ ), 20.4 ( $\text{CH}_2$ ), 18.8 ( $\text{CH}_3$ ); HRMS (ASAP)  $m/z$  calcd for  $\text{C}_{12}\text{H}_8\text{O}_2\text{Cl}_5$  358.8967, found 358.8938. Crystalline **1.105** was submitted for X-ray analysis. Recrystallization of enantiomerically enriched **1.105** resulted in enrichment of the mother liquor. After 2 x recrystallization from boiling heptanes and 1x recrystallization from boiling 1,2-DCE the mother liquor was enriched to ~90: 10 *er* as determined by SFC analysis of the amide derivative **2.87**.

SFC resolution of racemic **2.87** [Chiralpak IC column (250 x 4.6 mm), gradient elution 1% *i*PrOH (hold for 5 min), 2% *i*PrOH (hold for 5 min), 3% *i*PrOH (hold for 6 min), 4% *i*PrOH (hold for 3 min), 4.50% *i*PrOH (hold for 2 min), 5% *i*PrOH (hold for 3 min), 4 mL/min, 254 nm, P=110 (BAR)]:

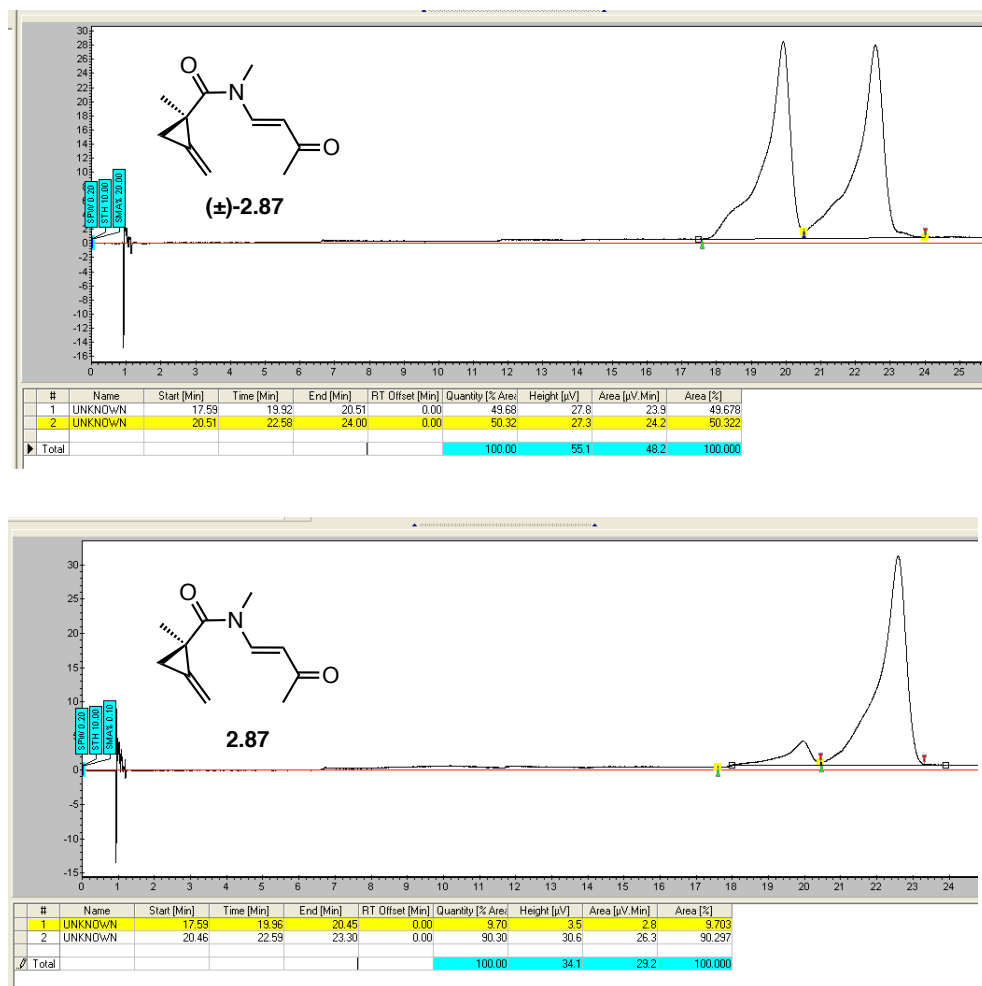
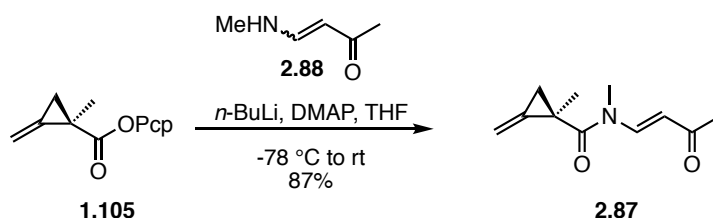


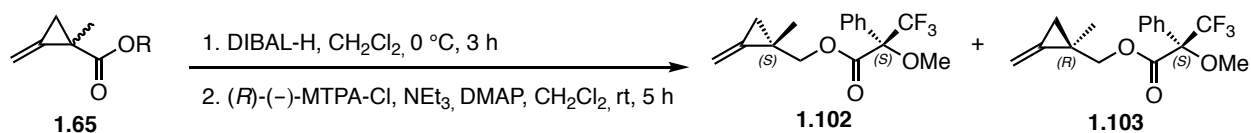
**Figure 3-6** SFC chromatograms of racemic standard and imide **2.87** derived from enantioenriched mother liquor sample of methylenecyclopropane **1.105**



**(*R,E*)-*N*,1-Dimethyl-2-methylene-*N*-(3-oxobut-1-en-1-yl)cyclopropane-1-**

**carboxamide (2.87).** A flask containing vinylogous amide **2.88** (0.0046 g, 0.046 mmol) was evacuated and backfilled with nitrogen. Freshly distilled THF (0.40 mL) was added and the resulting solution cooled to -78 °C and treated dropwise with *n*-BuLi (0.020 mL, 2.5 M solution in hexanes, 0.049 mmol) stirred for 5 min at -78°C then treated with a solution of pentachlorophenol ester **1.105** (0.018 g, 0.051 mmol) in THF (0.25 mL). The resulting solution was then treated with DMAP (0.00057 g, 0.0046 mmol) and stirred for 30 min at -78 °C. TLC analysis of the reaction mixture indicated product formation. The cold bath was removed and the reaction was warmed to room temperature. The reaction was directly subjected to purification by chromatography on SiO<sub>2</sub> (10-20% EtOAc/Hexanes) to deliver vinylogous amide **2.87** (0.0078 g, 87%) as a clear and colorless oil: <sup>1</sup>H NMR (300 MHz; CDCl<sub>3</sub>) δ 8.36 (d, *J* = 13.8 Hz, 1 H), 5.64 (d, *J* = 13.8 Hz, 1 H), 5.64 (ap. t, *J* = 2.7 Hz, 1 H), 5.53 (s, 1 H), 3.15 (s, 3 H), 2.29 (s, 3 H), 1.80 (dt, *J* = 9.6, 2.4 Hz, 1 H), 1.49 (s, 3 H), 1.33 (dt, *J* = 9.6, 2.3 Hz, 1 H).

**Mosher-acid chloride derivatization, representative procedure:**



**(1-Methyl-2-methylenecyclopropyl)methyl**

**(2*S*)-3,3,3-trifluoro-2-methoxy-2-**

**phenylpropanoate (1.102 and 1.103).** A solution of ethyl 1-methyl-2-methylenecyclopropane-1-carboxylate (**1.65**) (0.020 g, 0.14 mmol) in CH<sub>2</sub>Cl<sub>2</sub> (1 mL) was cooled to 0 °C, treated with

DIBAL-H (0.39 mL, 1 M solution in hexanes, 0.39 mmol) and stirred at 0 °C for 3 h. The reaction mixture was treated successively with H<sub>2</sub>O (15 µL), 15% NaOH (15 µL) and H<sub>2</sub>O (39 µL), dried (MgSO<sub>4</sub>) and filtered through a pad of Celite washing with EtOAc and concentrated. A solution of crude alcohol in CH<sub>2</sub>Cl<sub>2</sub> (1.1 mL) under an inert atmosphere was treated sequentially with a solution of (*R*)-(-)-MTPA-Cl<sup>47</sup> (0.028, 0.11 mmol) in CH<sub>2</sub>Cl<sub>2</sub> (0.5 mL), anhydrous NEt<sub>3</sub> (0.023 mL, 0.17 mmol) and DMAP (0.00070 g, 0.0055 mmol). The resulting clear and colorless solution was stirred at room temperature for 5 h after which time TLC analysis indicated complete consumption of the alcohol starting material. The reaction was filtered through a small pad of Florisil (washing with 30% Et<sub>2</sub>O/hexanes) and concentrated. <sup>1</sup>H NMR analysis of the crude reaction mixture showed a 1:1 mixture of ester diastereomers **1.102** and **1.103**.

**Racemic standard (500 MHz, CDCl<sub>3</sub>)**

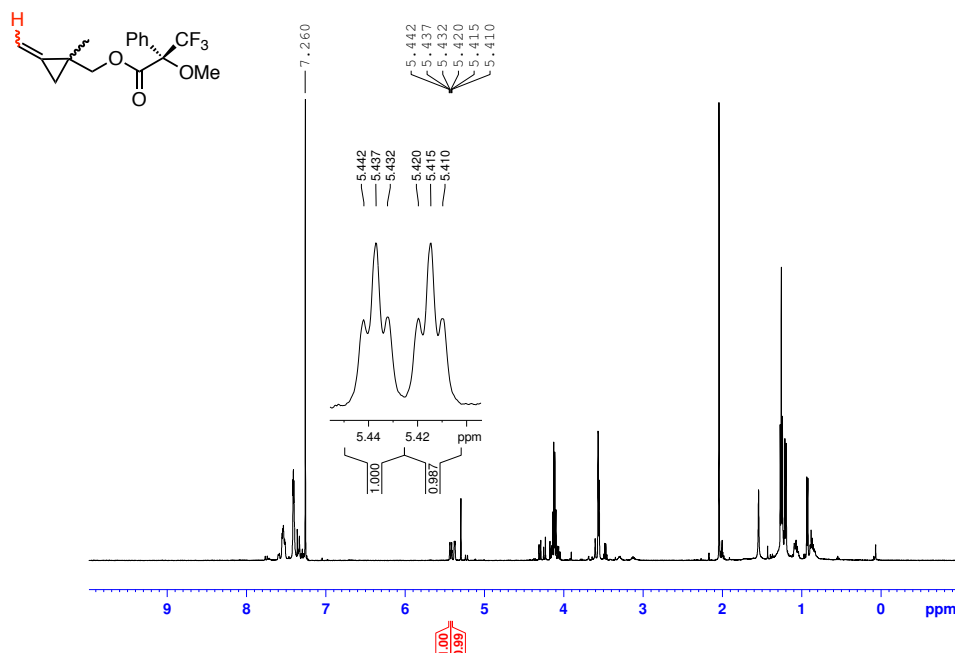


**Figure 3-7** Mosher ester derivative: racemic standard



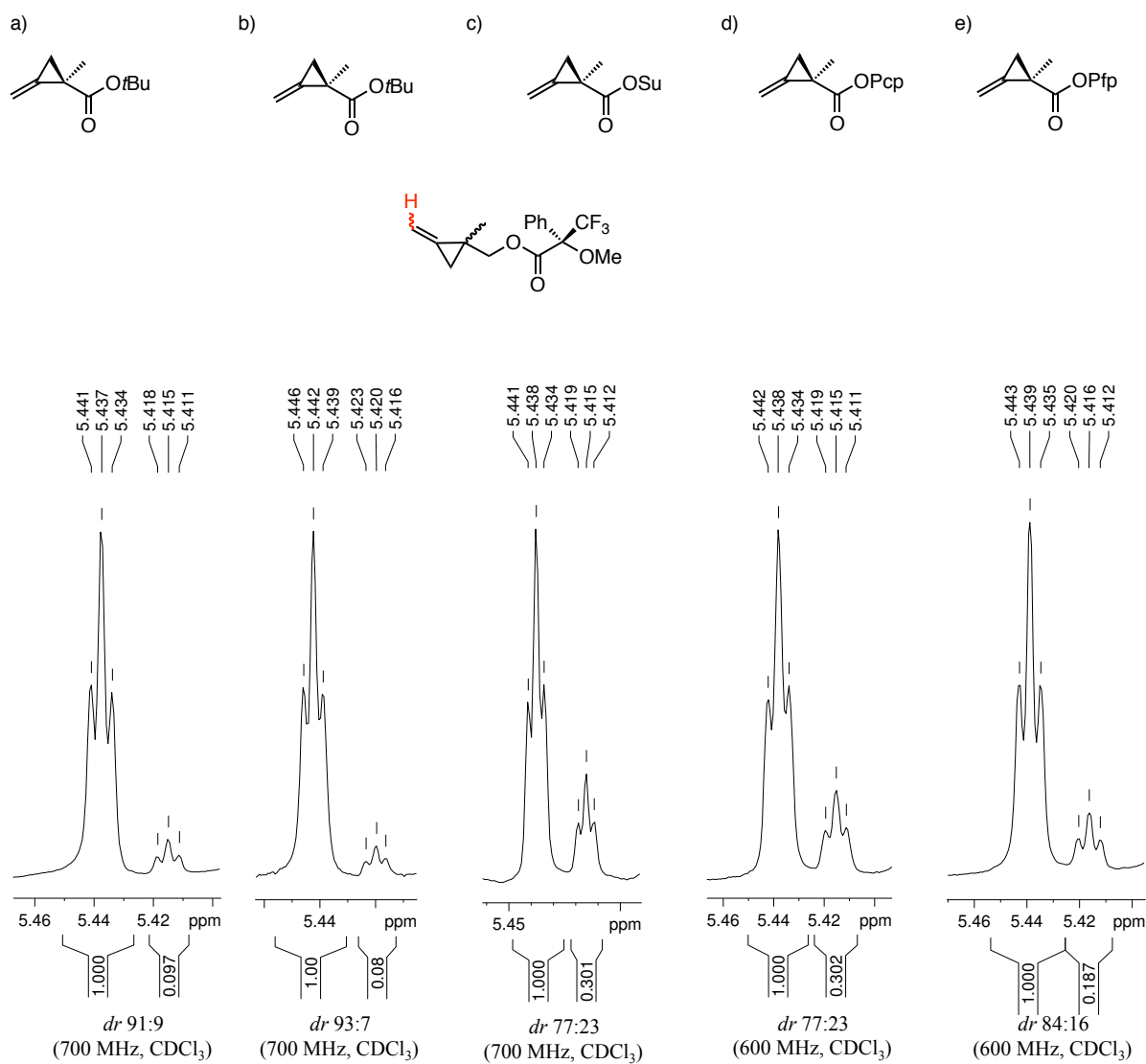
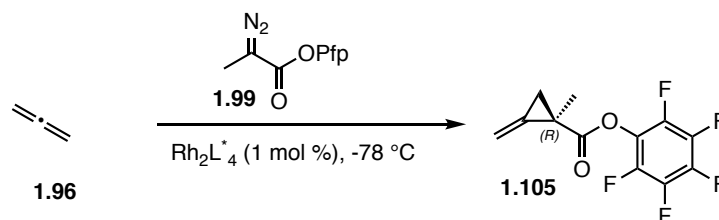


**Figure 3-8** Enantioenriched Mosher ester derivatives

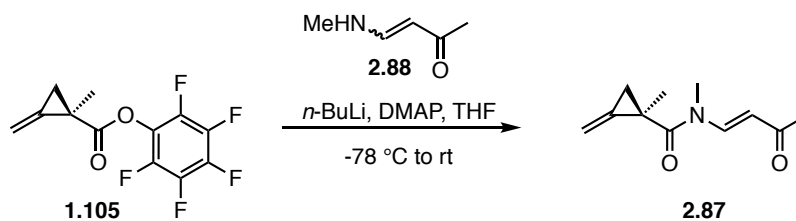
a) *t*-Butyl derivative (Table 1-3, entry 2, 700 MHz,  $\text{CDCl}_3$ ); (b) *t*-butyl derivative (Table 1-3, entry 3, 700 MHz,  $\text{CDCl}_3$ ); (c) succinimide derivative (Table 1-3, entry 6, 700 MHz); (d) pentachlorophenyl derivative (Table 1-3, entry 7, 600 MHz,  $\text{CDCl}_3$ ); pentafluorophenyl derivative (Table 1-3, entry 8, 600 MHz,  $\text{CDCl}_3$ ).

### Catalyst Screen: General Protocol for the Asymmetric Cyclopropanation of Allene:



**Perfluorophenyl (*R*)-1-methyl-2-methylenecyclopropane-1-carboxylate (1.105).** An oven-dried three neck flask charged with catalyst (0.0056 mmol) and hexanes or  $\text{CH}_2\text{Cl}_2$  (2.8 mL) and the resulting green solution was cooled to  $-78\text{ }^\circ\text{C}$  and treated dropwise with a large excess of condensed allene gas (1.96) (14 mmol). The reaction was then treated with a solution of perfluorophenyl 2-diazopropionate (1.99) (0.56 mmol) in hexanes or  $\text{CH}_2\text{Cl}_2$  (1.7 mL) via syringe pump at a rate of 1 mL/ h. After the addition was complete, the mixture was allowed to warm to room temperature. The reaction was concentrated under reduced pressure and the resulting residue purified by chromatography on  $\text{SiO}_2$  (0-2%  $\text{Et}_2\text{O}/\text{Hex}$ ) to deliver methylenecyclopropane (1.105):  $^1\text{H}$  NMR (400 MHz,  $\text{CD}_2\text{Cl}_2$ )  $\delta$  5.64 (t,  $J = 2.8$  Hz, 1 H), 5.56 (t,  $J = 2.2$  Hz, 1 H), 2.30 (dt,  $J = 9.2, 2.5$  Hz, 1 H), 1.63 (dt,  $J = 9.2, 2.4$  Hz, 1 H), 1.51 (s, 3 H).

### Catalyst Screen: General protocol for the conversion of methylenecyclopropanes to vinylogous imide 2.87 to assess enantiomeric excess:



**(*R,E*)-*N*,1-Dimethyl-2-methylene-*N*-(3-oxobut-1-en-1-yl)cyclopropane-1-carboxamide (2.87).** An oven-dried flask charged with vinylogous amide 2.87 (0.18 mmol, 1.0 eq.) was evacuated and backfilled with nitrogen (3x). Freshly distilled THF (0.6 mL) was added

and the resulting solution was cooled to -78 °C and treated dropwise with *n*-BuLi (2.29 M solution in hexanes, 0.19 mmol, 1.05 eq.). The resulting clear, pale yellow solution was stirred for 5 min at -78 °C, then treated with a solution of ester **1.105** (0.19 mmol, 1.05 eq) in THF (1 mL). The resulting bright yellow solution was treated with DMAP (0.19 mmol, 0.1 eq.) and stirred for 10 min at -78 °C. The cold bath was removed and the reaction mixture was allowed to stir, warming to room temperature. The reaction was quenched with sat. NaHCO<sub>3</sub>. After addition of EtOAc, the aqueous layer was extracted with EtOAc (3x) and the combined organic layers were dried (Na<sub>2</sub>SO<sub>4</sub>) and concentrated. The crude product was purified by chromatography on SiO<sub>2</sub> (10-15% EtOAc/hexanes) to deliver vinylogous imide **2.87** as a clear, pale yellow oil: <sup>1</sup>H NMR (300 MHz, CDCl<sub>3</sub>) δ 8.36 (d, *J* = 13.8 Hz, 1 H), 5.71 (d, *J* = 13.8 Hz, 1 H), 5.69 (ap. t, *J* = 3.0 Hz, 1 H), 5.53 (ap. s, 1 H), 3.15 (s, 3 H), 2.29 (s, 3 H), 1.79 (dt, *J* = 9.6, 2.2 Hz, 1 H), 1.49 (s, 3 H), 1.32 (dt, *J* = 9.6, 2.2 Hz, 1 H).

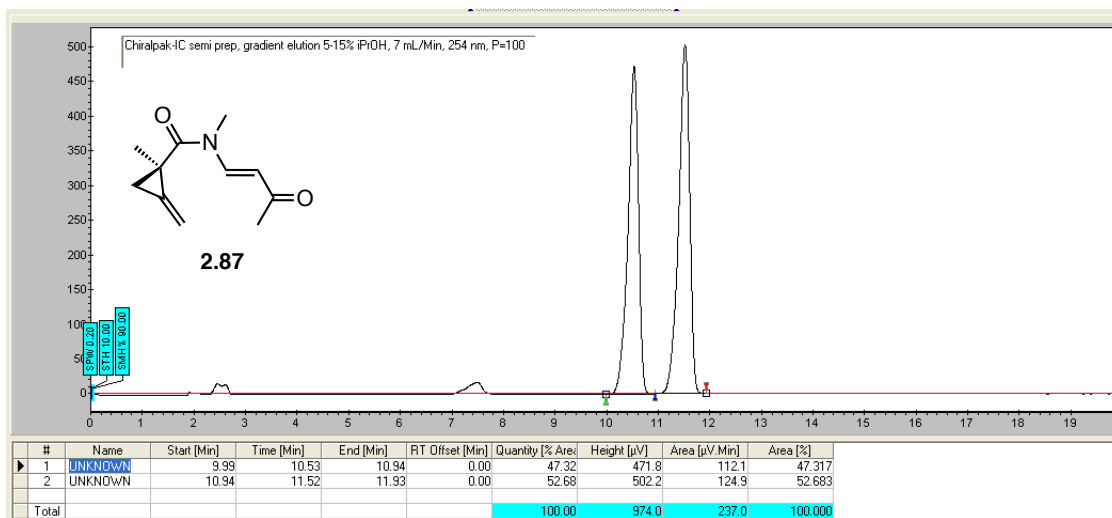


**Figure 3-9** SFC chromatogram of imide **2.87** derived from the reaction with Rh<sub>2</sub>(*R*-DOSP)<sub>4</sub>

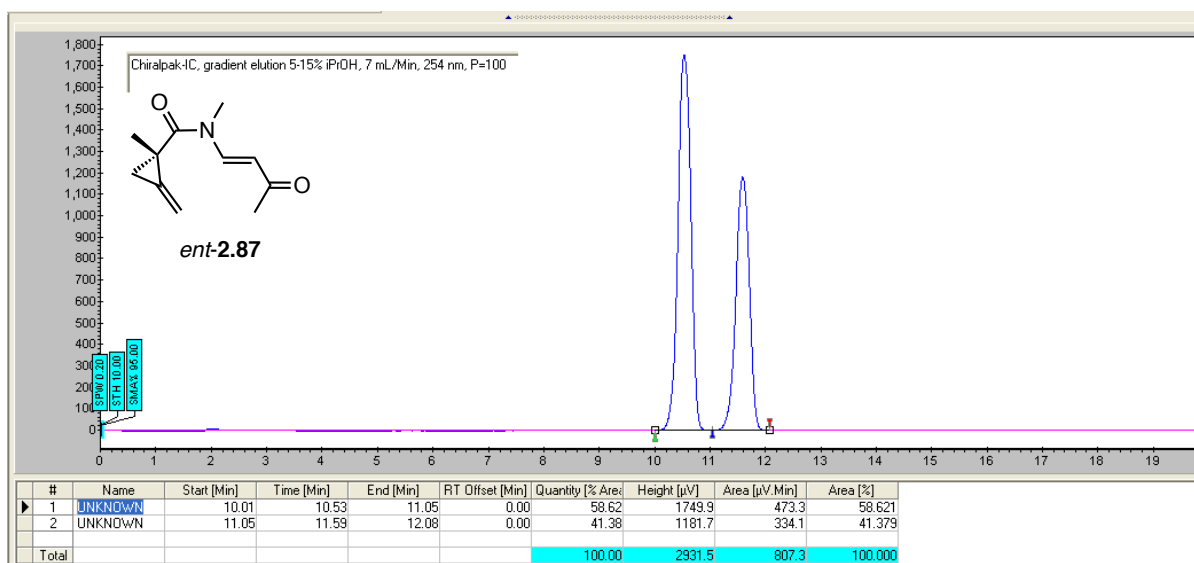


Figure 3-10 SFC chromatogram of imide **2.87** derived from the reaction with  $\text{Rh}_2(R\text{-BTCP})_4$

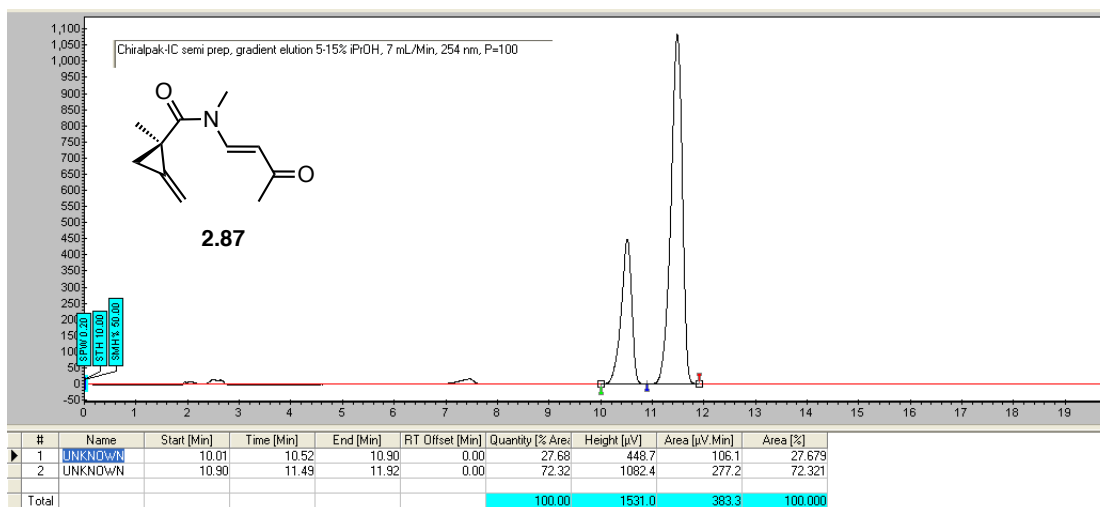


Figure 3-11 SFC chromatogram of imide **2.87** derived from the reaction with  $\text{Rh}_2(S\text{-PTTL})_4$

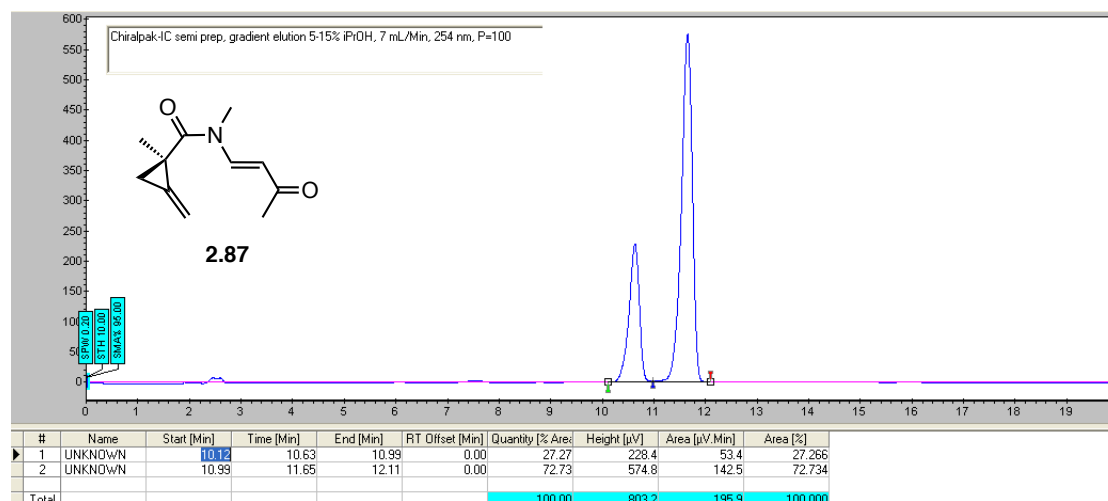
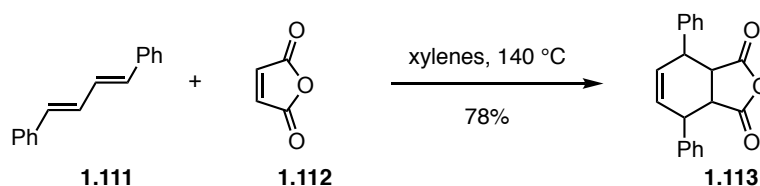
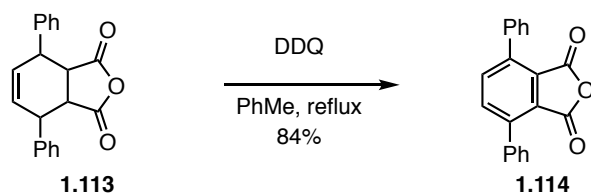


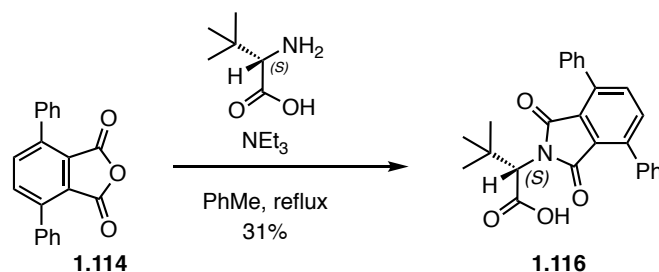
Figure 3-12 SFC chromatogram of imide **2.87** derived from the reaction with  $\text{Rh}_2(\text{S-PTAD})_4$



**4,7-Diphenyl-3a,4,7,7a-tetrahydroisobenzofuran-1,3-dione (1.113).** A clear, yellow solution of butadiene **1.111** (2.0 g, 9.6 mmol) and maleic anhydride **1.112** (1.1 g, 11 mmol) in xylenes (25 mL) was heated at 140 °C for 16 h. After this time, the reaction was cooled to 0 °C and the resulting white precipitate filtered to afford Diels-Alder adduct **1.113** (2.29 g, 78%) as a white solid:  $^1\text{H}$  NMR (500 MHz,  $\text{CDCl}_3$ )  $\delta$  7.43 (ap. t,  $J = 7.3$  Hz, 4 H), 7.39-7.36 (m, 6 H), 6.56 (s, 2 H), 3.84 (d,  $J = 4.0$  Hz, 2 H), 3.74, dd,  $J = 4.5, 2.0$  Hz, 2 H). The experimental data was consistent with the literature-reported data.<sup>133</sup>

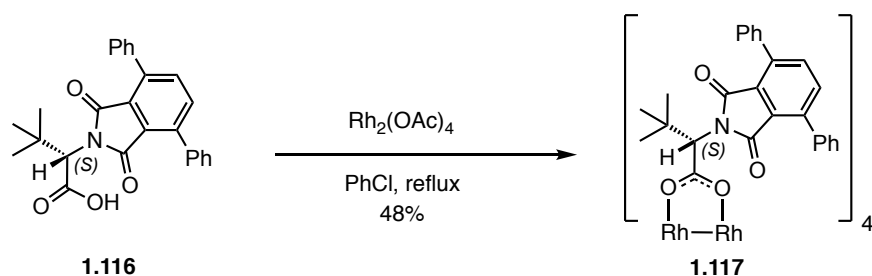


**4,7-Diphenylisobenzofuran-1,3-dione (1.114).** A red solution of anhydride **1.113** (1.0 g, 3.3 mmol) and DDQ (1.5 g, 6.6 mmol) in toluene (10 mL) was heated at 110 °C for 17 h. The reaction was concentrated and filtered washing with copious amounts of EtOH to deliver crude 4,7-diphenylisobenzofuran-1,3-dione **1.114** (0.832 g, 84%) as a light pink solid that was used directly:  $^1\text{H}$  NMR (300 MHz,  $\text{CDCl}_3$ )  $\delta$  7.85 (s, 2 H), 7.61-7.57 (m, 4 H), 7.54-7.51 (m, 6H). The experimental data was consistent with the literature-reported data.<sup>133</sup>



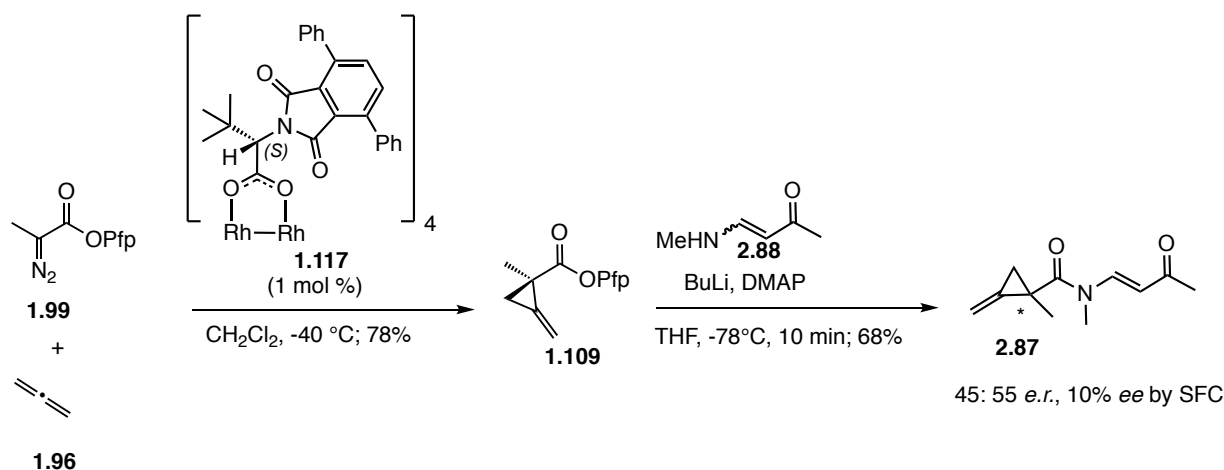
**(S)-2-(1,3-Dioxo-4,7-diphenylisoindolin-2-yl)-3,3-dimethylbutanoic acid (1.116).** An oven-dried microwave vial was charged sequentially with 4,7-diphenylisobenzofuran-1,3-dione (**1.114**) (0.300 g, 1.00 mmol), *L-tert*-leucine (0.199 g, 1.50 mmol) and triethylamine (0.0283 mL, 0.200 mmol) and the resulting heterogeneous brown solution heated at reflux for 19 h. The solution was cooled to room temperature, treated with 5% HCl and EtOAc. The separated aqueous layer was extracted with EtOAc (3x) and the combined organic layers, dried ( $\text{Na}_2\text{SO}_4$ ), filtered and concentrated. The resulting residue was purified by chromatography on  $\text{SiO}_2$  (0-20% Acetone/ $\text{CH}_2\text{Cl}_2$ ) to deliver carboxylic acid **1.116** (0.128 g, 31%) as a white foam: M.p. 142.7-

145 °C;  $[\alpha]_D^{19} -10.6$  ( $c$  0.17,  $\text{CHCl}_3$ ); IR (ATR) 2963, 1770, 1710, 1603, 1475, 1382, 1122, 903, 752, 698  $\text{cm}^{-1}$ ;  $^1\text{H}$  NMR (300 MHz,  $\text{CDCl}_3$ )  $\delta$  7.67 (s, 2 H), 7.56 (ap. dd,  $J = 7.6, 1.9$  Hz, 4 H), 7.52-7.45 (m, 6 H), 4.68 (s, 1 H), 1.14 (s, 9 H);  $^{13}\text{C}$  NMR (100 MHz,  $\text{CDCl}_3$ )  $\delta$  172.3, 167.3, 140.4, 136.5, 136.3, 129.6, 128.9, 128.3, 128.1, 60.0, 35.8, 28.2; HRMS (LCMS ESI+)  $m/z$  calcd for  $\text{C}_{26}\text{H}_{24}\text{NO}_4$  ( $\text{M}+\text{H}$ ) 414.1700, found 414.1698.



**Tetrakis(*S*)-2-(1,3-dioxo-4,7-diphenylisoindolin-2-yl)-3,3-dimethylbutanoic acid dirhodium(II) complex (1.117).** A microwave vial was charged with (*S*)-2-(1,3-dioxo-4,7-diphenylisoindolin-2-yl)-3,3-dimethylbutanoic acid **1.116** (0.090 g, 0.22 mmol),  $\text{Rh}_2(\text{OAc})_4$  (0.016 g, 0.036 mmol) and chlorobenzene (0.5 mL) and the resulting green solution heated at 145 °C (external temperature, oil bath). After heating overnight, the reaction was cooled and concentrated. The resulting green residue was purified by chromatography on  $\text{SiO}_2$  (0-2% acetone/ $\text{CH}_2\text{Cl}_2$ ) to deliver a green residue which was taken up in EtOAc and concentrated to deliver the bis EtOAc adduct **1.117** (35.5 mg, 48%) as an emerald green crystalline solid: M.p. 280-282.9 °C (dec.);  $[\alpha]_D^{20} +217$  ( $c$  0.03,  $\text{CHCl}_3$ ); IR (ATR) 2944, 1716, 1606, 1509, 1353, 1226, 1046, 737  $\text{cm}^{-1}$ ;  $^1\text{H}$  NMR (500 MHz,  $\text{CDCl}_3$ )  $\delta$  7.52 (bs, 8 H), 7.44-7.33 (m, 40 H), 4.20 (s, 4 H), 4.12 (q,  $J = 7.3$  Hz, 4 H, EtOAc), 2.04 (s, 6 H, EtOAc), 1.23 (t,  $J = 7.0$  Hz, 6 H, EtOAc), 0.84 (s, 36 H);  $^{13}\text{C}$  NMR (125 MHz,  $\text{CDCl}_3$ )  $\delta$  187.4 (8C), 171.9 (4C), 166.3 (4C), 166.1 (4C), 140.0 (4C), 139.3 (4C), 136.8 (8C), 136.3 (4C), 135.3 (4C), 129.9 (8 C), 128.2 (16C), 127.8

(16C), 60.7 (EtOAc), 60.6 (4C), 35.6 (4C), 28.2 (12C), 21.2 (EtOAc), 14.3 (EtOAc); HRMS (ESI+)  $m/z$  calcd for  $C_{104}H_{89}O_{16}N_4Rh_2$  (M+H) 1855.43782, found 1855.43183.



**Perfluorophenyl (S)-1-methyl-2-methylenecyclopropane-1-carboxylate (1.109).** An oven-dried three neck flask was charged with dirhodium catalyst **1.117** (0.0114 g, 0.00562 mmol) and  $CH_2Cl_2$  (2.8 mL) and the resulting green solution was cooled to  $-78\text{ }^{\circ}C$  (acetone/ dry ice bath) and treated dropwise with an large excess of condensed allene gas (10 drops,  $\sim 0.99$  g removed from lecture bottle, 24.7 mmol). The light grey reaction was then treated with perfluorophenyl 2-diazopropanoate **1.99** (0.150 g, 0.562 mmol) in  $CH_2Cl_2$  (1.7 mL) via syringe pump at a rate of 1 mL/h maintaining the temperature at  $-78\text{ }^{\circ}C$ . After the addition was complete TLC analysis showed starting material. The reaction was allowed to stir for a further hour at  $-78\text{ }^{\circ}C$  after which time TLC showed major starting material. Starting material was also observed after warming to  $-60\text{ }^{\circ}C$  for 30 min. After warming to  $-40\text{ }^{\circ}C$  for 30 min some conversion to a new spot was observed. After a further 30 min at  $-40\text{ }^{\circ}C$  full conversion was observed by TLC. The reaction was removed from the cold bath and allowed to warm to room temperature. The solvent was removed under reduced pressure and the residue was purified by chromatography on  $SiO_2$  (0-2%  $Et_2O$ /hexanes) to deliver perfluorophenyl 1-methyl-2-methylenecyclopropane-1-carboxylate **1.109** (0.121 g, 78%) as a clear and colorless oil:  $^1H$  NMR (300 MHz,  $CDCl_3$ )  $\delta$  5.64



(ap.t  $J = 2.7$  Hz, 1 H), 5.57 (ap. t,  $J = 2.1$  Hz, 1 H), 2.31 (dt,  $J = 9.1, 2.5$  Hz, 1 H), 1.61 (dt,  $J = 9.1, 2.5$  Hz, 1 H), 1.53 (s, 3 H).

**((S,E)-N,1-Dimethyl-2-methylene-N-(3-oxobut-1-en-1-yl)cyclopropane-1-carboxamide (2.87).** An oven-dried round bottom flask charged with vinylogous amide **2.88** (0.020 g, 0.20 mmol) was evacuated and backfilled with nitrogen (3x). Freshly distilled THF (1 mL) was added and the solution was cooled to  $-78$  °C (dry ice/acetone bath) and treated dropwise with *n*-BuLi (0.085 mL, 2.5 M solution in hexanes, 0.21 mmol) and stirred for 5 min at  $-78$  °C. The reaction was then treated dropwise with a solution of perfluorophenyl 1-methyl-2-methylenecyclopropane-1-carboxylate **1.109** (0.059 g, 0.21 mmol) in THF (0.5 mL) and then DMAP (0.0025 g, 0.020 mmol) and stirred for 10 min at  $-78$  °C. The cold bath was removed, allowing the reaction to warm to room temperature. The reaction was quenched with  $\text{NaHCO}_3$  and EtOAc was added. The separated aqueous phase was extracted with EtOAc (3x) and the combined organic phases were dried ( $\text{Na}_2\text{SO}_4$ ) and concentrated. The resulting residue was purified by chromatography on  $\text{SiO}_2$  (10-15% EtOAc/hexanes) to deliver ((S,E)-N,1-dimethyl-2-methylene-N-(3-oxobut-1-en-1-yl)cyclopropane-1-carboxamide **2.87** (0.0266 g, 0.138 mmol, 68%, *er* 45:55, 10% *ee*) as a clear and pale yellow oil:  $^1\text{H}$  NMR (300 MHz,  $\text{CDCl}_3$ )  $\delta$  8.37 (d,  $J = 13.8$  Hz, 1 H), 5.71 (d,  $J = 13.8$  Hz, 1 H), 5.70 (ap. d,  $J = 2.7$  Hz, 1 H), 5.53 (s, 1 H), 3.16 (s, 3 H), 2.29 (s, 3 H), 1.80 (dt,  $J = 9.6, 2.4$  Hz, 1 H), 1.50 (s, 3 H), 1.33 (dt,  $J = 9.7, 2.3$  Hz, 1 H). SFC conditions: Chiralpak-IC semi-prep column (250 x 10mm), gradient elution: 5-15% (rate 1.0), 7 mL/min, 254 nm, P=100 (BAR).

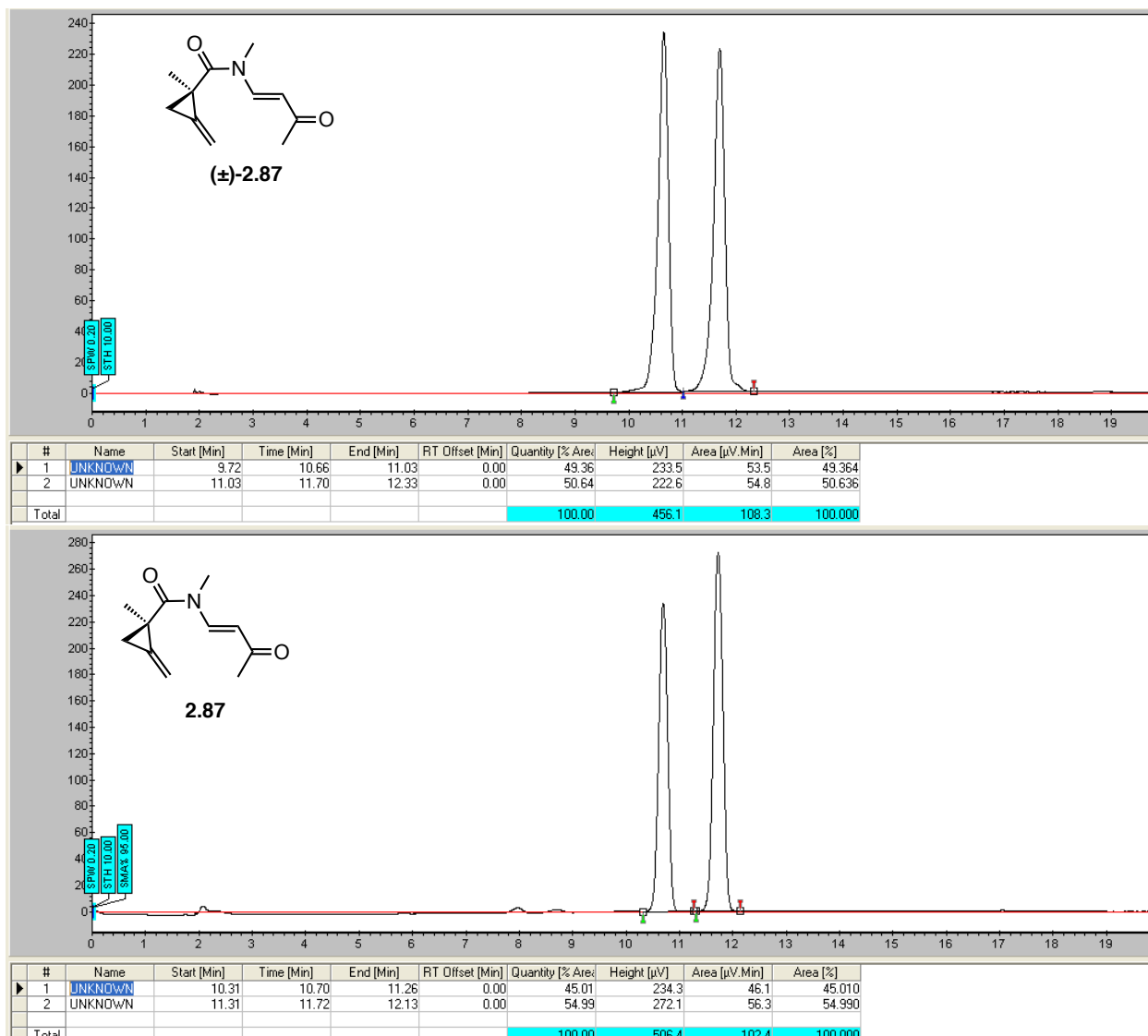
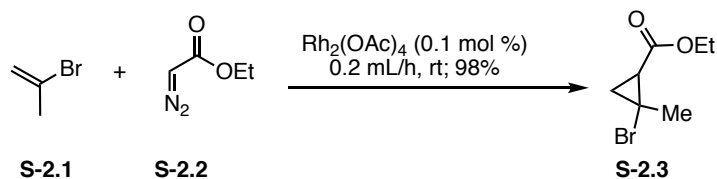
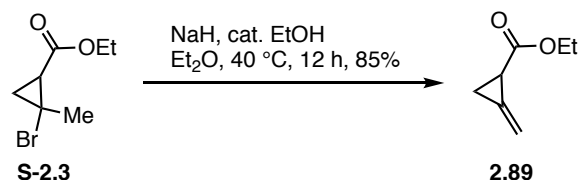


**Figure 3-13** SFC chromatograms of racemic standard and imide **2.87** derived from the cyclopropanation with dirhodium catalyst **1.117**

### 3.2.2 CHAPTER TWO EXPERIMENTAL PART: (±)-2.1

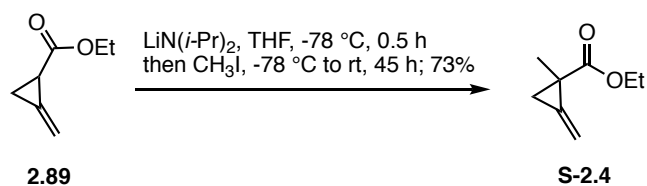


**Ethyl 2-bromo-2-methylcyclopropanecarboxylate (S-2.3).** An oven dried flask was charged with  $\text{Rh}_2(\text{OAc})_4$  (0.0695 g, 0.157 mmol) and 2-bromopropene **S-2.1** (30.4 mL, 343 mmol) under an atmosphere of nitrogen was treated with ethyl diazoacetate **S-2.2** (19.0 mL, 87% purity, 157 mmol) *via* syringe pump at a rate of 0.2 mL/ h. After the addition was complete the crude product was filtered through a pad of silica, washed with  $\text{Et}_2\text{O}$  and concentrated under reduced pressure to yield ester **S-2.3** (31.7 g, 98%) as a clear and yellow oil and mixture of diastereomers which was used directly:  $^1\text{H}$  NMR (400 MHz,  $\text{CDCl}_3$ )  $\delta$  4.21 (dq,  $J = 7.1, 1.3$  Hz, 2 H), 4.16 (q,  $J = 7.1$  Hz, 2 H), 2.30 (dd,  $J = 9.6, 6.8$  Hz, 1 H), 1.87 (s, 3 H), 1.84 (s, 3 H), 1.80-1.74-1.57 (m, 3 H), 1.44 (t,  $J = 6.6$  Hz, 1 H), 1.30 (t,  $J = 7.2$  Hz, 3 H), 1.29 (t,  $J = 7.0$  Hz, 3 H), 1.23 (dd,  $J = 6.4, 4.4$  Hz, 1 H);  $^{13}\text{C}$  NMR (125 MHz)  $\delta$  170.4, 169.5, 61.3, 61.2, 33.5, 33.1, 30.9, 29.8, 28.9, 24.5, 24.0, 23.1, 14.5, 14.4. The experimental  $^1\text{H}$  NMR was consistent with the literature-reported data.<sup>93</sup>



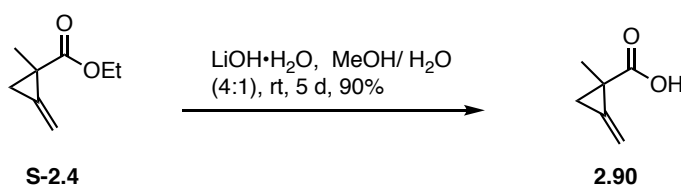
**Ethyl 2-methylenecyclopropanecarboxylate (2.89).** An oven-dried flask was charged with NaH (4.21 g, 158 mmol) and anhydrous diethyl ether (110 mL) under an atmosphere of

nitrogen and treated dropwise with carboxylic acid **S-2.3** (18.5 g, 89.1 mmol). The resulting light brown slurry was heated to reflux and treated dropwise with a catalytic amount of freshly distilled ethanol (1.15 mL, 19.6 mmol) upon the addition of which the solution immediately turned deep red/ brown in color. The resulting mixture was let stir at reflux overnight. The reaction was diluted with Et<sub>2</sub>O, filtered through a pad of Celite and concentrated under reduced pressure in an ice bath. The crude product was then distilled under reduced pressure (oil bath temperature ca. 130 °C, house vacuum ca. 100-120 mmHg) to yield the desired methylenecyclopropane ethyl ester **2.89** (9.98 g, 89% (96% pure), 85% yield) as a brown oil which was used directly without further purification: <sup>1</sup>H NMR (300 MHz, CDCl<sub>3</sub>) δ 5.52 (d, *J* = 1.8 Hz, 2 H), 4.15 (q, *J* = 7.0 Hz, 2 H) 2.25 (ap. bs, 1 H), 1.81 (ap. bs, 1 H), 1.63 (ap t, *J* = 9.2 Hz, 1 H), 1.26 (t, *J* = 7.2 Hz, 3 H); <sup>13</sup>C NMR (100 MHz) δ 172.1, 130.28, 104.6, 60.7, 18.1, 14.2, 11.5. The experimental <sup>1</sup>H NMR was consistent with the literature-reported data.<sup>93</sup>

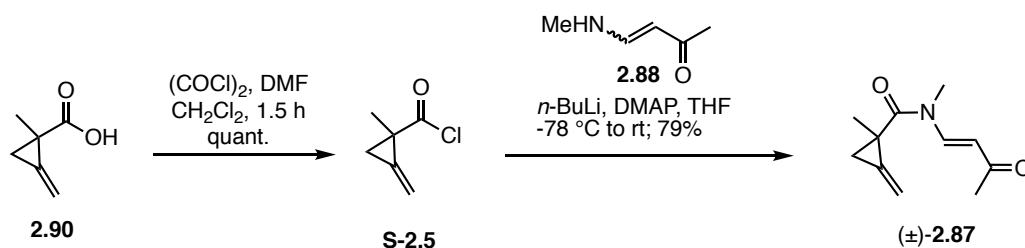


**Ethyl 1-methyl-2-methylenecyclopropanecarboxylate (S-2.4).** LDA was prepared *in situ* by the dropwise addition of *n*-BuLi (34.4 mL, 2.5 M solution of hexanes, 86.1 mmol) to a solution of diisopropylamine (13.3 mL, 93.9 mmol) in THF (136 mL) at -78 °C. The resulting solution was stirred at -78 °C for 20 min and 15 min at 0 °C before it was cooled to -78 °C and treated dropwise with ester **2.89** (9.87 g, 78.3 mmol). The resulting solution was stirred for 0.5 h at -78 °C and treated dropwise with CH<sub>3</sub>I (14.7 mL, 235 mmol). The solution was allowed to warm slowly to 0 °C over 4.5 h, quenched with a saturated solution of NH<sub>4</sub>Cl, extracted with Et<sub>2</sub>O, washed with brine, dried (Na<sub>2</sub>SO<sub>4</sub>), filtered and concentrated. The crude product was

purified by chromatography on SiO<sub>2</sub> (97:3 hexanes/ether) to deliver ester (±)-**S-2.4** (8.02 g, 73%) as a clear and pale yellow oil: IR (ATR) 2982, 2932, 2876, 1719, 1467, 1297, 1146 cm<sup>-1</sup>; <sup>1</sup>H NMR (500 MHz, CDCl<sub>3</sub>) δ 5.45 (ap. t, *J*=2.8 Hz, 1 H), 5.42 (ap. t, *J*= 2.0 Hz, 1 H), 4.15-4.08 (m, 2 H), 2.01 (dt, *J*= 8.7, 2.4 Hz, 1 H), 1.39 (s, 3 H), 1.31 (dt, *J*= 8.7, 2.4 Hz, 1 H), 1.23, (t, *J*= 7.0 Hz, 3 H); <sup>13</sup>C NMR (100 MHz, CDCl<sub>3</sub>) δ 173.7, 137.8, 102.7, 60.8, 23.2, 19.0, 18.9, 14.3; HRMS (LCMS) *m/z* calcd for C<sub>8</sub>H<sub>13</sub>NO<sub>2</sub>(M+H) 141.0916, found 141.0552.



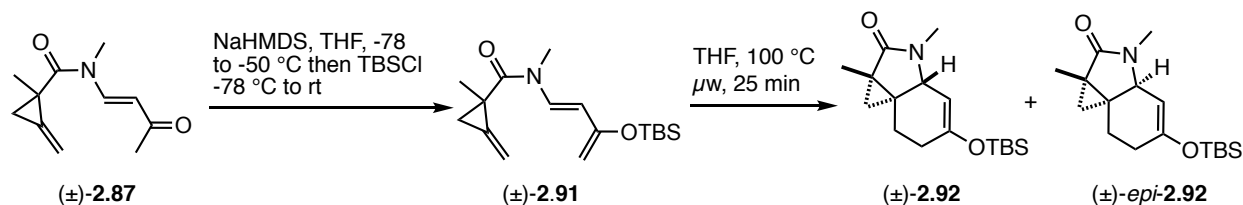
**1-Methyl-2-methylenecyclopropanecarboxylic acid (2.90).** A solution of methylenecyclopropane ethyl ester **S-2.4** (8.03 g, 57.3 mmol) in MeOH/H<sub>2</sub>O 4:1 (357 mL) was treated with lithium hydroxide monohydrate (12.0 g, 286 mmol). The resulting cloudy yellow solution was stirred at room temperature for 5 days, acidified by dropwise treatment with 2N HCl (pH 1-2), diluted with CH<sub>2</sub>Cl<sub>2</sub> and the resulting aqueous phase was extracted with CH<sub>2</sub>Cl<sub>2</sub>. The combined organic phases were dried (Na<sub>2</sub>SO<sub>4</sub>), filtered and concentrated under reduced pressure to yield carboxylic acid **2.90** (5.8 g, 90%) as a clear, orange oil which was used directly: IR (ATR) 2986, 2831, 1687, 1310, 1176, 911 cm<sup>-1</sup>; <sup>1</sup>H NMR (400 MHz, CDCl<sub>3</sub>) δ 5.49 (ap. t, *J*= 2.8 Hz, 1 H), 5.45 (ap. t, *J*= 2.0 Hz, 1 H), 2.10 (dt, *J*= 9.2, 2.4 Hz, 1 H), 1.40 (dt, *J*= 9.2, 2.7 Hz, 1 H), 1.38 (s, 3 H); <sup>13</sup>C NMR (125 MHz, CDCl<sub>3</sub>) δ 180.6, 137.4, 103.2, 77.2, 23.0, 19.8, 18.3; HRMS (ESI-) *m/z* calcd for C<sub>6</sub>H<sub>7</sub>O<sub>2</sub> (M-H) 111.04406, found 111.04413.



**1-Methyl-2-methylenecyclopropanecarbonyl chloride (S-2.5).** A solution of carboxylic acid **2.90** (1.38 g, 12.3 mmol) in  $\text{CH}_2\text{Cl}_2$  (24 mL) was cooled to 0 °C and treated with oxalyl chloride (1.13 mL, 12.9 mmol) and then DMF (0.0489 mL, 0.0481 mmol) upon the addition of which gas evolution was observed. The resulting solution was allowed to stir warming to room temperature.  $^1\text{H}$  NMR analysis of an aliquot ( $\text{CDCl}_3$ ) indicated the presence of the desired acid chloride. The resulting solution was concentrated to yield crude acid chloride **S-25** (1.61 g, quantitative), which was used directly. Characteristic  $^1\text{H}$  NMR signals of acid chloride in crude spectrum (300 MHz,  $\text{CDCl}_3$ )  $\delta$  5.64 (ap t,  $J = 2.7$  Hz, 1 H), 5.59 (ap. t,  $J = 2.3$  Hz, 1 H), 2.37 (dt,  $J = 9.6, 2.4$  Hz, 1 H), 1.62 (dt,  $J = 9.6, 2.6$  Hz, 1 H), 1.49 (s, 3 H)

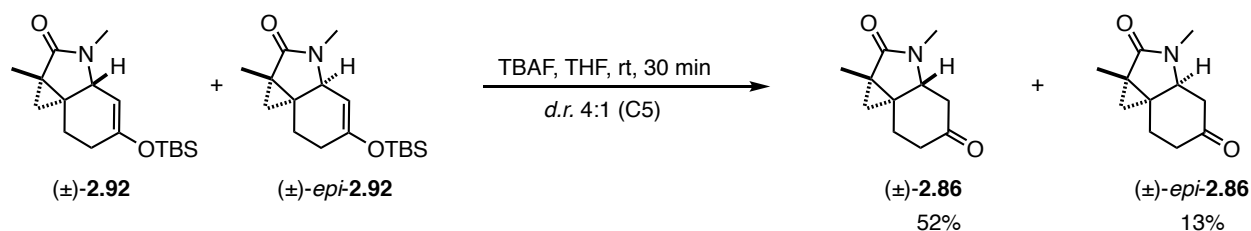
**N,1-Dimethyl-2-methylene-N-(3-oxobut-1-en-1-yl)cyclopropanecarboxamide (±)-2.87.** A flame-dried flask containing vinylogous amide **2.88** (1.02 g, 10.3 mmol) was evacuated and backfilled with an atmosphere of nitrogen. Anhydrous THF (34 mL) was added and the resulting solution was cooled to -78 °C and treated sequentially with *n*-BuLi (4.3 mL, 2.5 M solution in hexanes, 10.9 mmol), acyl chloride **S-25** (1.62 g, 12.4 mmol) and DMAP (0.126 g, 1.03 mmol). The cold bath was removed and the reaction let stir warming to room temperature. The reaction was concentrated and purified by chromatography on  $\text{SiO}_2$  (gradient elution 10% to 20% EtOAc/hexanes) to obtain amide (±)-**2.87** (1.58 g, 79%) as a clear and yellow oil: IR (ATR) 2975, 1676, 1614, 1577, 1247, 1074, 967  $\text{cm}^{-1}$ ;  $^1\text{H}$  NMR (400 MHz,  $\text{CDCl}_3$ )  $\delta$  8.35 (d,  $J = 14.0$ , 1 H), 5.69 (d,  $J = 13.6$  Hz, 1 H), 5.69 (ap. d,  $J = 2.8$  Hz, 1 H), 5.51 (ap t,  $J = 2.0$  Hz, 1 H), 3.13 (s, 3 H), 2.27 (s, 3 H), 1.78 (dt,  $J = 9.6, 2.4$  Hz, 1 H), 1.48 (s, 3 H), 1.31 (dt,  $J = 9.6, 2.4$  Hz, 1

H);  $^{13}\text{C}$  NMR (100 MHz,  $\text{CDCl}_3$ )  $\delta$  196.9, 172.3, 142.9, 134.8, 108.4, 104.9, 30.8, 28.9, 24.9, 21.8, 15.9; HRMS (LCMS)  $m/z$  calcd for  $\text{C}_{11}\text{H}_{16}\text{NO}_2$  ( $\text{M}+\text{H}$ ) 194.1176, found 194.1174



***N*-(3-((*tert*-Butyldimethylsilyl)oxy)buta-1,3-dien-1-yl)-*N*,1-dimethyl-2-methylenecyclopropanecarboxamide (±)-2.91.** A flame dried flask was charged with NaHMDS (0.782 g, 4.05 mmol) followed by anhydrous THF (40 mL) under an atmosphere of nitrogen. The resulting clear and colorless solution was stirred for 15 min at room temperature, cooled to  $-78\text{ }^{\circ}\text{C}$  and treated with vinylogous imide (±)-2.87 (0.712 g, 3.69 mmol) in THF (7.4 mL) slowly via syringe pump at a rate of 2 mL/h. During the slow addition of the amide the solution changed color from clear pale yellow, to clear and deep orange. The resulting clear, orange solution was stirred for 1 h warming to  $-50\text{ }^{\circ}\text{C}$ , cooled to  $-78\text{ }^{\circ}\text{C}$  and treated dropwise with a solution of TBSCl (0.673 g, 4.42 mmol) in THF (15 mL) over a period of 5 minutes. The solution was allowed to stir for 5 min at  $-78\text{ }^{\circ}\text{C}$  before the cold bath was removed and the solution allowed to reach room temperature. The reaction was concentrated to yield crude TBS enol ether (±)-2.91 (1.13 g, quantitative conversion), as an orange oil, which was used directly.

**Diels Alder adducts (±)-2.92 and (±)-*epi*-2.92.** A solution of crude enol ether (±)-2.91 (assumed 1.13 g, 3.69 mmol) in THF (11 mL) was heated under microwave irradiation at  $100\text{ }^{\circ}\text{C}$  for 25 min, concentrated under reduced pressure to obtain the Diels-Alder adducts (±)-2.92 and (±)-*epi*-2.92 which were used directly in the next reaction without purification.



***trans*-1a,3-Dimethylhexahydro-2*H*-cyclopropa[*c*]indole-2,5(3*H*)-dione (±)-(2.86) and *cis*-1a,3-dimethylhexahydro-2*H*-cyclopropa[*c*]indole-2,5(3*H*)-dione (±)-*epi*-2.86.** The Diels-Alder adducts (±)-2.92 and (±)-*epi*-2.92 (assumed 1.13 g, 3.69 mmol) were immediately taken up in THF (37 mL) and treated with TBAF (3.87 mL, 1 M solution in THF, 3.87 mmol). The resulting solution was stirred for 30 min at room temperature. The resulting residue was purified by chromatography on SiO<sub>2</sub> (gradient elution: 40% to 80% EtOAc/Hex) to deliver ketone (±)-2.86 (0.373 g, 52% over two steps from (±)-2.87) as a yellow solid and ketone (±)-*epi*-2.86 (0.0930 g, 13% over two steps from (±)-2.87) in an isolated *dr* of 4:1, (±)-2.86: (±)-*epi*-2.86.

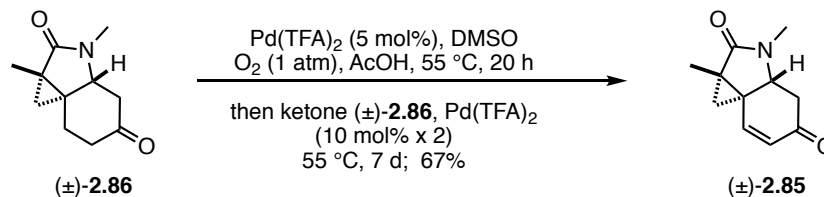
***trans*-1a,3-Dimethyl-3a,4-dihydro-1*H*-cyclopropa[*c*]indole-2,5(1*aH*,3*H*)-dione (±)-(2.86) .** Ketone (±)-2.86 was obtained as an oil which solidified at -20 °C to provide crystals of sufficient quality for X-ray analysis.

IR (ATR) 2951, 2933, 1705, 1676, 1359, 1230, 925 cm<sup>-1</sup>; <sup>1</sup>H NMR (400 MHz, CDCl<sub>3</sub>) δ 3.41 (dd, *J* = 13.0, 3.8 Hz, 1 H), 2.80 (ddd, *J* = 13.3, 4.1, 1.5 Hz, 1 H), 2.69 (ddt, *J* = 15.5, 5.0, 1.5 Hz, 1 H), 2.67 (s, 3 H), 2.54 (ddd, *J* = 15.4, 12.2, 7.2 Hz, 1 H), 2.35 (ap. t, *J* = 13.2 Hz, 1 H), 2.17-2.09 (m, 1 H), 1.72 (ddd, *J* = 13.1, 7.3, 1.9 Hz, 1 H), 1.38 (s, 3 H), 0.95 (d, *J* = 4.0 Hz, 1 H), 0.66 (d, *J* = 4.0 Hz, 1 H); <sup>13</sup>C NMR (100 MHz, CDCl<sub>3</sub>) 207.5, 178.9, 60.2, 45.1, 41.5, 31.9, 30.7, 27.2, 25.9, 22.8, 11.0; HRMS (LCMS) *m/z* calcd for C<sub>11</sub>H<sub>16</sub>NO<sub>2</sub> (M+H) 194.1176, found 194.1174.

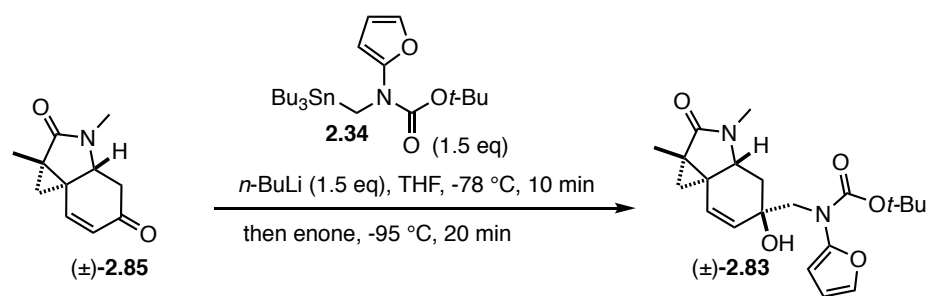
***cis*-1a,3-Dimethyltetrahydro-1*H*-cyclopropa[*c*]indole-2,5(1*aH*,3*H*)-dione (±)-*epi*-2.86.** <sup>1</sup>H NMR (500 MHz, CDCl<sub>3</sub>) δ 3.73 (ap. t, *J* = 6.5 Hz, 1 H), 2.84 (ddd, *J* = 15.3, 6.8, 0.7



Hz, 1 H), 2.72 (s, 3 H), 2.50 (dt,  $J = 16.6, 5.3$  Hz, 1 H), 2.43-2.36 (m, 2 H), 2.30 (ddd,  $J = 14.8, 10.0, 5.0$  Hz, 1 H), 1.83 (dt,  $J = 14.5, 5.8$  Hz, 1 H), 1.34 (s, 3 H), 0.93 (d,  $J = 4.5$  Hz, 1 H), 0.84 (d,  $J = 4.6$  Hz, 1 H). The experimental  $^1\text{H}$  NMR was consistent with the literature-reported data.<sup>134</sup>



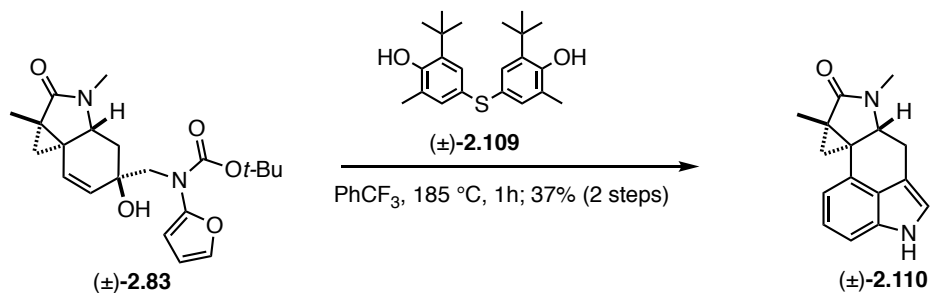
**1a,3-Dimethyl-3a,4-dihydro-1H-cyclopropa[*c*]indole-2,5(1a*H*,3*H*)-dione (±)-(2.85).** A microwave flask equipped with a stir bar was charged with  $\text{Pd(TFA)}_2$  (0.0129 g, 0.0384 mmol). The flask and the balloon were purged and filled with  $\text{O}_2$ , followed by the addition of DMSO (5.45  $\mu\text{L}$ , 0.0767 mmol) and AcOH (3.8 mL). The resulting brown solution was stirred at 55 °C under an atmosphere of oxygen (balloon) for 20 h prior to the addition of ketone (±)-**2.86** (0.148 g, 0.767 mmol). The resulting black solution was stirred for a further 7 days during which time two more portions of  $\text{Pd(TFA)}_2$  catalyst were added (2 x 0.1 equiv). The reaction was concentrated and purified by chromatography on  $\text{SiO}_2$  (50% EtOAc/Hex) to obtain enone (±)-**2.85** (0.098 g, 67%) as a white solid: IR (ATR) 2956, 2918, 2850, 1663, 1588, 1390, 1228, 1117  $\text{cm}^{-1}$ ;  $^1\text{H}$  NMR (500 MHz)  $\delta$  6.97 (d,  $J = 9.5$  Hz, 1 H), 6.13 (d,  $J = 10.0$  Hz, 1 H), 3.80 (dd,  $J = 14.0, 3.5$  Hz, 1 H), 2.89 (dd,  $J = 15.5, 3.5$  Hz, 1 H), 2.70 (s, 3 H), 2.43 (dd,  $J = 15.5, 14.0$  Hz, 1 H), 1.45 (s, 3 H), 1.33 (dd,  $J = 4.0$  Hz, 1 H), 0.85 (dd,  $J = 4.0$  Hz, 1 H);  $^{13}\text{C}$  NMR (100 MHz)  $\delta$  197.0, 177.8, 148.4, 131.4, 58.6, 41.9, 32.9, 32.1, 27.3, 23.5, 10.9; HRMS (LCMS)  $m/z$  calcd for  $\text{C}_{11}\text{H}_{14}\text{NO}_2$  ( $\text{M}+\text{H}$ ) 192.1019, found 192.1019.



**Alcohol (±)-2.83.** A flame-dried flask was charged with furanylamino stannane **2.34** (0.277 g, 0.570 mmol) and evacuated for 15 min under high vacuum prior to the introduction of a nitrogen atmosphere. THF (1.2 mL) was added and the solution cooled to  $-78\text{ }^{\circ}\text{C}$  and treated dropwise with *n*-BuLi (0.228 mL, 2.5 M solution in hexanes, 0.570 mmol). The resulting clear and colorless solution was stirred at  $-78\text{ }^{\circ}\text{C}$  for 10 min, cooled to  $-95\text{ }^{\circ}\text{C}$  (acetone/liquid nitrogen) and treated with a solution of ketone (±)-**2.85** (0.0738 g, 0.386 mmol) in THF (1.5 mL) over a period of 15 min. The resulting clear and yellow solution was stirred for a further 5 min at  $-95\text{ }^{\circ}\text{C}$ , diluted with EtOAc (2 mL) and quenched with saturated  $\text{NH}_4\text{Cl}$  (2 mL). The separated aqueous phase was extracted with EtOAc (3x) and the combined organic phases dried ( $\text{Na}_2\text{SO}_4$ ) and concentrated. The crude residue was filtered through  $\text{SiO}_2$  and washed with 15% EtOAc/Hex to elute tin byproducts then EtOAc to elute product. The EtOAc fraction was concentrated to yield crude alcohol (±)-**2.83** as a yellow oil, which was used directly without purification.

The tertiary alcohol (±)-**2.83** can be purified by chromatography on  $\text{SiO}_2$  (gradient elution 15% EtOAc/Hex to remove tin by-product and then 30% to 50% EtOAc/Hex) to deliver the desired tertiary alcohol (±)-**2.83** for full characterisation: IR (ATR) 3390, 2969, 2932, 2869, 1681, 1694, 1612, 1392, 1374, 1292, 1154,  $733\text{ cm}^{-1}$ ;  $^1\text{H}$  NMR (400 MHz,  $\text{CDCl}_3$ )  $\delta$  7.19 (s, 1 H), 6.35 (d,  $J = 2.0\text{ Hz}$ , 1 H), 6.01 (s, 1 H), 5.83 (d,  $J = 9.6\text{ Hz}$ , 1 H), 5.66 (d,  $J = 9.6\text{ Hz}$ , 1 H), 3.86 (d,  $J = 14.8\text{ Hz}$ , 1 H), 3.72 (d,  $J = 14.4\text{ Hz}$ , 1 H), 3.66 (dd,  $J = 12.8, 2.4\text{ Hz}$ , 1 H), 2.70 (s, 3 H), 2.19 (d,  $J = 12.0\text{ Hz}$ , 1 H), 1.59 (ap. t,  $J = 12.6\text{ Hz}$ , 1 H), 1.44 (s, 9 H), 1.35 (s, 3 H), 0.88 (d,

$J = 3.6$  Hz, 1 H), 0.58 (d,  $J = 3.6$  Hz, 1 H);  $^{13}\text{C}$  NMR (125 MHz,  $\text{CDCl}_3$ )  $\delta$  179.5, 149.1, 138.4, 131.1, 129.4, 111.3, 102.0, 82.6, 73.9, 59.5, 57.2, 37.3, 36.8, 32.3, 31.9, 28.2, 27.3, 23.5, 10.8; HRMS (LCMS ESI) $^+$   $m/z$  calcd for  $\text{C}_{21}\text{H}_{29}\text{N}_2\text{O}_5$  (M+H) 389.2071, found 389.2071.



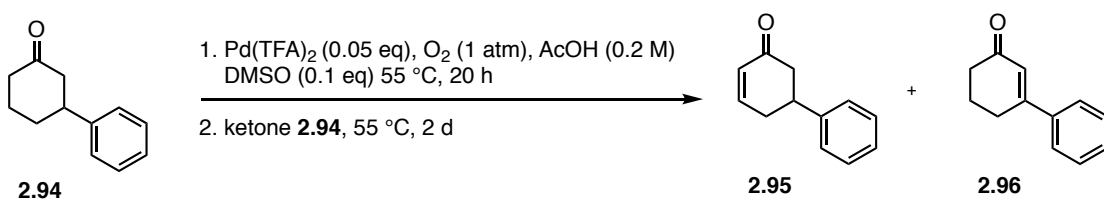
**Indole ( $\pm$ )-2.110.** A solution of crude alcohol ( $\pm$ )-2.83 (0.148 g, 0.381 mmol) in trifluorotoluene (3.5 mL) was treated with 4,4'-thiobis(6-tert-butyl-*o*-cresol) (0.0136 g, 0.0381 mmol) and heated at 185  $^\circ\text{C}$  under microwave irradiation for 1 h. The reaction mixture was concentrated under reduced pressure and the resulting crude product purified by chromatography on  $\text{SiO}_2$  (60% EtOAc/Hex) to deliver the desired indole ( $\pm$ )-2.110 (0.036 g, 37% over two steps): IR (ATR) 3292, 2937, 2850, 1681, 1446, 1372, 1238, 1074, 738  $\text{cm}^{-1}$ ;  $^1\text{H}$  NMR (400 MHz)  $\delta$  8.06 (bs, 1 H), 7.22 (d,  $J = 8.4$  Hz, 1 H), 7.12 (ap. t,  $J = 7.6$  Hz, 1 H), 7.0 (t,  $J = 1.6$  Hz, 1 H), 6.81 (d,  $J = 7.2$  Hz, 1 H), 3.83 (dd,  $J = 12.0, 4.0$  Hz, 1 H), 3.29 (dd,  $J = 14.0, 4.0$  Hz, 1 H), 2.84 (s, 3 H), 2.71 (ddd,  $J = 13.6, 12.0, 1.6$  Hz, 1 H), 1.85 (s, 3 H), 1.17 (d,  $J = 3.2$  Hz, 1 H), 0.90 (d,  $J = 3.6$  Hz, 1 H);  $^{13}\text{C}$  NMR (100 MHz)  $\delta$  179.0, 133.8, 133.2, 128.3, 123.3, 119.2, 111.3, 110.5, 109.2, 61.7, 32.8, 32.4, 29.1, 27.6, 25.5, 12.5; HRMS (LCMS)  $m/z$  calcd for  $\text{C}_{16}\text{H}_{17}\text{N}_2\text{O}$  (M+H) 253.1335, found 253.1335.



cyclohexanone **2.94** (0.040 g, 0.23 mmol). The flask was purged with O<sub>2</sub> and a balloon of oxygen attached. DMSO (1.6 μL, 0.023 mmol) and acetic acid (1.15 mL) were added. The resulting black solution was stirred at 80 °C under an atmosphere of O<sub>2</sub> for 12 h. <sup>1</sup>H NMR analysis of an aliquot (CDCl<sub>3</sub>) showed a diastereomeric ratio of 1.7: 1 **2.95**: **2.96**.

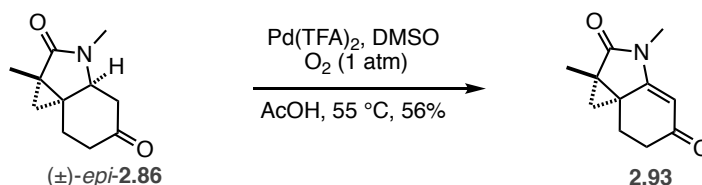
The reaction was concentrated and purified by chromatography on SiO<sub>2</sub> (gradient elution 0-20% EtOAc/Hex) to obtain cyclohexenones **2.95** and **2.96** as yellow oils for a characterisation standard: **1,6-Dihydro-[1,1'-biphenyl]-3(2H)-one (2.95)**. <sup>1</sup>H NMR (400 MHz) δ 7.34 (ap. d, *J* = 7.2 Hz, 2 H), 7.28-7.25 (m, 3 H), 7.05 (ddd, *J* = 10.1, 5.8, 2.5 Hz), 6.13 (dd, *J* = 10.0, 2.9 Hz 1 H) 3.36-3.34 (m, 1 H), 2.71-2.2.51 (m, 4 H). The experimental <sup>1</sup>H NMR was consistent with the literature-reported data.<sup>98</sup>

**5,6-Dihydro-[1,1'-biphenyl]-3(4H)-one (2.96)**. <sup>1</sup>H NMR (400 MHz) δ 7.50 (dd, *J* = 7.0, 3.1 Hz, 2 H), 7.41 (ap. t, *J* = 3.3 Hz, 3 H), 6.43 (ap. t, *J* = 1.4 Hz, 1 H), 2.80-2.77 (m, 2 H), 2.49 (t, *J* = 6.7 Hz, 2 H), 2.16 (dt, *J* = 12.9, 6.4 Hz, 2 H). The experimental <sup>1</sup>H NMR was consistent with the literature-reported data.<sup>98</sup>



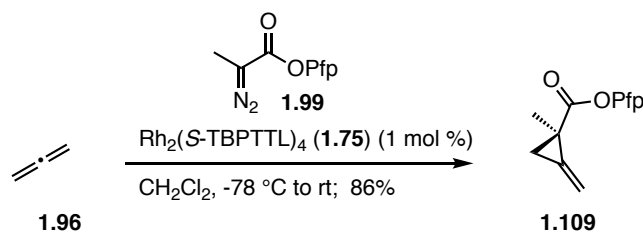
**1,6-Dihydro-[1,1'-biphenyl]-3(2H)-one (2.95) and 5,6-dihydro-[1,1'-biphenyl]-3(4H)-one (2.96)**. A flame dried microwave flask equipped with a stir bar and cooled under an atmosphere of nitrogen was charged with Pd(TFA)<sub>2</sub> (0.00393 g, 0.0115 mmol). The flask was purged with O<sub>2</sub> and a balloon of O<sub>2</sub> attached, followed by the addition of DMSO (1.63 μL, 0.0230 mmol) and AcOH (1.15 mL, 0.2 M w.r.t. ketone). The resulting black solution was stirred

at 55 °C under an atmosphere of oxygen for 20 h. After 20 h ketone **2.94** (0.0400 g, 0.230 mmol) was added and the resulting black solution stirred at 55 °C for 2 days. <sup>1</sup>H NMR analysis of an aliquot (CDCl<sub>3</sub>) showed a regioisomeric ratio of 2.17: 1.

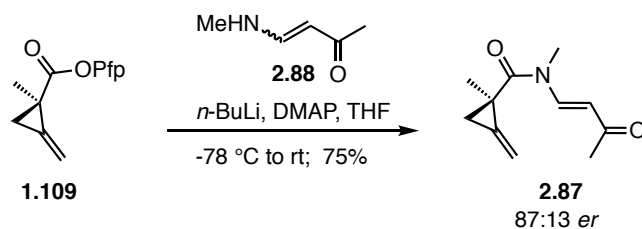


**1a,3-Dimethyl-1,1a,6,7-tetrahydro-2H-cyclopropa[c]indole-2,5(3H)-dione (2.93).** A microwave flask was charged with Pd(TFA)<sub>2</sub> (0.0092 g, 0.027 mmol). The flask was purged and filled with O<sub>2</sub>, followed by the addition of DMSO (1.9 μL) and AcOH (1.3 mL). The resulting brown solution was stirred at 55 °C under an atmosphere of oxygen (balloon) for 20 h then treated with ketone (±)-*epi*-**2.86** (0.052, 0.27 mmol). After 3 days <sup>1</sup>H NMR analysis of an aliquot (CDCl<sub>3</sub>) indicated exclusive formation of the undesired regioisomer. The reaction was concentrated and purified by chromatography on SiO<sub>2</sub> (50% EtOAc/Hex) to deliver vinylogous amide **2.93** (0.029 g, 56%) as a white solid: IR (ATR) 2956, 1732, 1607, 1458, 1241, 1074 cm<sup>-1</sup>; <sup>1</sup>H NMR (300 MHz, CDCl<sub>3</sub>) δ 5.49 (s, 1 H), 2.93 (s, 3 H), 2.68-2.65 (m, 1 H), 2.63 (d, *J* = 5.0 Hz, 1 H), 2.35 (td, *J* = 12.4, 6.8 Hz, 1 H), 1.73 (ddd, *J* = 13.0, 4.7, 2.8 Hz, 1 H), 1.41 (s, 3 H), 1.33 (d, *J* = 4.2 Hz, 1 H), 1.17 (d, *J* = 4.2 Hz, 1 H); <sup>13</sup>C NMR (100 MHz, CDCl<sub>3</sub>) δ 197.2, 177.1, 164.4, 101.4, 36.9, 30.1, 29.9, 29.2, 26.2, 24.5, 10.4; HRMS (LCMS ESI)<sup>+</sup> *m/z* calcd for C<sub>11</sub>H<sub>14</sub>O<sub>2</sub>N (M+H) 192.1019, found 192.1020. The experimental <sup>1</sup>H NMR was consistent with the literature-reported data.<sup>134</sup>

### 3.2.3 CHAPTER TWO EXPERIMENTAL PART: (-)-2.1



**Perfluorophenyl (*R*)-1-methyl-2-methylenecyclopropane-1-carboxylate (1.109).** An oven-dried three-neck flask fitted with a nitrogen inlet, a dry-ice condenser, and septum was charged with  $\text{Rh}_2(\text{S-TBPTTL})_4$  (**1.75**)<sup>55</sup> (0.236 g, 0.0939 mmol) and  $\text{CH}_2\text{Cl}_2$  (51 mL) and the resulting green solution was cooled to -78°C and treated dropwise with an excess of condensed allene gas (**1.96**, 2.23 g, 55.6 mmol). A solution of perfluorophenyl 2-diazopropanoate (**1.99**) (2.50 g, 9.39 mmol) in anhydrous  $\text{CH}_2\text{Cl}_2$  (9.0 mL) was then added slowly *via* syringe pump at a rate of ca. 1 mL/h, allowing the solution to run down the side of the flask into the reaction mixture. After the addition was complete, the mixture was allowed to stir at -78 °C for 1 h before warming to room temperature. The solution was concentrated and the resulting green residue was purified by chromatography on  $\text{SiO}_2$  (0-1%  $\text{Et}_2\text{O}$ /hexanes) to deliver methylenecyclopropane **1.109** (2.24 g, 86%) as a clear and pale yellow oil:  $[\alpha]_{\text{D}}^{20}$  -2.6 (*c* 1,  $\text{CHCl}_3$ ); IR (ATR) 2985, 2939, 1770, 1655, 1517, 1459, 1283, 1070, 1028, 993  $\text{cm}^{-1}$ ;  $^1\text{H}$  NMR (400 MHz,  $\text{CD}_2\text{Cl}_2$ )  $\delta$  5.64 (t, *J* = 2.8 Hz, 1 H), 5.56 (t, *J* = 2.2 Hz, 1 H), 2.30 (dt, *J* = 9.2, 2.5 Hz, 1 H), 1.63 (dt, *J* = 9.2, 2.4 Hz, 1 H), 1.51 (s, 3 H);  $^{13}\text{C}$  NMR (100 MHz,  $\text{CD}_2\text{Cl}_2$ )  $\delta$  170.4, 143.2-143.0 (m), 141.3-141.0 (m), 140.7-140.5 (m), 139.9-139.5 (m), 137.4-137.0 (m), 136.8, 126.2-123.8 (m), 104.5, 23.2, 20.6, 18.8; DEPT-135 (100 MHz,  $\text{CD}_2\text{Cl}_2$ )  $\delta$  104.5 ( $\text{CH}_2$ ), 20.6 ( $\text{CH}_2$ ), 18.8 ( $\text{CH}_3$ );  $^{19}\text{F}$  NMR (471 MHz,  $\text{CD}_2\text{Cl}_2$ )  $\delta$  -153.9 (m, 2 F), -59.4 (t, *J*<sub>F</sub> = 21.2 Hz, 1 F), -163.5 to -163.6 (m, 2 F); HRMS (APCI+) *m/z* calcd for  $\text{C}_{12}\text{H}_8\text{O}_2\text{F}_5$  (M+H) 279.04390, found 279.04312.



**(*R,E*)-*N*,1-Dimethyl-2-methylene-*N*-(3-oxobut-1-en-1-yl)cyclopropane-1-carboxamide**

**(2.87).** An oven-dried flask charged with vinylogous amide **2.88**<sup>41</sup> (0.700 g, 7.06 mmol) was evacuated and backfilled with nitrogen (3x). Freshly distilled THF (24 mL) was added and the resulting solution was cooled to -78 °C and treated dropwise with *n*-BuLi (3.24 mL, 2.29 M solution in hexanes, 7.42 mmol). The resulting clear, pale yellow solution was stirred for 5 min at -78 °C, then treated with a solution of ester **1.109** (2.06 g, 7.41 mmol) in THF (4 mL). The resulting bright yellow solution was treated with DMAP (0.0862 g, 0.706 mmol) and stirred for 10 min at -78 °C. The cold bath was removed and the reaction mixture was allowed to stir, warming to room temperature. The reaction was quenched with sat. NaHCO<sub>3</sub>. After addition of EtOAc, the aqueous layer was extracted with EtOAc (3x) and the combined organic layers were dried (Na<sub>2</sub>SO<sub>4</sub>) and concentrated. The crude product was purified by chromatography on SiO<sub>2</sub> (10-15% EtOAc/hexanes) to deliver the vinylogous imide **2.87** (1.03 g, 75%) as a clear, pale yellow oil: [ $\alpha$ ]<sub>D</sub><sup>20</sup> +214.4 (*c* 1, CHCl<sub>3</sub>); IR (ATR) 2968, 2932, 1680, 1615, 1578, 1516, 1355, 1262, 1247, 1072, 968 cm<sup>-1</sup>; <sup>1</sup>H NMR (400 MHz, CDCl<sub>3</sub>)  $\delta$  8.36 (d, *J* = 13.6 Hz, 1 H), 5.73-5.69 (m, 2 H), 5.53 (ap. s, 1 H), 3.15 (s, 3 H), 2.29 (s, 3 H), 1.79 (dt, *J* = 9.6, 2.2 Hz, 1 H), 1.49 (s, 3 H), 1.32 (dt, *J* = 9.6, 2.2 Hz, 1 H); <sup>13</sup>C NMR (125 MHz, CDCl<sub>3</sub>)  $\delta$  196.9, 172.4, 142.9, 134.9, 108.4, 104.9, 30.9, 28.9, 24.9, 21.8, 15.9; HRMS (ESI)<sup>+</sup> *m/z* calcd for C<sub>11</sub>H<sub>16</sub>O<sub>2</sub>N (M+H) 194.1176, found 194.1174.



The *er* of the imide product **2.87** was determined using chiral SFC. The following conditions were developed for resolution of the amide using a) a Chiralpak-IC analytical column and b) a Chiralpak-IC semi preparative column:

- a) Chiralpak-IC analytical column (250 x 4.6 mm), gradient elution: 1% *i*PrOH (hold for 5 min), 2% *i*PrOH (hold for 5 min), 3% *i*PrOH (hold for 6 min), 4% *i*PrOH (hold for 3 min), 4.50% *i*PrOH (hold for 2 min), 5% *i*PrOH (hold for 3 min), 4 mL/min, 254 nm, P=110 (BAR)]
- b) Chiralpak-IC semi prep column (250 x 10 mm), gradient elution: 5-15% (rate 1.0), 7 mL/min, 254 nm, P=100 (BAR).

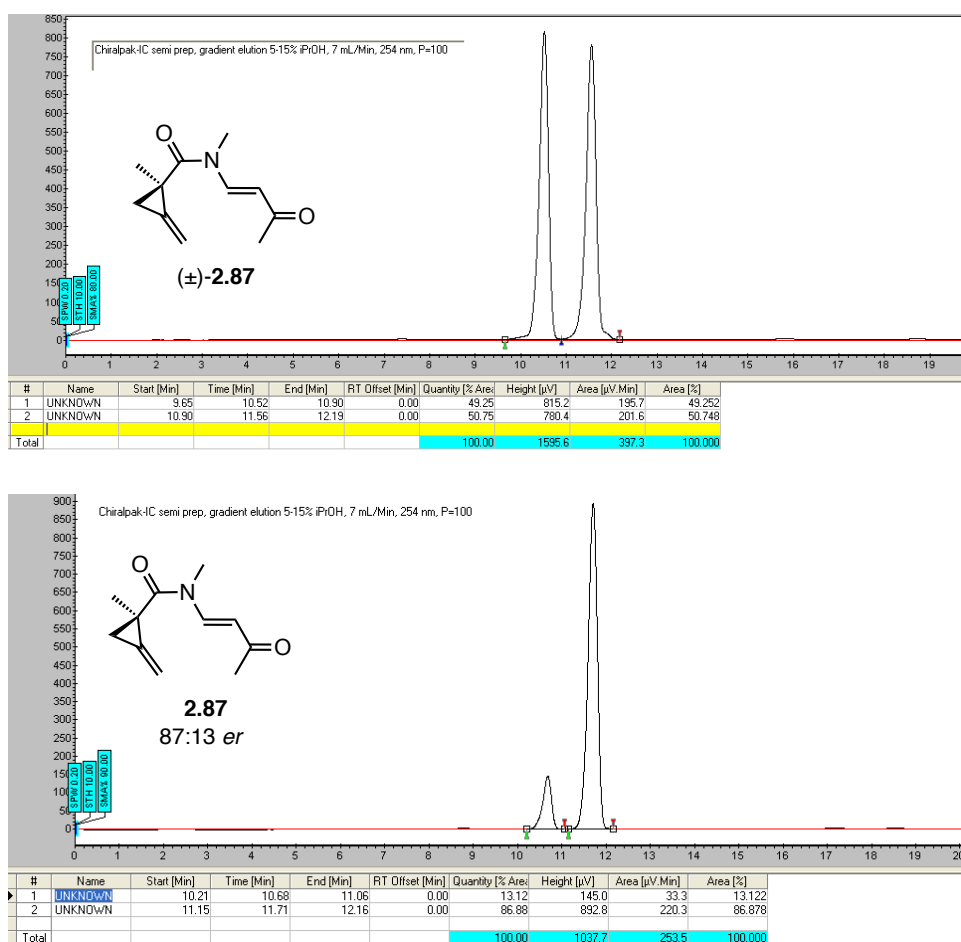
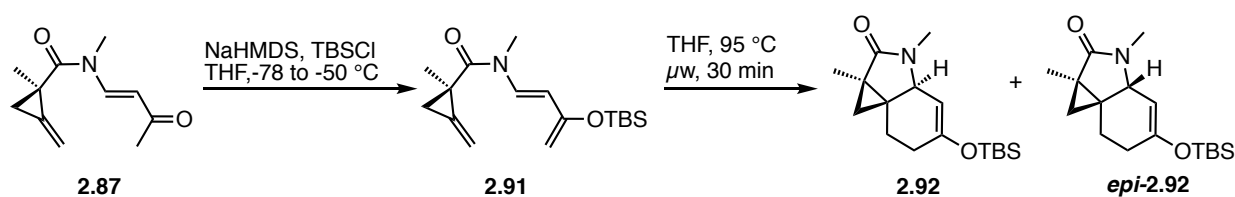
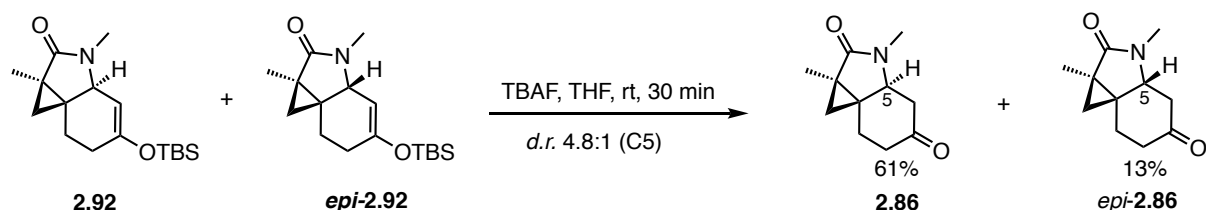


**Figure 3-14** Representative SFC chromatogram showing racemic standard and enantiomerically enriched imide **2.87** using conditions b)



(1*aR*,3*aS*,7*aS*)-5-((*tert*-Butyldimethylsilyl)oxy)-1*a*,3-dimethyl-1,1*a*,3,3*a*,6,7-hexahydro-2*H*-cyclopropa[*c*]indol-2-one (2.92) and (1*aR*,3*aR*,7*aS*)-5-((*tert*-butyldimethylsilyl)oxy)-1*a*,3-dimethyl-1,1*a*,3,3*a*,6,7-hexahydro-2*H*-cyclopropa[*c*]indol-2-one (*epi*-2.92). An oven-dried flask was charged with NaHMDS (0.611 g, 3.17 mmol) followed by anhydrous THF (31.5 mL) under an atmosphere of nitrogen. The resulting clear, colorless solution was stirred for 15 min at room temperature, cooled to -78 °C and stirred for a further 15 min prior to treatment with a solution of vinylogous amide **2.87** (0.556 g, 2.88 mmol) in THF (6.0 mL) that was added slowly via syringe pump at a rate of ca. 2 mL/h. During the slow addition of the amide, the solution changes color from clear pale yellow, to clear and gold to clear and deep orange. The resulting clear, orange solution was allowed to stir for 1 h while warming to -50 °C, cooled to -78 °C and treated dropwise with a solution of TBSCl (0.526 g, 3.45 mmol) in THF (11.5 mL) over a period of 5 min. The solution was allowed to stir for 5 min at -78 °C before the cold bath was removed and the solution allowed to reach room temperature. <sup>1</sup>H NMR analysis of an aliquot (CDCl<sub>3</sub>) indicated formation of the desired TBS enol ether. The reaction mixture was concentrated under reduced pressure to obtain crude enol ether as an orange gel, which was immediately taken up in THF (8.4 mL) and heated under microwave irradiation in a sealed vial at 95 °C for 30 min (3 x 2.8 mL batches). The combined batches were concentrated to deliver a mixture of crude enol ethers **2.92** and *epi*-**2.92** (assumed full conversion 0.885 g, 2.88 mmol).



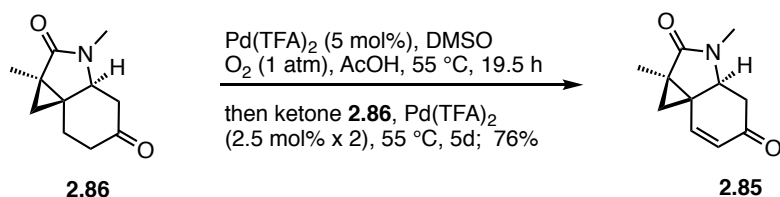
**(1a*R*,3a*S*,7a*S*)-1a,3-Dimethylhexahydro-2*H*-cyclopropa[*c*]indole-2,5(3*H*)-dione**

**(2.86) and (1a*R*,3a*R*,7a*S*)-1a,3-dimethylhexahydro-2*H*-cyclopropa[*c*]indole-2,5(3*H*)-dione (epi-2.86).** The crude enol ethers **2.92** and **epi-2.92** (0.885 g, 2.88 mmol) were taken up in THF (29 mL), treated dropwise with TBAF (2.88 mL, 1 M solution in THF, 2.88 mmol) and allowed to stir at room temperature for 30 min. The reaction mixture was filtered through a pad of Celite and concentrated. The resulting residue was purified by chromatography on SiO<sub>2</sub> (20% EtOAc/hexanes to elute recovered vinylogous amide **2.87**, then 50-70% EtOAc/hexanes to elute ketone **2.86** and then 90-100% EtOAc/hexanes to elute **epi-2.86**) to deliver recovered vinylogous amide **2.87** (0.0153 g) as a yellow oil along with *trans*-ketone **2.86** (0.339 g, 61% over two steps from amide **2.87**, (63% brsm)) as a yellow crystalline solid and *cis*-ketone **epi-2.86** (0.0711 g, 13% over two steps from amide **2.87** (13% brsm)) as a yellow oil.

***trans*-Ketone 2.86:**  $[\alpha]_D^{20} +83.9$  (*c* 1, CHCl<sub>3</sub>); Mp 95.5-98.4 °C; IR (ATR) 2955, 1706, 1676, 1414, 1395, 1359, 1292, 1230, 1123, 1072, 1042, 865 cm<sup>-1</sup>; <sup>1</sup>H NMR (300 MHz, CDCl<sub>3</sub>)  $\delta$  3.40 (dd, *J* = 13.1, 4.1 Hz, 1 H), 2.80 (ddd, *J* = 13.5, 4.1, 1.4 Hz, 1 H), 2.72-2.66 (m, 4 H), 2.53 (ddd, *J* = 15.2, 12.1, 7.3 Hz, 1 H), 2.35 (ap. t, *J* = 13.4 Hz, 1 H), 2.18-2.08 (m, 1 H), 1.72 (ddd, *J* = 13.2, 7.2, 1.8 Hz, 1 H), 1.38 (s, 3 H), 0.95 (d, *J* = 3.6 Hz, 1 H), 0.66 (d, *J* = 3.9 Hz, 1 H); <sup>13</sup>C NMR (100 MHz, CDCl<sub>3</sub>)  $\delta$  207.6, 178.9, 60.1, 45.1, 41.5, 31.8, 30.7, 27.2, 25.8, 22.7, 11.0; HRMS (LCMS-ESI) *m/z* calcd for C<sub>11</sub>H<sub>16</sub>O<sub>2</sub>N (M+H) 194.1176, found 194.1175.

***cis*-Ketone epi-2.86:**  $[\alpha]_D^{18} -9.1$  (*c* 1, CHCl<sub>3</sub>); <sup>1</sup>H NMR (300 MHz; CDCl<sub>3</sub>)  $\delta$  3.73 (ap. t, *J* = 6.6 Hz, 1 H), 2.83 (dd, *J* = 15.0, 6.3 Hz, 1 H), 2.72 (s, 3 H), 2.55-2.25 (m, 4 H), 1.82 (dt, *J* =

13.8, 5.1 Hz, 1 H), 1.34 (s, 3 H), 0.92 (d,  $J = 4.5$  Hz, 1 H), 0.84 (d,  $J = 4.5$  Hz, 1 H). The experimental  $^1\text{H}$  NMR was consistent with the literature-reported data.<sup>134</sup>



**(1a*R*,3a*S*,7a*R*)-1a,3-Dimethyl-1,1a,3a,4-tetrahydro-2*H*-cyclopropa[*c*]indole-2,5(3*H*)-dione (**2.85**).** A solution of  $\text{Pd(TFA)}_2$  (0.00940 g, 0.0274 mmol) and DMSO (3.90  $\mu\text{L}$ , 0.0549 mmol) in AcOH (2.74 mL) was heated at 55 °C under an atmosphere of  $\text{O}_2$  (balloon) to pre-activate the catalyst system. After 19.5 h, ketone **2.86** (0.106 g, 0.549 mmol) was added and the reaction was allowed to stir at 55 °C under an atmosphere of  $\text{O}_2$  (balloon). Additional  $\text{Pd(TFA)}_2$  was added at 48 h (4.7 mg) and 72 h (4.7 mg) after the addition of the ketone in order to drive the reaction to completion. After 5 d,  $^1\text{H}$  NMR of an aliquot ( $\text{CDCl}_3$ ) showed that the conversion was complete and the reaction mixture was concentrated and purified by chromatography on  $\text{SiO}_2$  (3-5% acetone/ $\text{CH}_2\text{Cl}_2$ ) to deliver enone **2.85** (0.0796 g, 76%) as a cream crystalline solid.

Protocol for the enantiomeric enrichment by recrystallization: Enone **2.85** (0.0610 g, 0.320 mmol) was dissolved in a 15:1 mixture of 1,2-dichloroethane: boiling MTBE ( $c$  0.08 M) and allowed to cool to room temperature prior to the addition of a seed crystal. The resulting solution was allowed to stand overnight at -20 °C during which time white needle-shaped crystals formed. The mother liquor was removed via pipette transfer and the crystals were washed with MTBE (2x) and placed under vacuum to remove trace solvents. The first recrystallization provided crystals of 100:0 *er*, the second recrystallization crystals were 99.5:0.5 *er* and the third recrystallization provided crystals of 96:4 *er*. Three rounds of recrystallization

delivered enone **2.85** (29.7 mg, 56% of theoretical maximum yield) as white, needle-shaped crystals. Only samples with *er* >98:2 were carried on in the subsequent reaction. The *er* of the combined material was >99.5:0.5 *er* by SFC analysis:  $[\alpha]_D^{18}$  -103.4 (*c* 1, CHCl<sub>3</sub>); Mp 131.7-134.1 °C; IR (ATR) 2966, 2929, 1683, 1664, 1618, 1585, 1452s, 1389, 1235, 1071, 688, 796 cm<sup>-1</sup>; <sup>1</sup>H NMR (500 MHz, CDCl<sub>3</sub>) δ 6.97 (d, *J* = 9.5 Hz, 1 H), 6.14 (d, *J* = 9.5 Hz, 1 H), 3.81 (dd, *J* = 13.8, 3.8 Hz, 1 H), 2.90 (dd, *J* = 15.5, 4.0 Hz, 1 H), 2.71 (s, 3 H), 2.44 (dd, *J* = 15.8, 14.3 Hz, 1 H), 1.46 (s, 3 H), 1.33 (d, *J* = 4.0 Hz, 1 H), 0.86 (d, *J* = 4.0 Hz, 1 H); <sup>13</sup>C NMR (125 MHz, CDCl<sub>3</sub>) δ 197.0, 177.8, 148.4, 131.4, 58.6, 41.9, 32.9, 32.1, 27.3, 23.5, 10.9; HRMS (ESI)<sup>+</sup> *m/z* calcd for C<sub>11</sub>H<sub>14</sub>O<sub>2</sub>N (M+H) 192.1019, found 192.1017. SFC conditions to separate enone **2.85** [Chiralpak-IC semi preparative column (250 x 10 mm), gradient elution: 1-30% *i*PrOH (rate 1.0), 5.5 mL/min, 254 nm, P=100 (BAR)]

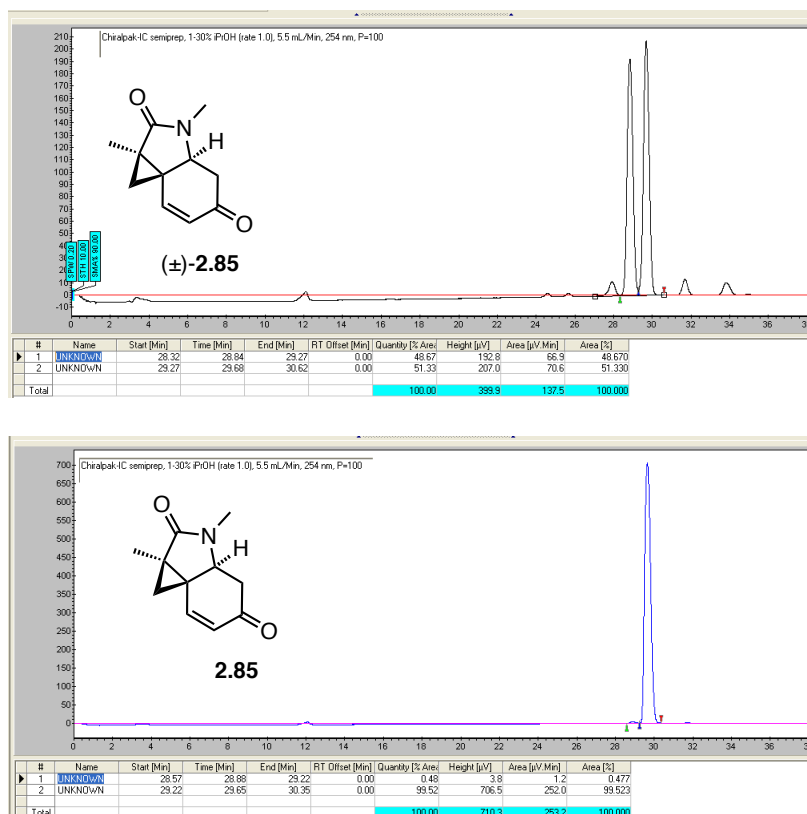
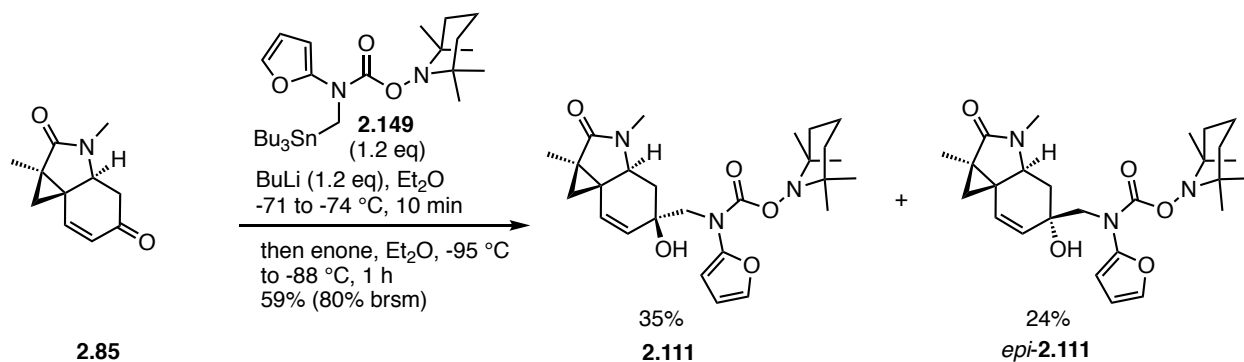


**Figure 3-15** SFC chromatograms of the racemic standard and enantioenriched enone **2.85** after recrystallization



**2,2,6,6-Tetramethylpiperidin-1-yl furan-2-yl(((1*R*,3*aS*,5*R*,7*aR*)-5-hydroxy-1*a*,3-dimethyl-2-oxo-1*a*,2,3,3*a*,4,5-hexahydro-1*H*-cyclopropa[*c*]indol-5-yl)methyl)carbamate (2.111) and 2,2,6,6-tetramethylpiperidin-1-yl furan-2-yl(((1*R*,3*aS*,5*S*,7*aR*)-5-hydroxy-1*a*,3-dimethyl-2-oxo-1*a*,2,3,3*a*,4,5-hexahydro-1*H*-cyclopropa[*c*]indol-5-yl)methyl)carbamate (*epi*-2.111).** An oven-dried 2-neck flask equipped with a septum fitted with a nitrogen inlet and a stopper was charged with stannane **2.149** (0.107 g, 0.188 mmol) and evacuated under high vacuum, then backfilled with nitrogen (3x). The stopper was exchanged for a thermocouple thermometer under a positive flow of nitrogen, and anhydrous Et<sub>2</sub>O (0.60 mL) was added. The clear, colorless solution was cooled to -74 °C (Et<sub>2</sub>O/dry ice), stirred for 10 min, then treated dropwise with *n*-BuLi (0.0753 mL, 2.5 M solution in hexanes, 0.188 mmol) during the slow addition of which the temperature increased to -71.4 °C. The resulting clear and colorless solution was stirred at -73 °C for 15 min then cooled to -94 °C (N<sub>2(l)</sub>/ Et<sub>2</sub>O) over a period of 10 min and treated dropwise with a solution of enone **2.85** (0.0300 g, 0.157 mmol) in THF/Et<sub>2</sub>O (1:1 , 600 μL). During this addition the temperature rose to -88 °C and the solution became clear yellow. The mixture was stirred for 1 h while the internal temperature was kept between -89 to -95 °C. The solution was then allowed to warm slowly to -75 °C over 20 min, diluted with EtOAc (0.50 mL) and quenched with sat. NH<sub>4</sub>Cl<sub>(aq)</sub> (1.0 mL), keeping the internal temperature below -50 °C. The cold bath was removed and the reaction mixture was warmed to room temperature.

The aqueous layer was extracted with EtOAc (3x). The combined organic layers were dried (Na<sub>2</sub>SO<sub>4</sub>) and concentrated. The resulting residue was purified by chromatography on SiO<sub>2</sub> (5-10% acetone/CH<sub>2</sub>Cl<sub>2</sub>) to deliver recovered starting material **71** (7.8 mg) as a white solid along with allylic alcohols **2.111** (0.026 g, 35%) and *epi*-**2.111** (0.0176 g, 24%) as a white foams.

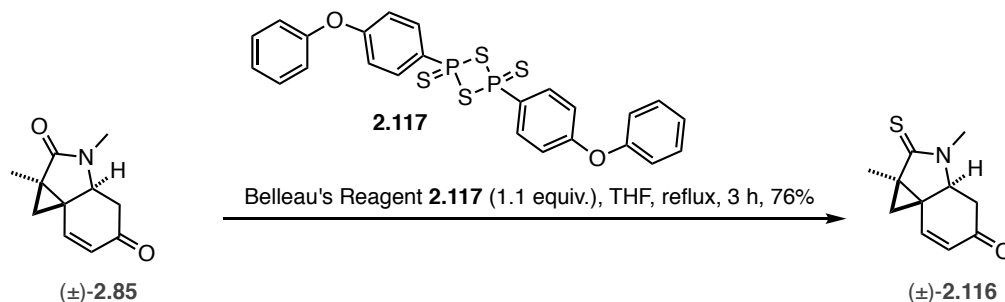
**Allylic alcohol 2.111**:  $[\alpha]_D^{17}$  -22.8 (*c* 1, CHCl<sub>3</sub>); IR (ATR) 3415, 2932, 1736, 1676, 1614, 1504, 1380, 1365, 1287, 1124, 915, 730 cm<sup>-1</sup>; <sup>1</sup>H NMR (400 MHz, C<sub>6</sub>D<sub>6</sub>)  $\delta$  6.81 (dd, *J* = 2.0, 0.8 Hz, 1 H), 5.99 (dd, *J* = 3.2, 2.4 Hz, 1 H), 5.90 (dd, 3.2, 0.8 Hz, 1 H), 5.43 (dd, *J* = 9.8, 0.6 Hz, 1 H), 5.36 (d, *J* = 9.6 Hz, 1 H), 3.76 (d, *J* = 14.8 Hz, 1 H), 3.54 (d, *J* = 14.0 Hz, 1 H), 3.37 (s, 1 H), 2.98 (dd, *J* = 13.2, 2.4 Hz, 1 H), 2.54 (s, 3 H), 2.42 (dd, *J* = 12.0, 0.8 Hz, 1 H), 1.68 (ap. t, *J* = 12.2 Hz, 1 H), 1.58-1.55 (m, 2 H), 1.31 (s, 3 H), 1.27-1.23 (m, 9 H), 1.08-1.05 (m, 1 H), 0.93 (s, 3 H), 0.92 (s, 3 H), 0.75 (d, *J* = 3.6 Hz, 1 H), 0.23 (d, *J* = 3.6 Hz, 1 H); <sup>13</sup>CNMR (100 MHz, CDCl<sub>3</sub>)  $\delta$  179.2, 159.0, 148.9, 139.5, 132.3, 128.8, 111.5, 103.1, 75.1, 60.9, 60.8, 59.5, 58.2, 39.1 (2C), 35.8, 32.4, 32.1, 31.9, 31.7, 27.2, 24.6, 20.5 (2C), 16.9, 10.8; HRMS (LCMS ESI+) *m/z* calcd for C<sub>26</sub>H<sub>38</sub>O<sub>5</sub>N<sub>3</sub> (M+H) 472.2806, found 472.2807. The relative configuration of allylic alcohol **2.111** was established through a combination of X-ray and <sup>1</sup>H NMR data. An X-ray crystal structure of (±)-**2.111** confirmed the assigned relative configuration. Crystals were grown by slow evaporation at room temperature from a mixture of Et<sub>2</sub>O/hexanes (1:1): Mp 91.4-94.3 °C.

**Allylic alcohol epi-2.111**:  $[\alpha]_D^{24}$  -1.0 (*c* 0.5, CHCl<sub>3</sub>); IR (ATR) 3413, 2932, 1744, 1677, 1611, 1504, 1451, 1381, 1364, 1287, 1177, 924, 736 cm<sup>-1</sup>; <sup>1</sup>H NMR (400 MHz, C<sub>6</sub>D<sub>6</sub>)  $\delta$  6.86 (dd, *J* = 2.0, 0.8 Hz, 1 H), 6.03 (dd, *J* = 3.2, 2.0 Hz, 1 H), 5.87 (dd, *J* = 3.2, 0.8 Hz, 1 H), 5.66 (dd, *J* = 9.8, 0.6 Hz, 1 H), 5.48 (d, *J* = 10.0 Hz, 1 H), 3.84, 3.80 (ABq, *J* = 14.4 Hz, 2 H), 3.53 (dd, *J* = 12.6, 2.6 Hz, 1 H), 3.48 (bs, 1 H), 2.47 (s, 3 H), 2.12 (ddd, *J* = 12.0, 2.8, 1.2 Hz, 1 H), 1.66-1.55



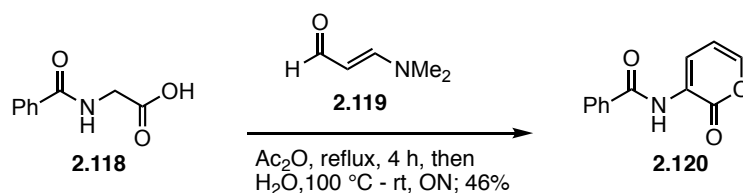


H), 2.36 (s, 3 H), 1.69 (s, 3 H), 1.60 (d,  $J = 3.6$  Hz, 1 H), 0.45 (d,  $J = 3.6$  Hz, 1 H);  $^{13}\text{C}$  NMR (100 MHz,  $\text{CDCl}_3$ )  $\delta$  135.6, 133.7, 128.8, 123.1, 118.2, 113.5, 110.5, 108.1, 69.8, 65.8, 40.1, 34.5, 27.9, 25.1, 24.4, 16.6; HRMS (LCMS ESI+)  $m/z$  calcd for  $\text{C}_{16}\text{H}_{19}\text{N}_2$  ( $\text{M}+\text{H}$ ) 239.1543, found 239.1541.

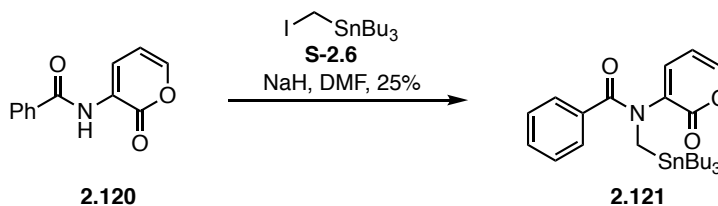


### 1a,3-Dimethyl-2-thioxo-1,1a,2,3,3a,4-hexahydro-5*H*-cyclopropa[*c*]indol-5-one

**(2.116).** A solution of enone  $(\pm)\text{-}\mathbf{2.85}$  (0.020 g, 0.11 mmol) in THF (2 mL) was treated with Belleau's reagent **2.117** (0.061 g, 0.12 mmol) and stirred at 66 °C under an atmosphere of nitrogen for 3 h. The reaction was quenched with  $\text{Na}_2\text{CO}_3$  and extracted with EtOAc (3x). The combined organic layers were dried ( $\text{Na}_2\text{SO}_4$ ), filtered and concentrated. The resulting residue was purified by chromatography on  $\text{SiO}_2$  (0-20% EtOAc/hexanes) to deliver thioamide **2.116** (0.016 g, 76%) as a yellow oil: IR (ATR) 2970, 2932, 2850, 1713, 1668, 1581, 1480, 1398, 1310, 1109  $\text{cm}^{-1}$ ;  $^1\text{H}$  NMR (400 MHz,  $\text{CDCl}_3$ )  $\delta$  7.02 (d,  $J = 9.6$  Hz, 1 H), 6.17 (d,  $J = 9.6$  Hz, 1 H), 4.10 (dd,  $J = 14.0, 4.0$  Hz, 1 H), 3.12 (s, 3 H), 3.03 (dd,  $J = 15.6, 4.0$  Hz, 1 H), 2.53 (ap. t,  $J = 14.8$  Hz, 1 H), 1.63 (s, 3 H), 1.20 (d,  $J = 4.0$  Hz, 1 H), 1.03 (d,  $J = 4.0$  Hz, 1 H);  $^{13}\text{C}$  NMR (100 MHz,  $\text{CDCl}_3$ )  $\delta$  208.1, 196.6, 148.1, 131.4, 64.3, 43.0, 42.1, 34.4, 32.3, 26.5, 14.1; HRMS (LCMS ESI) $^+$   $m/z$  calcd for  $\text{C}_{11}\text{H}_{14}\text{NOS}$  ( $\text{M}+\text{H}$ ) 208.0791, found 208.0790.

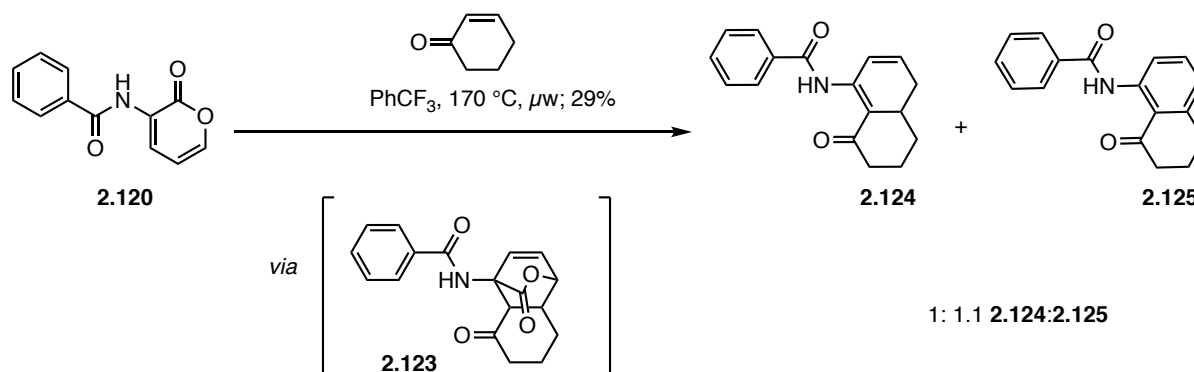


***N*-(2-Oxo-2*H*-pyran-3-yl)benzamide (2.120).** An oven-dried flask containing 3-dimethylaminoacrolein (**2.119**) (0.225 g, 2.27 mmol) in acetic anhydride (10 mL) was treated with hippuric acid (**2.118**) (0.407 g, 2.27 mmol) and the resulting orange solution heated to for 4 h during which time the solution became dark purple/black in color. The reaction was cooled to 100 °C and  $\text{H}_2\text{O}$  (10 mL) was added and the reaction was allowed to stir overnight cooling to room temperature. The resulting orange oil was concentrated under reduced pressure and filtered through a pad of  $\text{SiO}_2$  (washing with 20% EtOAc/hexanes), concentrated and purified by chromatography on  $\text{SiO}_2$  (10-25% EtOAc/hexanes) to deliver pyrone **2.120** (0.225 g, 46%) as a yellow solid:  $^1\text{H}$  NMR (400 MHz;  $\text{DMSO-d}_6$ )  $\delta$  9.56 (bs, 1 H), 8.07 (dd,  $J = 7.2, 2.0$  Hz, 1 H), 7.93 (d,  $J = 6.8$  Hz, 2 H), 7.68 (dd,  $J = 5.0, 1.8$  Hz, 1 H), 7.61 (d,  $J = 7.2$  Hz, 1 H), 7.54 (ap. t,  $J = 6.8$  Hz, 2 H), 6.54 (dd,  $J = 7.0, 5.0$  Hz, 1 H); HRMS (LCMS ESI) $^+$   $m/z$  calcd for  $\text{C}_{12}\text{H}_{10}\text{O}_3\text{N}$  (M+H) 216.0655, found 216.0654. The experimental  $^1\text{H}$  NMR was consistent with the literature-reported data.<sup>136</sup>



***N*-(2-Oxo-2*H*-pyran-3-yl)-*N*-((tributylstannyl)methyl)benzamide (2.121).** A solution of pyrone **2.120** (0.040 g, 0.19 mmol) in DMF (0.5 mL) at 0 °C was treated with NaH (0.0090 g, 60% dispersion in mineral oil, 0.22 mmol). The resulting mixture was stirred at 0 °C for 0.5 h

then treated with (iodomethyl)tributyltin (**S-2.6**) (0.084 g, 0.20 mmol) and stirred for 2 h warming to room temperature. The resulting brown solution reaction was diluted with Et<sub>2</sub>O and quenched with saturated aq. NH<sub>4</sub>Cl and the separated aqueous layer extracted with Et<sub>2</sub>O (2 x) and the combined organic layers dried (Na<sub>2</sub>SO<sub>4</sub>) and concentrated. The resulting residue was purified by chromatography on SiO<sub>2</sub> (0-15% EtOAc/hexanes) to deliver stannane **2.121** (0.024 g, 25%, 42% brsm) as a clear, yellow oil: IR (ATR) 2952, 2921, 2869, 2850, 1728, 1627, 1446, 1374, 911, 742 cm<sup>-1</sup>; <sup>1</sup>H NMR (400 MHz; CDCl<sub>3</sub>) δ 7.34 (dd, *J* = 5.1, 2.0 Hz, 1 H), 7.34-7.23 (m, 5 H), 6.74 (dd, *J* = 6.8, 1.8 Hz, 1 H), 5.99 (dd, *J* = 6.8, 5.2 Hz, 1 H), 3.22 (bs, 2 H), 1.57-1.49 (m, 6 H), 1.30 (dt, *J* = 14.7, 7.3 Hz, 6 H), 0.90 (ap. t, *J* = 8.2 Hz, 6 H), 0.88 (t, *J* = 7.3 Hz, 9 H); <sup>13</sup>C NMR (100 MHz; CDCl<sub>3</sub>) δ 170.4, 159.4, 150.4, 138.9, 135.6, 133.8, 130.2, 128.4, 127.7, 105.7, 36.4, 29.2, 27.6, 13.9, 11.1; HRMS (LCMS, ESI)<sup>+</sup> *m/z* calcd for C<sub>25</sub>H<sub>38</sub>O<sub>3</sub>NSn (M+H) 520.18682, found 520.18690.

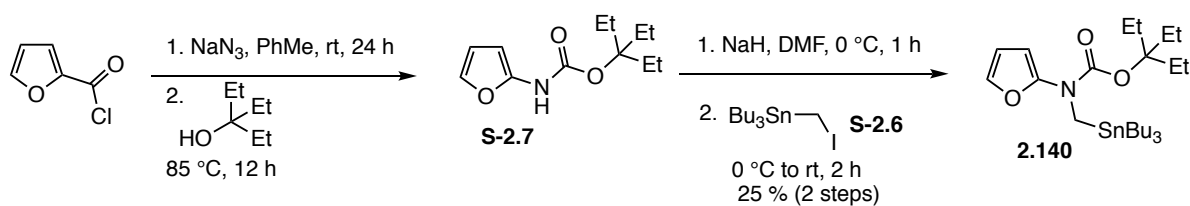


***N*-(8-Oxo-4,4a,5,6,7,8-hexahydronaphthalen-1-yl)benzamide (2.124) & *N*-(8-oxo-5,6,7,8-tetrahydronaphthalen-1-yl)benzamide (2.125).** A solution of pyrone **2.120** (0.028 g, 0.13 mmol) in PhCF<sub>3</sub> (0.5 mL) was treated with cyclohexenone (0.065 mL, 0.65 mmol) and the resulting solution heated under microwave irradiation in a sealed tube at 170 °C for 3 h. The reaction was concentrated and purified by chromatography on SiO<sub>2</sub> (5-10% EtOAc/ Hex) to

deliver dienone **2.124** (0.0040 mg, 12%, 23% brsm) as a white solid and protected aniline **2.125** (0.0060 mg, 17%, 35% brsm) as a yellow solid along with recovered starting material (14 mg).

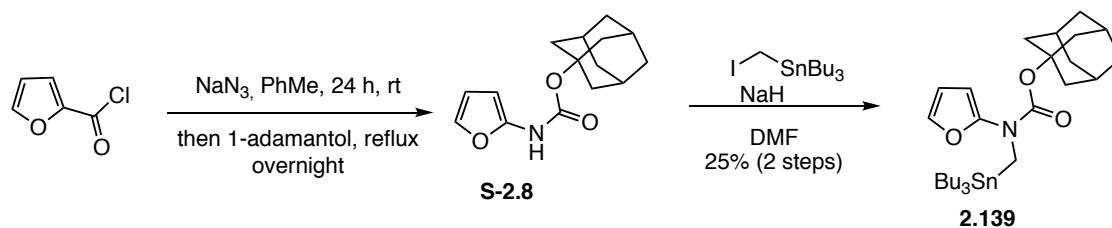
***N*-(8-Oxo-4,4a,5,6,7,8-hexahydronaphthalen-1-yl)benzamide (2.124):** IR (ATR) 2986, 2977, 2954, 2945, 2939, 2900, 2869, 1678, 1640, 1577, 1527, 1463, 1407, 1277, 1266, 1241, 1176, 1143  $\text{cm}^{-1}$ ;  $^1\text{H-NMR}$  (400 MHz;  $\text{CDCl}_3$ ):  $\delta$  13.81 (s, 1 H), 8.04-8.01 (m, 2 H), 7.57-7.47 (m, 3 H), 5.74-5.69 (m, 1 H), 5.66 (dtd,  $J = 9.9, 2.0, 0.84$  Hz, 1 H), 4.08 (dddd,  $J = 23.8, 6.6, 4.0, 0.80$  Hz, 1 H), 3.68 (ddt,  $J = 24.1, 9.7, 2.4$  Hz, 1 H), 3.23-3.13 (m, 1 H), 2.61 (dtd,  $J = 17.3, 6.6, 0.98$  Hz, 1 H), 2.46 (ap. dt,  $J = 17.3, 7.6$  Hz, 1 H), 2.05 (dq,  $J = 12.9, 4.7, 2.0$  Hz, 1 H), 1.94-1.87 (m, 2 H), 1.53-1.47 (m, 1 H);  $^{13}\text{C-NMR}$  (100 MHz,  $\text{CDCl}_3$ )  $\delta$  203.6, 166.5, 150.2, 134.5, 132.4, 128.9, 128.7, 128.0, 121.6, 112.8, 39.2, 35.5, 30.9, 29.7, 20.7; HRMS (LCMS)  $m/z$  calcd for  $\text{C}_{17}\text{H}_{18}\text{O}_2\text{N}$  ( $\text{M}+\text{H}$ ) = 268.1332, found 268.1330.

***N*-(8-Oxo-5,6,7,8-tetrahydronaphthalen-1-yl)benzamide (2.125):** IR (ATR) 2951, 2930, 2921, 2902, 2882, 2852, 1720, 1663, 1638, 1607, 1558, 1459, 1353, 1344, 1260, 1241, 1213, 1143, 1072, 794  $\text{cm}^{-1}$ ;  $^1\text{H-NMR}$  (400 MHz;  $\text{CDCl}_3$ ):  $\delta$  13.13 (s, 1 H), 8.85 (dd,  $J = 8.4, 1.1$  Hz, 1 H), 8.11-8.08 (m, 2 H), 7.54-7.52 (m, 4 H), 6.99 (dq,  $J = 7.6, 1.2$  Hz, 1 H), 3.02 (t,  $J = 6.0$  Hz, 2 H), 2.76 (dd,  $J = 6.9, 6.1$  Hz, 2 H), 2.14 (dq,  $J = 12.4, 6.0$  Hz, 2 H);  $^{13}\text{C-NMR}$  (125 MHz,  $\text{CDCl}_3$ ):  $\delta$  203.9, 166.4, 146.3, 142.5, 135.5, 135.2, 132.1, 128.9, 127.7, 123.4, 118.9, 118.6, 41.0, 31.2, 22.9; HRMS (LCMS)  $m/z$  calcd for  $\text{C}_{17}\text{H}_{16}\text{O}_2\text{N}$  ( $\text{M}+\text{H}$ ) = 266.1176, found 266.1173.



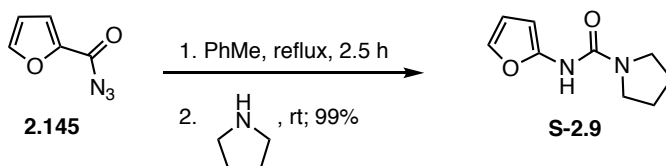
**3-Ethylpentan-3-yl furan-2-yl((tributylstannyl)methyl)carbamate (2.140).** A solution of sodium azide (0.39 g, 6.0 mmol) in toluene (4.8 mL) was treated with 2-furoyl chloride (0.53 mL, 5.3 mmol) and let stir at room temperature for 24 h. The resulting clear light yellow solution was treated with 3-ethyl-3-pentanol (1.85 g, 16 mmol) and stirred at 85 °C for 12 h during which time the solution became yellow then brown. The reaction was diluted with ethyl acetate and washed with NaHCO<sub>3</sub>. The separated aqueous layer was extracted (3x EtOAc) and the combined organic layers dried (Na<sub>2</sub>SO<sub>4</sub>) and concentrated. The resulting residue was purified by chromatography on SiO<sub>2</sub> (gradient elution 0-5% EtOAc/Hex) to deliver furan **S-2.7** (0.47 g, ca 40%, 81% pure, yield ~32%) with minor impurities as a yellow oil, which was used directly without further purification. <sup>1</sup>H NMR (300 MHz) δ 7.05 (s, 1 H), 6.61 (bs, 1 H), 6.33 (d, *J* = 2.1 Hz, 1 H), 6.02 (s, 1 H), 1.86 (q, *J* = 7.4 Hz, 6 H), 0.85 (t, *J* = 7.5 Hz, 9 H). A solution of furan **S-2.7** (0.072 g, 0.32 mmol) in dry DMF (1.3 mL) at 0 °C was treated with NaH (0.0077 g, 0.32 mmol) in portions. The reaction mixture was stirred at 0 °C for 1 h, at which time (iodomethyl)tributyltin **S-2.6** (0.15 g, 0.35 mmol) was added dropwise. The solution was stirred at 0 °C for 2 h, diluted with Et<sub>2</sub>O and quenched with saturated aq. NH<sub>4</sub>Cl. The separated aqueous layer was extracted with Et<sub>2</sub>O (2 x) and the combined organic layers were washed with brine, dried (Na<sub>2</sub>SO<sub>4</sub>) and concentrated. The resulting residue was purified by chromatography on SiO<sub>2</sub> (0-5% EtOAc/Hex) to deliver stannane **2.140** (0.055 g, 33%) as a clear and colorless oil: <sup>1</sup>H NMR (300 MHz) δ 7.14 (d, *J* = 1.2 Hz, 1 H), 6.32 (dd, *J* = 3.2, 2.3 Hz, 1 H), 5.92 (bs, 1 H), 3.35

(bs, 2 H), 1.79 (q,  $J = 7.2$  Hz, 6 H), 1.48-1.42 (m, 6 H), 1.27 (sextet,  $J = 7.2$  Hz, 6 H), 0.87 (t,  $J = 7.2$  Hz, 9 H), 0.86-0.76 (m, 15 H)

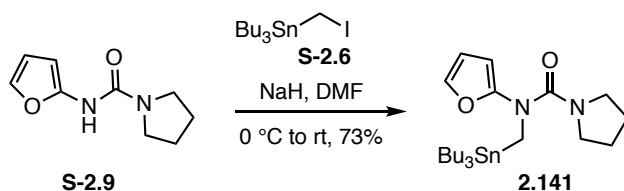


**(3*s*,5*s*,7*s*)-Adamantan-1-yl furan-2-yl((tributylstannyl)methyl)carbamate (2.139).** A stirred solution of 2-furoyl chloride (0.405 g, 3.10 mmol) in toluene (4.00 mL) was treated with sodium azide (0.230 g, 3.53 mmol) in one portion. After stirring the reaction mixture at room temperature for 24 h 1-adamantanol (1.42 g, 9.31 mmol) was added and the resulting solution was heated at reflux overnight. The reaction was diluted with ethyl acetate then treated with  $\text{NaHCO}_3$ . The separated aqueous phase was extracted with ethyl acetate (3x) and the combined organic layers dried ( $\text{Na}_2\text{SO}_4$ ), filtered and concentrated under reduced pressure. The residue was purified by chromatography on  $\text{SiO}_2$  (gradient elution 0-5%  $\text{EtOAc/Hex}$ ) to deliver carbamate **S-2.8** (0.376 g, 46%) as clear oil: IR (ATR) 3294, 2910, 2852, 1703, 1612, 1530, 1353, 1251, 1185, 1061  $\text{cm}^{-1}$ ;  $^1\text{H}$  NMR (300 MHz)  $\delta$  7.05 (dd,  $J = 2.0, 1.1$  Hz, 1 H), 6.60 (bs, 1 H), 6.33 (dd,  $J = 3.2, 2.3$  Hz, 1 H), 6.02 (bs, 1 H), 2.18 (s, 3 H), 2.15 (s, 6 H), 1.67 (s, 6 H);  $^{13}\text{C}$  NMR (125 MHz)  $\delta$  151.5, 145.6, 136.1, 111.5, 95.0, 41.6, 36.3, 31.0. A solution of carbamate **S-2.8** (0.10 g, 0.38 mmol) in dry  $\text{DMF}$  (1 mL) at 0  $^\circ\text{C}$  was treated with  $\text{NaH}$  (0.012 g, 0.46 mmol). The reaction mixture was stirred at 0  $^\circ\text{C}$  for 1 h, at which time (iodomethyl)tributyltin **S-2.6** (0.18 g, 0.42 mmol) was added dropwise. The solution was stirred at 0  $^\circ\text{C}$  for 2 h, diluted with  $\text{Et}_2\text{O}$  and quenched with saturated aq.  $\text{NH}_4\text{Cl}$ . The separated aqueous layer was extracted with  $\text{Et}_2\text{O}$  (3x) and the combined organic extracts were dried ( $\text{Na}_2\text{SO}_4$ ) and concentrated under reduced pressure. The resulting residue was purified by chromatography on  $\text{SiO}_2$  (0-5%  $\text{EtOAc/Hex}$ ) to

deliver stannane **2.139** (0.12 g, 57%) as a clear and colorless oil:  $^1\text{H}$  NMR (300 MHz)  $\delta$  7.12 (d,  $J = 0.9$  Hz, 1 H), 6.31 (dd,  $J = 3.2, 2.3$  Hz, 1H), 5.91 (bs, 1 H), 3.38 (bs 2 H), 2.15 (bs, 3 H), 2.10 (bs, 6 H), 1.65 (s, 6 H), 1.48–1.42 (m, 6 H), 1.27 (sextet,  $J = 7.2$  Hz, 6 H), 0.8 (t,  $J = 7.2$  Hz, 9 H), 0.84 (t,  $J = 8.1$  Hz, 6 H)

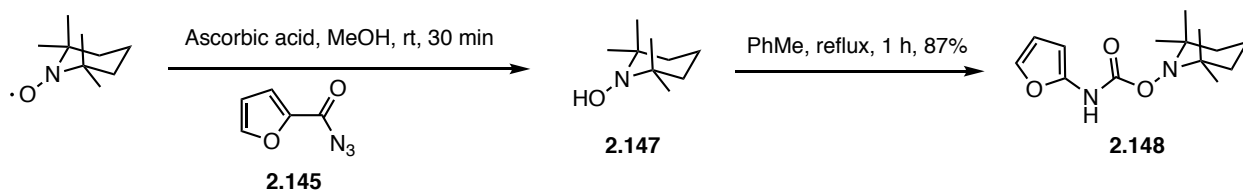


***N*-(Furan-2-yl)pyrrolidine-1-carboxamide (**S-2.9**)**. A solution of furan-2-carbonyl azide<sup>111</sup> (**2.145**) (0.500 g, 3.65 mmol) in anhydrous toluene (18 mL) was heated to reflux for 2.5 h. The reaction was cooled to 0 °C and treated with pyrrolidine (0.306 mL, 3.65 mmol) upon the addition of which a white gas evolved. The resulting solution was filtered through neutral alumina and concentrated to deliver urea **S-2.9** (0.650 g, 99%) as a pale yellow solid: Mp 129.2–134.8 °C; IR (ATR) 3219, 3174, 2867, 1646, 1532, 1519, 1471, 1349, 1234, 1204, 1003, 772  $\text{cm}^{-1}$ ;  $^1\text{H}$  NMR (400 MHz;  $\text{CDCl}_3$ )  $\delta$  7.05 (dd,  $J = 2.0, 0.8$  Hz, 1 H), 6.38 (bs, 1H), 6.34 (dd,  $J = 3.2, 2.0$  Hz, 1 H), 6.13 (dd,  $J = 3.2, 0.8$  Hz, 1 H), 3.43 (t,  $J = 5.8$  Hz, 4 H), 1.96 (t,  $J = 6.6$  Hz, 4H);  $^{13}\text{C}$  NMR (100 MHz;  $\text{CDCl}_3$ )  $\delta$  152.6, 146.5, 135.8, 111.6, 95.4, 46.0, 25.7; HRMS (ESI)<sup>+</sup>  $m/z$  calcd for  $\text{C}_9\text{H}_{13}\text{O}_2\text{N}_2$  (M+H) 181.09715, found 181.09663.



***N*-(Furan-2-yl)-*N*-((tributylstannyl)methyl)pyrrolidine-1-carboxamide (**2.141**)**. A solution of furanyl urea **S-2.9** (0.500 g, 2.77 mmol) in DMF (4.5 mL) at 0 °C was treated with NaH (0.0888 g, 90% dispersion in mineral oil, 3.33 mmol). The resulting mixture was stirred at 0

°C for 0.5 h then treated with (iodomethyl)tributyltin **S-2.6** (1.26 g, 2.91 mmol) and stirred for 1 h warming to room temperature. The reaction was diluted with Et<sub>2</sub>O and quenched with saturated aq. NH<sub>4</sub>Cl. The separated aqueous layer was extracted with Et<sub>2</sub>O (2 x) and the combined organic layers dried (Na<sub>2</sub>SO<sub>4</sub>) and concentrated. The resulting residue was purified by chromatography on SiO<sub>2</sub> (0-5% EtOAc/hexanes) to deliver stannane **2.141** (0.981 g, 73%) as a clear and colorless oil: IR (ATR) 2951, 2919, 2869, 2850, 1631, 1603, 1504, 1452, 1392, 1074, 999, 913, 733 cm<sup>-1</sup>; <sup>1</sup>H NMR (300 MHz; CDCl<sub>3</sub>) δ 7.18 (dd, *J* = 2.0, 1.1 Hz, 1 H), 6.31 (dd, *J* = 3.0, 2.1 Hz, 1 H), 5.82 (dd, *J* = 3.2, 0.8 Hz, 1 H), 3.19 (s, 2 H), 3.06 (t, *J* = 6.6 Hz, 4 H), 1.71 (t, *J* = 6.6 Hz, 4 H), 1.50-1.41 (m, 6 H), 1.28 (sextet, *J* = 7.2 Hz, 6 H), 0.87 (t, *J* = 7.2 Hz, 9 H), 0.88-0.83 (m, 6 H); <sup>13</sup>C NMR (100 MHz, CDCl<sub>3</sub>) δ 158.6, 152.2, 138.2, 111.1, 101.1, 47.7, 37.8, 29.2, 27.6, 25.6, 13.9, 10.4; HRMS (ESI) *m/z* calcd for C<sub>22</sub>H<sub>41</sub>O<sub>2</sub>N<sub>2</sub>Sn (M+H) 485.21845, found 485.21635.

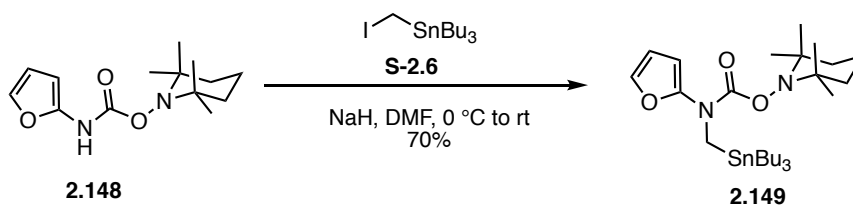


**2,2,6,6-Tetramethylpiperidin-1-ol (2.147).** Prepared based on protocols reported by Paleos and Dais<sup>137</sup> and Wipf<sup>138</sup>. A solution of TEMPO (2.00 g, 96% purity, 12.3 mmol) in deoxygenated MeOH (104 mL) was treated with ascorbic acid (2.60 g, 14.8 mmol) upon the addition of which the solution immediately changed color from clear and orange to a clear pale yellow solution. The solution was allowed to stir for 30 min, then concentrated under reduced pressure. The resulting residue was diluted with deoxygenated Et<sub>2</sub>O (60 mL) and water (60 mL) and transferred to a separatory funnel. The aqueous phase was further extracted with deoxygenated Et<sub>2</sub>O (4 x 30 mL) and the combined organic layers were dried (MgSO<sub>4</sub>) under



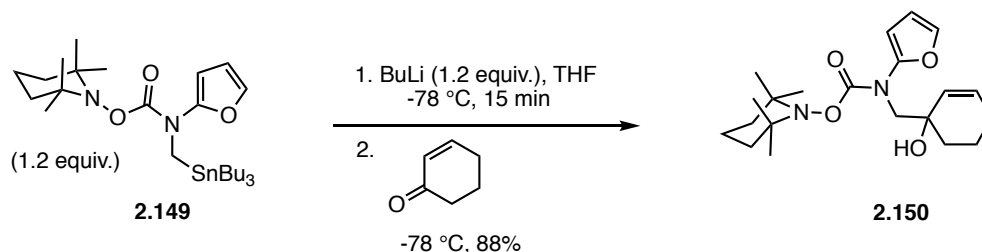
nitrogen, filtered and concentrated to deliver crude 2,2,6,6-tetramethylpiperidin-1-ol (**2.147**) (1.55 g, 80% crude yield), which was carried on without further purification.

**2,2,6,6-Tetramethylpiperidin-1-yl furan-2-ylcarbamate (2.148).** A solution of acyl azide **2.145**<sup>111</sup> (0.800 g, 5.84 mmol) in PhMe (45 mL) was heated at reflux for 1 h then cooled to room temperature. IR analysis of the reaction mixture indicated isocyanate formation ( $\nu_{\text{NCO}}$  2265  $\text{cm}^{-1}$ ). The reaction mixture was then treated with a solution of 2,2,6,6-tetramethylpiperidin-1-ol (**2.147**) (1.55 g, 9.86 mmol) in PhMe (12 mL). The resulting orange/brown solution was stirred for 1 h and concentrated. The residue was purified by chromatography on  $\text{SiO}_2$  (0-4% EtOAc/hexanes) to deliver TEMPO-carbamate **2.148** (1.35 g, 87%) as a white solid: Mp 101.4-102.8 °C; IR (ATR) 3256, 2936, 2924, 2921, 1715, 1620, 1506, 1439, 1379, 1251, 1154, 1010, 719  $\text{cm}^{-1}$ ;  $^1\text{H}$  NMR (500 MHz,  $\text{CDCl}_3$ )  $\delta$  9.00 (bs, 1 H), 7.10 (d,  $J = 1.0$  Hz, 1 H), 6.38 (dd,  $J = 3.3, 2.3$  Hz, 1 H), 6.17 (d,  $J = 3.0$  Hz, 1 H), 1.71-1.55 (m, 5 H), 1.48-1.44 (m, 1 H), 1.26 (s, 6 H), 1.19 (s, 6 H);  $^{13}\text{C}$  NMR (125 MHz,  $\text{CDCl}_3$ )  $\delta$  154.6, 144.9, 136.4, 111.7, 95.6, 61.5, 39.9, 31.7, 20.9, 16.9; HRMS (ESI+)  $m/z$  calcd for  $\text{C}_{14}\text{H}_{23}\text{O}_3\text{N}_2$  (M+H) 267.17032, found 267.17137.



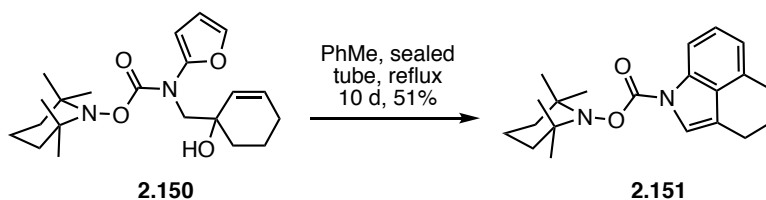
**2,2,6,6-Tetramethylpiperidin-1-yl furan-2-yl((tributylstannyl)methyl)carbamate (2.149).** A solution of furan **2.148** (0.150 g, 0.563 mmol) in DMF (0.9 mL) was cooled to 0 °C and treated with NaH (0.0270 g, 60% dispersion in mineral oil, 0.675 mmol). The resulting solution was stirred at 0 °C for 0.5 h then treated with (iodomethyl)tributyltin **S-2.6**<sup>139</sup> (0.255 g, 0.591 mmol). The resulting brown solution was stirred for 1 h while warming to room

temperature, diluted with Et<sub>2</sub>O and quenched with sat. NH<sub>4</sub>Cl<sub>(aq)</sub>. The aqueous layer was extracted with Et<sub>2</sub>O (2x) and the combined organic layers were dried (Na<sub>2</sub>SO<sub>4</sub>) and concentrated. The resulting residue was purified by chromatography on SiO<sub>2</sub> (0-3% EtOAc/hexanes) to deliver stannane **2.149** (0.223 g, 70%) as a clear, pale yellow oil: IR (ATR) 2947, 2926, 2923, 2869, 1728, 1609, 1502, 1430, 1377, 1349, 1185, 1072, 986 cm<sup>-1</sup>; <sup>1</sup>H NMR (400 MHz, C<sub>6</sub>D<sub>6</sub>) δ 6.90 (dd, *J* = 2.0, 0.80 Hz, 1 H), 6.05 (dd, *J* = 3.2, 2.0 Hz, 1 H), 5.93 (bs, 1 H), 3.35 (s, 2 H, <sup>2</sup>*J*<sup>117/119</sup>Sn-<sup>1</sup>H = 27.6 Hz), 1.69-1.54 (m, 9 H), 1.44-1.35 (m, 7 H), 1.33 (s, 6 H), 1.27-1.23 (m, 2 H), 1.09-1.05 (m, 6 H), 0.97-0.94 (m, 15 H); <sup>13</sup>C NMR (100 MHz, C<sub>6</sub>D<sub>6</sub>) δ 157.2, 151.1, 138.8, 111.3, 101.5, 60.4, 39.4, 36.7, 32.0, 29.6 (*J*<sup>117/119</sup>Sn-<sup>13</sup>C = 20 Hz), 27.9 (*J*<sup>117/119</sup>Sn-<sup>13</sup>C = 57 Hz), 20.6, 17.2, 14.0, 11.0 (<sup>1</sup>*J*<sup>119</sup>Sn-<sup>13</sup>C = 334 Hz, <sup>1</sup>*J*<sup>117</sup>Sn-<sup>13</sup>C = 319 Hz); HRMS (ESI+) *m/z* calcd for C<sub>27</sub>H<sub>51</sub>O<sub>3</sub>N<sub>2</sub>Sn (M+H) 571.29162, found 571.28963.



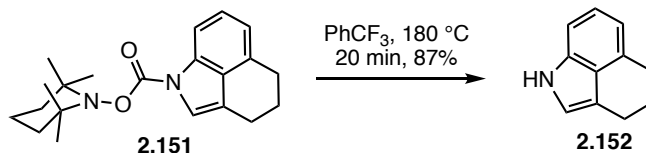
**2,2,6,6-Tetramethylpiperidin-1-ylfuran-2-yl((1-hydroxycyclohex-2-en-1-yl)methyl)carbamate (2.150).** A flame-dried flask cooled under an inert atmosphere was charged with stannane **2.149** (0.142 g, 0.250 mmol) and evacuated under high vacuum then backfilled with nitrogen (3x). THF (0.5 mL) was added and the resulting clear and colorless solution cooled to -78 °C, stirred for 10 min and treated dropwise with *n*-BuLi (0.100 mL, 2.5 M solution in hexanes, 0.250 mmol). The resulting clear, very pale yellow solution was stirred at -78 °C for 15 min then treated dropwise with enone (0.0201 mL, 0.208 mmol). The reaction was stirred for 30 min at -78 °C, diluted with EtOAc (2 mL) and quenched with NH<sub>4</sub>Cl (2 mL). The

separated aqueous layer was extracted (3 x EtOAc), dried (Na<sub>2</sub>SO<sub>4</sub>) and concentrated. The residue was purified by chromatography on SiO<sub>2</sub> (10-15% EtOAc/Hexanes) to yield allylic alcohol **2.150** (0.0691 g, 88%) as a white solid: Mp 114.8-116.5 °C; IR (ATR) 3443, 2967, 2930, 2883, 1730, 1610, 1502, 1363, 1284, 1172, 984, 733; <sup>1</sup>H NMR (500 MHz; CDCl<sub>3</sub>) δ 7.24 (d, *J* = 1.5 Hz, 1 H), 6.37 (dd, *J* = 3.3, 2.3 Hz, 1 H), 6.10 (d, *J* = 3.0 Hz, 1 H), 5.81 (dt, *J* = 10.0, 3.5 Hz, 1 H), 5.62 (d, *J* = 10.0 Hz, 1 H), 3.75 (d, *J* = 14.5 Hz, 1 H), 3.67 (d, *J* = 14.5 Hz, 1H), 3.50 (bs, 1 H), 2.03 (dd, *J* = 18.0, 5.0 Hz, 1 H), 1.91 (dd, *J* = 17.9, 3.1 Hz, 1 H), 1.78-1.53 (m, 7 H), 1.47 (dt, *J* = 13.2, 2.3 Hz, 2 H), 1.36 (dt, *J* = 13.3, 3.0 Hz, 1 H), 1.13 (s, 6 H), 0.92 (s, 6 H); <sup>13</sup>C NMR (100 MHz; CDCl<sub>3</sub>) δ 158.7, 149.1, 139.3, 130.6, 130.2, 111.2, 103.1, 70.9, 60.7, 60.7, 39.1, 33.9, 31.8, 31.8, 25.3, 20.4, 19.1, 17.0; HRMS (LCMS) *m/z* calcd for C<sub>21</sub>H<sub>33</sub>O<sub>4</sub>N<sub>2</sub> (M+H) 377.2435, found 377.2437.



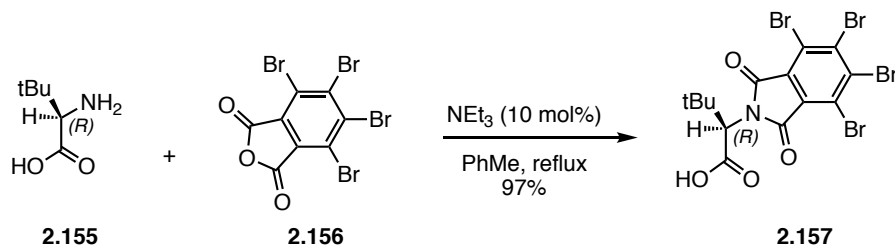
**2,2,6,6-Tetramethylpiperidin-1-yl 4,5-dihydrobenzo[*cd*]indole-1(3*H*)-carboxylate (2.151).** Allylic alcohol **2.150** (0.050 g, 0.13 mmol) in dry degassed toluene (10 mL) was heated in a sealed tube at reflux, during which time the solution became clear and brown. The reaction was stirred for 10 days and filtered through a pad of florisil (2% EtOAc/Hex) to deliver crude indole (0.039 g). The brown residue was purified by chromatography on SiO<sub>2</sub> (0-5% EtOAc/Hex) to deliver indole **2.151** (0.023 g, 51%) as a white film: IR (ATR) 2969, 2928, 2889, 2865, 1756, 1437, 1377, 1355, 1230, 1131, 1094, 753 cm<sup>-1</sup>; <sup>1</sup>H NMR (300 MHz; CD<sub>2</sub>Cl<sub>2</sub>) δ 7.81 (d, *J* = 8.1 Hz, 1 H), 7.30 (s, 1 H), 7.23 (t, *J* = 7.8 Hz, 1 H), 6.98 (d, *J* = 7.2 Hz, 1 H), 2.91 (t, *J* =

6.0 Hz, 2 H), 2.82 (t,  $J = 6.1$  Hz, 2 H), 2.03 (p,  $J = 6.1$  Hz, 2 H), 1.73-1.61 (m, 6 H), 1.31 (s, 6 H), 1.15 (s, 6 H);  $^{13}\text{C}$  NMR (100 MHz,  $\text{C}_6\text{D}_6$ , 70 °C)  $\delta$  152.3, 134.8, 132.6, 130.1, 125.6, 120.3, 119.2, 118.6, 113.4, 60.8, 39.9, 31.9 (broad), 27.5, 24.5, 22.1, 21.5 (broad) 17.4; HRMS (LCMS,  $\text{ESI}^+$ )  $m/z$  calcd for  $\text{C}_{21}\text{H}_{29}\text{O}_2\text{N}_2$  ( $\text{M}+\text{H}$ ) 341.22235, found 341.22141.



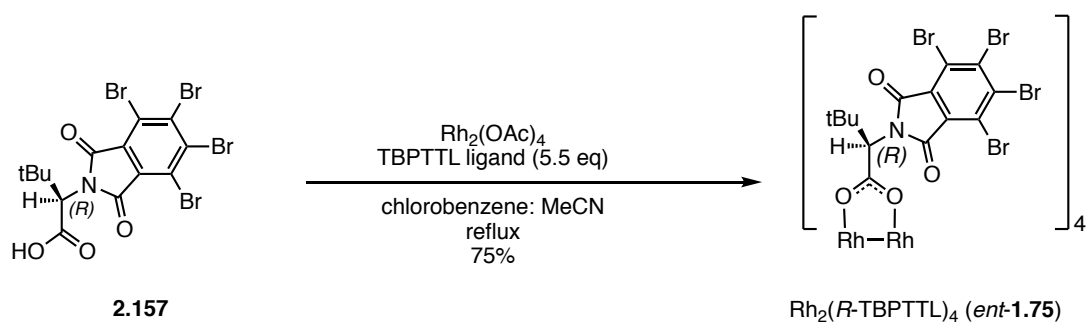
**1,3,4,5-Tetrahydrobenzo[*cd*]indole (138).** A solution of protected indole **2.151** (0.0040 g, 0.012 mmol) in  $\text{PhCF}_3$  (1 mL) was heated at 180 °C in the microwave for 1 h 20 min. The reaction was concentrated & purified by chromatography on  $\text{SiO}_2$  (2% EtOAc/hexanes) to deliver indole **2.152** (0.0016 g, 87%) as a white film:  $^1\text{H}$  NMR (500 MHz;  $\text{CDCl}_3$ )  $\delta$  7.80 (bs, 1 H), 7.15 (d,  $J = 8.5$ , 1 H), 7.10 (ap. t,  $J = 7.5$  Hz, 1 H), 6.85 (d,  $J = 1.0$  Hz, 1 H), 6.83 (dd,  $J = 6.8$ , 0.8 Hz, 1 H), 2.94 (t,  $J = 6.0$  Hz, 2 H), 2.87 (t,  $J = 6.2$  Hz, 2 H), 2.07 (ap. quintet,  $J = 6.1$  Hz, 2 H). The experimental  $^1\text{H}$  NMR was consistent with the literature-reported data.<sup>83</sup>

### 3.2.4 CHAPTER TWO EXPERIMENTAL PART: (+)-2.1



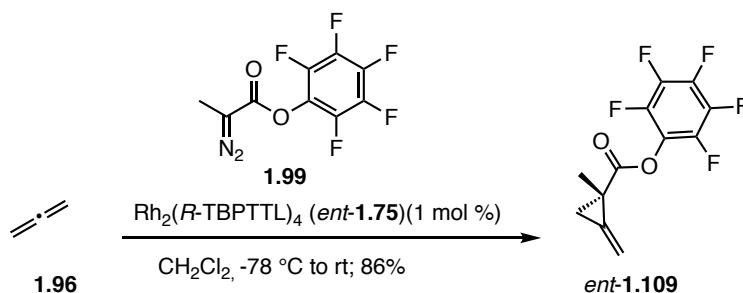
***N*-Tetrabromophthaloyl-(*R*)-*tert*-leucine (2.157).** An oven-dried round bottom flask topped with a Dean Stark apparatus and condenser was charged sequentially with D-*tert*-leucine

**2.155** (0.500 g, 3.77 mmol), tetrabromophthalic anhydride **2.156** (1.79 g, 3.77 mmol), anhydrous toluene (10 ml) and triethylamine (0.0536 mL, 0.377 mmol) and the resulting heterogeneous mixture heated at reflux while the solvent was removed at a rate of  $\sim 1$  mL/h. The resulting solution was cooled to room temperature and treated with 5% HCl (6 mL) and EtOAc (15 mL). The separated aqueous layer was extracted with EtOAc (6 mL) and the combined organic layers were dried ( $\text{Na}_2\text{SO}_4$ ) and concentrated to deliver N-tetrabromophthaloyl-(*R*)-*tert*-leucine (**2.157**) (2.11 g, 97%) as a white solid:  $[\alpha]_{\text{D}}^{20} +22.3$  ( $c$  0.40, EtOH);  $^1\text{H}$  NMR (300 MHz, acetone- $d_6$ )  $\delta$  4.68 (s, 1 H), 1.19 (s, 9 H). The experimental  $^1\text{H}$  NMR was consistent with the literature-reported data for the enantiomer.<sup>55</sup>



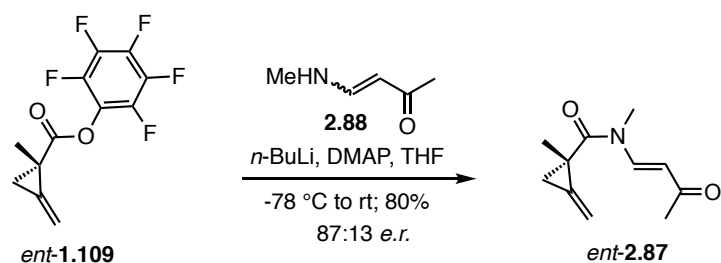
**Dirhodium(II) tetrakis[N-tetrabromophthaloyl-(*R*)-*tert*-leucinate] [ $\text{Rh}_2(\text{R-TBPTTL})_4$ ] (**ent-1.75**). An oven dried flask topped with a dean stark apparatus and condenser was charged with  $\text{Rh}_2(\text{OAc})_4$  (0.130 g, 0.294 mmol) and N-tetrabromophthaloyl-(*R*)-*tert*-leucine **2.157** (0.933 g, 1.62 mmol) and a solution of chlorobenzene/  $\text{CH}_3\text{CN}$  (9:1, 13 mL). The resulting dark purple mixture was heated at reflux while the solvent was removed at a rate of  $\sim 1$  mL/ h for 5 h during which time the solution becomes emerald green. After 5 h the reaction was cooled to room temperature and treated sequentially with toluene (40 mL) and sat.  $\text{NaHCO}_3$  (40 mL). The separated organic layer was washed with  $\text{NaHCO}_3$  (1x 40mL), brine (1 x 40mL), filtered and dried ( $\text{Na}_2\text{SO}_4$ ) to deliver  $\text{Rh}_2(\text{R-TBPTTL})_4$  **ent-1.75** (0.555 g, 75%) as a green solid which was**

used directly without further purification:  $^1\text{H}$  NMR (300 MHz, benzene- $d_6$ )  $\delta$  5.37 (s, 4 H), 1.45 (s, 36 H). The experimental  $^1\text{H}$  NMR was consistent with the literature-reported data for the enantiomer.<sup>55</sup>



**Perfluorophenyl (*S*)-1-methyl-2-methylenecyclopropane-1-carboxylate (*ent*-1.109).**

An oven-dried three neck flask fitted with a nitrogen inlet, a dry-ice condenser and a septum was charged with  $\text{Rh}_2(\text{R-TBPTTL})_4$  (*ent*-1.75) (0.566 g, 0.226 mmol) and  $\text{CH}_2\text{Cl}_2$  (141 mL) and the resulting green solution cooled to  $-78\text{ }^\circ\text{C}$  (dry ice/acetone bath) and treated dropwise with an excess of condensed allene gas (**1.96**) (~65 drops, approx. 5.14 g, ~ 5.52 mmol). The resulting solution was then treated with a solution of perfluorophenyl 2-diazopropanoate (**1.99**) (6.00 g, 22.6 mmol) in  $\text{CH}_2\text{Cl}_2$  (12 mL) via syringe pump at a rate of ~ 2 mL/h. The resulting solution was allowed to stir at  $-78\text{ }^\circ\text{C}$  for 1 h before warming to room temperature. The resulting green residue was purified by chromatography on  $\text{SiO}_2$  (0-1%  $\text{Et}_2\text{O}/\text{Hex}$ ) to deliver methylenecyclopropane *ent*-1.109 (5.41 g, 86%) as a clear and pale yellow oil:  $[\alpha]_{\text{D}}^{19} +2.8$  ( $c$  7.6,  $\text{CHCl}_3$ );  $^1\text{H}$  NMR (500 MHz,  $\text{CD}_2\text{Cl}_2$ )  $\delta$  5.64 (ap. t,  $J = 2.8$  Hz, 1 H); 5.56 (ap. t,  $J = 2.3$  Hz, 1 H), 2.30 (dt,  $J = 9.5, 2.5$  Hz, 1 H), 1.63 (dt,  $J = 9.2, 2.4$  Hz, 1 H), 1.51 (s, 3 H); HRMS (ESI+)  $m/z$  calcd for  $\text{C}_{12}\text{H}_8\text{O}_2\text{F}_5$  ( $\text{M}+\text{H}$ ) 279.04390, found 279.04502. The experimental data was consistent with the reported data for the enantiomer.<sup>140</sup>



**(*S,E*)-*N*,1-Dimethyl-2-methylene-*N*-(3-oxobut-1-en-1-yl)cyclopropane-1-carboxamide (*ent*-2.87).** An oven-dried round bottom flask was charged with vinylogous amide **2.88** (2.77 g, 27.9 mmol) and evacuated and backfilled with nitrogen (3x). Distilled THF (93 mL) was added and the resulting solution cooled to -78 °C and treated dropwise with *n*-BuLi (11.7 mL, 2.5 M solution of hexanes, 29.3 mmol) and stirred for 5 min at -78 °C then treated dropwise with a solution of perfluorophenyl (*S*)-1-methyl-2-methylenecyclopropane-1-carboxylate *ent*-1.109 (8.15 g, 29.3 mmol) in THF (15 mL). The resulting solution was then treated with DMAP (0.0341 g, 0.279 mmol) and stirred for 10 min at -78 °C. The cold bath was removed and the reaction was allowed to warm to room temperature. The reaction was treated with sat. NaHCO<sub>3</sub> and EtOAc was added. The separated aqueous layer was extracted with EtOAc (3 x) and the combined organic layers dried and concentrated. The crude product was purified by chromatography on SiO<sub>2</sub> (10-15% EtOAc/Hex) to deliver (*S,E*)-*N*,1-dimethyl-2-methylene-*N*-(3-oxobut-1-en-1-yl)cyclopropane-1-carboxamide (*ent*-2.87) (4.30 g, 80%, *er* 87:13) as a clear and pale yellow oil:  $[\alpha]_{\text{D}}^{19} -243.2$  (*c* 2.24, CHCl<sub>3</sub>); <sup>1</sup>H NMR (500 MHz, CDCl<sub>3</sub>)  $\delta$  8.37 (d, *J* = 14.0 Hz, 1 H), 5.73 (d, *J* = 13.5 Hz, 1 H), 5.71 (ap. t, *J* = 2.8 Hz, 1 H), 5.53 (s, 1 H), 3.15 (s, 3 H), 2.29 (s, 3 H), 1.80 (dt, *J* = 9.8, 2.4 Hz, 1 H), 1.50 (s, 3 H), 1.33 (dt, *J* = 9.7, 2.4 Hz, 1 H); HRMS (ESI)+ *m/z* calcd for C<sub>11</sub>H<sub>16</sub>O<sub>2</sub>N (M+H) 194.1176, found 194.1175.

SFC conditions: Chiralpak-IC semi-prep column (250 x 10mm), gradient elution: 5-15% (rate 1.0), 7 mL/min, 254 nm, P=100 (BAR).

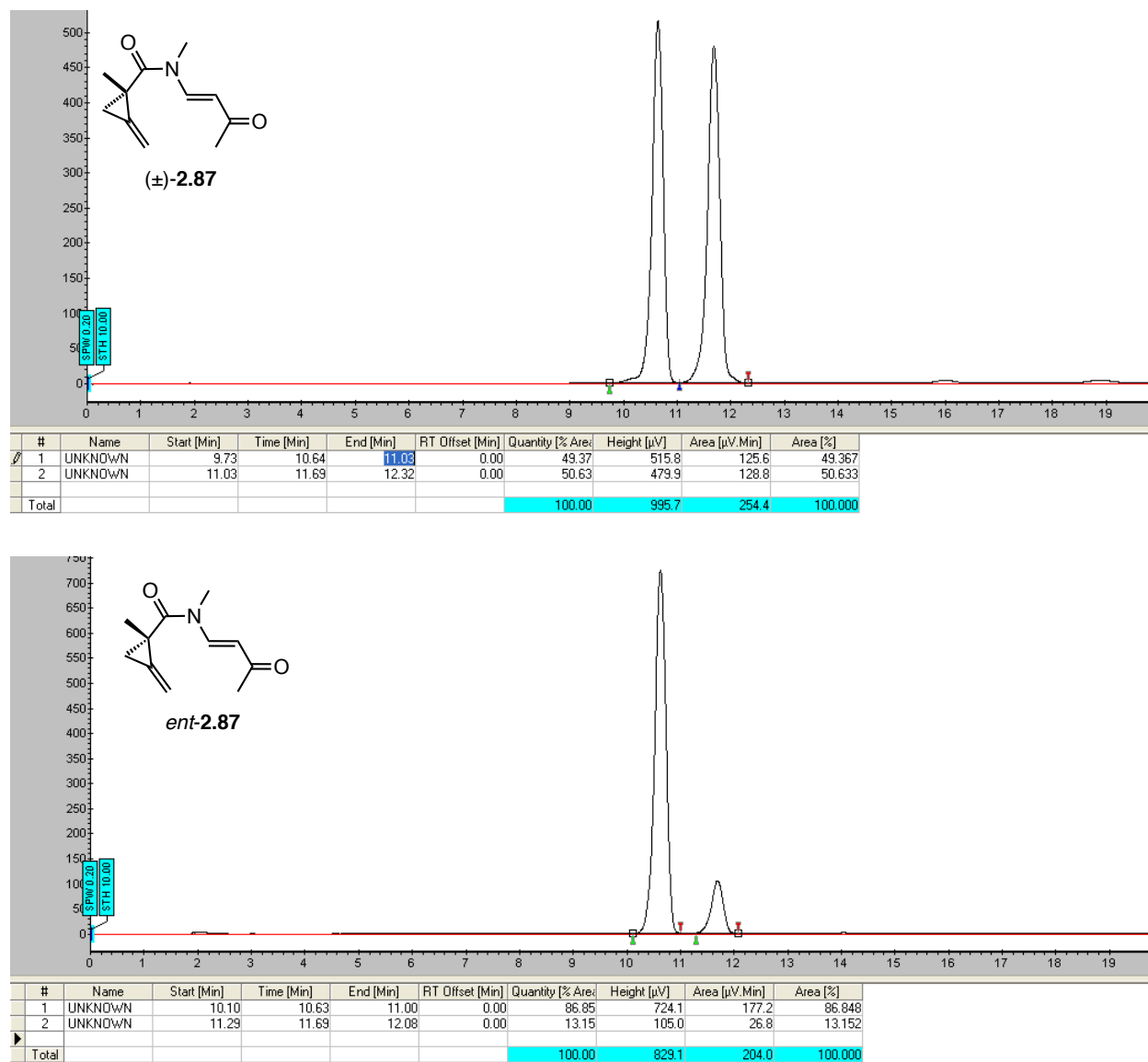
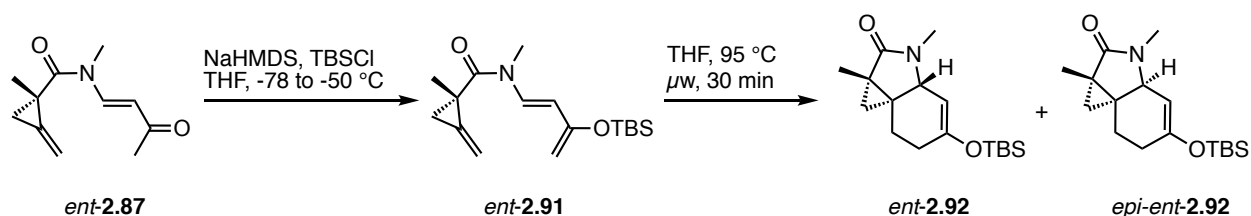


Figure 3-16 SFC chromatogram of racemic standard and enantioenriched amide *ent*-2.87 (87:13 *er*)

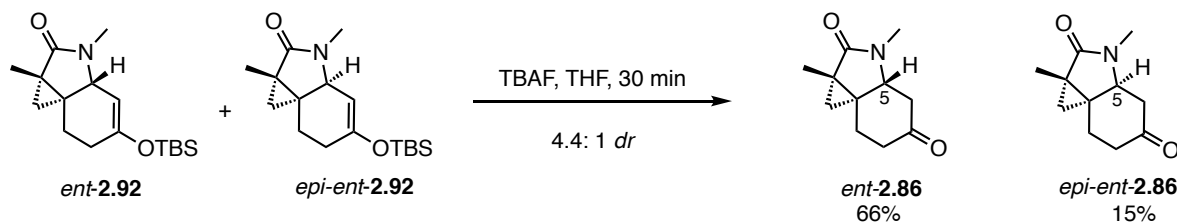




**(1a*S*,3a*R*,7a*R*)-5-((*tert*-Butyldimethylsilyl)oxy)-1a,3-dimethyl-1,1a,3,3a,6,7-hexahydro-2*H*-cyclopropa[*c*]indol-2-one (*ent*-2.92) and (1a*S*,3a*S*,7a*R*)-5-((*tert*-butyldimethylsilyl)oxy)-1a,3-dimethyl-1,1a,3,3a,6,7-hexahydro-2*H*-cyclopropa[*c*]indol-2-one (*epi-ent*-2.92).**

An oven-dried flask was charged with NaHMDS (2.50 g, 12.9 mmol) followed by anhydrous THF (150 mL) under an atmosphere of nitrogen. The resulting clear and colorless solution was stirred for 15 min at room temperature then cooled to -78 °C and stirred for a further 15 min at this temperature prior to treatment with vinylogous amide *ent*-2.87 (2.75 g, 14.2 mmol) in THF (20 mL) slowly at a rate of ~4 mL/h maintaining the temperature of the acetone/dry ice bath below -50 °C. During the slow addition of the amide the solution changes color from clear and pale yellow to clear and orange. The resulting clear, orange solution was allowed to warm to -50 °C over 1 h, cooled to -78 °C and treated dropwise with a solution of TBSCl (2.36 g, 15.5 mmol) in THF (52 mL). The reaction was allowed to stir for a further 5 min at -78 °C before the cold bath was removed and the reaction allowed to reach room temperature. <sup>1</sup>H NMR analysis of an aliquot (CDCl<sub>3</sub>) indicated conversion to enol ether *ent*-2.91. The reaction was concentrated and directly subjected to the following reaction: <sup>1</sup>H NMR (300 MHz, CDCl<sub>3</sub>) δ 7.65 (d, *J* = 13.5 Hz, 1 H), 5.67 (ap. s, 1 H), 5.52 (d, *J* = 13.8 Hz, 1 H), 5.45 (ap. s, 1 H), 4.23 (s, 2 H), 3.13 (s, 3 H), 1.73 (dt, *J* = 9.6, 2.1 Hz, 1 H), 1.47 (s, 3 H), 1.25 (dt, *J* = 9.4, 2.2 Hz, 1 H), 1.00 (s, 9 H), 0.24 (d, *J* = 2.7 Hz, 6 H). A solution of crude amide *ent*-2.91 (assumed 3.98 g, 12.9 mmol) in THF (28 mL, 3.5 mL x 8 batches) was heated under microwave irradiation at 95 °C for

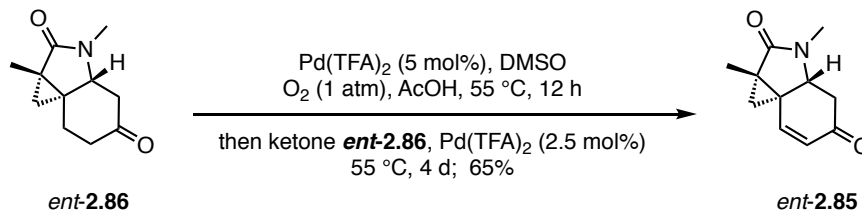
30 min then concentrated to deliver the crude Diels-Alder adducts *ent*-**2.92** and *epi-ent*-**2.92** (assumed 3.98 g, 12.9 mmol) as orange oils which were used directly in the next reaction.



**(1a*S*,3a*R*,7a*R*)-1a,3-Dimethylhexahydro-2*H*-cyclopropa[*c*]indole-2,5(3*H*)-dione (*ent*-**2.86**) & (1a*S*,3a*S*,7a*R*)-1a,3-dimethylhexahydro-2*H*-cyclopropa[*c*]indole-2,5(3*H*)-dione (*epi-ent*-**2.86**).** The crude enol ether adducts *ent*-**2.92** and *epi-ent*-**2.92** (assumed 3.98 g, 12.9 mmol) were immediately taken up in THF (130 mL) was treated dropwise with TBAF (12.9 mL, 1M solution in THF, 12.9 mmol) and stirred at room temperature for 30 min. The reaction mixture was filtered through a pad of florisil (washing with EtOAc) and concentrated. The resulting residue was purified by chromatography on SiO<sub>2</sub> (20% to elute RSM, then 50-70% EtOAc/Hex to elute *trans*-diastereomer, then 90-100% EtOAc/Hexanes to elute *cis*-diastereomer) to deliver *trans*-ketone *ent*-**2.86** (1.64 g, 66%) as a pale yellow solid and *cis*-ketone *epi-ent*-**2.86** (0.371 g, 15%) as a yellow oil.

***trans*-Ketone (*ent*-**2.86**):**  $[\alpha]_D^{19} -104.3$  (*c* 0.93 CHCl<sub>3</sub>); <sup>1</sup>H NMR (400 MHz, CDCl<sub>3</sub>)  $\delta$  3.41 (dd, *J* = 12.8, 4.0 Hz, 1 H), 2.80 (ddd, *J* = 13.6, 4.0, 1.6 Hz, 1 H), 2.69 (ddt, *J* = 15.5, 4.8, 1.6 Hz, 1 H), 2.66 (s, 3 H), 2.54 (ddd, *J* = 15.4, 12.2, 7.2 Hz, 1 H), 2.35 (ap.t, *J* = 13.4 Hz, 1 H), 2.13 (tdd, *J* = 12.6, 5.0, 1.4 Hz, 1 H), 1.72 (ddd, *J* = 13.1, 7.3, 1.9 Hz, 1 H), 1.38 (s, 3 H), 0.95 (d, *J* = 3.6 Hz, 1 H), 0.66 (d, *J* = 4.0 Hz, 1 H); HRMS (ESI)<sup>+</sup> *m/z* calcd for C<sub>11</sub>H<sub>16</sub>O<sub>2</sub>N (M+H) 194.11756, found 194.11786.

**cis-ketone (*epi-ent-2.86*):**  $[\alpha]_D^{19} +11.0$  ( $c$  0.15  $\text{CHCl}_3$ );  $^1\text{H}$  NMR (300 MHz,  $\text{CDCl}_3$ )  $\delta$  3.73 (ap. t,  $J = 6.5$  Hz, 1 H), 2.84 (dd,  $J = 15.0, 6.0$  Hz, 1 H), 2.72 (s, 3 H), 2.53-2.25 (m, 4 H), 1.83 (dt,  $J = 14.2, 5.2$  Hz, 1 H), 1.34 (s, 3 H), 0.93 (d,  $J = 4.5$  Hz, 1 H), 0.84 (d,  $J = 4.5$  Hz, 1 H); HRMS (ESI)+  $m/z$  calcd for  $\text{C}_{11}\text{H}_{16}\text{O}_2\text{N}$  ( $\text{M}+\text{H}$ ) 194.11756, found 194.11777



**(1*aS*,3*aR*,7*aS*)-1*a*,3-Dimethyl-1,1*a*,3*a*,4-tetrahydro-2*H*-cyclopropa[*c*]indole-2,5(3*H*)-dione (*ent-2.85*).** A solution of  $\text{Pd}(\text{TFA})_2$  (0.0441 g, 0.129 mmol) and DMSO (0.0184 mL, 0.259 mmol) in AcOH (13 mL) was heated at 55 °C under an atmosphere of oxygen (balloon). After stirring at 55 °C overnight ketone *ent-2.86* (0.500 g, 2.59 mmol) was added and the reaction allowed to stir at room 55 °C for 4 days during which time additional catalyst (2x 0.11 g) was added after 24 and 48 h to drive the reaction to completion. The reaction was concentrated and purified by chromatography (50-70% EtOAc/Hexanes) to deliver enone *ent-2.85* (0.320 g, 65%) as a pale yellow solid.

Representative protocol for the enantiomeric enrichment by recrystallization: Enone *ent-2.85* (0.110 g, 0.573 mmol) was dissolved in boiling MTBE (9.5 mL) and 1,2-dichloroethane (0.4 mL) and allowed to cool to room temperature. The resulting solution was allowed to stand overnight at -20 °C during which time white needle-shaped crystals formed. The mother liquor was removed via pipette transfer and the crystals were washed with MTBE (2x) and placed under vacuum to remove trace solvents. The first recrystallization provided crystals of >99.5:0.5 *er*, the second recrystallization provided crystals of 95.4:4.6 *er* and the third recrystallization

provided crystals of 98:2 *er* to deliver a combined yield of enone *ent*-**2.85** (0.0654 g, 60%, 69% of theoretical maximum) as a white crystalline solid. Only combined samples with *er* >97.5:2.5 were carried on in the subsequent reaction:  $[\alpha]_D^{17} + 111.1$  (*c* 0.484, CHCl<sub>3</sub>); <sup>1</sup>H NMR (400 MHz, CDCl<sub>3</sub>)  $\delta$  6.98 (d, *J* = 9.6 Hz, 1 H), 6.15 (d, *J* = 9.6 Hz, 1 H), 3.82 (dd, *J* = 14.2, 3.8 Hz, 1 H), 2.91 (dd, *J* = 15.9, 3.6 Hz, 1 H), 2.72 (s, 3 H), 2.44 (dd, *J* = 15.6, 14.0 Hz, 1 H), 1.47 (s, 3 H), 1.34 (d, *J* = 4.0 Hz, 1 H), 0.86 (d, *J* = 4.0 Hz, 1 H); HRMS (ESI)+ *m/z* calcd for C<sub>11</sub>H<sub>14</sub>O<sub>2</sub>N (M+H) 192.1019, found 192.1018. SFC analysis: Chiralpak-IC semiprep column (250 x 10 mm), gradient elution: 1-30% *i*PrOH (rate 1.0), 5.5 mL/min, 254 nm, P=100 (BAR).

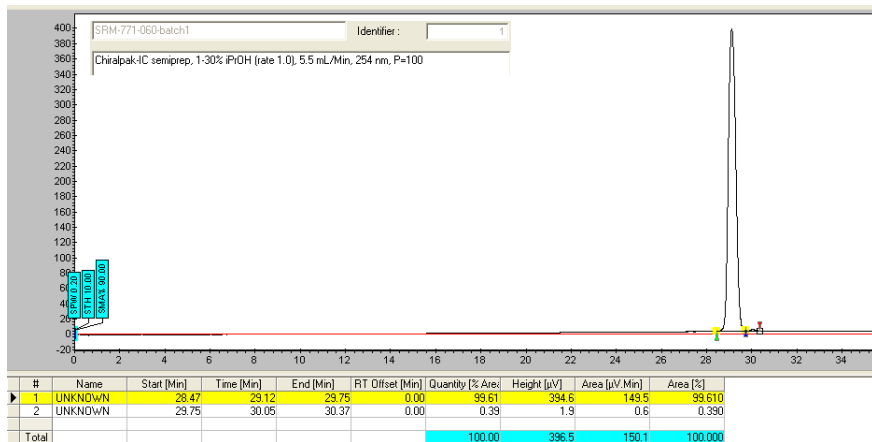
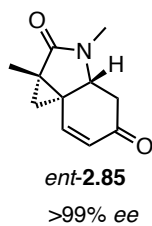
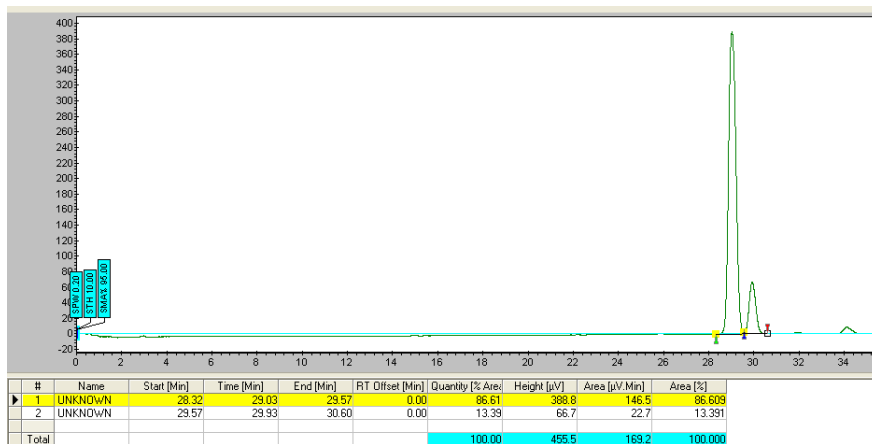
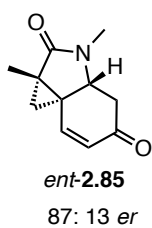
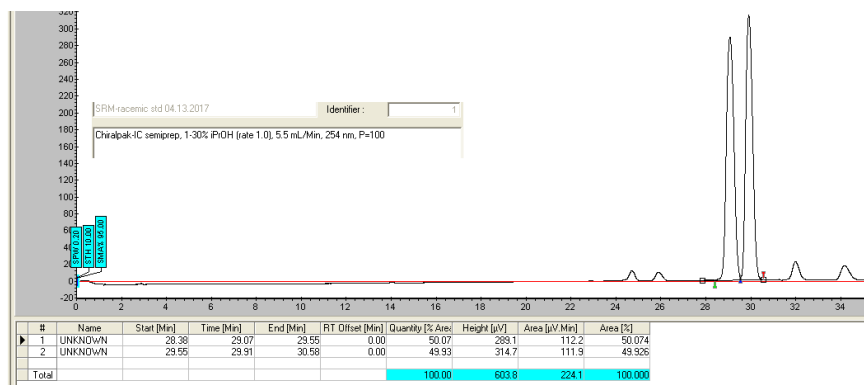
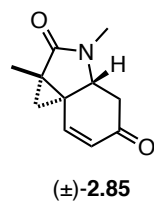
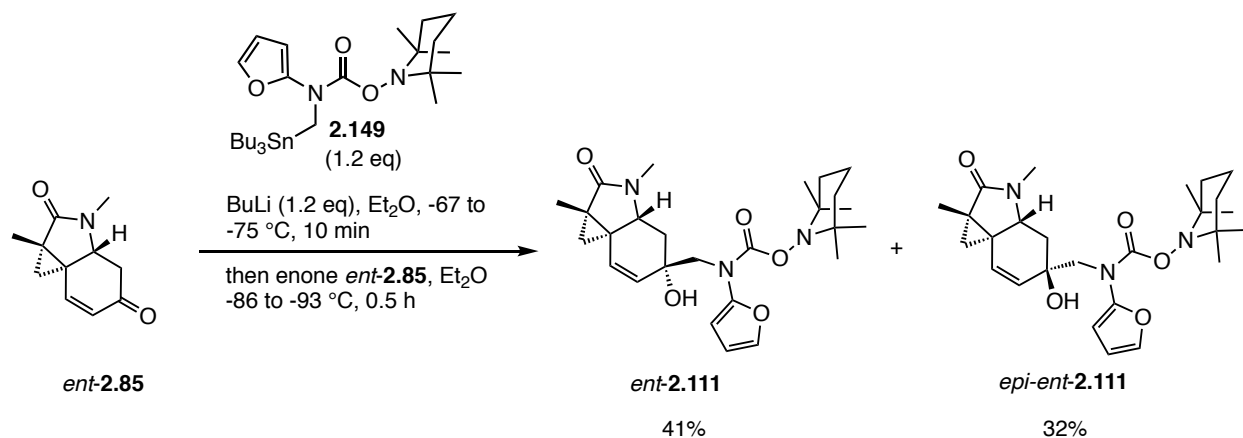


**Figure 3-17** Representative SFC chromatograms of a) racemic standard b) enone *ent*-2.85 before recrystallization and c) enantioenriched enone *ent*-2.85 after recrystallization (batch 1)

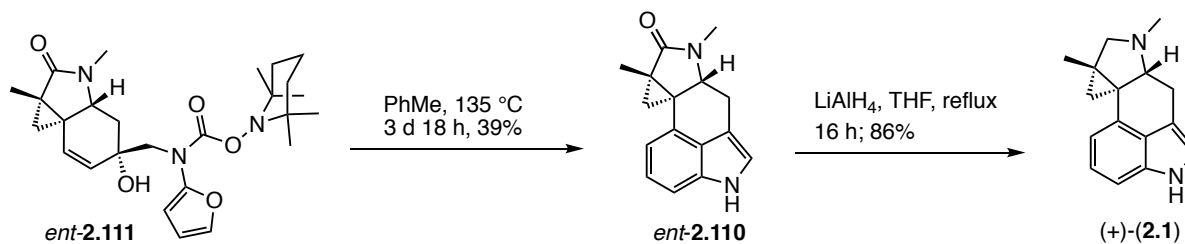


**Allylic alcohols *ent*-2.111 and *epi-ent*-2.111.** An oven-dried 3-neck 25 mL flask fitted with two stoppers and nitrogen inlet was charged with stannane **2.149** (0.893 g, 1.57 mmol) and evacuated under high vacuum then backfilled with nitrogen (3x). A stopper was exchanged for a thermocouple thermometer and anhydrous  $\text{Et}_2\text{O}$  (5 mL) was added. The clear, pale yellow solution was cooled to -70.5 °C ( $\text{Et}_2\text{O}$ /dry ice) and stirred for 10 min then treated dropwise with *n*-BuLi (0.628 mL, 2.5 M solution in hexanes, 1.57 mmol) during which time the temperature rose to -67.4 °C. The resulting clear, yellow solution was stirred for 15 min maintaining the internal temperature between -67.4 and -74.5 °C then cooled to -93.1 °C (liquid nitrogen/ $\text{Et}_2\text{O}$  bath) and treated with enone **ent-2.85** (0.250 g, 1.31 mmol) in anhydrous THF/ $\text{Et}_2\text{O}$  1:1 (3.5 mL) slowly over 10 min in 0.4 mL portions during which time the temperature rose to -86 °C. The reaction was stirred for 30 min maintaining the temperature below -90 °C, then stirred for a further hour warming to -76 °C. The reaction was then diluted with EtOAc and quenched with  $\text{NH}_4\text{Cl}$  maintaining the internal temperature below -50 °C. The separated aqueous layer was extracted (5 x EtOAc), dried ( $\text{Na}_2\text{SO}_4$ ) and concentrated. The residue was purified by chromatography on  $\text{SiO}_2$  (gradient elution 5% acetone/ $\text{CH}_2\text{Cl}_2$  to elute enone **ent-2.85** recovered starting material then alcohol **ent-2.111**, then 10% acetone/ $\text{CH}_2\text{Cl}_2$  to elute alcohol **epi-ent-2.111**)

to deliver enone *ent*-**2.85** (3 mg) as a white solid, alcohol *ent*-**2.111** (0.250 g, 41%) as a white foam and alcohol *epi-ent*-**2.111** (0.196 g, 32%) as a white foam.

**Allylic alcohol *ent*-2.111:**  $[\alpha]_D^{18} +30.1$  ( $c$  0.2,  $\text{CHCl}_3$ );  $^1\text{H}$  NMR (500 MHz,  $\text{C}_6\text{D}_6$ )  $\delta$  6.81 (d,  $J$  = 1.0 Hz, 1 H), 5.98 (dd,  $J$  = 3.3, 2.3 Hz, 1 H), 5.89 (d,  $J$  = 2.5 Hz, 1 H), 5.43 (d,  $J$  = 9.5 Hz, 1 H), 5.36 (d,  $J$  = 9.5 Hz, 1 H), 3.74 (d,  $J$  = 14.5 Hz, 1 H), 3.54 (d,  $J$  = 15.0 Hz, 1 H), 3.30 (s, 1 H), 2.97 (dd,  $J$  = 13.3, 2.3 Hz, 1 H), 2.53 (s, 3 H), 2.40 (ap. t,  $J$  = 10.8 Hz, 1 H), 1.67 (ap. t,  $J$  = 12.3 Hz, 1 H), 1.54 (ap. t,  $J$  = 13.0 Hz, 2 H), 1.31 (s, 3 H), 1.27-1.23 (m, 9 H), 1.06 (dt,  $J$  = 13.5, 2.8 Hz, 1 H), 0.93 (s, 3 H), 0.92 (s, 3 H), 0.75 (d,  $J$  = 3.5 Hz, 1 H), 0.23 (d,  $J$  = 3.5 Hz, 1 H); HRMS (ESI+)  $m/z$  calcd for  $\text{C}_{26}\text{H}_{38}\text{O}_5\text{N}_3$  ( $\text{M}+\text{H}$ ) 472.28060, found 472.28102.

**Allylic alcohol *epi-ent*-2.111:**  $[\alpha]_D^{18} +2.0$  ( $c$  0.3,  $\text{CHCl}_3$ );  $^1\text{H}$  NMR (300 MHz,  $\text{C}_6\text{D}_6$ )  $\delta$  6.84 (dd,  $J$  = 1.8, 0.9 Hz, 1 H), 6.02 (dd,  $J$  = 3.2, 2.0 Hz, 1 H), 5.86 (dd,  $J$  = 3.2, 0.8 Hz, 1 H), 5.60 (d,  $J$  = 9.6 Hz, 1 H), 5.45 (d,  $J$  = 9.6 Hz, 1 H), 3.74 (ap. s, 2 H), 3.45 (d,  $J$  = 13.2 Hz, 1 H), 3.12 (ap. d,  $J$  = 9.4 Hz, 1 H), 2.46 (s, 3 H), 2.08 (d,  $J$  = 13.8 Hz, 1 H), 1.58 (t,  $J$  = 13.0 Hz, 3 H), 1.30-1.23 (m, 12 H), 1.08 (ap. dd,  $J$  = 11.5, 3.4 Hz, 1 H), 0.93 (ap. s, 6 H), 0.76 (d,  $J$  = 3.3 Hz, 1 H), 0.21 (d,  $J$  = 3.6 Hz, 1 H); HRMS (ESI+)  $m/z$  calcd for  $\text{C}_{26}\text{H}_{38}\text{O}_5\text{N}_3$  ( $\text{M}+\text{H}$ ) 472.28060, found 472.28147.



**(+)-Cycloclavine (+)-2.1.** A solution of allylic alcohol *ent*-**2.111** (0.128 g, 0.272 mmol) in anhydrous, degassed toluene (10 mL) was heated to 135 °C in a sealed tube for 3 d 18 h. The reaction was cooled, concentrated and filtered through a pad of  $\text{SiO}_2$  washing with 2-5%

acetone/CH<sub>2</sub>Cl<sub>2</sub> to deliver crude indole *ent*-**2.110** (27 mg, 39%) which was used directly: <sup>1</sup>H NMR (400 MHz, CD<sub>2</sub>Cl<sub>2</sub>) δ 8.14 (bs, 1H), 7.21 (d, *J* = 8.0 Hz, 1 H), 7.09 (dd, *J* = 8.0, 7.2 Hz, 1 H), 7.02 (ap. s, 1 H), 6.80 (d, *J* = 6.8 Hz, 1 H), 3.78 (dd, *J* = 11.8, 4.2 Hz, 1 H), 3.29 (dd, *J* = 13.6, 4.0 Hz, 1 H), 2.79 (s, 3 H), 2.71-2.64 (m, 1 H), 1.80 (s, 3 H), 1.14 (d, *J* = 3.6 Hz, 1 H), 0.84 (d, *J* = 3.2 Hz, 1 H). A microwave vial was charged with crude indole *ent*-**2.110** (0.0270 g, 0.107 mmol) in anhydrous THF (1.2 mL) under an atmosphere of nitrogen was cooled to 0 °C and treated dropwise with LiAlH<sub>4</sub> (0.535 mL, 1M solution in Et<sub>2</sub>O, 0.535 mmol) and the resulting solution stirred at reflux in a sealed tube for 16 h. The reaction was diluted with Et<sub>2</sub>O, cooled to 0 °C and treated sequentially with DI H<sub>2</sub>O (0.020 mL), 15% NaOH<sub>(aq)</sub> (0.020 mL) and DI H<sub>2</sub>O (0.061 mL), warmed to room temperature and stirred for 15 min. Anhydrous MgSO<sub>4</sub> was then added and the solution allowed to stir rigorously for 15 min, then filtered through a pad of Celite. The crude residue was purified by chromatography on SiO<sub>2</sub> (pre-washed column with 0.1% NEt<sub>3</sub>/CH<sub>2</sub>Cl<sub>2</sub> then gradient elution 0-2% MeOH/CH<sub>2</sub>Cl<sub>2</sub> with 0.1% NEt<sub>3</sub> added to each eluent) to deliver (+)-cycloclavine (+)-**2.1** (21.95 mg, 86% or 34% 2 steps) as a white solid. [α]<sub>D</sub><sup>18</sup> +61.4 (c 0.2, CHCl<sub>3</sub>); literature [α]<sub>D</sub><sup>20</sup> +63 (c 1, CHCl<sub>3</sub>)<sup>72</sup>; M.p. 161.1 to 163.8 °C (dark brown liquid, dec.); IR (ATR) 3409, 3166, 3103, 3062, 2942, 2885, 2843, 2788, 1617, 1590, 1442, 1322, 1165, 1095, 922, 749 cm<sup>-1</sup>; <sup>1</sup>H NMR (500 MHz, CDCl<sub>3</sub>) δ 7.89 (bs, 1 H), 7.13 (dd, *J* = 8.0, 0.5 Hz, 1 H), 7.09 (ap. t, *J* = 7.8 Hz, 1 H), 6.90 (ap. t, *J* = 1.8 Hz, 1 H), 6.82 (dd, *J* = 7.0, 0.5 Hz, 1 H), 3.15 (d, *J* = 9.0 Hz, 1 H), 3.13 (dd, *J* = 13.8, 3.8 Hz, 1 H), 2.78 (dd, *J* = 11.5, 4.0 Hz, 1 H), 2.63-2.57 (m, 1 H), 2.40 (d, *J* = 8.5 Hz, 1 H), 2.36 (s, 3 H), 1.69 (s, 3 H), 1.60 (d, *J* = 3.5 Hz, 1 H), 0.45 (d, *J* = 3.5 Hz, 1 H); <sup>13</sup>C NMR (150 MHz, CDCl<sub>3</sub>) δ 135.6, 133.7, 128.8, 123.1, 118.2, 113.5, 110.5, 108.1, 69.8, 65.7, 40.1, 34.5, 27.9, 25.1, 24.4, 16.6; DEPT-135 (100 MHz, CDCl<sub>3</sub>) δ 123.1 (CH), 118.2 (CH), 110.5 (CH), 108.1 (CH), 69.8 (CH), 65.8 (CH<sub>2</sub>), 40.1 (N-CH<sub>3</sub>), 25.1 (CH<sub>2</sub>), 24.4



(CH<sub>2</sub>), 16.6 (CH<sub>3</sub>); HRMS (LCMS ESI+)  $m/z$  calcd for C<sub>16</sub>H<sub>19</sub>N<sub>2</sub> (M+H) 239.1543, found 239.1544.

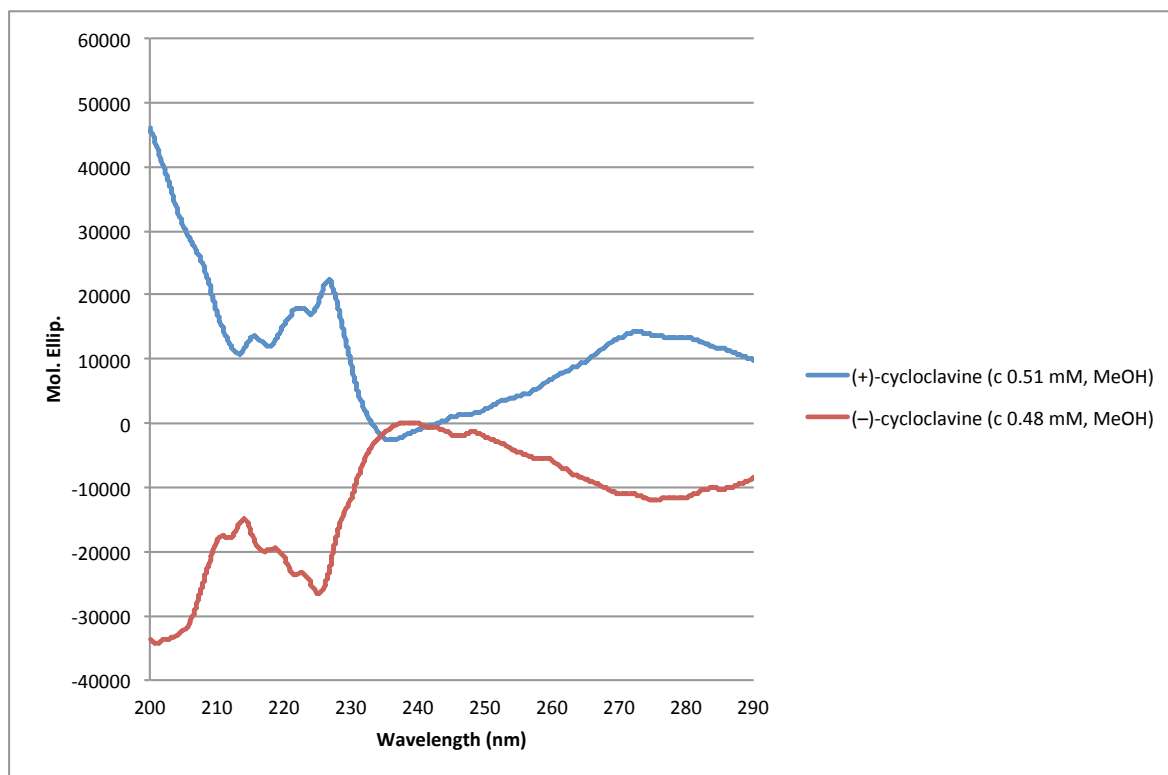
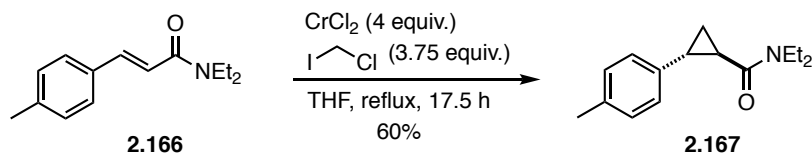
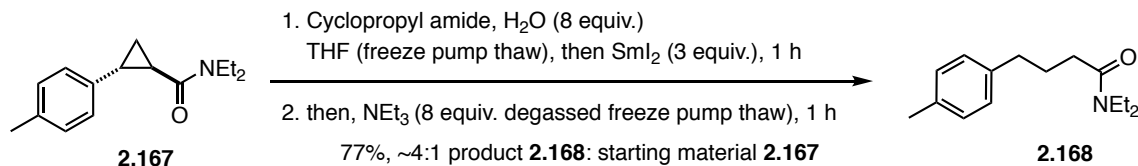


**Figure 3-18** Overlaid CD spectra of (-)- and (+)-cycloclavine



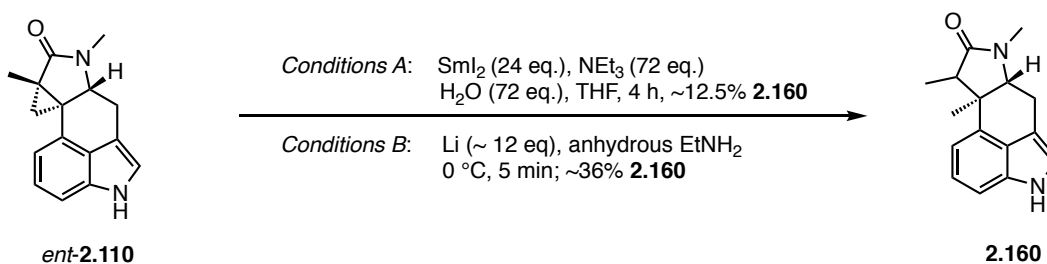
***trans*-N,N-Diethyl-2-(*p*-tolyl)cyclopropane-1-carboxamide (2.167).** A suspension of CrCl<sub>2</sub> (2.33 g, 18.4 mmol) in THF (46 mL) was treated dropwise with (*E*)-N,N-diethyl-3-(*p*-tolyl)acrylamide<sup>141</sup> **2.166** (1.00 g, 4.60 mmol) in THF (23 mL) followed by CH<sub>2</sub>Cl<sub>2</sub> (1.28 mL, 17.3 mmol) at room temperature under an inert atmosphere. After stirring for 17.5 h at reflux, the reaction was quenched with 1.0 M HCl and extracted with diethyl ether. The combined organic

layers were washed with sat.  $\text{NH}_4\text{Cl}_{(\text{aq})}$ ,  $\text{H}_2\text{O}$  and dried ( $\text{Na}_2\text{SO}_4$ ) and concentrated. The residue was purified by chromatography on  $\text{SiO}_2$  (0-15% Hex/EtOAc) to deliver *trans*-*N,N*-diethyl-2-phenylcyclopropane-1-carboxamide **2.167** (0.64 g, 60%) as a clear, yellow oil: IR (ATR) 2974, 2931, 1629, 1518, 1481, 1459, 1427, 1362, 1254, 1139, 1074, 809  $\text{cm}^{-1}$ ;  $^1\text{H}$  NMR (300 MHz,  $\text{CDCl}_3$ )  $\delta$  7.09 (d,  $J = 8.1$  Hz, 2 H), 7.02 (d,  $J = 8.1$  Hz, 2 H), 3.40 (q,  $J = 7.0$  Hz, 4 H), 2.44 (qd,  $J = 6.9, 4.2$  Hz, 1 H), 2.32 (s, 3 H), 1.89 (dt,  $J = 8.2, 4.8$  Hz, 1H), 1.63 (ap. p,  $J = 4.7$  Hz, 1 H), 1.22-1.14 (m, 1 H), 1.18 (t,  $J = 7.1$  Hz, 3 H), 1.13 (t,  $J = 7.4$  Hz, 3 H);  $^{13}\text{C}$  NMR (100 MHz,  $\text{CDCl}_3$ )  $\delta$  171.3, 138.3, 135.9, 129.2, 126.2, 42.3, 41.1, 25.3, 23.3, 21.1, 16.2, 15.1, 13.4; HRMS (LCMS, ESI+)  $m/z$  calcd for  $\text{C}_{15}\text{H}_{22}\text{NO}$  ( $\text{M}+\text{H}$ ) 232.1696, found 232.1694



**(*E*)-*N,N*-Diethyl-3-(*p*-tolyl)acrylamide (2.168).** An oven-dried Schlenck tube cooled under an atmosphere of argon was charged sequentially with (*trans*)-*N,N*-diethyl-2-phenylcyclopropane-1-carboxamide **2.167** (0.0607 g, 0.262 mmol), HPLC grade  $\text{H}_2\text{O}$  (0.0378 mL, 2.10 mmol) and THF (1.0 mL). The clear yellow solution was subjected to 6 cycles of freeze pump thaw (liquid nitrogen). After the last cycle an atmosphere of argon was introduced. The reaction was then treated with  $\text{SmI}_2$  (7.87 mL, 0.1 M solution in THF, 0.787 mmol, syringe flushed 3x with argon) and the resulting dark blue solution stirred under an atmosphere of argon at room temperature. After stirring at room temperature for 1 h, no reaction had occurred. The reaction was then treated with degassed  $\text{NEt}_3$  (0.293 mL, 0.210 mmol, degassed by freeze pump thaw) after the addition of which the solution became a dark green color. The solution was stirred for 1 h during which time the reaction turned color from dark to light green and then an

aliquot was taken and analyzed by  $^1\text{H}$  NMR ( $\text{CDCl}_3$ ) indicating consumption of the starting material. The excess  $\text{Sm}(\text{II})$  was oxidized by bubbling through compressed air then the reaction was diluted with  $\text{CH}_2\text{Cl}_2$  and  $\text{NaOH}$  (1N) was added. The separated aqueous layer was extracted with  $\text{CH}_2\text{Cl}_2$  (3x) and the combined organic layers dried, filtered and concentrated.  $^1\text{H}$  NMR analysis of the crude (~64 mg crude) showed ~ 4:1 ratio of acyclic amide **2.168**: cyclopropane starting material **2.167**). The crude reaction mixture was purified by chromatography on  $\text{SiO}_2$  (0-15%  $\text{EtOAc/Hex}$ ) to deliver an inseparable 4:1 mixture (0.047 g, ~77%) of amide product **2.168**: cyclopropane **2.167**. Characterization data for the major amide product **2.168** of the mixture: IR (ATR) 2973, 2932, 2872, 1634, 1515, 1480, 1449, 1428, 1258, 1137, 808  $\text{cm}^{-1}$ ;  $^1\text{H}$  NMR (400 MHz,  $\text{CDCl}_3$ )  $\delta$  7.08 (s, 4 H), 3.37 (q,  $J = 7.1$  Hz, 2 H), 3.24 (q,  $J = 7.2$  Hz, 2 H), 2.41 (t,  $J = 7.2$  Hz, 2 H), 2.31 (s, 3 H), 2.29 (ap. d,  $J = 7.6$  Hz, 2 H), 1.97 (ap. pentet,  $J = 7.6$  Hz, 2 H), 1.12 (t,  $J = 7.2$  Hz, 3 H), 1.11 (t,  $J = 7.0$  Hz, 3 H);  $^1\text{H}$  NMR (100 MHz,  $\text{CDCl}_3$ )  $\delta$  172.0, 139.0, 135.4, 129.2, 128.5, 42.1, 40.2, 35.1, 32.4, 27.1, 21.1, 14.5, 13.3; HRMS (ASAP)  $m/z$  calcd for  $\text{C}_{15}\text{H}_{24}\text{NO}$  ( $\text{M}+\text{H}$ ) 234.1858, found 234.1830.

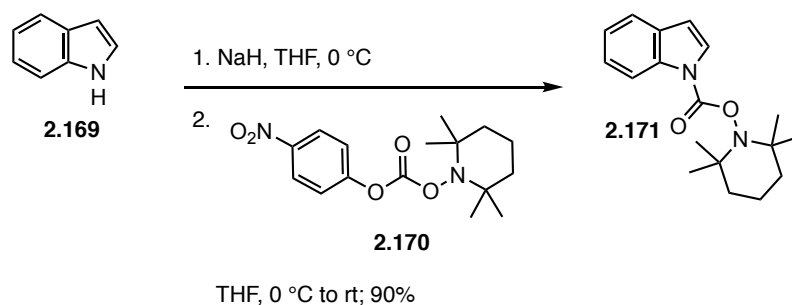


**(6aR,9aR)-7,9,9a-Trimethyl-4,6,6a,7,9,9a-hexahydro-8H-indolo[6,5,4-cd]indol-8-one.**

*Conditions A.* An oven-dried flask containing a stir bar was charged with a dark blue solution of  $\text{SmI}_2$  in THF (1.9 mL, 0.1 M solution, 1.9 mmol, 8 Eq.) under an atmosphere of nitrogen, followed by degassed  $\text{Et}_3\text{N}$  (0.24 mL, 1.7 mmol, 72 Eq.) and degassed water (0.031 mL, 1.7 mmol, 72 Eq.) and stirred vigorously. The resulting dark brown solution was treated dropwise

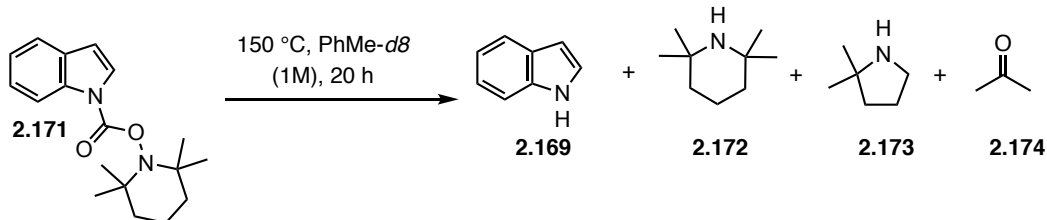
with a solution of amide *ent*-**2.110** (0.0060 g, 0.024 mmol, 1 Eq.) in THF (0.2 mL) and the resulting reaction stirred at room temperature for 30 min during which time the solution became a light green color then white. LCMS indicated mostly starting material amide *ent*-**2.110**. The reaction was stirred at room temperature for an additional 3.5 h during which time additional equivalence of SmI<sub>2</sub> (2 x 1.9 mL, 2 x 8 equiv) was added. After which time LCMS showed consumption of starting material. Excess SmI<sub>2</sub> was quenched by bubbling compressed air through solution, which turned yellow. The reaction was diluted with CH<sub>2</sub>Cl<sub>2</sub> and 1M NaOH. The separated aqueous layer was extracted (3x CH<sub>2</sub>Cl<sub>2</sub>) and the combined organic layers dried (Na<sub>2</sub>SO<sub>4</sub>) and concentrated. The resulting residue was purified by chromatography to deliver the tentatively assigned cyclopropane cleavage product **2.160** (0.75 mg, ~12.5%) as a white film: <sup>1</sup>H NMR (500 MHz, CD<sub>2</sub>Cl<sub>2</sub>) δ 8.16 (bs, 1 H), 7.23 (d, *J* = 8.0 Hz, 1 H), 7.11 (ap. t, *J* = 7.8 Hz, 1 H), 7.03 (s, 1 H), 6.96 (d, *J* = 7.0 Hz, 1 H), 3.52 (dd, *J* = 12.8, 4.8 Hz, 1 H), 3.32 (dd, *J* = 14.0, 4.5 Hz, 1 H), 2.88 (s, 3 H), 2.84 (ap. td, *J* = 13.5, 2.4 Hz, 1 H), 2.69 (q, *J* = 7.0 Hz, 1 H), 1.47 (d, *J* = 7.0 Hz, 3 H), 1.00 (s, 3 H); HRMS (LCMS ESI+) *m/z* calcd for C<sub>16</sub>H<sub>19</sub>NO<sub>2</sub> (M+H) 255.1492, found 255.1489.

*Conditions B:* A solution of amide *ent*-**2.110** (0.0060 g, 0.024 mmol) in anhydrous ethylamine (1.2 mL) was cooled to 0 °C under an atmosphere of argon and treated with approx. 2 mg of Li and stirred until the solution color remained dark blue. After 5 min the solution was quenched with a small amount of sat. NH<sub>4</sub>Cl solution and Et<sub>2</sub>O, stirred for 30 min then evaporated to dryness, suspended in CH<sub>2</sub>Cl<sub>2</sub>, dried with Na<sub>2</sub>SO<sub>4</sub>, filtered and concentrated. The resulting residue was purified by chromatography on SiO<sub>2</sub> (0-5% MeOH/CH<sub>2</sub>Cl<sub>2</sub>) delivering the tentatively assigned amide **2.160** (~2.16 mg, 36%) and an unidentified byproduct.



**2,2,6,6-Tetramethylpiperidin-1-yl 1*H*-indole-1-carboxylate (2.171).** An oven-dried round bottom flask charged with 90% NaH (0.147 g, 5.49 mmol) in THF (30 mL) was cooled to 0 °C, stirred at this temperature for 5 min and then treated with a solution of indole **2.169** (0.500 g, 4.23 mmol) in THF (2 mL). The off-white, cloudy mixture was stirred for 30 min at 0 °C then treated with a solution of mixed anhydride **2.170** (1.64 g, 5.07 mmol) in THF (10 mL). The bright orange reaction was then stirred for 1 h while allowing the solution to slowly warm to room temperature. After 1 h the reaction was quenched with DI H<sub>2</sub>O. EtOAc and Na<sub>2</sub>CO<sub>3</sub> were added. The separated organic layer was extracted with EtOAc (2x) and the combined organic layers washed with brine, dried and concentrated under reduced pressure to afford a yellow residue which was purified by chromatography on SiO<sub>2</sub> (0-2% EtOAc/Hex) to afford protected indole **2.171** (1.14 g, 90%) as a white solid: <sup>1</sup>H NMR (300 MHz, CD<sub>2</sub>Cl<sub>2</sub>) δ 8.21 (d, *J* = 8.4 Hz, 1 H), 7.68 (d, *J* = 3.9 Hz, 1 H), 7.60 (d, *J* = 7.2 Hz, 1 H), 7.34 (td, *J* = 7.7, 1.3 Hz, 1 H), 7.25 (td, *J* = 7.5, 1.4 Hz, 1 H), 6.65 (dd, *J* = 3.8, 0.8 Hz, 1 H), 1.75-1.62 (m, 5 H), 1.49-1.47 (m, 1 H), 1.32 (s, 6 H), 1.16 (s, 6 H); HRMS (LCMS ESI+) *m/z* calcd for C<sub>18</sub>H<sub>25</sub>N<sub>2</sub>O<sub>2</sub> (M+H) 301.1911, found 301.1906.

## Thermolysis of TEMPOC-protected indole



**Thermolysis Experiment 1 (Entry 1):** A microwave vial was charged with protected indole **2.171** (0.150 g, 0.499 mmol) in C<sub>6</sub>D<sub>5</sub>CD<sub>3</sub> (0.5 mL) was heated in a sealed tube in an oil bath maintaining the external temperature at 150 C °C. After 20 h, the brown reaction was removed from the oil bath and allowed to cool to room temperature. <sup>1</sup>H NMR analysis of the crude reaction showed ~ 3.6: 1 ratio of pyrrolidine **2.173**: tetramethylpiperidine **2.172**.

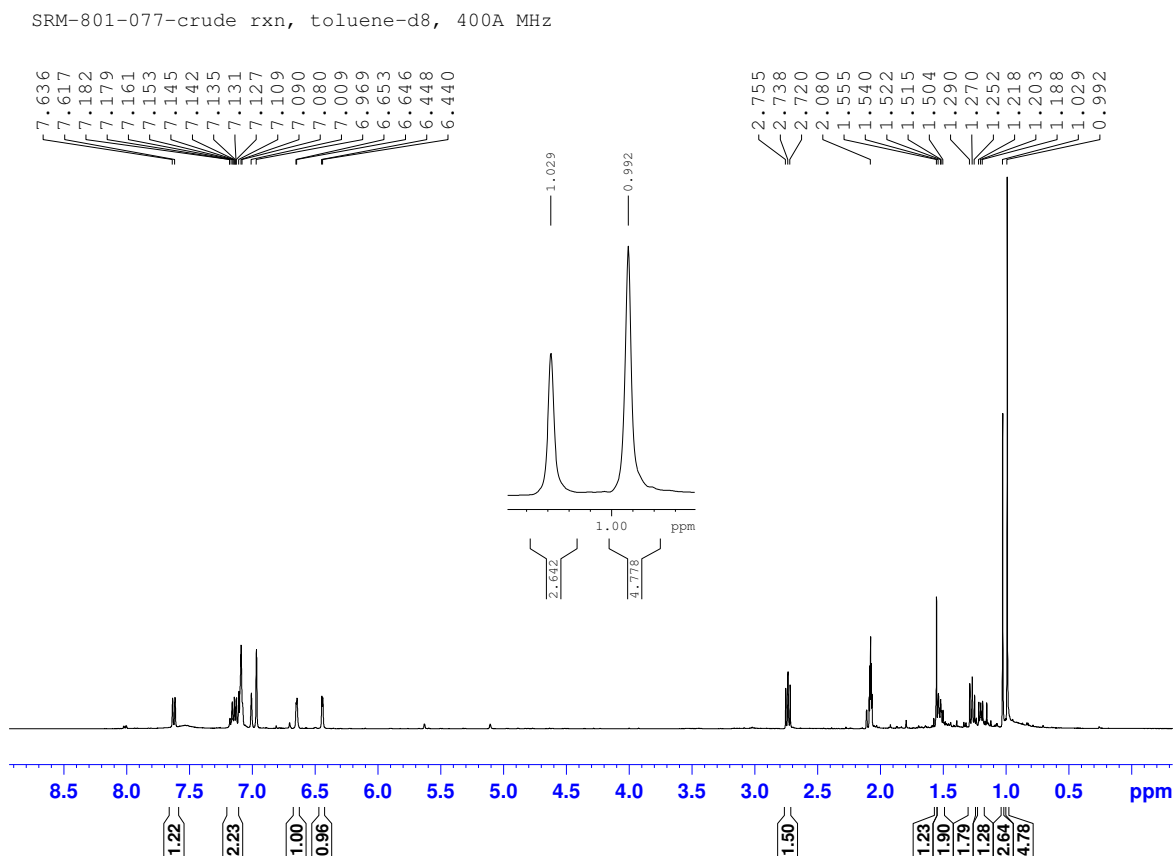
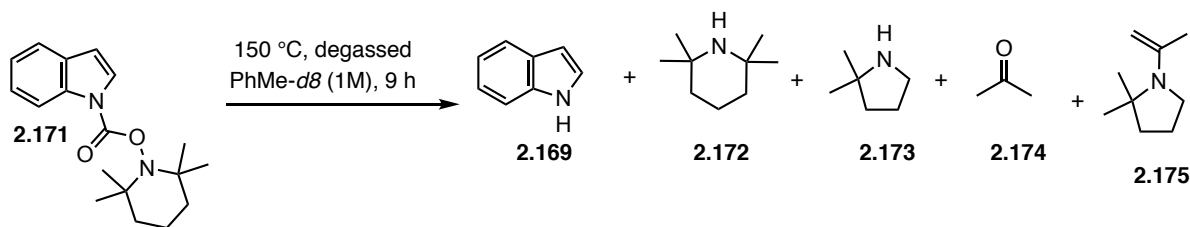


**Figure 3-19** Thermolysis experiment 1: crude <sup>1</sup>H NMR spectrum



**Thermolysis Experiment 2 (Entry 2):** A microwave vial charged with protected indole **2.171** (0.150 g, 0.499 mmol) in  $\text{C}_6\text{D}_5\text{CD}_3$  (0.5 mL) was subjected to 4 cycles of freeze pump thaw and on the last cycle an atmosphere of nitrogen introduced and the capped microwave vial sealed with additional teflon and parafilm. The reaction was then heated in a silicone oil bath maintaining the external temperature at 150 C °C for 9 h during which time the reaction turned from clear and colorless to dark brown. The reaction was cooled to room temperature. TLC indicated reaction completion.  $^1\text{H}$  NMR analysis of the crude reaction showed 1.0: 2.3: 0.98 ratio of tetramethylpiperidine **2.169**: pyrrolidine **2.172**: pyrrolidine enamine **2.175**.

SRM-801-080-cr

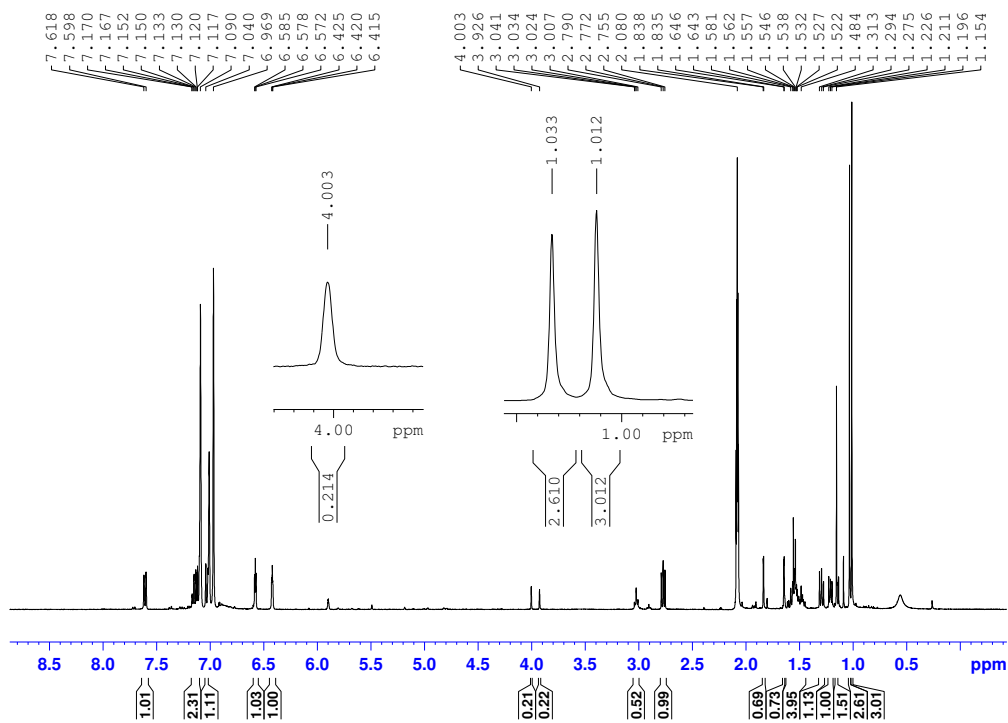
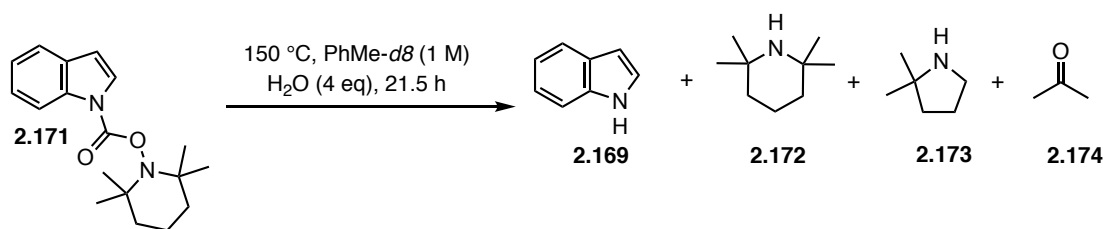


**Figure 3-20** Thermolysis experiment 2: crude  $^1\text{H}$  NMR spectrum



**Thermolysis Experiment 3 (Entry 3):** A microwave vial charged with protected indole **2.171** (0.100 g, 0.332 mmol) and HPLC grade water (0.024 mL, 1.33 mmol) in  $\text{C}_6\text{D}_5\text{CD}_3$  (0.33 mL). The reaction was then heated in a silicone oil bath in the sealed microwave tube maintaining the external temperature at 150 °C. After heating 21.5h the brown reaction was cooled to room temperature and  $^1\text{H}$  NMR analysis of the reaction showed conversion to indole **2.169** and a ~ 3.4: 1 ratio of pyrrolidine **2.173**: tetramethylpiperidine **2.172**. The reaction was concentrated and the resulting brown residue purified by chromatography on  $\text{SiO}_2$  (0-10% EtOAc/Hex) to deliver indole **2.169** (0.034 g, 87%) as a tan solid:  $^1\text{H}$  NMR (400 MHz,  $\text{CDCl}_3$ )  $\delta$  8.15 (bs, 1 H), 7.66 (d,  $J = 7.2$  Hz, 1 H), 7.41 (d,  $J = 8.0$  Hz, 1 H), 7.40-7.18 (m, 2 H), 7.14-7.10 (m, 1 H), 6.57 (t,  $J = 2.2$  Hz, 1 H).

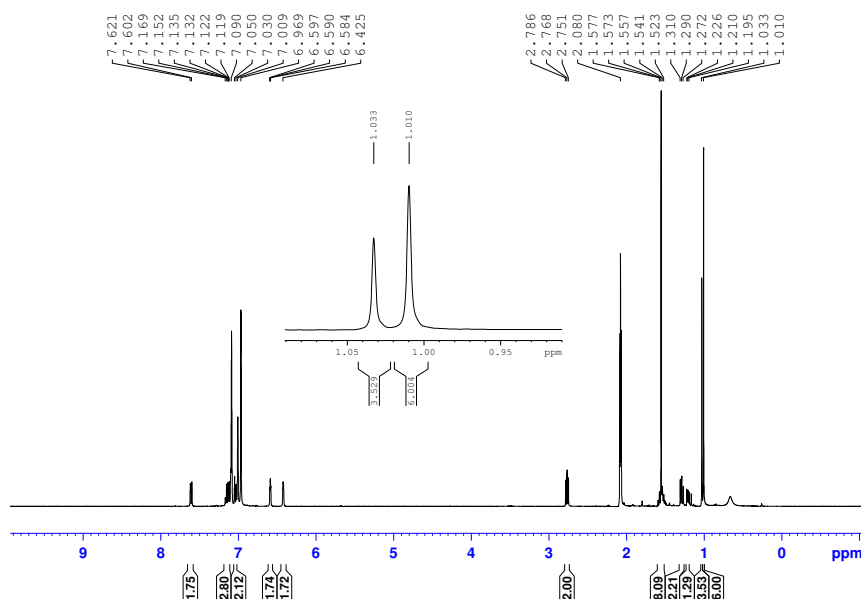
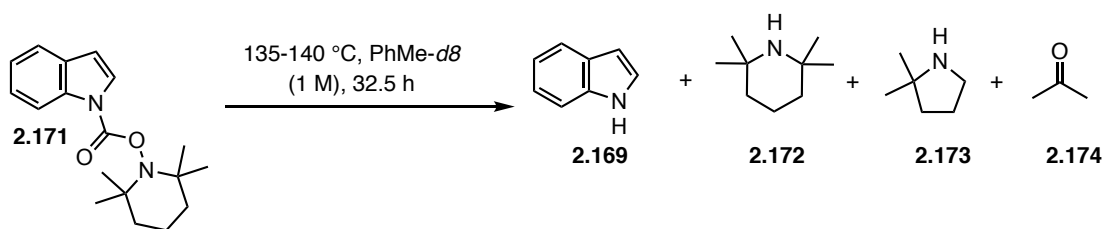


**Figure 3-21** Thermolysis experiment 3: crude  $^1\text{H}$  NMR spectrum





**Thermolysis Experiment 4 (Entry 4):** A microwave vial was charged with protected indole **2.171** (0.100 g, 0.332 mmol) in  $\text{C}_6\text{D}_5\text{CD}_3$  (0.33 mL). The reaction was then heated in a silicone oil bath maintaining the external temperature between 135-140 °C for 32.5 h during which time the reaction turns from clear and colorless to dark brown. After heating for 32.5 h the reaction was cooled to room temperature.  $^1\text{H}$  NMR analysis of the crude reaction showed ~ 1.8:1 ratio of pyrrolidine **2.173**: tetramethylpiperidine **2.172**.

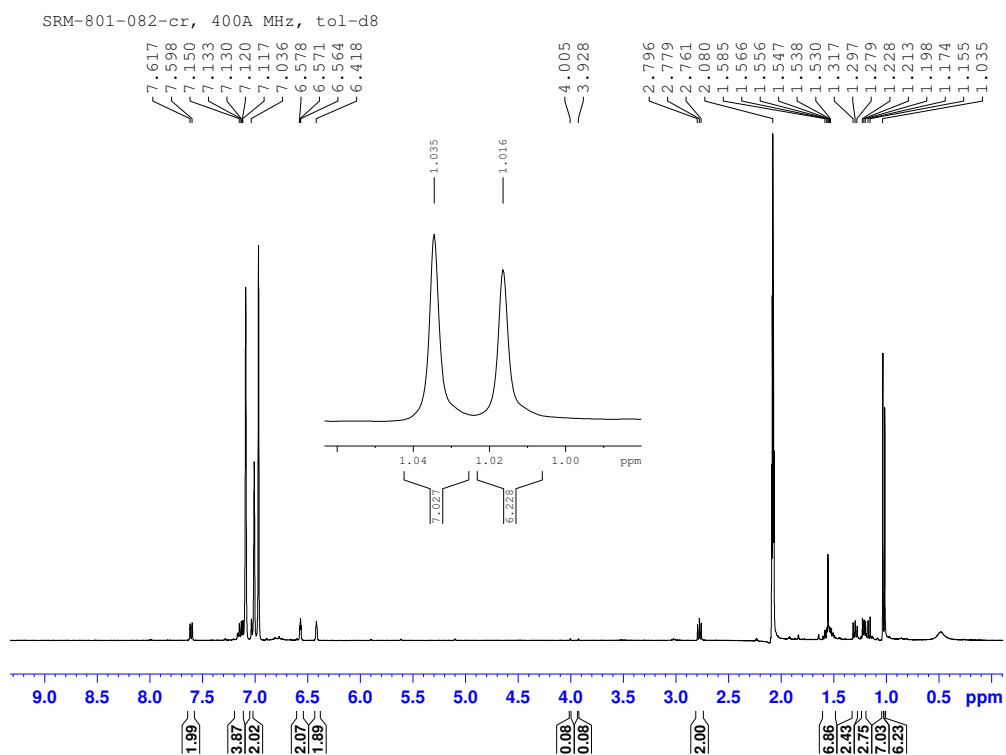
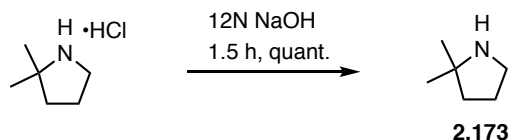
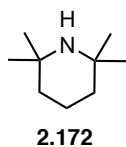


**Figure 3-22** Thermolysis experiment 4: crude  $^1\text{H}$  NMR spectrum



**2,2-Dimethylpyrrolidine Standard.** A solution of commercially available 2,2-dimethylpyrrolidine•HCl (0.050 g, 0.35 mmol) in NaOH (1.25 mL, 12N) was stirred vigorously at room temperature. After 1.5 h the solution was treated with tol-d8 (1 mL) and stirred vigorously. The separated organic layer was dried (Na<sub>2</sub>SO<sub>4</sub>). <sup>1</sup>H NMR analysis of the organic layer showed full conversion to the free base **2.173**: <sup>1</sup>H NMR (400 MHz, PhMe-*d*8) δ 2.77 (t, *J* = 7.0 Hz, 2 H), 1.57 (p, *J* = 7.3 Hz, 2 H), 1.30 (t, *J* = 7.6 Hz, 2 H), 1.01 (s, 6 H); <sup>13</sup>C NMR (100 MHz, tol-d8) δ 58.8, 46.3, 39.9, 28.9, 26.4



**Tetramethylpiperidine Standard.** <sup>1</sup>H NMR (400 MHz, PhMe-*d*8) δ 1.55-1.49 (m, 2 H), 1.23-1.20 (m, 4 H), 1.03 (s, 12 H); <sup>13</sup>C NMR (100 MHz, tol-d8) δ 49.6, 38.7, 32.0, 18.9

## **APPENDIX A**

### **X-RAY DATA**

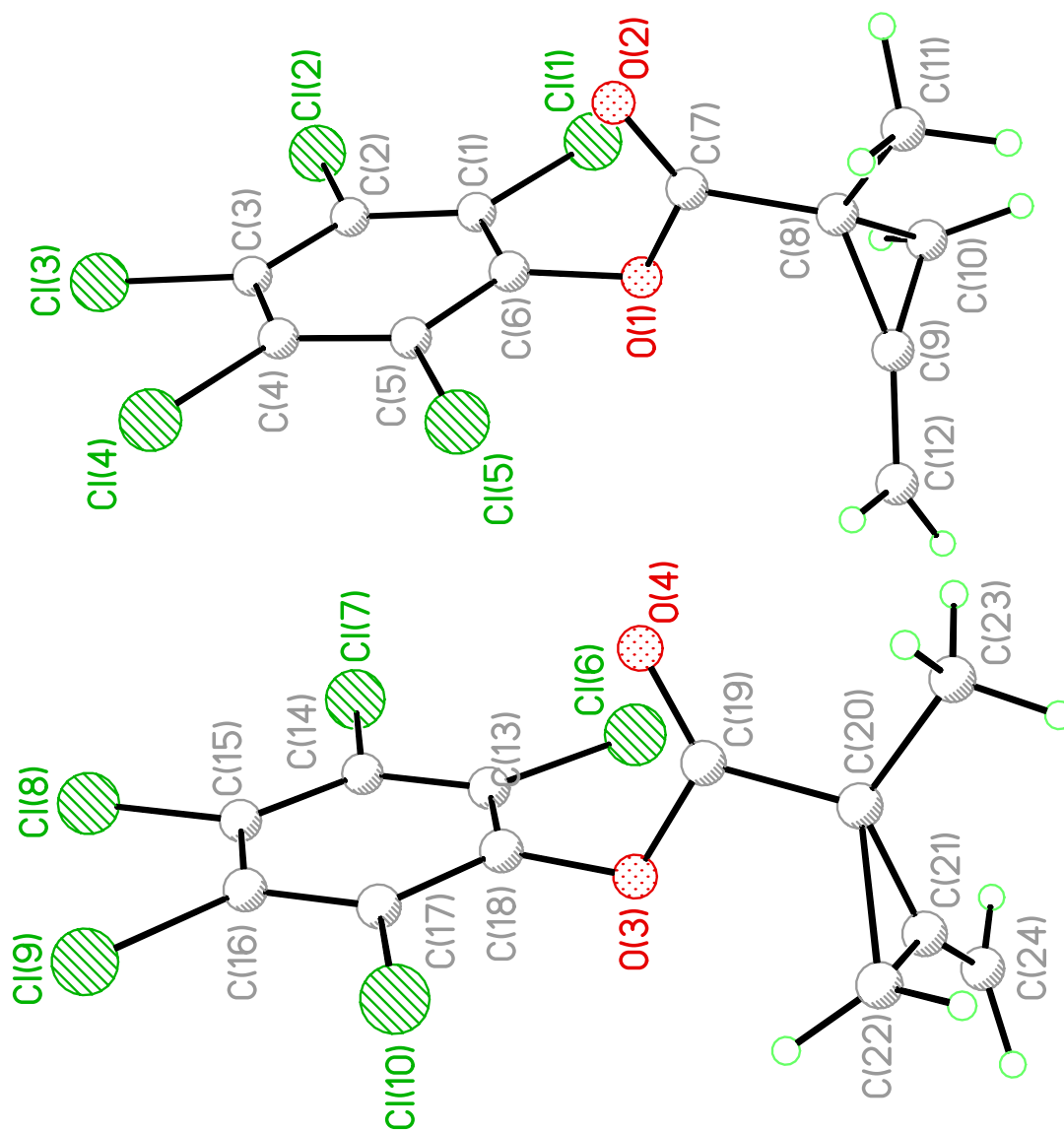


Figure A-1 ORTEP structure of methylenecyclopropane 1.105.

**Table A-1** Data Collection and Structure Refinement for Methylene cyclopropane **1.105**

<b>Diffractometer</b>	Bruker Apex II CCD
<b>Radiation source</b>	IMuS micro-focus source, Cu
<b>Theta range for data collection</b>	4.09 to 68.86°
<b>Index ranges</b>	-9<= <i>h</i> <=8, -10<= <i>k</i> <=10, -13<= <i>l</i> <=13
<b>Reflections collected</b>	11743
<b>Independent reflections</b>	4546 [R(int) = 0.0323]
<b>Absorption correction</b>	multi-scan
<b>Max. and min. transmission</b>	0.6100 and 0.2500
<b>Structure solution technique</b>	direct methods
<b>Structure solution program</b>	SHELXS-97 (Sheldrick, 2008)
<b>Refinement method</b>	Full-matrix least-squares on F <sup>2</sup>
<b>Refinement program</b>	SHELXL-97 (Sheldrick, 2008)
<b>Function minimized</b>	$\sum w(F_o^2 - F_c^2)^2$
<b>Data / restraints / parameters</b>	4546 / 3 / 346
<b>Goodness-of-fit on F<sup>2</sup></b>	1.582
<b>Final R indices</b>	4118 data; I>2σ(I)     R1 = 0.0508, wR2 = 0.1505 all data                     R1 = 0.0555, wR2 = 0.1550
<b>Weighting scheme</b>	$w=1/[\sigma^2(F_o^2)+(0.0680P)^2]$ where $P=(F_o^2+2F_c^2)/3$
<b>Absolute structure parameter</b>	0.1(0)
<b>Largest diff. peak and hole</b>	0.566 and -0.447 eÅ <sup>-3</sup>
<b>R.M.S. deviation from mean</b>	0.063 eÅ <sup>-3</sup>

**Table A-2** Atomic Coordinates and Equivalent Isotropic Atomic Displacement Parameters ( $\text{\AA}^2$ ) for Methylenecyclopropane **1.105**

U(eq) is defined as one third of the trace of the orthogonalized  $U_{ij}$  tensor.

	<b>x/a</b>	<b>y/b</b>	<b>z/c</b>	<b>U(eq)</b>
C1	0.9094(8)	0.0898(7)	0.4000(6)	0.0522(13)
C2	0.0077(9)	0.1080(8)	0.2794(6)	0.0561(14)
C3	0.0366(9)	0.2483(9)	0.2261(5)	0.0591(16)
C4	0.9642(9)	0.3759(8)	0.2934(6)	0.0573(14)
C5	0.8631(9)	0.3594(7)	0.4130(5)	0.0514(13)
C6	0.8380(8)	0.2166(7)	0.4665(5)	0.0463(12)
C7	0.8026(9)	0.2339(7)	0.6823(5)	0.0512(13)
C8	0.6645(9)	0.2187(7)	0.7977(5)	0.0549(13)
C9	0.4752(10)	0.2287(9)	0.7897(6)	0.0663(17)
C10	0.5378(14)	0.0806(11)	0.8090(8)	0.090(3)
C11	0.7246(14)	0.2727(12)	0.9130(6)	0.089(3)
C12	0.3468(12)	0.3220(15)	0.7723(7)	0.100(3)
C13	0.3673(9)	0.6379(8)	0.4052(6)	0.0574(15)
C14	0.4666(10)	0.6342(9)	0.2870(7)	0.0662(18)
C15	0.5368(9)	0.7653(10)	0.2269(6)	0.0655(18)
C16	0.5014(10)	0.9021(9)	0.2879(6)	0.0629(16)
C17	0.4022(10)	0.9071(8)	0.4086(6)	0.0615(16)
C18	0.3384(9)	0.7744(8)	0.4670(5)	0.0547(14)
C19	0.3090(9)	0.7541(8)	0.6820(6)	0.0561(14)
C20	0.1741(12)	0.7621(12)	0.7997(6)	0.084(2)
C21	0.9899(12)	0.7618(12)	0.7959(7)	0.086(2)
C22	0.0345(19)	0.9124(14)	0.8119(11)	0.120(4)
C23	0.2460(15)	0.7232(12)	0.9130(7)	0.093(3)
C24	0.863(2)	0.664(2)	0.7811(10)	0.144(6)
Cl1	0.8717(3)	0.9173(2)	0.4685(2)	0.0826(6)
Cl2	0.0908(3)	0.9516(3)	0.1955(2)	0.0900(7)
Cl3	0.1551(3)	0.2691(3)	0.07691(16)	0.0921(7)
Cl4	0.9979(3)	0.5523(3)	0.2305(2)	0.0940(7)
Cl5	0.7679(3)	0.5103(2)	0.49704(18)	0.0748(5)
Cl6	0.2764(4)	0.4812(3)	0.4833(3)	0.1008(8)
Cl7	0.5065(4)	0.4643(4)	0.2138(3)	0.1213(11)
Cl8	0.6578(3)	0.7588(5)	0.07831(18)	0.1178(12)
Cl9	0.5781(4)	0.0647(4)	0.2134(3)	0.1207(11)
Cl10	0.3587(4)	0.0727(3)	0.4860(3)	0.1085(9)
O1	0.7294(6)	0.1998(6)	0.5810(4)	0.0594(11)

	<b>x/a</b>	<b>y/b</b>	<b>z/c</b>	<b>U(eq)</b>
O2	0.9540(6)	0.2677(7)	0.6725(4)	0.0685(12)
O3	0.2320(7)	0.7838(9)	0.5817(4)	0.086(2)
O4	0.4647(7)	0.7296(6)	0.6689(4)	0.0691(12)

**Table A-3** Bond Lengths (Å) for Methylenecyclopropane **1.105**

C1-C6	1.394(9)	C1-C2	1.396(10)
C1-Cl1	1.707(7)	C2-C3	1.377(11)
C2-Cl2	1.717(7)	C3-C4	1.405(11)
C3-Cl3	1.717(6)	C4-C5	1.393(9)
C4-Cl4	1.712(7)	C5-C6	1.396(9)
C5-Cl5	1.705(6)	C6-O1	1.369(7)
C7-O2	1.175(8)	C7-O1	1.380(7)
C7-C8	1.483(8)	C8-C9	1.461(10)
C8-C11	1.518(9)	C8-C10	1.557(11)
C9-C12	1.317(12)	C9-C10	1.427(13)
C10-H10A	0.98	C10-H10B	0.98
C11-H11A	0.97	C11-H11B	0.97
C11-H11C	0.97	C12-H12A	0.94
C12-H12B	0.94	C13-C14	1.367(10)
C13-C18	1.389(11)	C13-Cl6	1.711(7)
C14-C15	1.395(12)	C14-Cl7	1.713(8)
C15-C16	1.392(12)	C15-Cl8	1.708(7)
C16-C17	1.390(10)	C16-Cl9	1.708(7)
C17-C18	1.385(11)	C17-Cl10	1.703(7)
C18-O3	1.358(7)	C19-O4	1.181(8)
C19-O3	1.375(7)	C19-C20	1.483(9)
C20-C21	1.409(13)	C20-C23	1.499(11)
C20-C22	1.688(16)	C21-C24	1.343(18)
C21-C22	1.406(17)	C22-H22A	0.98
C22-H22B	0.98	C23-H23A	0.97
C23-H23B	0.97	C23-H23C	0.97
C24-H24A	0.94	C24-H24B	0.94

**Table A-4** Bond Angles (°) for Methylenecyclopropane **1.105**

C6-C1-C2	118.9(6)	C6-C1-C11	118.8(5)
C2-C1-C11	122.3(5)	C3-C2-C1	121.3(6)
C3-C2-C12	119.6(5)	C1-C2-C12	119.1(6)
C2-C3-C4	119.7(6)	C2-C3-C13	120.9(6)
C4-C3-C13	119.4(6)	C5-C4-C3	119.7(6)
C5-C4-C14	119.3(6)	C3-C4-C14	121.0(5)
C4-C5-C6	119.9(6)	C4-C5-C15	121.5(5)
C6-C5-C15	118.6(5)	O1-C6-C1	119.6(6)
O1-C6-C5	119.7(6)	C1-C6-C5	120.5(5)
O2-C7-O1	122.2(6)	O2-C7-C8	127.8(5)
O1-C7-C8	110.0(5)	C9-C8-C7	118.5(5)
C9-C8-C11	120.1(6)	C7-C8-C11	114.1(6)
C9-C8-C10	56.3(6)	C7-C8-C10	117.4(6)
C11-C8-C10	118.5(6)	C12-C9-C10	150.8(10)
C12-C9-C8	143.9(9)	C10-C9-C8	65.2(6)
C9-C10-C8	58.4(5)	C9-C10-H10A	117.9
C8-C10-H10A	117.9	C9-C10-H10B	117.9
C8-C10-H10B	117.9	H10A-C10-H10B	115.1
C8-C11-H11A	109.5	C8-C11-H11B	109.5
H11A-C11-H11B	109.5	C8-C11-H11C	109.5
H11A-C11-H11C	109.5	H11B-C11-H11C	109.5
C9-C12-H12A	120.0	C9-C12-H12B	120.0
H12A-C12-H12B	120.0	C14-C13-C18	119.4(7)
C14-C13-C16	123.3(6)	C18-C13-C16	117.4(5)
C13-C14-C15	121.1(7)	C13-C14-C17	118.8(7)
C15-C14-C17	120.1(6)	C16-C15-C14	119.1(6)
C16-C15-C18	120.5(6)	C14-C15-C18	120.4(7)
C17-C16-C15	120.3(7)	C17-C16-C19	119.9(6)
C15-C16-C19	119.7(6)	C18-C17-C16	119.2(6)
C18-C17-C110	119.5(6)	C16-C17-C110	121.3(6)
O3-C18-C17	117.8(7)	O3-C18-C13	121.0(7)
C17-C18-C13	120.9(6)	O4-C19-O3	120.9(6)
O4-C19-C20	127.7(6)	O3-C19-C20	111.4(6)
C21-C20-C19	119.1(6)	C21-C20-C23	123.7(8)
C19-C20-C23	114.5(8)	C21-C20-C22	53.1(7)
C19-C20-C22	114.7(8)	C23-C20-C22	116.0(8)



C24-C21-C22	147.4(13)	C24-C21-C20	138.9(12)
C22-C21-C20	73.7(9)	C21-C22-C20	53.3(7)
C21-C22-H22A	118.4	C20-C22-H22A	118.4
C21-C22-H22B	118.4	C20-C22-H22B	118.4
H22A-C22-H22B	115.7	C20-C23-H23A	109.5
C20-C23-H23B	109.5	H23A-C23-H23B	109.5
C20-C23-H23C	109.5	H23A-C23-H23C	109.5
H23B-C23-H23C	109.5	C21-C24-H24A	120.0
C21-C24-H24B	120.0	H24A-C24-H24B	120.0
C6-O1-C7	117.0(5)	C18-O3-C19	117.9(5)

**Table A-5** Anisotropic Atomic Displacement Parameters ( $\text{\AA}^2$ ) for Methylenecyclopropane **1.105**.  
The anisotropic atomic displacement factor exponent takes the form:  $-2\pi^2 [h^2 a^{*2} U_{11} + \dots + 2 h k a^* b^* U_{12}]$

	$U_{11}$	$U_{22}$	$U_{33}$	$U_{23}$	$U_{13}$	$U_{12}$
C1	0.046(3)	0.057(3)	0.055(3)	-0.003(3)	-0.013(2)	-0.002(3)
C2	0.045(3)	0.071(4)	0.055(3)	-0.013(3)	-0.016(2)	-0.002(3)
C3	0.047(3)	0.093(5)	0.039(3)	0.002(3)	-0.011(2)	-0.003(3)
C4	0.054(4)	0.068(4)	0.050(3)	0.008(3)	-0.011(2)	-0.003(3)
C5	0.053(3)	0.053(3)	0.049(3)	0.001(2)	-0.011(2)	-0.001(3)
C6	0.040(3)	0.060(3)	0.039(3)	-0.005(2)	-0.007(2)	-0.003(2)
C7	0.056(4)	0.054(3)	0.046(3)	0.000(2)	-0.016(2)	-0.003(3)
C8	0.062(3)	0.061(3)	0.039(3)	0.008(2)	-0.004(2)	-0.007(3)
C9	0.070(4)	0.084(5)	0.041(3)	0.004(3)	-0.002(3)	-0.005(4)
C10	0.112(7)	0.080(5)	0.070(5)	0.012(4)	0.003(4)	-0.035(5)
C11	0.113(6)	0.117(7)	0.039(3)	-0.008(4)	-0.018(4)	-0.017(6)
C12	0.078(5)	0.154(10)	0.062(4)	-0.004(5)	-0.004(4)	0.021(6)
C13	0.051(3)	0.069(4)	0.054(3)	0.012(3)	-0.015(3)	-0.011(3)
C14	0.063(4)	0.076(4)	0.065(4)	-0.019(3)	-0.027(3)	0.009(3)
C15	0.048(3)	0.109(6)	0.040(3)	0.007(3)	-0.011(2)	-0.007(4)
C16	0.058(4)	0.079(4)	0.057(3)	0.019(3)	-0.024(3)	-0.009(3)
C17	0.064(4)	0.062(4)	0.064(4)	-0.006(3)	-0.027(3)	0.009(3)
C18	0.045(3)	0.080(4)	0.040(3)	0.002(3)	-0.011(2)	0.001(3)
C19	0.058(4)	0.067(4)	0.044(3)	-0.002(2)	-0.013(2)	-0.003(3)
C20	0.083(5)	0.128(7)	0.040(3)	-0.011(4)	-0.005(3)	-0.007(5)
C21	0.075(5)	0.112(7)	0.060(4)	-0.001(4)	0.011(3)	0.003(5)
C22	0.162(11)	0.101(8)	0.086(6)	-0.013(6)	0.003(6)	0.025(8)
C23	0.133(8)	0.103(7)	0.045(3)	-0.002(4)	-0.022(4)	-0.012(6)
C24	0.127(10)	0.213(18)	0.086(7)	-0.017(8)	-0.003(6)	-0.057(11)

	<b>U<sub>11</sub></b>	<b>U<sub>22</sub></b>	<b>U<sub>33</sub></b>	<b>U<sub>23</sub></b>	<b>U<sub>13</sub></b>	<b>U<sub>12</sub></b>
Cl1	0.0941(14)	0.0611(10)	0.0946(13)	0.0072(8)	-0.0234(11)	-0.0079(9)
Cl2	0.0849(14)	0.0986(15)	0.0863(13)	-0.0462(12)	-0.0164(10)	0.0180(11)
Cl3	0.0751(11)	0.153(2)	0.0425(8)	-0.0028(9)	0.0027(7)	-0.0093(12)
Cl4	0.1016(16)	0.0896(14)	0.0872(13)	0.0377(11)	-0.0114(11)	-0.0045(12)
Cl5	0.0804(11)	0.0656(10)	0.0768(10)	-0.0124(8)	-0.0127(8)	0.0182(9)
Cl6	0.1095(18)	0.0903(15)	0.1139(16)	0.0408(13)	-0.0483(14)	-0.0462(13)
Cl7	0.128(2)	0.112(2)	0.132(2)	-0.0714(18)	-0.0449(18)	0.0266(17)
Cl8	0.0748(12)	0.232(4)	0.0412(8)	0.0095(12)	0.0018(7)	0.0085(16)
Cl9	0.115(2)	0.1187(19)	0.144(2)	0.0796(18)	-0.0628(17)	-0.0474(16)
Cl10	0.120(2)	0.0815(14)	0.138(2)	-0.0419(14)	-0.0598(17)	0.0295(14)
O1	0.049(2)	0.088(3)	0.039(2)	-0.0031(19)	-0.0029(16)	-0.012(2)
O2	0.054(3)	0.096(4)	0.057(2)	0.000(2)	-0.0156(19)	-0.015(3)
O3	0.058(3)	0.162(6)	0.037(2)	0.000(3)	-0.0049(19)	0.013(3)
O4	0.068(3)	0.087(3)	0.055(2)	-0.004(2)	-0.018(2)	0.005(3)

**Table A-6** Hydrogen Atomic Coordinates and Isotropic Atomic Displacement Parameters ( $\text{\AA}^2$ ) for Methylenecyclopropane **1.105**

	<b>x/a</b>	<b>y/b</b>	<b>z/c</b>	<b>U(eq)</b>
H10A	0.5545	0.0102	0.7394	0.108
H10B	0.4986	0.0349	0.8910	0.108
H11A	0.7418	0.3806	0.9080	0.134
H11B	0.8369	0.2234	0.9192	0.134
H11C	0.6336	0.2487	0.9856	0.134
H12A	0.2322	0.2850	0.7694	0.12
H12B	0.3697	0.4254	0.7628	0.12
H22A	-0.0059	0.9581	0.8936	0.144
H22B	0.0452	0.9811	0.7411	0.144
H23A	0.2965	0.6224	0.9049	0.139
H23B	0.1492	0.7280	0.9855	0.139
H23C	0.3386	0.7941	0.9220	0.139
H24A	-0.2539	0.6978	0.7791	0.173
H24B	-0.1092	0.5605	0.7727	0.173

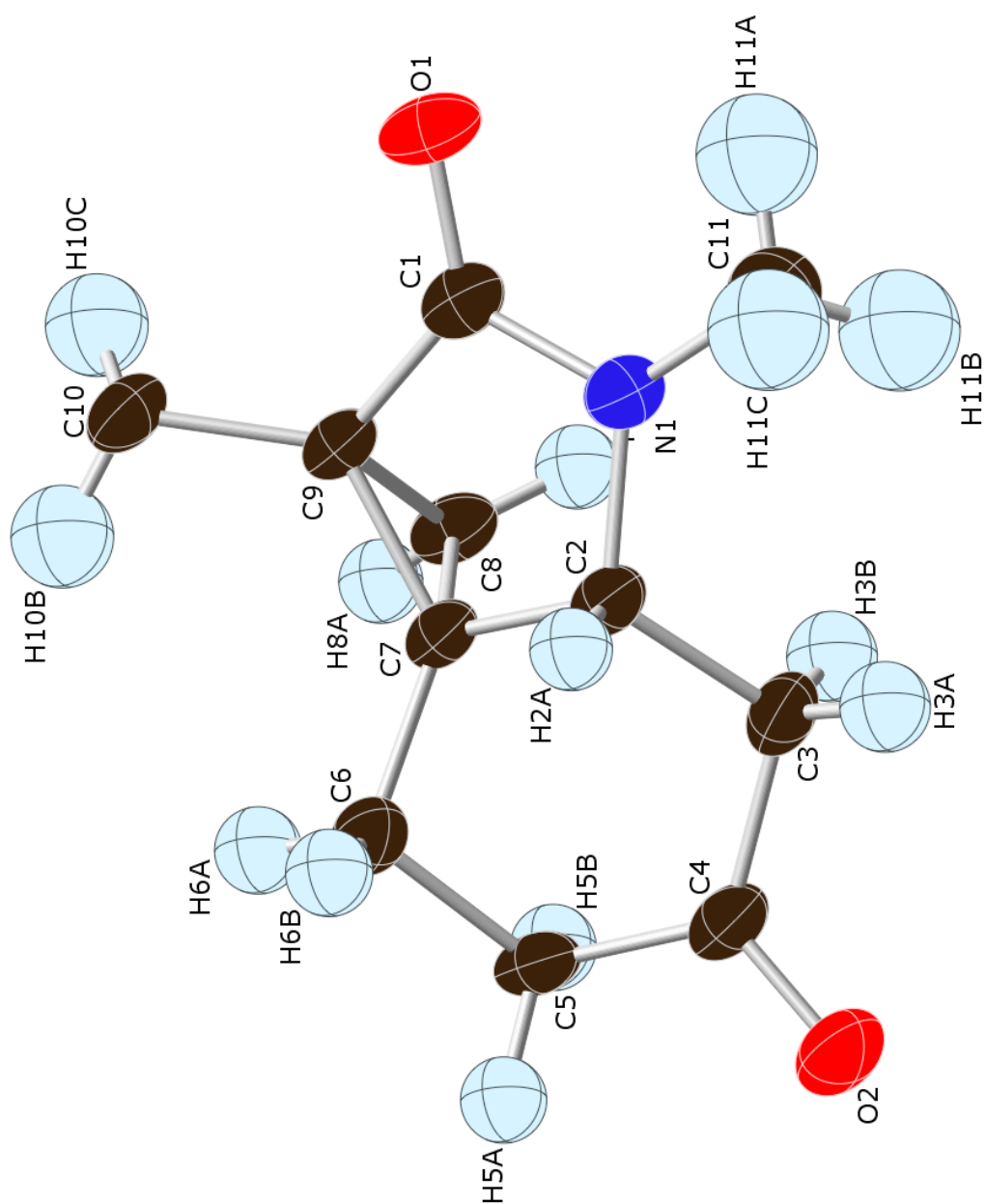


**Figure A-2** ORTEP structure of ketone (±)-2.86

**Table A-7** Data Collection and Structure Refinement for Ketone ( $\pm$ )-**2.86**

<b>Diffractometer</b>	Bruker Apex II CCD
<b>Radiation source</b>	IMuS micro-focus, Cu
<b>Theta range for data collection</b>	5.23 to 68.22°
<b>Index ranges</b>	-7<= <i>h</i> <=8, -12<= <i>k</i> <=13, -15<= <i>l</i> <=16
<b>Reflections collected</b>	6297
<b>Independent reflections</b>	1762 [R(int) = 0.0394]
<b>Coverage of independent reflections</b>	96.9%
<b>Absorption correction</b>	multi-scan
<b>Max. and min. transmission</b>	0.8980 and 0.7200
<b>Refinement method</b>	Full-matrix least-squares on $F^2$
<b>Refinement program</b>	SHELXL-2013 (Sheldrick, 2013)
<b>Function minimized</b>	$\sum w(F_o^2 - F_c^2)^2$
<b>Data / restraints / parameters</b>	1762 / 0 / 127
<b>Goodness-of-fit on <math>F^2</math></b>	3.255
<b>Final R indices</b>	1639 data; $I > 2\sigma(I)$ R1 = 0.1109, wR2 = 0.2851 all data R1 = 0.1135, wR2 = 0.2861
<b>Weighting scheme</b>	$w = 1/[\sigma^2(F_o^2) + (0.0680P)^2]$ where $P = (F_o^2 + 2F_c^2)/3$
<b>Largest diff. peak and hole</b>	0.650 and -0.432 eÅ <sup>-3</sup>
<b>R.M.S. deviation from mean</b>	0.126 eÅ <sup>-3</sup>

**Table A-8** Atomic Coordinates and Equivalent Isotropic Atomic Displacement Parameters ( $\text{\AA}^2$ ) for Ketone ( $\pm$ )-**2.86**.  
 $U(\text{eq})$  is defined as one third of the trace of the orthogonalized  $U_{ij}$  tensor.

	<b>x/a</b>	<b>y/b</b>	<b>z/c</b>	<b>U(eq)</b>
O1	0.0224(4)	0.9844(2)	0.7226(2)	0.0381(7)
O2	0.9272(4)	0.6922(3)	0.6518(2)	0.0512(9)
N1	0.3009(4)	0.9050(3)	0.6553(2)	0.0315(7)
C1	0.1848(5)	0.9371(3)	0.7317(2)	0.0292(8)
C2	0.4996(5)	0.8724(3)	0.6886(2)	0.0291(8)
C3	0.5962(6)	0.7631(3)	0.6392(2)	0.0348(9)
C4	0.7842(5)	0.7290(3)	0.6951(3)	0.0331(9)
C5	0.7852(5)	0.7314(3)	0.8077(3)	0.0319(8)
C6	0.6745(5)	0.8406(3)	0.8527(2)	0.0324(8)
C7	0.4814(5)	0.8480(3)	0.7981(2)	0.0263(8)
C8	0.3199(5)	0.7594(3)	0.8246(3)	0.0302(8)
C9	0.2853(5)	0.8985(3)	0.8271(2)	0.0270(8)
C10	0.2416(6)	0.9656(3)	0.9212(3)	0.0361(9)
C11	0.2457(7)	0.9283(4)	0.5531(3)	0.0498(11)

**Table A-9** Bond Lengths ( $\text{\AA}$ ) for Ketone ( $\pm$ )-**2.86**.

O1-C1	1.224(4)	O2-C4	1.218(5)
N1-C1	1.362(4)	N1-C11	1.439(5)
N1-C2	1.459(5)	C1-C9	1.499(5)
C2-C7	1.507(4)	C2-C3	1.521(4)
C2-H2A	1.0	C3-C4	1.513(5)
C3-H3A	0.99	C3-H3B	0.99
C4-C5	1.516(5)	C5-C6	1.540(4)
C5-H5A	0.99	C5-H5B	0.99
C6-C7	1.491(5)	C6-H6A	0.99
C6-H6B	0.99	C7-C8	1.514(4)
C7-C9	1.507(4)	C8-C9	1.531(4)
C8-H8A	0.99	C8-H8B	0.99
C9-C10	1.500(4)	C10-H10A	0.98
C10-H10B	0.98	C10-H10C	0.98
C11-H11A	0.98	C11-H11B	0.98
C11-H11C	0.98		

**Table A-10** Bond Angles (°) for Ketone (±)-**2.86**

C1-N1-C11	122.5(3)	C1-N1-C2	112.6(3)
C11-N1-C2	123.5(3)	O1-C1-N1	125.2(3)
O1-C1-C9	126.4(3)	N1-C1-C9	108.4(3)
N1-C2-C7	104.0(2)	N1-C2-C3	117.7(3)
C7-C2-C3	109.8(3)	N1-C2-H2A	108.3
C7-C2-H2A	108.3	C3-C2-H2A	108.3
C2-C3-C4	110.1(3)	C2-C3-H3A	109.6
C4-C3-H3A	109.6	C2-C3-H3B	109.6
C4-C3-H3B	109.6	H3A-C3-H3B	108.1
O2-C4-C5	120.3(4)	O2-C4-C3	121.3(3)
C5-C4-C3	118.2(3)	C4-C5-C6	114.7(3)
C4-C5-H5A	108.6	C6-C5-H5A	108.6
C4-C5-H5B	108.6	C6-C5-H5B	108.6
H5A-C5-H5B	107.6	C7-C6-C5	106.4(3)
C7-C6-H6A	110.4	C5-C6-H6A	110.4
C7-C6-H6B	110.4	C5-C6-H6B	110.4
H6A-C6-H6B	108.6	C6-C7-C8	119.1(3)
C6-C7-C2	113.3(3)	C8-C7-C2	115.1(3)
C6-C7-C9	132.0(3)	C8-C7-C9	60.9(2)
C2-C7-C9	106.8(3)	C7-C8-C9	59.34(19)
C7-C8-H8A	117.8	C9-C8-H8A	117.8
C7-C8-H8B	117.8	C9-C8-H8B	117.8
H8A-C8-H8B	115.0	C1-C9-C10	119.4(3)
C1-C9-C7	105.4(2)	C10-C9-C7	126.6(3)
C1-C9-C8	109.0(3)	C10-C9-C8	122.2(3)
C7-C9-C8	59.8(2)	C9-C10-H10A	109.5
C9-C10-H10B	109.5	H10A-C10-H10B	109.5
C9-C10-H10C	109.5	H10A-C10-H10C	109.5
H10B-C10-H10C	109.5	N1-C11-H11A	109.5
N1-C11-H11B	109.5	H11A-C11-H11B	109.5
N1-C11-H11C	109.5	H11A-C11-H11C	109.5
H11B-C11-H11C	109.5		

**Table A-11** Anisotropic Atomic Displacement Parameters ( $\text{\AA}^2$ ) for Ketone ( $\pm$ )-**2.86**

The anisotropic atomic displacement factor exponent takes the form:  $-2\pi^2 [h^2 a^{*2} U_{11} + \dots + 2 h k a^* b^* U_{12}]$

	$U_{11}$	$U_{22}$	$U_{33}$	$U_{23}$	$U_{13}$	$U_{12}$
O1	0.0285(13)	0.0263(13)	0.0595(16)	0.0047(9)	0.0047(11)	0.0067(9)
O2	0.0309(16)	0.0590(18)	0.0644(18)	-0.0273(14)	0.0112(13)	0.0050(12)
N1	0.0289(16)	0.0321(14)	0.0336(14)	0.0020(10)	0.0033(11)	0.0035(11)
C1	0.0275(17)	0.0176(14)	0.0429(18)	-0.0003(11)	0.0059(13)	-0.0020(12)
C2	0.0250(17)	0.0277(16)	0.0350(16)	-0.0030(11)	0.0059(12)	0.0020(12)
C3	0.035(2)	0.0364(18)	0.0336(16)	-0.0076(12)	0.0091(14)	0.0029(13)
C4	0.0255(18)	0.0251(15)	0.0491(19)	-0.0113(12)	0.0095(14)	-0.0026(12)
C5	0.0208(17)	0.0279(16)	0.0471(19)	-0.0030(12)	0.0025(13)	0.0029(12)
C6	0.0275(18)	0.0332(17)	0.0369(16)	-0.0056(12)	0.0051(13)	-0.0010(12)
C7	0.0227(17)	0.0230(15)	0.0336(15)	-0.0033(10)	0.0064(12)	0.0015(11)
C8	0.0236(17)	0.0238(16)	0.0437(17)	0.0017(11)	0.0068(13)	-0.0003(11)
C9	0.0232(17)	0.0240(15)	0.0341(16)	-0.0016(11)	0.0076(12)	0.0021(11)
C10	0.0364(19)	0.0353(18)	0.0371(17)	-0.0047(13)	0.0118(14)	0.0058(13)
C11	0.050(3)	0.059(3)	0.040(2)	0.0046(16)	0.0004(17)	0.0117(19)

**Table A-12** Hydrogen Atomic Coordinates and Isotropic Atomic Displacement Parameters ( $\text{\AA}^2$ ) for Ketone ( $\pm$ )-**2.86**

	<b>x/a</b>	<b>y/b</b>	<b>z/c</b>	<b>U(eq)</b>
H2A	0.5857	0.9460	0.6804	0.035
H3A	0.6255	0.7840	0.5697	0.042
H3B	0.5053	0.6921	0.6384	0.042
H5A	0.9231	0.7335	0.8328	0.038
H5B	0.7259	0.6540	0.8314	0.038
H6A	0.6552	0.8270	0.9244	0.039
H6B	0.7494	0.9178	0.8444	0.039
H8A	0.3327	0.7155	0.8889	0.036
H8B	0.2555	0.7118	0.7702	0.036
H10A	0.2236	1.0533	0.9068	0.054
H10B	0.3512	0.9550	0.9691	0.054
H10C	0.1215	0.9324	0.9491	0.054
H11A	0.1059	0.9489	0.5480	0.075
H11B	0.2707	0.8546	0.5134	0.075
H11C	0.3231	0.9971	0.5282	0.075



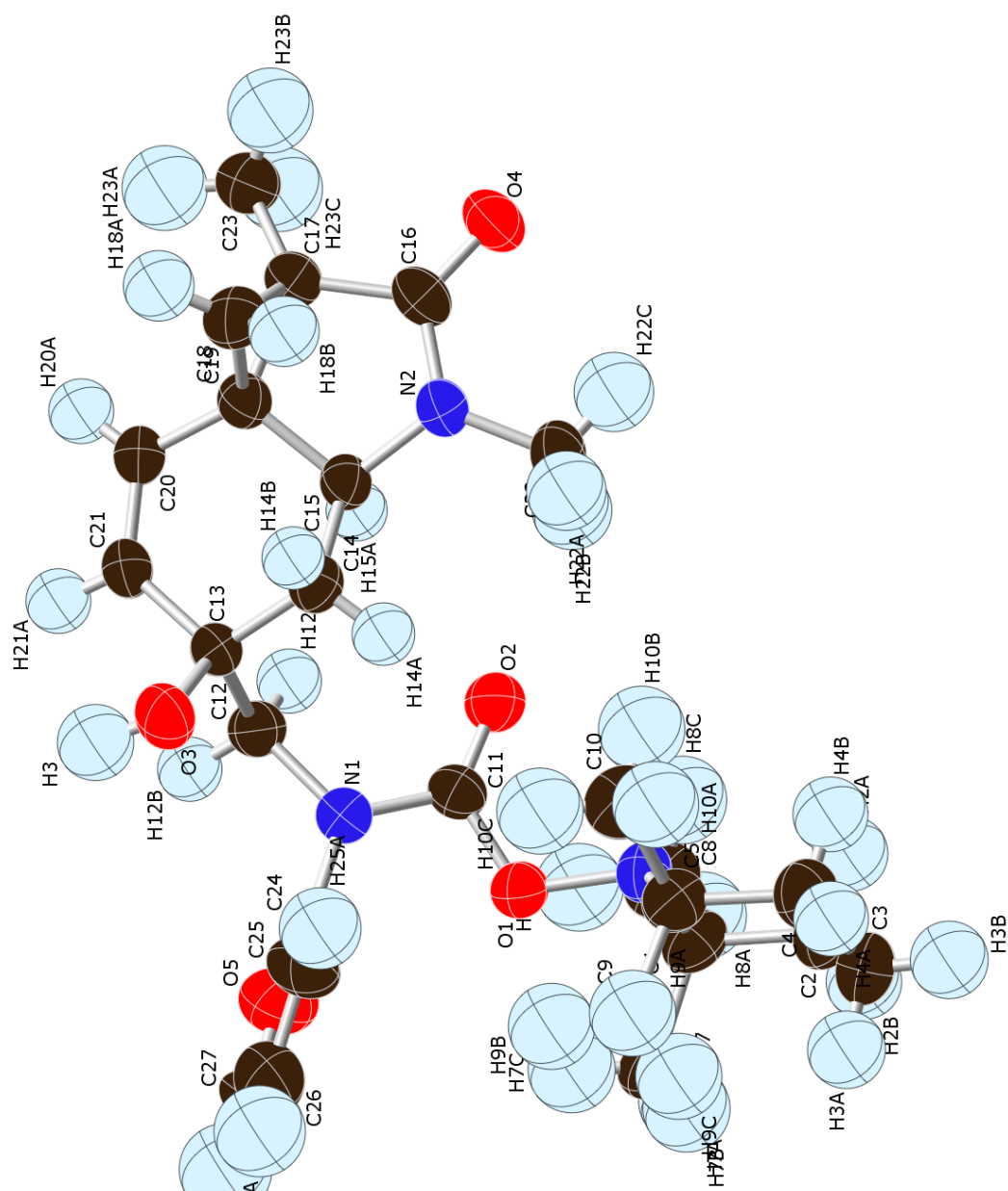


**Figure A-3** ORTEP structure of allylic alcohol (±)-2.111

**Table A-13** Date Collection and Structure Refinement for Allylic Alcohol ( $\pm$ )-**2.111**

<b>Diffractometer</b>	Bruker Apex II CCD
<b>Radiation source</b>	IMuS micro-focus, Cu
<b>Theta range for data collection</b>	3.76 to 68.50°
<b>Index ranges</b>	-10<= <i>h</i> <=10, -23<= <i>k</i> <=22, -16<= <i>l</i> <=18
<b>Reflections collected</b>	14241
<b>Independent reflections</b>	4735 [R(int) = 0.1006]
<b>Coverage of independent reflections</b>	98.8%
<b>Absorption correction</b>	multi-scan
<b>Max. and min. transmission</b>	0.9540 and 0.8820
<b>Structure solution technique</b>	direct methods
<b>Structure solution program</b>	SHELXL-2014/6 (Sheldrick, 2014)
<b>Refinement method</b>	Full-matrix least-squares on $F^2$
<b>Refinement program</b>	SHELXL-2014/6 (Sheldrick, 2014)
<b>Function minimized</b>	$\sum w(F_o^2 - F_c^2)^2$
<b>Data / restraints / parameters</b>	4735 / 0 / 317
<b>Goodness-of-fit on <math>F^2</math></b>	1.152
<b><math>\Delta/\sigma_{\max}</math></b>	0.444
<b>Final R indices</b>	2672 data; $I > 2\sigma(I)$ R1 = 0.0922, wR2 = 0.1973 all data                    R1 = 0.1407, wR2 = 0.2252
<b>Weighting scheme</b>	$w = 1/[\sigma^2(F_o^2) + (0.0680P)^2]$ where $P = (F_o^2 + 2F_c^2)/3$
<b>Largest diff. peak and hole</b>	0.544 and -0.279 eÅ <sup>-3</sup>
<b>R.M.S. deviation from mean</b>	0.113 eÅ <sup>-3</sup>

**Table A-14** Atomic Coordinates and Equivalent Isotropic Atomic Displacement Parameters ( $\text{\AA}^2$ ) for Allylic Alcohol ( $\pm$ )-2.111

U(eq) is defined as one third of the trace of the orthogonalized  $U_{ij}$  tensor.

	<b>x/a</b>	<b>y/b</b>	<b>z/c</b>	<b>U(eq)</b>
O1	0.3718(3)	0.71375(13)	0.52526(16)	0.0516(6)
N1	0.5116(3)	0.64695(15)	0.63095(19)	0.0496(7)
C1	0.2265(5)	0.81229(19)	0.4733(3)	0.0568(9)
O2	0.2715(3)	0.67526(13)	0.64034(17)	0.0552(6)
N2	0.1017(3)	0.51393(16)	0.7153(2)	0.0502(7)
C2	0.0738(5)	0.8347(2)	0.4110(3)	0.0678(11)
O3	0.6186(3)	0.50353(15)	0.67015(19)	0.0611(7)
C3	0.0408(5)	0.8023(2)	0.3182(3)	0.0720(12)
O4	0.9160(3)	0.48706(15)	0.78893(18)	0.0625(7)
C4	0.0416(5)	0.7250(2)	0.3283(3)	0.0668(11)
O5	0.7218(4)	0.7042(2)	0.6037(3)	0.0996(12)
C5	0.1922(4)	0.69733(19)	0.3868(3)	0.0559(9)
N3	0.2205(3)	0.73570(14)	0.47447(19)	0.0482(7)
C7	0.3604(5)	0.8431(2)	0.4429(3)	0.0720(12)
C8	0.2333(6)	0.8356(2)	0.5698(3)	0.0736(12)
C9	0.3164(5)	0.7003(2)	0.3358(3)	0.0704(11)
C10	0.1692(5)	0.6225(2)	0.4119(3)	0.0710(12)
C11	0.3728(4)	0.67788(17)	0.6028(2)	0.0458(8)
C12	0.5498(4)	0.61392(19)	0.7211(2)	0.0490(8)
C13	0.5255(4)	0.53573(18)	0.7206(2)	0.0454(8)
C14	0.3612(4)	0.51508(18)	0.6747(2)	0.0466(8)
C15	0.2649(4)	0.52448(17)	0.7410(2)	0.0439(8)
C16	0.0485(4)	0.48754(19)	0.7840(2)	0.0496(9)
C17	0.1795(4)	0.45581(19)	0.8527(2)	0.0504(8)
C18	0.2570(5)	0.40365(19)	0.8060(3)	0.0590(10)
C19	0.3184(4)	0.47538(17)	0.8191(2)	0.0463(8)
C20	0.4791(4)	0.48566(19)	0.8650(2)	0.0496(8)
C21	0.5722(4)	0.51259(19)	0.8194(2)	0.0501(9)
C22	0.0055(4)	0.5512(2)	0.6400(3)	0.0603(10)
C23	0.1694(5)	0.4478(2)	0.9491(3)	0.0688(11)
C24	0.6214(4)	0.6528(2)	0.5824(3)	0.0621(11)
C25	0.6469(5)	0.6171(3)	0.5111(3)	0.0795(13)
C26	0.7654(6)	0.6461(4)	0.4848(4)	0.0994(18)
C27	0.8131(5)	0.6977(4)	0.5412(4)	0.102(2)

**Table A-15** Bond lengths (Å) for Allylic Alcohol ( $\pm$ )-**2.111**

O1-C11	1.368(4)	O1-N3	1.462(4)
N1-C11	1.366(5)	N1-C24	1.383(5)
N1-C12	1.476(4)	C1-N3	1.497(5)
C1-C8	1.521(6)	C1-C7	1.525(6)
C1-C2	1.534(6)	O2-C11	1.196(4)
N2-C16	1.354(5)	N2-C15	1.448(4)
N2-C22	1.452(5)	C2-C3	1.505(6)
C2-H2A	0.98	C2-H2B	0.98
O3-C13	1.419(4)	O3-H3	0.87(5)
C3-C4	1.517(6)	C3-H3A	0.98
C3-H3B	0.98	O4-C16	1.222(4)
C4-C5	1.531(6)	C4-H4A	0.98
C4-H4B	0.98	O5-C24	1.339(6)
O5-C27	1.412(7)	C5-N3	1.494(5)
C5-C9	1.517(6)	C5-C10	1.538(6)
C7-H7A	0.97	C7-H7B	0.97
C7-H7C	0.97	C8-H8A	0.97
C8-H8B	0.97	C8-H8C	0.97
C9-H9A	0.97	C9-H9B	0.97
C9-H9C	0.97	C10-H10A	0.97
C10-H10B	0.97	C10-H10C	0.97
C12-C13	1.542(5)	C12-H12A	0.98
C12-H12B	0.98	C13-C21	1.524(5)
C13-C14	1.534(5)	C14-C15	1.497(5)
C14-H14A	0.98	C14-H14B	0.98
C15-C19	1.509(5)	C15-H15A	0.99
C16-C17	1.506(5)	C17-C23	1.497(5)
C17-C18	1.509(5)	C17-C19	1.519(5)
C18-C19	1.502(5)	C18-H18A	0.98
C18-H18B	0.98	C19-C20	1.465(5)
C20-C21	1.326(5)	C20-H20A	0.94
C21-H21A	0.94	C22-H22A	0.97
C22-H22B	0.97	C22-H22C	0.97
C23-H23A	0.97	C23-H23B	0.97
C23-H23C	0.97	C24-C25	1.354(7)
C25-C26	1.358(7)	C25-H25A	0.94
C26-C27	1.324(9)	C26-H26A	0.94
C27-H27A	0.94		

**Table A-16** Bond Angles (°) for Allylic Alcohol ( $\pm$ )-2.111

C11-O1-N3	114.2(2)	C11-N1-C24	121.7(3)
C11-N1-C12	118.1(3)	C24-N1-C12	119.8(3)
N3-C1-C8	106.3(3)	N3-C1-C7	115.6(3)
C8-C1-C7	109.1(3)	N3-C1-C2	105.2(3)
C8-C1-C2	109.0(4)	C7-C1-C2	111.4(3)
C16-N2-C15	112.4(3)	C16-N2-C22	122.6(3)
C15-N2-C22	121.0(3)	C3-C2-C1	113.5(4)
C3-C2-H2A	108.9	C1-C2-H2A	108.9
C3-C2-H2B	108.9	C1-C2-H2B	108.9
H2A-C2-H2B	107.7	C13-O3-H3	120.(3)
C2-C3-C4	109.2(3)	C2-C3-H3A	109.9
C4-C3-H3A	109.8	C2-C3-H3B	109.8
C4-C3-H3B	109.8	H3A-C3-H3B	108.3
C3-C4-C5	113.0(3)	C3-C4-H4A	109.0
C5-C4-H4A	109.0	C3-C4-H4B	109.0
C5-C4-H4B	109.0	H4A-C4-H4B	107.8
C24-O5-C27	104.2(5)	N3-C5-C9	116.8(3)
N3-C5-C4	105.8(3)	C9-C5-C4	111.0(4)
N3-C5-C10	105.0(3)	C9-C5-C10	109.0(3)
C4-C5-C10	108.8(3)	O1-N3-C1	105.5(2)
O1-N3-C5	104.8(3)	C1-N3-C5	119.3(3)
C1-C7-H7A	109.5	C1-C7-H7B	109.5
H7A-C7-H7B	109.5	C1-C7-H7C	109.5
H7A-C7-H7C	109.5	H7B-C7-H7C	109.5
C1-C8-H8A	109.5	C1-C8-H8B	109.5
H8A-C8-H8B	109.5	C1-C8-H8C	109.5
H8A-C8-H8C	109.5	H8B-C8-H8C	109.5
C5-C9-H9A	109.5	C5-C9-H9B	109.5
H9A-C9-H9B	109.5	C5-C9-H9C	109.5
H9A-C9-H9C	109.5	H9B-C9-H9C	109.5
C5-C10-H10A	109.5	C5-C10-H10B	109.5
H10A-C10-H10B	109.5	C5-C10-H10C	109.5
H10A-C10-H10C	109.5	H10B-C10-H10C	109.5
O2-C11-O1	126.2(3)	O2-C11-N1	126.0(3)
O1-C11-N1	107.8(3)	N1-C12-C13	115.3(3)
N1-C12-H12A	108.5	C13-C12-H12A	108.5
N1-C12-H12B	108.5	C13-C12-H12B	108.5
H12A-C12-H12B	107.5	O3-C13-C21	110.0(3)
O3-C13-C14	106.2(3)	C21-C13-C14	111.8(3)
O3-C13-C12	109.8(3)	C21-C13-C12	106.5(3)
C14-C13-C12	112.6(3)	C15-C14-C13	108.9(3)

C15-C14-H14A	109.9	C13-C14-H14A	109.9
C15-C14-H14B	109.9	C13-C14-H14B	109.9
H14A-C14-H14B	108.3	N2-C15-C14	121.9(3)
N2-C15-C19	103.2(3)	C14-C15-C19	108.9(3)
N2-C15-H15A	107.4	C14-C15-H15A	107.4
C19-C15-H15A	107.4	O4-C16-N2	126.3(3)
O4-C16-C17	125.0(3)	N2-C16-C17	108.7(3)
C23-C17-C16	119.4(3)	C23-C17-C18	122.5(3)
C16-C17-C18	109.3(3)	C23-C17-C19	127.7(3)
C16-C17-C19	103.9(3)	C18-C17-C19	59.5(2)
C19-C18-C17	60.6(2)	C19-C18-H18A	117.7
C17-C18-H18A	117.7	C19-C18-H18B	117.7
C17-C18-H18B	117.7	H18A-C18-H18B	114.8
C20-C19-C18	118.9(3)	C20-C19-C15	112.1(3)
C18-C19-C15	116.9(3)	C20-C19-C17	133.1(3)
C18-C19-C17	59.9(2)	C15-C19-C17	107.0(3)
C21-C20-C19	119.4(3)	C21-C20-H20A	120.3
C19-C20-H20A	120.3	C20-C21-C13	125.0(3)
C20-C21-H21A	117.5	C13-C21-H21A	117.5
N2-C22-H22A	109.5	N2-C22-H22B	109.5
H22A-C22-H22B	109.5	N2-C22-H22C	109.5
H22A-C22-H22C	109.5	H22B-C22-H22C	109.5
C17-C23-H23A	109.5	C17-C23-H23B	109.5
H23A-C23-H23B	109.5	C17-C23-H23C	109.5
H23A-C23-H23C	109.5	H23B-C23-H23C	109.5
O5-C24-C25	109.8(4)	O5-C24-N1	117.9(4)
C25-C24-N1	132.2(4)	C26-C25-C24	108.9(6)
C26-C25-H25A	125.5	C24-C25-H25A	125.5
C27-C26-C25	106.4(5)	C27-C26-H26A	126.8
C25-C26-H26A	126.8	C26-C27-O5	110.5(4)
C26-C27-H27A	124.7	O5-C27-H27A	124.7

**Table A-17** Anisotropic Atomic Displacement Parameters ( $\text{\AA}^2$ ) for Allylic Alcohol ( $\pm$ )-**2.111**The anisotropic atomic displacement factor exponent takes the form:  $-2\pi[h^* a^* U_{11} + \dots + 2 h^* k^* a^* b^* U_{12}]$ 

	$U_{11}$	$U_{22}$	$U_{33}$	$U_{23}$	$U_{13}$	$U_{12}$
O1	0.0494(13)	0.0528(15)	0.0509(14)	0.0085(10)	0.0090(11)	0.0004(11)
N1	0.0460(16)	0.0529(18)	0.0498(17)	0.0047(13)	0.0115(13)	-0.0013(13)
C1	0.072(2)	0.041(2)	0.054(2)	0.0015(15)	0.0103(18)	-0.0050(18)
O2	0.0563(15)	0.0517(15)	0.0601(15)	0.0054(11)	0.0191(12)	0.0061(11)
N2	0.0383(14)	0.0550(18)	0.0546(18)	0.0060(13)	0.0064(13)	0.0002(13)
C2	0.075(3)	0.047(2)	0.076(3)	0.0079(18)	0.008(2)	0.0086(19)
O3	0.0521(15)	0.0726(19)	0.0608(17)	0.0011(13)	0.0184(13)	0.0117(13)
C3	0.074(3)	0.071(3)	0.064(3)	0.015(2)	0.004(2)	0.003(2)
O4	0.0415(14)	0.082(2)	0.0639(17)	-0.0004(13)	0.0131(12)	-0.0044(12)
C4	0.069(3)	0.066(3)	0.058(2)	-0.0028(19)	0.0009(19)	-0.007(2)
O5	0.078(2)	0.121(3)	0.094(2)	0.024(2)	0.0105(18)	-0.035(2)
C5	0.063(2)	0.049(2)	0.053(2)	-0.0044(15)	0.0083(17)	-0.0076(17)
N3	0.0487(16)	0.0405(16)	0.0515(17)	0.0004(12)	0.0051(13)	-0.0008(12)
C7	0.083(3)	0.057(3)	0.070(3)	0.0068(19)	0.010(2)	-0.018(2)
C8	0.097(3)	0.048(2)	0.071(3)	-0.0113(18)	0.011(2)	-0.003(2)
C9	0.084(3)	0.072(3)	0.055(2)	-0.0025(19)	0.018(2)	0.002(2)
C10	0.091(3)	0.046(2)	0.073(3)	-0.0142(18)	0.014(2)	-0.009(2)
C11	0.0458(18)	0.0427(19)	0.050(2)	-0.0045(15)	0.0144(16)	-0.0033(15)
C12	0.0461(18)	0.055(2)	0.0433(19)	0.0024(15)	0.0070(15)	-0.0037(16)
C13	0.0383(16)	0.051(2)	0.0484(19)	0.0062(15)	0.0136(14)	0.0035(15)
C14	0.0480(18)	0.0424(18)	0.0468(19)	0.0012(14)	0.0069(15)	0.0019(15)
C15	0.0391(16)	0.0395(18)	0.0505(19)	0.0024(14)	0.0060(14)	-0.0005(14)
C16	0.0396(19)	0.053(2)	0.056(2)	-0.0105(16)	0.0111(15)	-0.0069(15)
C17	0.0439(18)	0.052(2)	0.054(2)	0.0026(15)	0.0101(15)	-0.0044(16)
C18	0.063(2)	0.044(2)	0.067(2)	0.0049(16)	0.0109(18)	-0.0031(17)
C19	0.0432(17)	0.0421(19)	0.053(2)	0.0015(14)	0.0109(15)	0.0011(14)
C20	0.0441(18)	0.054(2)	0.049(2)	0.0071(15)	0.0078(15)	0.0064(16)
C21	0.0385(17)	0.060(2)	0.049(2)	0.0057(16)	0.0053(15)	0.0041(16)
C22	0.0469(19)	0.064(3)	0.062(2)	0.0065(18)	-0.0016(17)	-0.0004(17)
C23	0.061(2)	0.082(3)	0.063(3)	0.013(2)	0.0139(19)	-0.010(2)
C24	0.0425(19)	0.076(3)	0.066(3)	0.027(2)	0.0112(18)	-0.0012(19)
C25	0.071(3)	0.104(4)	0.074(3)	0.019(3)	0.039(2)	0.014(3)
C26	0.072(3)	0.142(6)	0.088(4)	0.028(4)	0.026(3)	0.011(3)
C27	0.048(2)	0.149(6)	0.111(4)	0.057(4)	0.024(3)	-0.023(3)

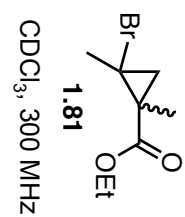
**Table A-18** Hydrogen atomic coordinates and isotropic atomic displacement parameters ( $\text{\AA}^2$ ) for allylic alcohol ( $\pm$ )-2.111.

	<b>x/a</b>	<b>y/b</b>	<b>z/c</b>	<b>U(eq)</b>
H2A	-0.0081	0.8228	0.4400	0.081
H2B	0.0740	0.8846	0.4042	0.081
H3	0.715(6)	0.498(3)	0.694(3)	0.083(15)
H3A	0.1181	0.8162	0.2867	0.086
H3B	-0.0588	0.8175	0.2821	0.086
H4A	0.0219	0.7040	0.2679	0.08
H4B	-0.0412	0.7115	0.3558	0.08
H7A	0.3642	0.8921	0.4540	0.108
H7B	0.3479	0.8346	0.3786	0.108
H7C	0.4544	0.8223	0.4769	0.108
H8A	0.2218	0.8849	0.5708	0.11
H8B	0.3307	0.8227	0.6094	0.11
H8C	0.1519	0.8139	0.5908	0.11
H9A	0.3026	0.6630	0.2922	0.106
H9B	0.4151	0.6959	0.3785	0.106
H9C	0.3110	0.7437	0.3041	0.106
H10A	0.1255	0.5966	0.3571	0.106
H10B	0.1009	0.6209	0.4520	0.106
H10C	0.2666	0.6027	0.4424	0.106
H12A	0.4879	0.6350	0.7584	0.059
H12B	0.6568	0.6236	0.7504	0.059
H14A	0.3220	0.5435	0.6209	0.056
H14B	0.3581	0.4671	0.6554	0.056
H15A	0.2833	0.5715	0.7658	0.053
H18A	0.3161	0.3674	0.8435	0.071
H18B	0.2043	0.3895	0.7444	0.071
H20A	0.5159	0.4733	0.9263	0.06
H21A	0.6750	0.5178	0.8504	0.06
H22A	0.0136	0.5309	0.5831	0.09
H22B	0.0381	0.5987	0.6422	0.09
H22C	-0.0994	0.5491	0.6443	0.09
H23A	0.2653	0.4304	0.9856	0.103
H23B	0.0883	0.4160	0.9515	0.103
H23C	0.1481	0.4920	0.9726	0.103
H25A	0.5916	0.5786	0.4843	0.095
H26A	0.8055	0.6322	0.4362	0.119
H27A	0.8963	0.7261	0.5398	0.122



## **APPENDIX B**

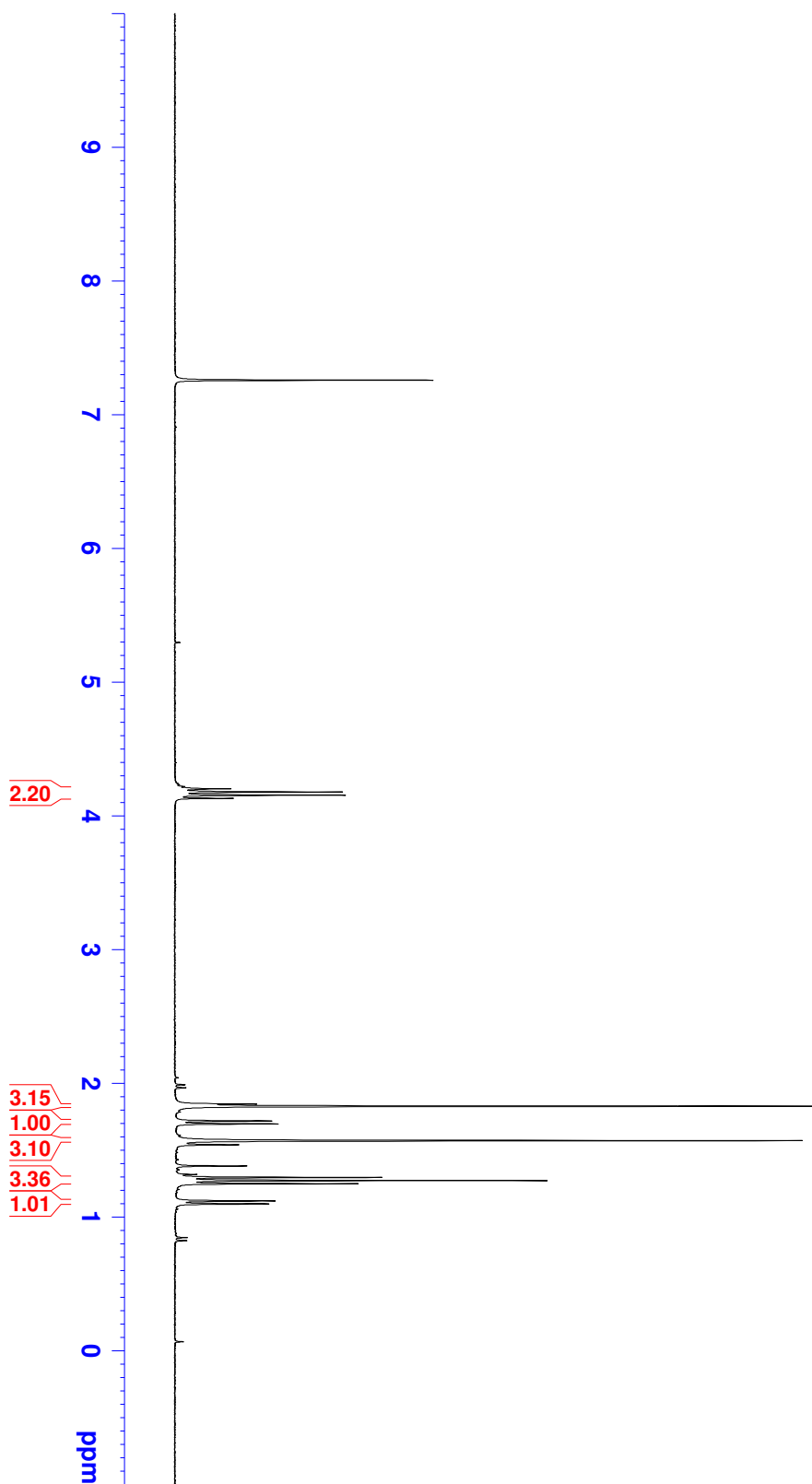
### **SELECTED NMR SPECTRA**

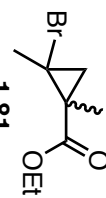


— 7.260

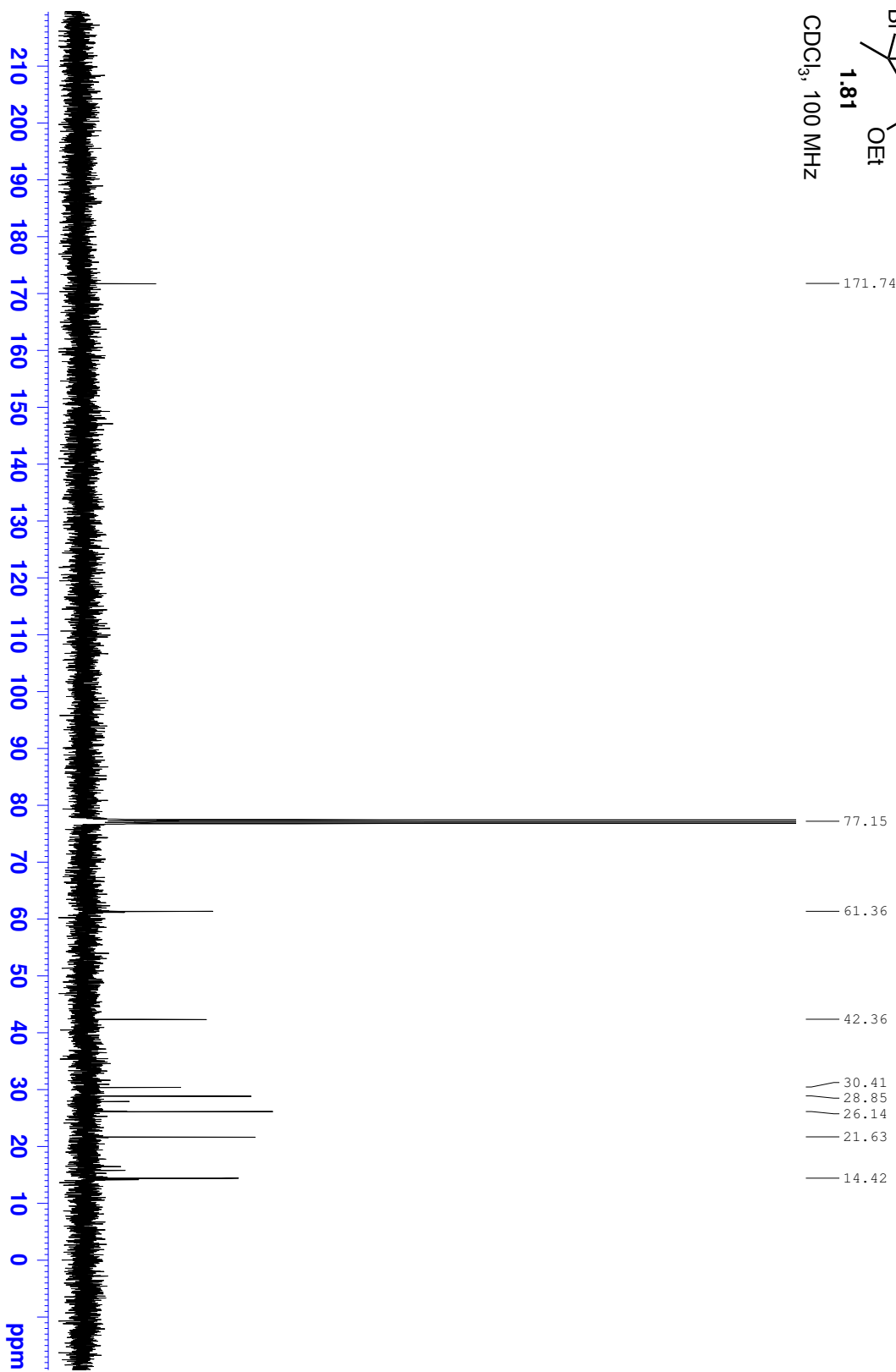
4.204  
 4.180  
 4.157  
 4.133

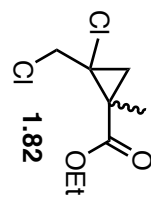
1.830  
 1.720  
 1.698  
 1.572  
 1.298  
 1.274  
 1.250  
 1.121  
 1.100



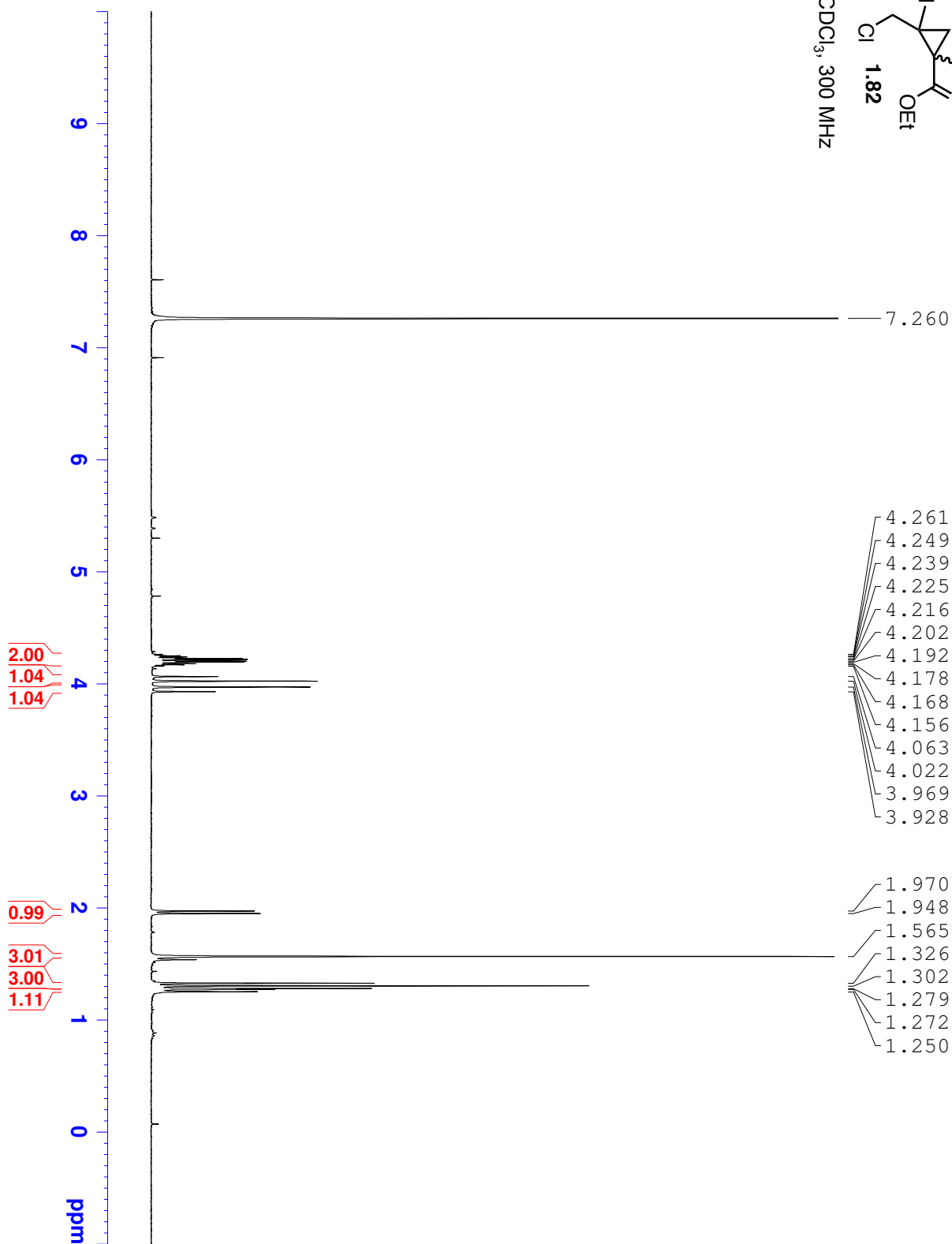


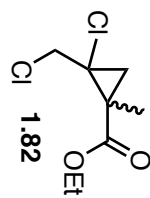
CDCl<sub>3</sub>, 100 MHz



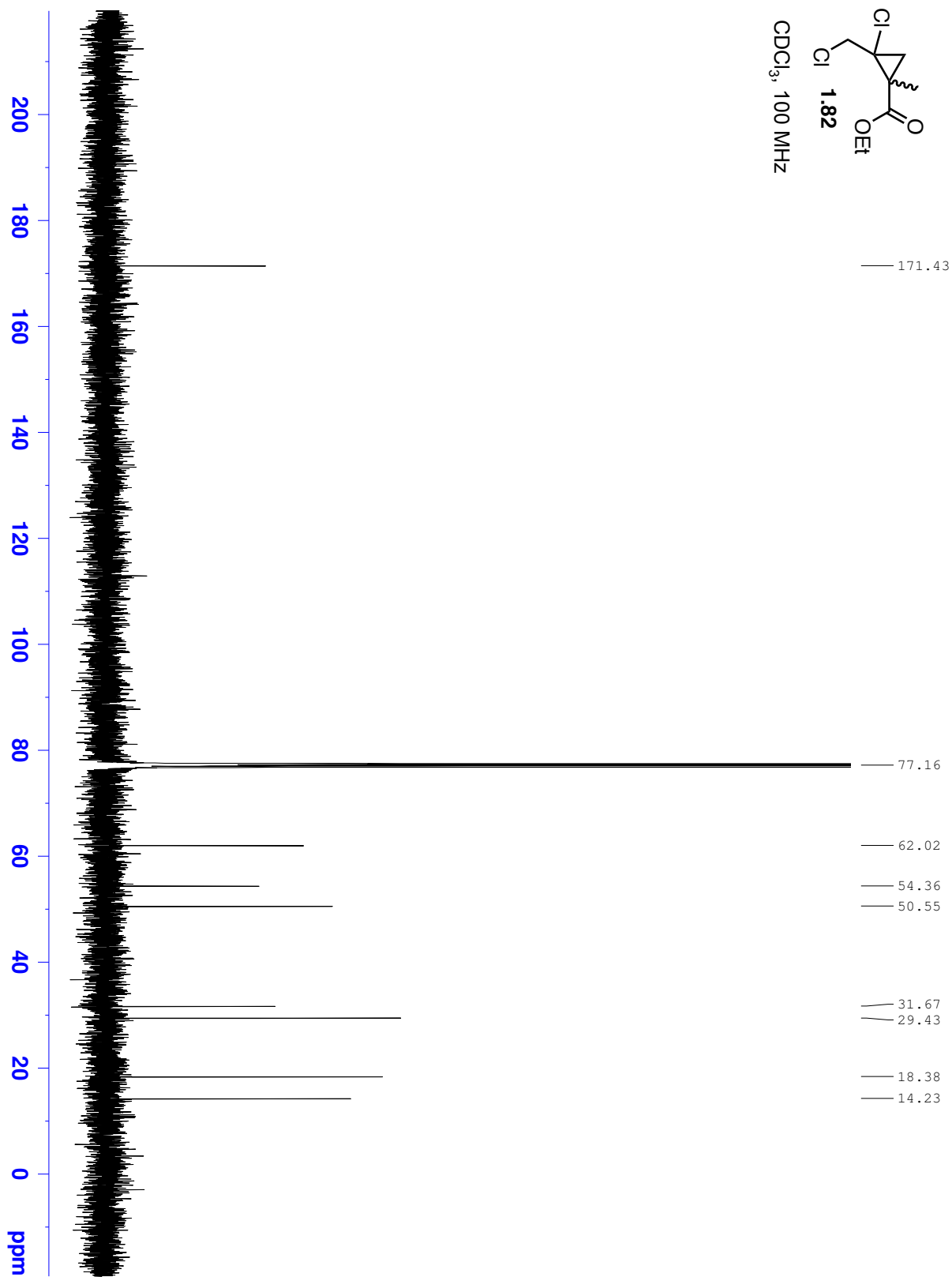


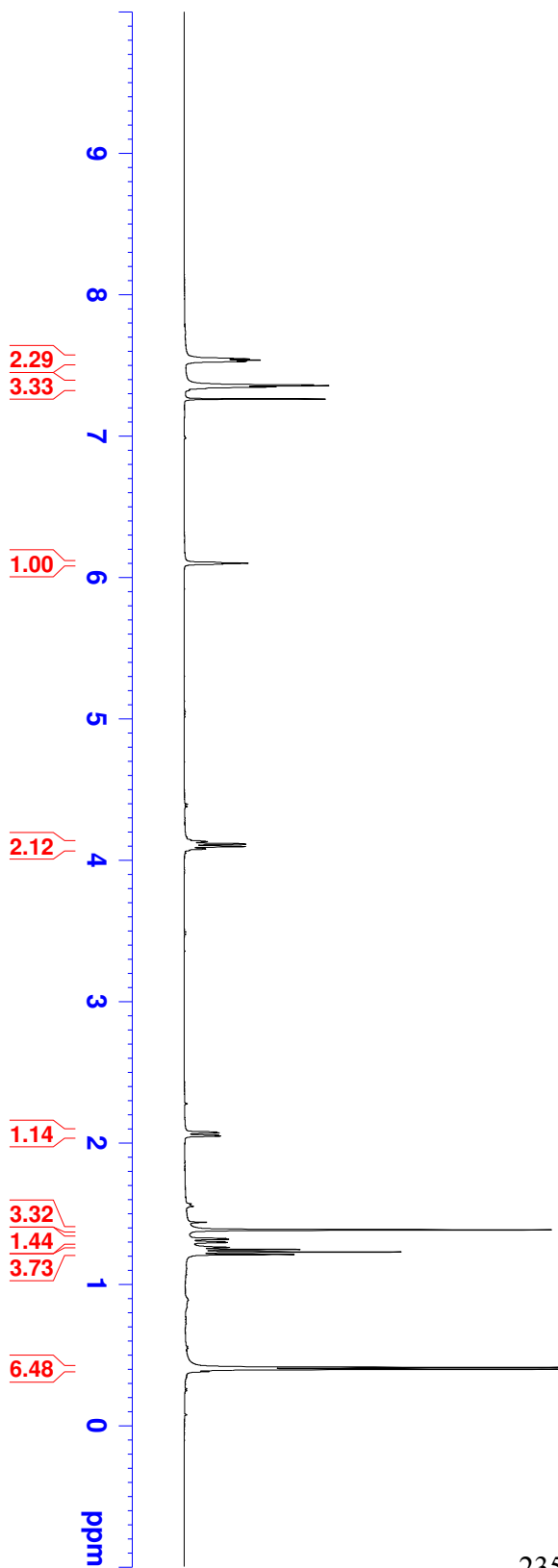
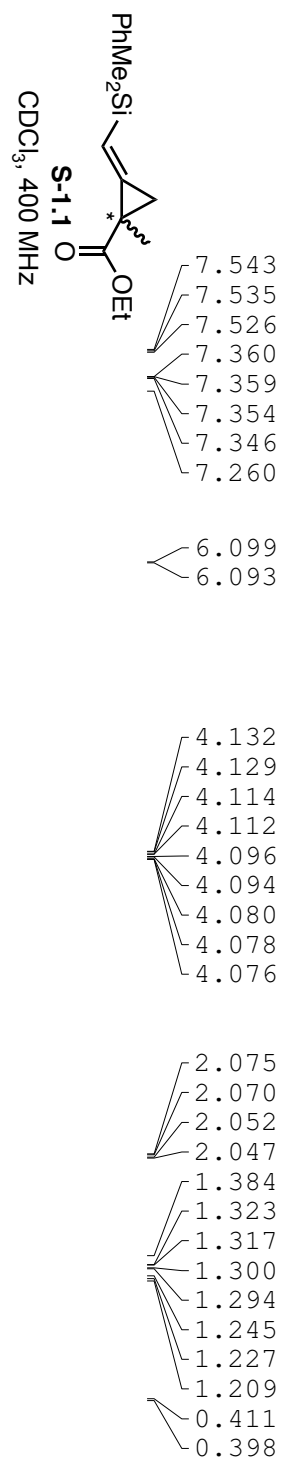
CDCl<sub>3</sub>, 300 MHz

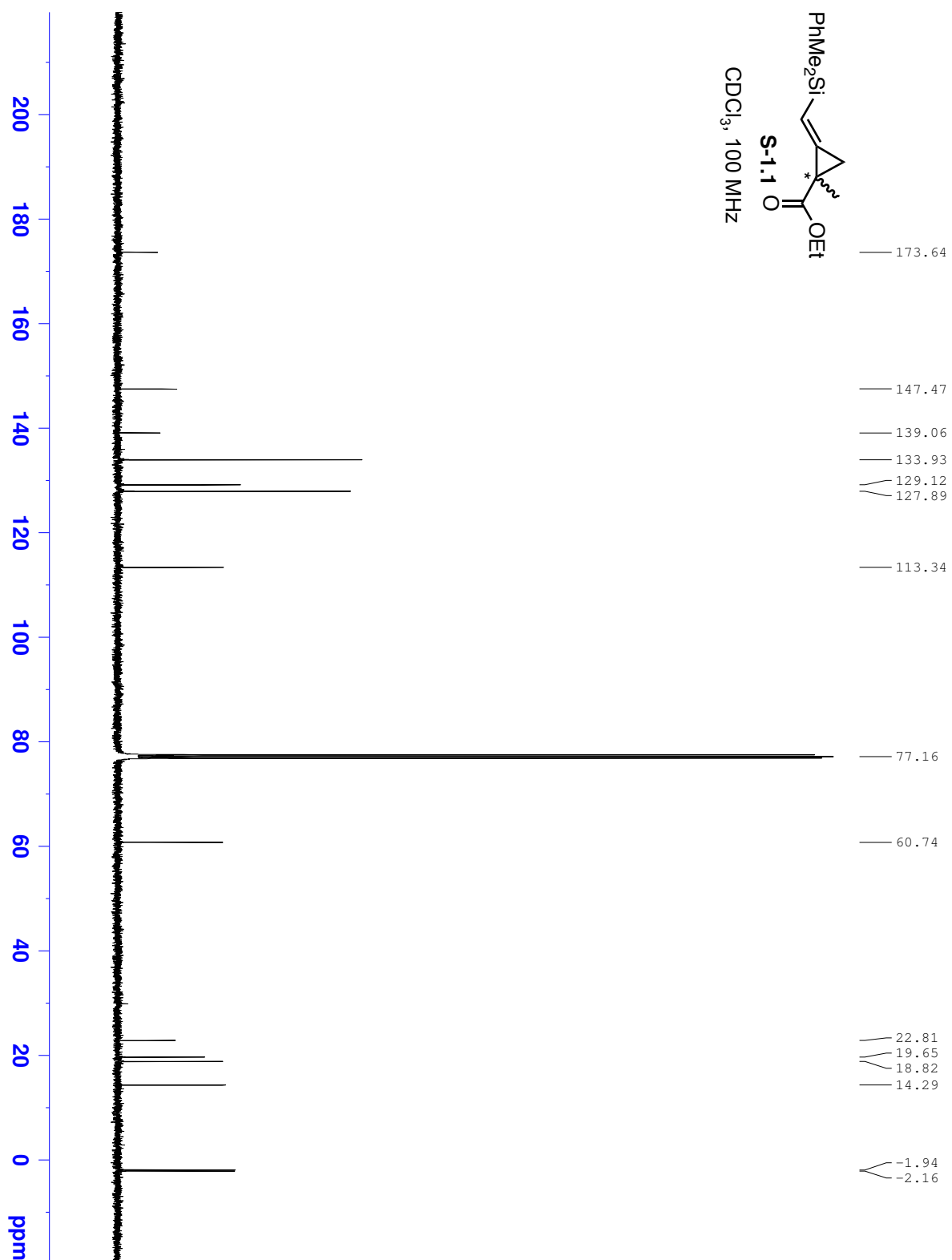


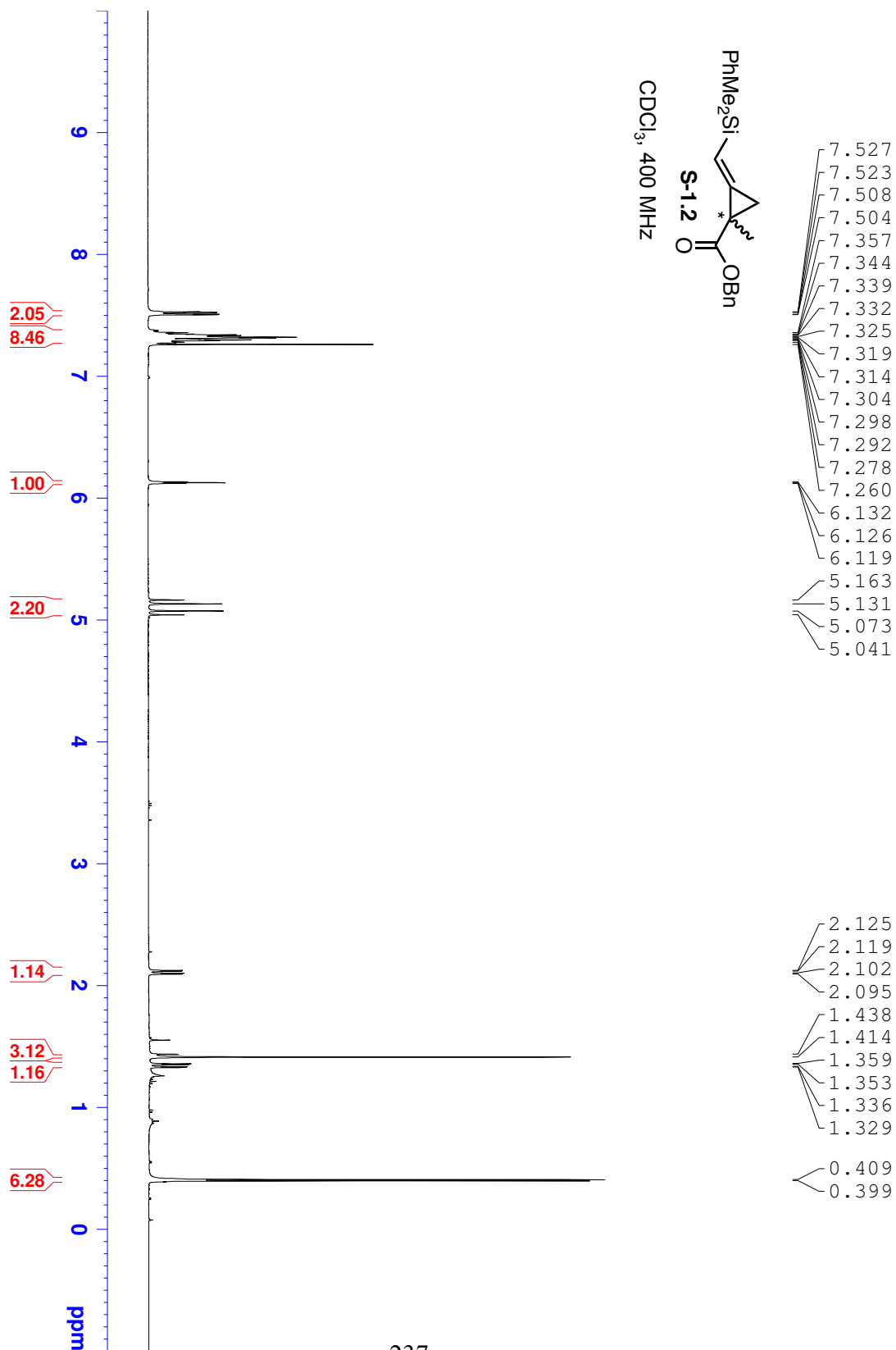


CDCl<sub>3</sub>, 100 MHz

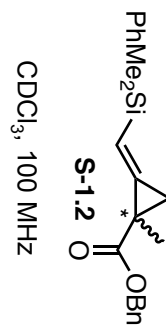












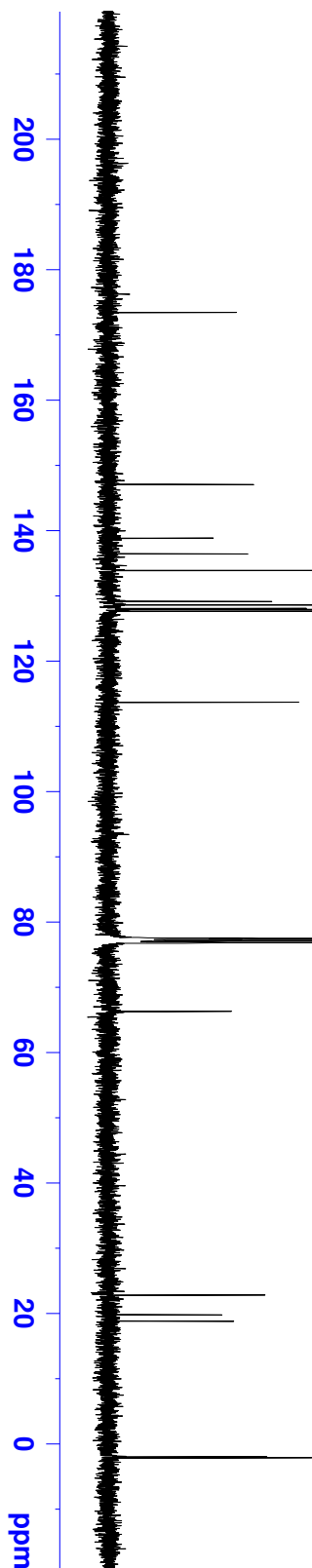
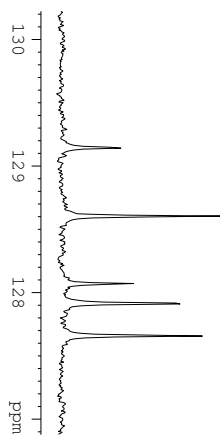
173.45  
 147.09  
 138.86  
 136.44  
 133.91  
 129.14  
 128.60  
 128.07  
 127.91  
 127.65  
 113.69

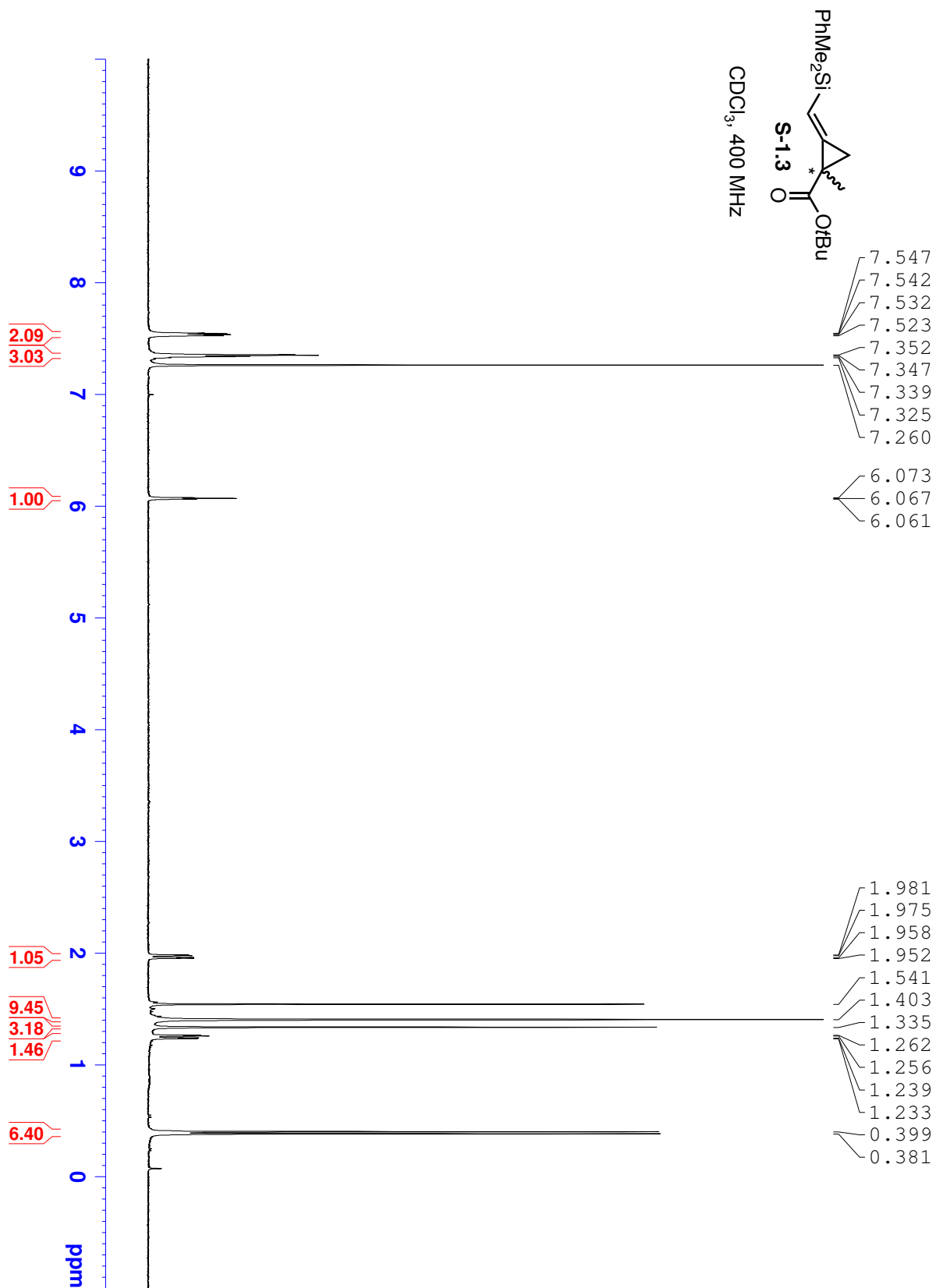
129.143  
 128.601  
 128.069  
 127.912  
 127.655

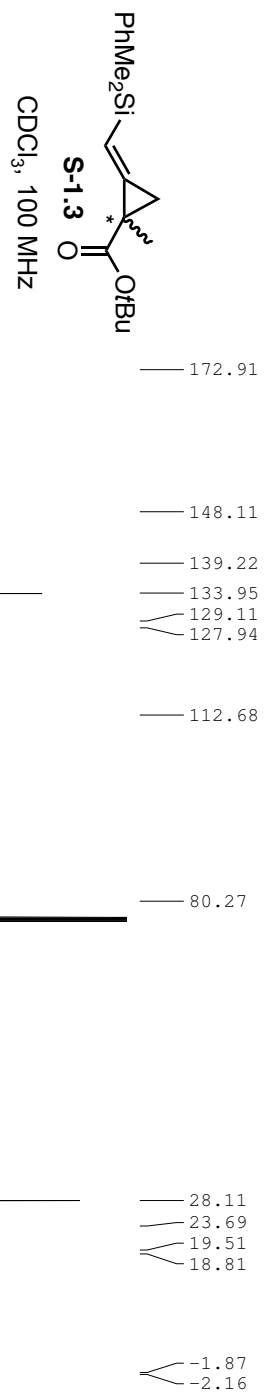
77.16  
 66.29

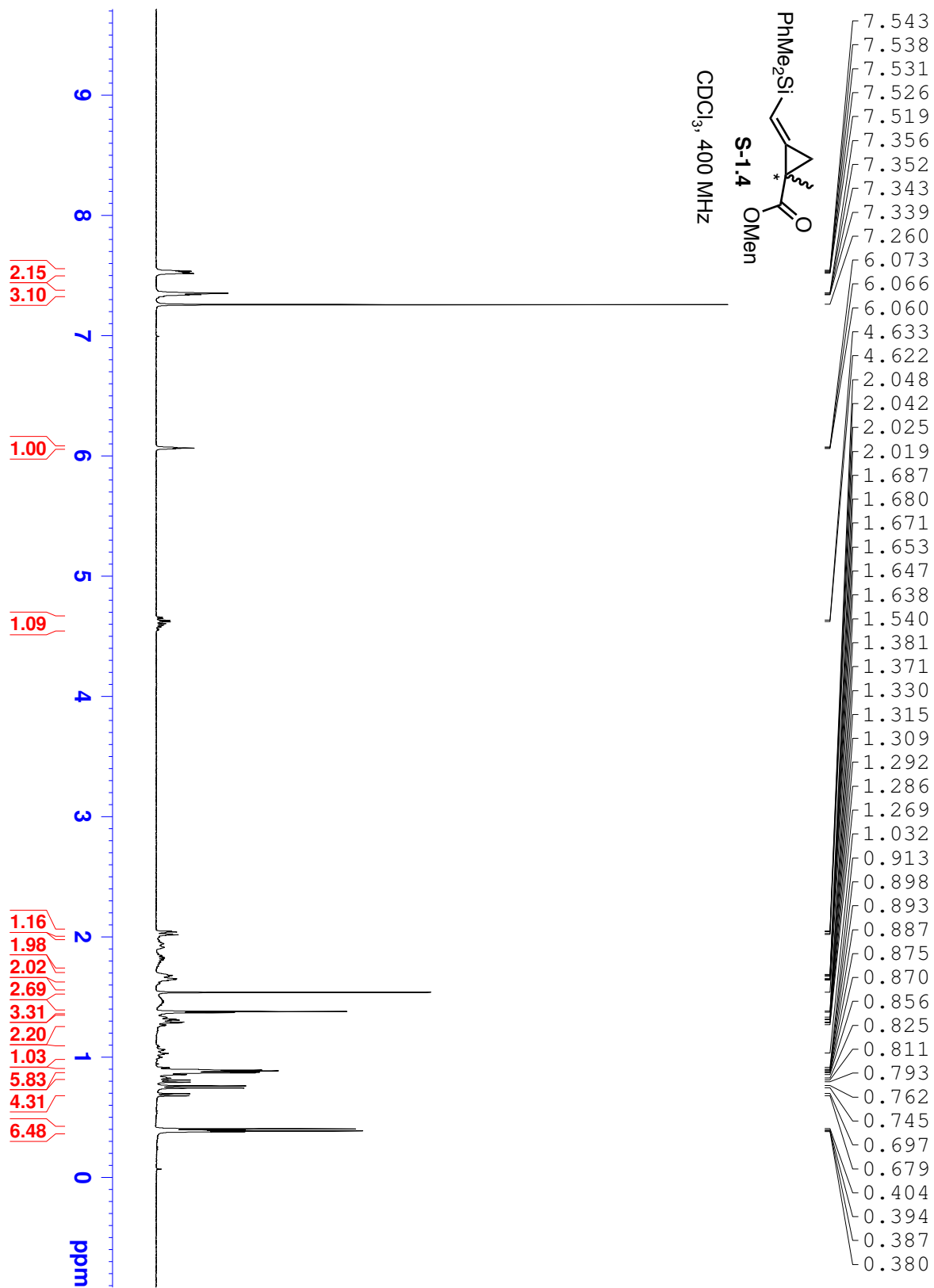
22.82  
 19.79  
 18.81

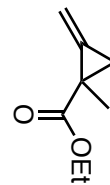
-1.97  
 -2.15





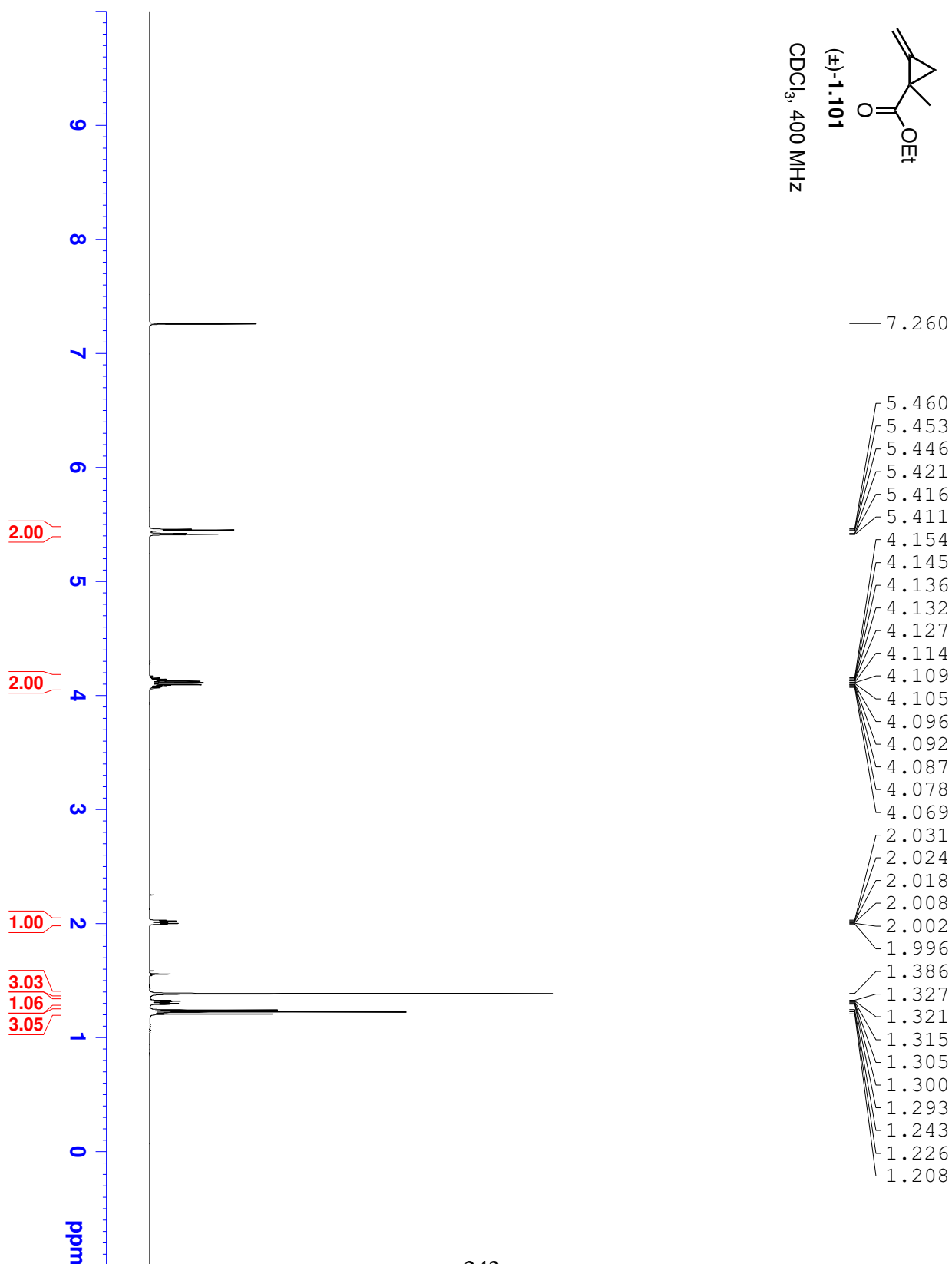


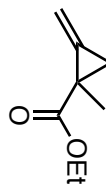




(±)-1.101

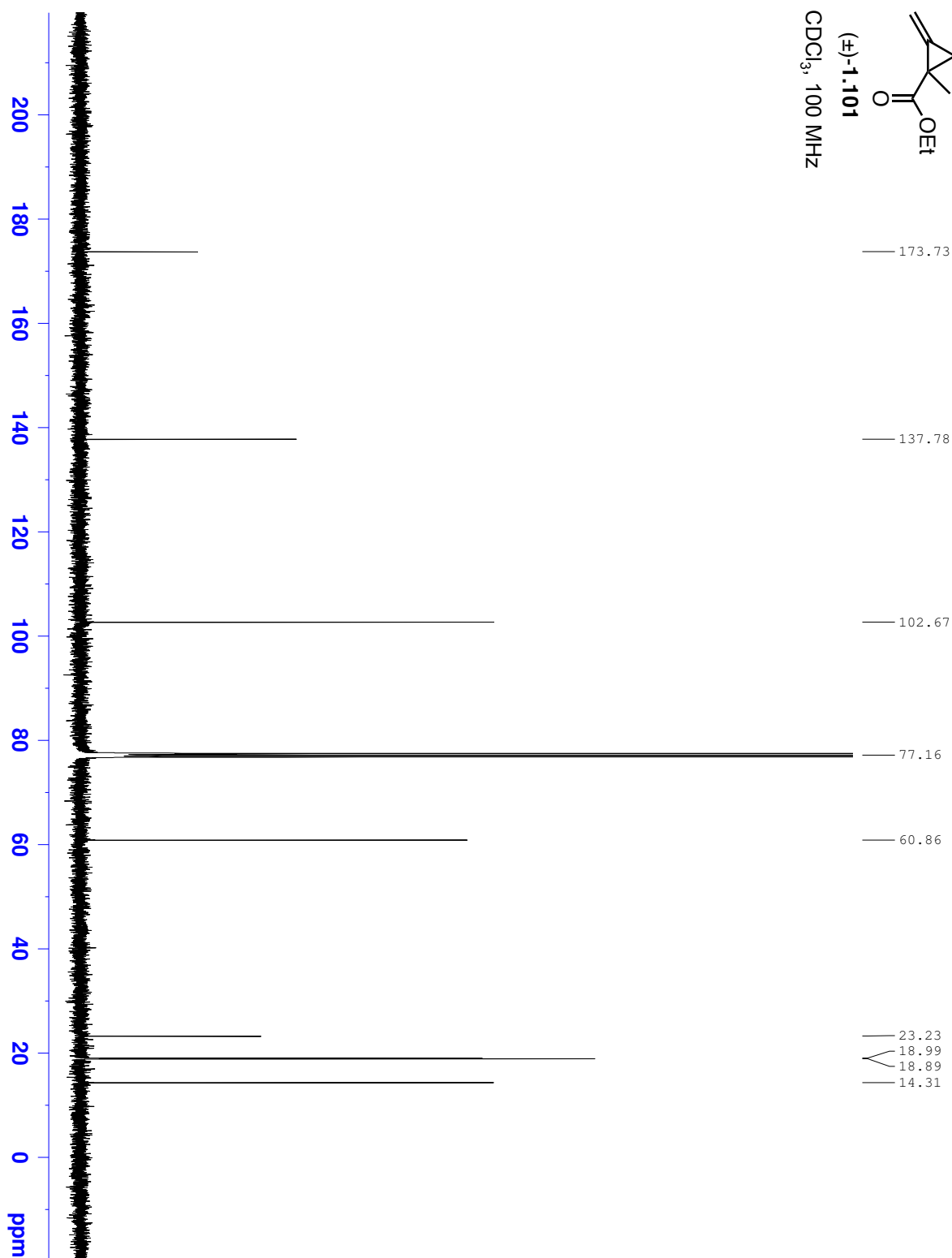
CDCl<sub>3</sub>, 400 MHz

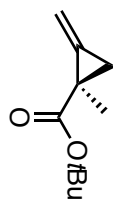




(±)-1.101

CDCl<sub>3</sub>, 100 MHz





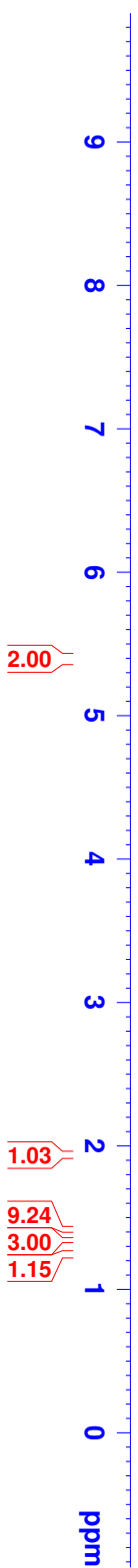
S-1.7

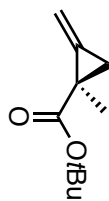
CDCl<sub>3</sub>, 400 MHz

7.260

5.429  
5.422  
5.415  
5.372  
5.367  
5.362

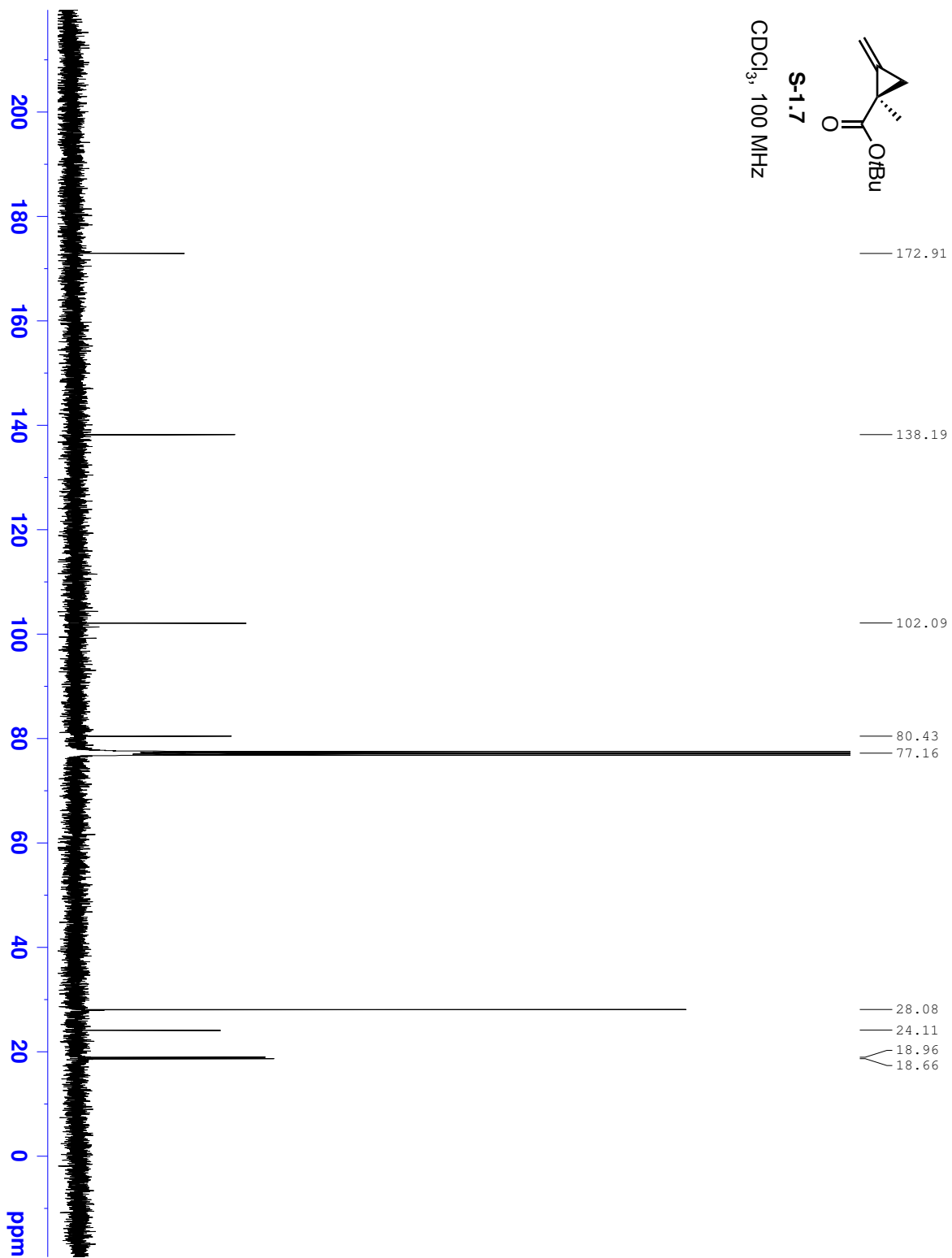
1.412  
1.338  
1.257  
1.252  
1.246  
1.236  
1.230  
1.224



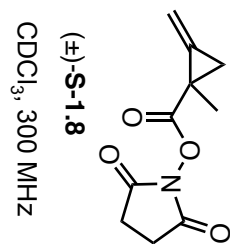


**S-1.7**

$\text{CDCl}_3$ , 100 MHz



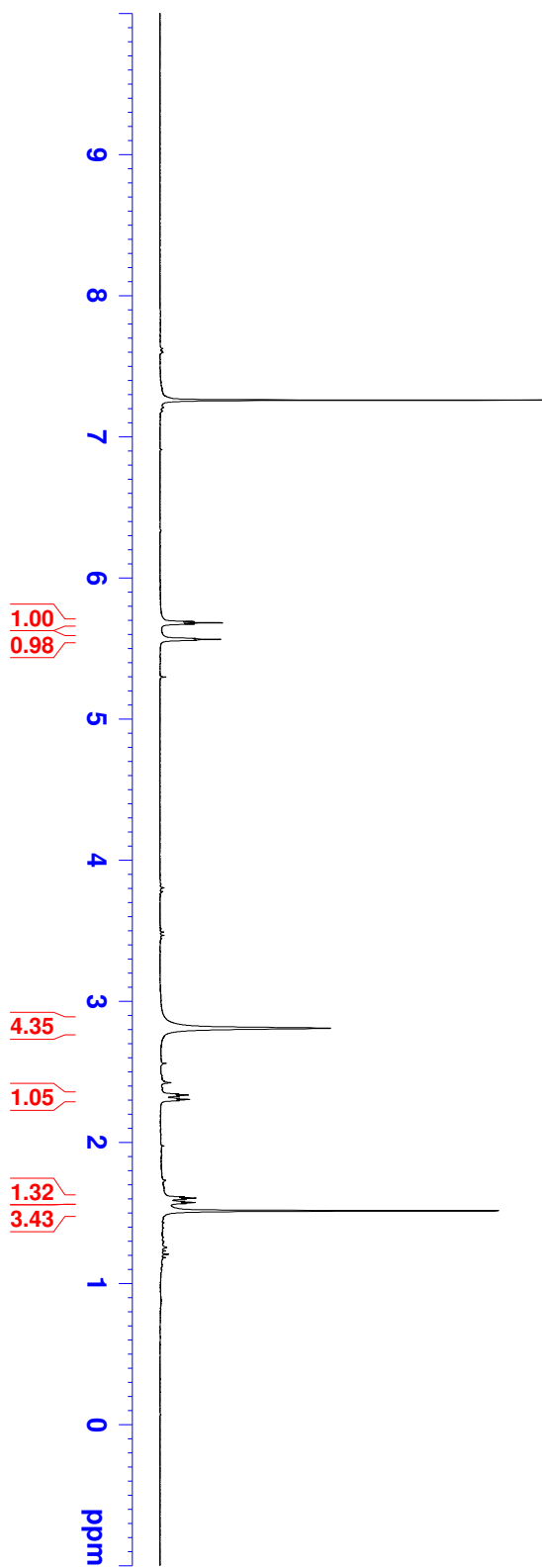


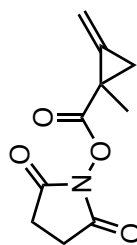


— 7.260

5.691  
 5.682  
 5.673  
 5.571  
 5.565  
 5.558

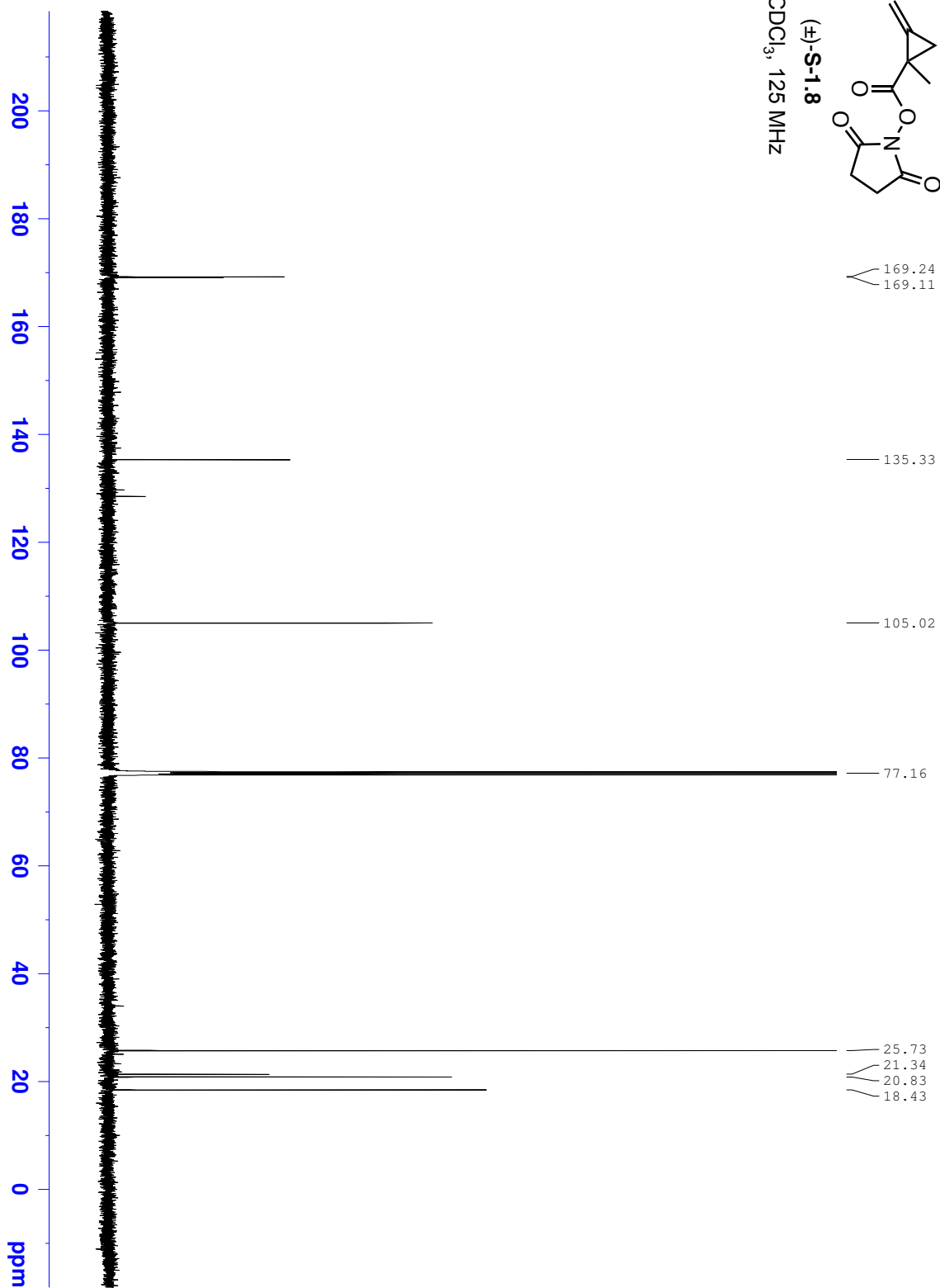
2.808  
 2.343  
 2.334  
 2.326  
 2.312  
 2.303  
 2.295  
 1.613  
 1.604  
 1.596  
 1.581  
 1.573  
 1.565  
 1.514

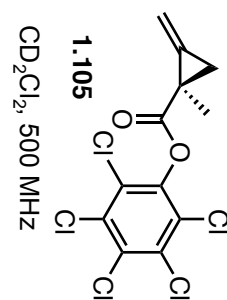




(±)-**S-1.8**

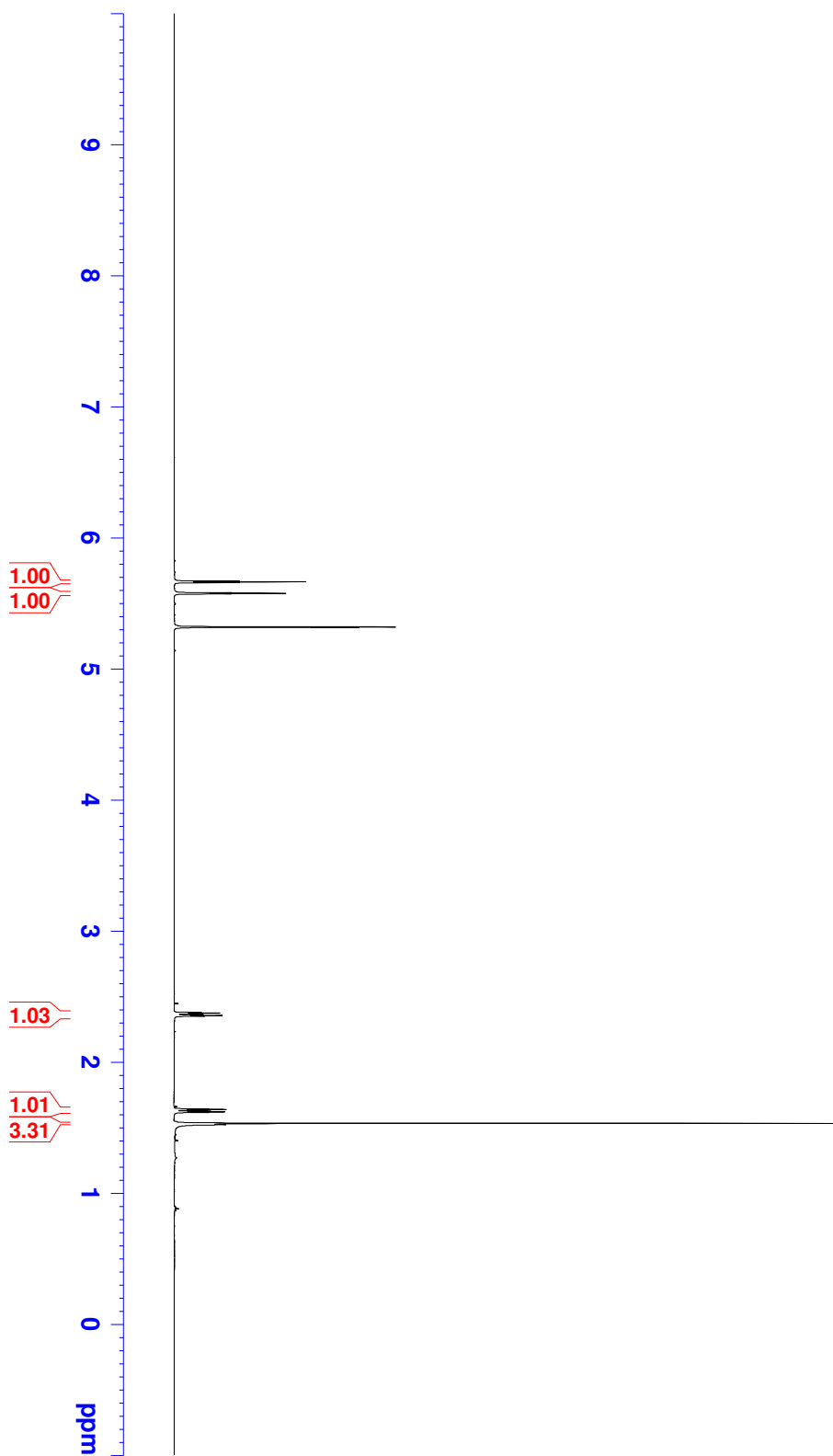
CDCl<sub>3</sub>, 125 MHz

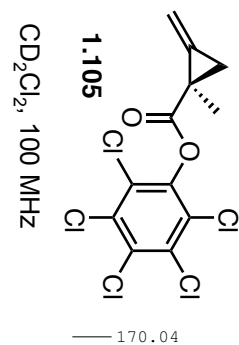




5.670  
 5.665  
 5.659  
 5.581  
 5.577  
 5.573  
 5.320

2.379  
 2.374  
 2.369  
 2.360  
 2.355  
 2.350  
 1.644  
 1.639  
 1.634  
 1.625  
 1.621  
 1.615  
 1.533





— 170.04

— 144.88

— 136.81

— 132.37

— 131.74

— 128.41

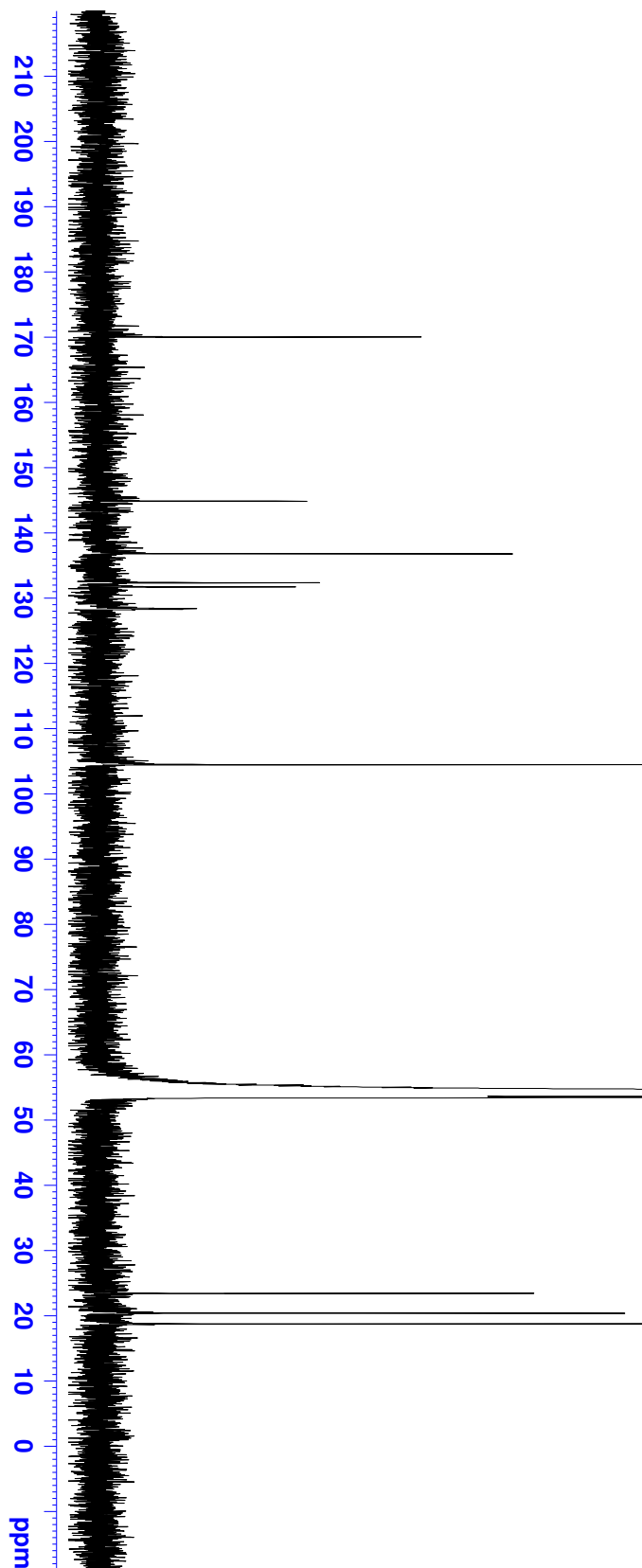
— 104.48

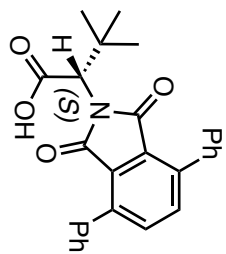
— 54.00

— 23.43

— 20.39

— 18.76



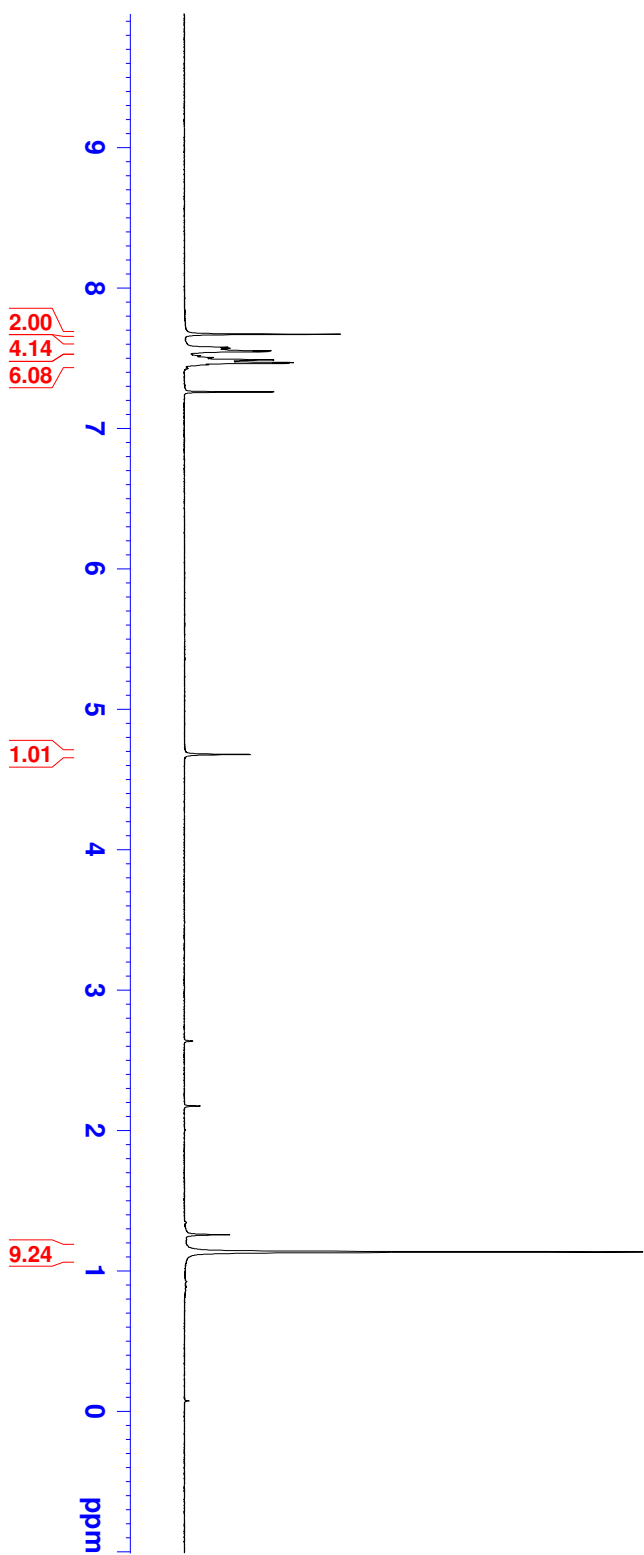


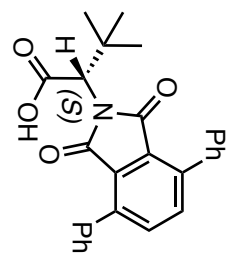
**1.116**  
CDCl<sub>3</sub>, 300 MHz

7.671  
7.579  
7.571  
7.553  
7.547  
7.517  
7.505  
7.499  
7.488  
7.478  
7.469  
7.464  
7.454  
7.260

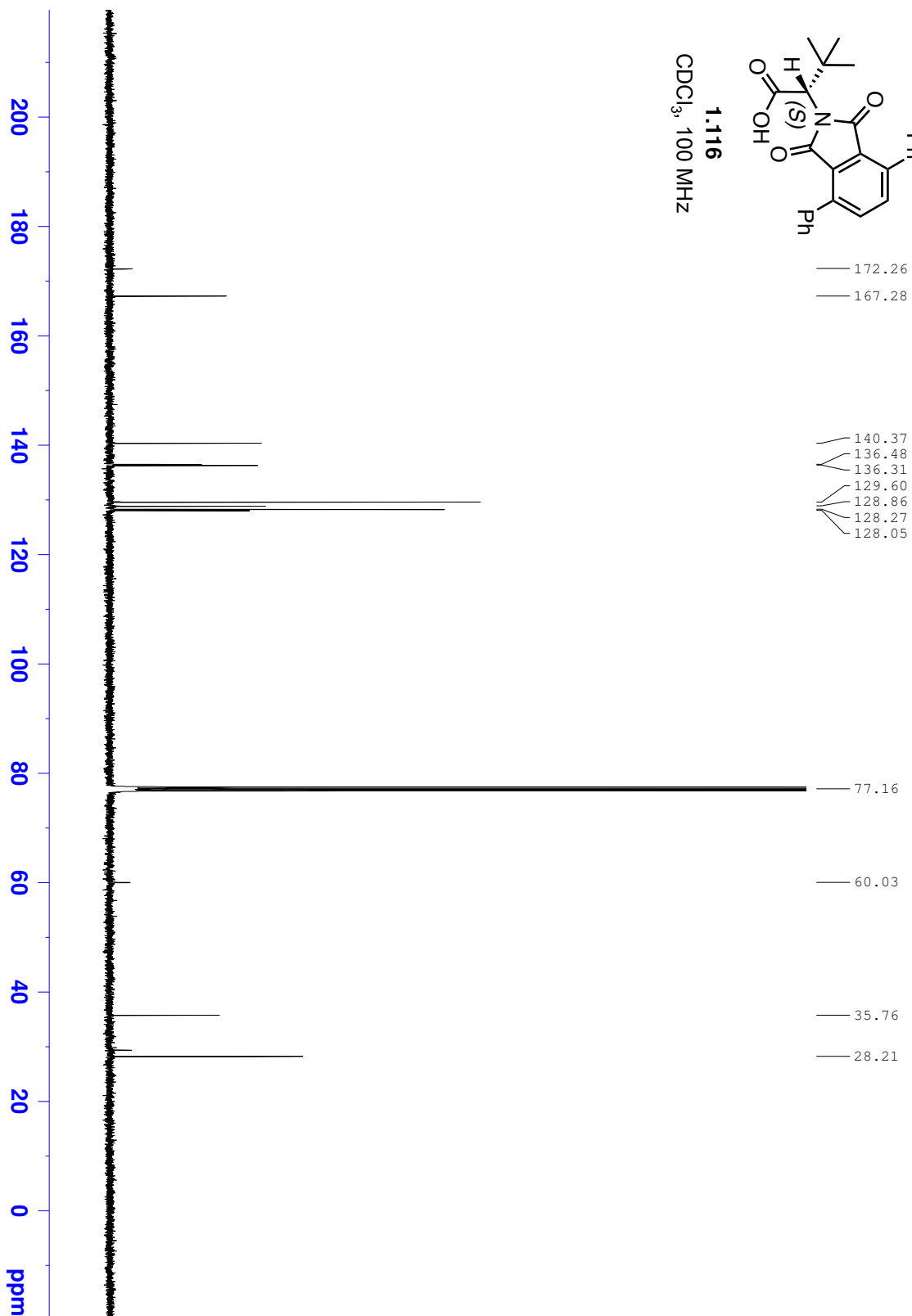
— 4.678

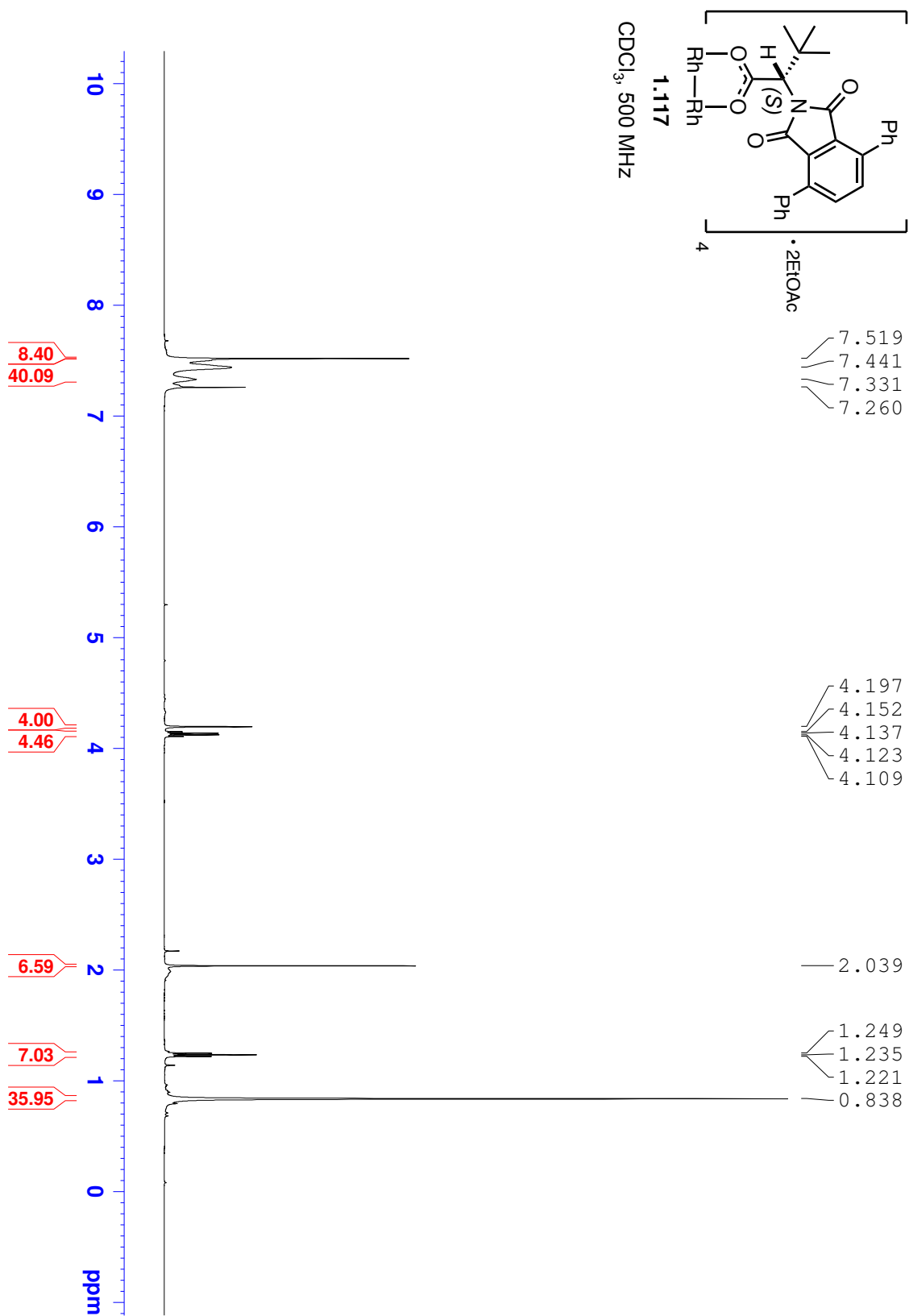
— 1.136

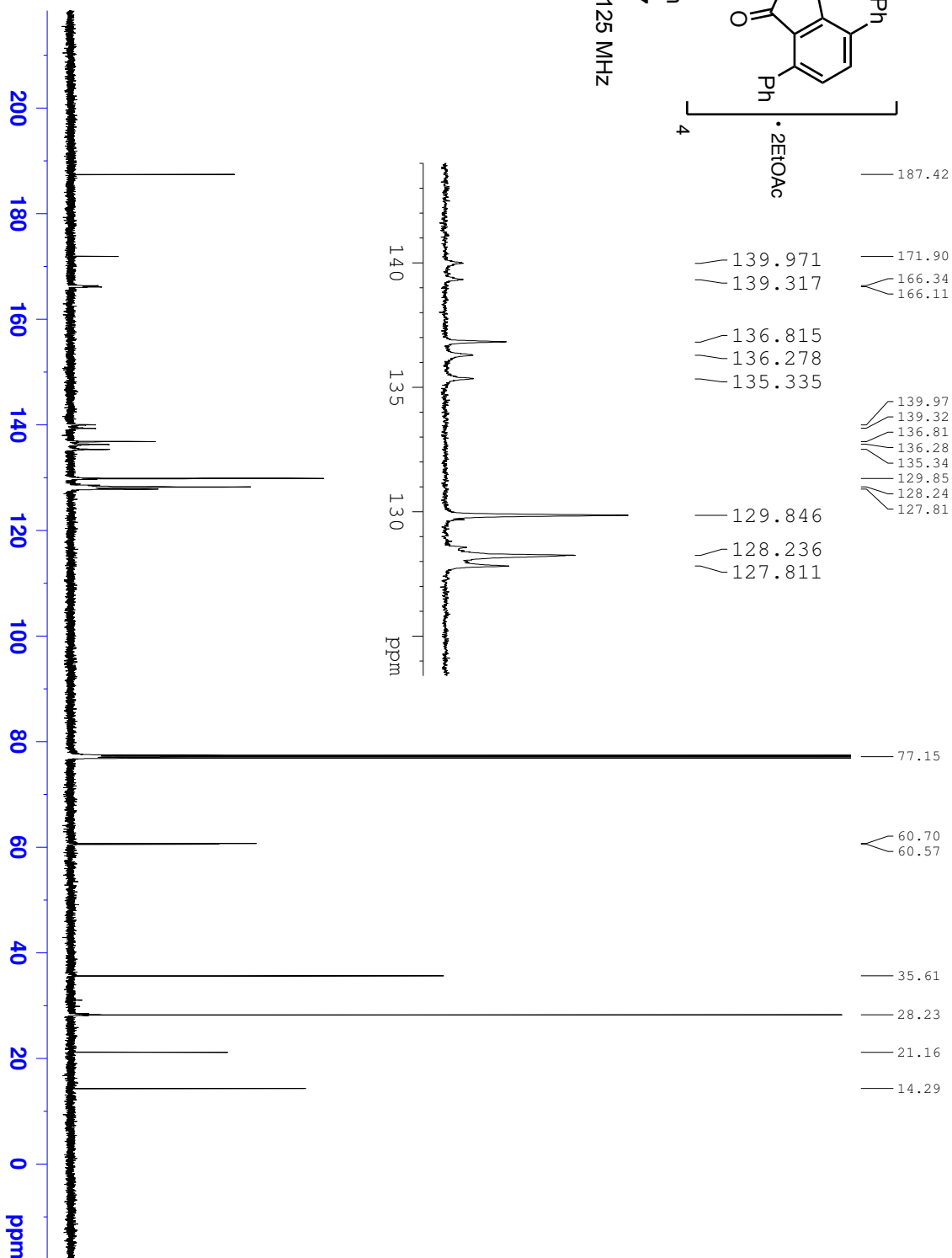
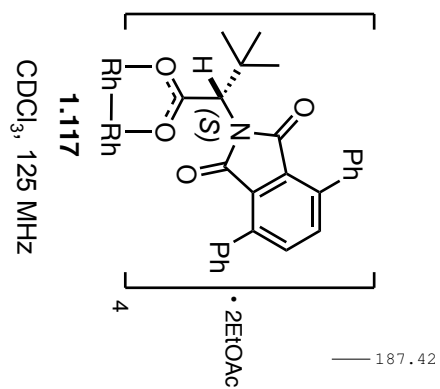




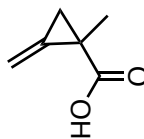
1.116  
CDCl<sub>3</sub>, 100 MHz











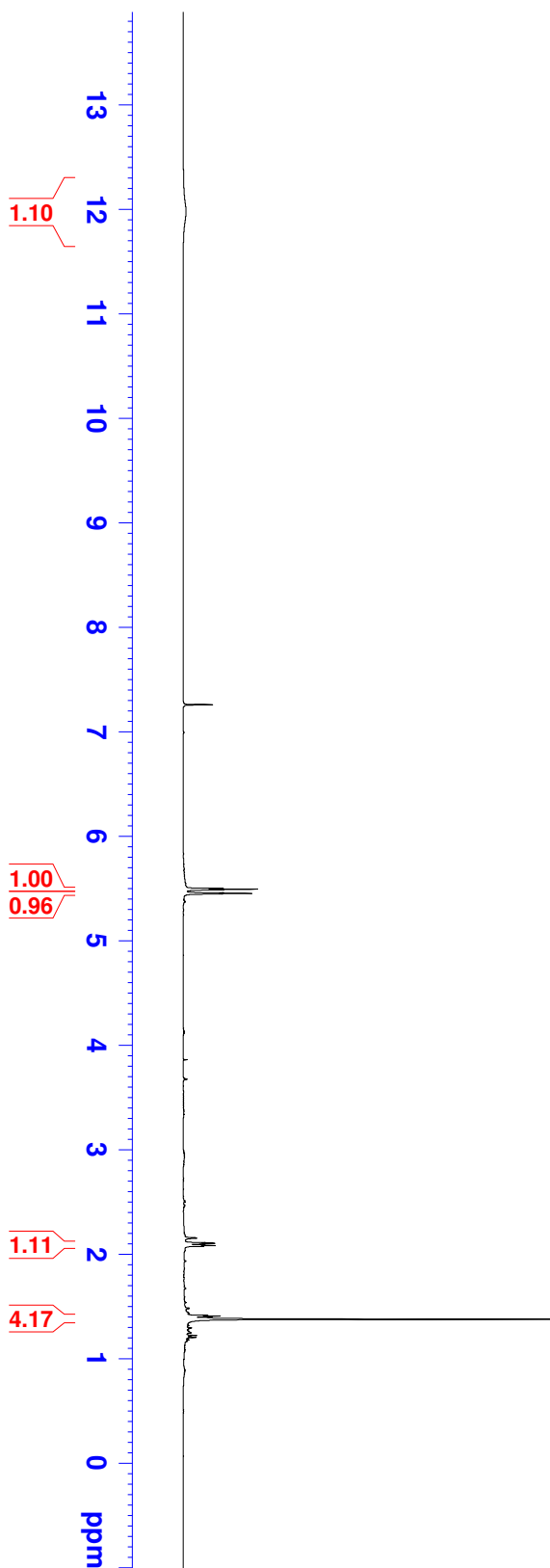
2.90  
CDCl<sub>3</sub>, 400 MHz

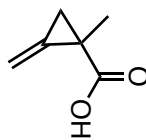
— 11.987

— 7.260

5.501  
5.494  
5.487  
5.459  
5.454  
5.449

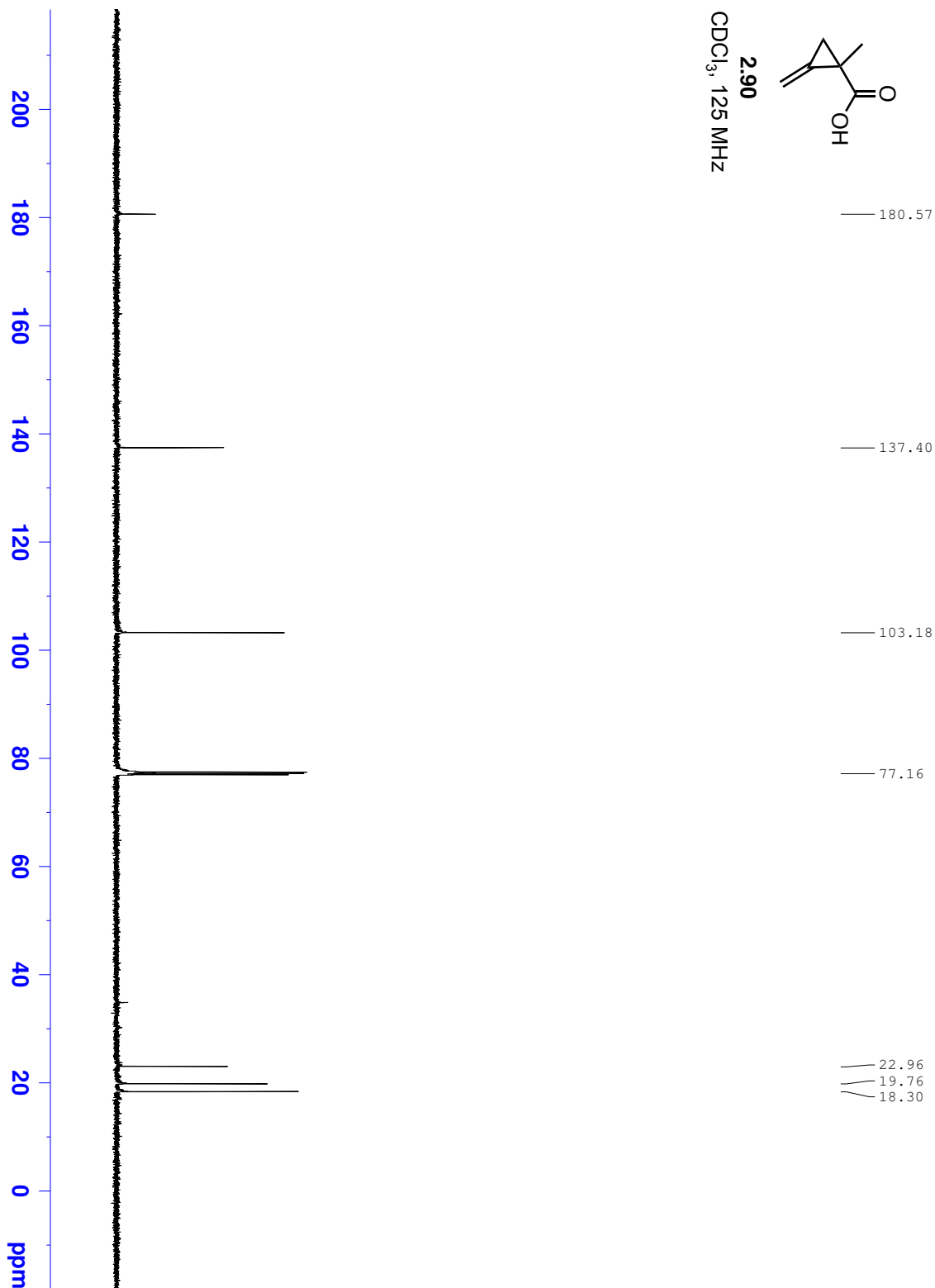
2.111  
2.105  
2.099  
2.088  
2.082  
2.076  
1.414  
1.408  
1.402  
1.392  
1.378

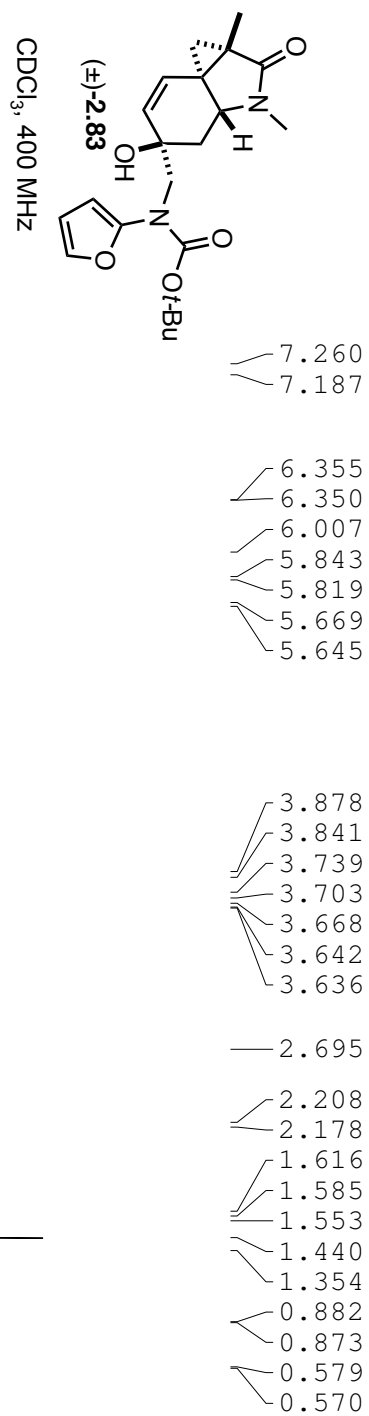


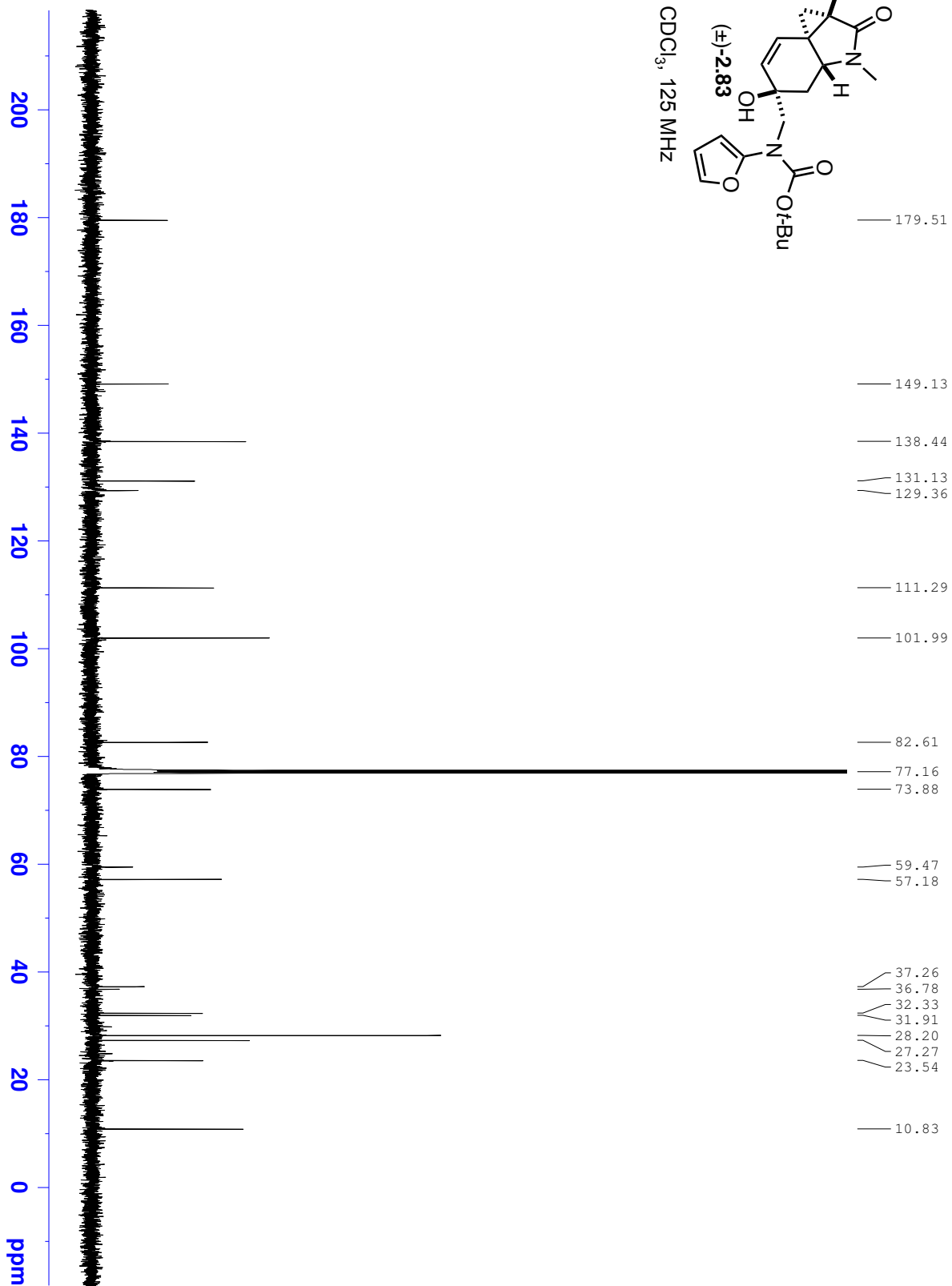
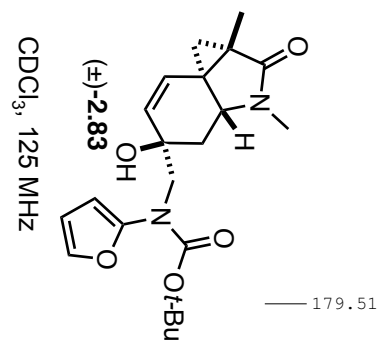


2.90

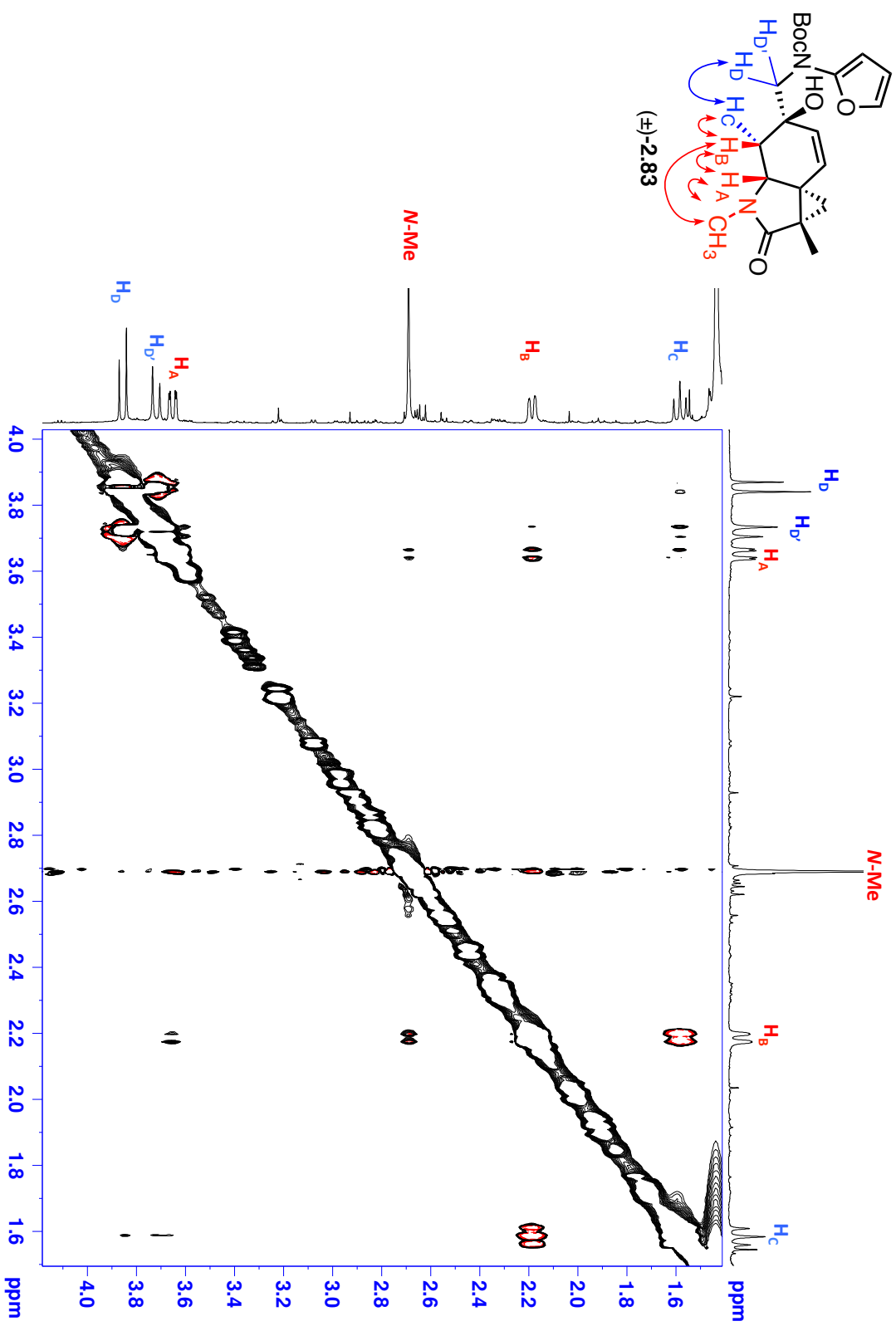
CDCl<sub>3</sub>, 125 MHz



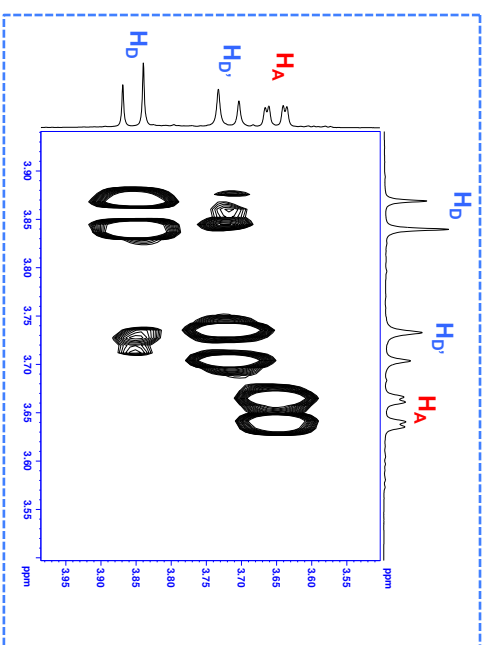
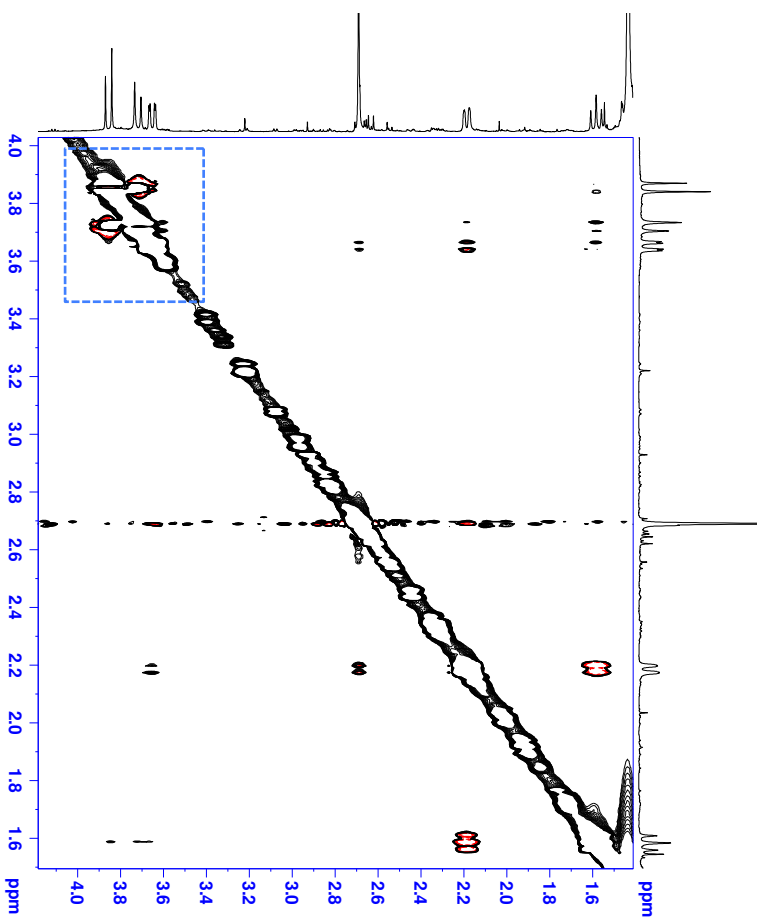
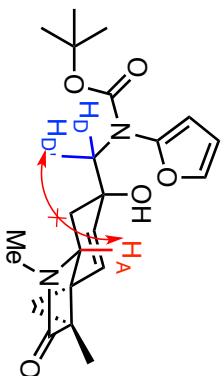


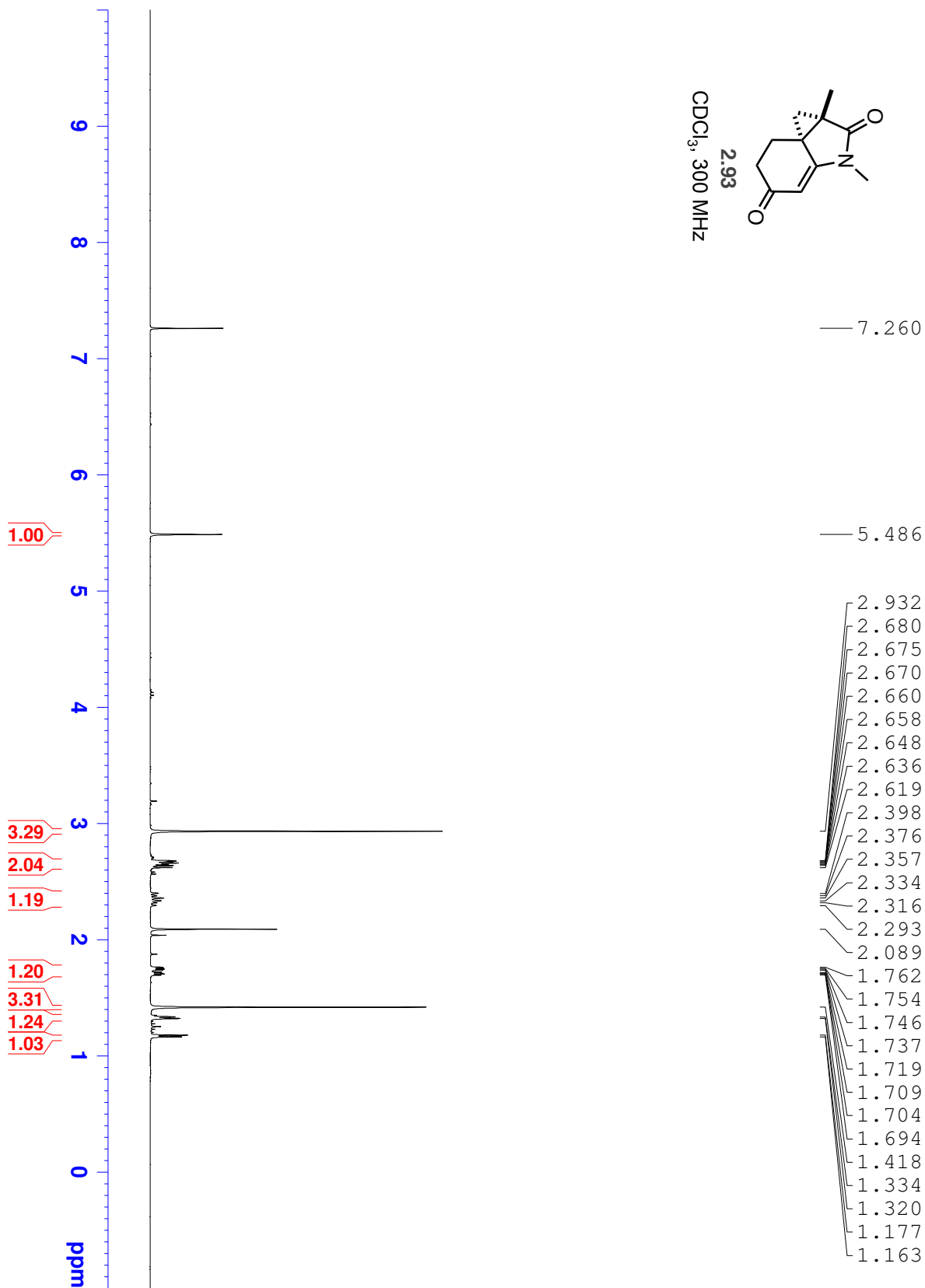
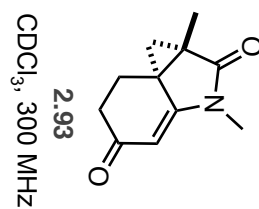


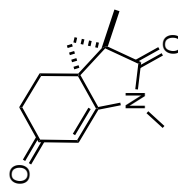
key NOESY correlations in (±)-**2.83** (CDCl<sub>3</sub>, 500 MHz)



Lack of key NOESY correlations in ( $\pm$ )-**2.83** (CDCl<sub>3</sub>, 500 MHz)

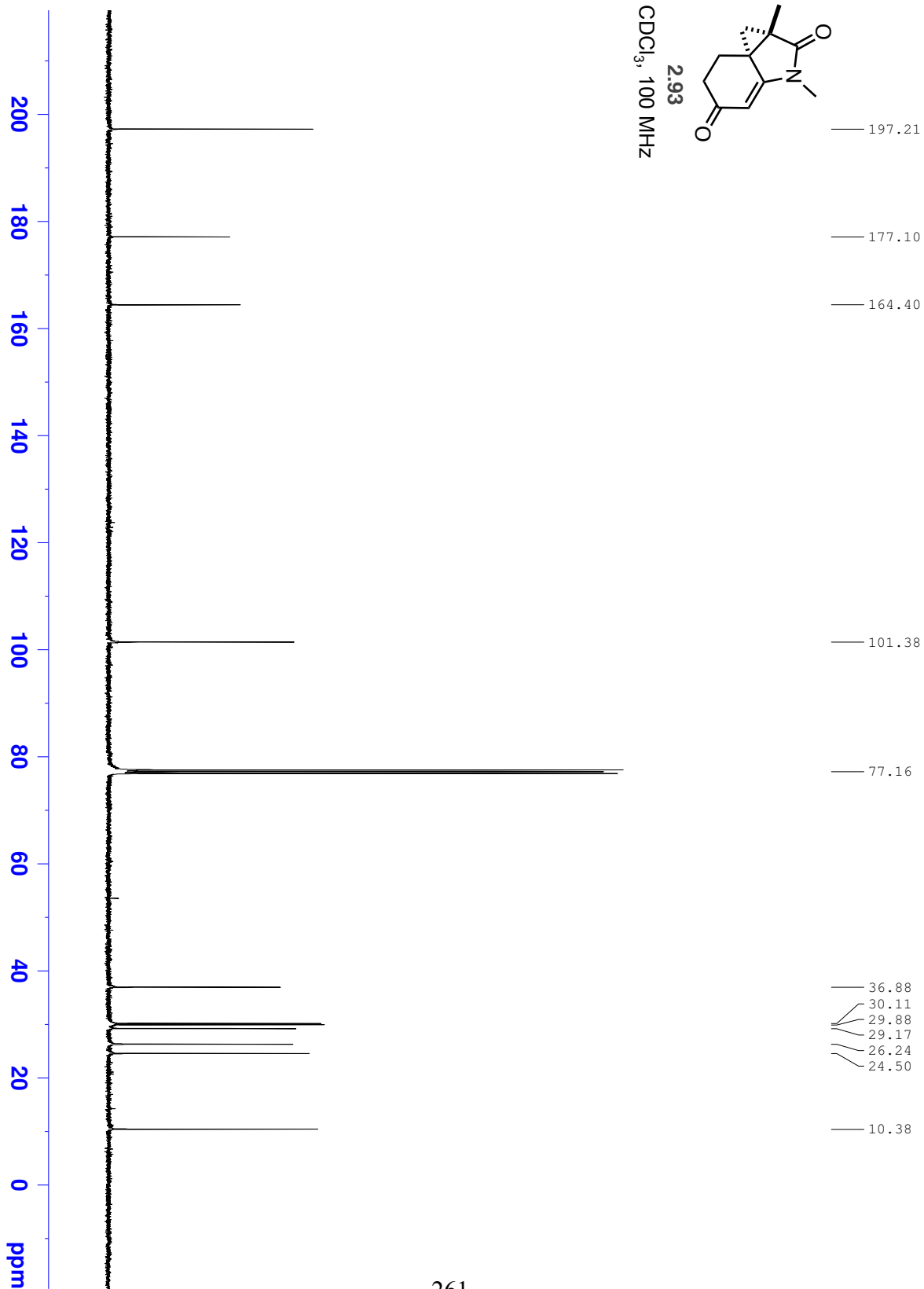




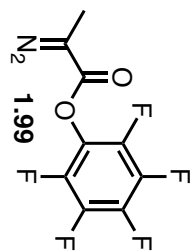


2.93

CDCl<sub>3</sub>, 100 MHz





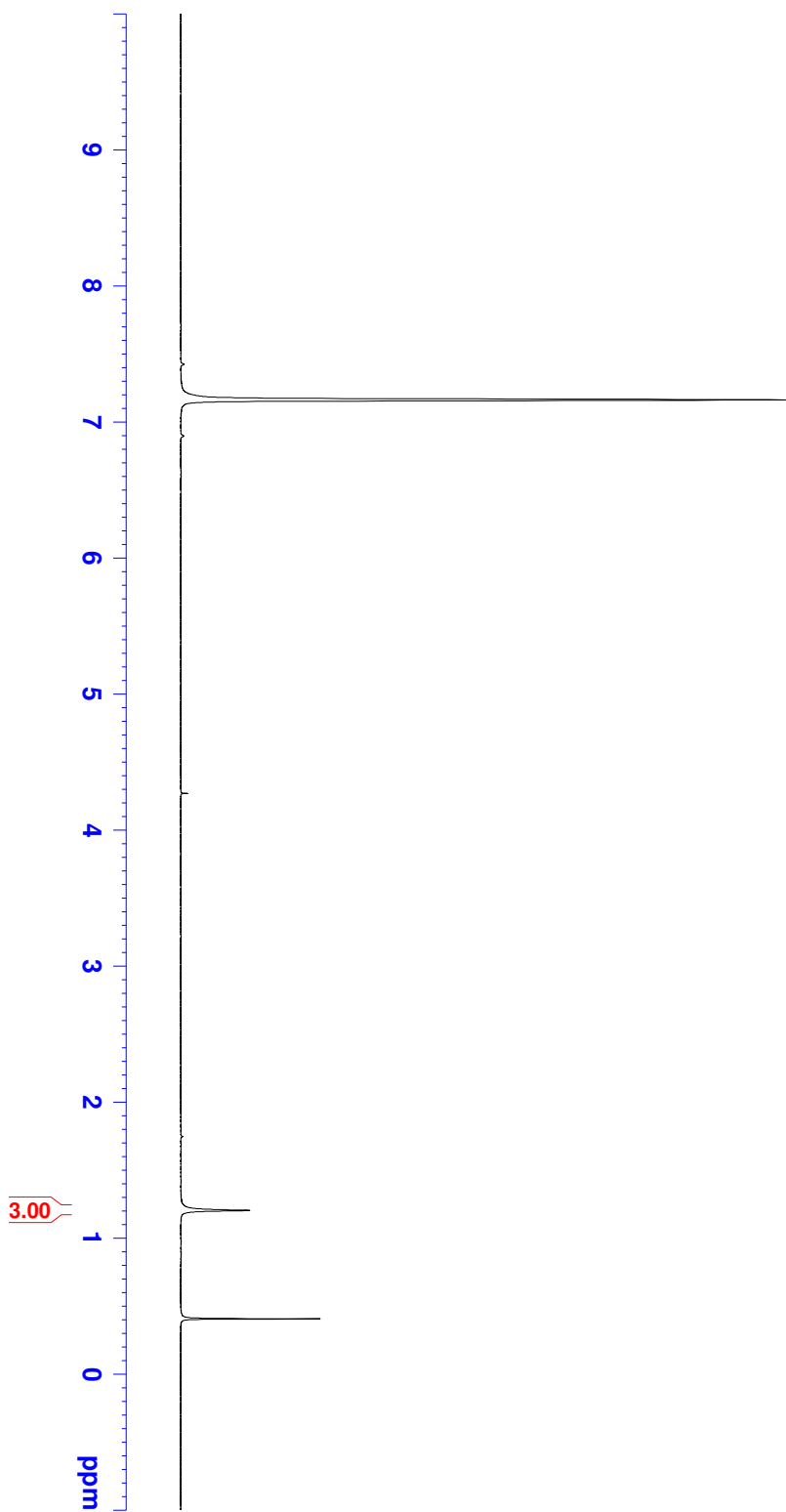


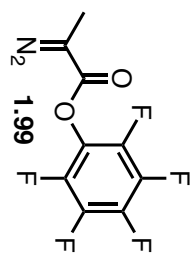
C<sub>6</sub>D<sub>6</sub>, 300 MHz

— 7.160

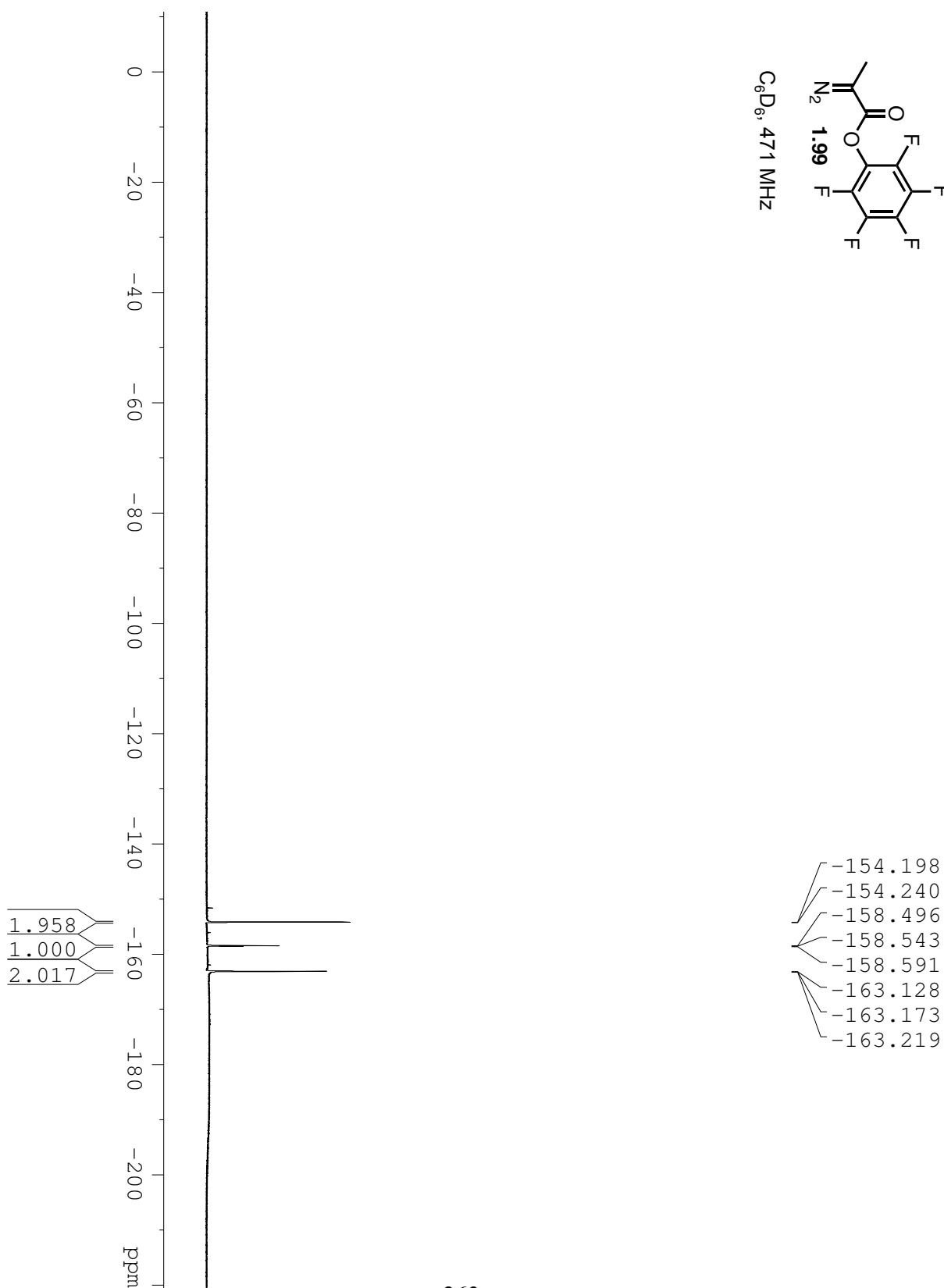
— 1.204

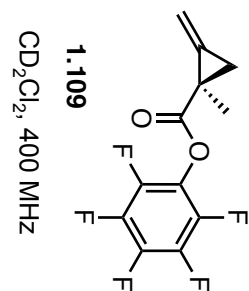
— 0.406





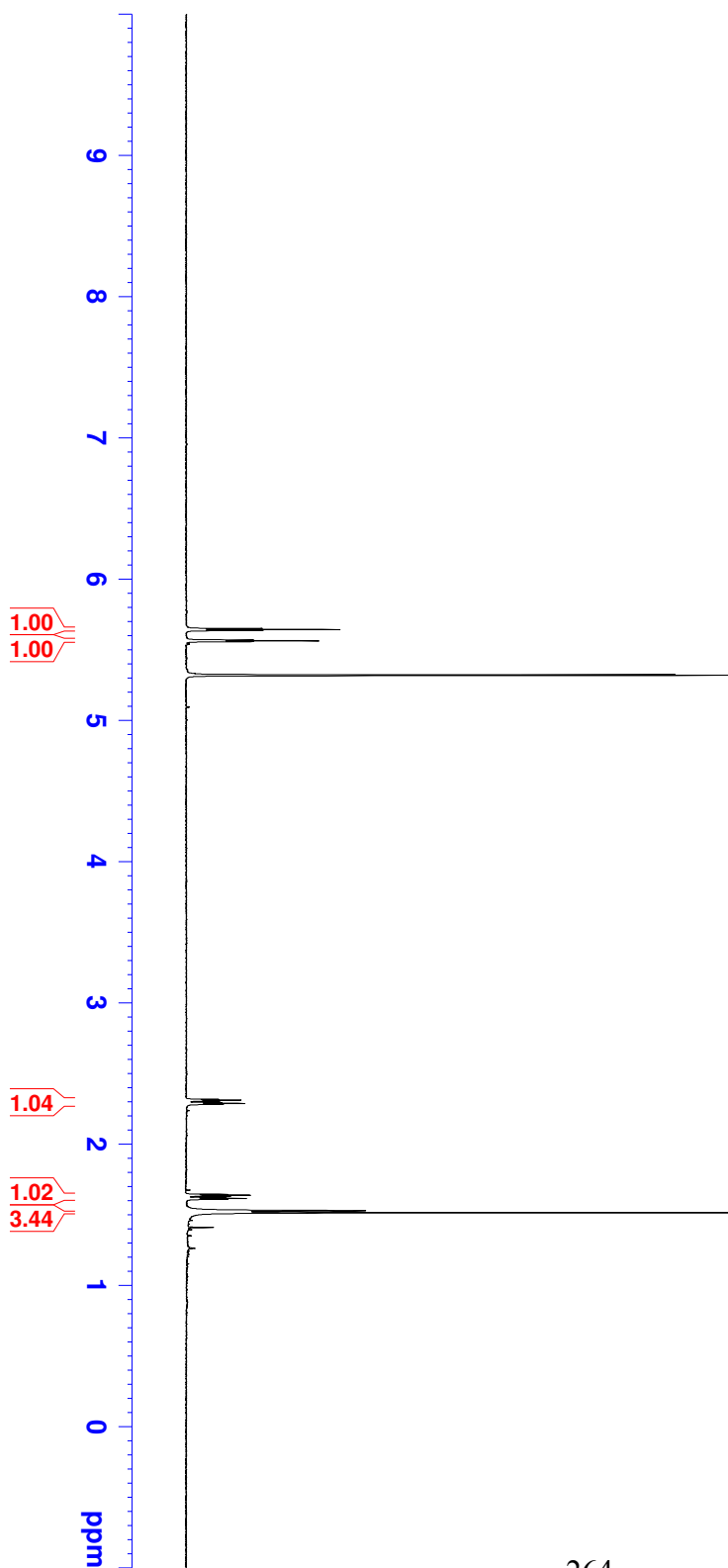
C<sub>6</sub>D<sub>6</sub>, 471 MHz

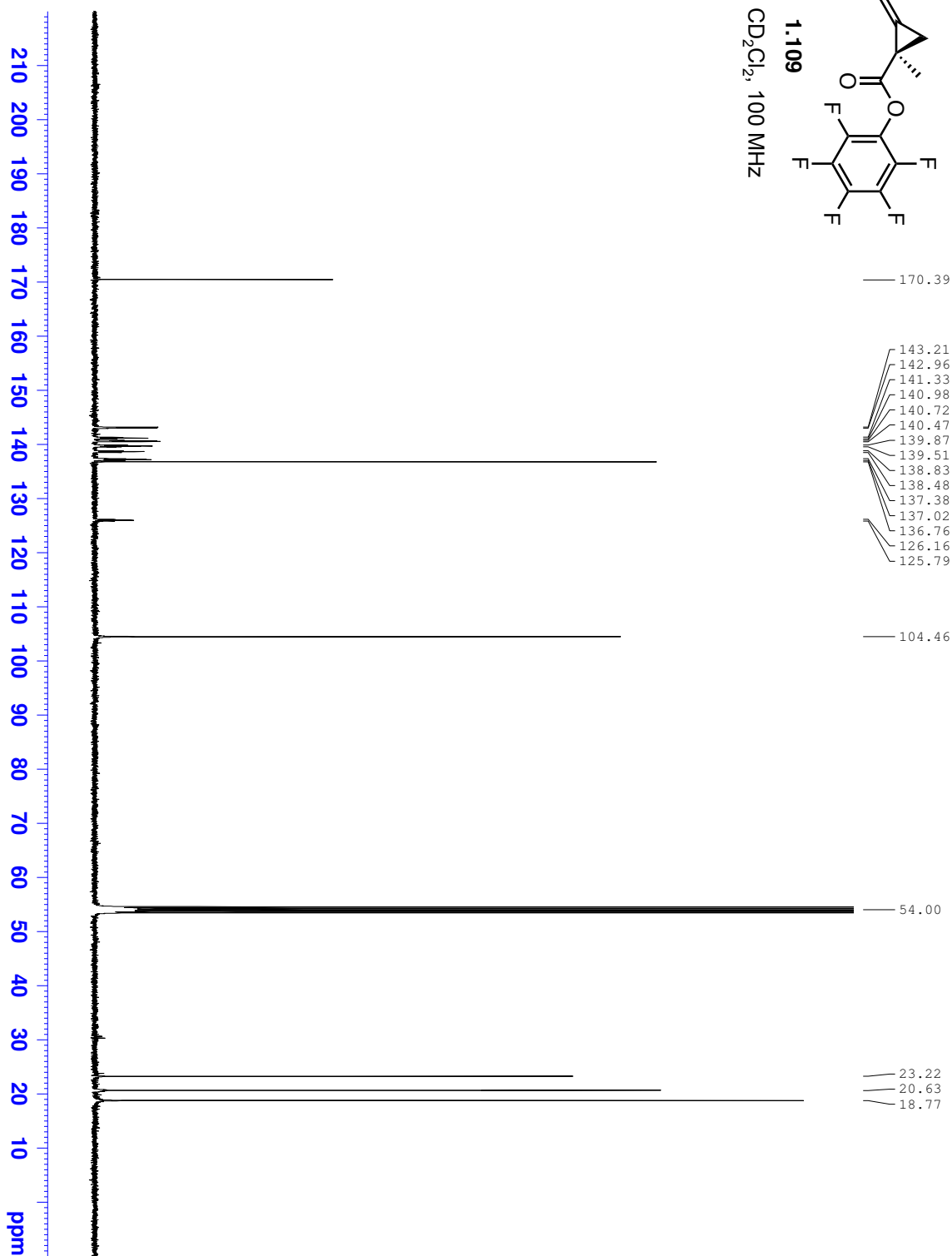
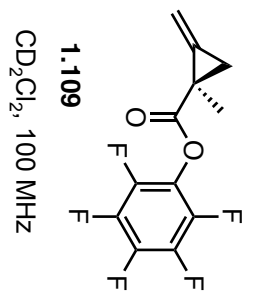


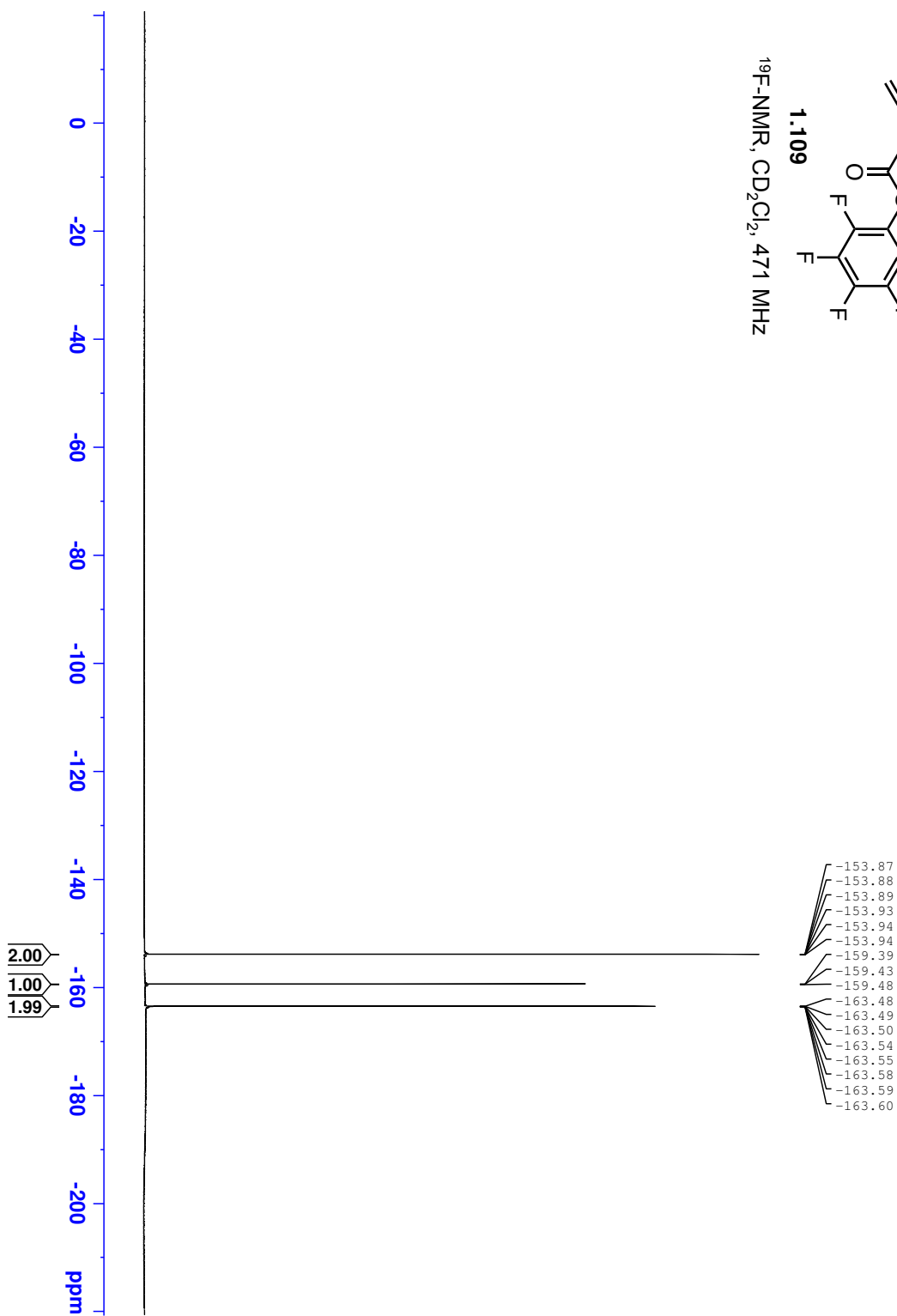
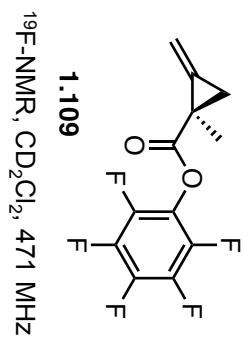


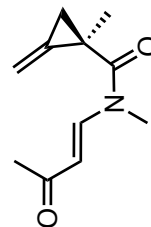
5.651  
5.644  
5.637  
5.569  
5.564  
5.558  
5.320

2.317  
2.311  
2.305  
2.294  
2.288  
2.281  
1.644  
1.638  
1.632  
1.621  
1.615  
1.609  
1.528  
1.514









2.87

CDCl<sub>3</sub>, 400 MHz

8.380  
8.346

7.260

5.728  
5.707  
5.700  
5.693  
5.527

3.152

2.289

1.811

1.805

1.800

1.787

1.781

1.776

1.494

1.343

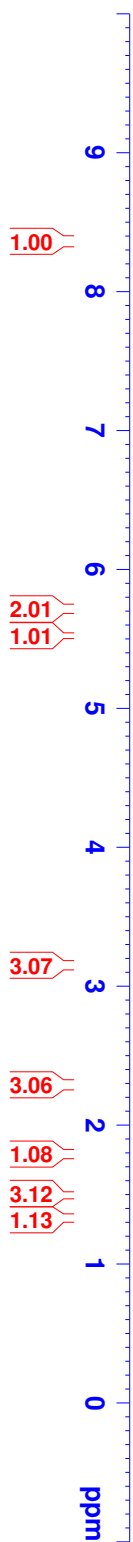
1.338

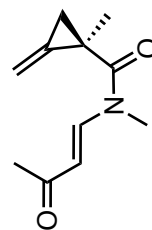
1.332

1.319

1.314

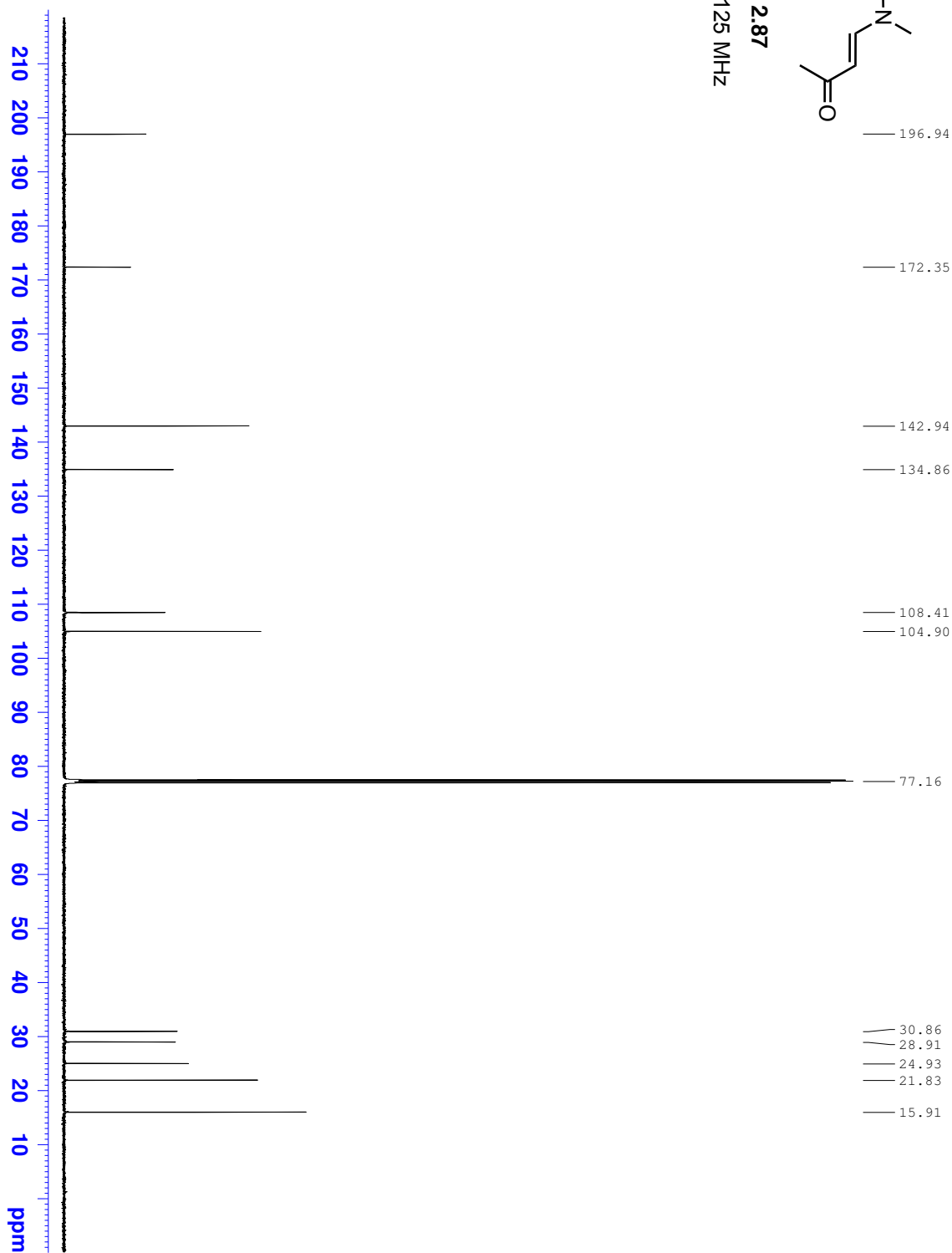
1.308

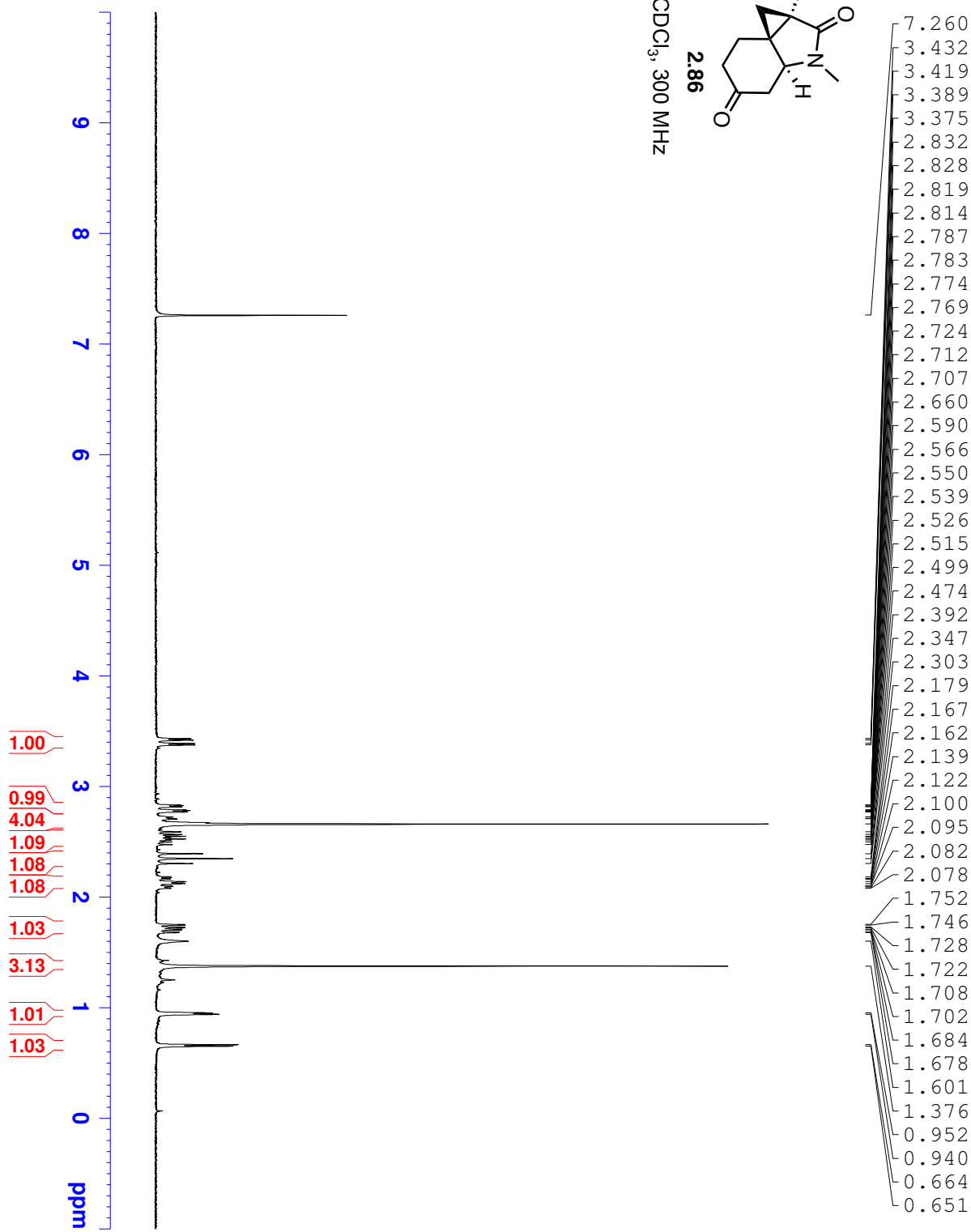
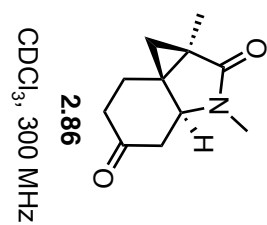




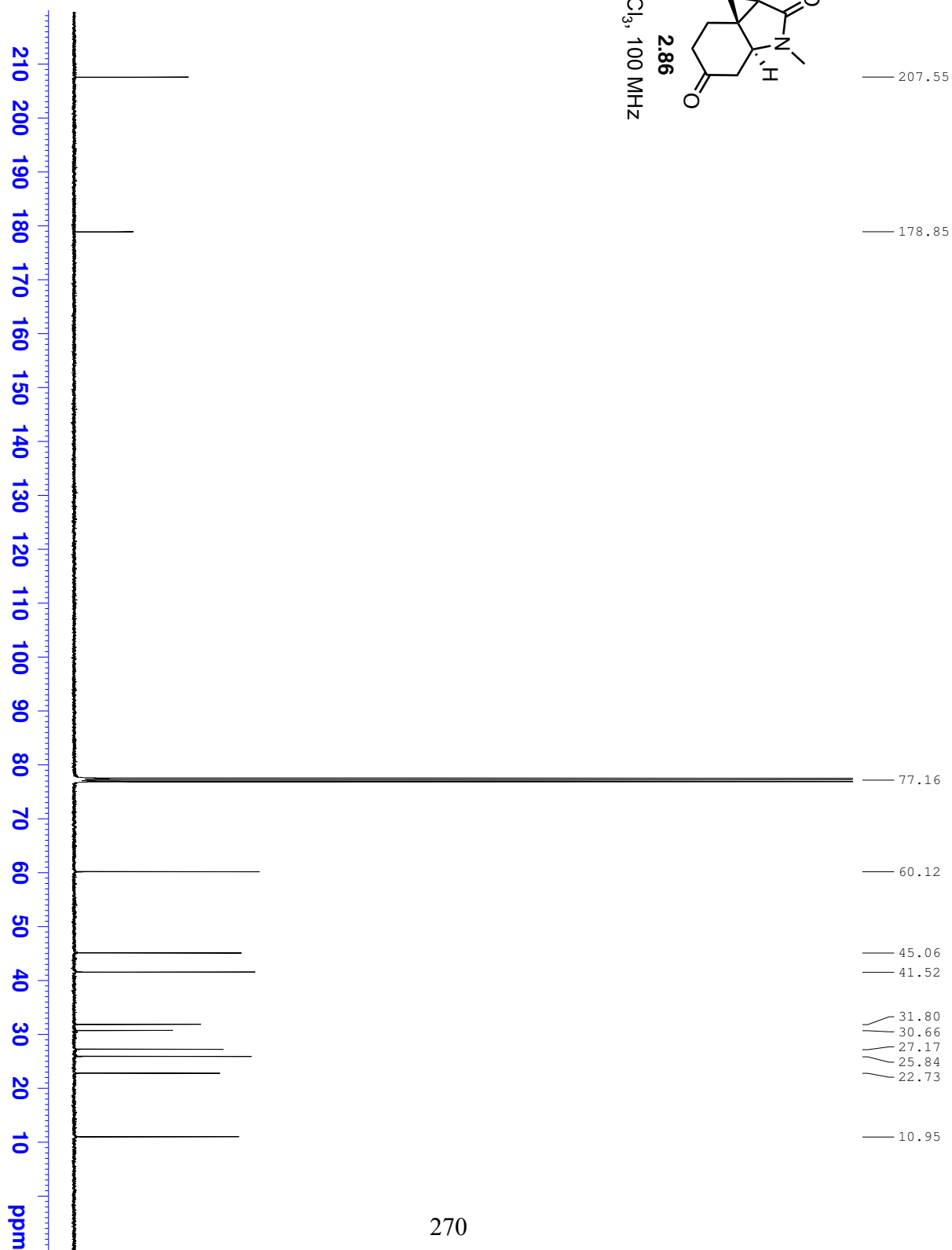
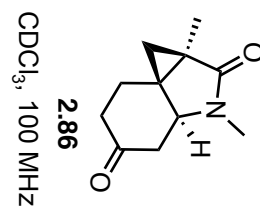
2.87

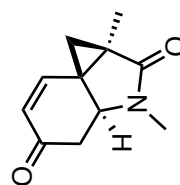
CDCl<sub>3</sub>, 125 MHz



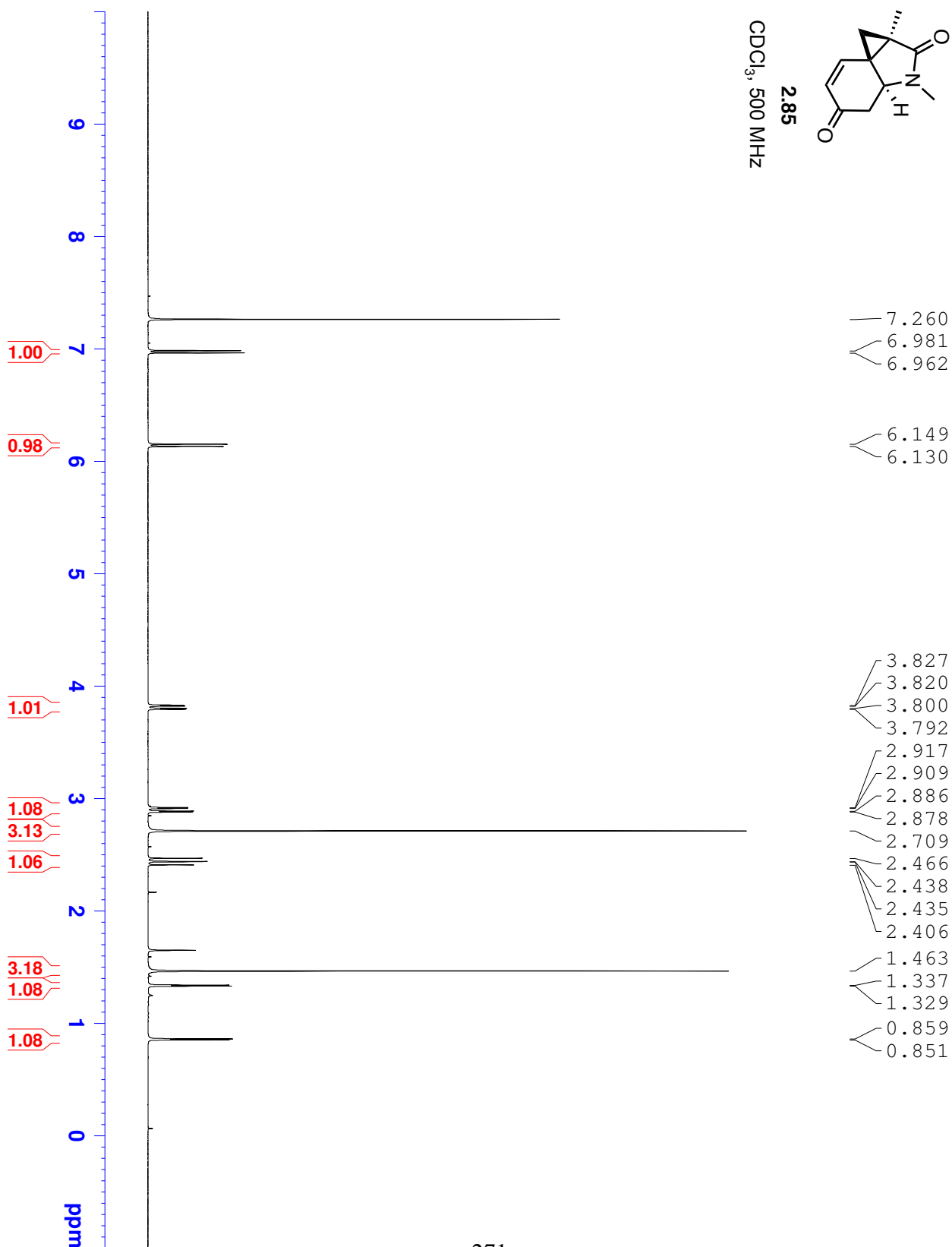


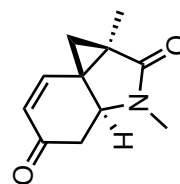






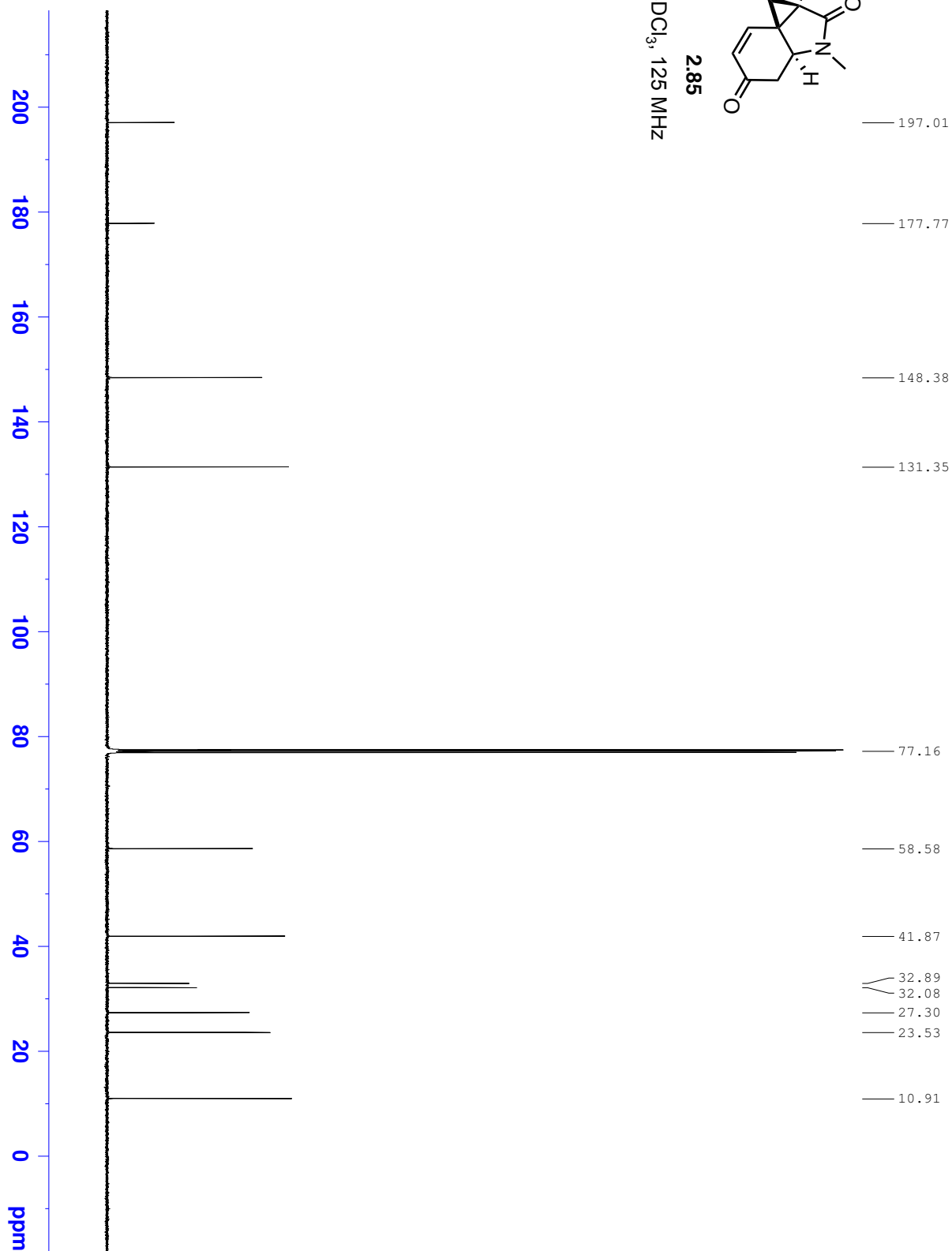
2.85  
CDCl<sub>3</sub>, 500 MHz

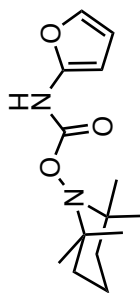




CDCl<sub>3</sub>, 125 MHz

2.85





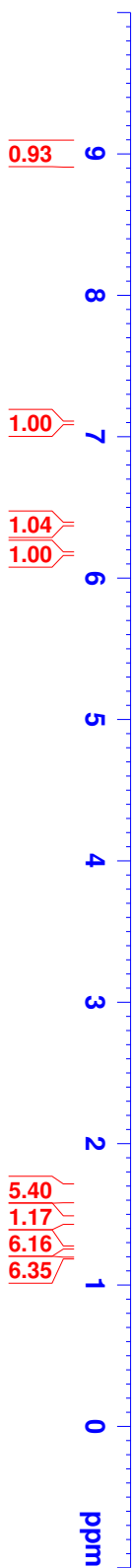
2.148

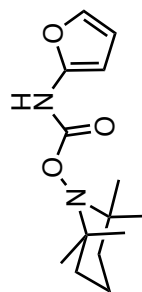
CDCl<sub>3</sub>, 500 MHz

— 9.003

7.260  
7.097  
7.095  
6.385  
6.380  
6.378  
6.374  
6.175  
6.169

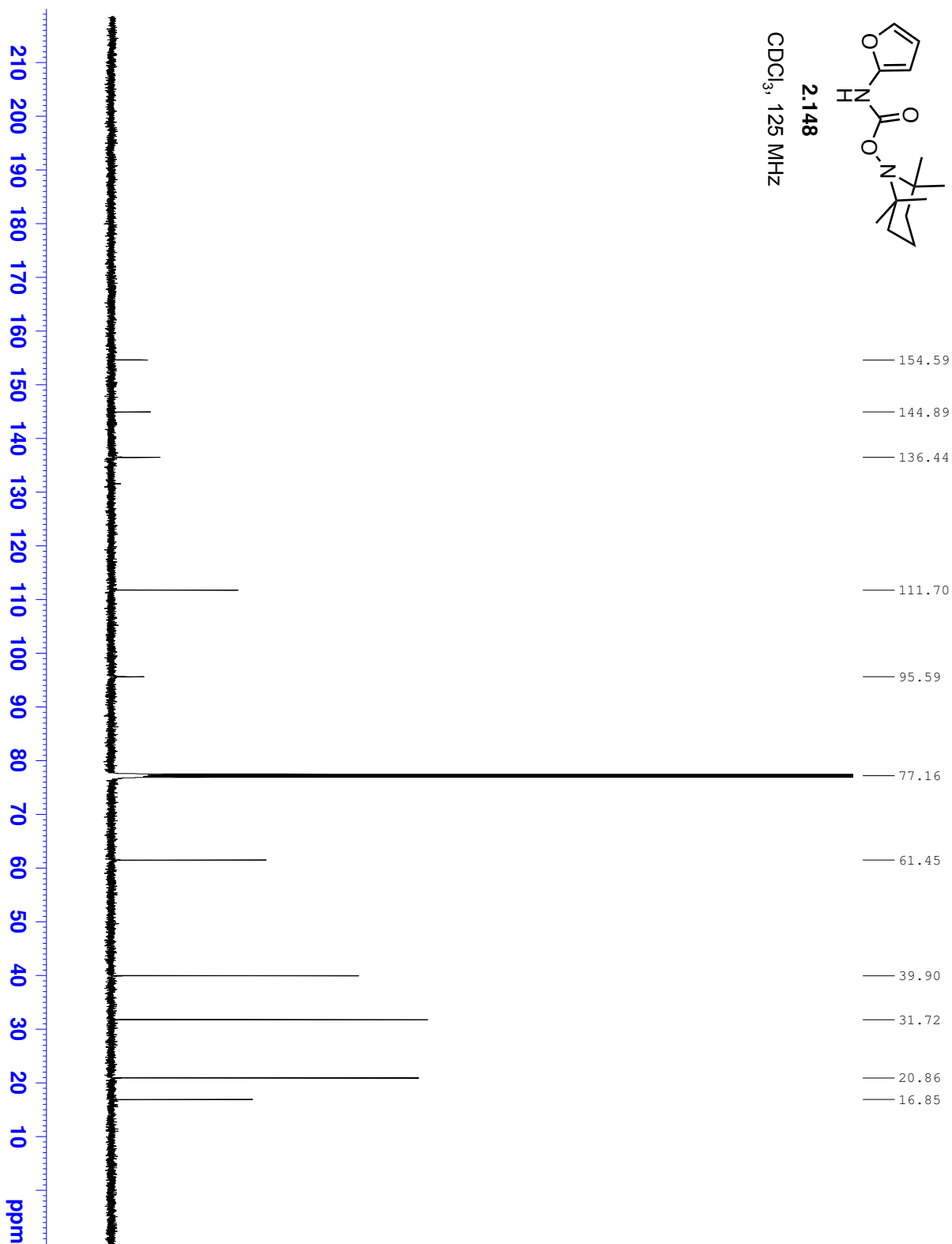
1.707  
1.681  
1.676  
1.655  
1.650  
1.623  
1.596  
1.570  
1.549  
1.484  
1.477  
1.470  
1.464  
1.458  
1.451  
1.445  
1.438  
1.264  
1.190

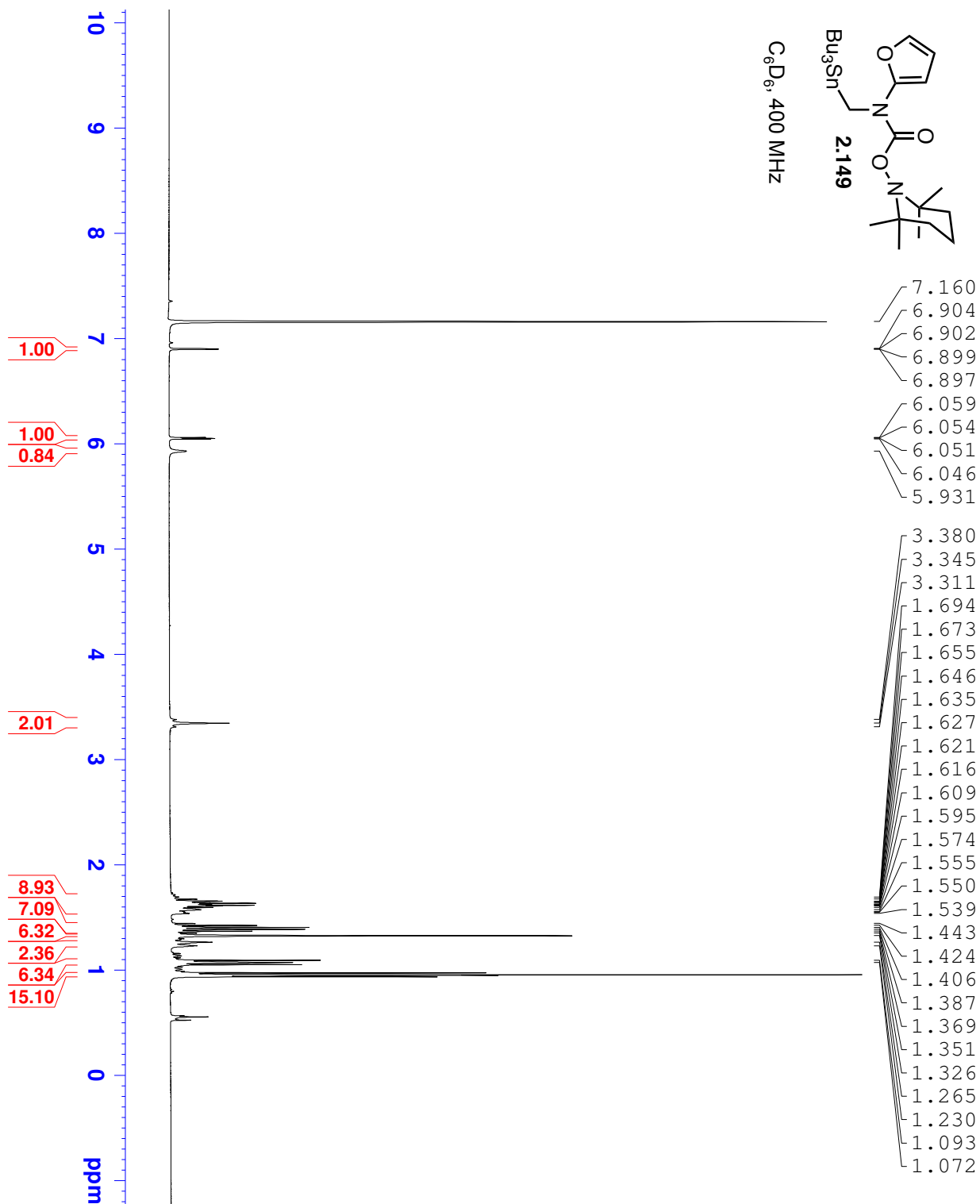


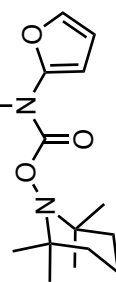


2.148

CDCl<sub>3</sub>, 125 MHz

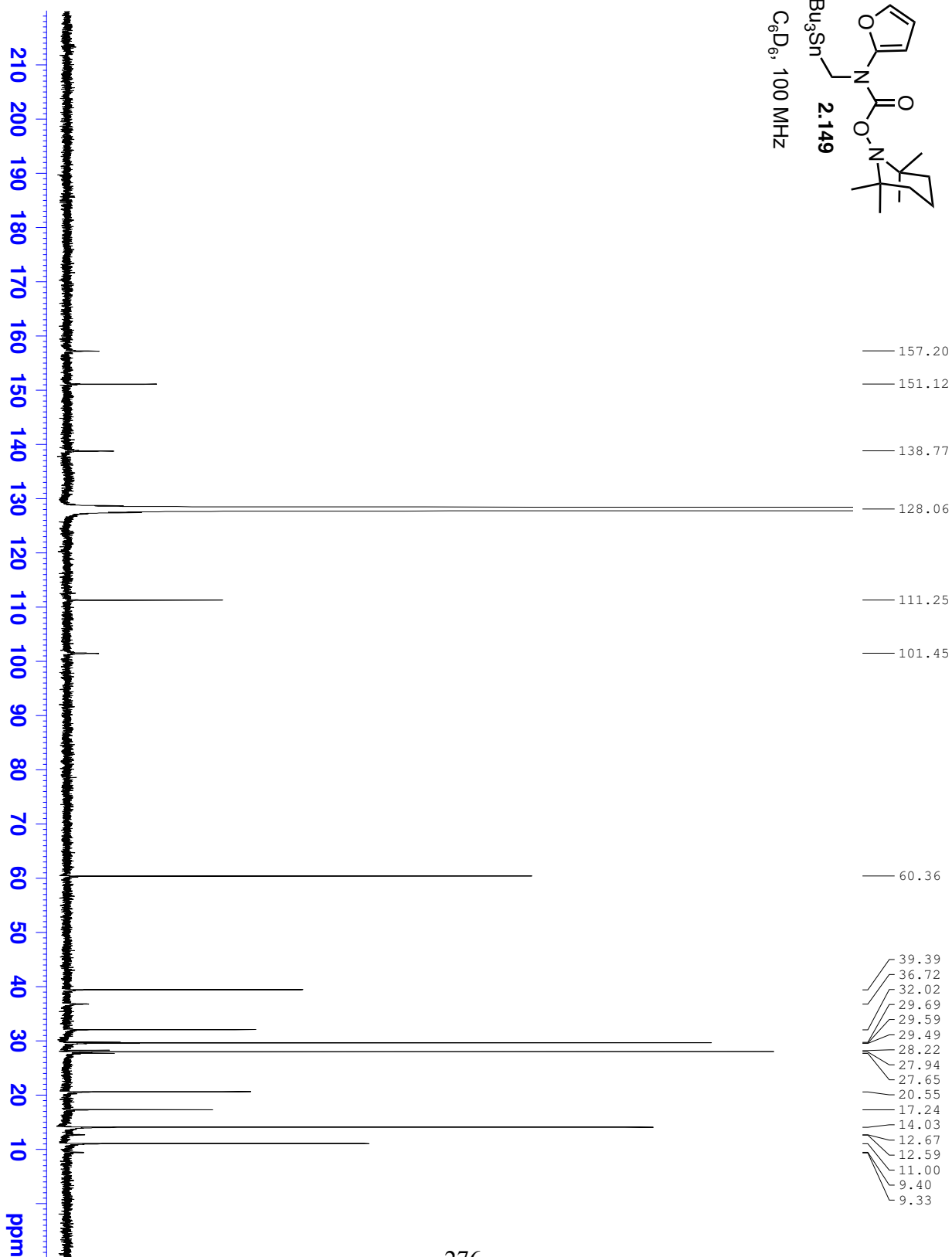






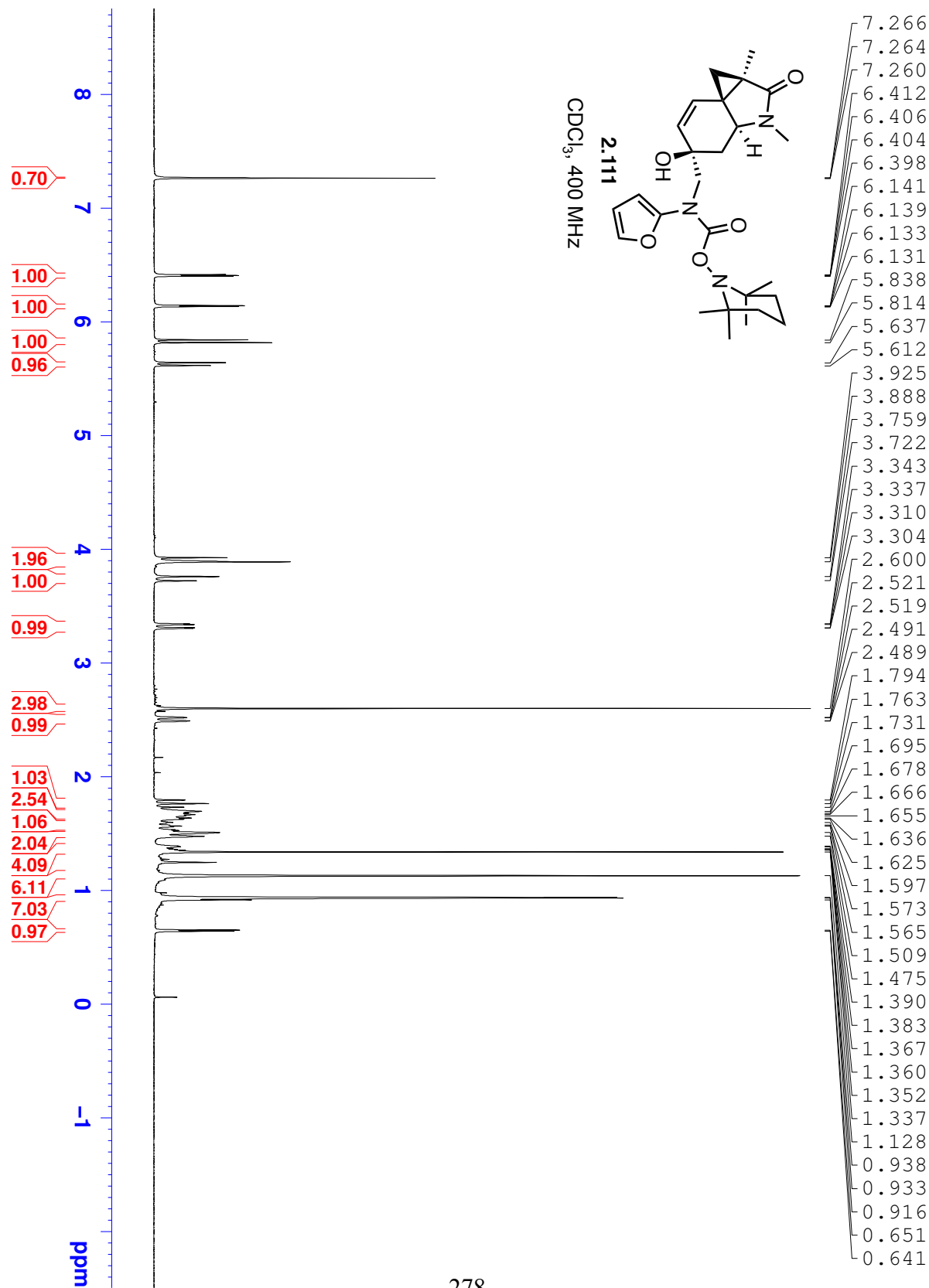
**2.149**

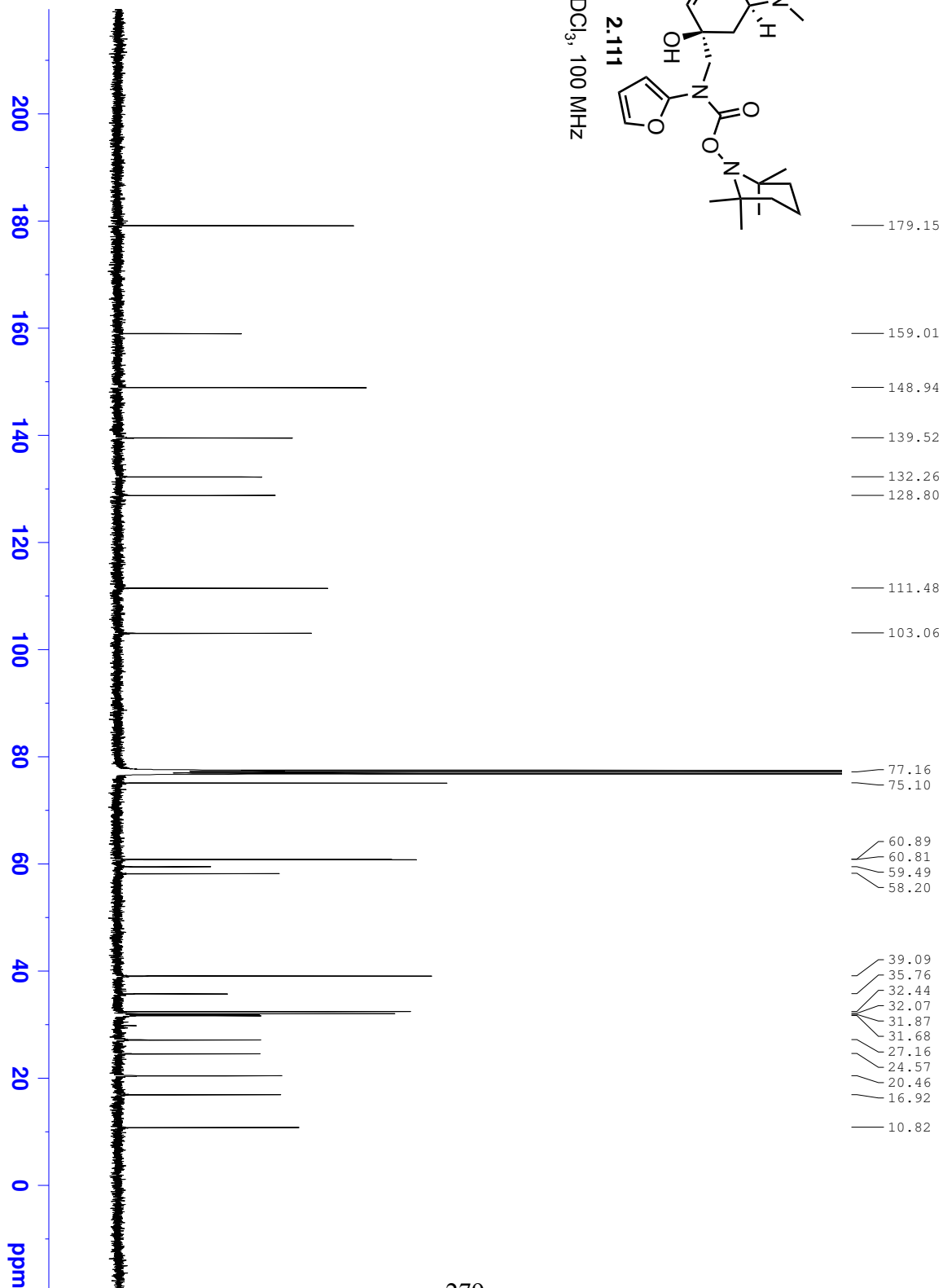
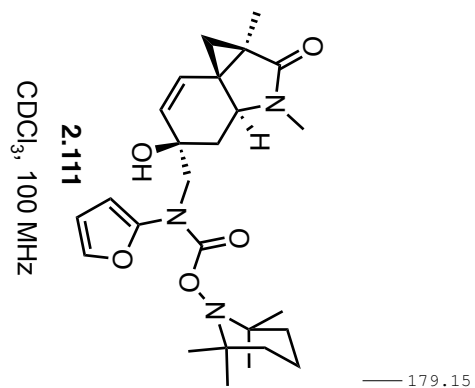
$C_6D_6$ , 100 MHz

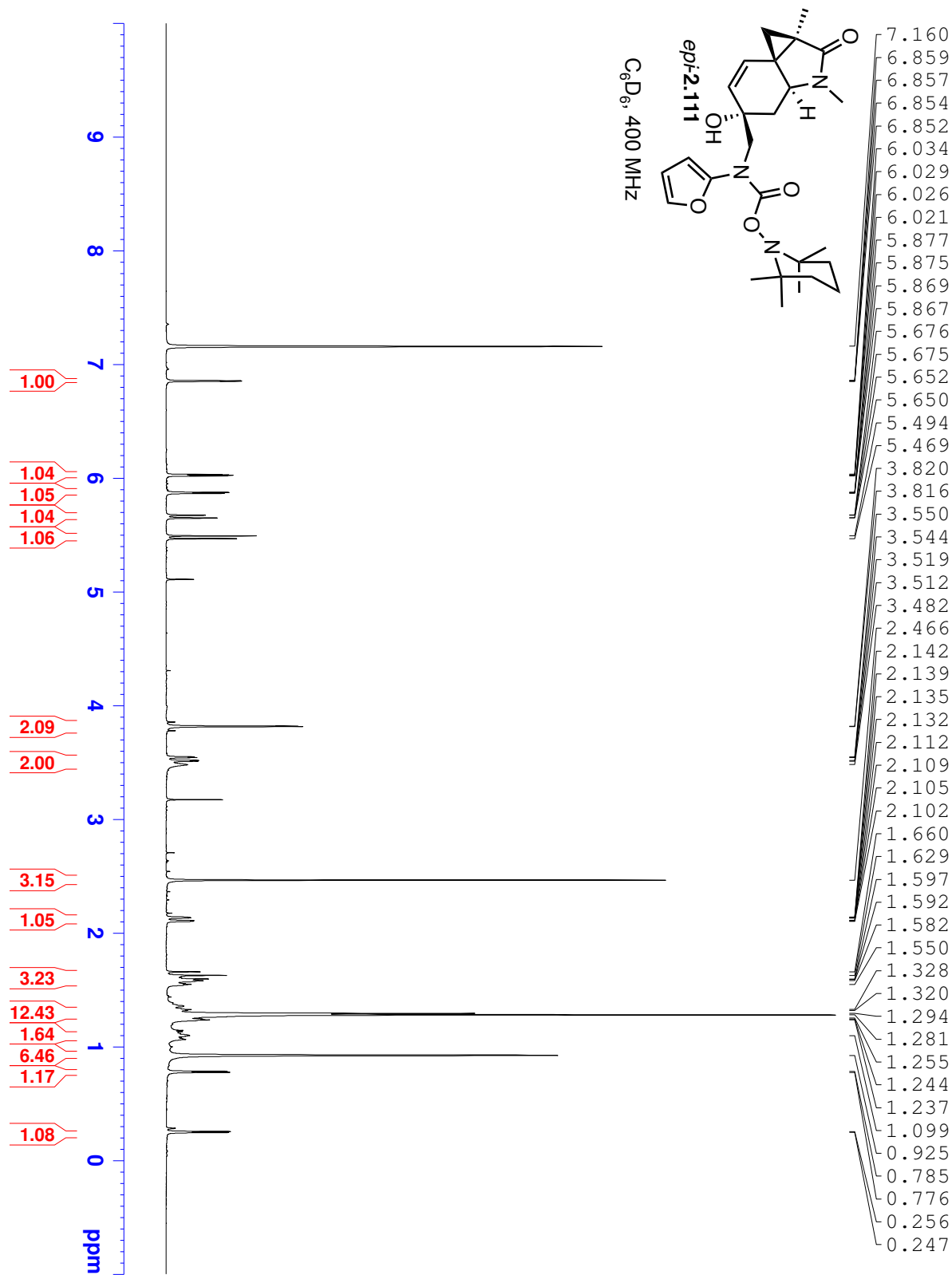


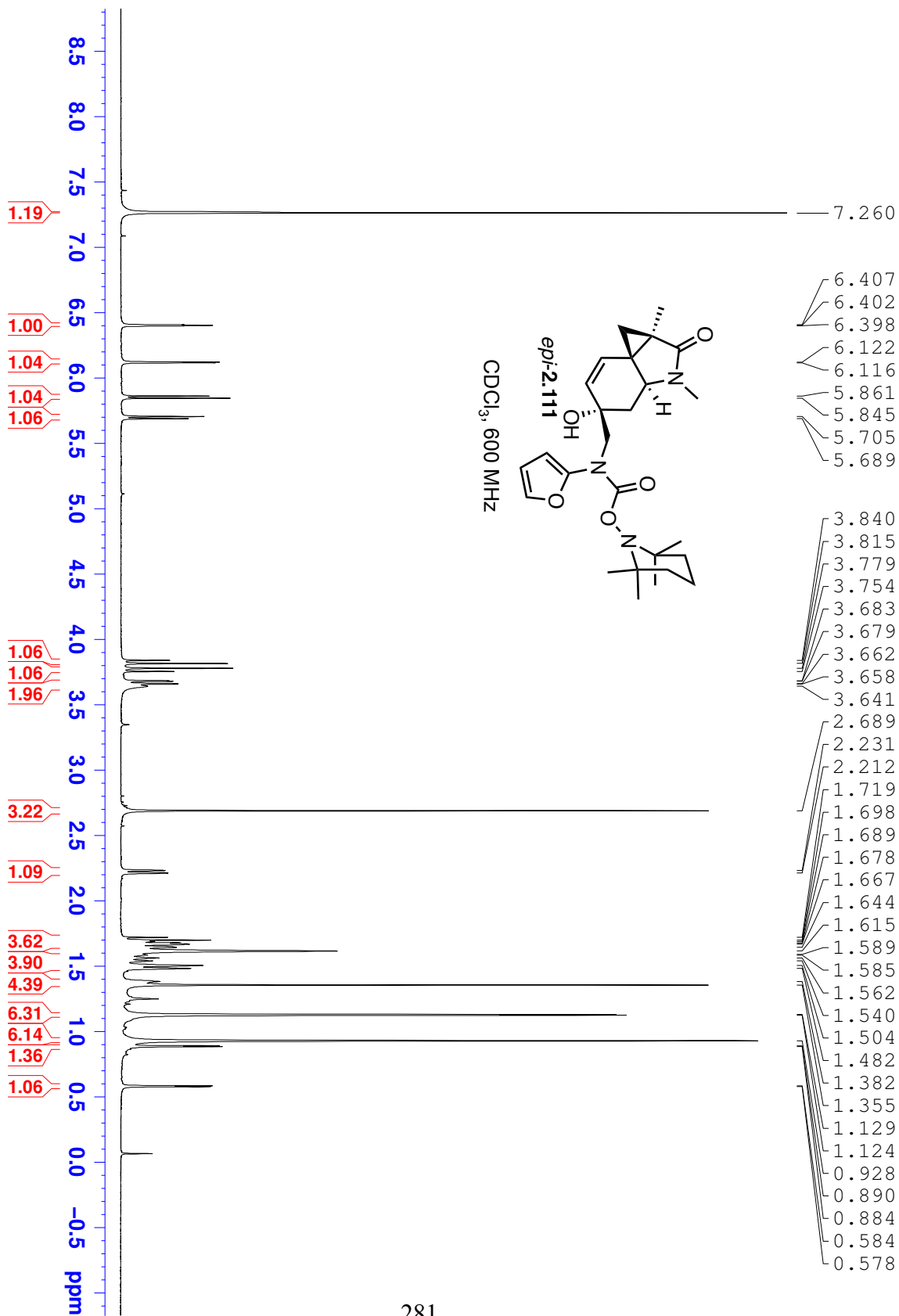


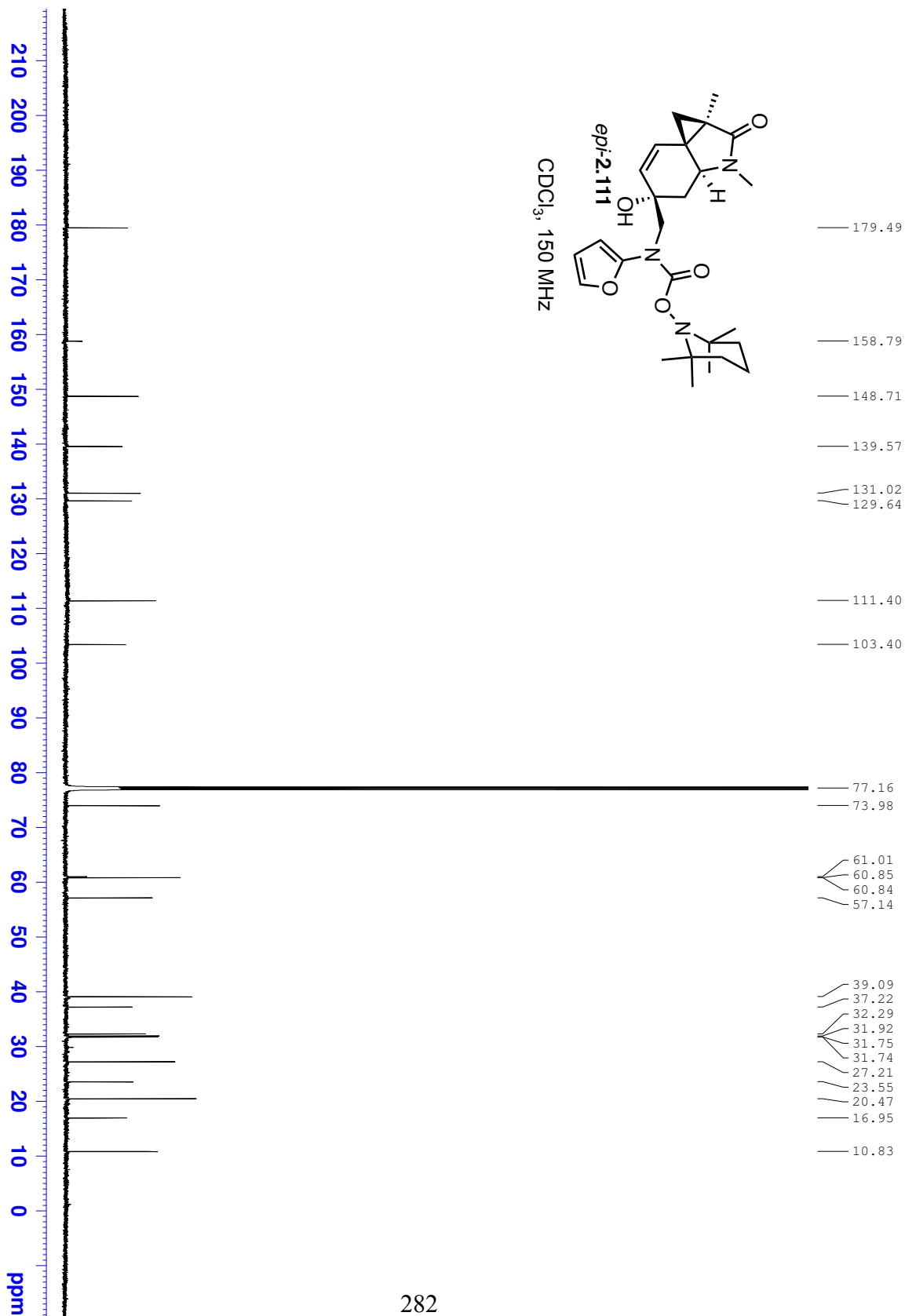




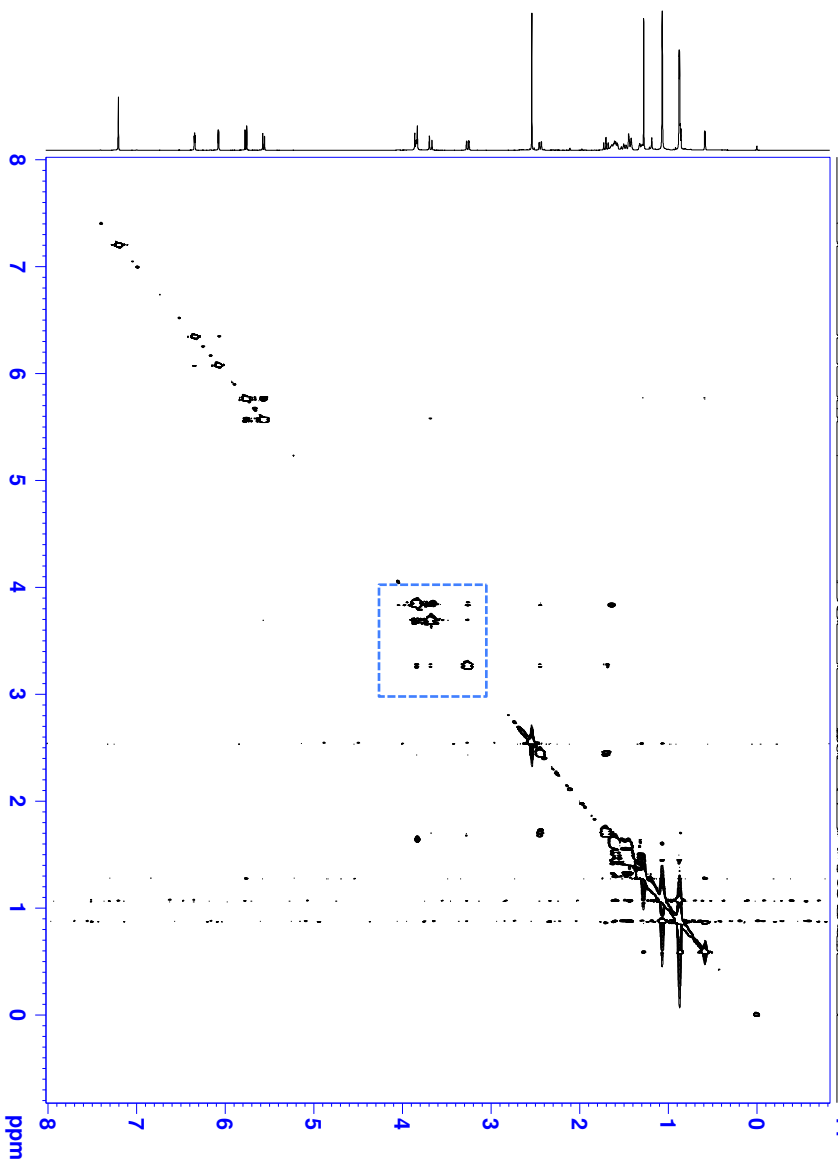
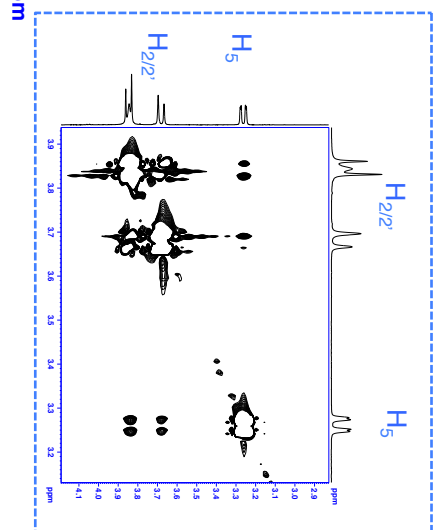
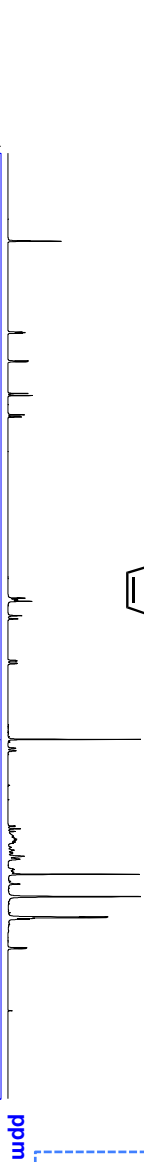
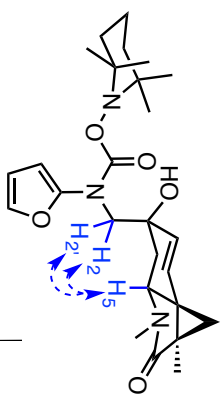




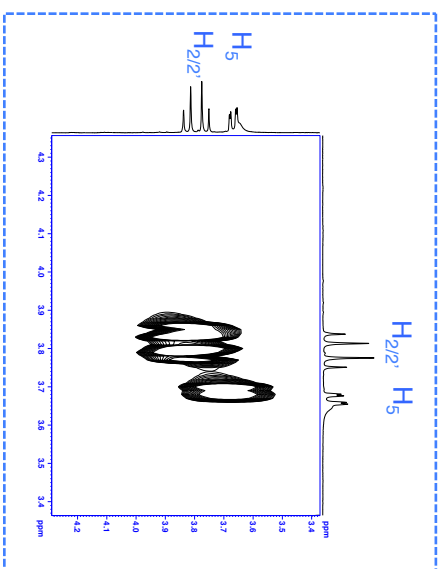
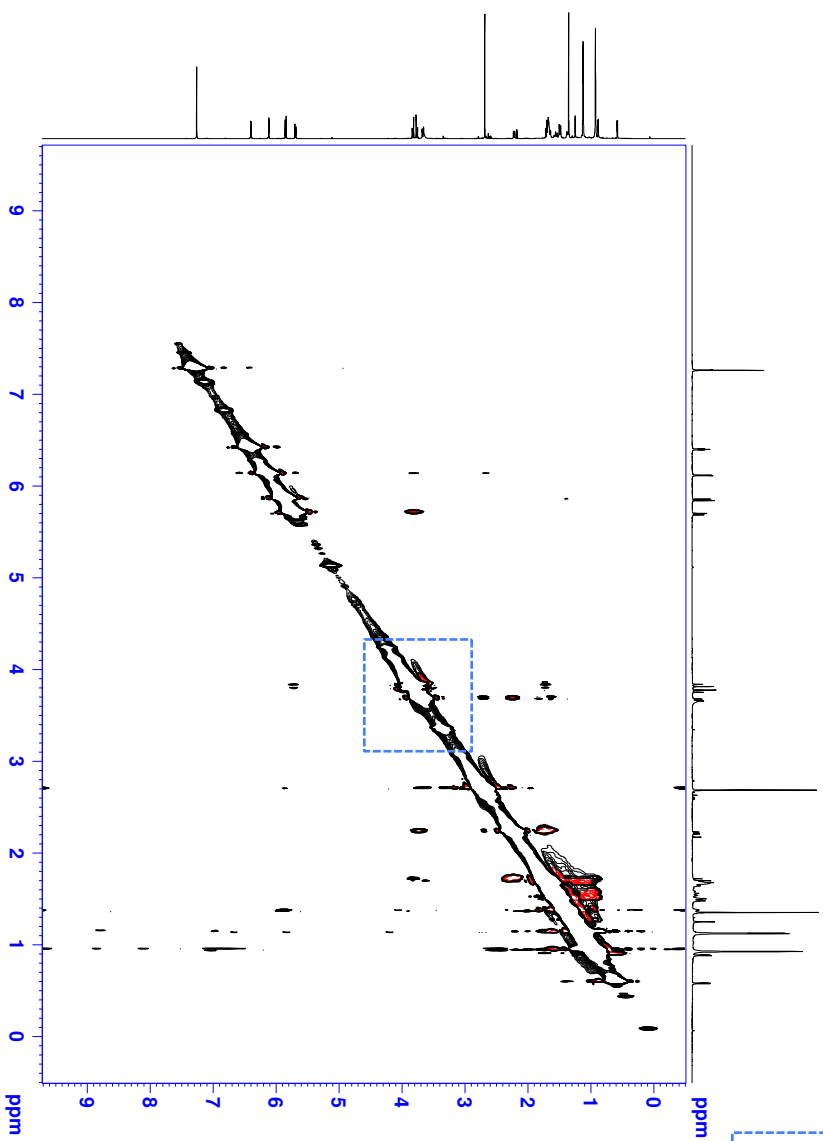
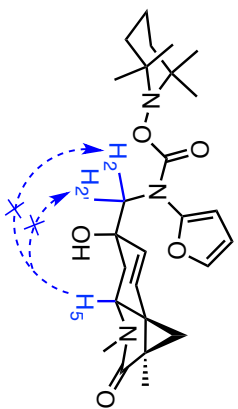




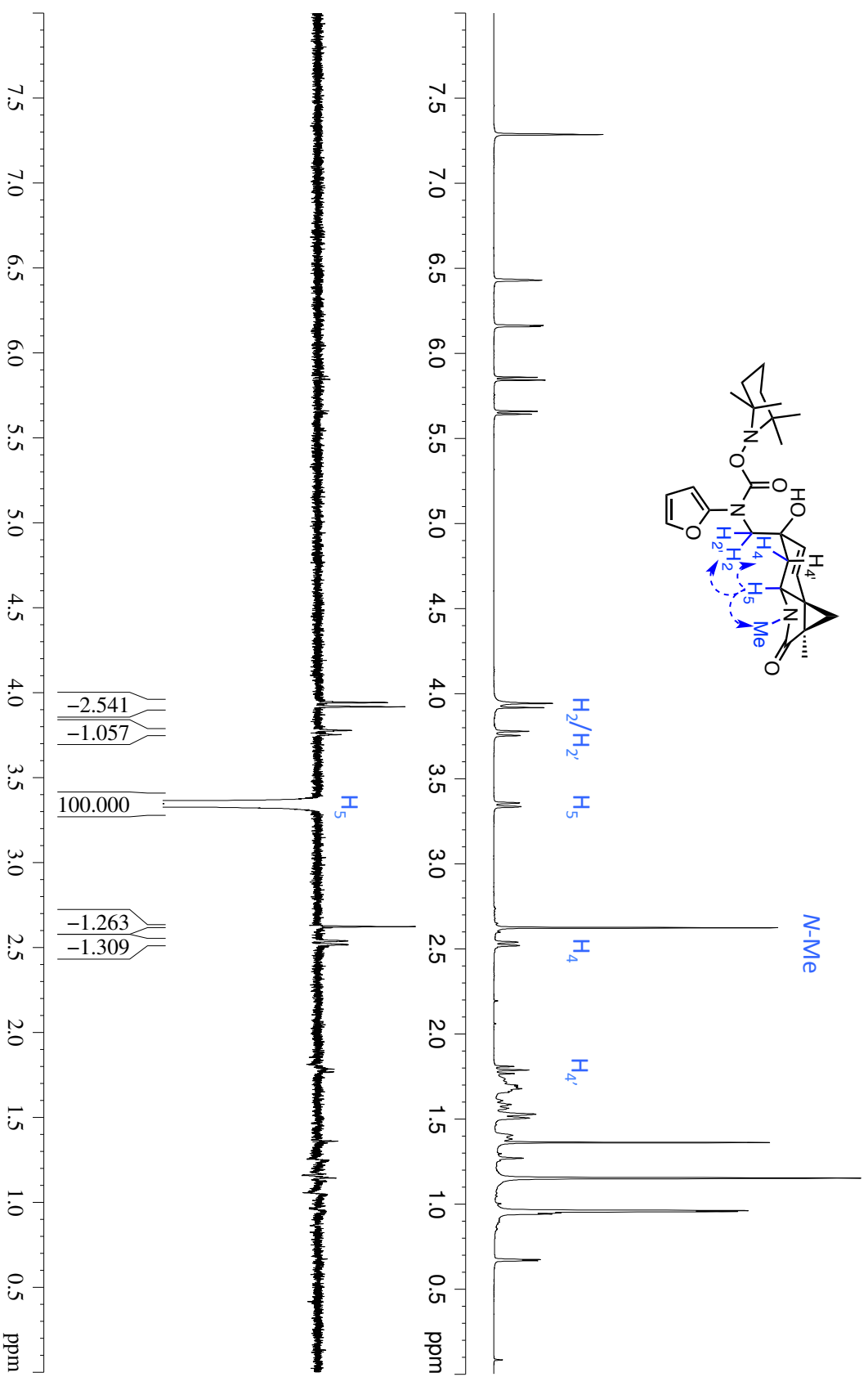
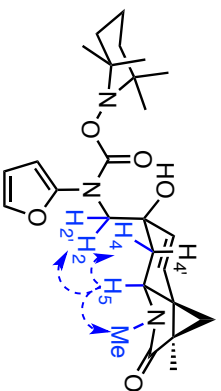
Key ROESY correlations in **2.111** (CDCl<sub>3</sub>, 500 MHz)



Lack of key ROESY correlations in *epi*-**2.III** (CDCl<sub>3</sub>, 600 MHz)

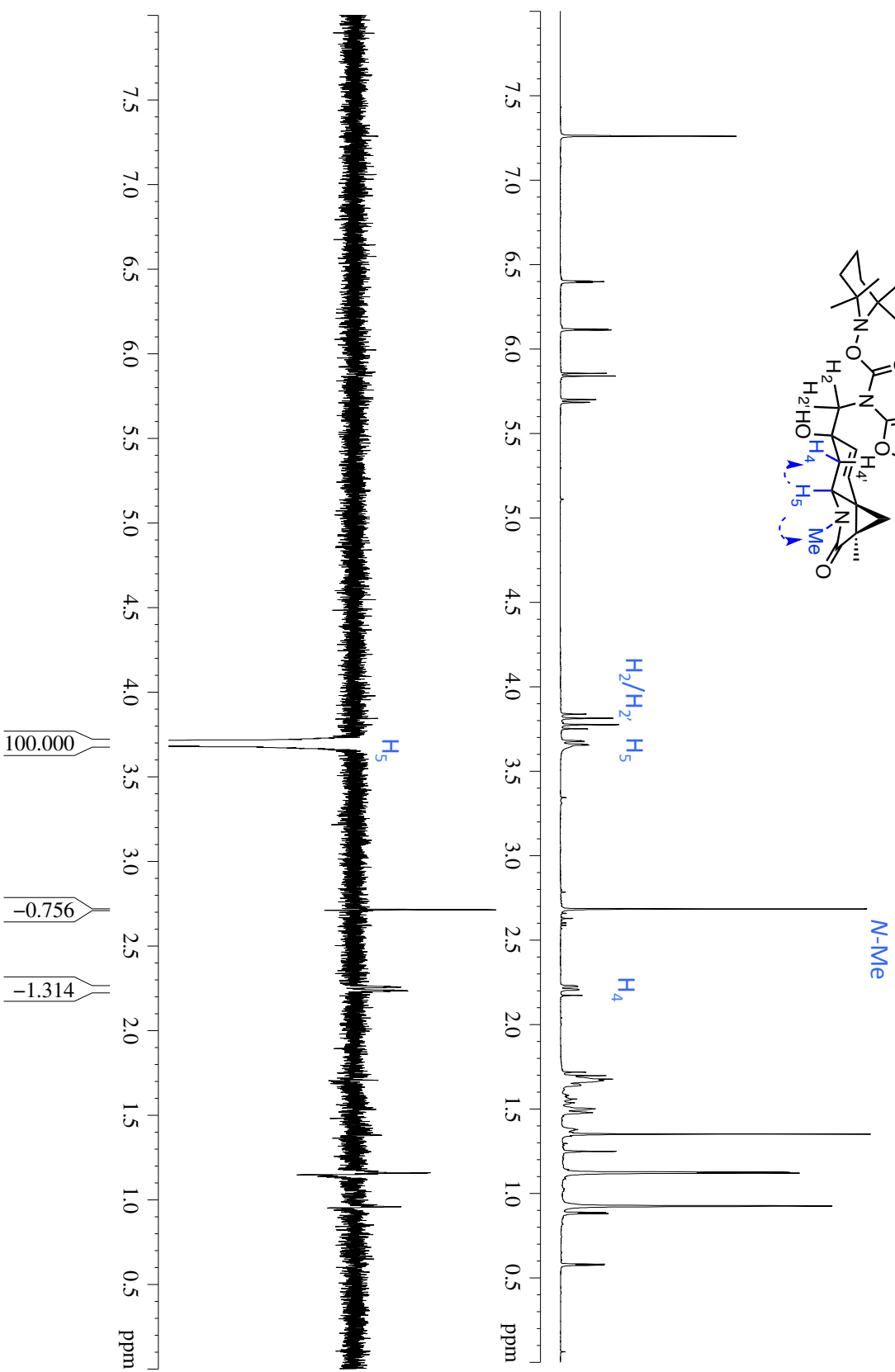
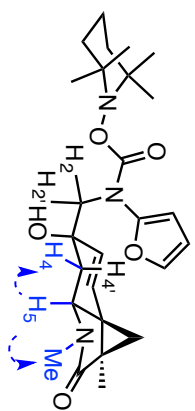


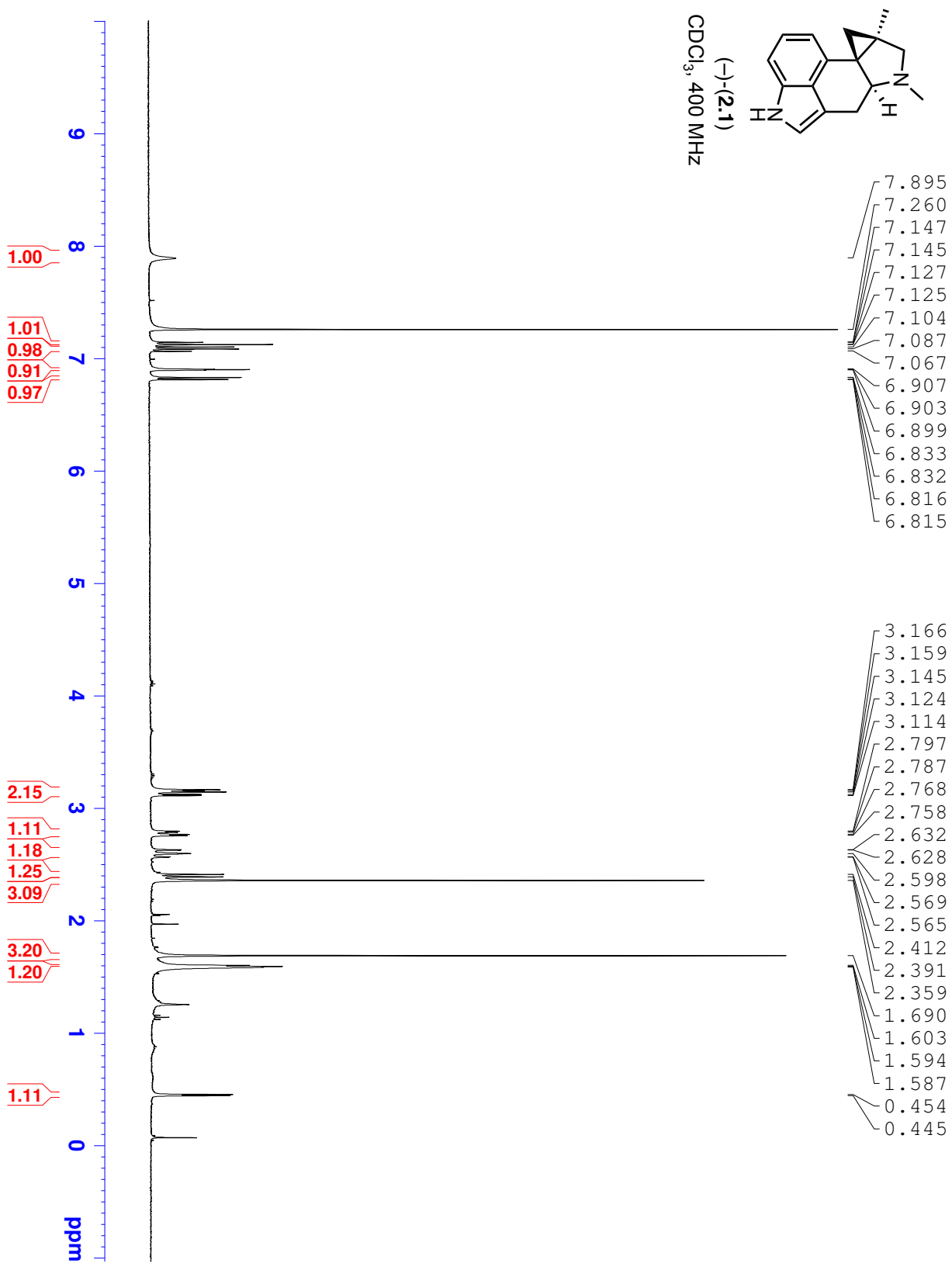
Key 1D-NOE correlations in **2.111** (CDCl<sub>3</sub>, 600 MHz)

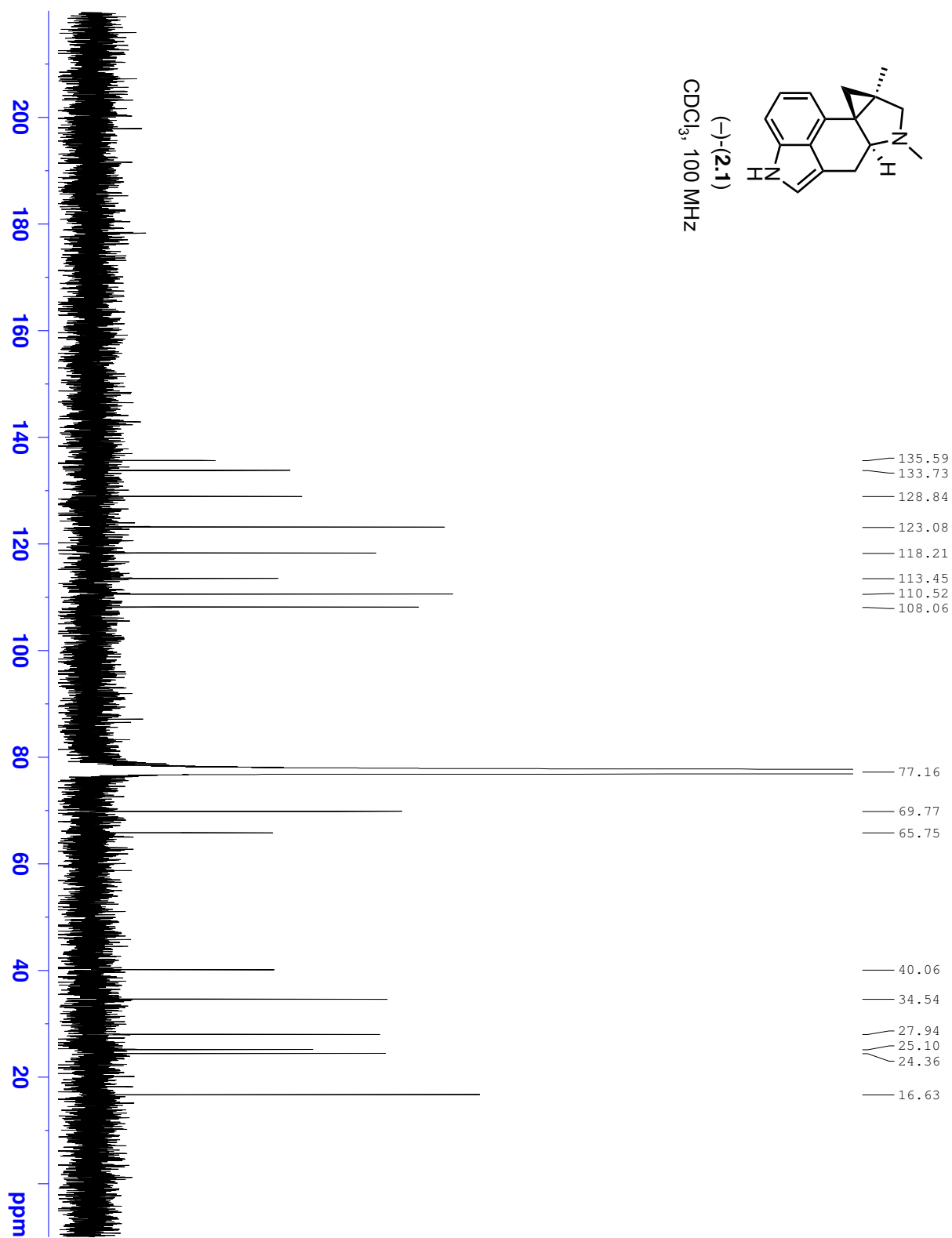


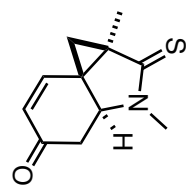


Key 1D-NOE correlations in *epi*-**2.111** (CDCl<sub>3</sub>, 600 MHz)

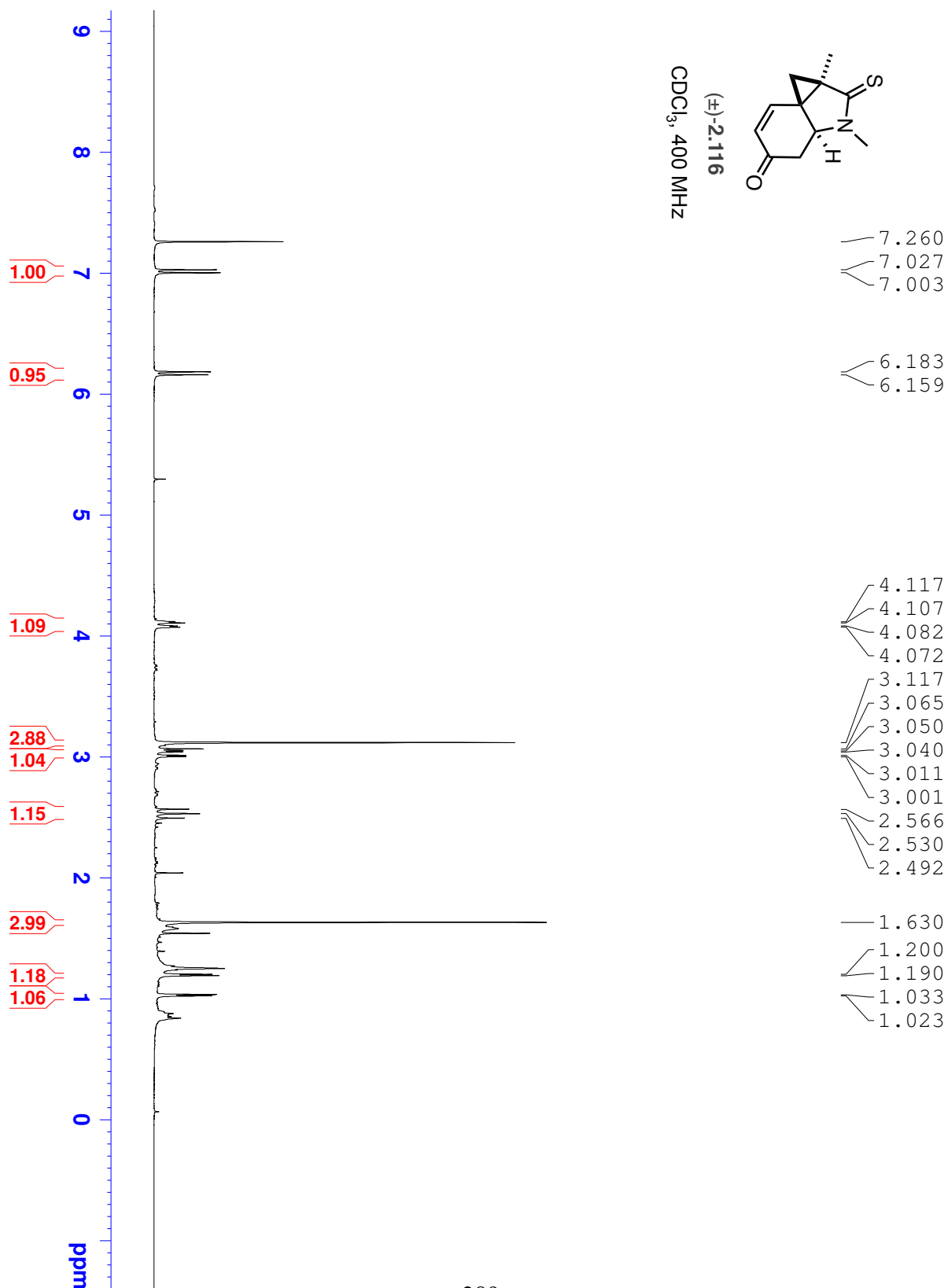


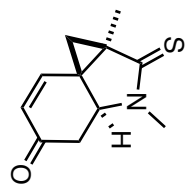






(±)-2.116  
CDCl<sub>3</sub>, 400 MHz





(±)-2.116

CDCl<sub>3</sub>, 100 MHz

— 208.07

— 196.59

— 148.13

— 131.44

— 77.16

— 64.32

— 42.99

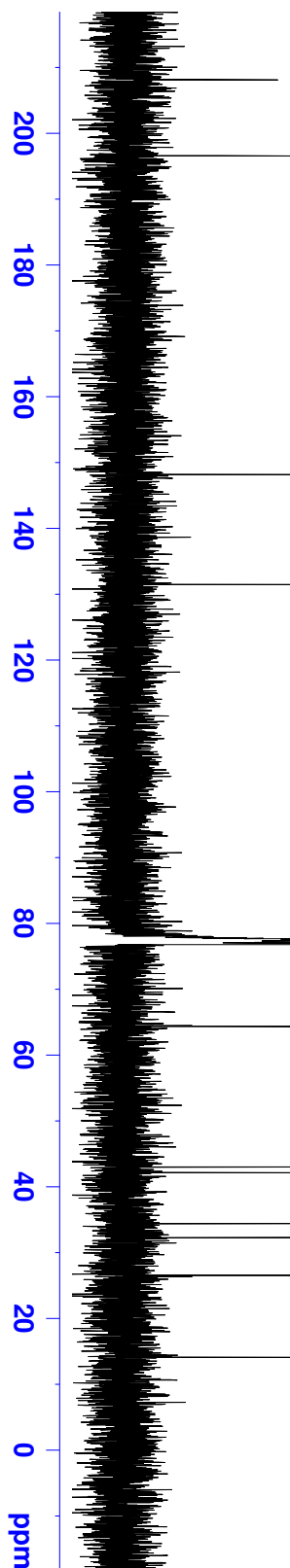
— 42.08

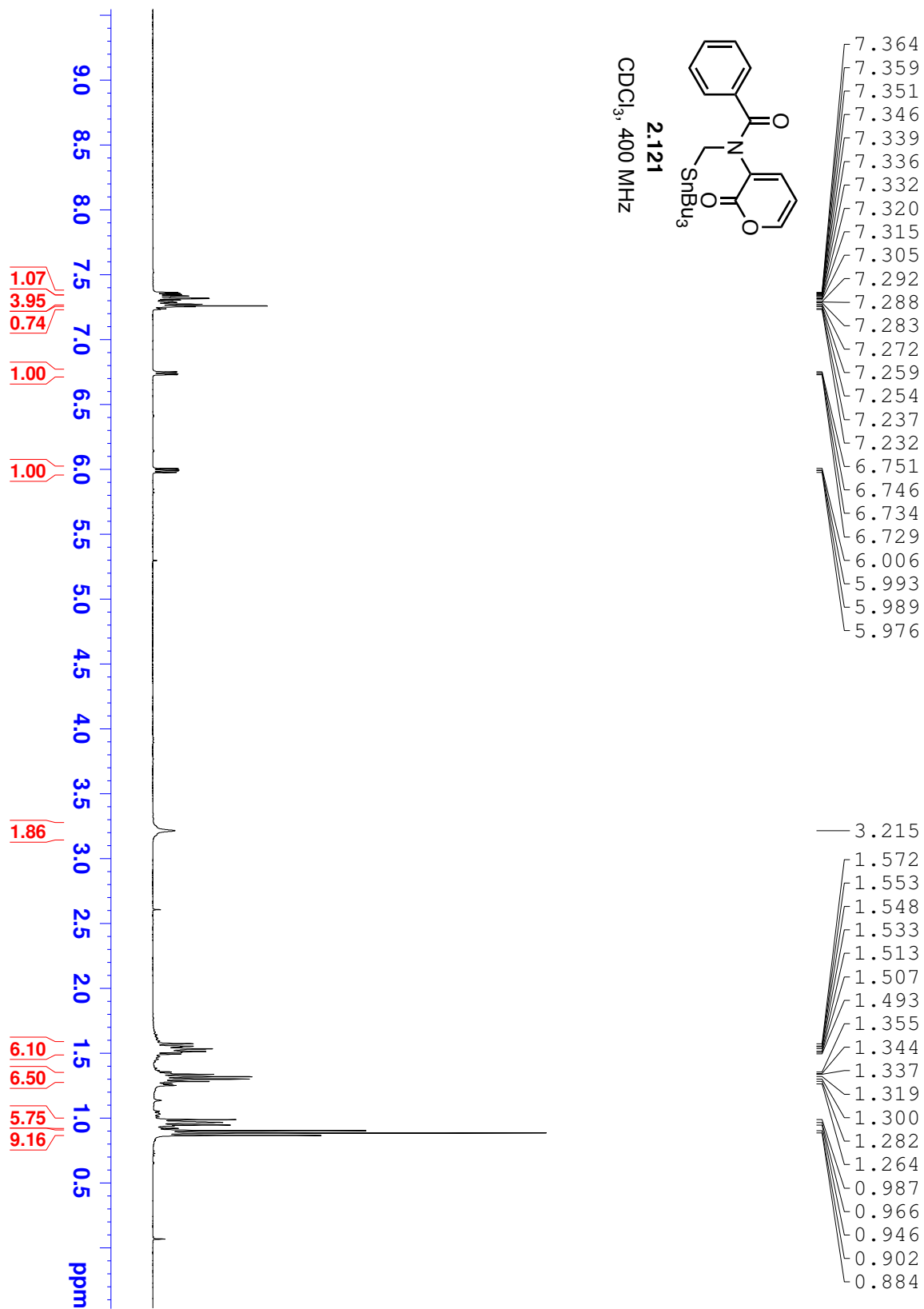
— 34.40

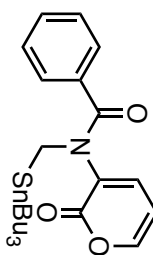
— 32.25

— 26.51

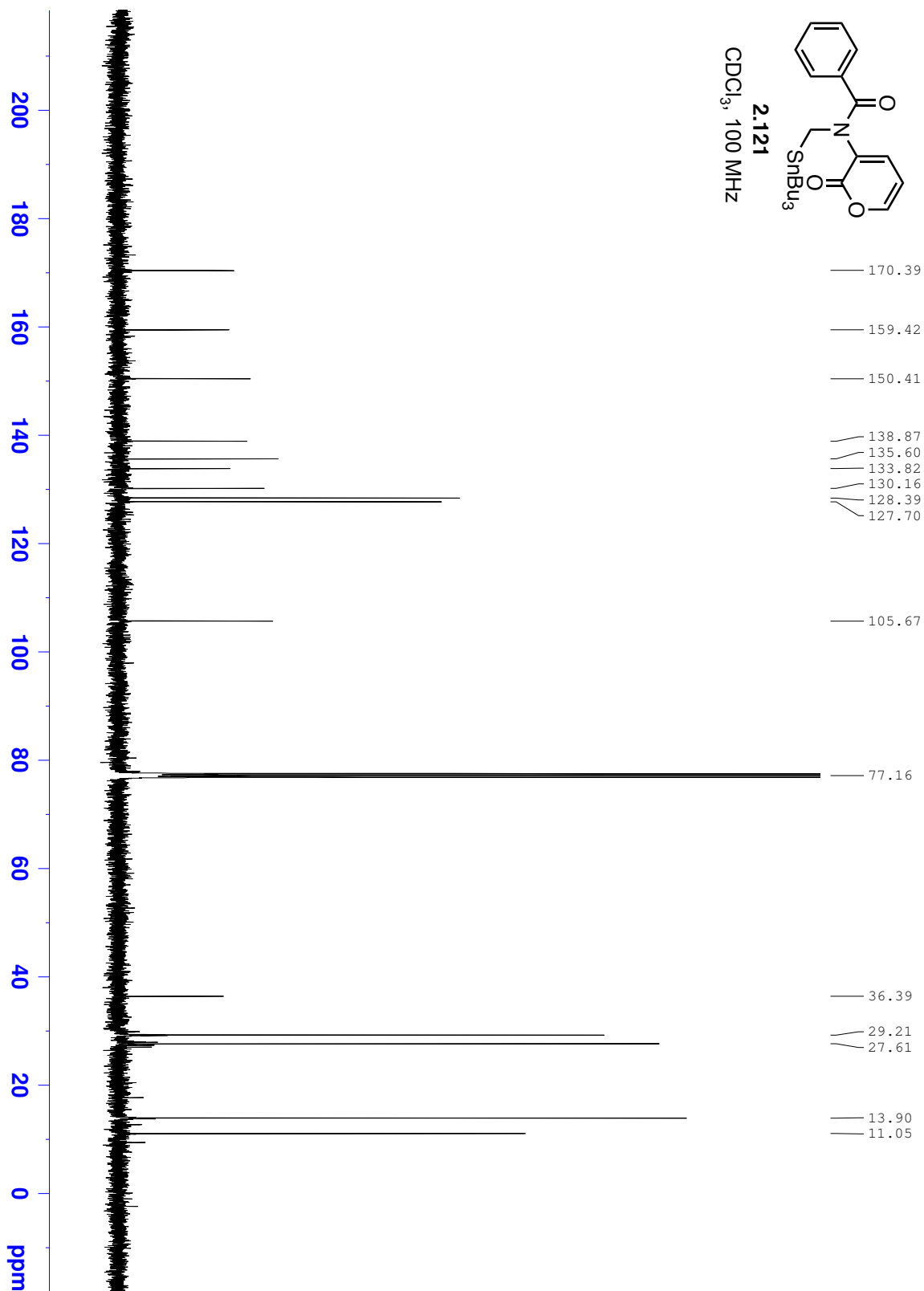
— 14.05

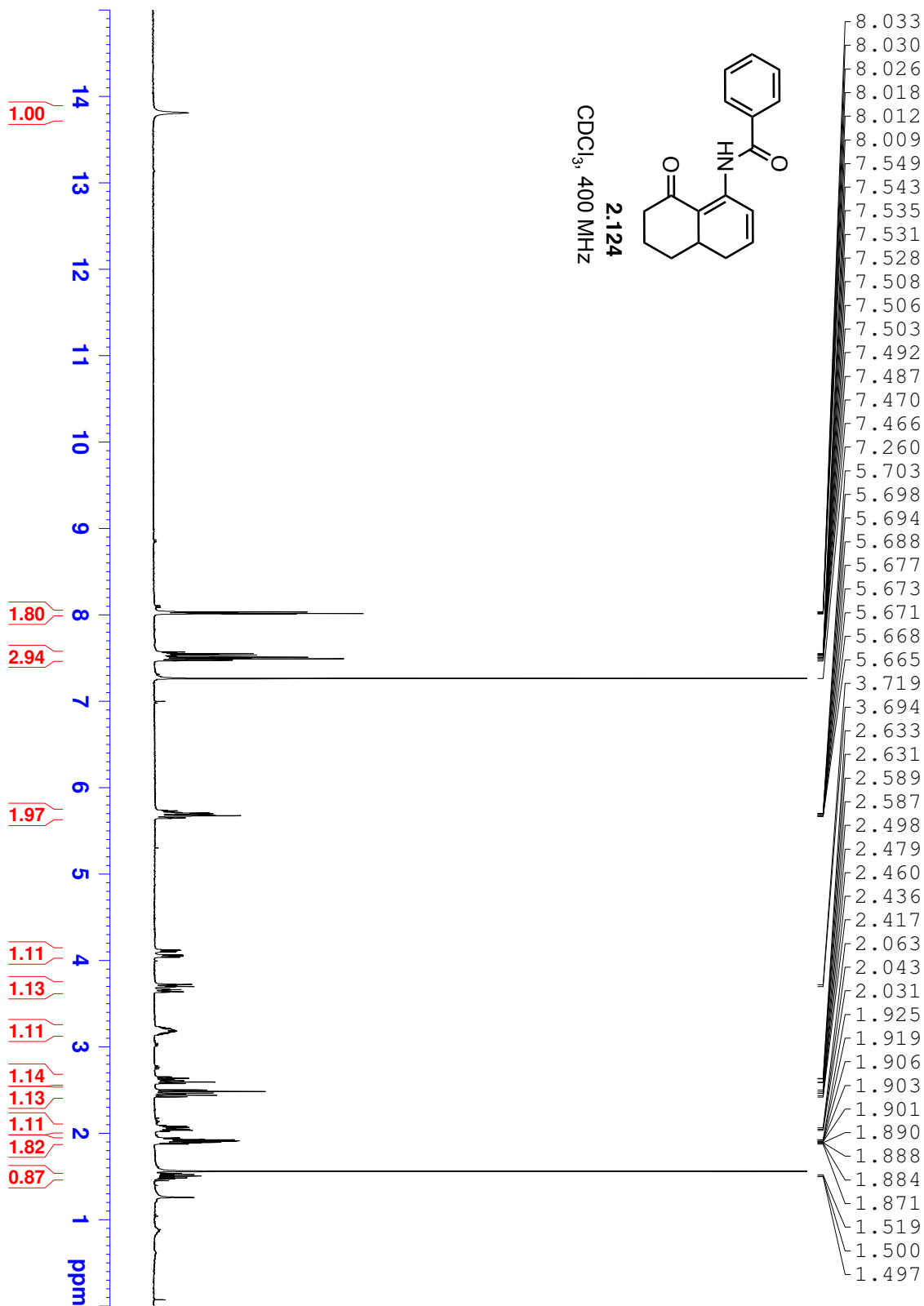




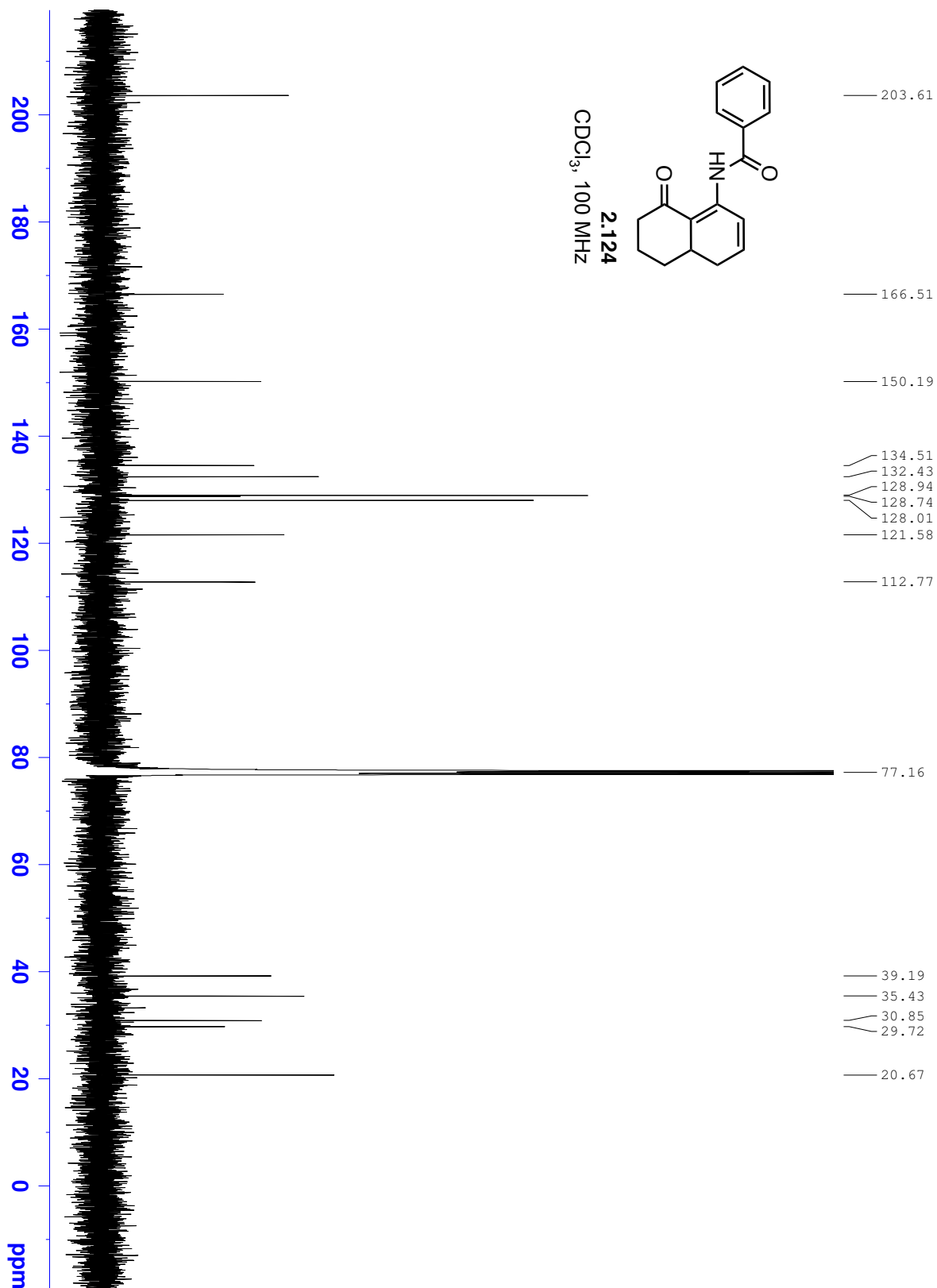


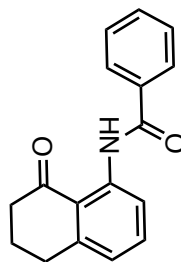
**2.121**  
CDCl<sub>3</sub>, 100 MHz







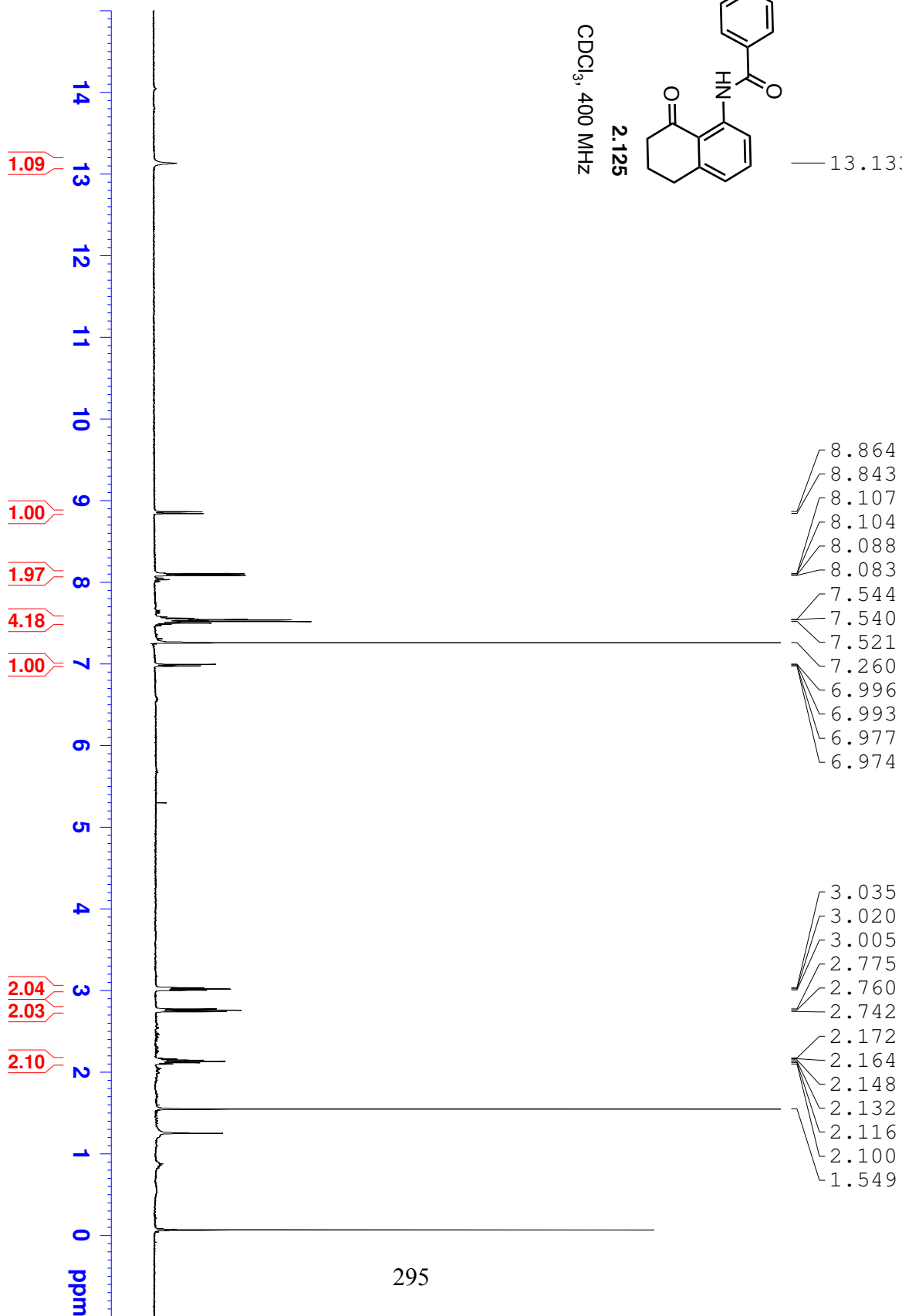


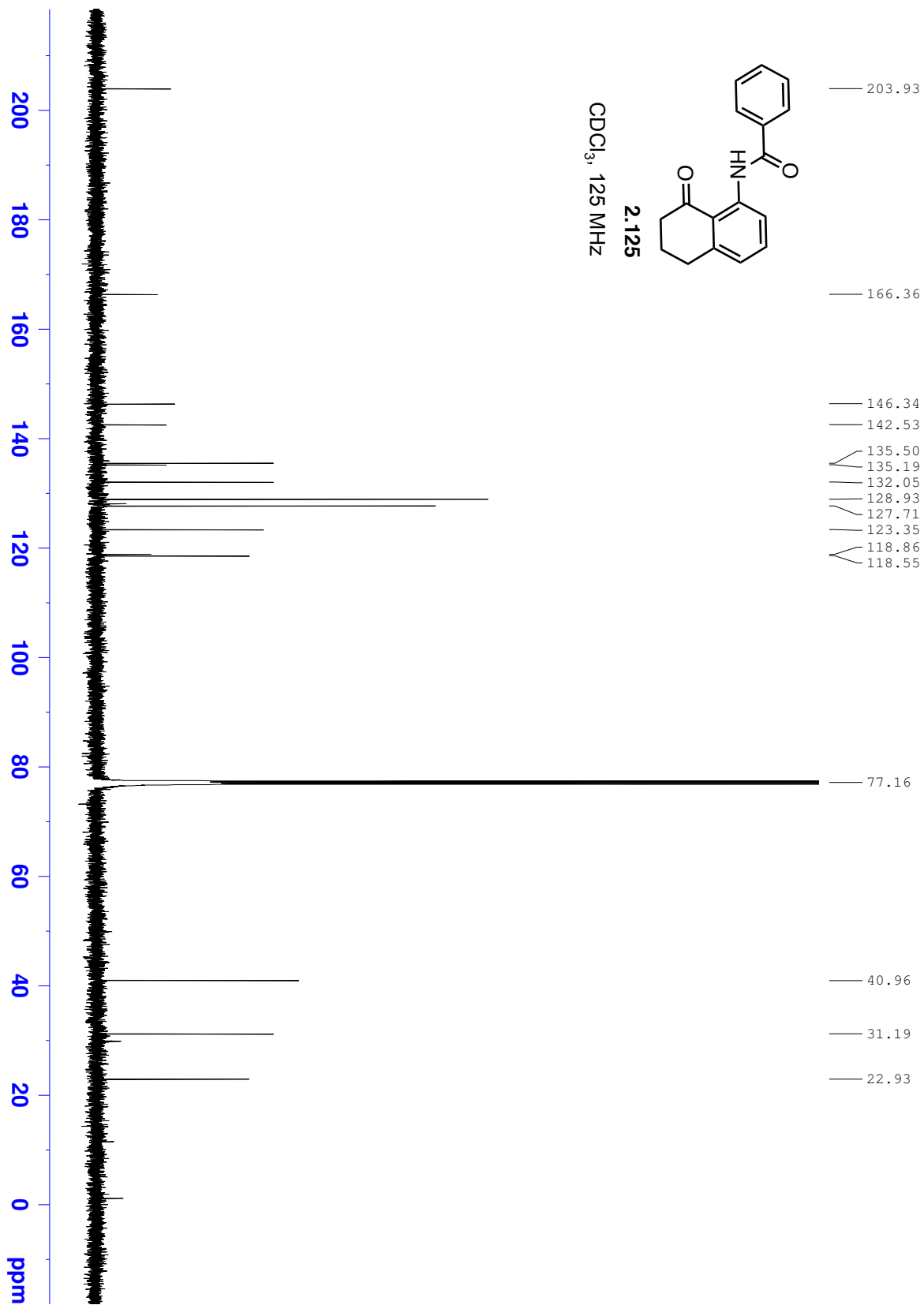


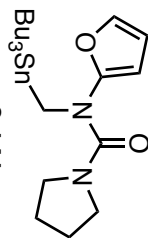
2.125

CDCl<sub>3</sub>, 400 MHz

— 13.133

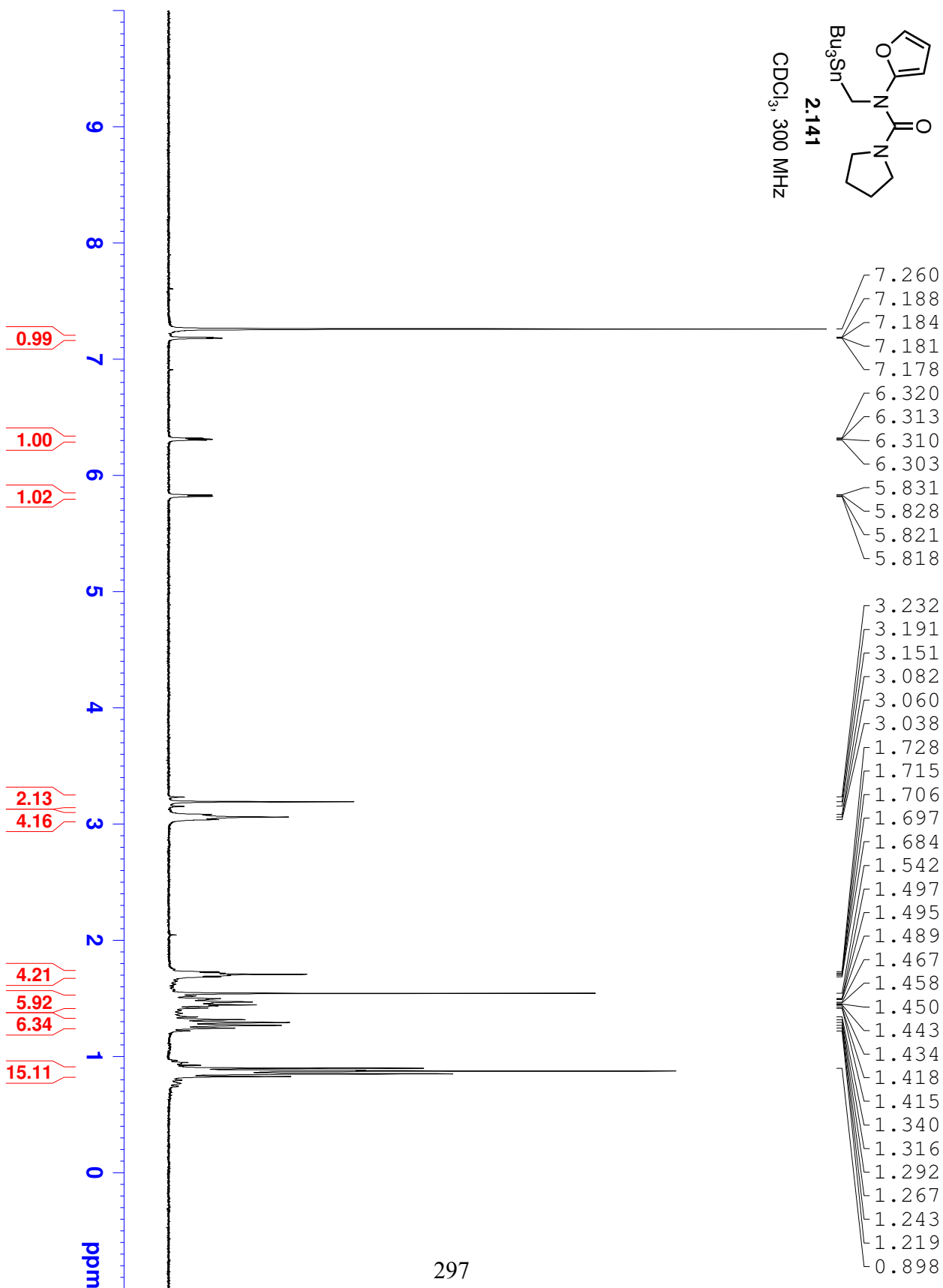


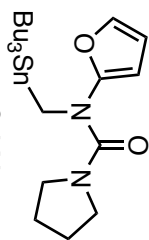




2.141

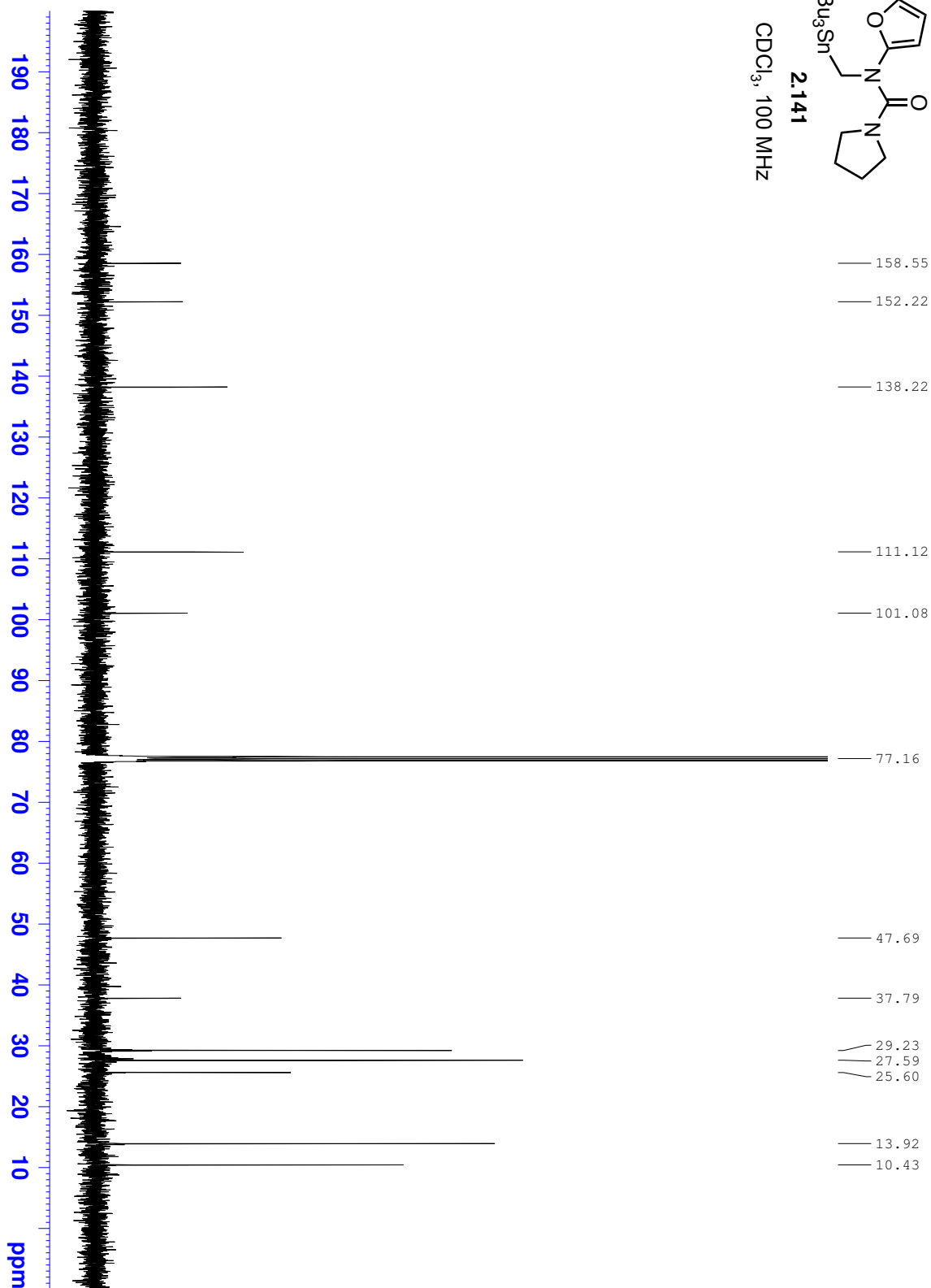
CDCl<sub>3</sub>, 300 MHz

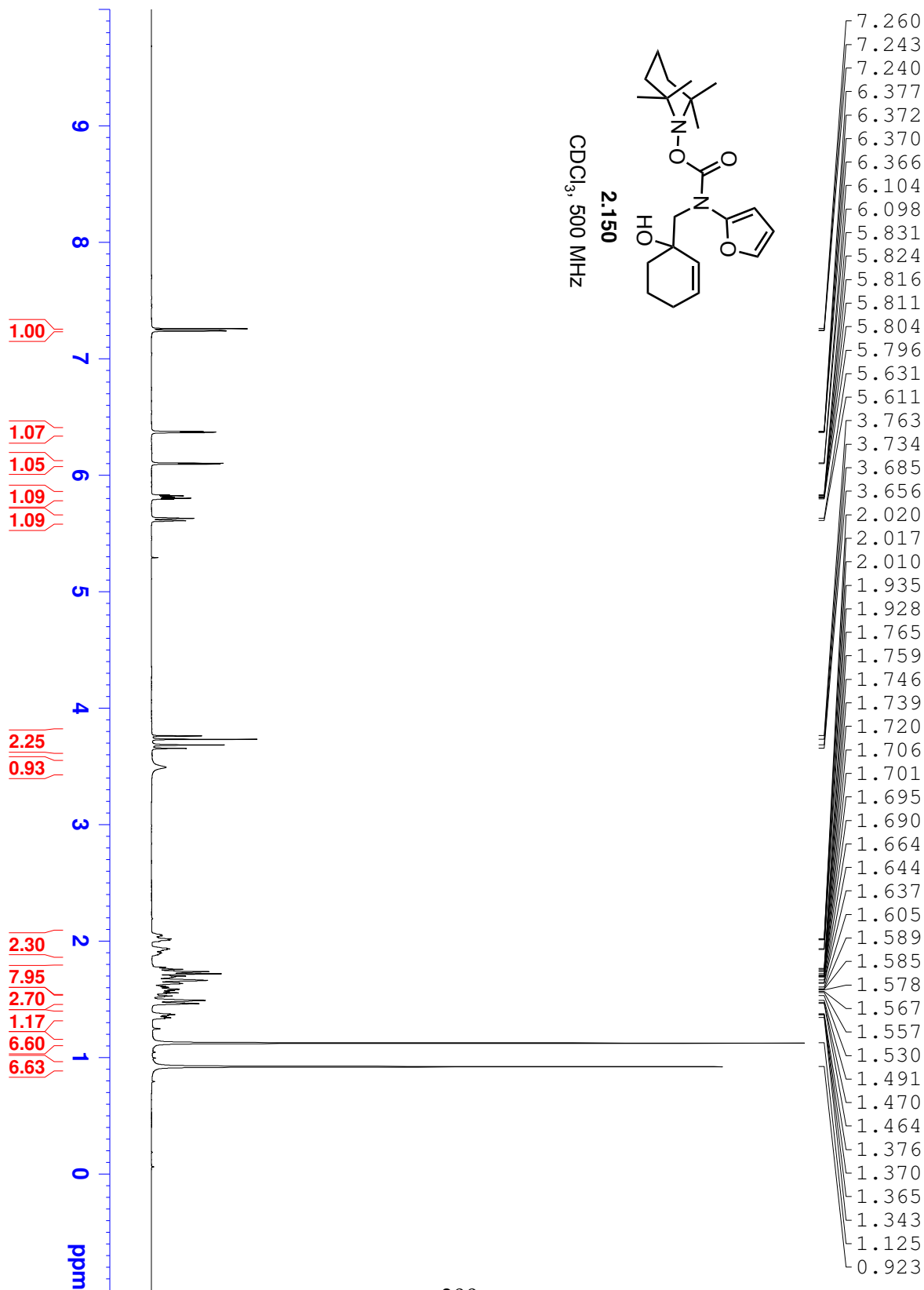


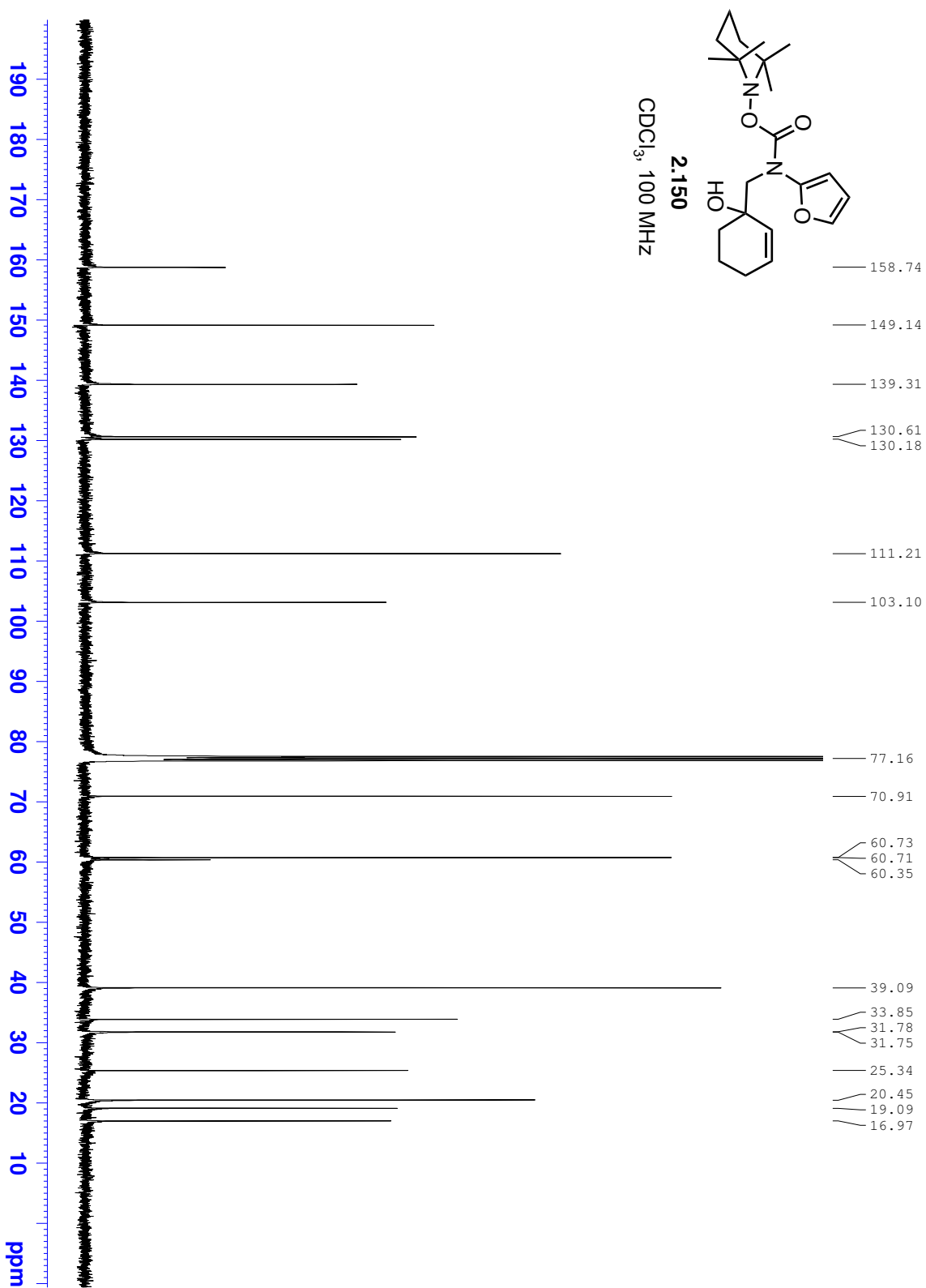


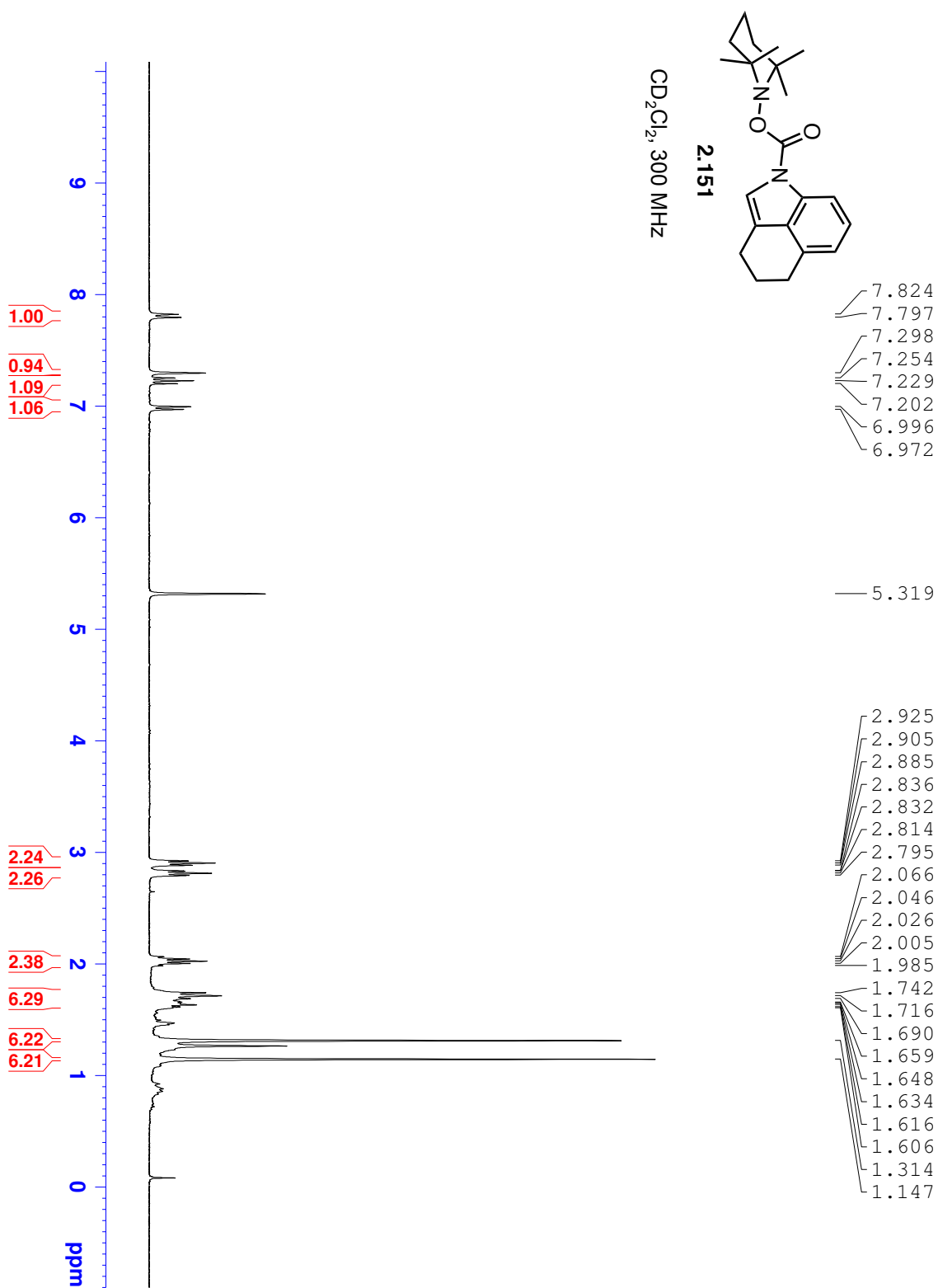
**2.141**

CDCl<sub>3</sub>, 100 MHz

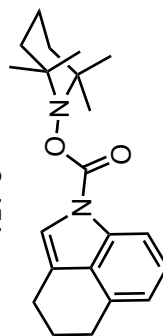












2.151

CDCl<sub>3</sub>, 100 MHz  
70 °C

31.936  
27.488  
24.528  
22.065  
21.494  
17.400

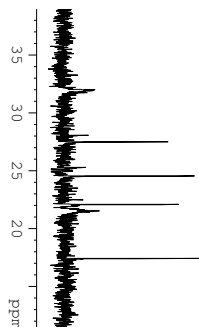
152.33

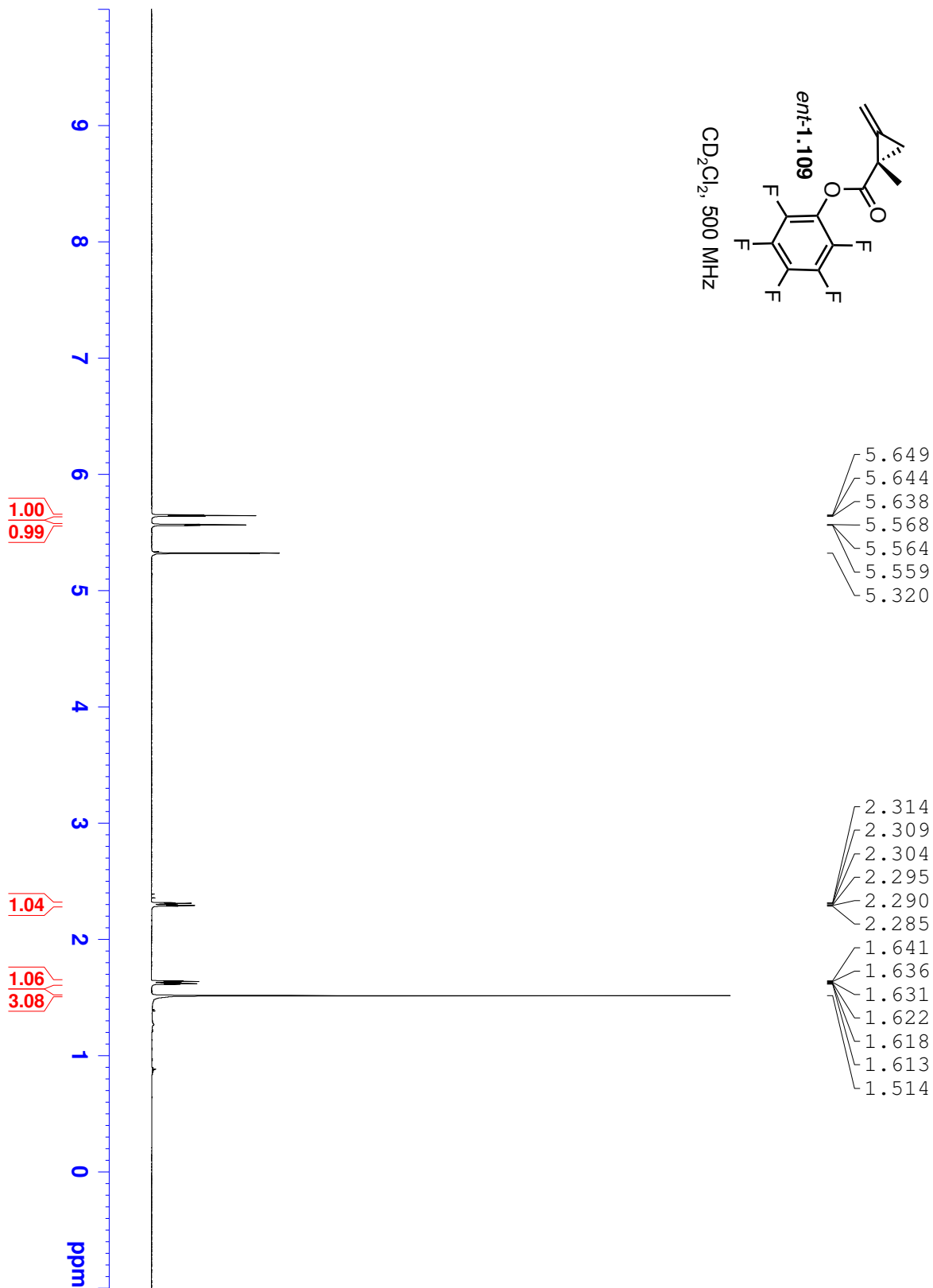
134.84  
132.63  
130.07  
128.06  
125.59  
120.34  
119.21  
118.55  
113.43

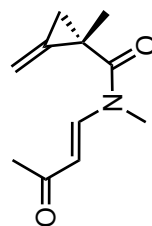
60.78

39.86

31.94  
27.49  
24.53  
22.06  
21.49  
17.40

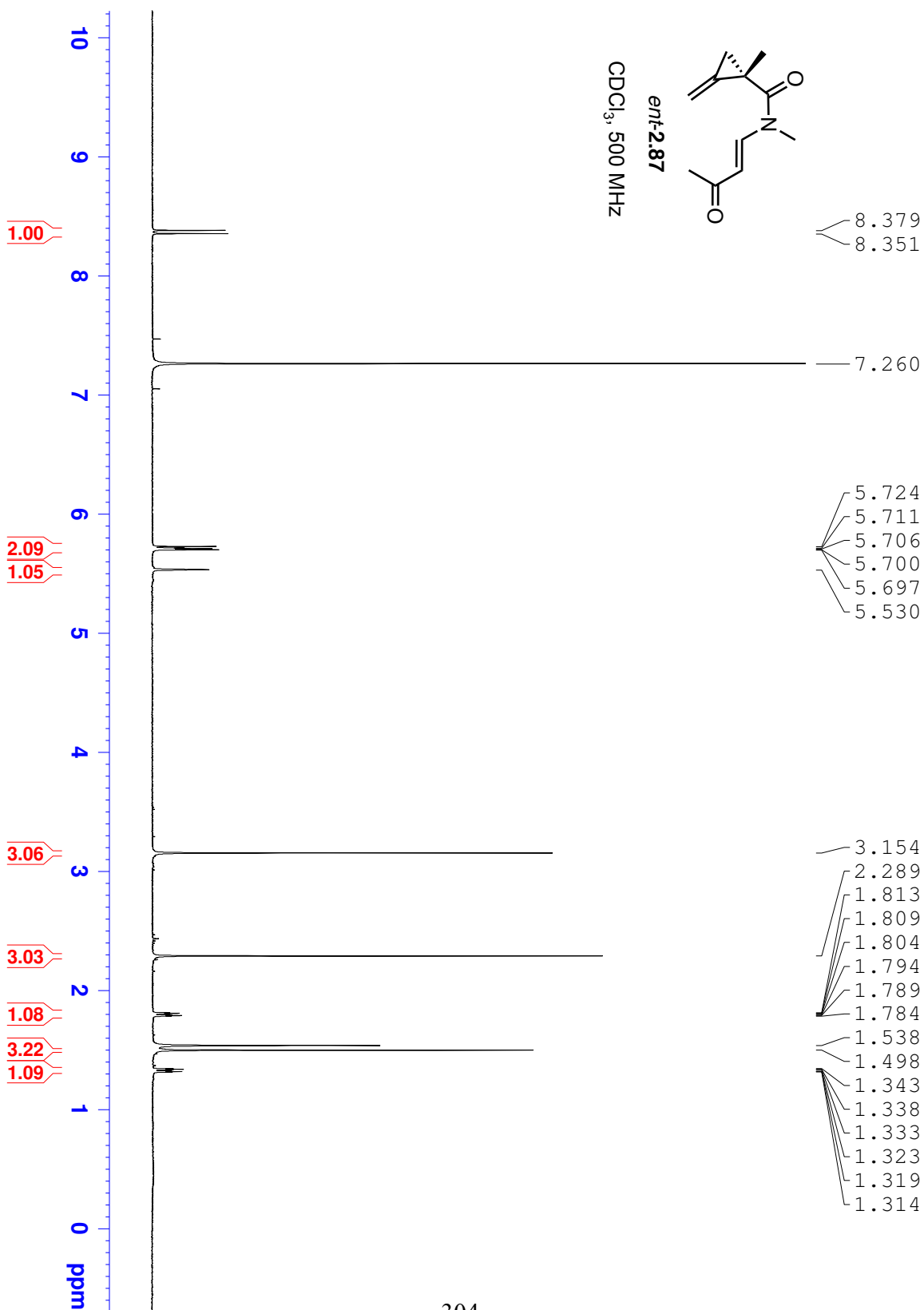


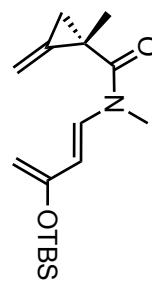




*ent*-2.87

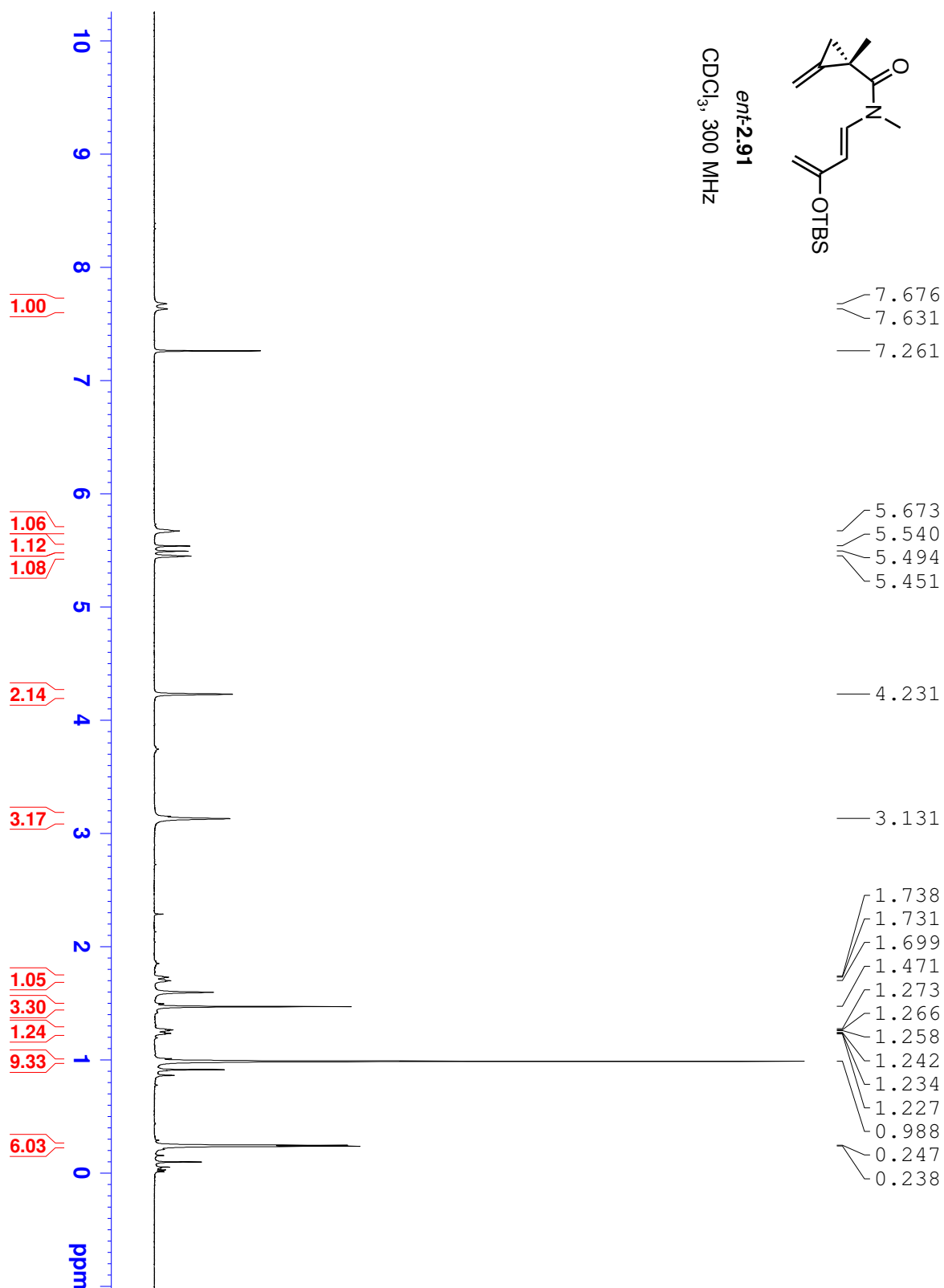
CDCl<sub>3</sub>, 500 MHz

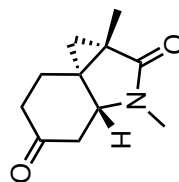




*ent*-2.91

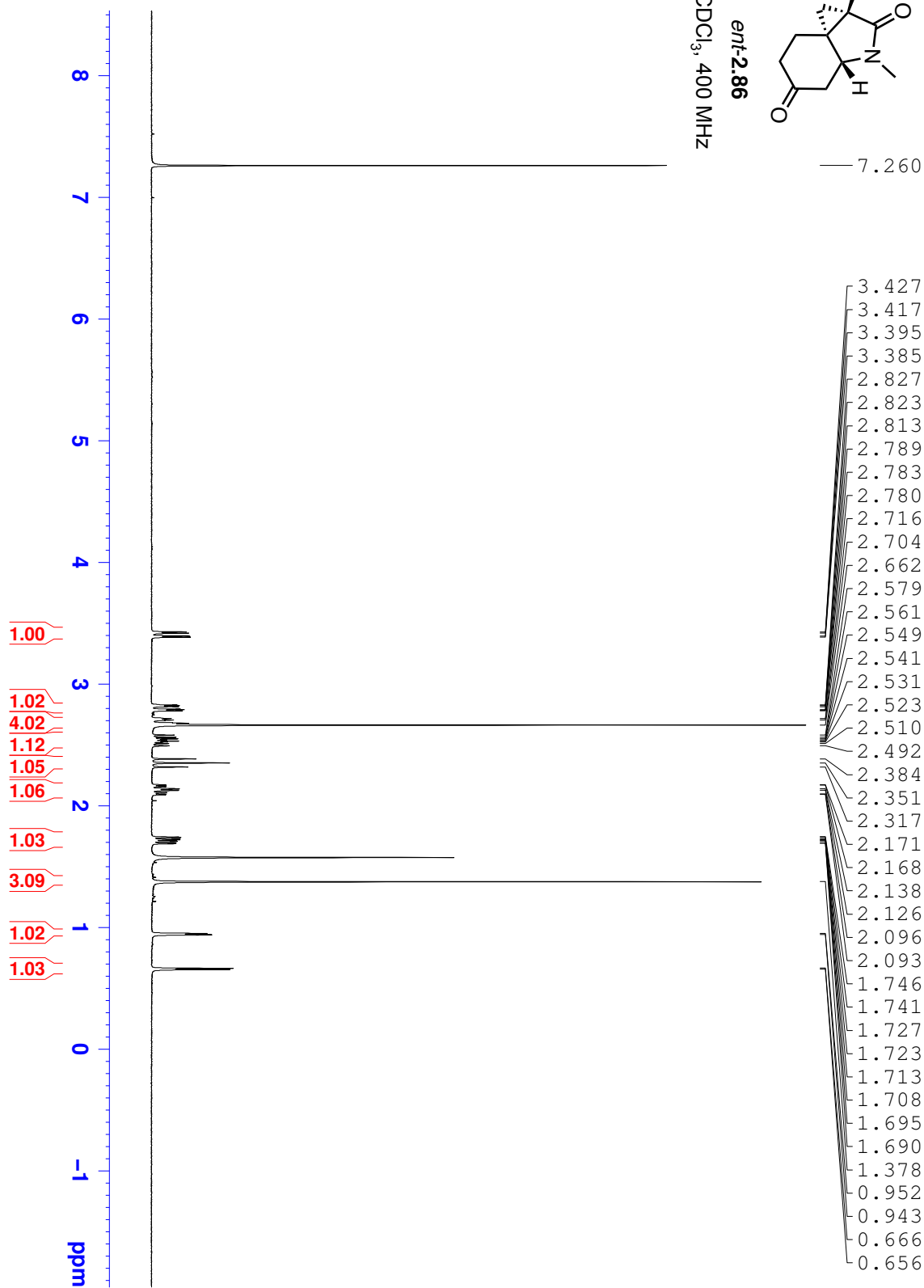
CDCl<sub>3</sub>, 300 MHz

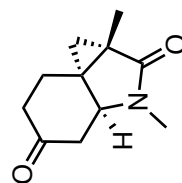




*ent*-2.86

CDCl<sub>3</sub>, 400 MHz



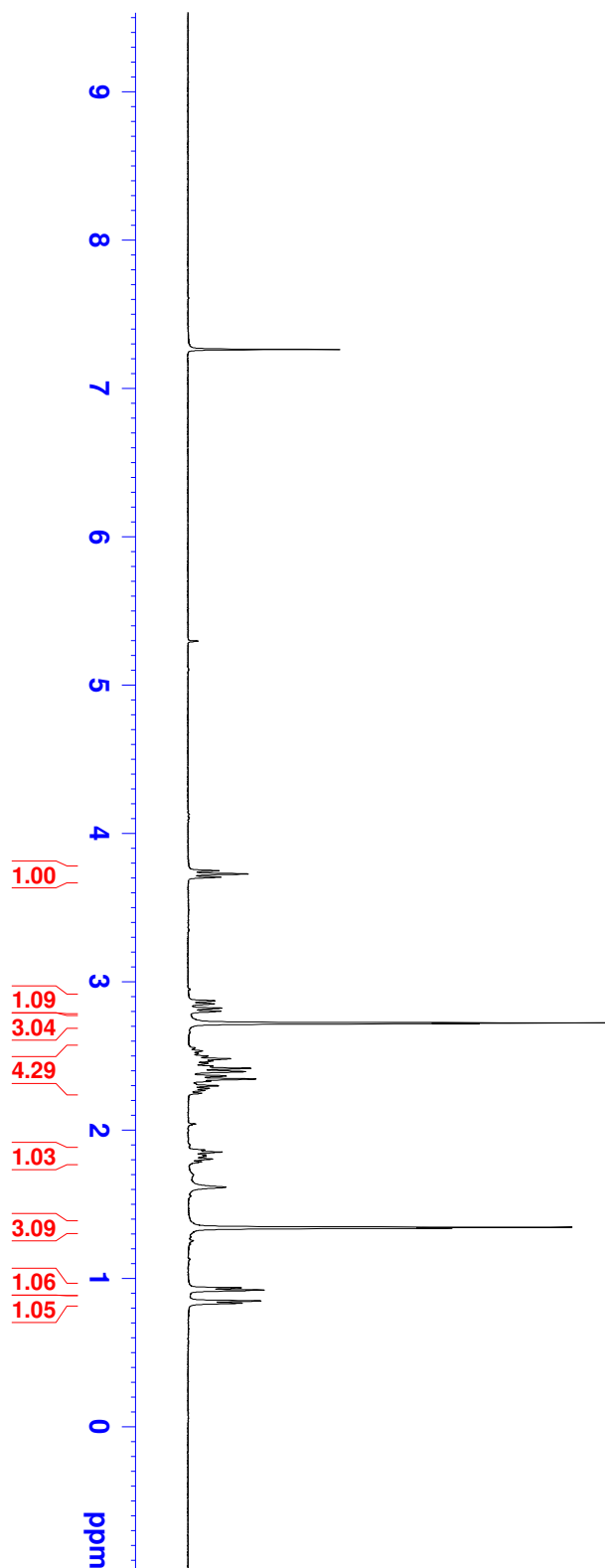


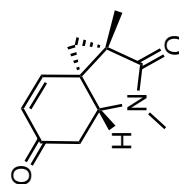
*epi-ent*-2.86

CDCl<sub>3</sub>, 300 MHz

— 7.260

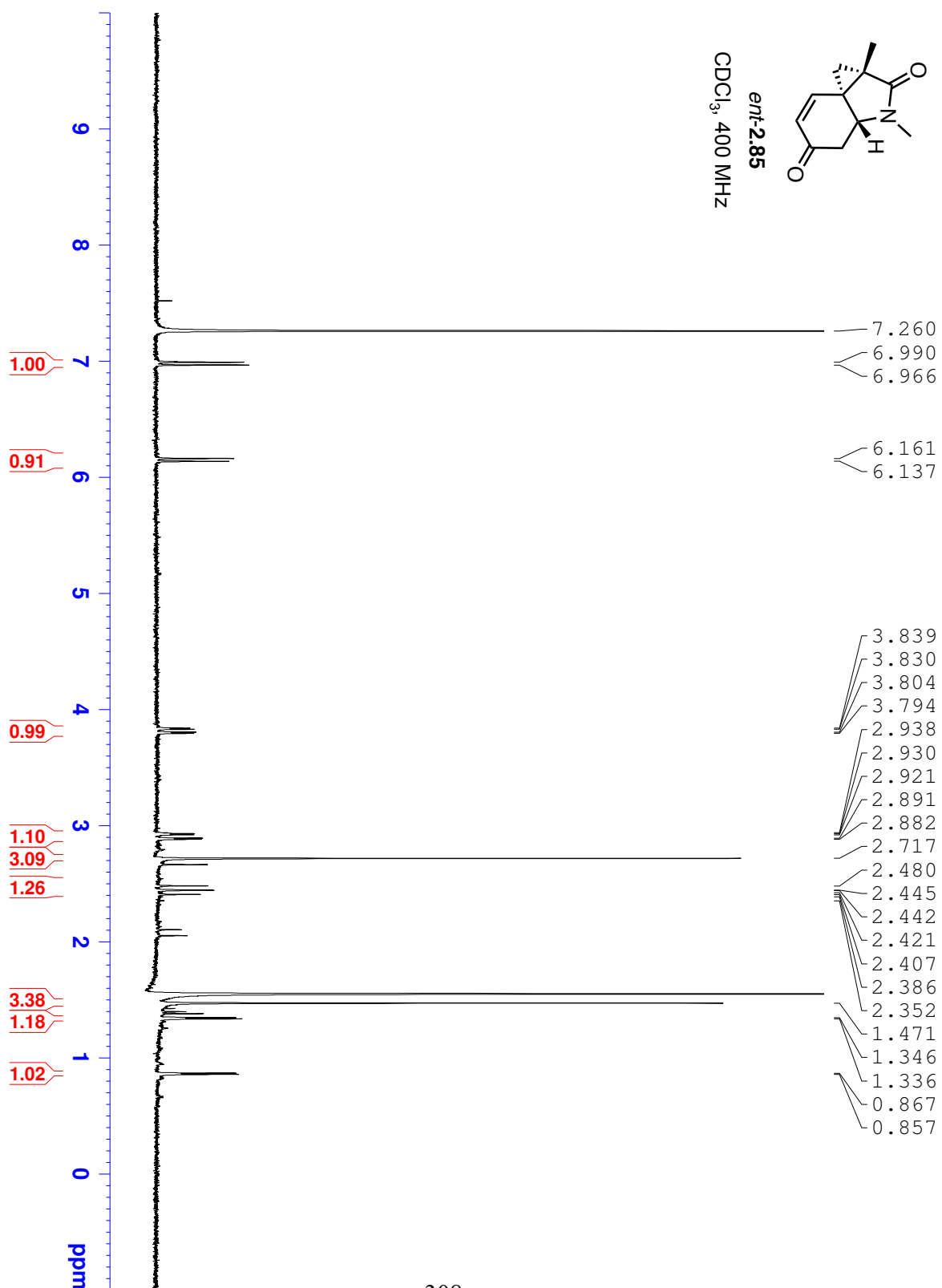
3.748  
3.726  
3.705  
2.871  
2.851  
2.821  
2.801  
2.722  
2.533  
2.499  
2.481  
2.465  
2.449  
2.430  
2.416  
2.394  
2.364  
2.344  
2.329  
2.298  
2.281  
2.267  
2.248  
1.866  
1.859  
1.851  
1.833  
1.827  
1.822  
1.804  
1.785  
1.343  
0.936  
0.921

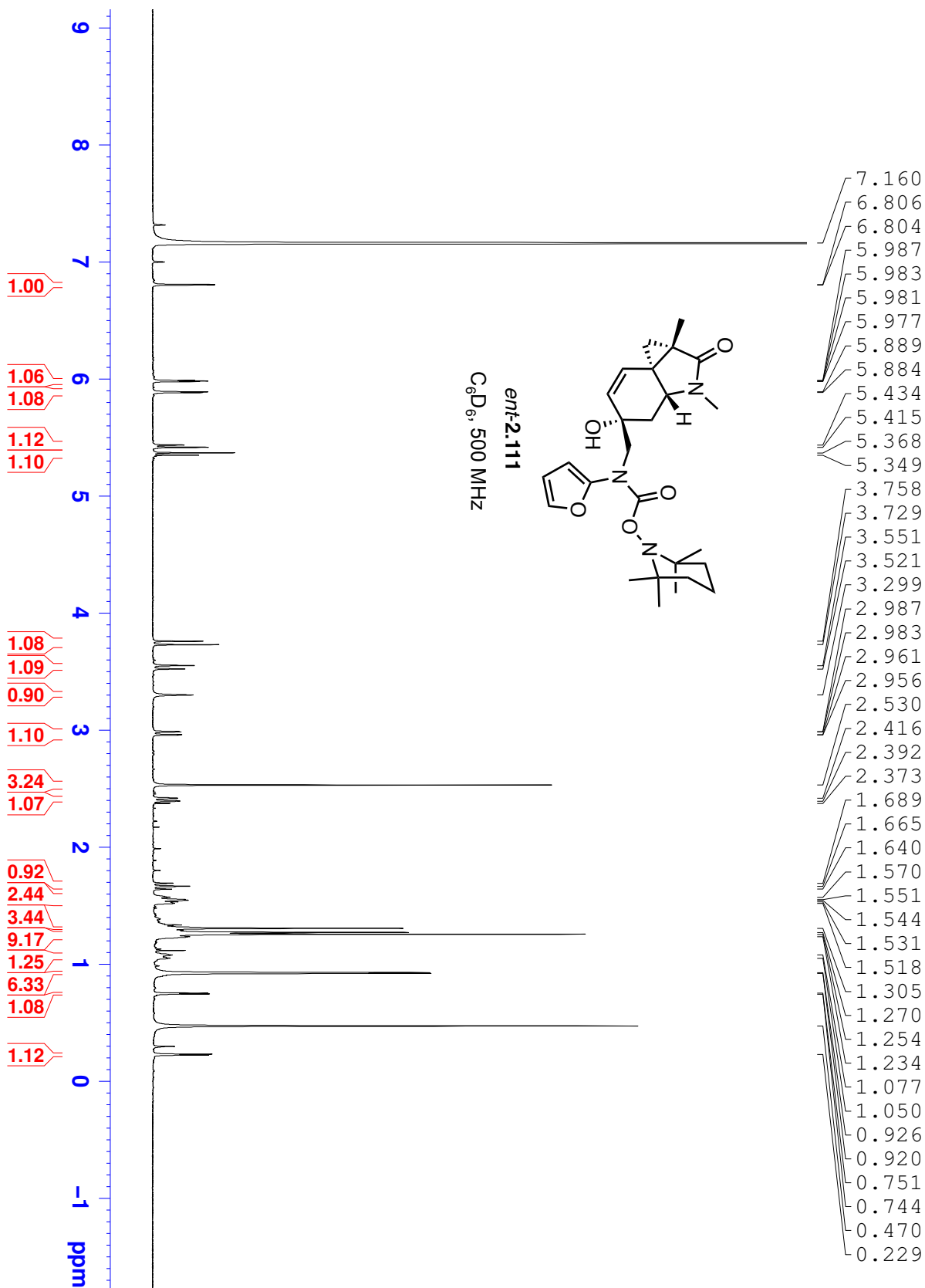




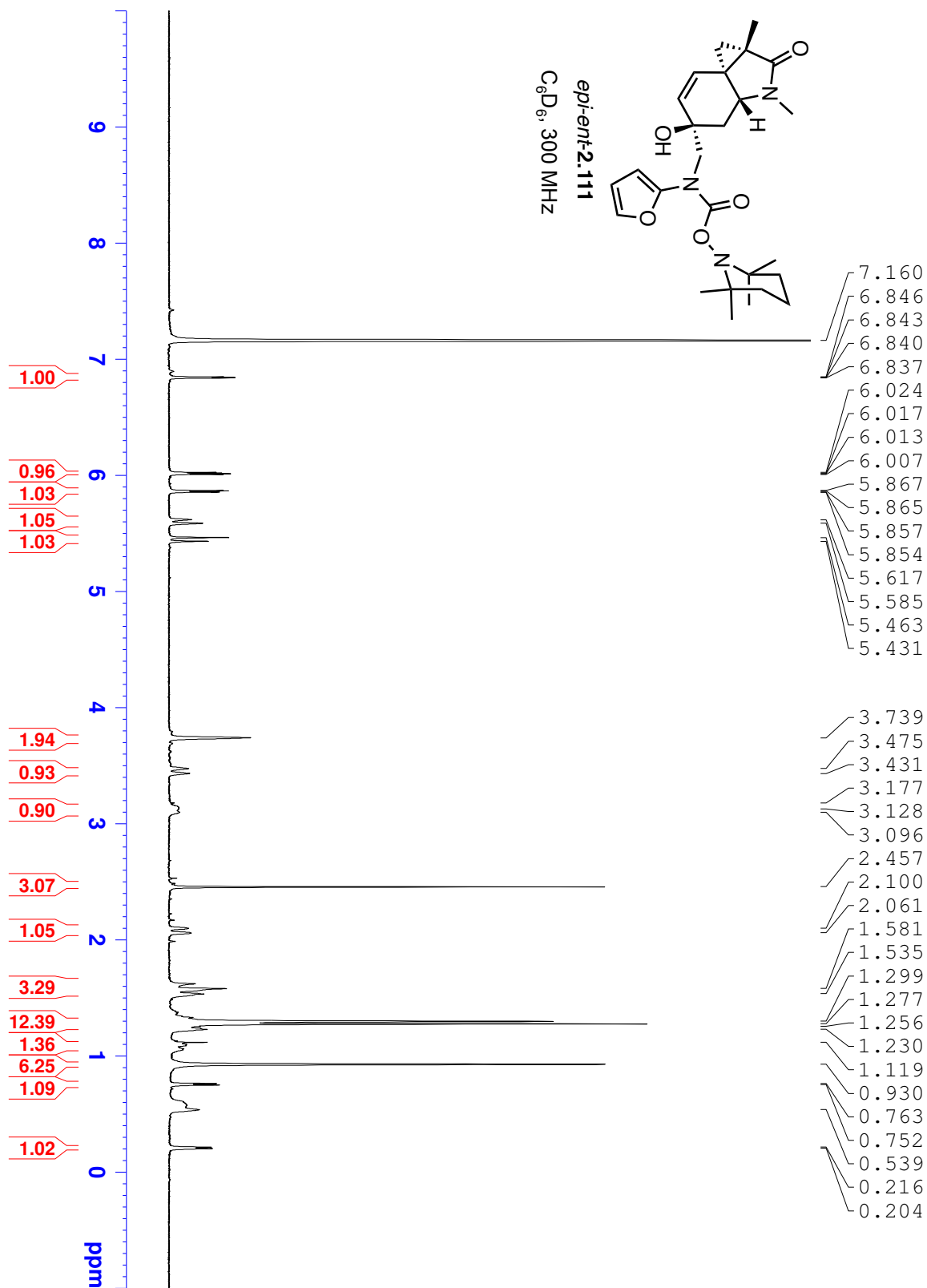
*ent*-2.85

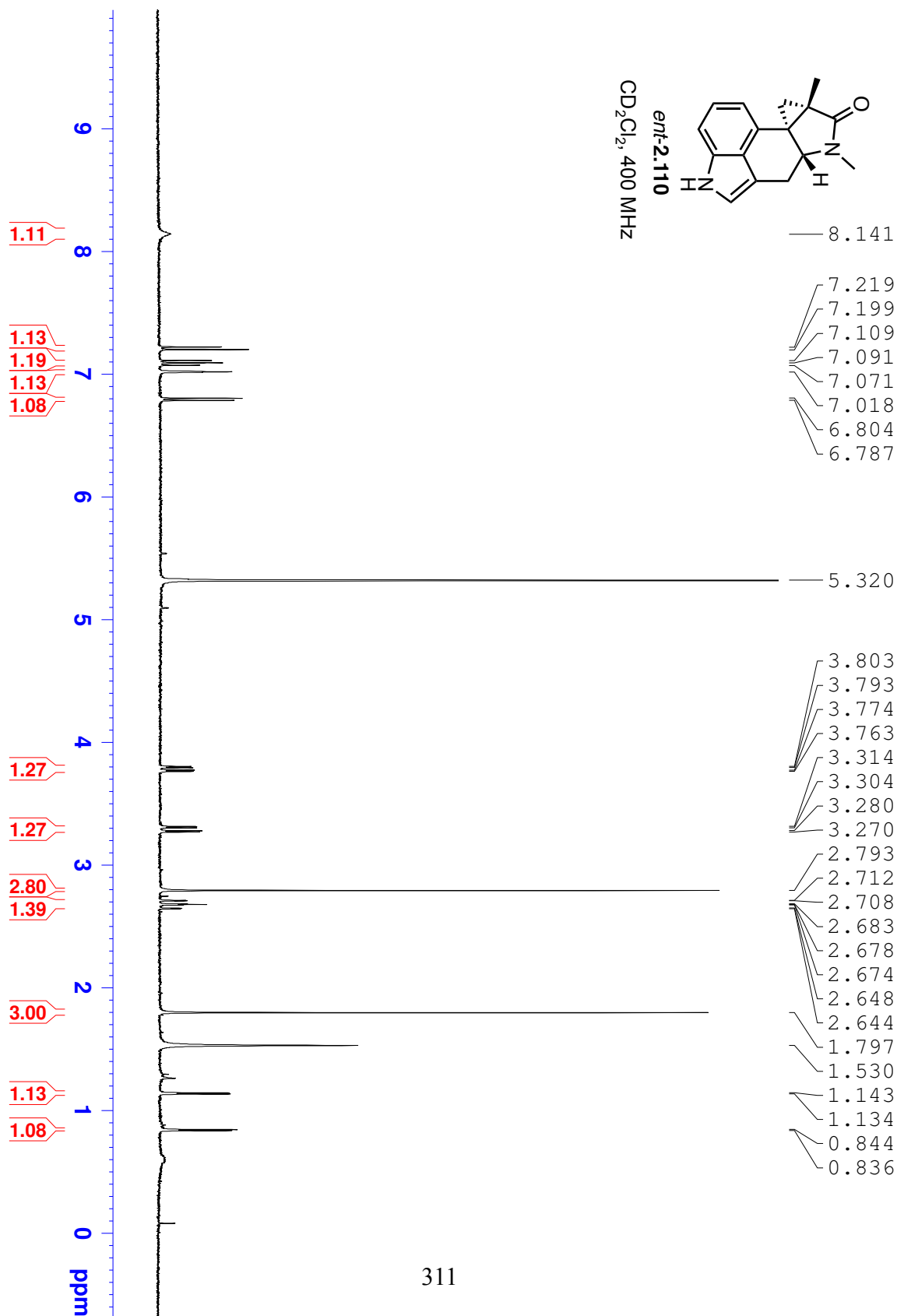
CDCl<sub>3</sub>, 400 MHz

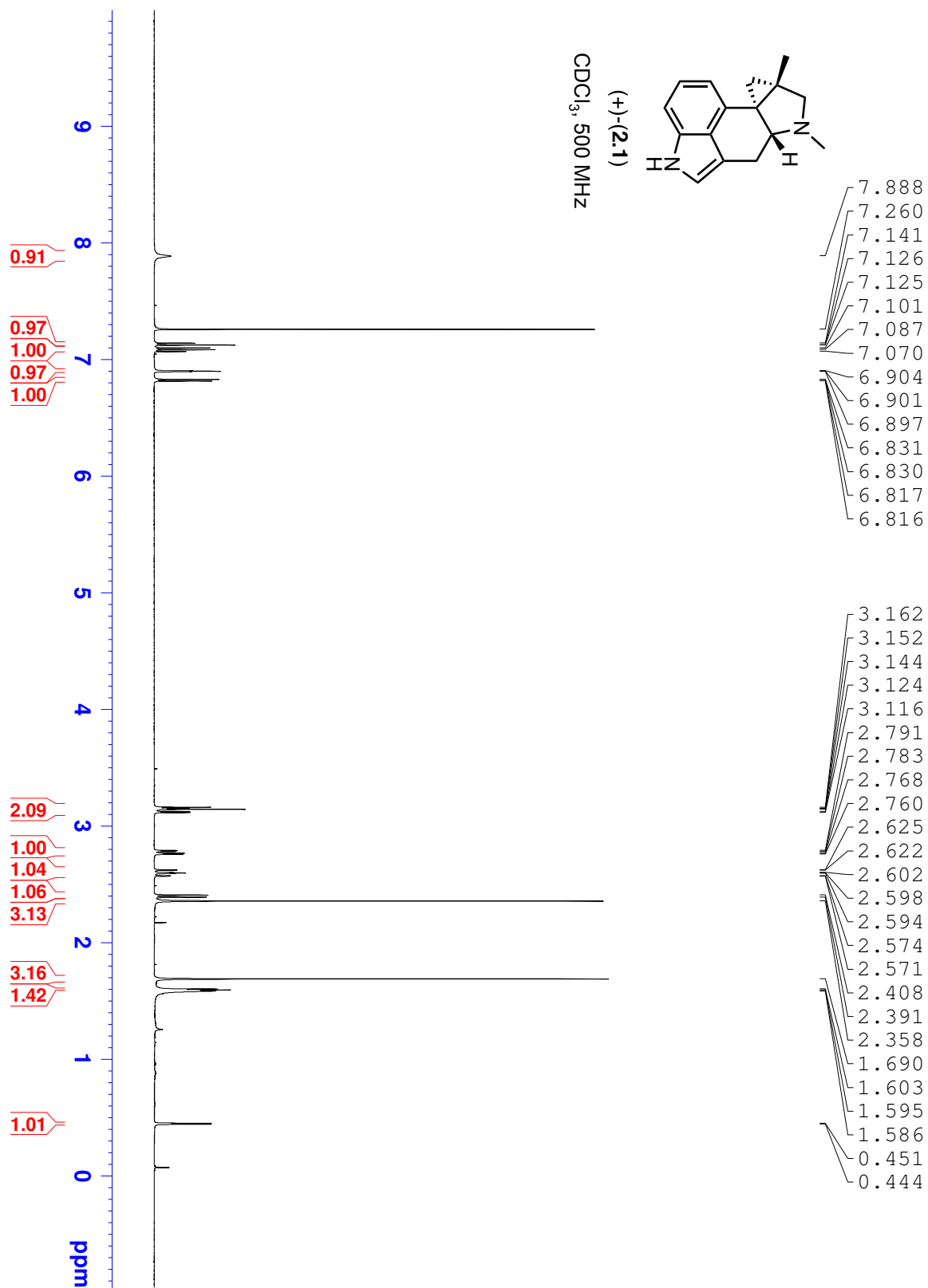


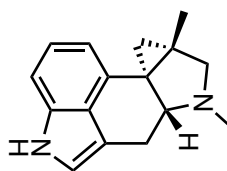






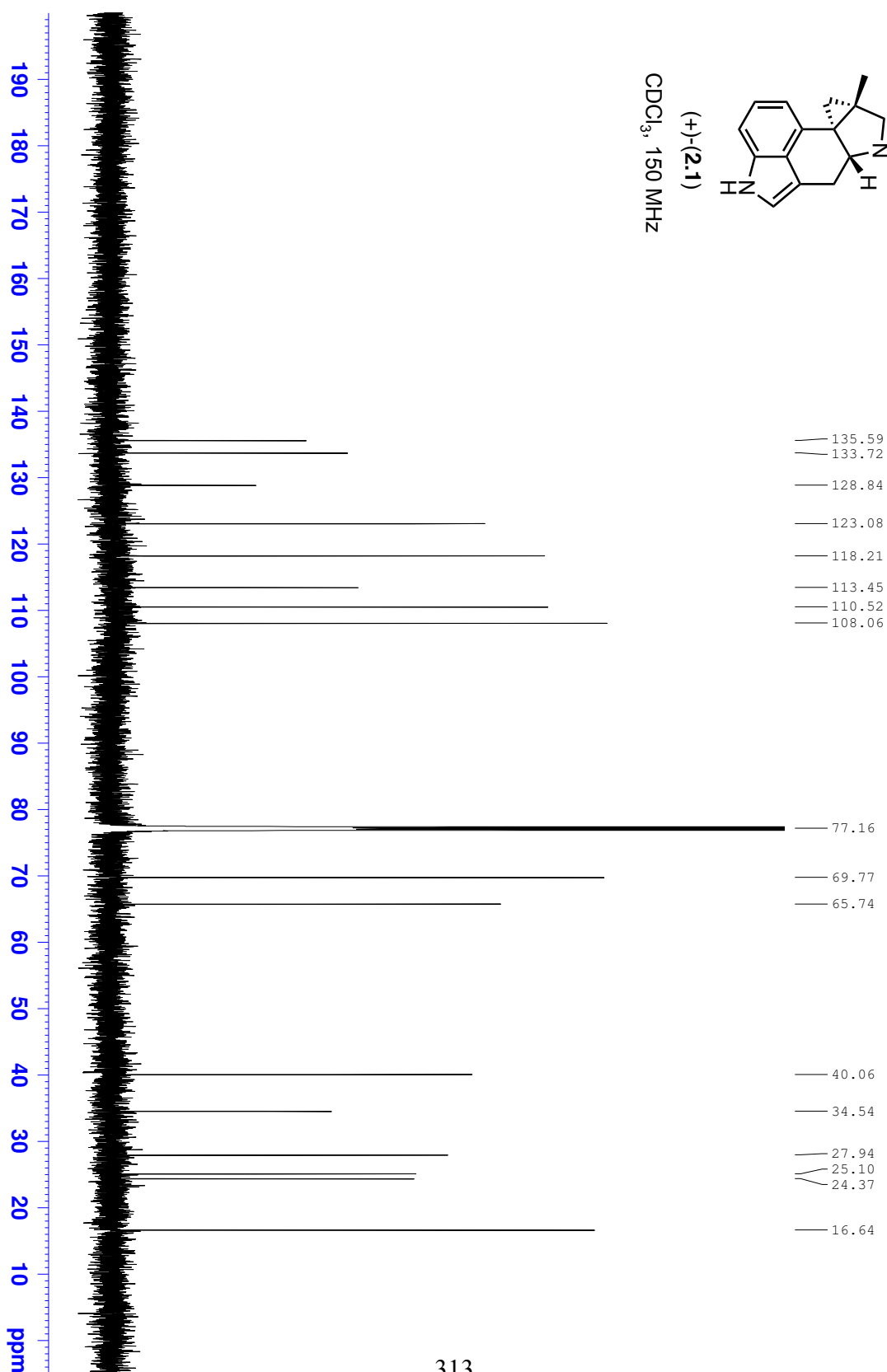


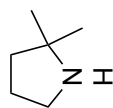




(+)-(2.1)

CDCl<sub>3</sub>, 150 MHz





2.173

PhMe-d8, 400 MHz

7.082  
6.999  
6.964

2.788  
2.771  
2.753

2.080

1.601  
1.583  
1.565  
1.546  
1.528  
1.315  
1.295  
1.277

1.008

2.788  
2.771  
2.753

2.080  
1.601  
1.583  
1.565  
1.546  
1.528  
1.315  
1.295  
1.277  
1.008

1.815

2.000

2.319

5.725

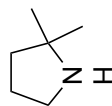
1.82

2.00

2.32

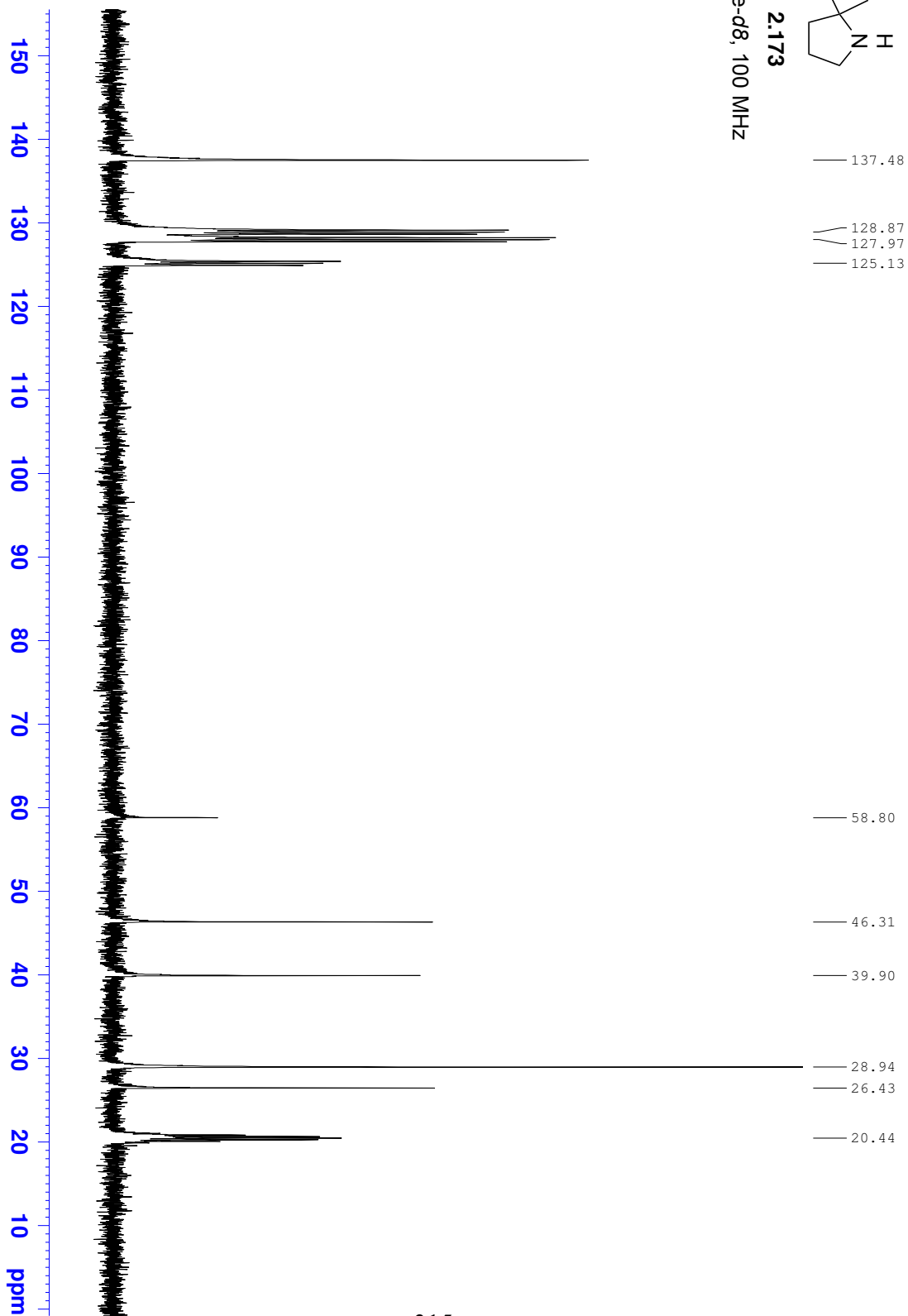
5.72

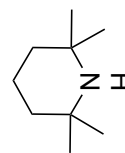
9.5 9.0 8.5 8.0 7.5 7.0 6.5 6.0 5.5 5.0 4.5 4.0 3.5 3.0 2.5 2.0 1.5 1.0 0.5 ppm



2.173

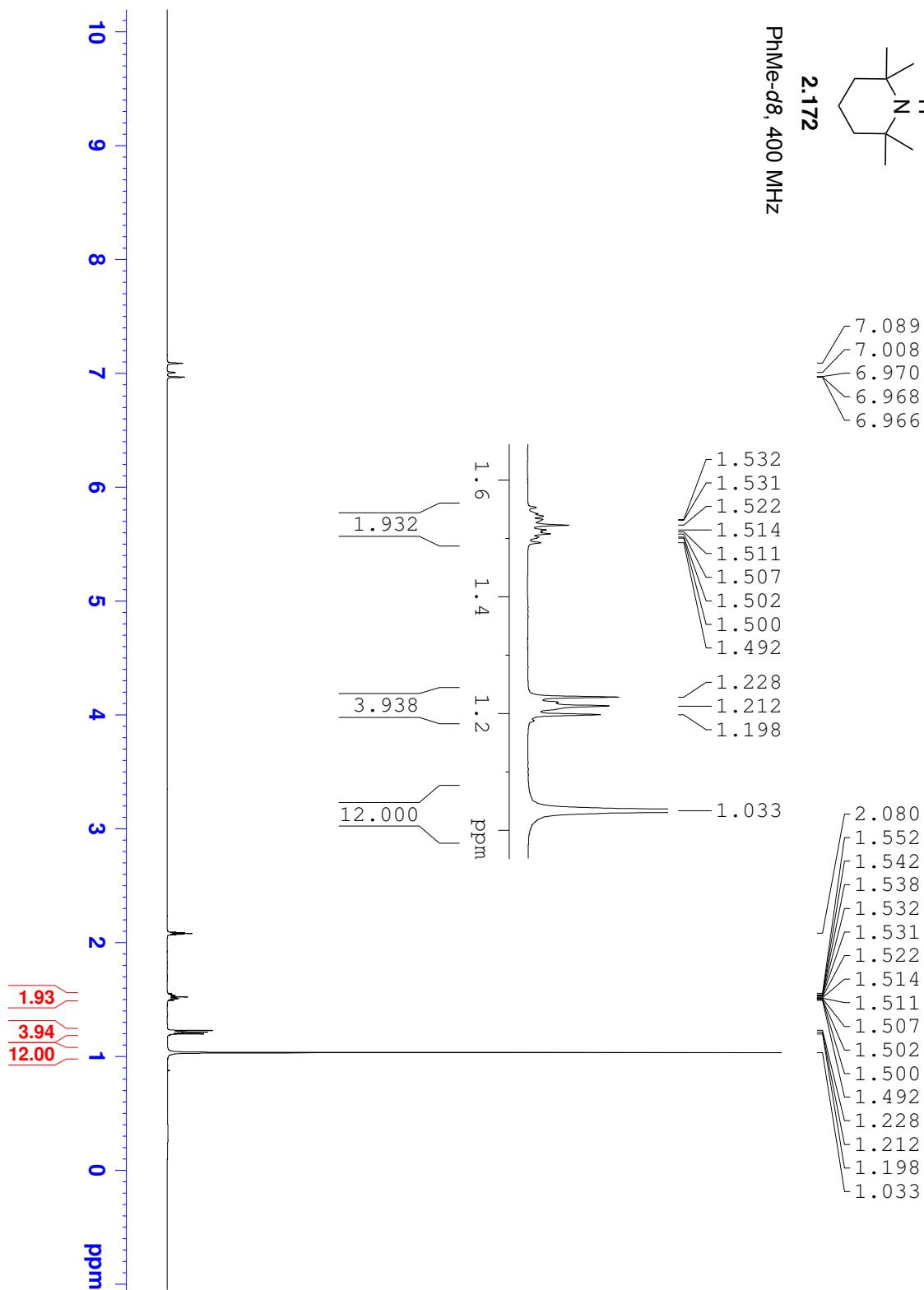
PhMe-d<sub>8</sub>, 100 MHz

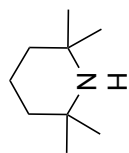




2.172

PhMe-*d*8, 400 MHz





2.172

PhMe-d<sub>8</sub>, 100 MHz

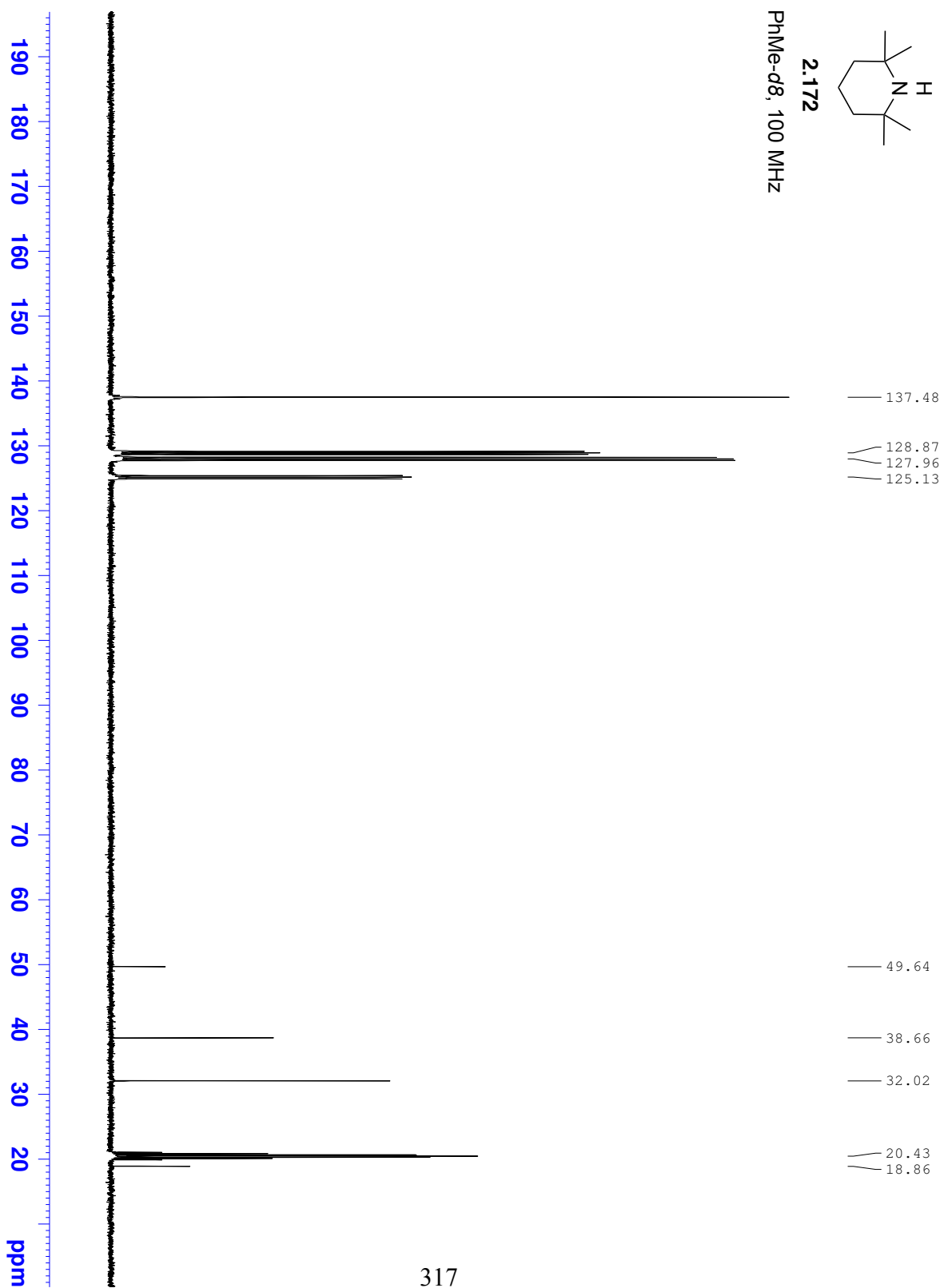




Table 2-9 Entry 1

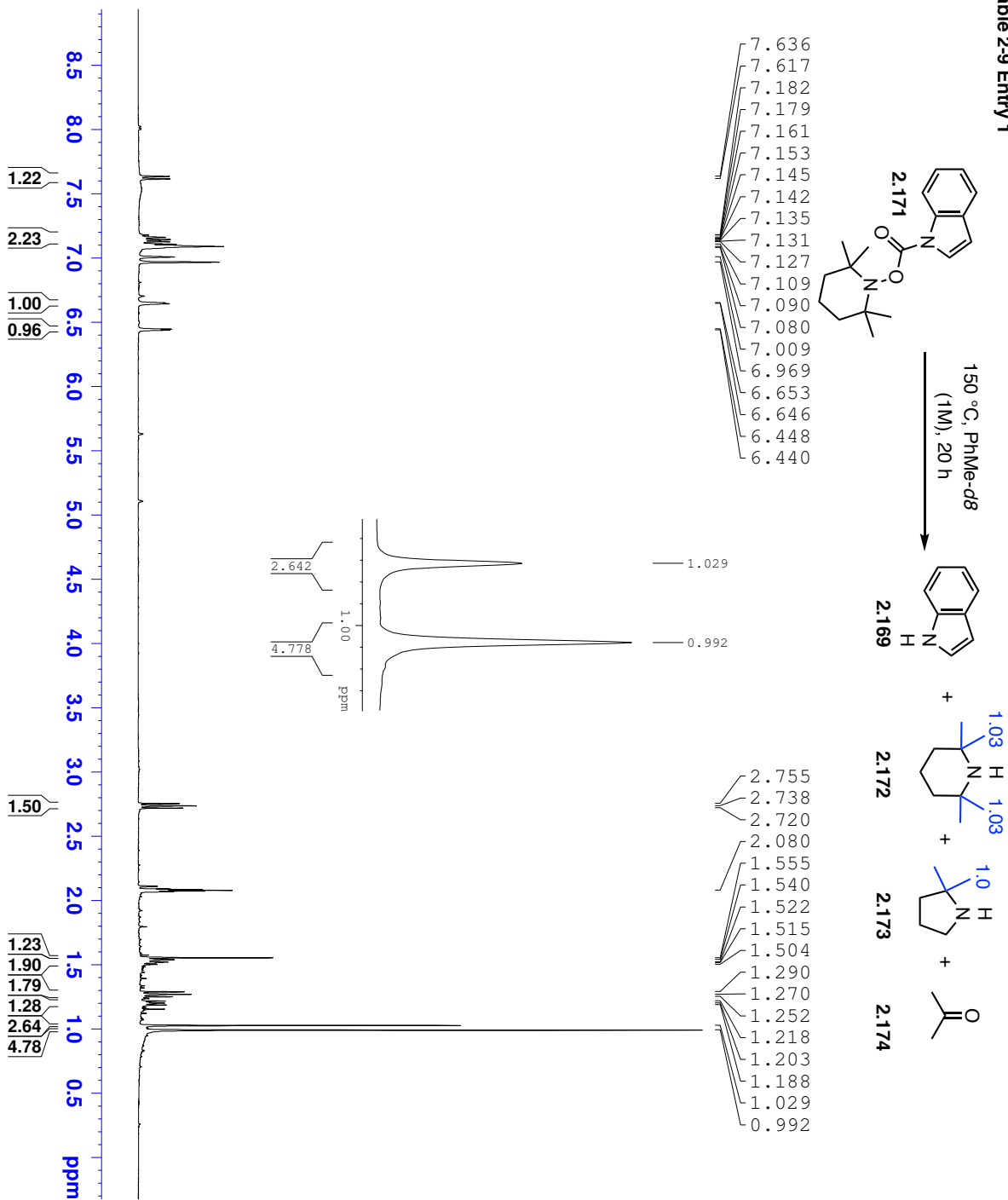


Table 2-9 Entry 1

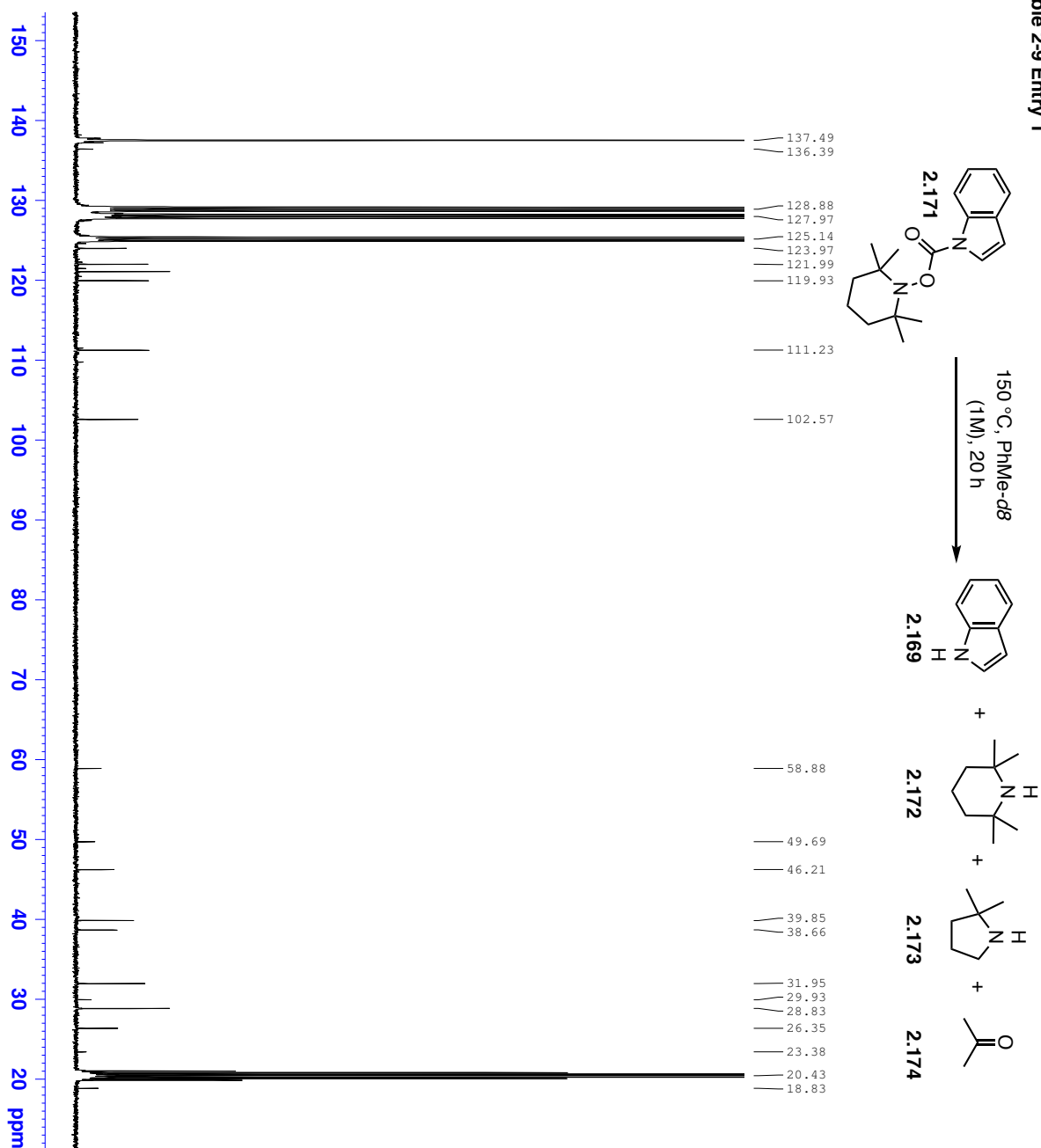
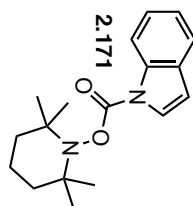
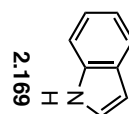


Table 2-9, Entry 2

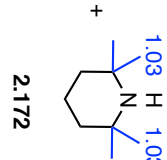


2.171

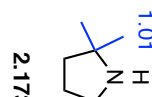
150 °C, degassed  
PhMe-d8 (1M), 9 h



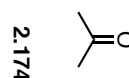
2.169



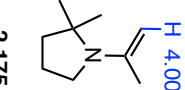
2.172



2.173



2.174



2.175

7.618  
7.598  
7.170  
7.167  
7.152  
7.150  
7.133  
7.130  
7.120  
7.117  
7.090  
7.040  
6.969  
6.585  
6.578  
6.572  
6.425  
6.420  
6.415

4.003  
3.926  
3.041  
3.034  
3.024  
3.007  
2.790  
2.772  
2.755  
2.080  
1.838  
1.835  
1.646  
1.643  
1.581  
1.562  
1.557  
1.546  
1.538  
1.532  
1.527  
1.522  
1.484  
1.313  
1.294  
1.275  
1.226  
1.211  
1.196  
1.154

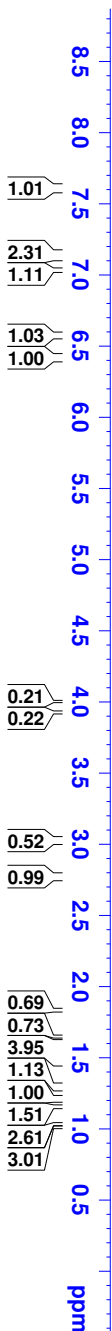
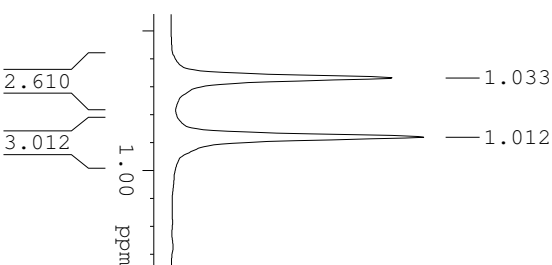
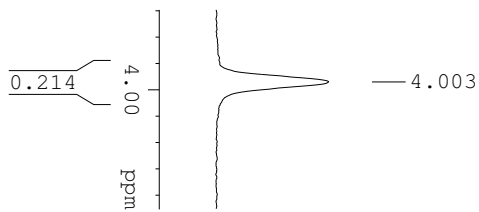
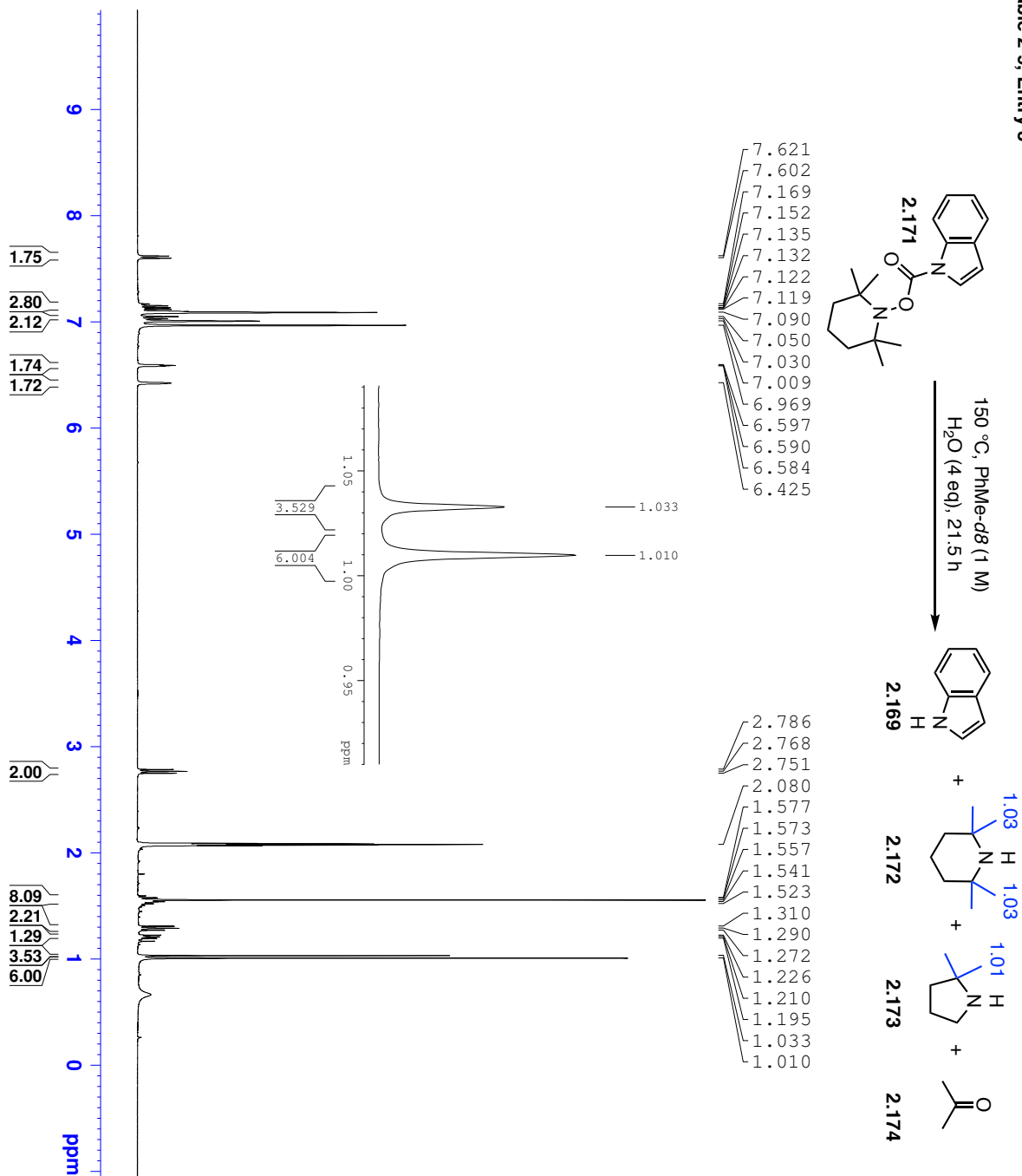
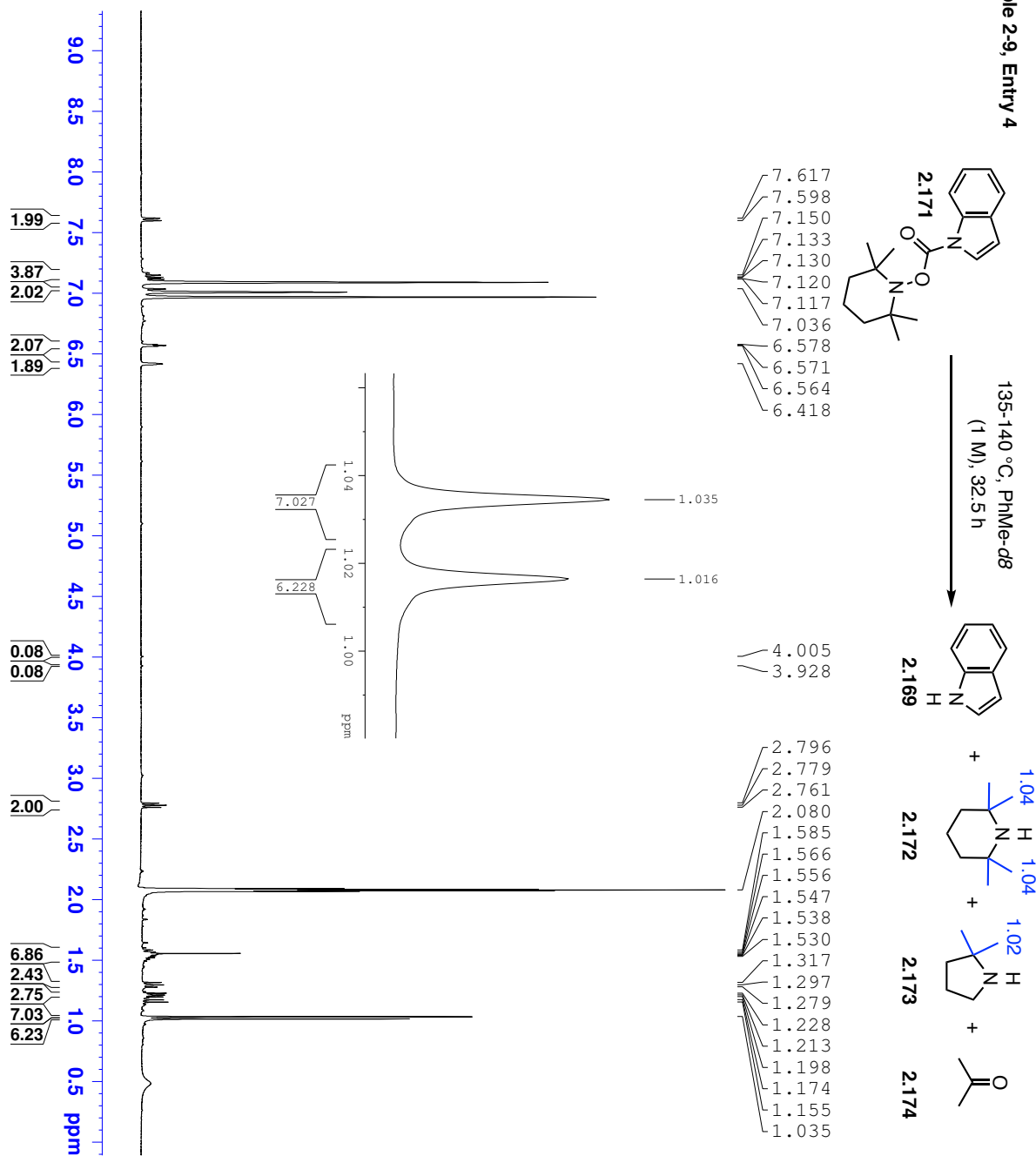


Table 2-9, Entry 3



**Table 2-9, Entry 4**



## BIBLIOGRAPHY

- (1) Baeyer, A. *Ber. Dtsch. Chem. Ges.* **1885**, *18*, 2269.
- (2) Wiberg, K. B. *Angew. Chem. Int. Ed.* **1986**, *25*, 312.
- (3) Wiberg, K. B.; Fenoglio, R. A. *J. Am. Chem. Soc.* **1968**, *90*, 3395.
- (4) Bach, R. D.; Dmitrenko, O. *J. Am. Chem. Soc.* **2004**, *126*, 4444.
- (5) Deakyne, C. A.; Allen, L. C.; Laurie, V. W. *J. Am. Chem. Soc.* **1977**, *99*, 1343.
- (6) Nemoto, T.; Yoshino, G.; Ojika, M.; Sakagami, Y. *Tetrahedron* **1997**, *53*, 16699.
- (7) R Evans, J.; J. Napier, E.; A Fletton, R. *J. Antibiot.* **1978**, *31*, 952.
- (8) Manchester, K. L. *FEBS Lett.* **2001**, *40*, S128.
- (9) Feng P, C.; Patrick S, J. *Br. J. Pharmacol. Chemother.* **2012**, *13*, 125.
- (10) Baldwin, J. E.; Adlington, R. M.; Bebbington, D.; T. Russell, A. *Tetrahedron* **1994**, *50*, 12015.
- (11) Gentry, B. G.; Vollmer, L. E.; Hall, E. D.; Borysko, K. Z.; Zemlicka, J.; Kamil, J. P.; Drach, J. C. *Antimicrob. Agents Chemother.* **2013**, *57*, 4343.
- (12) Prichard, M. N.; Williams, J. D.; Komazin-Meredith, G.; Khan, A. R.; Price, N. B.; Jefferson, G. M.; Harden, E. A.; Hartline, C. B.; Peet, N. P.; Bowlin, T. L. *Antimicrob. Agents Chemother.* **2013**, *57*, 3518.
- (13) Gragson, J. T.; Greenlee, K. W.; Derfer, J. M.; Boord, C. E. *J. Am. Chem. Soc.* **1953**, *75*, 3344.
- (14) Brandi, A.; Goti, A. *Chem. Rev.* **1998**, *98*, 589.
- (15) Audran, G.; Pellissier, H. *Adv. Synth. Catal.* **2010**, *352*, 575.
- (16) Yu, L.; Guo, R. *Org. Prep. Proced. Int.* **2011**, *43*, 209.
- (17) Brandi, A.; Cicchi, S.; Cordero, F. M.; Goti, A. *Chem. Rev.* **2014**, *114*, 7317.

- (18) Hartzler, H. D. *J. Am. Chem. Soc.* **1964**, *86*, 526.
- (19) Goldberg, A. F. G.; Craig, R. A.; O'Connor, N. R.; Stoltz, B. M. *Tetrahedron Lett.* **2015**, *56*, 2983.
- (20) Xu, L.; Huang, X.; Zhong, F. *Org. Lett.* **2006**, *8*, 5061.
- (21) Lai, M. T.; Liu, H. W. *J. Am. Chem. Soc.* **1990**, *112*, 4034.
- (22) de Meijere, A.; Leonov, A.; Heiner, T.; Noltemeyer, M.; Bes, M. T. *Eur. J. Org. Chem.* **2003**, *2003*, 472.
- (23) Zhao, Z.; Liu, H.-w. *J. Org. Chem.* **2002**, *67*, 2509.
- (24) de Meijere, A.; Teichmann, S.; Seyed-Mahdavi, F.; Kohlstruck, S. *Liebigs Ann.* **2006**, *1996*, 1989.
- (25) Prieto, J. A.; Pallarés, M. T.; Larson, G. L. *Synlett* **1993**, *1993*, 199.
- (26) Taguchi, T.; Okada, M. *J. Fluorine Chem.* **2000**, *105*, 279.
- (27) Sang, R.; Yang, H.-B.; Shi, M. *Tetrahedron Lett.* **2013**, *54*, 3591.
- (28) Simaan, S.; Marek, I. *Chem. Commun.* **2009**, 292.
- (29) Obame, G.; Pellissier, H.; Vanthuyne, N.; Bongui, J.-B.; Audran, G. *Tetrahedron Lett.* **2011**, *52*, 1082.
- (30) Nakaya, N.; Sugiyama, S.; Satoh, T. *Tetrahedron Lett.* **2009**, *50*, 4212.
- (31) Masarwa, A.; Stanger, A.; Marek, I. *Angew. Chem. Int. Ed.* **2007**, *46*, 8039.
- (32) Simaan, S.; Masarwa, A.; Bertus, P.; Marek, I. *Angew. Chem. Int. Ed.* **2006**, *45*, 3963.
- (33) Weatherhead-Kloster, R. A.; Corey, E. J. *Org. Lett.* **2006**, *8*, 171.
- (34) Yang, Z.; Xie, X.; Fox Joseph, M. *Angew. Chem. Int. Ed.* **2006**, *45*, 3960.
- (35) Xie, X.; Fox, J. M. *Synthesis* **2013**, *45*, 1807.
- (36) Reitel, K.; Lippur, K.; Järving, I.; Kudrjašova, M.; Lopp, M.; Kanger, T. *Synthesis* **2013**, *45*, 2679.
- (37) Chanthamath, S.; Iwasa, S. *Acc. Chem. Res.* **2016**, *49*, 2080.
- (38) Gregg, T. M.; Farrugia, M. K.; Frost, J. R. *Org. Lett.* **2009**, *11*, 4434.
- (39) Chanthamath, S.; Chua, H. W.; Kimura, S.; Shibatomi, K.; Iwasa, S. *Org. Lett.* **2014**, *16*, 3408.

- (40) Lindsay, V. N. G.; Fiset, D.; Gritsch, P. J.; Azzi, S.; Charette, A. B. *J. Am. Chem. Soc.* **2013**, *135*, 1463.
- (41) Petronijevic, F. R.; Wipf, P. *J. Am. Chem. Soc.* **2011**, *133*, 7704.
- (42) Panne, P.; DeAngelis, A.; Fox, J. M. *Org. Lett.* **2008**, *10*, 2987.
- (43) Goto, T.; Takeda, K.; Anada, M.; Ando, K.; Hashimoto, S. *Tetrahedron Lett.* **2011**, *52*, 4200.
- (44) Tsutsui, H.; Abe, T.; Nakamura, S.; Anada, M.; Hashimoto, S. *Chem. Pharm. Bull.* **2005**, *53*, 1366.
- (45) Schwartz, B. D.; Denton, J. R.; Lian, Y.; Davies, H. M. L.; Williams, C. M. *J. Am. Chem. Soc.* **2009**, *131*, 8329.
- (46) Osako, T.; Panichakul, D.; Uozumi, Y. *Org. Lett.* **2012**, *14*, 194.
- (47) Ward, D. E.; Rhee, C. K. *Tetrahedron Lett.* **1991**, *32*, 7165.
- (48) Applequist, D. E.; Johnston, M. R.; Fisher, F. *J. Am. Chem. Soc.* **1970**, *92*, 4614.
- (49) Davies Huw, M. L.; Antoulinakis Evan, G. *Org. React.* **2004**.
- (50) Elsner Martin, P.; Ziomek, G.; Seidel-Morgenstern, A. *AIChE J.* **2009**, *55*, 640.
- (51) Davies, H. M. L.; Stafford, D. G.; Doan, B. D.; Houser, J. H. *J. Am. Chem. Soc.* **1998**, *120*, 3326.
- (52) Qin, C.; Boyarskikh, V.; Hansen, J. H.; Hardcastle, K. I.; Musaev, D. G.; Davies, H. M. L. *J. Am. Chem. Soc.* **2011**, *133*, 19198.
- (53) DeAngelis, A.; Dmitrenko, O.; Yap, G. P. A.; Fox, J. M. *J. Am. Chem. Soc.* **2009**, *131*, 7230.
- (54) Uchida, T.; Katsuki, T. *Synthesis* **2006**, *2006*, 1715.
- (55) Goto, T.; Takeda, K.; Shimada, N.; Nambu, H.; Anada, M.; Shiro, M.; Ando, K.; Hashimoto, S. *Angew. Chem. Int. Ed.* **2011**, *50*, 6803.
- (56) Lindsay, V. N. G.; Lin, W.; Charette, A. B. *J. Am. Chem. Soc.* **2009**, *131*, 16383.
- (57) Davies, H. M. L.; Bruzinski, P. R.; Lake, D. H.; Kong, N.; Fall, M. J. *J. Am. Chem. Soc.* **1996**, *118*, 6897.
- (58) Hansen, J.; Davies, H. M. L. *Coord. Chem. Rev.* **2008**, *252*, 545.
- (59) McCabe, S. R.; Wipf, P. *Org. Biomol. Chem.* **2016**, *14*, 5894.



- (60) Miedaner, T.; Geiger, H. H. *Toxins* **2015**, *7*, 659.
- (61) Coufal-Majewski, S.; Stanford, K.; McAllister, T.; Blakley, B.; McKinnon, J.; Chaves, A. V.; Wang, Y. *Front. Vet. Sci.* **2016**, *3*, 1.
- (62) Eadie, M. J. *Lancet Neurol.* **2003**, *2*, 429.
- (63) Tittlemier, S. A.; Drul, D.; Roscoe, M.; McKendry, T. *J. Agric. Food Chem.* **2015**, *63*, 6644–6650.
- (64) Wallwey, C.; Li, S. M. *Nat. Prod. Rep.* **2011**, *28*, 496.
- (65) de Groot, A. N. J. A.; van Dongen, P. W. J.; Vree, T. B.; Hekster, Y. A.; van Roosmalen, J. *Drugs* **1998**, *56*, 523.
- (66) Beekman, A.; Barrow, R. *Aus. J. Chem.* **2014**, *67*, 827.
- (67) Makarieva, T. N.; Dmitrenok, A. S.; Dmitrenok, P. S.; Grebnev, B. B.; Stonik, V. A. *J. Nat. Prod.* **2001**, *64*, 1559.
- (68) Li, Y.-X.; Himaya, S. W. A.; Dewapriya, P.; Zhang, C.; Kim, S.-K. *Mar. Drugs* **2013**, *11*, 5063.
- (69) Dockery, L. E.; Gunderson, C. C.; Moore, K. N. *Onco. Targets Ther.* **2017**, *10*, 3029.
- (70) Cabri, W.; Roletto, J.; Olmo, S.; Fonte, P.; Ghetti, P.; Songia, S.; Mapelli, E.; Alpegiani, M.; Paissoni, P. *Org. Proc. Res. Dev.* **2006**, *10*, 198.
- (71) Korber, K.; Song, D.; Rheinheimer, J.; Kaiser, F.; Dickhaut, J.; Narine, A.; Culbertson, D. L.; Thompson, S.; Rieder, J; WO2014096238 A1: 2014.
- (72) Stauffacher, D.; Niklaus, P.; Tschertter, H.; Weber, H. P.; Hofmann, A. *Tetrahedron* **1969**, *25*, 5879.
- (73) Furuta, T.; Koike, M.; Abe, M. *Agric. Biol. Chem.* **1982**, *46*, 1921.
- (74) Schroeder, H.; Hoff, B.; WO 2012116935A2 20120907, 2012.
- (75) Jakubczyk, D.; Caputi, L.; Hatsch, A.; Nielsen, C. A. F.; Diefenbacher, M.; Klein, J.; Molt, A.; Schröder, H.; Cheng, J. Z.; Naesby, M.; O'Connor, S. E. *Angew. Chem. Int. Ed.* **2015**, *54*, 5117.
- (76) Jakubczyk, D.; Caputi, L.; Stevenson, C. E. M.; Lawson, D. M.; O'Connor, S. E. *Chem. Commun.* **2016**, *52*, 14306.
- (77) Coyle, C. M.; Cheng Jz Fau - O'Connor, S. E.; O'Connor Se Fau - Panaccione, D. G.; Panaccione, D. G. *Appl. Environ. Microbiol.* **2010**, *76*(3898).
- (78) Havemann, J.; Vogel, D.; Loll, B.; Keller, U. *Chem. Biol.*, *21*, 146.

- (79) Thibodeaux, C. J.; Chang, W.-c.; Liu, H.-w. *Chem. Rev.* **2012**, *112*, 1681.
- (80) Incze, M.; Dörnyei, G.; Moldvai, I.; Temesvári-Major, E.; Egyed, O.; Szántay, C. *Tetrahedron* **2008**, *64*, 2924.
- (81) Moldvai, I.; Temesvári-Major, E.; Incze, M.; Szentirmay, É.; Gács-Baitz, E.; Szántay, C. *J. Org. Chem.* **2004**, *69*, 5993.
- (82) Teranishi, K.; Hayashi, S.; Nakatsuka, S.-i.; Goto, T. *Tetrahedron Lett.* **1994**, *35*, 8173.
- (83) Petronijevic, F.; Timmons, C.; Cuzzupe, A.; Wipf, P. *Chem. Commun.* **2008**, 106.
- (84) LaPorte, M.; Hong, K. B.; Xu, J.; Wipf, P. *J. Org. Chem.* **2013**, *78*, 167.
- (85) Xu, J.; Wipf, P. *Org. Biomol. Chem.* **2017**, *15*, 7093.
- (86) Boonsompat, J.; Padwa, A. *J. Org. Chem.* **2011**, *76*, 2753.
- (87) Jabre, N. D.; Watanabe, T.; Brewer, M. *Tetrahedron Lett.* **2014**, *56*, 197.
- (88) Draghici, C.; Huang, Q.; Brewer, M. *J. Org. Chem.* **2009**, *74*, 8410.
- (89) Wang, W.; Lu, J. T.; Zhang, H. L.; Shi, Z. F.; Wen, J.; Cao, X. P. *J. Org. Chem.* **2014**, *79*, 122.
- (90) Netz, N.; Opatz, T. *J. Org. Chem.* **2016**.
- (91) Chen, J.-Q.; Song, L.-L.; Li, F.-X.; Shi, Z.-F.; Cao, X.-P. *Chem. Commun.* **2017**, *53*, 12902.
- (92) Chaudhuri, S.; Ghosh, S.; Bhunia, S.; Bisai, A. *Chem. Commun.* **2018**, *54*, 940.
- (93) Scott, M. E.; Lautens, M.; Dubé, M.; Ragan, J. A. *Org. Synth.* **2008**, *85*, 172.
- (94) Miller, B.; Wong, H.-S. *Tetrahedron* **1972**, *28*, 2369.
- (95) Stotter, P. L.; Hill, K. A. *J. Org. Chem.* **1973**, *38*, 2576.
- (96) Sharpless, K. B.; Lauer, R. F.; Teranishi, A. Y. *J. Am. Chem. Soc.* **1973**, *95*, 6137.
- (97) Ito, Y.; Hirao, T.; Saegusa, T. *J. Org. Chem.* **1978**, *43*, 1011.
- (98) Diao, T.; Stahl, S. S. *J. Am. Chem. Soc.* **2011**, *133*, 14566.
- (99) Wang, D.; Weinstein, A. B.; White, P. B.; Stahl, S. S. *Chem. Rev.* **2018**, *118*, 2636.
- (100) Konnick, M. M.; Stahl, S. S. *J. Am. Chem. Soc.* **2008**, *130*, 5753.
- (101) Steinhoff, B. A.; Fix, S. R.; Stahl, S. S. *J. Am. Chem. Soc.* **2002**, *124*, 766.

- (102) House, H. O.; Trost, B. M. *J. Org. Chem.* **1965**, *30*, 1341.
- (103) Velluz, L.; Valls, J.; Nominé, G. *Angew. Chem. Int. Ed.* **1965**, *4*, 181.
- (104) Nasipuri, D. *Stereochemistry of Organic Compounds: Principles and Applications*, 1994.
- (105) Maruoka, K.; Imoto, H.; Yamamoto, H. *Synlett* **1995**, 1995, 719.
- (106) Das, S.; Addis, D.; Junge, K.; Beller, M. *Chem. Eur. J.* **2011**, *17*, 12186.
- (107) Reeves, J. T.; Tan, Z.; Marsini, M. A.; Han, Z. S.; Xu, Y.; Reeves, D. C.; Lee, H.; Lu, B. Z.; Senanayake, C. H. *Adv. Synth. Catal.* **2013**, *355*, 47.
- (108) Wipf, P.; Rector, S. R.; Takahashi, H. *J. Am. Chem. Soc.* **2002**, *124*, 14848.
- (109) Wipf, P.; Spencer, S. R. *J. Am. Chem. Soc.* **2005**, *127*, 225.
- (110) Rosenker, C. J.; Krenske, E. H.; Houk, K. N.; Wipf, P. *Org. Lett.* **2013**, *15*, 1076.
- (111) Padwa, A.; Crawford, K. R.; Rashatasakhon, P.; Rose, M. *J. Org. Chem.* **2003**, *68*, 2609.
- (112) Barham, J. P.; John, M. P.; Murphy, J. A. *J. Am. Chem. Soc.* **2016**, *138*, 15482.
- (113) Kraft, S.; Ryan, K.; Kargbo, R. B. *J. Am. Chem. Soc.* **2017**, *139*, 11630.
- (114) Akahori, Y.; Yamakoshi, H.; Hashimoto, S.; Nakamura, S. *Org. Lett.* **2014**, *16*, 2054.
- (115) Szostak, M.; Spain, M.; Eberhart, A. J.; Procter, D. J. *J. Org. Chem.* **2014**, *79*, 11988.
- (116) Szostak, M.; Spain, M.; Eberhart, A. J.; Procter, D. J. *J. Am. Chem. Soc.* **2014**, *136*, 2268.
- (117) Roth, B. L.; Baner, K.; Westkaemper, R.; Siebert, D.; Rice, K. C.; Steinberg, S.; Ernsberger, P.; Rothman, R. B. *PNAS* **2002**, *99*, 11934.
- (118) Beaulieu, J.-M.; Gainetdinov, R. R. *Pharmacol. Rev.* **2011**, *63*, 182.
- (119) Joyce, J. N.; Millan, M. J. *Drug Discov. Today* **2005**, *10*, 917.
- (120) Maramai, S.; Gemma, S.; Brogi, S.; Campiani, G.; Butini, S.; Stark, H.; Brindisi, M. *Front. Neurosci.* **2016**, *10*, 451.
- (121) Banibrata, D.; Gyan, M.; Alope, D. *Curr. Top. Med. Chem.* **2015**, *15*, 908.
- (122) Heiser, J. F. W., C.S. *Mol. Diag. Ther.* **1998**, *10*, 343.
- (123) Dahlf, C.; Maassen Van Den Brink, A. *Headache* **2012**, *52*, 707.
- (124) Cho, R.; Kapur, S.; Du, L.; Hrdina, P. *Neurosci. Lett.* **1999**, *261*, 139.

- (125) Kaumann, A. J.; Levy, F. O. *Pharmacol. Ther.* **2006**, *111*, 674.
- (126) Wacker, D.; Wang, S.; McCorvy, J. D.; Betz, R. M.; Venkatakrisnan, A. J.; Levit, A.; Lansu, K.; Schools, Z. L.; Che, T.; Nichols, D. E.; Shoichet, B. K.; Dror, R. O.; Roth, B. L. *Cell*, *168*, 377.
- (127) Nichols, D. E. *Pharmacol. Ther.* **2004**, *101*, 131.
- (128) González-Maeso, J.; Weisstaub, N. V.; Zhou, M.; Chan, P.; Ivic, L.; Ang, R.; Lira, A.; Bradley-Moore, M.; Ge, Y.; Zhou, Q.; Sealton, S. C.; Gingrich, J. A. *Neuron* **2007**, *53*, 439.
- (129) Schmidt, C. J.; Sorensen, S. M.; Kenne, J. H.; Carr, A. A.; Palfreyman, M. G. *Life Sci.* **1995**, *56*, 2209.
- (130) Meltzer, H. Y.; Massey, B. W. *Curr. Opin. Pharmacol.* **2011**, *11*, 59.
- (131) Chapman, M. E.; Wideman, J. R. F. *Poult. Sci.* **2006**, *85*, 777.
- (132) Hashimoto, T.; Miyamoto, H.; Naganawa, Y.; Maruoka, K. *J. Am. Chem. Soc.* **2009**, *131*, 11280.
- (133) Rainbolt, J. E.; Miller, G. P. *J. Org. Chem.* **2007**, *72*, 3020.
- (134) Petronijevic, F. *Dissertation, University of Pittsburgh* **2012**.
- (135) Lu, X.; Lin, S. *J. Org. Chem.* **2005**, *70*, 9651.
- (136) Al-Saleh, B.; Makhseed, S.; Hassaneen, H. M. E.; Elnagdi, M. H. *Synthesis* **2006**, *2006*, 59.
- (137) Paleos, C. M.; Dais, P. *J. Chem. Soc. Chem. Commun*, **1977**, 345.
- (138) Frantz, M.-C.; Pierce, J. G.; Pierce, J. M.; Kangying, L.; Qingwei, W.; Johnson, M.; Wipf, P. *Org. Lett.* **2011**, *13*, 2318.
- (139) Åhman, J.; Somfai, P. *Synth. Commun.* **1994**, *24*, 1117.
- (140) McCabe, S. R.; Wipf, P. *Angew. Chem. Int. Ed.* **2017**, *56*, 324.
- (141) Shi, R.; Zhang, H.; Lu, L.; Gan, P.; Sha, Y.; Zhang, H.; Liu, Q.; Beller, M.; Lei, A. *Chem. Commun.* **2015**, *51*, 3247.